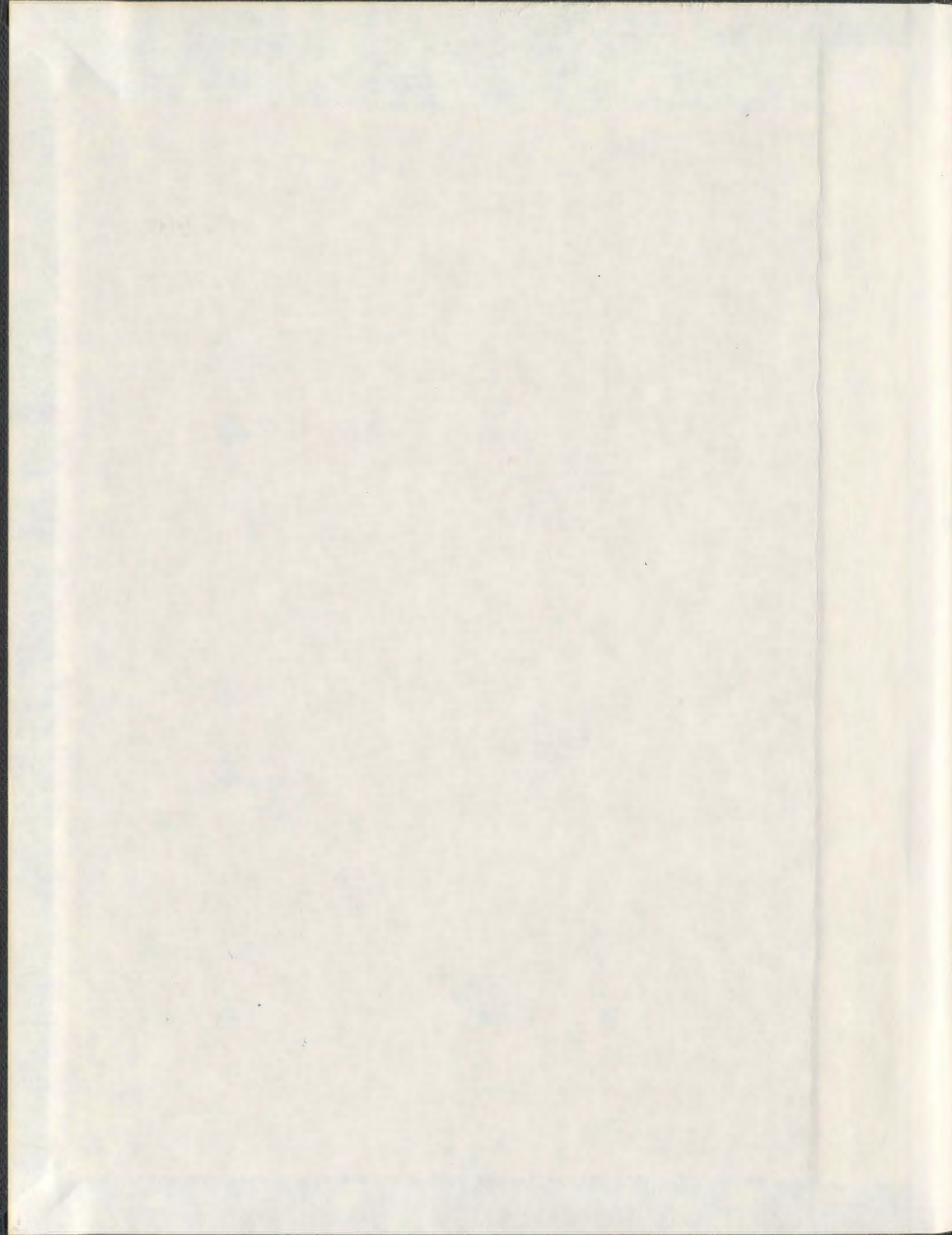


INVERSE ELECTRON DEMAND DIELS-ALDER  
(IEDDA)-DRIVEN DOMINO REACTIONS OF  
CHROMONE-FUSED ELECTRON DEFICIENT DIENES:  
NEW METHODOLOGY FOR THE SYNTHESIS OF  
XANTHONES AND XANTHONE-BASED POLYCYCLIC  
HETEROAROMATIC MOLECULES

ANH-THU T. DANG





001311



**Inverse Electron Demand Diels-Alder (IEDDA)-Driven Domino  
Reactions of Chromone-fused Electron Deficient Dienes:  
New Methodology for the Synthesis of Xanthenes and Xanthone-based  
Polycyclic Heteroaromatic Molecules**

by

**Anh-Thu T. Dang**

(B.Sc.) University of Natural Sciences,  
National University of Hochiminh City, Vietnam

A thesis submitted to the School of Graduate Studies  
in partial fulfillment of the requirements for  
the degree of Doctor of Philosophy

Department of Chemistry  
Memorial University  
St. John's, Newfoundland and Labrador, Canada

October 2009



## **Dedication**

I would like to dedicate this work to

My late Father Dang Gia Khanh who wished to wait for my graduation, but could not...

My Mother Pham Thi Dong Hoa

My Mother-in-law Nguyen Thi Minh Nguyet

My husband Tran Huu-Anh

And to all my brothers and sisters in my family.

## Abstract

The research described in this thesis mainly dealt with methodology development, design and synthesis, as well as the study of the physical properties of new xanthenes and xanthone-based molecules. An offshoot of this work was concerned with the development of a synthetic approach to novel cyclic oligophenylenes. The inverse electron demand Diels-Alder (IEDDA)-based methodology was employed in all of the projects.

The first objective was to employ the IEDDA reaction in a new approach to xanthenes. Specifically, nine new 2-substituted-4-methoxyxanthenes **1.228a-i** and eight new 2-substituted-3,4-dimethoxyxanthenes **1.229a-h** were synthesized using IEDDA-driven domino reactions between chromone-fused dienes **1.15** and the corresponding electron-rich dienophiles **1.225** and **1.226**, respectively. This work is described in Chapter 2. This methodology was also employed for the synthesis of arylxanthenes in Chapter 3. A series of 2-aryl-4-methoxyxanthenes **3.9a-c** and 2-substituted-4-phenylxanthone, such as **3.18**, was obtained from the reactions of the corresponding dienes **3.8a-c** or **1.15b** with dienophile **1.227**. However, the desired 2,4-diaryl-xanthenes **3.10** could not be synthesized by this method.

The second objective was to synthesize two different types of hetero[5]acenes from appropriate xanthone frameworks, *i.e.* 3,4-dimethoxyxanthenes and 4-methoxyxanthenes, which were successfully obtained by the established IEDDA methodology. For example, Chapter 4 describes the synthesis of xanthonoid hetero[5]acenes **4.22** and **4.12-4.14** from the key intermediate 3,4-dimethoxyxanthone



**4.23** via a selective demethylation, followed by an intramolecular nucleophilic aromatic substitution. Among these newly-synthesized compounds, hetero[5]acene-based crown ether **4.14** was designed for future complexation studies with ions toward chemosensor applications. The attempted synthesis of hetero[*n*]acenes (*n* = 5, 9) using double IEDDA reactions suffered from difficulties in the isolation of bis(diene) intermediate **4.26**. At best, trace amounts only of hetero[5]acene **4.25b** (mass spectroscopic analysis) were obtained.

In Chapter 5, another class of hetero[5]acenes, referred to as “donor-acceptor xanthone-carbazole hybrid systems”, was constructed from key intermediate 2-*o*-nitrophenyl-4-methoxyxanthenes **5.31a–f** and **5.38**, via microwave-assisted Cadogan reactions, followed by *N*-alkylation. A series of xanthone-carbazoles with or without substituents (OMe, Br) was synthesized, in which the “angular” isomers are the major product and the “linear” isomers are the minor ones in all cases. Suzuki couplings were effective in the synthesis of aryl-substituted xanthone-carbazole compounds. Physical studies on newly-synthesized xanthone-carbazoles showed some interesting features. For instance, the angular isomers show green fluorescence and quasi-reversible redox behaviour, while the linear ones show blue fluorescence in most cases and irreversible redox behaviour. Most of the xanthone-carbazoles exhibit moderate fluorescence quantum yields, narrow HOMO-LUMO energy gaps, low HOMO energies, and some of them have close interplanar distances in solid-state packing (X-ray analysis), which make them very promising candidates in OLED or OFET applications.

Finally, in Chapter 6, the synthesis of a cyclic oligophenylene was attempted using a six-fold IEDDA reaction. Although this project was unsuccessful, investigations aimed at the improvement of the reaction conditions as well as the design of a more reactive bis(diene) should be informative to future work.



## Acknowledgements

Foremost, I am extremely grateful to my supervisor, Dr. Graham J. Bodwell, who has inspired me immensely with his expertise and research insights. His guidance, support and encouragement in my professional and personal lives will forever be remembered and appreciated.

I would also like to thank Dr. Sunil V. Pansare and Dr. Raymond A. Poirier, my supervisory committee members, for their helpful discussions and diligent review of the thesis. The examiners of this thesis work are acknowledged for their time and critical evaluation.

I would like to thank Dr. Bernhard Witulski at Johannes-Gutenberg-Universität Mainz for providing me with not only a good research environment but also with kind instructions and encouragement during my short tenure in his laboratory in the Summer of 2007. Dr. Carole Witulski-Alayrac, Jörg Moritz, and Dr. Dieter Schollmeyer are acknowledged for their contributions to the microwave-assisted Cadogan reactions and X-ray crystallography, respectively, as described in Chapter 5.

I would also like to express my appreciation to Dr. Paris E. Georgiou, Dr. Yuming Zhao, and Dr. David W. Thompson for their thoughtful advice and support over the course of my PhD program. Thanks are extended to Ms. Linda Winsor, Dr. Celine Schneider, and Dr. Dawe Louise, respectively for their assistance with the mass spectral analysis, NMR service, and X-ray crystallography. Dr. Robert Davis as well as the Faculty and Staff of the Chemistry Department are acknowledged for their kindness and willingness to assist when needed.

I am deeply grateful to my family for their love and encouragement. Throughout my studies, my husband, Dr Huu-Anh Tran has been an unyielding source of strength, understanding, patience and support that I could always draw on. With him by my side, anything would be possible for me.

I wish to thank Drs. Lan Gien, Tran Gien, Mr. and Mrs. McIntyre, the Pham and the Kim Le families for their assistance, encouragement and giving me a "home" in St. John's during my studies. Sincere thanks goes to my friends all over the world whose friendships and support I can always rely on during the most difficult days. All students, past and present, in the Bodwell group as well as in others are remembered for their kindness and friendship.

Financial support from the Department of Chemistry, School of Graduate Studies (including J. Beryl Truscott Graduate Scholarship) at Memorial University, and Natural Sciences and Engineering Research Council (NSERC) of Canada is gratefully acknowledged.



## Table of Contents

<b>Title.....</b>	<b>i</b>
<b>Dedication .....</b>	<b>ii</b>
<b>Abstract.....</b>	<b>iii</b>
<b>Acknowledgements .....</b>	<b>vi</b>
<b>Tables of Contents.....</b>	<b>viii</b>
<b>List of Figures.....</b>	<b>xiv</b>
<b>List of Schemes .....</b>	<b>xviii</b>
<b>List of Tables .....</b>	<b>xxiv</b>
<b>List of Symbols, Abbreviations and Acronyms.....</b>	<b>xxvi</b>

### **Chapter 1    Introduction**

1.1 A Brief Review of the Diels-Alder Reaction.....	1
1.2 IEDDA Reactions of the 1,3-Disubstituted Electron-deficient Dienes .....	3
1.3 The IEDDA Reaction Studies in the Bodwell Group .....	5
1.3.1 IEDDA Reactions of Dienes 1.11 .....	5
1.3.2 Coumarin-based Dienes 1.12 .....	7
1.3.3 Azadienes 1.13 and 1.14 .....	9
1.3.4 Chromone-based Dienes 1.15 .....	11
1.4 Xanthone.....	13
1.4.1 Structure, Nomenclature, Classification, and Properties .....	13
1.4.2 Methodologies for the Synthesis of Xanthones .....	15

1.5 Heteroacenes .....	32
1.5.1 Historical Development of Heteroacenes .....	32
1.5.2 Classifications and Nomenclatures of Heteroacenes .....	34
1.5.3 Common Acene-type Packing Motifs.....	36
1.5.4 Relationships between Charge Carrier Mobility and Molecular Structures .....	37
1.5.5 Major Interest: Xanthonoid Hetero[5]acenes.....	40
1.6 Aims of This Work .....	45
1.7 References and Notes.....	47
 <b>Chapter 2     Synthesis and Physical Properties of 2-Substituted                   4-Methoxyxanthenes and 3,4-Dimethoxyxanthenes</b>	
2.1 Introduction.....	56
2.1.1 A Proposed Mechanism for the Synthesis of Xanthenes via the IEDDA Reaction .....	57
2.1.2 Retrosynthetic Analysis of 4-Methoxy- and 3,4-Dimethoxyxanthenes .....	59
2.2 Results and Discussion .....	60
2.2.1 Synthesis of HWE Phosphonates and Wittig Reagent.....	60
2.2.2 Synthesis of Chromone-fused Electron-deficient Dienes <b>1.15</b> .....	61
2.2.3 Synthesis of Dienophiles <b>1.225</b> and <b>1.226</b> .....	63
2.2.4 Synthesis of 2-Substituted 4-Methoxyxanthenes.....	64
2.2.5 Synthesis of 2-Substituted 3,4-Dimethoxyxanthenes.....	65



2.2.6 Physical Properties of 2-Substituted 4-Methoxy- and 3,4-Dimethoxyxanthones .....	72
2.3 Conclusions.....	75
2.4 Experimental Section.....	76
2.4.1 Experimental Procedures .....	77
2.4.2 UV and Fluorescence Measurements.....	105
2.4.3 Crystallographic Data for <b>2.46e</b> and <b>2.49d</b> .....	108
2.5 References and Notes.....	111
Appendix: Selected NMR Spectra of Synthesized Compounds .....	115

### **Chapter 3     Synthesis and Physical Properties of 2-Aryl-4-methoxyxanthones                   and the Attempted Synthesis of 2,4-Diarylxanthones**

3.1 Introduction.....	145
3.2 Results and Discussion .....	147
3.2.1 Synthesis of Dienes <b>3.8</b> .....	147
3.2.2 Synthesis of Dienophile <b>1.227</b> .....	148
3.2.3 Synthesis of 2-Aryl-4-methoxyxanthones .....	149
3.2.4 Attempted Synthesis of 2,4-Diarylxanthones .....	151
3.2.5 Physical Properties of Arylxanthones <b>3.9a–c</b> and <b>3.18</b> .....	153
3.3 Conclusions.....	154
3.4 Experimental Section .....	155
3.4.1 Experimental Procedures .....	155





## **Chapter 5    Synthesis and Physical Properties of**

### **New Donor-Acceptor Xanthone-Carbazole Hybrid Systems**

5.1 Introduction.....	238
5.2 Synthetic Approach to Xanthone-Carbazole Hybrid Systems.....	243
5.3 Results and Discussion .....	248
5.3.1 Synthesis of the Parent Xanthone-Carbazole Hybrid Systems .....	248
5.3.2 Synthesis of Substituted Xanthone-Carbazole Hybrid Systems .....	252
5.3.3 Synthesis of Aryl-substituted Xanthone-Carbazole Hybrid Systems .....	261
5.3.4 Structures and X-ray Packing Motifs of Xanthone-Carbazole Hybrid Systems .....	263
5.3.5 Physical Properties of Xanthone-Carbazole Hybrid Systems.....	267
5.4 Conclusions and Proposal for Future Work.....	288
5.5 Experimental Section.....	290
5.5.1 Experiment Procedures .....	290
5.5.2 Crystallographic Data for Compounds 5.39–5.42. ....	337
5.5.3 UV and Fluorescence Experiments.....	364
5.5.4 Cyclic Voltammetry Experiments .....	367
5.5.5 Aggregation Studies on Compound 5.45 .....	368
5.6 References and Notes.....	369
Appendix: Selected NMR Spectra of Synthesized Compounds .....	375

## **Chapter 6    Attempted Synthesis of Cyclic Oligophenylenes**

### **Using IEDDA Chemistry**

6.1 Introduction.....	428
6.2 Retrosynthetic Analysis of Cyclic Oligophenylenes .....	433
6.3 Results and Discussion .....	436
6.2.1 Synthesis of 2-Hydroxybenzophenone <b>6.21</b> as a Model Study .....	436
6.2.2 Synthesis of Bis(diene) <b>6.15</b> .....	437
6.2.3 Synthesis of Bis(enamine) <b>6.16</b> .....	439
6.2.4 Attempted Synthesis of Cyclic Oligophenylene <b>1.233</b> .....	440
6.3 Conclusions.....	441
6.4 Experimental Section.....	442
6.5 References and Notes.....	447
Appendix: Selected NMR Spectra of Synthesized Compounds.....	449



## List of Figures

<b>Figure 1.1</b> Frontier molecular orbital representation of a [4+2] cycloaddition reaction.....	1
<b>Figure 1.2</b> Three types of Diels-Alder reactions.....	3
<b>Figure 1.3</b> Electron-deficient dienes <b>1.11–1.15</b> investigated by the Bodwell group. ....	5
<b>Figure 1.4</b> The relative average torsion angles of <b>1.25</b> , <b>1.34</b> , and <b>1.35</b> . ....	9
<b>Figure 1.5</b> X-ray crystal structure of xanthone <b>1.51</b> . ....	13
<b>Figure 1.6</b> The xanthone skeleton with the IUPAC numbering recommendation.....	13
<b>Figure 1.7</b> Examples of the six different classifications of naturally-occurring xanthones. ....	14
<b>Figure 1.8</b> Some examples of “hit” xanthone compounds.....	15
<b>Figure 1.9</b> Useful approaches to xanthones. ....	16
<b>Figure 1.10</b> Examples of linear acenes. ....	33
<b>Figure 1.11</b> Examples of modified pentacene systems. ....	34
<b>Figure 1.12</b> Examples of hetero[ <i>n</i> ]acenes.....	36
<b>Figure 1.13</b> “Herringbone” ( <i>top</i> ) and $\pi$ -stacking ( <i>bottom</i> ) arrangements of pentacenes <b>1.180–1.182</b> . ....	37
<b>Figure 1.14</b> Dienes <b>1.15</b> and selected electron-rich dienophiles <b>1.225–1.227</b> .....	46
<b>Figure 1.15</b> Target structures via IEDDA approaches.....	47
<b>Figure 2.1</b> Examples of naturally-occurring 4-methoxy- and 3,4-dimethoxyxanthones <b>2.1–2.7</b> .....	56
<b>Figure 2.2</b> Dienophiles used in the synthesis of 2-substituted xanthones.....	59
<b>Figure 2.3</b> ORTEP presentation of <b>2.46e</b> .....	67

<b>Figure 2.4</b> X-ray structure of <b>2.49e</b> .....	69
<b>Figure 2.5</b> Absorption spectra of <b>1.228a–f</b> ( <i>left</i> ) and <b>1.228g–i</b> ( <i>right</i> ) in CHCl <sub>3</sub> (2 x 10 <sup>-5</sup> M).....	73
<b>Figure 2.6</b> Emission spectra of <b>1.228a–g</b> ( <i>left</i> ) and <b>1.228h–i</b> ( <i>right</i> ) in CHCl <sub>3</sub> (2 x 10 <sup>-5</sup> M).....	73
<b>Figure 2.7</b> Absorption ( <i>left</i> ) and emission spectra ( <i>right</i> ) of <b>1.229a–h</b> in CHCl <sub>3</sub> (2 x 10 <sup>-5</sup> M). ....	74
<b>Figure 3.1</b> Absorption and emission spectra of arylxanthenes <b>1.228h</b> , <b>3.9a–c</b> and <b>3.18</b> in CHCl <sub>3</sub> (3 x 10 <sup>-5</sup> M).....	154
<b>Figure 4.1</b> Known xanthone-based heteroacenes.....	173
<b>Figure 4.2</b> IUPAC names of compounds <b>1.214</b> and <b>1.218</b> . ....	174
<b>Figure 4.3</b> Xanthonoid hetero[ <i>n</i> ]acenes. ....	175
<b>Figure 4.4</b> New xanthonoid hetero[5]acene derivatives <b>4.12–4.14</b> . ....	175
<b>Figure 4.5</b> Absorption spectra of <b>4.12–4.14</b> and <b>4.22</b> in CHCl <sub>3</sub> (2 x 10 <sup>-5</sup> M).....	187
<b>Figure 4.6</b> Emission spectra of <b>4.12–4.14</b> and <b>4.22</b> in CHCl <sub>3</sub> (2 x 10 <sup>-5</sup> M).....	187
<b>Figure 4.7</b> Modeling structure of <b>4.22</b> ( <i>top</i> ) and its predicted packing motif ( <i>bottom</i> ). ....	189
<b>Figure 4.8</b> Representation of the HOMO and LUMO of <b>4.22</b> .....	190
<b>Figure 4.9</b> Modeling structure of <b>4.14</b> : front view ( <i>left</i> ) and side view ( <i>right</i> ). ....	190
<b>Figure 5.1</b> Target structures and IUPAC names. ....	243
<b>Figure 5.2</b> X-ray structures of <b>5.39</b> and <b>5.40</b> . ....	249
<b>Figure 5.3</b> Hydrogen bonds of in X-ray structures of <b>5.39</b> ( <i>left</i> ) and <b>4.40</b> ( <i>right</i> ). ....	251
<b>Figure 5.4</b> Xanthenes bearing substituents <b>5.31</b> . ....	252



<b>Figure 5.5</b> The relative average torsion angles of <b>5.39–5.41</b> (X-ray calculations).....	264
<b>Figure 5.6</b> X-ray packing motif of angular isomer <b>5.39</b> (R = H).....	265
<b>Figure 5.7</b> X-ray packing motif of angular isomer <b>5.42</b> (R = CH <sub>3</sub> ).....	265
<b>Figure 5.8</b> X-ray packing motif of linear isomer <b>5.40</b> (R = H).....	266
<b>Figure 5.9</b> X-ray packing motif of linear isomer <b>5.41</b> (R = C <sub>2</sub> H <sub>5</sub> ). ....	266
<b>Figure 5.10</b> Absorption spectra ( <i>left</i> ) and emission spectra ( <i>right</i> ) of xanthone-carbazoles <b>5.39</b> , <b>5.40</b> , <b>5.42</b> and <b>5.43</b> in CHCl <sub>3</sub> (2 x 10 <sup>-5</sup> M).....	269
<b>Figure 5.11</b> Absorption spectra ( <i>left</i> ) and emission spectra ( <i>right</i> ) of the angular <b>5.42</b> , <b>5.44</b> , <b>5.45</b> (solid lines) and the linear <b>5.43</b> , <b>5.41</b> , <b>5.46</b> (dotted lines) in CHCl <sub>3</sub> (2 x 10 <sup>-5</sup> M).....	270
<b>Figure 5.12</b> Absorption spectra ( <i>left</i> ) and emission spectra ( <i>right</i> ) of angular <b>5.42</b> (solid lines) and linear <b>5.43</b> (dotted lines) in cyclohexane, diethyl ether, dichloromethane, and acetonitrile (4 × 10 <sup>-5</sup> M). ....	272
<b>Figure 5.13</b> Cyclic voltammograms of angular isomer <b>5.42</b> ( <i>left</i> ) and linear isomer <b>5.43</b> ( <i>right</i> ). ....	273
<b>Figure 5.14</b> Aromatic proton shifts in <sup>1</sup> H NMR spectra of compound <b>5.45</b> . ....	277
<b>Figure 5.15</b> Proton shifts of methoxy group in <sup>1</sup> H NMR spectra of compound <b>5.45</b> . ....	278
<b>Figure 5.16</b> Representative stacking of <b>5.45</b> based on aggregation studies.....	279
<b>Figure 5.17</b> HOMO and LUMO maps of <b>5.42</b> ( <i>left</i> ) and linear isomer <b>5.43</b> ( <i>right</i> ).....	280
<b>Figure 5.18</b> Absorption ( <i>left</i> ) and emission ( <i>right</i> ) spectra of angular isomers <b>5.52a–f</b> .....	282
<b>Figure 5.19</b> Absorption ( <i>left</i> ) and emission ( <i>right</i> ) spectra of linear	

isomers 5.53b–d,f. ....	282
<b>Figure 5.20</b> Absorption ( <i>left</i> ) and emission ( <i>right</i> ) spectra of aryl substituted xanthone-carbazole hybrid systems 5.67–5.69. ....	284
<b>Figure 5.21</b> HOMO ( <i>left</i> ) and LUMO ( <i>right</i> ) maps of 5.69a–c. ....	287
<b>Figure 5.22</b> Quantum yields of substituted xanthone-carbazoles and the parent compound 5.70. ....	288
<b>Figure 5.23</b> Future target structure 5.71. ....	290
<b>Figure 6.1</b> Examples of hexagonal cyclic oligophenylenes 6.1–6.3. ....	429
<b>Figure 6.2</b> Target structures. ....	433
<b>Figure 6.3</b> Computed structure (MMFF) of cyclic oligophenylene 1.233. ....	435
<b>Figure 6.4</b> Suggested bis(diene) 6.29 and bis(dienophile) 6.30. ....	442



## List of Schemes

<b>Scheme 1.1</b> 1,3-Electron-deficient dienes <b>1.2a–d</b> .....	4
<b>Scheme 1.2</b> Generation and IEDDA reactions of the electron-deficient diene <b>1.5</b> .....	4
<b>Scheme 1.3</b> IEDDA reactions of diene <b>1.11</b> (EWG = CO <sub>2</sub> Et) with dienophiles <b>1.16</b> and <b>1.18</b> .....	6
<b>Scheme 1.4</b> IEDDA-driven domino reaction between diene <b>1.11</b> (EWG = CO <sub>2</sub> Et) and enamine <b>1.20</b> .....	6
<b>Scheme 1.5</b> IEDDA reactions between diene <b>1.12</b> (EWG = CO <sub>2</sub> Me) and enamines <b>1.24</b> , <b>1.26</b> , <b>1.29</b> .....	7
<b>Scheme 1.6</b> Plausible explanation for the formation of non-aromatized products <b>1.27</b> and <b>1.28</b> .....	8
<b>Scheme 1.7</b> IEDDA reactions of 1-azadienes <b>1.13a–c</b> with enamine <b>1.24</b> .....	10
<b>Scheme 1.8</b> IEDDA reaction of 2-azadiene <b>1.14</b> ( <i>p</i> -C <sub>6</sub> H <sub>4</sub> NO <sub>2</sub> ) with enamine <b>1.24</b> .....	11
<b>Scheme 1.9</b> Employment of the Povarov reaction for the synthesis of pyrido[2,3- <i>c</i> ]coumarin <b>1.45</b> .....	11
<b>Scheme 1.10</b> IEDDA reaction of diene <b>1.15</b> (EWG = CO <sub>2</sub> Et) with enamine <b>1.24</b> .....	12
<b>Scheme 1.11</b> Synthesis of xanthone <b>1.66</b> via the GSS reaction.....	17
<b>Scheme 1.12</b> Synthesis of xanthenes <b>1.68</b> via the modified GSS reaction.....	17
<b>Scheme 1.13</b> Friedel-Crafts-based approach to xanthone <b>1.72</b> .....	18
<b>Scheme 1.14</b> Synthesis of $\alpha$ -mangostin <b>1.59a</b> .....	18
<b>Scheme 1.15</b> Synthesis of xanthone <b>1.80</b> from ester <b>1.79</b> via pyrolysis.....	19

<b>Scheme 1.16</b> Synthesis of xanthone <b>1.84</b> from ester <b>1.85</b> involving photo-Fries rearrangement. ....	20
<b>Scheme 1.17</b> Synthesis of xanthone <b>1.95</b> from ester <b>1.92</b> involving Smiles rearrangement. ....	20
<b>Scheme 1.18</b> Synthesis of xanthonones <b>1.100</b> and <b>1.101</b> via Ullmann coupling and cyclization reactions.....	21
<b>Scheme 1.19</b> Synthesis of “dixanthone” <b>1.106</b> from <b>1.102</b> and <b>1.103</b> . ....	22
<b>Scheme 1.20</b> Synthesis of xanthone <b>1.51</b> via aryl ether <b>1.108</b> and an anionic cascade reaction. ....	22
<b>Scheme 1.21</b> Synthesis of xanthone <b>1.51</b> via a tandem coupling-cyclization strategy. ....	23
<b>Scheme 1.22</b> Synthesis of xanthonones <b>1.120</b> via a palladium migration process. ....	24
<b>Scheme 1.23</b> Larock’s proposed mechanism for synthesis of xanthone <b>1.120</b> via a palladium migration process. ....	25
<b>Scheme 1.24</b> Tandem coupling-cyclization of salicylaldehyde <b>1.126</b> and silylaryl triflate <b>1.111</b> . ....	25
<b>Scheme 1.25</b> Normal Diels-Alder reaction between diene <b>1.132</b> and dienophile <b>1.133</b> ...	27
<b>Scheme 1.26</b> Normal Diels-Alder reaction between dienes <b>1.132</b> and DMAD ( <b>1.136</b> ). ...	27
<b>Scheme 1.27</b> Normal Diels-Alder reaction between diene <b>1.141</b> and DMAD ( <b>1.136</b> ). ....	28
<b>Scheme 1.28</b> IEDDA reaction between dienes <b>1.144</b> and dienophiles <b>1.145</b> . ....	29
<b>Scheme 1.29</b> Postulated mechanism to explain the formation of xanthonones <b>1.147</b> and dienes <b>1.148</b> . ....	29
<b>Scheme 1.30</b> Synthesis of xanthonones <b>1.156</b> and <b>1.159</b> from reactions of	

organolithium reagents <b>1.152</b> or <b>1.157</b> with compounds <b>1.151</b> .....	30
<b>Scheme 1.31</b> Synthesis of xanthenes <b>1.162</b> from <b>1.160</b> and <b>1.161</b> .....	31
<b>Scheme 1.32</b> Synthesis of benzofuroxanthone <b>1.192</b> .....	41
<b>Scheme 1.33</b> Syntheses of benzofuroxanthenes <b>1.196</b> and <b>1.198</b> .....	42
<b>Scheme 1.34</b> Synthesis of the angular indoloxanthone <b>1.203</b> .....	43
<b>Scheme 1.35</b> Synthesis of the linear indoloxanthone <b>1.206</b> .....	43
<b>Scheme 1.36</b> Multi-step synthesis of dixanthone <b>1.210</b> .....	44
<b>Scheme 1.37</b> Two-step synthesis of dixanthone <b>1.214</b> .....	44
<b>Scheme 1.38</b> Two-step synthesis of dixanthone <b>1.218</b> .....	45
<b>Scheme 1.39</b> The synthesis of dixanthone <b>1.224</b> .....	45
<b>Scheme 2.1</b> Synthesis of 2-methyl-4-methoxyxanthone <b>2.10</b> via a palladium migration process.....	57
<b>Scheme 2.2</b> Synthesis of 2-hydroxybenzophenones (path A) and the proposed synthesis of xanthenes (path B) via an IEDDA / elimination / elimination sequence. .	58
<b>Scheme 2.3</b> Retrosynthetic analysis of xanthenes <b>1.228</b> and <b>1.229</b> .....	59
<b>Scheme 2.4</b> Synthesis of substrates for HWE and Wittig reactions.....	60
<b>Scheme 2.5</b> Attempted synthesis of phosphonate <b>2.32</b> from literature. ....	61
<b>Scheme 2.6</b> Reported syntheses of diene <b>1.15</b> (EWG = CO <sub>2</sub> Et).....	61
<b>Scheme 2.7</b> Synthesis of dienes <b>1.15a–e</b> .....	62
<b>Scheme 2.8</b> Synthesis of dienes <b>1.15f–i</b> .....	62
<b>Scheme 2.9</b> Synthesis of dienophile <b>1.225</b> .....	63
<b>Scheme 2.10</b> Synthesis of tetramethoxyethene (TME) <b>1.226</b> .....	64



<b>Scheme 2.11</b> IEDDA reaction between diene <b>1.15e</b> and <b>1.226</b> in solvent-free conditions.....	66
<b>Scheme 2.12</b> Proposed pathways to <b>1.229</b> and <b>2.49d,f</b> .....	69
<b>Scheme 2.13</b> Proposed mechanism for the formation of <b>2.49d,f</b> .....	71
<b>Scheme 2.14</b> Possible elaboration of the useful compound <b>2.53</b> .....	76
<b>Scheme 3.1</b> Synthesis of arylxanthenes <b>3.3</b> and <b>3.7</b> .....	145
<b>Scheme 3.2</b> Retrosynthetic analysis of target arylxanthenes <b>3.9</b> and <b>3.10</b> .....	146
<b>Scheme 3.3</b> Synthesis of dienophile <b>1.227</b> .....	149
<b>Scheme 3.4</b> Attempted synthesis of 2,4-diphenylxanthenes <b>3.17</b> .....	151
<b>Scheme 3.5</b> Synthesis of arylxanthenes <b>3.18</b> .....	151
<b>Scheme 4.1</b> Retrosynthetic analysis of <i>syn</i> xanthonoid hetero[5]acene <b>4.22</b> via a one-directional approach.....	179
<b>Scheme 4.2</b> Retrosynthetic analysis of <i>syn</i> - and <i>anti</i> -xanthonoid hetero[5]acenes <b>4.25</b> and <b>4.29</b> via a two-directional approach.....	180
<b>Scheme 4.3</b> Retrosynthetic analysis of <i>syn</i> -xanthonoid hetero[9]acene <b>4.31</b> via a two-directional approach.....	180
<b>Scheme 4.4</b> Synthesis of xanthonoid hetero[5]acenes <b>4.22</b> and <b>4.37</b> via one-directional approach.....	182
<b>Scheme 4.5</b> Synthesis of tosylated polyethylene oxide chains <b>4.42</b> and <b>4.44</b> .....	183
<b>Scheme 4.6</b> Synthesis of xanthonoid hetero[5]acene derivatives <b>4.12–4.14</b> .....	184
<b>Scheme 4.7</b> Synthesis of xanthenes-based <b>4.18</b> and <b>4.19</b> via dialkylation.....	185
<b>Scheme 4.8</b> New donor and acceptor systems <b>4.49</b> and <b>4.50</b> .....	186

<b>Scheme 4.9</b> Synthesis of dialdehyde <b>4.27</b> . .....	191
<b>Scheme 4.10</b> Synthesis of phosphonate <b>4.55</b> . .....	191
<b>Scheme 4.11</b> Attempted synthesis of bis(diene) <b>4.26a</b> . .....	192
<b>Scheme 4.12</b> Attempted synthesis of bis(diene) <b>4.26b</b> . .....	192
<b>Scheme 4.13</b> Synthesis of <i>syn</i> -xanthonoid hetero[5]acene <b>4.25b</b> via a two-directional approach. ....	193
<b>Scheme 4.14</b> Attempted synthesis of dienes <b>4.26c–e</b> . .....	194
<b>Scheme 4.15</b> Synthesis route toward diene <b>4.59</b> . .....	195
<b>Scheme 4.16</b> Toward the synthesis of hexasubstituted benzene <b>4.57</b> . .....	196
<b>Scheme 4.17</b> Product of the double-acylation reaction of <b>4.64</b> . .....	196
<b>Scheme 4.18</b> Alternative approach to the target <b>4.57</b> . .....	197
<b>Scheme 4.19</b> Proposed step-wise approach to <i>syn</i> -xanthonoid hetero[ <i>n</i> ]acenes ( <i>n</i> = 5, 6, 7, 9). .....	199
<b>Scheme 4.20</b> Proposed step-wise approach to <i>syn</i> -xanthonoid hetero[ <i>n</i> ]acenes ( <i>n</i> = 4–9). .....	200
<b>Scheme 5.1</b> Synthesis of indolocarbazole <b>5.30</b> via microwave-assisted Cadogan reaction. ....	246
<b>Scheme 5.2</b> Retrosynthetic analysis of target xanthone-carbazole compounds <b>5.6</b> and <b>5.7</b> . ....	247
<b>Scheme 5.3</b> Synthesis of the parent xanthone-carbazole compounds <b>5.39–5.41</b> . ....	248
<b>Scheme 5.4</b> Synthesis of <i>N</i> -alkylated xanthone-carbazole compounds <b>5.41–5.46</b> . ....	250
<b>Scheme 5.5</b> Synthesis of 3-formylchromone derivatives <b>5.34a</b> and <b>5.34b</b> . ....	252

<b>Scheme 5.6</b> Synthesis of <i>o</i> -nitrophenylacetic acid derivatives <b>5.33a</b> and <b>5.33b</b> . .....	253
<b>Scheme 5.7</b> Mechanisms of the Cadogan reaction proposed by Cadogan. ....	260
<b>Scheme 5.8</b> Suzuki coupling of <b>5.52f</b> with 2-thienylboronic acid <b>5.66b</b> . ....	262
<b>Scheme 6.1</b> Staab and Binning's synthesis of cyclic hexaphenylene <b>6.1</b> . ....	430
<b>Scheme 6.2</b> Schülter's synthesis of cyclic dodecaphenylene <b>6.2</b> . ....	431
<b>Scheme 6.3</b> Synthesis of macrocycle <b>6.10</b> using the thermodynamic approach. ....	432
<b>Scheme 6.4</b> Synthesis of 2-hydroxyacetophenone <b>6.13</b> and diacid <b>6.14</b> . ....	433
<b>Scheme 6.5</b> Retrosynthetic analysis of cyclic oligophenylene <b>1.233</b> via a six-fold IEDDA-driven domino reaction. ....	434
<b>Scheme 6.6</b> Retrosynthetic analysis of bis(diene) <b>6.15</b> and bis(enamine) <b>6.16</b> . ....	436
<b>Scheme 6.7</b> IEDDA reaction between monodiene <b>1.15h</b> and monoenamine <b>6.12</b> . ....	437
<b>Scheme 6.8</b> Synthesis of bis(diene) <b>6.15</b> . ....	438
<b>Scheme 6.9</b> Synthesis of intermediates <b>6.18</b> and <b>6.19</b> . ....	439
<b>Scheme 6.10</b> Synthesis of bis(aldehyde) <b>6.20</b> as a prospective precursor to bis(enamine) <b>6.16</b> . ....	439
<b>Scheme 6.11</b> An attempted six-fold IEDDA reaction between bis(diene) <b>6.15</b> and bis(enamine) <b>6.16</b> . ....	441



## List of Tables

<b>Table 1.1</b> Classifications and general nomenclatures of heteroacenes. ....	35
<b>Table 1.2</b> Relationship between charge carrier mobility and molecular structures. ....	39
<b>Table 1.3</b> Relationship between charge carrier mobility and molecular structures. ....	40
<b>Table 2.1</b> Reactions of dienes <b>1.15a–i</b> with dienophile <b>1.225</b> . ....	65
<b>Table 2.2</b> Reactions of dienes <b>1.15a–i</b> with dienophile <b>1.226</b> . ....	68
<b>Table 2.3</b> Physical data of 4-methoxyxanthenes <b>1.228a–i</b> . ....	74
<b>Table 2.4</b> Physical data of 3,4-dimethoxyxanthenes <b>1.229a–h</b> . ....	75
<b>Table 3.1</b> Synthesis of dienes <b>3.8a–c</b> . ....	148
<b>Table 3.2</b> Synthesis of 2-aryl-4-methoxyxanthenes <b>3.9a–c</b> . ....	150
<b>Table 3.3</b> HOMO–LUMO gap calculations. ....	152
<b>Table 3.4</b> Physical data of xanthenes <b>3.9a–c</b> and <b>3.18</b> in comparison with <b>1.228h</b> . ....	154
<b>Table 4.1</b> Examples of chromophore-based crown ethers. ....	177
<b>Table 4.2</b> Examples of xanthone-based crown ethers. ....	178
<b>Table 5.1</b> Xanthone-based compounds. ....	240
<b>Table 5.2</b> Carbazole-based compounds. ....	241
<b>Table 5.3</b> Methodologies for the synthesis of carbazole framework. ....	245
<b>Table 5.4</b> Synthesis of <i>o</i> -nitrophenyl dienes <b>5.32a–f</b> . ....	254
<b>Table 5.5</b> Synthesis of <i>o</i> -nitrophenyl xanthenes <b>5.31a–f</b> . ....	256
<b>Table 5.6</b> Synthesis of substituted xanthone-carbazole hybrid systems. ....	257
<b>Table 5.7</b> Synthesis of aryl-substituted xanthone-carbazole hybrid systems. ....	261
<b>Table 5.8</b> Photophysical data of compounds <b>5.39–5.46</b> . ....	271

<b>Table 5.9</b> UV/Vis absorption and emission data for <b>5.42</b> and <b>5.43</b> in different solvents.....	272
<b>Table 5.10</b> Photophysical and electrochemical data for <b>5.41–5.43</b> , selected hetero[5]acenes and pentacene. ....	275
<b>Table 5.11</b> Photophysical data of substituted compounds <b>5.52</b> and <b>5.53</b> in comparison with their parent compound <b>5.70</b> and <b>5.46</b> , respectively. ....	283
<b>Table 5.12</b> Photophysical data of parent <b>5.70</b> and aryl substituted compounds <b>5.67–5.69</b> . ....	285

## List of Symbols, Abbreviations and Acronyms

3-21G(d)	Split-valence Basis Set (d-type)
6-31G(d)	Polarization Basis Set (d-type)
<i>A</i>	absorbance
Å	angstrom unit
Ac	acetyl
Ac <sub>2</sub> O	acetic anhydride
AcOH	acetic acid
AM1	Austin model 1
APCI (-)	Atmospheric Pressure Chemical Ionization in negative mode
APCI (+)	Atmospheric Pressure Chemical Ionization in positive mode
aq.	aqueous
b.p.	boiling point
B3LYP	Becher 3 parameter Lee Yaing Pan
Bn	benzyl
borsm	based on recovery of starting material
br	broad (in IR or NMR)
Bu	butyl
BzCl	benzoyl chloride
c	concentration
<i>ca.</i>	circa
calcd	calculated



cat.	catalytic
CI (+)	chemical ionization
conc.	concentrated
$\delta$	chemical shift in ppm down field from tetramethylsilane
$\Delta$	heat (in reaction conditions)
$\Delta$	Stokes shifts
$\Phi$	relative average torsion angle
$\Phi_{em}$	emission quantum yield
d	doublet (in NMR)
DA	Diels-Alder
dd	doublet of doublets (in NMR)
DDQ	2,3-dichloro-5,6-dicyano-1,4-benzoquinone
DFT	density functional theory
DMAD	dimethyl acetylenedicarboxylate
DMF	<i>N,N</i> -dimethylformamide
DMP	Dess-Martin periodinane
DMSO	dimethyl sulfoxide
DMXAA	5,6-dimethoxyxanthenone-4-acetic acid
DOM	directed ortho metalation
$\epsilon$	coefficient (extinction)
$E_a$	activation energy
$E_{abs}$	absorption energy

EDG	electron-donating group
$E_{em}$	emission energy
$E_g$	energy gap
$E_{HOMO}$	HOMO energy level
EI (-)	electron impact in negative mode
EI (+)	electron impact in positive mode
$E_{ox}^{onset}$	potential of oxidation onset
$E_{pa}$	potential at anodic peak
$E_{pc}$	potential at cathodic peak
equiv.	equivalent(s)
Et	Ethyl
Et <sub>3</sub> N	Triethylamine
EtOAc	ethyl acetate
EWG	electron-withdrawing group
FD	field desorption (mass spectrum)
FETs	field-effect transistors
FGI	functional group interchange
FMO	frontier molecular orbital
GCMS	Gas Chromatography mass spectrometry
GSS	Grover, Shah and Shah (name of reaction)
h	hour(s)
HOMO	Highest Occupied Molecular Orbital

HRMS	high-resolution mass spectrum (spectra)
HWE	Horner-Wadsworth-Emmons
Hz	hertz
h $\nu$	light
$I$	the integrated intensity of the emission band
IBX	2-iodoxybenzoic acid
IEDDA	inverse electron demand Diels-Alder
$i_{pa}$	anodic peak current
$i_{pc}$	cathodic peak current
IR	infrared
IUPAC	International Union of Pure and Applied Chemistry
$J$	coupling constant (Hz, in NMR)
K	Kelvin (degree)
$k_{nr}$	non-radiative decay rate
$k_r$	radiative rate
$\lambda_{max}$	maxima wavelength (in UV or fluorescence)
$\lambda_{max} (abs)$	maxima absorption wavelength
$\lambda_{max} (em)$	maxima emission wavelength
$\lambda_o$	solvent reorganization energy
$\lambda_t$	total reorganization energy
$\lambda_{vib}$	vibrational energy
$l$	optical path length
LDA	lithium diisopropylamine



lit.	literature
LUMO	Lowest Unoccupied Molecular Orbital
$\mu$ W	microwave
m	multiplet (in NMR)
<i>m</i>	<i>meta</i>
m	medidum (in IR)
M <sup>+</sup>	molecular ion
MALDI-TOF	Matrix-Assisted Laser Desorption Ionization-Time of Flight
Me	methyl
Me <sub>4</sub> Si	tetramethylsilane
MeCN	acetonitrile
min	minute(s)
MMFF	Merck Molecular Force Field
MO	molecular orbital
MOM	methoxymethyl ether
mp	melting point
MS	mass spectrum (spectra)
<i>n</i> -BuLi	<i>n</i> -butyllithium
<i>n</i> <sub>D</sub>	refractive index of the solvent
NMP	<i>N</i> -methylpyrrolidone
NMR	nuclear magnetic resonance
Nphth	<i>N</i> -phthalimido
Nu	nucleophile

<i>o</i>	<i>ortho</i>
OFETs	organic field-effect transistors
OLEDs	organic light-emitting diodes
OPVs	organic photovoltaic devices
ORTEP	Oak Ridge thermal ellipsoid plot
OTf	trifluoromethanesulfonate
<i>p</i>	<i>para</i>
PCC	pyridinium chlorochromate
Ph	phenyl
PPA	poly(phosphoric acid)
ppm	parts per million
Pr	propyl
<i>p</i> -TsOH	<i>p</i> -toluenesulfonic acid
q	quartet (in NMR)
R <sub>f</sub>	retention factor (in tlc)
RHF	restricted Hartree-Fock
rt	room temperature
s	singlet (in NMR)
s	strong (in IR)
<i>s</i> -BuLi	<i>sec</i> -butyllithium
SiMe <sub>3</sub>	trimethylsilyl
SM	starting material
std	standard

t	triplet (in NMR)
TBSOTf	<i>tert</i> -butyldimethylsilyl trifluoromethanesulfonate
<i>t</i> -Bu	<i>tert</i> -butyl
<i>tert</i>	tertiary
TFTs	thin-film transistors
THF	tetrahydrofuran
tlc	thin-layer chromatography
TME	tetramethoxyethene
TMEDA	<i>N,N,N',N'</i> -Tetramethylethylenediamine
TMS	tetramethylsilane
Ts	tosyl
TsCl	<i>p</i> -toluenesulfonyl chloride
u	unknown sample
UV-vis	ultraviolet-visible (spectroscopy)
w	weak
X5	2,3,4,5,6-pentamethoxyxanthone



## Chapter 1

### Introduction

#### 1.1 A Brief Review of the Diels-Alder Reaction

In organic synthesis, the Diels-Alder reaction,<sup>1</sup> a [4+2] cycloaddition, is one of the most powerful tools to construct six-membered rings. This electrocyclic reaction occurs between a conjugated diene, which contributes  $4\pi$  electrons, and a dienophile, which contributes  $2\pi$  electrons. According to Frontier Molecular Orbital (FMO) theory,<sup>2</sup> the Diels-Alder reaction proceeds through the interaction of the  $\text{HOMO}_{\text{diene}}$  with the  $\text{LUMO}_{\text{dienophile}}$  or vice versa (Figure 1.1). Both reaction partners undergo bond formation on the same side of their respective  $\pi$  planes. As such, this reaction is said to be suprafacial in both components.



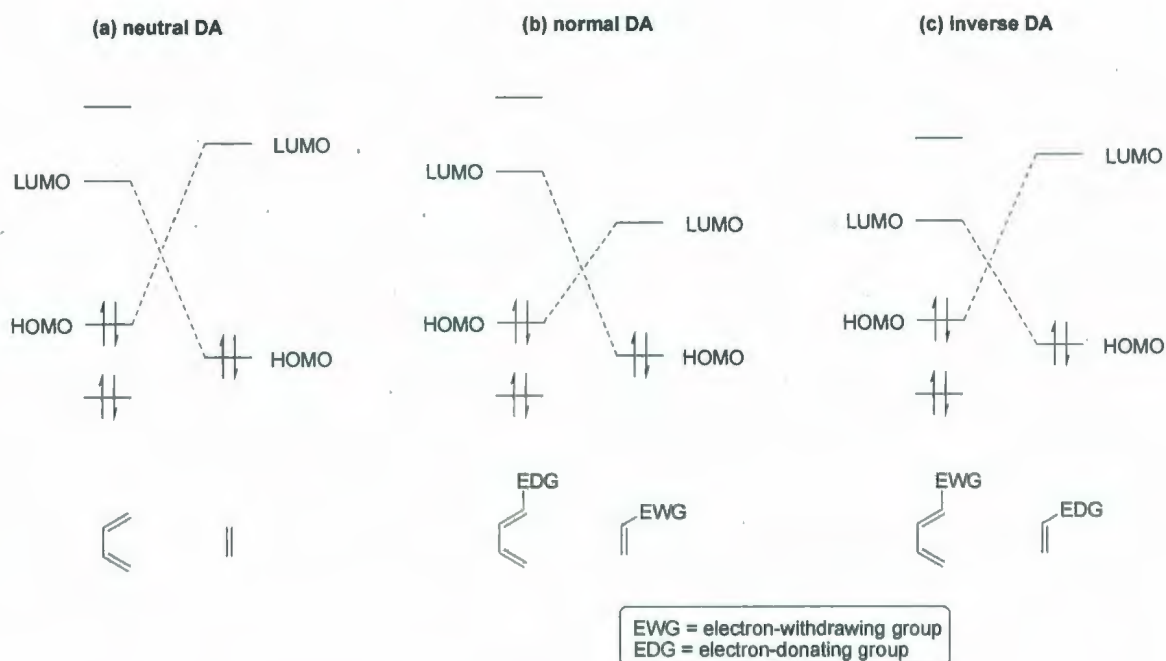
**Figure 1.1** Frontier molecular orbital representation of a [4+2] cycloaddition reaction.

Whichever of the above-mentioned HOMO-LUMO interactions has the smaller energy gap will dictate what type of Diels-Alder reaction it is. The parent Diels-Alder reaction between 1,3-butadiene and ethene (Figure 1.2) has large energy gaps for both interactions and occurs only under very harsh conditions to give cyclohexene as the product in low yield.<sup>3</sup> In general, the attachment of an electron-withdrawing group (EWG) to a  $\pi$ -system lowers the energy of the LUMO while the attachment of an

electron-donating group (EDG) raises the energy of the HOMO. Thus, when the diene and dienophile are complementarily modified with electron-withdrawing and donating groups, one of the HOMO-LUMO gaps becomes smaller, allowing the reaction to proceed under milder conditions.

Diels-Alder reactions are typically divided into three categories based on their dominant HOMO-LUMO interactions (Figure 1.2):

- (a) The neutral Diels-Alder reaction: the diene and dienophile bear no substituents and/or electron-neutral substituents. Thus, the interactions of  $\text{HOMO}_{\text{diene}}\text{-LUMO}_{\text{dienophile}}$  and  $\text{HOMO}_{\text{dienophile}}\text{-LUMO}_{\text{diene}}$  have large gaps and are similar in energy.
- (b) The normal electron demand Diels-Alder reaction: the diene bears at least one EDG, and the dienophile bears at least one EWG. Thus, the interaction of  $\text{HOMO}_{\text{electron-rich diene}}\text{-LUMO}_{\text{electron-deficient dienophile}}$  is dominant.
- (c) The inverse electron demand Diels-Alder (IEDDA) reaction: the diene bears at least one EWG, and the dienophile bears at least one EDG. Thus, the interaction of  $\text{HOMO}_{\text{electron-rich dienophile}}\text{-LUMO}_{\text{electron-deficient diene}}$  is dominant.



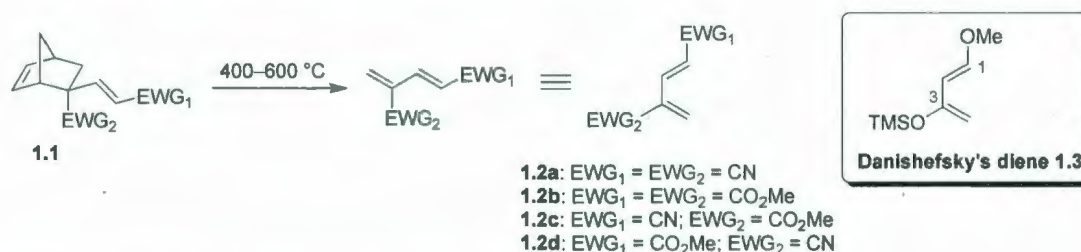
**Figure 1.2** Three types of Diels-Alder reactions.

## 1.2 IEDDA Reactions of 1,3-Disubstituted Electron-deficient Dienes

The IEDDA reaction was discovered much later (1959)<sup>4</sup> than the normal Diels-Alder reaction (1928),<sup>1</sup> and has gained much attention since the 1980s.<sup>5</sup> Numerous electron-deficient dienes, including acyclic and cyclic dienes and heterodienes, have been found to undergo IEDDA reactions with a broad range of electron-rich dienophiles. Among these electron-deficient dienes, those that bear EWGs at the 1- and 3-positions are especially interesting, *e.g.* **1.2a–d** (Scheme 1.1). In such systems, the EWGs work cooperatively to electronically bias the diene unit. This would be expected to endow the diene with high reactivity and regioselectivity in its IEDDA chemistry, much like Danishefsky's diene **1.3**<sup>6</sup> in the normal Diels-Alder reaction. However, dienes of this type are rare, presumably because the low-lying LUMO also renders them prone to

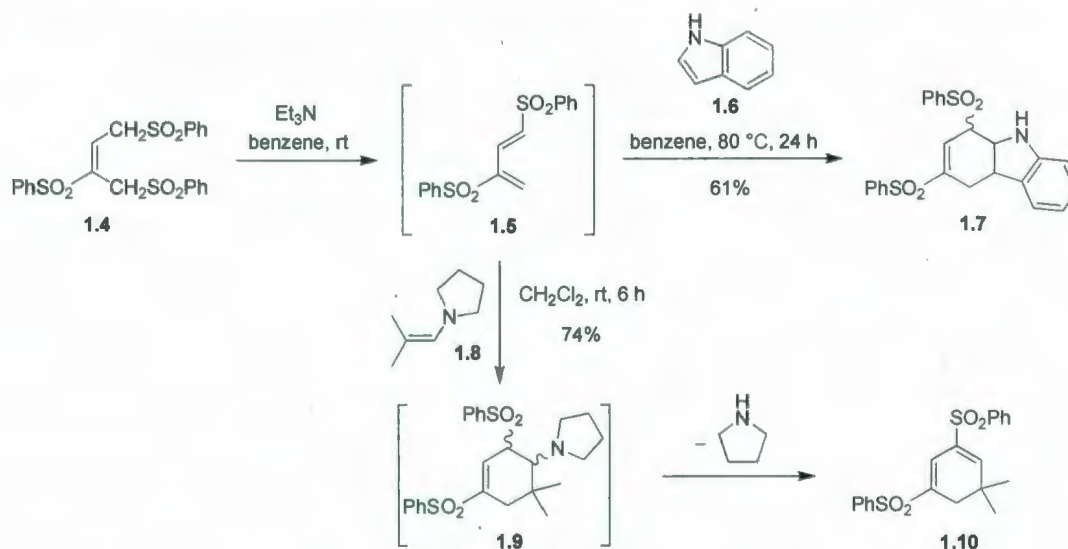


polymerization. For example, dienes **1.2a–d**<sup>7</sup> obtained from thermolysis-induced retro-Diels-Alder reactions readily polymerized (Scheme 1.1).



**Scheme 1.1** 1,3-Electron-deficient dienes **1.2a–d**.

Reaction of **1.4** with Et<sub>3</sub>N generated diene **1.5**<sup>8</sup> (Scheme 1.2), which dimerized in the absence of a dienophile, but reacted *in situ* with electron-rich dienophiles such as **1.6** and **1.8** to give a mixture of epimers **1.7** and **1.10** (via **1.9**), respectively.

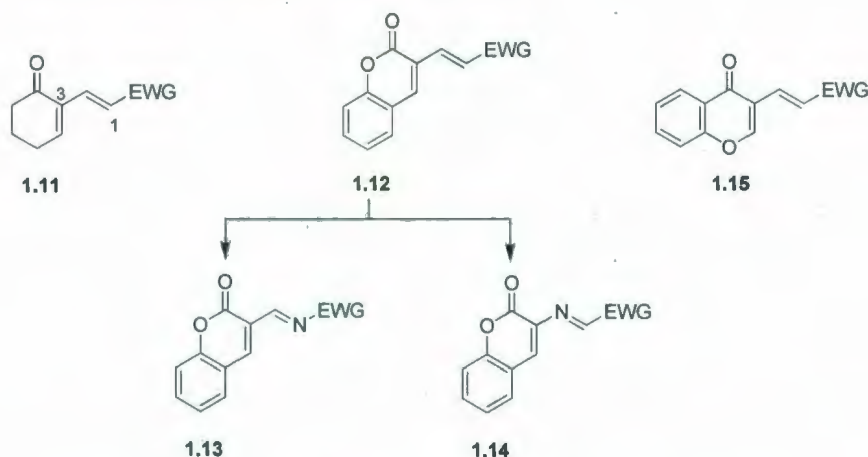


**Scheme 1.2** Generation and IEDDA reactions of the electron-deficient diene **1.5**.

Only a few other examples<sup>9</sup> of 1,3-activated electron-deficient dienes had been reported until the Bodwell group developed a series of such dienes to explore their IEDDA chemistry.

### 1.3 IEDDA Reaction Studies in the Bodwell Group

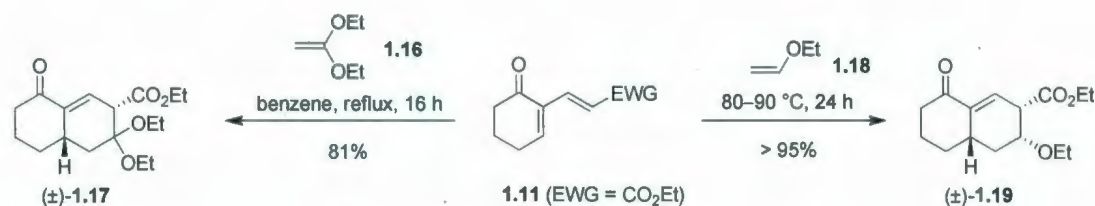
Since 1993, the Bodwell group at Memorial University has been investigating IEDDA reactions of electron-deficient dienes **1.11**–**1.15** (Figure 1.3) which bear electron-withdrawing groups at the 1 and 3 positions of the diene unit, to construct various carbocyclic and heterocyclic systems. These semicyclic dienes are, to varying degrees, more stable than the acyclic dienes **1.2a–d** and **1.5**.



**Figure 1.3** Electron-deficient dienes **1.11**–**1.15** investigated by the Bodwell group.

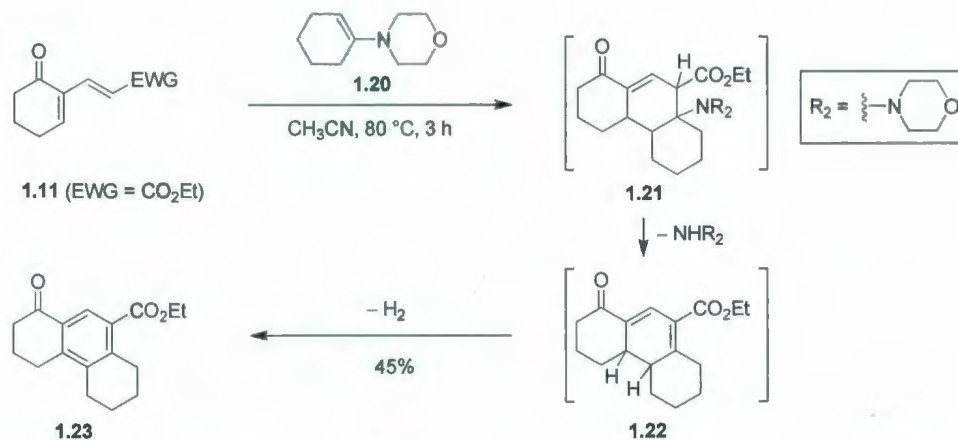
#### 1.3.1 IEDDA Reactions of Dienes **1.11**

Dienes **1.11** (EWG = CO<sub>2</sub>Et, CO<sub>2</sub>Bn, CN, C(=O)Ph)<sup>10</sup> are relatively stable and can be stored at –20 °C under a nitrogen atmosphere for at least two weeks without significant decomposition. Electron-deficient diene **1.11** (EWG = CO<sub>2</sub>Et) was found to react with electron-rich dienophiles such as 1,1-diethoxyethylene (**1.16**) or ethyl vinyl ether (**1.18**) to afford adducts **1.17** and **1.19**, respectively in good yields (Scheme 1.3).<sup>11</sup> Both reactions proceeded with complete regioselectivity, and the reaction with ethyl vinyl ether was completely *endo* selective.



**Scheme 1.3** IEDDA reactions of diene **1.11** (EWG = CO<sub>2</sub>Et) with dienophiles **1.16** and **1.18**.

Diene **1.11** (EWG = CO<sub>2</sub>Et) also reacted with enamine **1.20** to afford tricycle **1.23** (Scheme 1.4).<sup>12</sup> Neither the IEDDA adduct **1.21** nor the new electron-deficient diene **1.22**, which would result from the elimination of morpholine from **1.22**, was observed. An interesting feature of this reaction is that a new aromatic system was formed, presumably via a domino IEDDA / elimination / transfer hydrogenation sequence (the enamine is the hydrogen acceptor). Over the ensuing decade, this very productive reaction was applied to other types of electron-deficient dienes (*i.e.* **1.12–1.15**) by the Bodwell group.

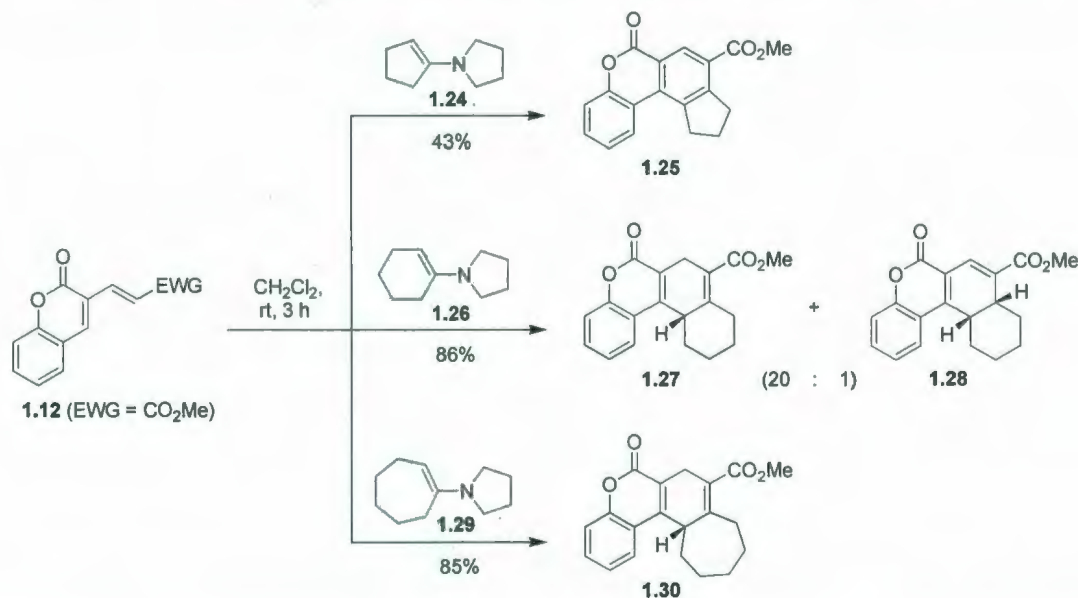


**Scheme 1.4** IEDDA-driven domino reaction between diene **1.11** (EWG = CO<sub>2</sub>Et) and enamine **1.20**.



### 1.3.2 Coumarin-based Dienes 1.12

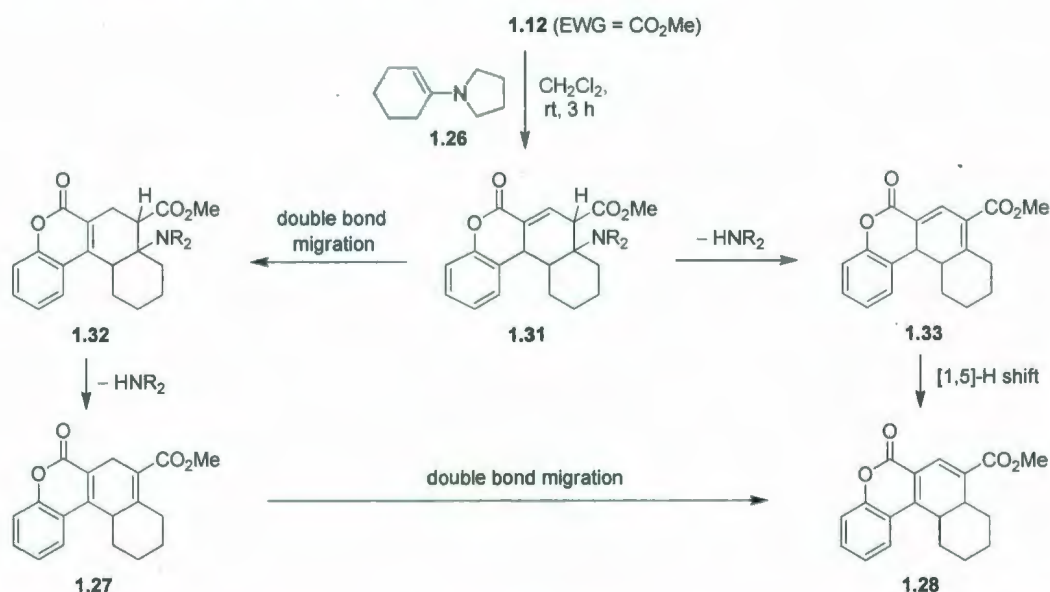
Dienes **1.12** (EWG = CO<sub>2</sub>Me, CN, COMe, SO<sub>2</sub>Ph)<sup>13</sup> are much more stable (more than six months at room temperature under air) than dienes **1.11**. Presumably, the partial aromatic character of the 2-pyrone moiety in **1.12** contributes to the enhancement of stability. As expected, the higher stability is accompanied by lower reactivity. Diene **1.12** (EWG = CO<sub>2</sub>Me) did not react with ethyl vinyl ether (**1.18**) under a variety of conditions. However, **1.12** (EWG = CO<sub>2</sub>Me) did react with a range of enamines including **1.24**, **1.26**, and **1.29** (Scheme 1.5), which have higher HOMO energies (−7.48 eV, −7.50 eV, −7.47 eV, respectively) than that of ethyl vinyl ether (**1.18**) (−9.09 eV).<sup>14</sup>



**Scheme 1.5** IEDDA reactions between diene **1.12** (EWG = CO<sub>2</sub>Me) and enamines **1.24**, **1.26**, and **1.29**.

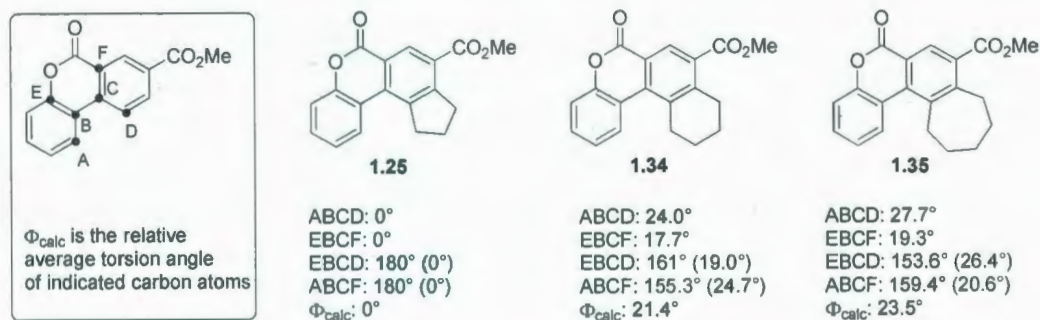
The reaction of diene **1.12** (EWG = CO<sub>2</sub>Me) with relatively unhindered enamines gave aromatized products, presumably via an IEDDA /  $\beta$ -elimination / transfer

hydrogenation process. For example, the reaction of **1.12** (EWG = CO<sub>2</sub>Me) with enamine **1.24** afforded the aromatized product **1.25** (Scheme 1.5). On the other hand, reactions with relatively hindered enamines afforded dihydroaromatic products. For instance, in the reaction of **1.12** (EWG = CO<sub>2</sub>Me) with enamine **1.26**, new dienes **1.27** and **1.28** were formed. Similarly, diene **1.30** was obtained from the reaction of **1.12** (EWG = CO<sub>2</sub>Me) with enamine **1.29**. In these cases, an initial IEDDA reaction presumably affords tetracycle **1.31** (Scheme 1.6), and this could be followed by a double bond migration process to give **1.32** or a  $\beta$ -elimination of pyrrolidine to give **1.33**. A  $\beta$ -elimination of pyrrolidine from **1.32** would afford diene **1.27**. Diene **1.28** could come either from **1.27** via a double bond migration or from **1.33** via either a [1,5]-H shift or two successive double bond migrations. The activation energy ( $E_a$ ) to [1,5]-H shift in 1,3-cyclohexadiene has been calculated to be very high (41.9 kcal/mol),<sup>15</sup> so it seemed more likely at this stage that **1.28** originated from **1.27**.



**Scheme 1.6** Plausible explanation for the formation of non-aromatized products **1.27** and **1.28**.

The reason that **1.27**, **1.28** and **1.30** did not undergo a transfer hydrogenation to afford aromatized products **1.34** and **1.35** (Figure 1.4) is most likely due to steric interactions across the bay region. Although it has been reported that the benzocoumarin framework can twist to reduce such steric interactions,<sup>16</sup> this process is most likely accompanied by the accumulation of some strain energy. AM1 calculations<sup>17</sup> showed that compound **1.25** is planar ( $\Phi_{\text{calc}} = 0^\circ$ ), while **1.34** and **1.35** are nonplanar. Both compounds have relative average torsion angles ( $\Phi_{\text{calc}}$ ) of more than  $20^\circ$  (Figure 1.4). It thus appears that the amount of strain energy present in **1.34** and **1.35** is enough to render the respective transfer hydrogenation steps unfavourable.



**Figure 1.4** The relative average torsion angles of **1.25**, **1.34**, and **1.35** (AM1 calculation).

### 1.3.3 Azadienes **1.13** and **1.14**

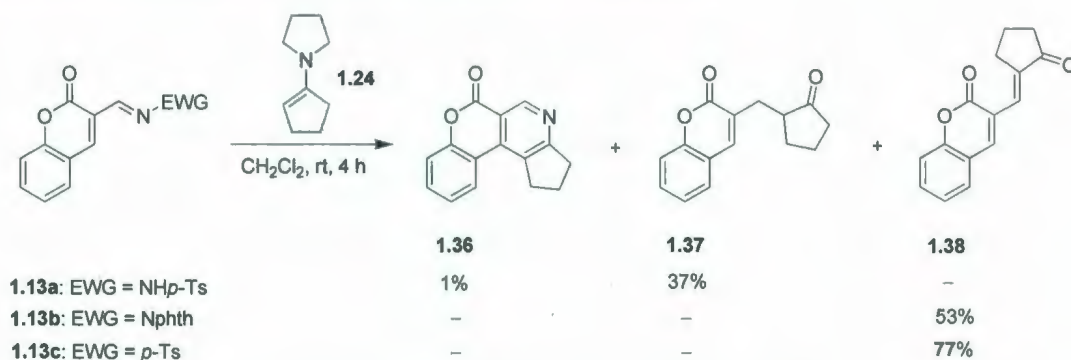
Like dienes **1.12**, azadienes **1.13** and **1.14** (Figure 1.3) are quite stable. These systems were investigated with the original aim of generating pyridocoumarins by way of IEDDA reactions with enamine dienophiles.<sup>18</sup>

#### 1.3.3.1 1-Azadienes **1.13**

Reaction of diene **1.13a** with enamine **1.24** gave a mixture of **1.36** (1%) and **1.37** (37%), while dienes **1.13b** and **1.13c** both yielded **1.38** as the only isolated product



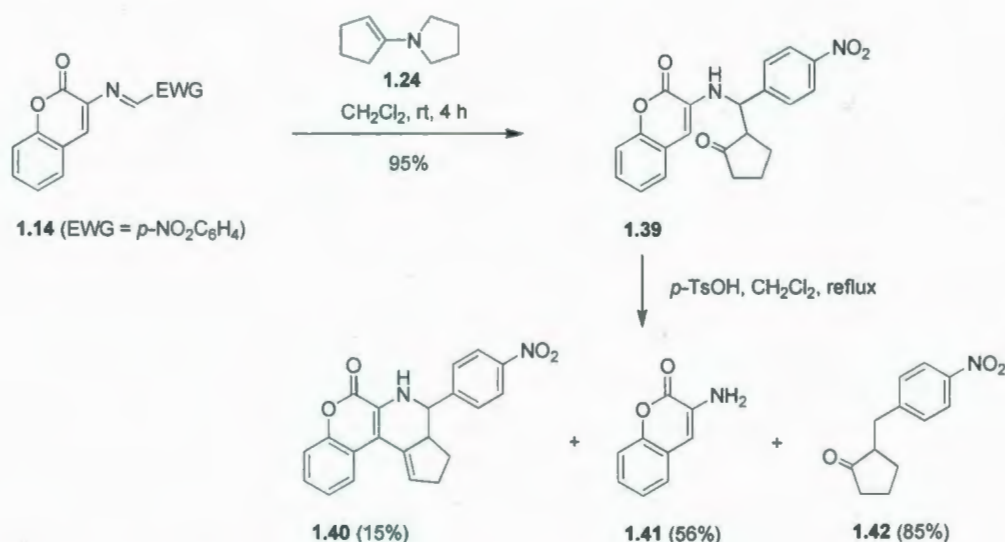
(Scheme 1.7). Formation of the desired product **1.36** can be explained by an IEDDA reaction, followed by eliminations of *p*-toluenesulfonamide and pyrrolidine (in either order). On the other hand, the more abundant products **1.37** and **1.38** were formed through pathways involving an initial 1,2-addition of the enamine **1.24** to the imine units of **1.13b–c**. Clearly, the replacement of carbon by nitrogen at 1-position of the diene unit caused 1,2-addition to be favoured over cyclization either via a concerted (IEDDA) reaction or a stepwise (1,4-addition / Mannich) mechanism.



**Scheme 1.7** IEDDA reactions of 1-azadienes **1.13a–c** with enamine **1.24**.

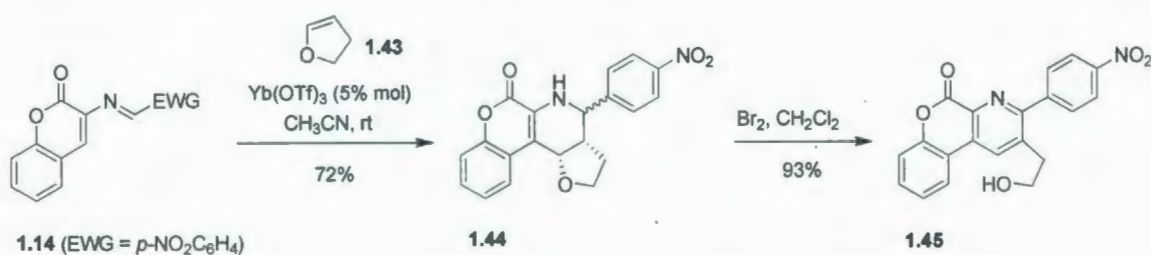
### 1.3.3.2 2-Azadiene 1.14

As in the case of 1-azadiene **1.13**, enamine **1.24** participated in a 1,2-addition to the imine unit of 2-azadiene **1.14** (EWG = *p*-C<sub>6</sub>H<sub>4</sub>NO<sub>2</sub>) to afford product **1.39** in 95% yield (Scheme 1.8). Although **1.39** appeared to be poised to undergo cyclization, refluxing **1.39** in dichloromethane in the presence of *p*-TsOH met with only very limited success. A mixture of products **1.40** (15%), **1.41** (56%), and **1.42** (85%) was obtained, in which ring-closure occurred only in the least abundant product, **1.40**.



**Scheme 1.8** IEDDA reaction of 2-azadiene **1.14** ( $p\text{-NO}_2\text{C}_6\text{H}_4$ ) with enamine **1.24**.

Alternatively, 2-azadiene **1.14** (EWG =  $p\text{-NO}_2\text{C}_6\text{H}_4$ ) reacted with vinyl ethers such as dihydrofuran (**1.43**) in the presence of a Lewis acid to afford a mixture of diastereomer **1.44**. This is actually an example of the Povarov reaction.<sup>19</sup> Povarov adduct mixture **1.44** was then aromatized upon treatment with bromine to give pyrido[2,3-*c*]coumarin **1.45** in good yield (Scheme 1.9).<sup>20</sup>

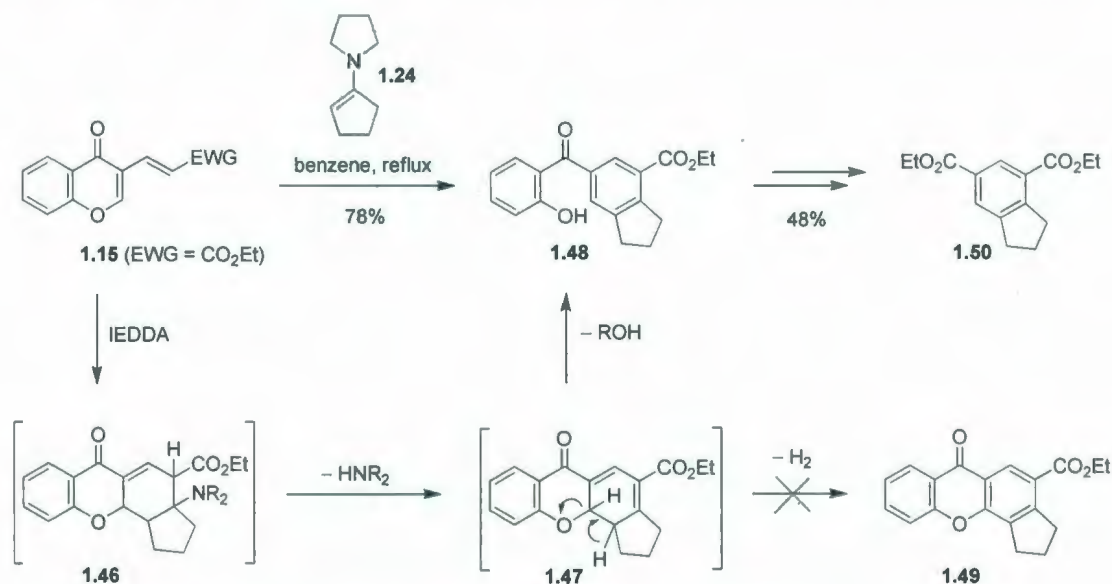


**Scheme 1.9** Employment of the Povarov reaction for the synthesis of pyrido[2,3-*c*]coumarin **1.45**.

### 1.3.4 Chromone-based Dienes **1.15**

Chromone-fused electron-deficient dienes such as **1.15** (EWG =  $\text{CO}_2\text{Et}$ )<sup>21</sup> are very stable in air and were also found to undergo IEDDA reaction with enamine **1.24**

(Scheme 1.10). 2-Hydroxybenzophenone **1.48** was obtained as a single product, the origin of which can be accounted for by an IEDDA reaction, followed by  $\beta$ -elimination of pyrrolidine and an internal elimination. Presumed intermediates **1.46** and **1.47** were not observed by tlc. The expected transfer hydrogenation process to give the desired xanthone **1.49** did not occur. However, 2-hydroxybenzophenone **1.48** could be converted into diester **1.50**,<sup>11,12,22</sup> which is a useful precursor for the synthesis of metacyclophanes.



**Scheme 1.10** IEDDA reaction of diene **1.15** (EWG = CO<sub>2</sub>Et) with enamine **1.24**.

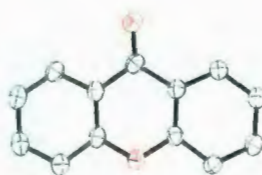
In summary, electron-deficient dienes **1.11–1.15** (Figure 1.3) have been developed by the Bodwell group and their IEDDA chemistry has been investigated. The heterocyclic moieties dramatically increase the stability of these dienes. In the cases of dienes **1.11** and **1.15**, an IEDDA-driven domino reaction occurred smoothly to afford aromatized products such as **1.23** (Scheme 1.4) and **1.48** (Scheme 1.10), respectively. As described in the following Chapters, similar approaches were employed in this work to synthesize xanthenes and xanthonoid aromatic systems.



## 1.4 Xanthone

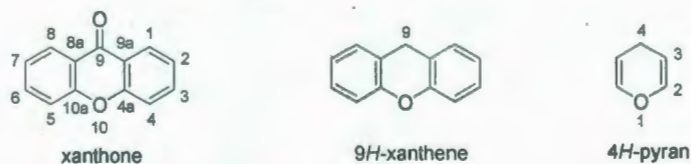
### 1.4.1 Structure, Nomenclature, Classification, and Properties

The crystal structure of the parent xanthone **1.51** (Figure 1.5) was first reported in 1982<sup>23</sup> and then redetermined eight years later.<sup>24</sup> This tricyclic aromatic compound has two benzenoid rings and one pyranoid ring, in which the central ring has a partial, albeit slight, aromatic character due to the conjugation of C=O bond with the endocyclic oxygen atom. The molecule is essentially planar in the crystal, containing torsion angles of 3.7° and 2.0° between the pyranoid ring and the two benzene rings, which adopt a very flattened boat conformation.<sup>25</sup>



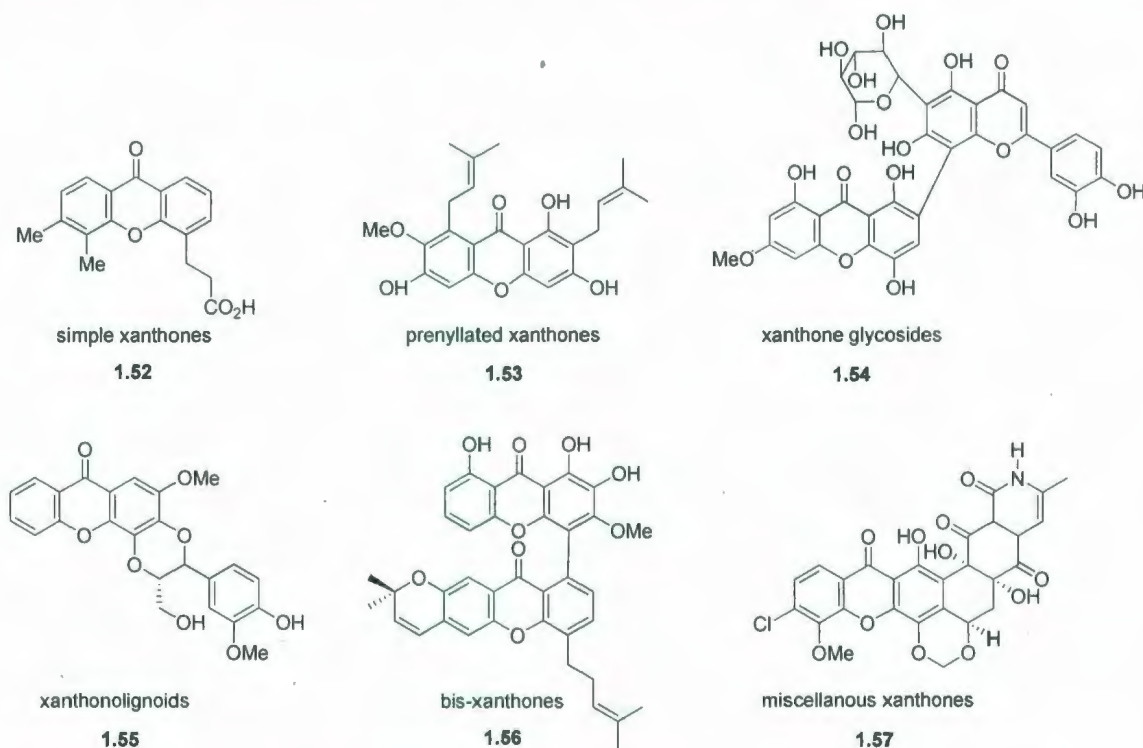
**Figure 1.5** X-ray crystal structure of xanthone **1.51**.<sup>23–25</sup>

Three different names have been used to describe compound **1.51**: xanthone, 9*H*-xanthene-9-one and dibenzo-4*H*-pyran-4-one.<sup>26</sup> The first two names are the most commonly used in the literature. The numbering of xanthone is also not always consistent in the literature.<sup>27</sup> In this thesis, the IUPAC provisional recommendation in the year 2004<sup>28</sup> will be employed (Figure 1.6).



**Figure 1.6** The xanthone skeleton with the IUPAC numbering recommendation.

More than 500 naturally-occurring xanthenes, which have been isolated from higher plants, fungi and lichens, were reported in only a four-year period (2000–2004).<sup>27</sup> Depending on the nature of the substituents on the xanthone scaffold, naturally-occurring xanthenes are classified into six main categories: simple xanthenes, prenylated xanthenes, xanthone glycosides, xanthonolignoids, bis-xanthenes, and miscellaneous xanthenes. Representative examples **1.52**–**1.57** are shown in Figure 1.7.



**Figure 1.7** Examples of the six different classifications of naturally-occurring xanthenes.<sup>27</sup>

Xanthenes have attracted the attention of chemists and biochemists because of their potentially useful biological and pharmaceutical properties. Many naturally-occurring and synthetic xanthenes exhibit antioxidant, antibacterial, antitumor, and antimalarial behavior. Some “hit” compounds are listed in Figure 1.8. For example, compounds **1.58** and **1.59**, extracted from *Mangifera indica* L. (mango) and *Garcinia*

*mangostana* (mangosteen), were respectively commercialized as antioxidants under the names of Vimang<sup>®</sup> and Xango<sup>®</sup>. Psorospermin **1.60** and 5,6-dimethoxyxanthone-4-acetic acid (DMXAA) (**1.61**) are antitumor agents, while 2,3,4,5,6-pentamethoxyxanthone (X5) **1.62** is an antimalarial agent.



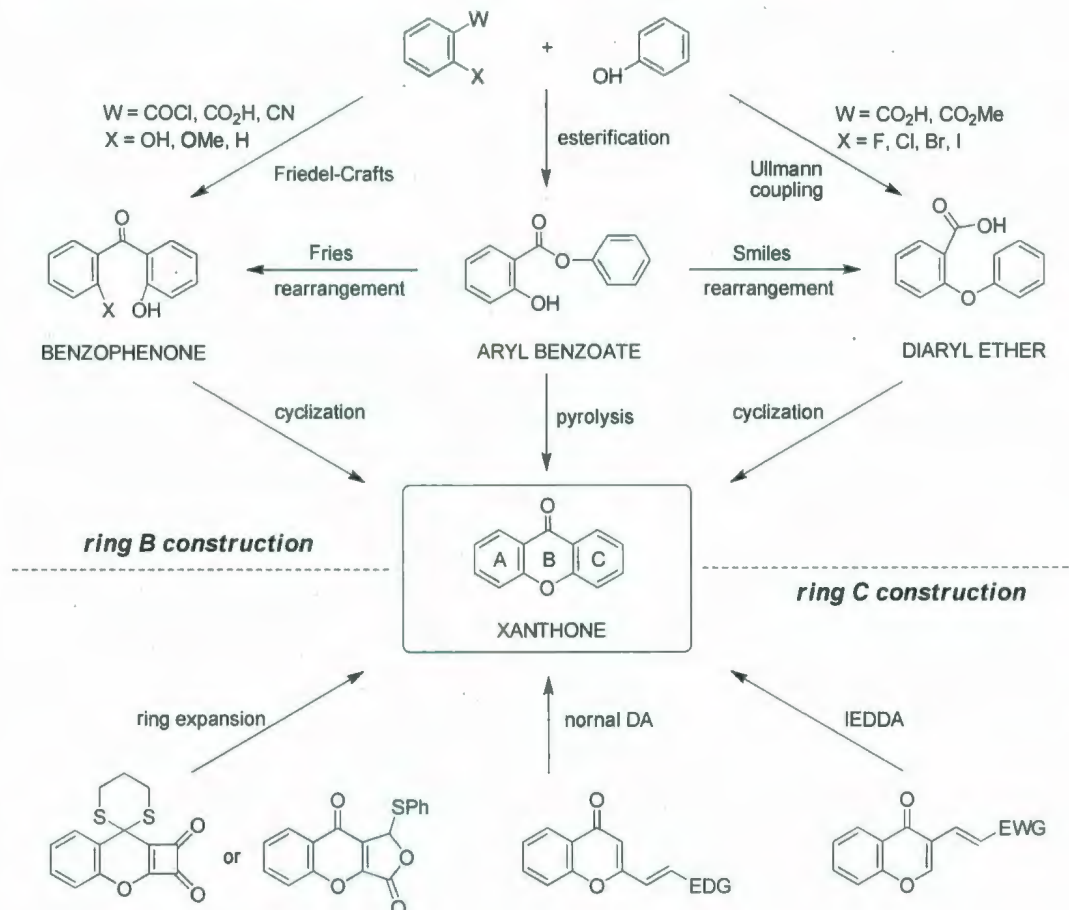
**Figure 1.8** Some examples of “hit” xanthone compounds.<sup>26</sup>

#### 1.4.2 Methodologies for the Synthesis of Xanthenes

The synthesis of xanthone derivatives has garnered much interest from organic chemists for more than a century. In the 1880s, an approach to xanthenes involving distillation of a mixture of a phenol, an *o*-hydroxybenzoic acid and acetic anhydride was reported.<sup>29</sup> Since then, a variety of other synthetic routes with higher yields have been developed. The most useful methodologies<sup>30</sup> can be divided into two main types, namely “ring B construction” and “ring C construction” (Figure 1.9). The former involves the cyclization of benzophenone, aryl benzoate<sup>31</sup> or diaryl ether intermediates, while the



latter relies upon ring expansion or cycloaddition reactions. Typical examples of each approach to xanthenes are discussed below in chronological order.

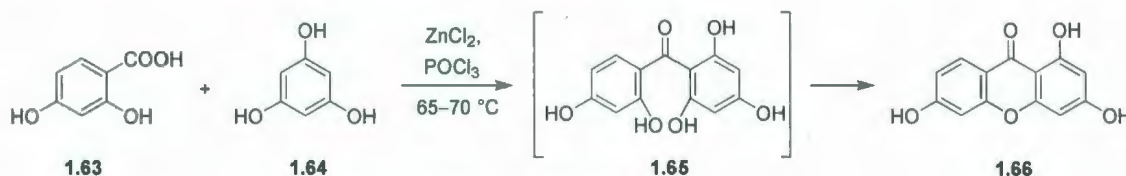


**Figure 1.9** Useful approaches to xanthenes.

#### 1.4.2.1 Synthesis of Xanthenes via “ring B construction”

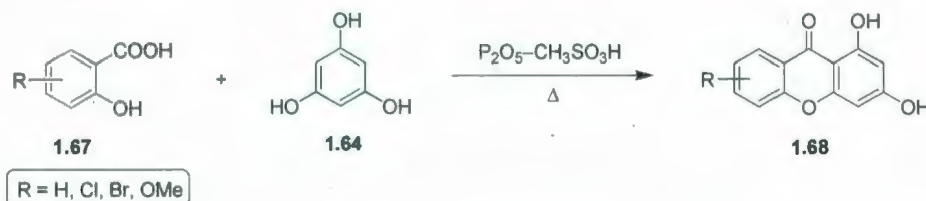
Prior to the development of more practical two-step syntheses of xanthenes, which proceed via benzophenone, aryl benzoate or diaryl ether intermediates, a one-pot reaction was reported in 1955. This method, which came to be known as the Grover, Shah and Shah (GSS) reaction,<sup>32</sup> directly produced xanthenes. For example, upon heating of salicylic acid **1.63** and phenol **1.64** in the presence of zinc chloride and

phosphoryl chloride, xanthone **1.66** was obtained, albeit in low yield, either with or without the observation of intermediate **1.65** (Scheme 1.11).



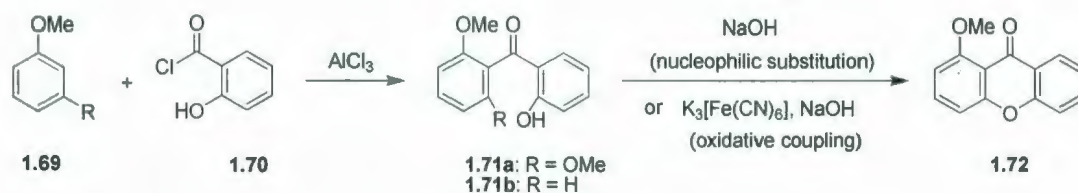
**Scheme 1.11** Synthesis of xanthone **1.66** via the GSS reaction.

More than 30 years later, it was discovered that the yields of the desired xanthenes could be significantly improved by using Eaton's reagent ( $\text{P}_2\text{O}_5\text{-CH}_3\text{SO}_3\text{H}$ )<sup>33</sup> instead of  $\text{ZnCl}_2\text{-POCl}_3$ . For instance, xanthenes **1.68** (Scheme 1.12) were obtained in much higher yields (73–93%) than when using the original conditions (18–48%).<sup>34</sup>



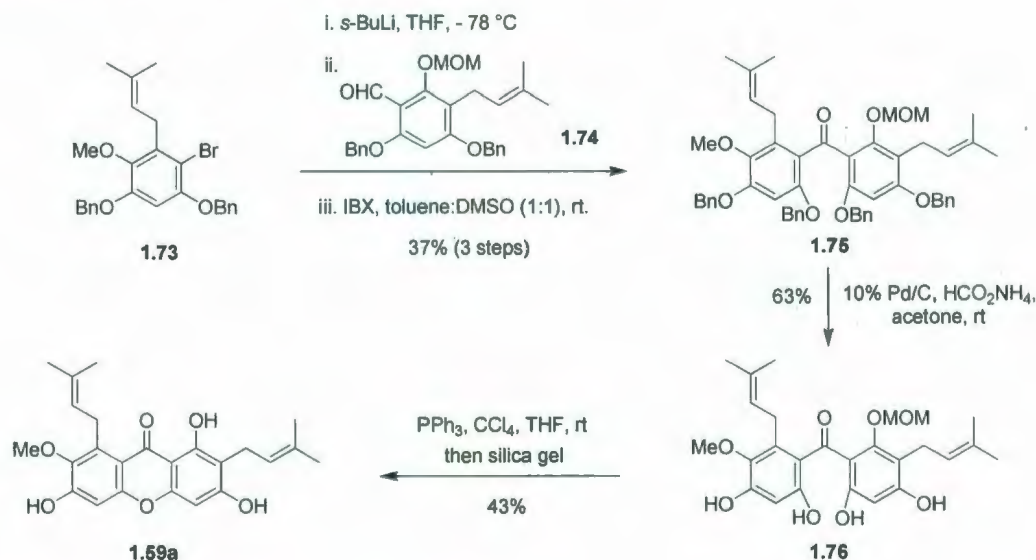
**Scheme 1.12** Synthesis of xanthenes **1.68** via the modified GSS reaction.

In the meantime, various two-step reactions involving benzophenone, aryl benzoate and diaryl ether intermediates were being developed. First, benzophenone derivatives were commonly obtained by a Friedel-Crafts acylation of a phenol derivative **1.69** with 2-hydroxybenzoyl chloride (**1.70**) (Scheme 1.13). The subsequent cyclization step could then proceed via a nucleophilic substitution ( $\text{R} = \text{OMe}$ )<sup>35</sup> or an oxidative coupling ( $\text{R} = \text{H}$ ).<sup>36</sup>



**Scheme 1.13** Friedel-Crafts-based approach to xanthone **1.72**.

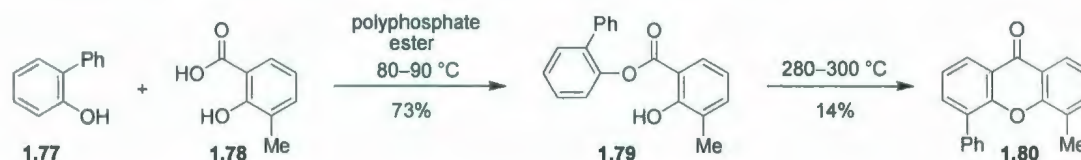
A naturally-occurring xanthone,  $\alpha$ -mangostin (**1.59a**) (Scheme 1.14)<sup>37</sup> was also synthesized via a benzophenone intermediate **1.75**, but this intermediate was formed using the 1,2-addition of the carbanion derived from **1.73** to aldehyde **1.74**, followed by an oxidation. Removal of the benzyl protecting groups in **1.75** afforded tetraol **1.76** which underwent a cyclization and deprotection of the MOM group upon treatment with  $\text{PPh}_3$ - $\text{CCl}_4$  and silica gel.<sup>38</sup> The cyclization might have been initiated by phosphorylation of the phenol, followed by abstraction of triphenylphosphine oxide, whereas removal of the MOM protecting group was simultaneously effected by the presumed active species ( $\text{Ph}_3\text{P}^+\cdot\text{CCl}_3\cdot\text{Cl}^-$ ).



**Scheme 1.14** Synthesis of  $\alpha$ -mangostin **1.59a**.

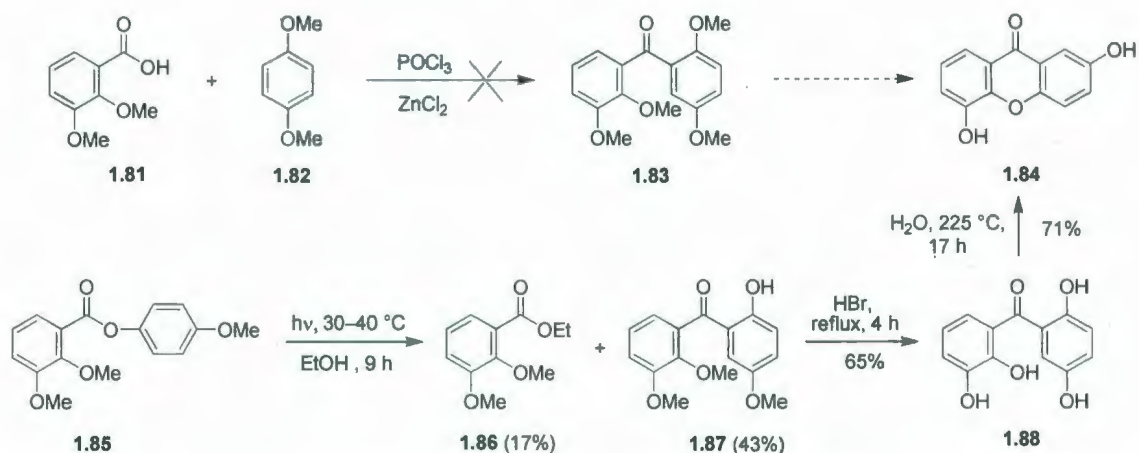


Relatively few syntheses of xanthenes via an aryl benzoate intermediate, either as a direct or an indirect precursor, have been reported. For example, xanthone **1.80** (Scheme 1.15) was obtained from ester **1.79** via pyrolysis.<sup>39</sup> Under these very harsh conditions, the desired xanthone was formed, but in a very low yield (14%).



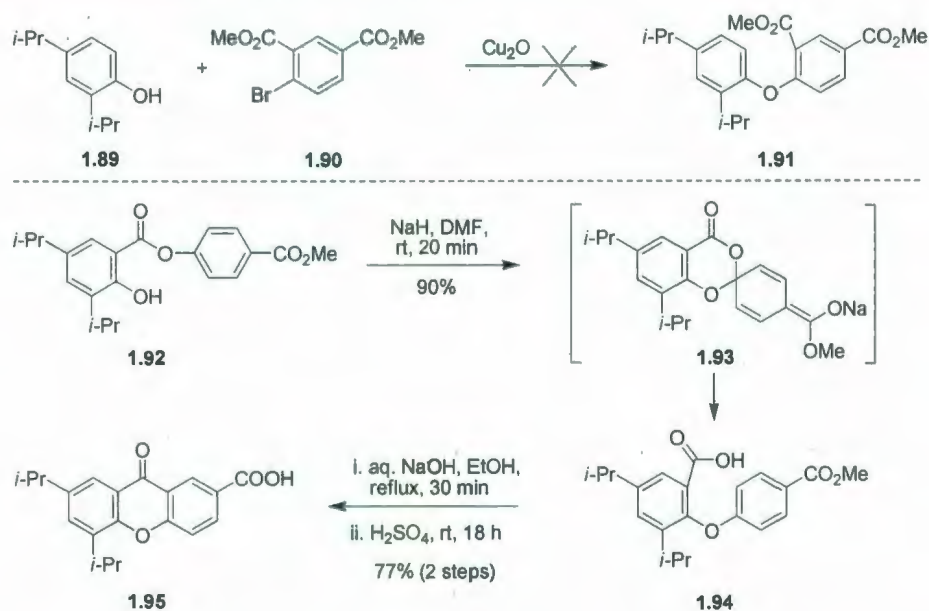
**Scheme 1.15** Synthesis of xanthone **1.80** from ester **1.79** via pyrolysis.

Aryl benzoates can be transformed into the corresponding benzophenones or diaryl ethers through photo-Fries rearrangement or Smiles rearrangement. This approach is usually taken when benzophenones or diaryl ethers cannot be prepared satisfactorily using conventional methods. For example, Friedel-Crafts reaction between 2,3-dimethoxybenzoic acid (**1.81**) and *p*-dimethoxybenzene (**1.82**) failed to produce benzophenone **1.83**, which is a potential precursor of xanthone **1.84** (Scheme 1.16). Therefore, an alternative route to **1.84** involving photo-Fries rearrangement of ester **1.85** was employed. Benzophenone **1.87** was obtained in moderate yield and then converted into the desired xanthone **1.84** via an acid-promoted demethylation (65%), and cyclization of **1.88** (71%).<sup>40</sup>



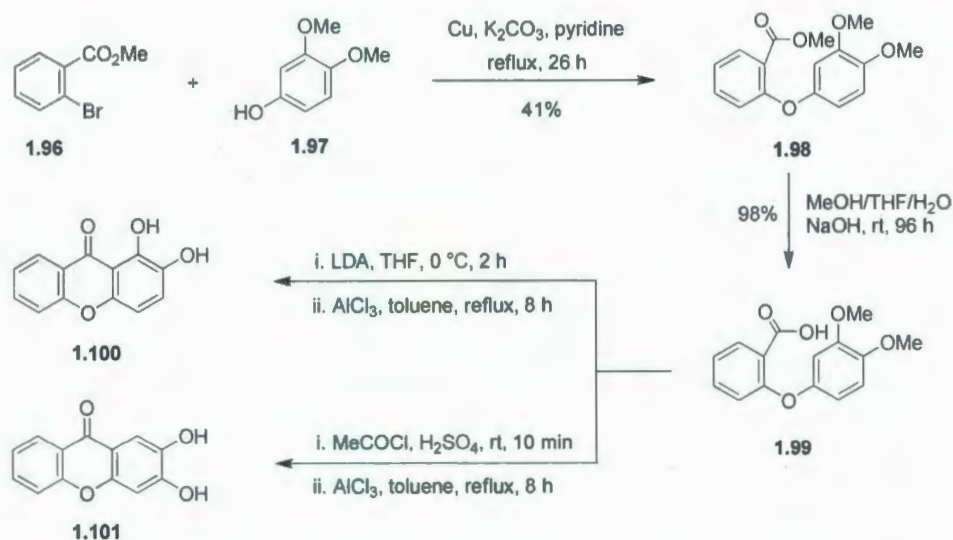
**Scheme 1.16** Synthesis of xanthone **1.84** from ester **1.85** involving photo-Fries rearrangement.

Similarly, diaryl ether **1.91** could not be formed from sterically-hindered phenol **1.89** and aryl bromide **1.90** via an Ullmann coupling (Scheme 1.17). Thus, diaryl ether **1.94** was prepared from aryl benzoate **1.92** via a Smiles rearrangement. Saponification of **1.94**, followed by an intramolecular Friedel-Crafts acylation of the resulting carboxylic acid furnished xanthone **1.95** in good yield.<sup>41</sup>



**Scheme 1.17** Synthesis of xanthone **1.95** from ester **1.92** involving Smiles rearrangement.

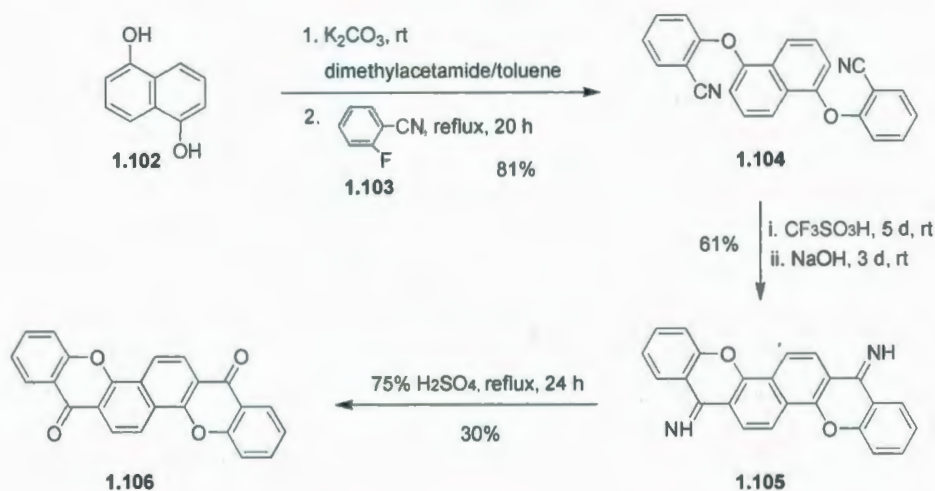
A typical example of a xanthone synthesis proceeding through a diaryl ether intermediate commenced with an Ullmann coupling between aryl halide **1.96** and phenol **1.97** to give diaryl ether **1.98** (Scheme 1.18). The subsequent hydrolysis of **1.98** gave carboxylic acid **1.99**, which underwent a cyclization either via a directed metalation<sup>42</sup> or a Friedel-Crafts acylation to afford xanthenes **1.100** and **1.101**, respectively.<sup>43</sup>



**Scheme 1.18** Synthesis of xanthenes **1.100** and **1.101** via Ullmann coupling and cyclization reactions.

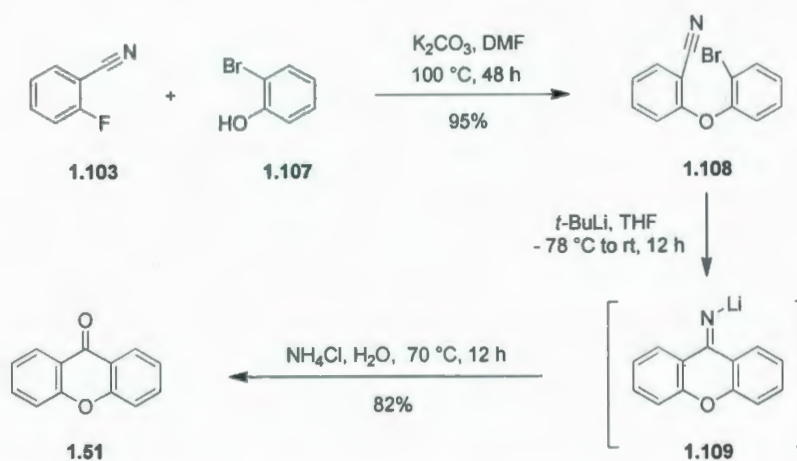
Dixanthone [*sic*]<sup>44</sup> **1.106** was also synthesized via diaryl ether intermediate **1.104**, which was obtained from 1,5-dihydroxynaphthalene (**1.102**) and 1-cyano-2-fluorobenzene (**1.103**) through nucleophilic aromatic substitution (Scheme 1.19).<sup>45</sup> The cyclization steps involved the superacid-promoted Houben-Hoesch reaction.<sup>46</sup> The acidic hydrolysis of the resulting diimine **1.105** gave dixanthone **1.106** in low yield, 30%.





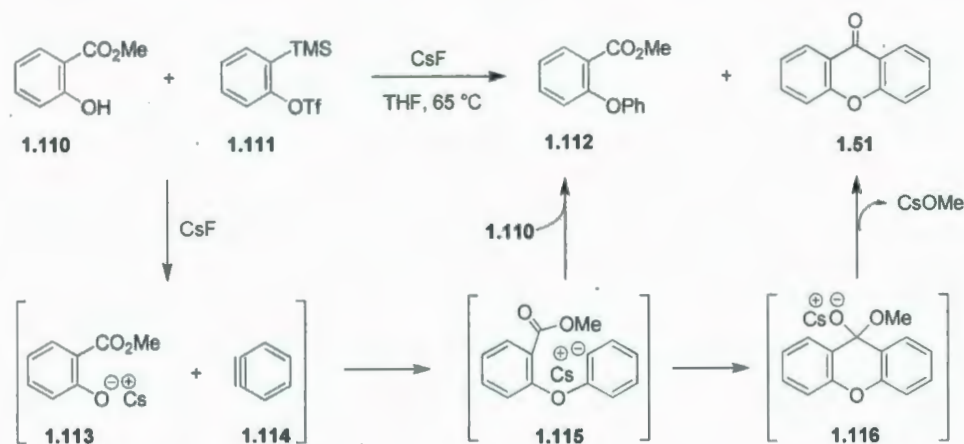
**Scheme 1.19** Synthesis of “dixanthone” **1.106** from **1.102** and **1.103**.

A more efficient variant of the diaryl ether approach is exemplified by a synthesis of the parent xanthone **1.51**, in which diaryl ether **1.108** was first obtained from a nucleophilic substitution reaction between 1-cyano-2-fluorobenzene (**1.103**) and 2-bromophenol (**1.107**) (Scheme 1.20).<sup>47</sup> A ring closure of **1.108** to give xanthone **1.51** in 82% yield was then achieved using an anionic cascade process initiated by halogen-metal exchange and ended with hydrolysis of intermediate **1.109**.



**Scheme 1.20** Synthesis of xanthone **1.51** via aryl ether **1.108** and an anionic cascade reaction.

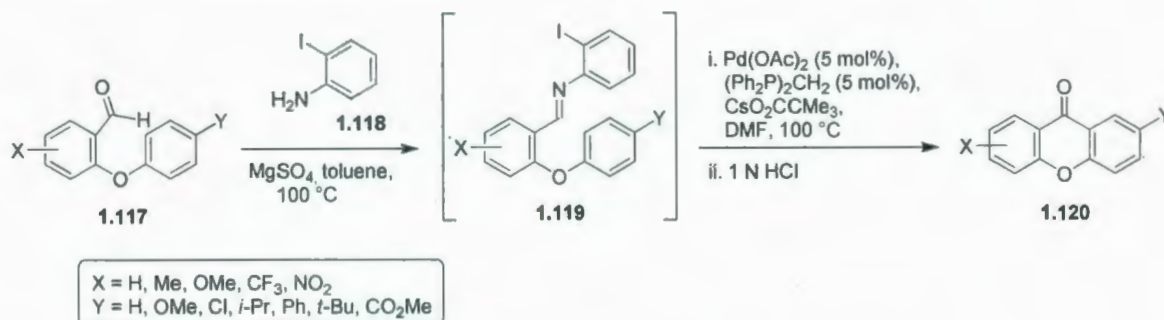
Recently, Larock *et al.* reported two new approaches to xanthenes via diaryl ether intermediates using a tandem coupling-cyclization and a palladium migration process. In the first method, the coupling occurred via a nucleophilic addition of phenolate **1.113** to benzyne (**1.114**), which had been derived from methyl salicylate (**1.110**) and silylaryl triflate **1.111**, respectively (Scheme 1.21). The resulting anion **1.115** underwent cyclization via a nucleophilic 1,2-addition to the carbonyl group, followed by an elimination of CsOMe to furnish xanthone **1.51**. The yields of xanthone derivatives obtained through this method ranged from 51 to 83%.<sup>48</sup> Diaryl ether **1.112** was formed as a byproduct, likely as a result of the protonation of intermediate **1.115** with phenol **1.110**.



**Scheme 1.21** Synthesis of xanthone **1.51** via a tandem coupling-cyclization strategy.

Larock's second method involved an intramolecular C-H activation via a palladium migration process. Imine **1.119**, which was generated *in situ* from aldehyde **1.117** and amine **1.118**, underwent a Pd-catalyzed cyclization, followed by an acidic

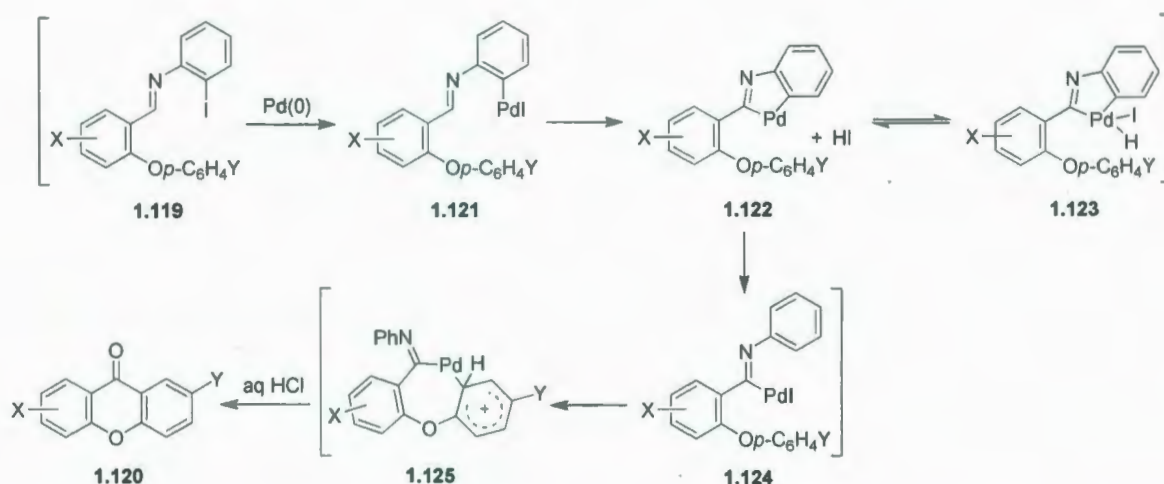
hydrolysis to afford xanthone **1.120** in yields ranging from 10 to 80%, depending upon the nature of the substituents (Scheme 1.22).<sup>49</sup>



**Scheme 1.22** Synthesis of xanthenes **1.120** via a palladium migration process.

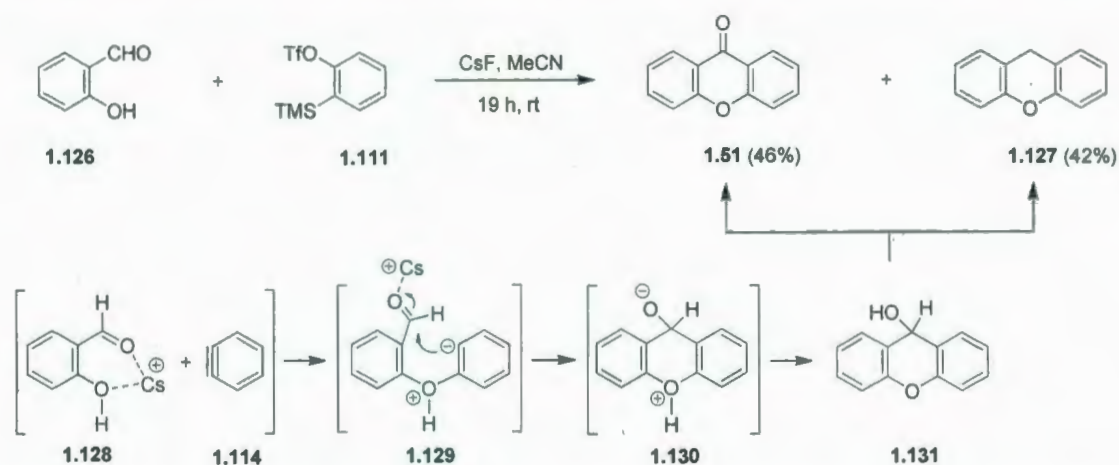
Larock's proposed mechanism for the formation of xanthone **1.120** (Scheme 1.23) commenced with an oxidative addition in the C-I bond, followed by a migration of the palladium atom from the initial aryl site in intermediate **1.121** to the imidoyl position in intermediate **1.124** via palladacycle **1.122**. Intermediate **1.125** could then be obtained from **1.124** via intramolecular arylation, which presumably proceed through an electrophilic aromatic substitution<sup>50</sup> or a proton-transfer mechanism.<sup>51</sup> Thus, the cyclization step would be disfavoured in the presence of an EWG (X or Y) and be favoured in the presence of an EDG. Indeed, xanthenes bearing an EWG were obtained in low or moderate yields (10–56%) while xanthenes bearing an EDG were formed in good yields (72–80%).





**Scheme 1.23** Larock's proposed mechanism for synthesis of xanthone **1.120** via a palladium migration process.

Most recently, another tandem coupling-cyclization involving salicylaldehydes (instead of salicylates in Larock's work) and silylaryl triflates was reported (Scheme 1.24).<sup>52</sup> The reaction between **1.126** and **1.111** occurred in a fashion analogous to that of **1.110** and **1.111** (Scheme 1.21). However, xanthone **1.51** and xanthene **1.127** were obtained from xanthol **1.131** as a mixture in low to moderate, and roughly equal yields.



**Scheme 1.24** Tandem coupling-cyclization of salicylaldehyde **1.126** and silylaryl triflate **1.111**.

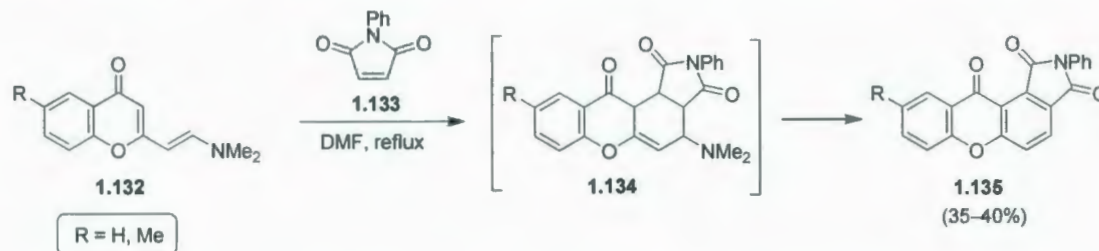
In summary, syntheses of xanthenes via “ring B construction” have been established for over one hundred years. This two-step strategy involves the formation of either a benzophenone or a diaryl ether as a key intermediate, followed by a cyclization. In the first strategy, Friedel-Crafts reaction, or an addition of a carbanion to an aldehyde, followed by an oxidation, can be used to form benzophenone intermediates. The cyclization can occur via dehydration, nucleophilic aromatic substitution, or oxidative coupling. In the second route, a diaryl ether can be prepared by Ullmann coupling, nucleophilic aromatic substitution, or nucleophilic addition. The cyclization can then be carried out by a Friedel-Crafts reaction, a nucleophilic addition to an ester carbonyl, or a palladium-catalyzed ring closure. In the event that a benzophenone or a diaryl ether cannot be prepared using the conventional methods, photo-Fries or Smiles rearrangements can be used.

#### 1.4.2.2 Synthesis of Xanthenes via “ring C construction”

In this approach, xanthenes can be formed in only one step from the final precursors via a Diels-Alder reaction, a cascade-type reaction, or a Michael reaction.

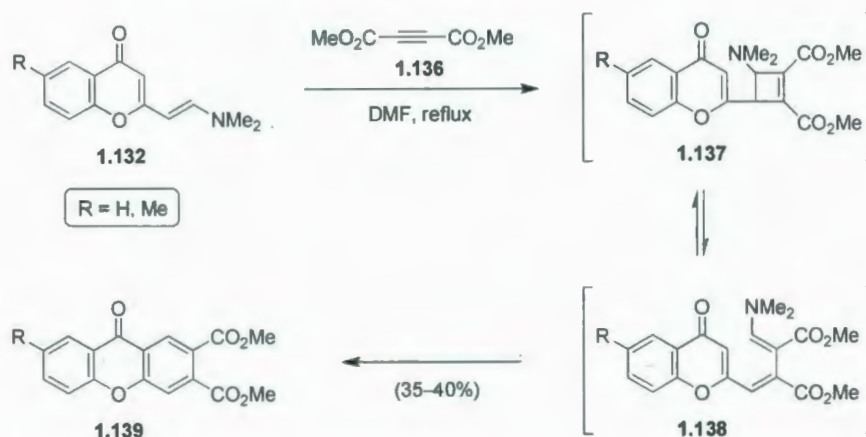
Initial work using the Diels-Alder reaction to achieve xanthenes found that both normal and inverse electron demand Diels-Alder reactions between 2-vinylchromones and dienophiles gave [4+2] adducts (so-called xanthone derivatives), but they did not react further to afford xanthenes with aromatized C-rings.<sup>53</sup> However, aromatization could be achieved when the dienes and dienophiles were appropriately modified. For example, in the normal Diels-Alder reaction between electron-rich dienes **1.132** and electron-deficient dienophiles such as **1.133** (Scheme 1.25),<sup>54</sup> the elimination of

dimethylamine aided the aromatization of adduct intermediates **1.134** to form xanthenes **1.135**. It seems likely that a transfer hydrogenation step completed the aromatization.



**Scheme 1.25** Normal Diels-Alder reaction between diene **1.132** and dienophile **1.133**.

Surprisingly, when dienes **1.132** reacted with dimethyl acetylenedicarboxylate (DMAD) (**1.136**), a [2+2] cycloaddition occurred instead of the anticipated [4+2] cycloaddition (Scheme 1.26). A subsequent cascade reaction then took place, including a  $4\pi$ -electrocyclic ring opening to give **1.138**, a  $6\pi$ -electrocyclic ring closure and a  $\beta$ -elimination of dimethylamine to form xanthenes **1.139**.<sup>54</sup>

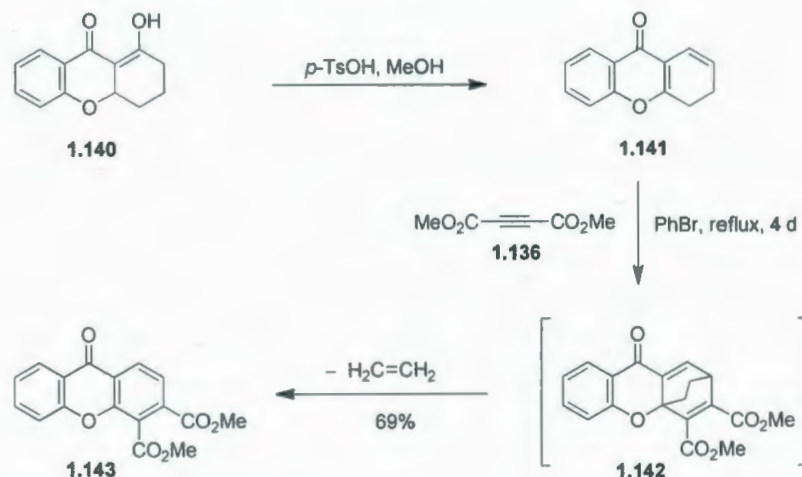


**Scheme 1.26** Normal Diels-Alder reaction between dienes **1.132** and DMAD (**1.136**).

In a related example, diene **1.141**, which was a minor product obtained from the reaction of xanthone derivative **1.140**<sup>55</sup> with *p*-TsOH in methanol, participated in a Diels-

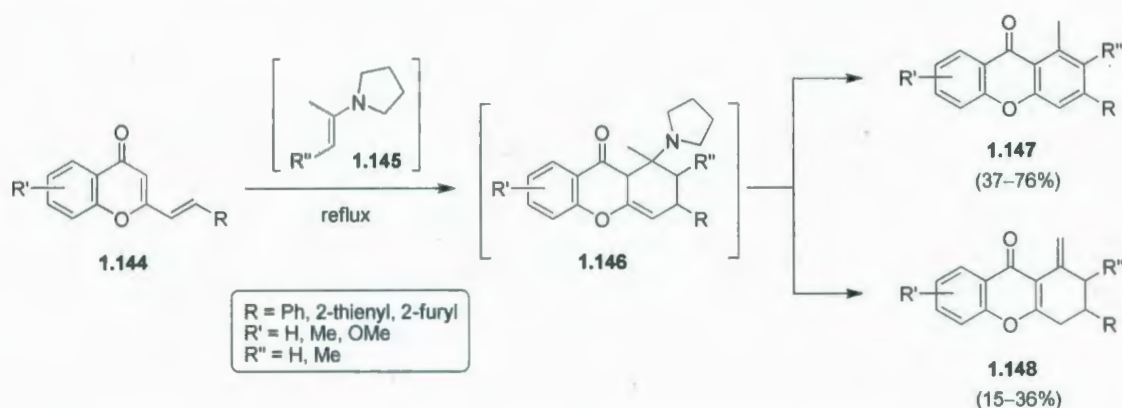


Alder reaction with DMAD (**1.136**), followed by a retro Diels-Alder elimination of ethylene to afford xanthone diester **1.143** in 69% yield (Scheme 1.27).<sup>56</sup>



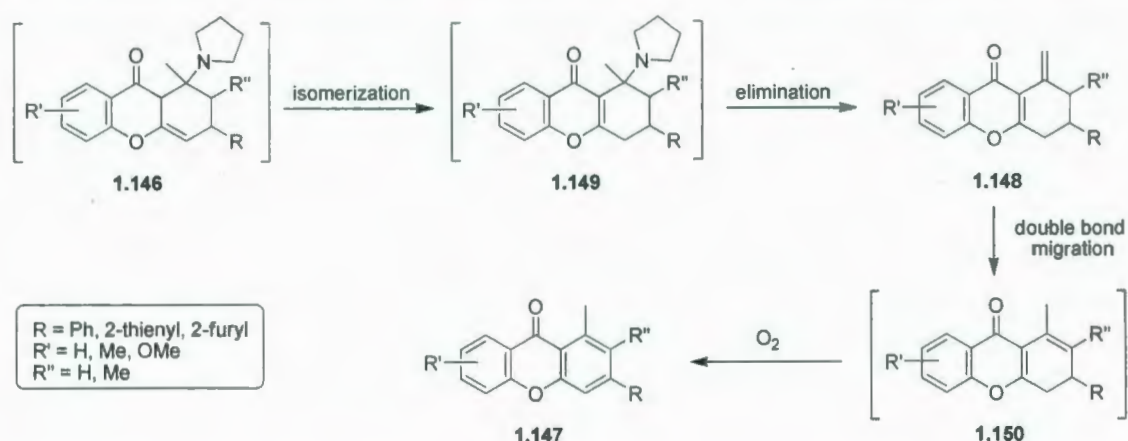
**Scheme 1.27** Normal Diels-Alder reaction between diene **1.141** and DMAD (**1.136**).

The IEDDA-based approach to xanthenes resembles the normal Diels-Alder-based approach in that a dialkylamino group was used to both activate the electron-rich component and serve as a leaving group after the cycloaddition. Enamines, which can be easily prepared from the reaction between an aldehyde or a ketone with an amine, have been employed as dienophiles in these IEDDA reactions. For example, IEDDA reactions between dienes **1.144** and enamines **1.145**, which were obtained by refluxing the corresponding ketones with a catalytic amount of pyrrolidine, provided a mixture of xanthenes **1.147** and dienes **1.148** in moderate to good yields (Scheme 1.28).<sup>57</sup>



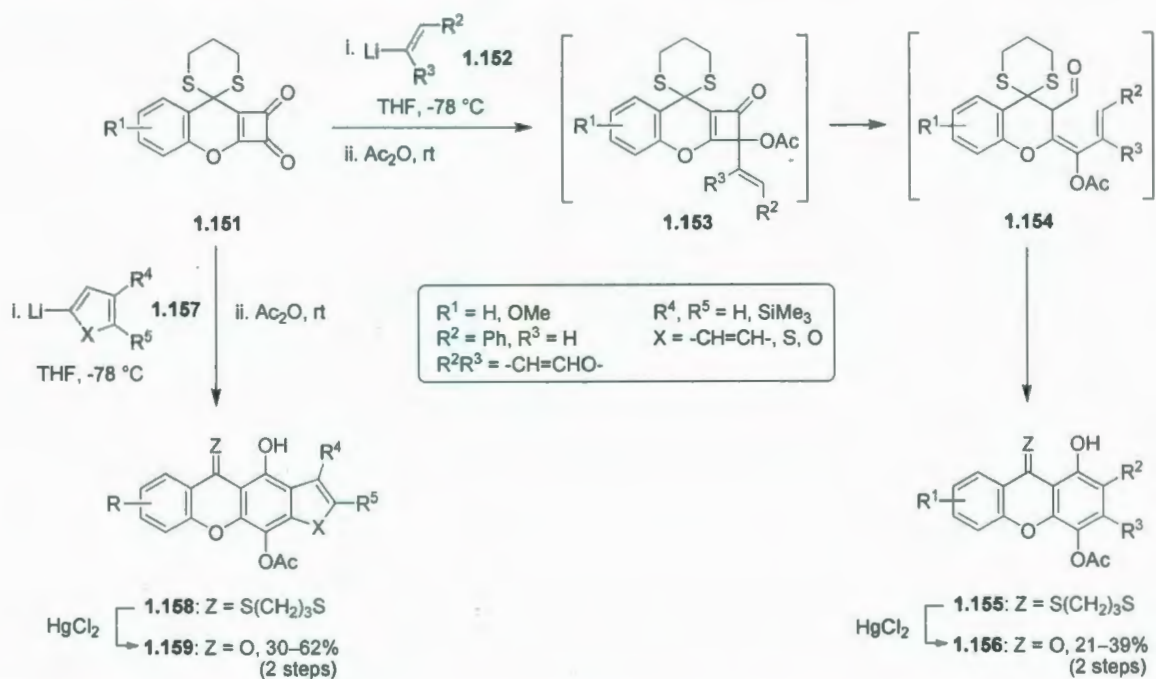
**Scheme 1.28** IEDDA reaction between dienes **1.144** and dienophiles **1.145**.

The formation of the desired xanthenes **1.147** was postulated to proceed through byproducts **1.148**, which were presumed to come from adducts **1.146** through an isomerization and an elimination of pyrrolidine at the less-hindered site (Scheme 1.29). The exocyclic double bond in **1.148** then migrated into the ring to form intermediates **1.150**, which underwent an oxidation reaction to afford xanthenes **1.147**. The minor products **1.148**, which were not completely converted into **1.147**, could be then converted into the desired xanthenes **1.147** by treatment with strong acids such as AcOH / H<sub>2</sub>SO<sub>4</sub>.



**Scheme 1.29** Postulated mechanism to explain the formation of xanthenes **1.147** and dienes **1.148**.

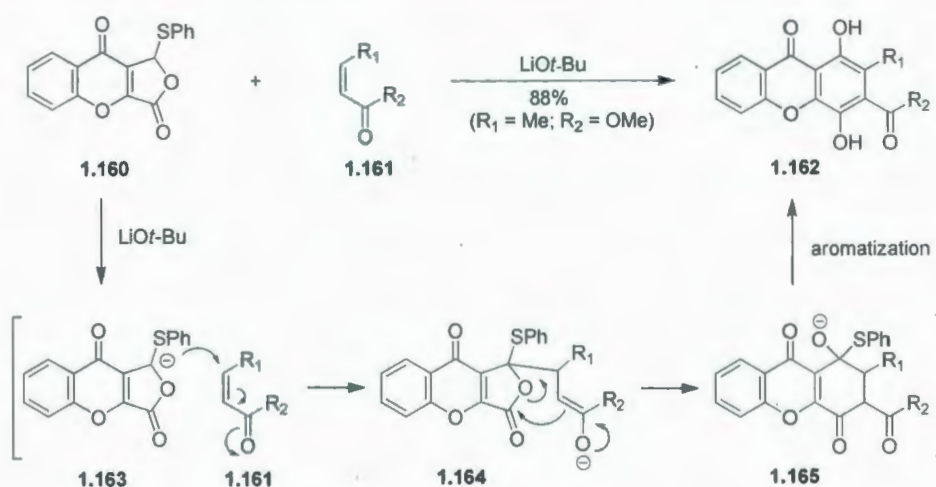
Another method to synthesize xanthenes involved the 1,2-addition of organolithium reagents to dithiane-protected  $\gamma$ -benzopyrone-fused cyclobutenediones (Scheme 1.30).<sup>58</sup> Addition of an organolithium compound to the less-hindered carbonyl group in **1.151**,<sup>59</sup> followed by an *O*-acylation of the resulting alkoxide gave intermediates **1.153**. These unstable cyclobutenes immediately underwent a  $4\pi$ -electrocyclic ring opening and a subsequent  $6\pi$ -electrocyclic ring closure / tautomerization to afford dithiane-protected compounds **1.155**. Dethianation under standard conditions<sup>59</sup> furnished the desired xanthenes **1.156** in moderate yields. Similarly, xanthone-fused heteroaromatic systems such as **1.159** were synthesized in moderate to good yields from dithianes **1.151** and organolithium reagents **1.157**.



**Scheme 1.30** Synthesis of xanthenes **1.156** and **1.159** from reactions of organolithium reagents **1.152** or **1.157** with compounds **1.151**.



The most recent report of a new xanthone synthesis described the condensation of a benzopyranophthalide with acyclic or cyclic Michael acceptors (Scheme 1.31).<sup>60</sup> Carbanion **1.163**, which was derived from **1.160**, underwent a conjugate addition to **1.161**, followed by a nucleophilic ring closure to give tricyclic intermediate **1.165**, which then aromatized to form xanthone **1.162** in excellent yield. The precursor **1.160** was prepared in five steps from the commercially available compounds *o*-hydroxypropiophenone and ethyl chlorooxoacetate.<sup>60,61</sup>



**Scheme 1.31** Synthesis of xanthenes **1.162** from **1.160** and **1.161**.

In summary, xanthenes have been synthesized via the “ring C construction” approach using both normal and inverse Diels-Alder reactions, 1,2-addition of organolithium reagents to dithiane-protected  $\gamma$ -benzopyrone-fused cyclobutenediones, or condensation of benzopyranophthalides with acyclic or cyclic Michael acceptors.

Overall, a variety of synthetic approaches to xanthenes through ring B or ring C are available. The older methods are reliable and can usually be performed on a larger scale, but can be limited in their scope and / or give only moderate yields. The more

modern methods (developed since the 1990s) tend to involve more impressive transformations, have broader scope and / or allow access to more elaborate xanthoness.

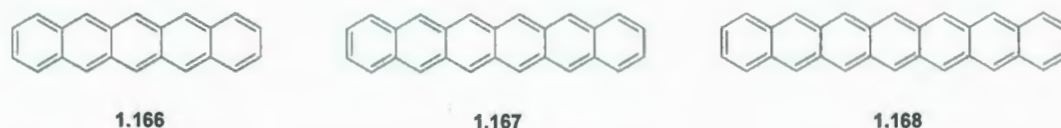
## 1.5 Heteroacenes

### 1.5.1 Historical Development of Heteroacenes

The importance and performance of organic electronic / optoelectronic devices have both significantly increased over the last twenty years. Three common classes of such devices are organic field-effect transistors (OFETs, also known as thin-film transistors, TFTs), organic photovoltaic devices (OPVs) and organic light-emitting diodes (OLEDs). Organic systems used for OLEDs must have a high fluorescence quantum yield, and all of the above devices require the organic system to have high charge carrier mobility for optimal performance. This latter property is strongly correlated to molecular packing in the solid state as well as the energies and intermolecular overlap between HOMOs and LUMOs.<sup>62,63</sup> In general, charge carrier mobility, which reflects the ease with which an electron (or hole) can be transferred from the HOMO of one molecule to the LUMO of its neighbour, tends to increase as face-to-face molecular packing becomes closer and more compact. The same is true as the HOMO-LUMO gap becomes narrower. However, a high-lying HOMO in conjunction with a narrow band gap renders an organic molecule sensitive to photooxidation, resulting in the deterioration of semiconductor performance under ambient conditions. As such, the requirements for an ideal organic molecular candidate in organic device applications are (1) close (face-to-face) molecular packing in the solid state; (2) narrow HOMO-LUMO gap; (3) low

HOMO energy; and (4) reasonable solubility in common solvents, which facilitates processing and device fabrication.

Acene-type compounds are one of the most widely studied classes of organic molecules for the applications in the devices discussed above. For example, high-quality FET devices made from thin films of pentacene (**1.166**) (Figure 1.10) have shown much higher levels of charge carrier mobility ( $5 \text{ cm}^2 \text{ V}^{-1} \text{ s}^{-1}$ )<sup>64</sup> compared to that of amorphous silicon ( $0.5 \text{ cm}^2 \text{ V}^{-1} \text{ s}^{-1}$ ).<sup>62</sup> Presumably, the high mobility of pentacene originates from its highly ordered and close molecular packing in the solid state, which promotes  $\pi$ - $\pi$  interactions between adjacent molecules.<sup>65</sup> Higher acenes, such as hexacene (**1.167**) and heptacene (**1.168**), which show smaller HOMO-LUMO gaps than that of pentacene, are predicted to exhibit superior electronic properties.<sup>66</sup> However, the low solubility and inherent instability of these higher, linearly-fused and solely carbon-based acenes have limited their accessibility for proper study for applications.

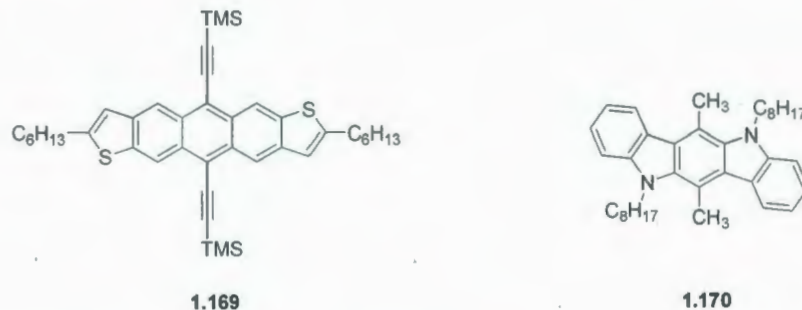


**Figure 1.10** Examples of linear acenes.

A current scientific challenge is to develop new organic materials, which exhibit both high charge carrier mobility and high stability under ambient conditions. The introduction of heteroatoms into fused-ring systems has been one of the recent major approaches to modify the physical and chemical properties of “ladder-type” acenes.<sup>67</sup> Modified systems such as anthradithiophenes **1.169**<sup>68</sup> and indolocarbazoles **1.170**<sup>69</sup>



(Figure 1.11) are more stable than pentacene and show relatively high charge carrier mobility ( $0.14\text{--}1.0\text{ cm}^2\text{ V}^{-1}\text{ s}^{-1}$ ).



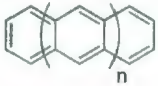
**Figure 1.11** Examples of modified pentacene systems.

Several types of ladder-type heteroacenes (see below for a definition of this term) have been developed and studied. Among the heteroatoms (S, N, O, B, P, Si, Se, and Te) that have been used to modify acene systems, the first three of these have been widely employed, whereas the others have been used infrequently.

### 1.5.2 Classifications and Nomenclatures of Heteroacenes

The term “heteroacenes” refers to acene derivatives in which one or more of the carbocyclic rings is replaced by a heteroaromatic ring. Therefore, heteroacenes are, like the parent acenes, classified according to the total number of rings in the system. The prefix “hetero” is added before the name of acenes to denote the presence of at least one heteroaromatic ring (Table 1.1).

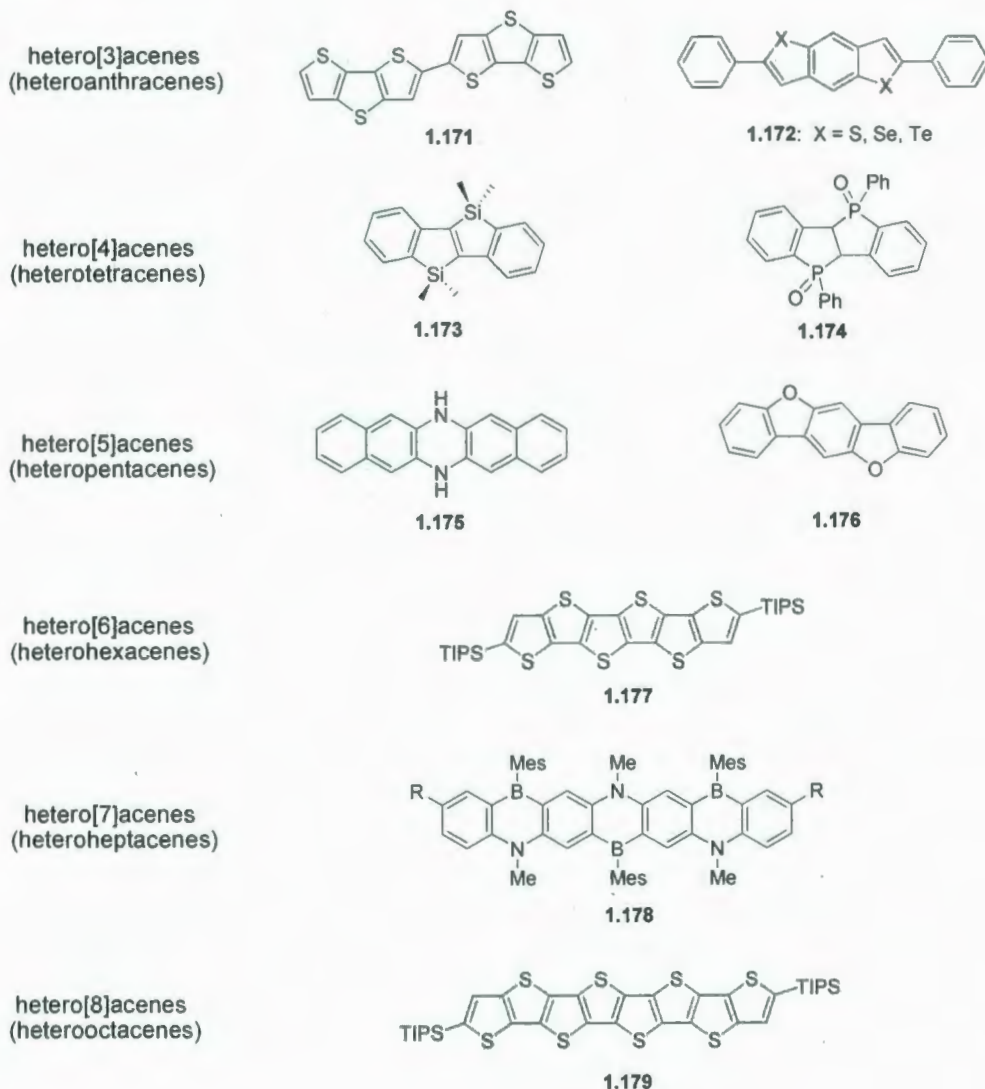
**Table 1.1** Classifications and general nomenclatures of heteroacenes.

	Acenes	Heteroacenes (literature)	Heteroacenes (this work)
$n = 1$	anthracene	heteroanthracene	hetero[3]acene
$n = 2$	tetracene	heterotetracene	hetero[4]acene
$n = 3$	pentacene	heteropentacene	hetero[5]acene
$n = 4$	hexacene	heterohexacene	hetero[6]acene
$n = n$			hetero[n]acene

In this thesis, the Greek *prefix* (such as tetra, penta, etc.) indicating the number of rings will be replaced by an Arabic number in square brackets.<sup>70</sup> For example, a heteropentacene will be named as a hetero[5]acene. As such, the general term hetero[n]acenes ( $n \geq 1$ ) can be used for all types of heteroacenes, some examples of which are given in Figure 1.12.

Because of the great diversity of heteroacenes, individual heteroacenes are called by common names in most cases. For example: “bis(dithienothiophene)” **1.171**,<sup>71</sup> “diphenyldi(chalcogenophene)s” **1.172**,<sup>72</sup> “bis-silicon-bridged stilbene” **1.173**,<sup>73</sup> “bis-phosphoryl-bridged stilbene” **1.174**,<sup>74</sup> “diazadihydropentacene” **1.175**,<sup>75</sup> “dibenzo[*d,d'*]-benzo[1,2-*b*:4,5-*b'*]difurans” (**1.176**),<sup>76</sup> “thiophene-based heteroacenes” **1.177** and **1.179**,<sup>77</sup> “ladder-type fused-azaborine” **1.178**.<sup>78</sup> Clearly, these names convey the desired information, but they are not consistent with one another. The development of an unambiguous system of nomenclature for heteroacenes would be a timely and useful

contribution. However, this will be a very challenging and potentially contentious undertaking.

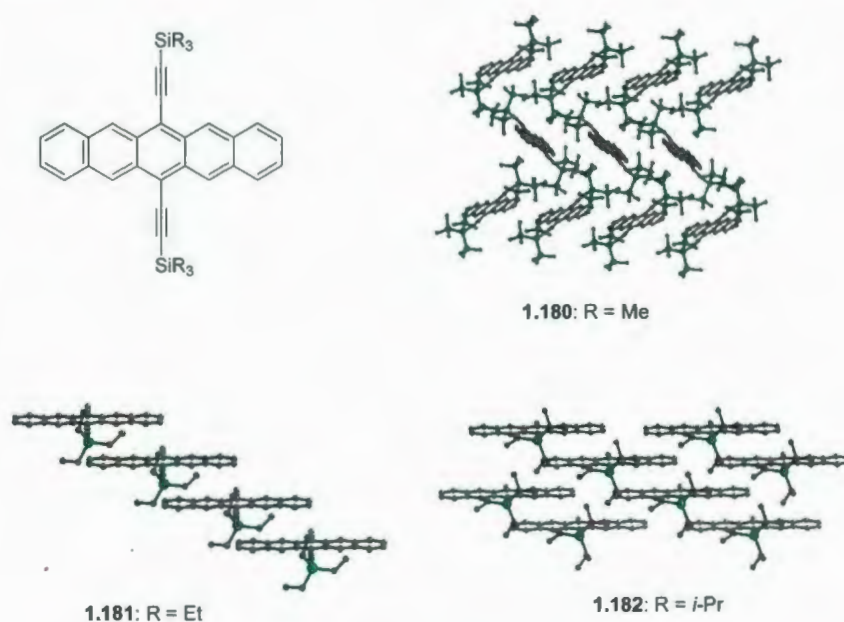


**Figure 1.12** Examples of hetero[*n*]acenes.

### 1.5.3 Common Acene-type Packing Motifs

There are two common packing motifs adopted by acene-type compounds in the solid state that result in strong intermolecular interactions, *i.e.*, the “herringbone” and  $\pi$ -stacking motifs (Figure 1.13).<sup>62</sup>





**Figure 1.13** “Herringbone” (*top*) and  $\pi$ -stacking (*bottom*) arrangements of pentacenes 1.180–1.182.

In the classic “herringbone” arrangement, the edge of one acene molecule interacts with the face of another acene molecule. This arrangement is also called “edge-to-face”. Alternatively, the molecules can adopt a parallel arrangement, which is referred to as “face-to-face” or “ $\pi$ -stacking”. The herringbone arrangement yields two-dimensional electronic coupling while  $\pi$ -stacking one can yield one- or two-dimensional interactions.

#### 1.5.4 Relationships between Charge Carrier Mobility and Molecular Structures

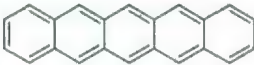
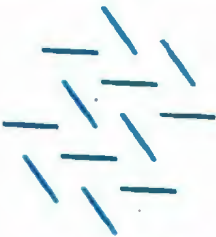
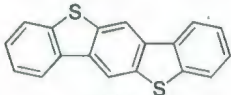
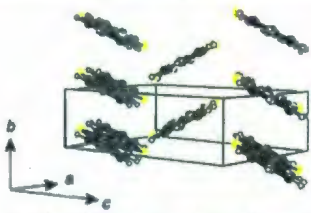
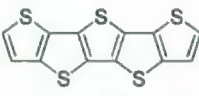

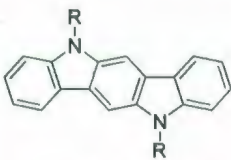
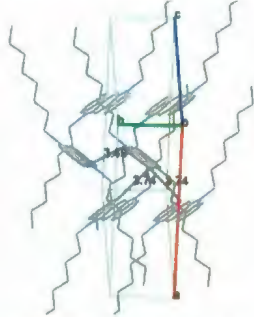
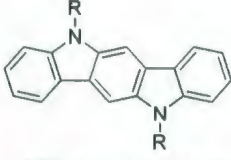

It has been known that charge carrier mobility depends on molecular packing, HOMO energies and the HOMO-LUMO gap. However, it has proved to be very difficult to exploit any of these benchmarks to effectively tune the charge-carrier-mobility of a parent system because even small changes in molecular structure can significantly affect

the key properties (especially solid state packing), but not necessarily in complementary ways. A further complication is that charge carrier mobility measurements obtained using different methods tend to vary for the same molecule. The error depends heavily on the specific technique and the level of the worker's expertise. Therefore, charge carrier mobility values should be viewed cautiously.

Generally, it is very hard to pinpoint which feature of the molecular packing motif, distance between two molecules (interplanar distance), or HOMO-LUMO gap more strongly affects the charge carrier mobility. Among its derivatives (Table 1.2), pentacene, which has the longest interplanar distance and smallest HOMO-LUMO gap, showed the highest charge carrier mobility. In this case, it seems that the HOMO-LUMO gap plays the most important role. Compounds **1.183**<sup>79</sup> and **1.184**<sup>80</sup> have essentially the same interplanar distances. However, due to the  $\pi$ -stacking arrangement and a slightly smaller HOMO-LUMO gap, the latter has charge carrier mobility 4.5 times higher than that of the former. Apparently, both the packing motif and HOMO-LUMO gap were involved in this case.

It is interesting to note that different substituents can strongly influence charge carrier mobility. For example, compound **1.186**,<sup>81,82</sup> which bears *p*-octylphenyl groups exhibited a twelve-fold higher charge carrier mobility than **1.185**,<sup>81,82</sup> which bears an *n*-octyl group. In this case, the HOMO-LUMO gap was not a dominant factor as **1.186** has a significantly larger band gap. Presumably, the compact molecular packing resulting from  $\pi$ -stacking between the acene frameworks as well as between the phenyl groups enhanced the charge carrier ability.

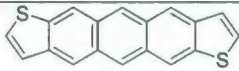
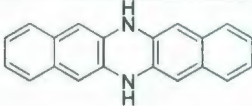
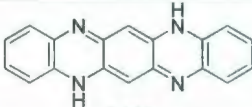
**Table 1.2** Relationship between charge carrier mobility and molecular structures.

Acene-type compounds	Packing motifs (single crystal)	Minimal interplanar distance (Å)	HOMO-LUMO gap (exp, eV)	Mobility ( $\text{cm}^2 \text{V}^{-1} \text{s}^{-1}$ )
 1.166	 herringbone	6.27	1.85 <sup>80</sup>	$500 \times 10^{-2}$
 1.183	 $\pi$ -stacking + herringbone	3.52	3.3	$1 \times 10^{-2}$
 1.184	 $\pi$ -stacking	3.50	3.2	$4.5 \times 10^{-2}$
 1.185: R = <i>n</i> -octyl	 $\pi$ -stacking + herringbone	3.49	2.65	$0.3 \times 10^{-2}$
 1.186: R = <i>p</i> -octylphenyl	 $\pi$ -stacking	3.44	2.80	$12 \times 10^{-2}$



In some cases in which a single crystal could not be obtained, polycrystals on a thin film were subjected directly to charge carrier mobility measurement (Table 1.3).

**Table 1.3** Relationship between charge carrier mobility and molecular structures.<sup>83</sup>

Acene-type compounds	Packing motifs	Mobility ( $\text{cm}^2 \text{V}^{-1} \text{s}^{-1}$ )
 1.187	Polycrystals (thin film)	$9 \times 10^{-2}$
 1.175	Polycrystals (thin film)	$5 \times 10^{-5}$
 1.188	Polycrystals (thin film)	$2 \times 10^{-2}$

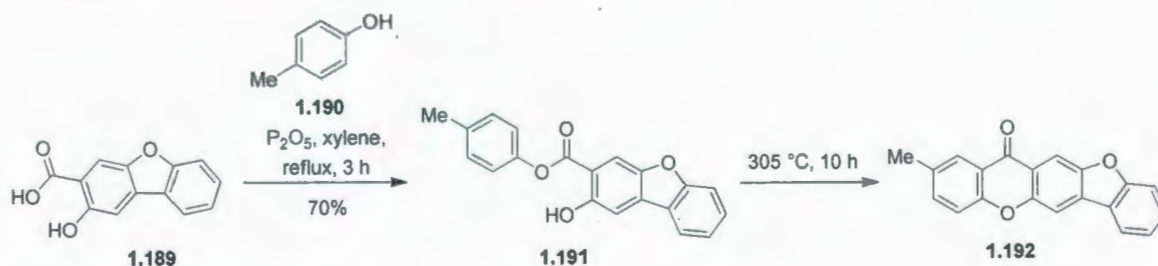
Although the charge carrier mobility of a molecule is not predictable based on the packing motif, interplanar distance, or HOMO-LUMO gap, these factors are nevertheless important, not only for the fundamental purposes of broadly characterizing new compounds and understanding their physical and chemical properties, but also in the broader context of developing new organic systems for potential applications in optoelectronic devices.

### 1.5.5 Major Interest: Xanthonoid Hetero[5]acenes

Only three types of xanthonoid hetero[5]acenes have been reported, namely benzofuroxanthenes, indoloxanthenes, and dixanthenes. These heteroacene systems attracted interest because of their pharmaceutical properties rather than physical

properties. In particular, dibenzofurans are known to exhibit antifungal and antibacterial activity.<sup>84</sup> Likewise, the indole nucleus is associated with a broad range of pharmaceutical properties such as antibacterial,<sup>85</sup> anticancer,<sup>85</sup> antibiotic,<sup>86</sup> antifungal,<sup>87</sup> and central nervous system modulating.<sup>88</sup> Thus, the combination of a xanthone moiety, which also exhibits a variety of biological activities (see Section 1.4.1), and either benzofuran or indole moieties might be expected to give rise to new biologically-active molecular frameworks.

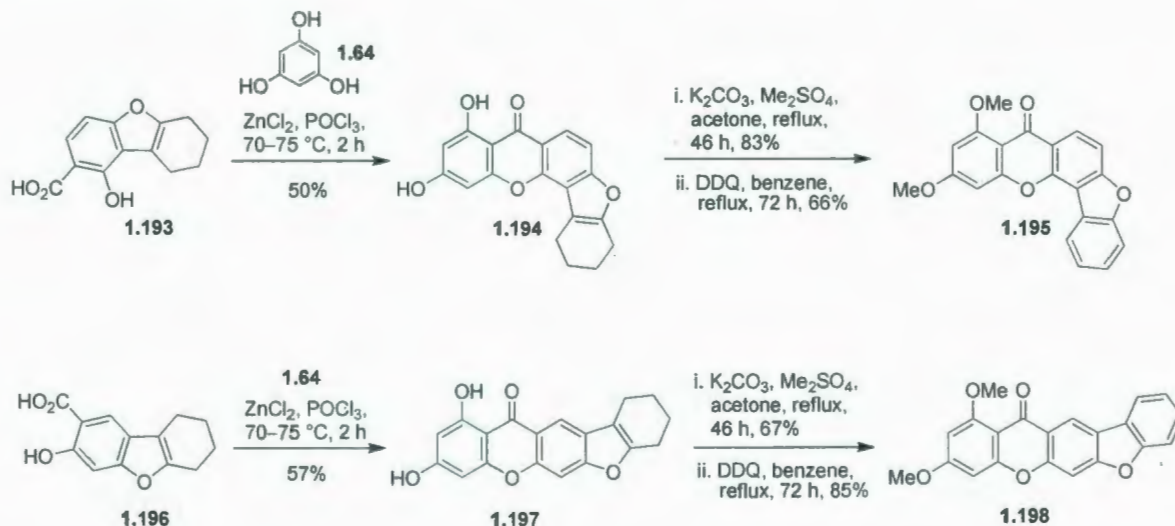
One of the first xanthonoid heteroacenes to be synthesized was benzofuroxanthone **1.192**, which was reported by Kamel *et al.* in 1973 (Scheme 1.32).<sup>89</sup> The xanthone moiety in **1.192** was constructed via a pyrolysis of ester **1.191**, which was obtained from *o*-hydroxy acid **1.189** and 4-methylphenol (**1.190**) via an esterification. The isolated yield of **1.192** was not reported.



**Scheme 1.32** Synthesis of benzofuroxanthone **1.192**.

Alternatively, the GSS reaction<sup>32</sup> was employed to build xanthone moieties in the angular benzofuroxanthone **1.195** and the linear one **1.198** (Scheme 1.33).<sup>90</sup> Xanthone derivative **1.194** was obtained in 50% yield from phloroglucinol (**1.64**) and 2-hydroxyacid **1.193** via a GSS reaction. Methylation of **1.194**, followed by an aromatization of the resulting diether gave the desired benzofuroxanthone **1.195** in good

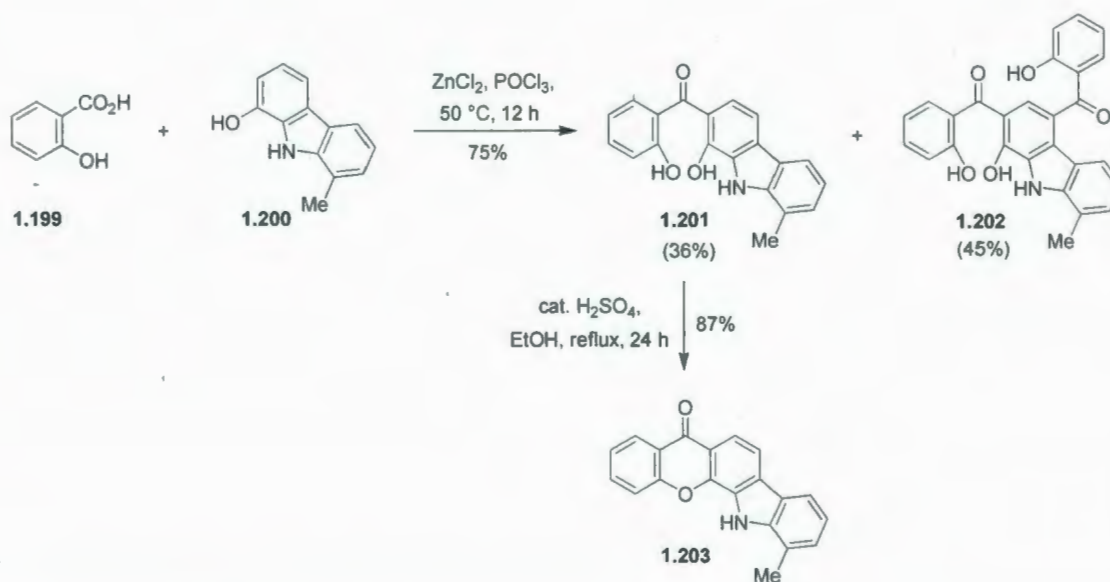
yield. Linear benzo-furoxanthone **1.198** was synthesized in the same fashion from dibenzofuran ester **1.196**.



**Scheme 1.33** Syntheses of benzofuroxanthones **1.196** and **1.198**.

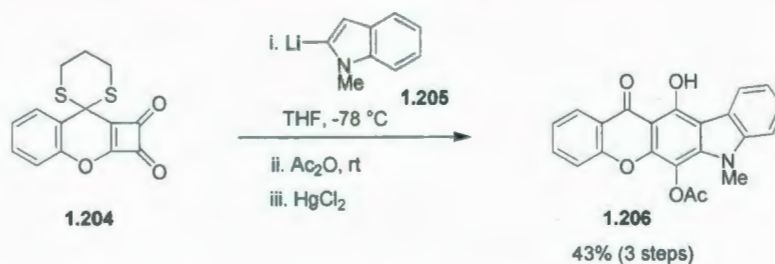
The GSS reaction was also attempted for synthesis of the angular indoloxanthone **1.203** (Scheme 1.34),<sup>91</sup> but only Friedel-Crafts reaction occurred between hydroxyacid **1.199** and carbazole **1.200** to give mono- and di-acylation products **1.201** and **1.202**, respectively. Dehydration of intermediate **1.201** under acid catalysis afforded the angular indoloxanthone **1.203** in good yield.





**Scheme 1.34** Synthesis of the angular indoloxanthone **1.203**.

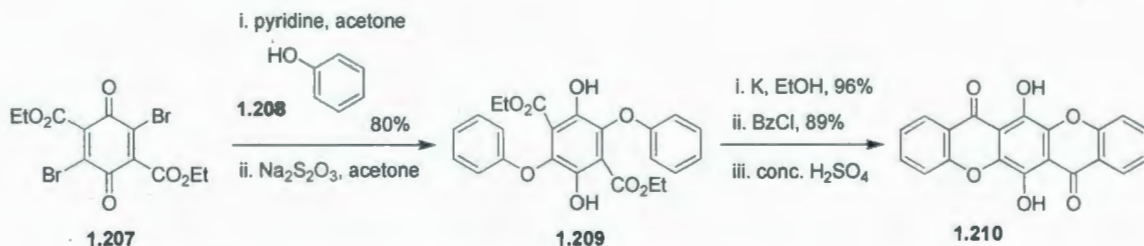
Another approach to indoloxanthones involved the 1,2-addition of an organolithium reagent **1.205** to dithiane-protected  $\gamma$ -benzopyrone-fused cyclobutenediones, such as **1.204** (Scheme 1.35).<sup>58</sup> The linear indoloxanthone **1.206** was obtained in 43% yield (see Scheme 1.31 for the proposed mechanism).



**Scheme 1.35** Synthesis of the linear indoloxanthone **1.206**.

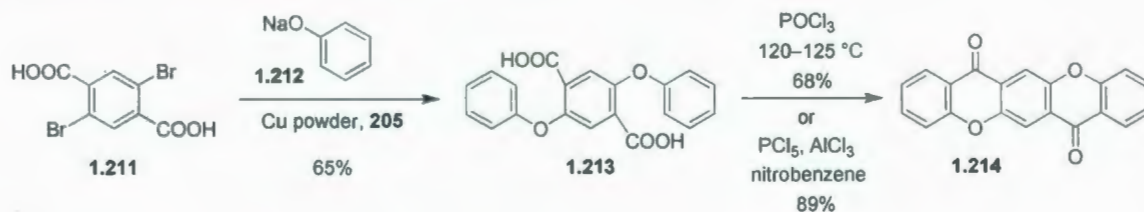
Chromonoxanthones or so-called dixanthones have also received some interest. In 1934, a multi-step synthesis of **1.210** was reported including a condensation of dibromo compound **1.207** with phenol (**1.209**), followed by functional group

interchanges and a cyclization. Some yields were not mentioned but the reported yields were good (Scheme 1.36).<sup>92</sup>



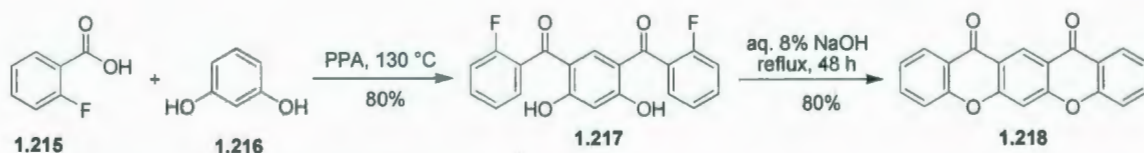
**Scheme 1.36** Multi-step synthesis of dixanthone **1.210**.

Using the same strategy as the synthesis of **1.210**, *i.e.* via an intermediate diaryl ether, compound **1.214** was also obtained via two steps in comparable yields (Scheme 1.37).<sup>93</sup> The yield of the cyclization step was much improved using  $\text{PCl}_5$  and  $\text{AlCl}_3$  in comparison with  $\text{POCl}_3$ .



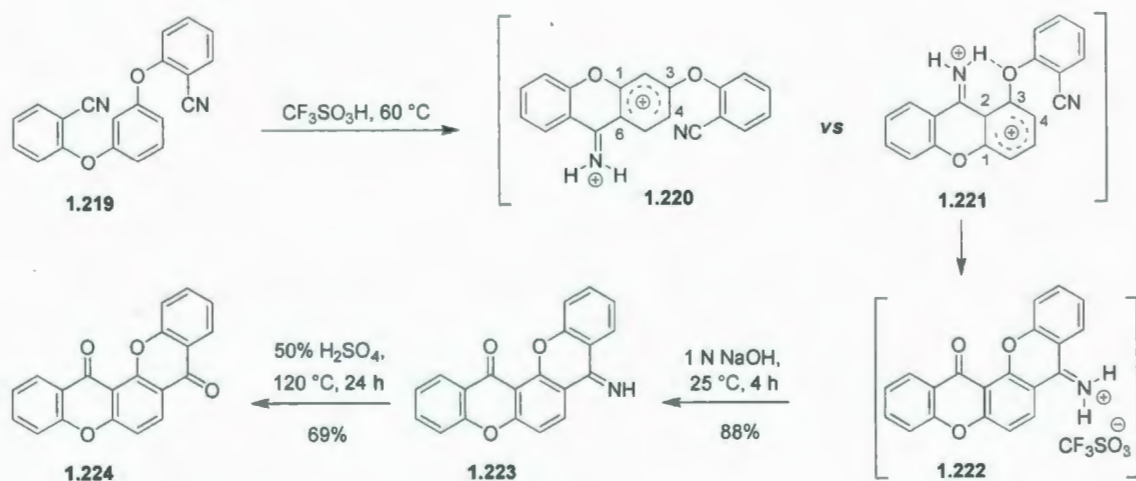
**Scheme 1.37** Two-step synthesis of dixanthone **1.214**.

Alternatively, a high-yielding two-step synthesis of dixanthone **1.218** was achieved via a dibenzophenone intermediate, which consisted of a double Friedel-Crafts acylation between 2-fluorobenzoic acid (**1.215**) and resorcinol **1.216** (80%) in the presence of poly(phosphoric acid) (PPA), followed by a double intramolecular nucleophilic aromatic substitution of intermediate **1.217** (80%) (Scheme 1.38).<sup>94</sup>



**Scheme 1.38** Two-step synthesis of dixanthone **1.218**.

The angular dixanthone **1.224** (Scheme 1.39)<sup>45</sup> was synthesized using the approach for compound **1.106** (Scheme 1.19). In this case, the regioselectivity of cyclization onto the resorcinol-derived dinitrile **1.219** (1,2,3,4- rather than 1,3,4,6-substitution) may result from stabilization of the intermediate **1.221** by intramolecular hydrogen bonding.



**Scheme 1.39** The synthesis of dixanthone **1.224**.

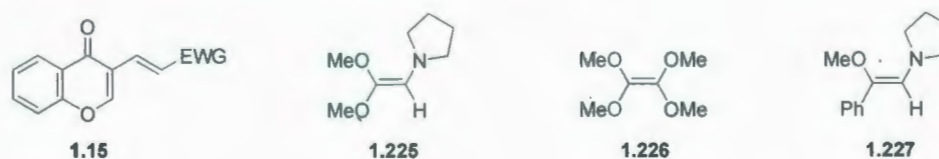
## 1.6 Aims of This Work

The research described in this dissertation deals primarily with the development of new methodology for the synthesis of xanthenes as well as the design, synthesis and physical properties of new xanthenes and more elaborate xanthone-containing molecules.



An offshoot of this work was concerned with the development of synthetic approaches to novel cyclooligophenylenes.

The first objective was to employ the IEDDA reaction in a new approach to xanthenes. Specifically, IEDDA-driven domino reactions between chromone-fused dienes **1.15** and electron-rich dienophiles such as **1.225–1.227** (Figure 1.14) were investigated as a means of forming 4-methoxyxanthenes **1.228**, 3,4-dimethoxyxanthenes **1.229**, and 4-phenylxanthenes **1.230** (Figure 1.15).

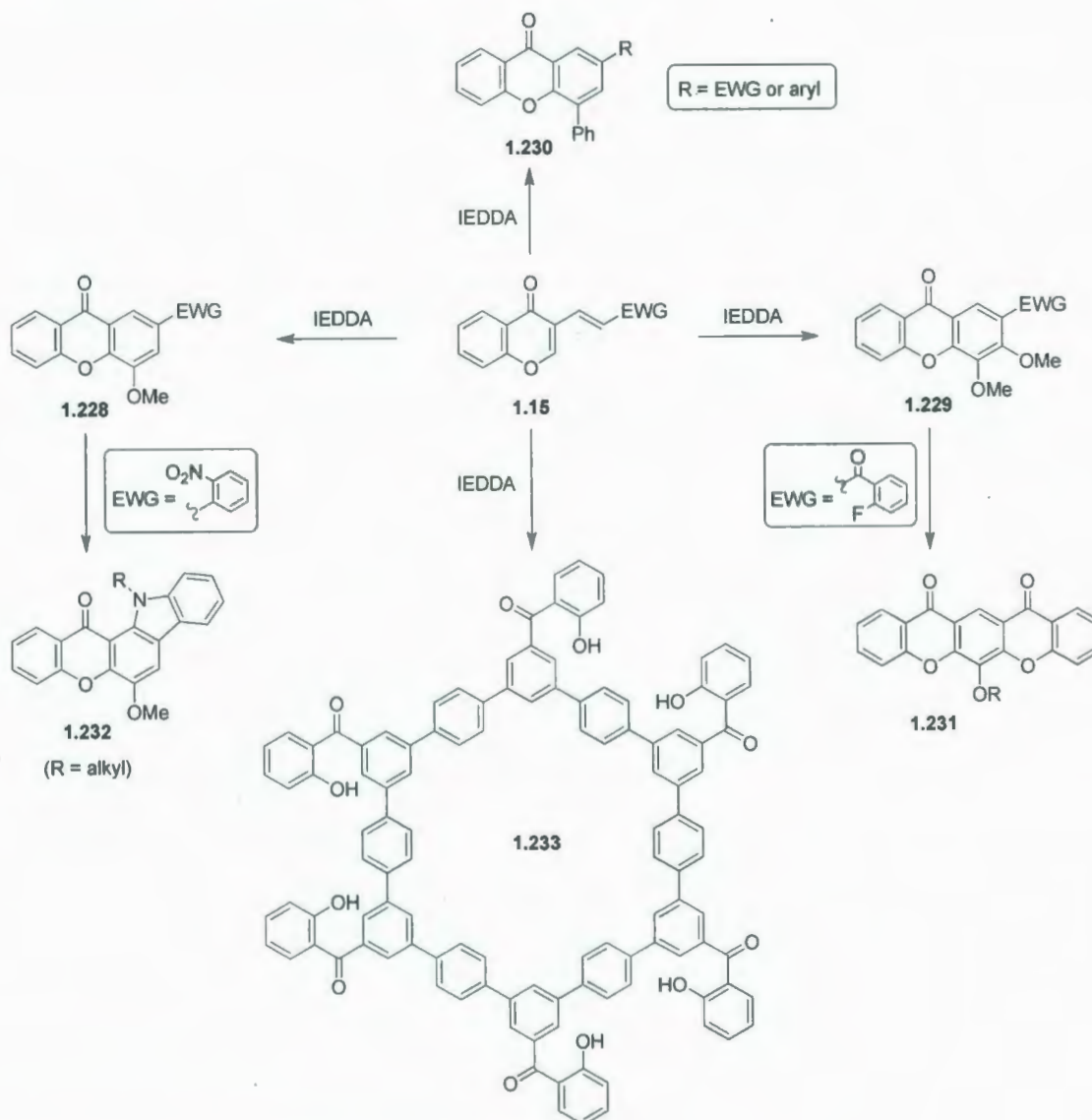


**Figure 1.14** Dienes **1.15** and selected electron-rich dienophiles **1.225–1.227**.

The second objective was to extend some of the newly-synthesized xanthenes into more complex structures, which may exhibit potentially exploitable physical properties. For example, hetero[5]acenes **1.231** and **1.232** were selected as targets because they may have potential applications in electronic and optoelectronic devices.

The initial targets, *i.e.* **1.228** and **1.229**, were chosen with an eye toward subsequent extension of the methodology. For instance, 3,4-dimethoxyxanthone **1.229** (EWG = 2-fluorobenzoyl) was envisioned as being a precursor to xanthonoid hetero[5]acene **1.231** (so-called dixanthone).<sup>94</sup> Other xanthonoid hetero[5]acenes, such as **1.232** (an indoloxanthone)<sup>91</sup> could conceivably be obtained from **1.228** (EWG = *o*-nitrophenyl). The novel cyclooligophenylene **1.233** was slated also to be constructed

using the synthetic methodology used previously in the Bodwell group for the formation of 2-hydroxybenzophenones (see Scheme 1.10).



**Figure 1.15** Target structures via IEDDA approaches.

## 1.7 References and Notes

- [1] Diels, O.; Alder, K. *Justus Liebigs Ann. Chem.* **1928**, 460, 98–122.

- 
- [2] Bruice, P. Y., 4<sup>th</sup> Ed., *Organic Chemistry*, Pearson Education, Inc.: New York, USA, **2004**, pp. 1190.
- [3] Joshel, L. M.; Butz, L. W. *J. Am. Chem. Soc.* **1941**, *63*, 3350–3351.
- [4] Carboni, R. A.; Lindsey, R. V., Jr. *J. Am. Chem. Soc.* **1959**, *81*, 4342–4346.
- [5] (a) Weinreb, S. M.; Staib, R. R. *Tetrahedron* **1982**, *38*, 3087–3128. (b) Boger, D. L. *Tetrahedron* **1983**, *39*, 2869–2939. (c) Danishefsky, S.; Webb, R. R. *J. Org. Chem.* **1984**, *49*, 1955–1958. (d) Whitesell, M. A.; Kyba, E. P. *Tetrahedron Lett.* **1984**, *25*, 2119–2120. (e) Weinreb, S. M. *Acc. Chem. Res.* **1985**, *18*, 16–21. (f) Schmidt, R. R. *Acc. Chem. Res.* **1986**, *19*, 250–259. (g) Boger, D. L. *Chem. Rev.* **1986**, *86*, 781–793. (h) Boger, D. L.; Weinreb, S. M. *Hetero Diels-Alder Methodology in Organic Synthesis*, Academic Press: New York, **1987**. (i) Kametani, T.; Hibino, S. *Advances in Heterocyclic Chemistry*, Katritzky, A. R., Ed.; Academic Press: New York, **1987**, Vol. 42, pp. 246–335. (j) Teng, M.; Fowler, F. W. *J. Org. Chem.* **1990**, *55*, 5646–5653. (k) Tietze, L. F.; Schneider, C. K. *Org. Chert.* **1991**, *56*, 2476–2481. (l) Benson, S. C.; Lee, L.; Snyder, J. K. *Tetrahedron Lett.* **1996**, *37*, 5061–5064.
- [6] Danishefsky, S.; Kitahara, T. *J. Am. Chem. Soc.* **1974**, *96*, 7807–7808.
- [7] Ahn, K.-D.; Hall, H. K. *J. Polym. Sci. Polym. Chem. Ed.* **1981**, *19*, 629–644.
- [8] Padwa, A.; Gareau, Y.; Harrison, B.; Rodriguez, A. *J. Org. Chem.* **1992**, *57*, 3540–3545.
- [9] (a) Padwa, A.; Gareau, Y.; Harrison, B. H. *J. Org. Chem.* **1991**, *56*, 2713–2720. (b) Padwa, A.; Harrison, B. *Tetrahedron Lett.* **1989**, *30*, 3259–3262. (c) Padwa, A.;



- 
- Norman, B. H. *Tetrahedron Lett.* **1988**, 29, 2417–2420. (d) Prinzbach, H.; Auge, W.; Basbudak, M. *Helv. Chim. Acta* **1971**, 54, 759–764.
- [10] (a) Langille, J. D. *M.Sc. Thesis* **1999**, Memorial Univeristy. (b) Pi, Z. *M.Sc. Thesis* **1996**, Memorial University.
- [11] Bodwell, G. J.; Pi, Z. *Tetrahedron Lett.* **1997**, 38, 309–312.
- [12] Bodwell, G. J.; Pi, Z.; Pottie, I. R. *Synlett* **1999**, 477–479.
- [13] Pottie, I. R. *Ph.D. Thesis* **2002**, Memorial Univeristy.
- [14] SPARTAN '08 software from Wavefunction, Inc. Irvine, CA, USA (RHF/3-21G\*//AM1/toluene).
- [15] Hess, B. A.; Baldwin, J. E. *J. Org. Chem.* **2002**, 67, 6025–6033.
- [16] Bringmann, G.; Stefan, T. *Tetrahedron* **2001**, 57, 331–344.
- [17] CambridgeSoft Chem 3D
- [18] Kendall, J. *M.Sc. Thesis* **2002**, Memorial University.
- [19] Povarov, L. S. *Russ. Chem. Rev.* **1967**, 36, 656–670.
- [20] Kudale, A. A.; Kendall, J.; Miller, D. O.; Collins, J. L.; Bodwell, G. J. *J. Org. Chem.* **2008**, 73, 8437–8447.
- [21] Bodwell, G. J.; Hawco, K. M.; da Silva, R. P. *Synlett* **2003**, 179–182.
- [22] Bodwell, G. J.; Hawco, K. M.; Satou, T. *Synlett* **2003**, 879–881.
- [23] Biswas, S. C.; Sen, R. K. *Indian J. Pure Appl. Phys.* **1982**, 20, 414–415.
- [24] Onuma, S.; Iijima, K.; Oonishi, I. *Acta Crystallogr. Sect. C Cryst. Struct. Commun.* **1990**, 46, 1725–1727.

- 
- [25] A review: Gales, L.; Damas, A. M. *Curr. Med. Chem.* **2005**, *12*, 2499–2515 and references cited therein.
- [26] A review: Pinto, M. M. M.; Sousa, M. E.; Nascimento, M. S. J. *Curr. Med. Chem.* **2005**, *12*, 2517–2538.
- [27] A review: Vieira, L. M. M.; Kijjoo, A. *Curr. Med. Chem.* **2005**, *12*, 2413–2446 and references cited therein.
- [28]     *About     Constructing     Preferred     IUPAC     Names     URL*  
[http://www.iupac.org/reports/provisional/](http://www.iupac.org/reports/provisional/abstract_04/BB-prs310305/Chapter2-sec25.pdf) abstract\_04/BB-prs310305/Chapter2-sec25.pdf
- [29] (a) Michael, A. *Ann. Chem. J.* **1883**, *5*, 81. (b) Kostanecki, S. *Ber. Dtsch. Chem. Ges.* **1891**, *24*, 1898.
- [30] A review: Sousa, M. E.; Pinto, M. M. M. *Curr. Med. Chem.* **2005**, *12*, 2447–2479 and up-to-date references which will be cited for each reaction.
- [31] The term “diaryl ester” was used by other authors.
- [32] Grover, P. K.; Shah, G. D.; Shah, R. C. *J. Chem. Soc.* **1955**, 3982–3985.
- [33] Eaton, P. E.; Carlson, G. R.; Lee, J. T. *J. Org. Chem.* **1973**, *38*, 4071–4073.
- [34] Pillai, R. K. M.; Naiksatam, P.; Johnson, F.; Rajagopalan, R.; Watts, P. C.; Cricchio, R.; Borrás, S. *J. Org. Chem.* **1986**, *51*, 717–723.
- [35] Quillinan, A. J.; Scheinmann, F. *J. Chem. Soc. Perkin Trans. 1*, **1973**, *13*, 1329–1337.
- [36] Lewis, J. R. *Proc. Chem. Soc.* **1963**, 373.

- [37] Likubo, K.; Ishikawa, Y.; Ando, N.; Umezawa, K.; Nishiyama, S. *Tetrahedron Lett.* **2002**, *43*, 291–293.
- [38] (a) Arimoto, H.; Nishiyama, S.; Yamamura, S. *Tetrahedron Lett.* **1990**, *31*, 5619–5620. (b) Yamamura, S.; Nishiyama, S. *Bull. Chem. Soc. Jpn.* **1997**, *70*, 2025–2037.
- [39] Atwell, G. J.; Rewcastle, G. W.; Baguley, B. C.; Denny, W. A. *J. Med. Chem.* **1990**, *33*, 1375–1379.
- [40] Finnegan, R. A.; Merkel, K. E. *J. Org. Chem.* **1972**, *37*, 2986–2989.
- [41] Pfister, J. R. *J. Heterocyclic Chem.* **1982**, *19*, 1255–1256.
- [42] For the initial idea of cyclization via metalation, see: Familoni, O. B.; Ionica, I.; Bower, J. F.; Snieckus, V. *Synlett* **1997**, 1081–1083.
- [43] (a) Gales, L.; Sousa, M. E.; Pinto, M. M. M.; Kijjioa, A.; Damas, A. M. *Acta. Cryst.* **2001**, *C57*, 1319–1323. (b) Sousa, E. P.; Silva, A. M. S.; Pinto, M. M. M.; Pedro, M. M.; Cerqueira, F. A. M.; Nascimento, M. S. *J. Helv. Chim. Acta* **2002**, *85*, 2862–2876.
- [44] In writing, [sic] indicates an incorrect or uncommon spelling. See: <http://en.wikipedia.org/wiki/Sic>
- [45] Colquhoun, H. M.; Lewis, D. F.; Williams, D. J. *Org. Lett.* **2001**, *3*, 2337–2340.
- [46] Kürti, L.; Czako, B., *Strategic Applications of Names of Reactions in Organic Synthesis*, Elsevier Inc., London, UK, **2005**, pp. 216.
- [47] Kristensen, J. L.; Vedo, P.; Begtrup, M. *J. Org. Chem.* **2003**, *68*, 4091–4092.
- [48] (a) Zhao, J.; Larock, R. C. *Org. Lett.* **2005**, *7*, 4273–4275. (b) Zhao, J.; Larock, R. C. *J. Org. Chem.* **2007**, *72*, 583–588.



- 
- [49] Zhao, J.; Yue, D.; Campo, M. A.; Larock, R. C. *J. Am. Chem. Soc.* **2007**, *129*, 5288–5295.
- [50] (a) Dyker, G. *Angew. Chem. Int. Ed.* **1999**, *38*, 1698–1712. (b) Martín-Matute, B.; Mateo, C.; Caardenas, D. J.; Echavarren, A. M. *Chem. Eur. J.* **2001**, *7*, 2341–2348 and references cited therein.
- [51] (a) Campeau, L.; Parisien, M.; Jean, A.; Fagnou, K. *J. Am. Chem. Soc.* **2006**, *128*, 581–590. (b) Garcia-Cuadrado, D.; Braga, A.; Maseras, F.; Echavarren, A. M. *J. Am. Chem. Soc.* **2006**, *128*, 1066–1067.
- [52] Okuma, K.; Nojima, A.; Matsunaga, N.; Shioji, K. *Org. Lett.* **2009**, *11*, 169–171.
- [53] (a) Schonberg, A.; Mustafa, A. Aziz, G. *J. Am. Chem. Soc.* **1954**, *76*, 4576–4577. (b) Mustafa, A.; Ali, A. I. *J. Org. Chem.* **1956**, *21*, 849–851. (c) Letcher, R. M.; Yue, T.-Y. *J. Chem. Soc., Chem. Commun.* **1992**, 1310–1311.
- [54] Ghosh, C. K.; Bhattacharyya, S.; Patra, A. *J. Chem. Soc., Perkin Trans. 1*, **1997**, 2167–2168.
- [55] Gabbutt, C. D.; Hepworth, J. D.; Urquhart, M. W. J.; Vazquez de Miguel, L. M. *J. Chem. Soc., Perkin Trans 1*, **1997**, *12*, 1819–1824.
- [56] Gabbutt, C. D.; Hepworth, J. D.; Urquhart, M. W. J.; Vasquez de Miguel, L. M. *J. Chem. Soc., Perkin Trans 1* **1998**, 1547–1554.
- [57] Kelkar, A. S.; Letcher, R. M.; Cheung, K. K.; Chiu, K. F.; Brown, G. D. *J. Chem. Soc., Perkin Trans 1* **2000**, 3732–3741.
- [58] Sun, L.; Liebeskind, L. S. *J. Am. Chem. Soc.* **1996**, *118*, 12473–12474.
- [59] Corey, E. J.; Seebach, D. *Angew. Chem., Int. Ed. Engl.* **1965**, *4*, 1075–1077.

- 
- [60] Hauser, K. M.; Dorsch, W. A. *Org. Lett.* **2003**, *5*, 3753–3754.
- [61] Zagorevskii, V. A.; Zykov, D. A.; Orlova, E. K. *Zh. Obshh. Khim. (Engl. Trans.)* **1961**, *31*, 568–574.
- [62] Anthony, J. E. *Chem. Rev.* **2006**, *106*, 5028–5048.
- [63] Bendikov, M.; Wudl, F.; Perepichka, D. F. *Chem. Rev.* **2004**, *104*, 4891–4946.
- [64] Kelley, T. W.; Boardman, L. D.; Dunbar, T. D.; Muiers, D. V.; Pellerite, M. J.; Smith, T. Y. P. *J. Phys. Chem. B* **2003**, *107*, 5887–5893.
- [65] (a) Moon, H.; Zeis, R.; Borkent, E. J.; Besnard, C.; Lovinger, A. J.; Siegrist, T.; Kloc, C.; (b) Bao, Z. N. *J. Am. Chem. Soc.* **2004**, *126*, 15322–15323. (c) Curtis, M. D.; Cao, J.; Kampf, J. W. *J. Am. Chem. Soc.* **2004**, *126*, 4318–4328.
- [66] Bendikov, M.; Wudl, F.; Perepichka, D. F. *Chem. Rev.* **2004**, *104*, 4891–4946.
- [67] The name “acene” was first coined by Clar. See: (a) Clar, E. *Ber.* **1939**, *72B*, 2137–2139. (b) Briggs, J. B.; Miller, G. P. *C. R. Chimie* **2006**, *9*, 916–927. Poly(acene) is called “ladder” polymer, see: (c) Lowe, J. P.; Kafafi, S. A.; LaFemina, J. P. *J. Phys. Chem.* **1986**, *90*, 6602–6610. (d) Freund, T.; Scherf, U.; Müllen, K. *Angew. Chem. Int. Ed. Engl.* **1994**, *33*, 2424–2426. Thus, the term “ladder-type” acenes originates from these references.
- [68] Payne, M. M.; Parkin, S. R.; Anthony, J. E.; Kuo, C. C.; Jackson, T. N. *J. Am. Chem. Soc.* **2005**, *127*, 4986–4987.
- [69] (a) Li, Y. N.; Wu, Y. L.; Gardner, S.; Ong, B. *Adv. Mater.* **2005**, *17*, 849–853. (b) Wakim, S.; Bouchard, J.; Simard, M.; Drolet, N.; Tao, Y.; Leclerc, M. *Chem. Mater.*

- 
- 2004**, *16*, 4386–4388. (c) Wakim, S.; Bouchard, J.; Blouin, N.; Michaud, A.; Leclerc, M. *Org. Lett.* **2004**, *6*, 3413–3416.
- [70] Horn, T.; Wegener, S.; Mullen, K. *Macromol. Chem. Phys.* **1995**, *196*, 2463–2474.
- [71] Li, X.-C.; Sirringhaus, H.; Garnier, F.; Holmes, A. B.; Moratti, S. C.; Feeder, N.; Clegg, W.; Teat, S. J.; Friend, R. H. *J. Am. Chem. Soc.* **1998**, *120*, 2206–2207.
- [72] Takimiya, K.; Kunugi, Y.; Konda, Y.; Niihara, N.; Otsubo, T. *J. Am. Chem. Soc.* **2004**, *126*, 5084–5085.
- [73] Yamaguchi, S.; Xu, C.; Tamao, K. *J. Am. Chem. Soc.* **2003**, *125*, 13662–13663.
- [74] Fukazawa, A.; Hara, M.; Okamoto, T.; Son, E.-C.; Xu, C.; Tamao, K.; Yamaguchi, S. *Org. Lett.* **2008**, *10*, 913–916.
- [75] Miao, Q.; Nguyen, T.-Q.; Someya, T.; Blanchet, G. B.; Nuckolls, C. *J. Am. Chem. Soc.* **2003**, *125*, 10284–10287.
- [76] Kawaguchi, K.; Nakano, K.; Nozaki, K. *J. Org. Chem.* **2007**, *72*, 5119–5128.
- [77] Okamoto, T.; Kudoh, K.; Wakamiya, A.; Yamaguchi, S. *Chem. Eur. J.* **2007**, *13*, 548–556.
- [78] Agou, T.; Kobayashi, J.; Kawashima, T. *Org. Lett.* **2006**, *8*, 2241–2244.
- [79] Ebata, H.; Miyazaki, E.; Yamamoto, T.; Takimiya, K. *Org. Lett.* **2007**, *9*, 4499–4502.
- [80] Xiao, K.; Liu, Y.; Qi, T.; Zhang, W.; Wang, F.; Gao, J.; Qiu, W.; Ma, Y.; Cui, G.; Chen, S.; Zhan, X.; Yu, G.; Qin, J.; Hu, W.; Zhu, D. *J. Am. Chem. Soc.* **2005**, *127*, 13281–13286.
- [81] Wu, Y.; Li, Y.; Gardner, S.; Ong, B. *J. Am. Chem. Soc.* **2005**, *127*, 614–618.



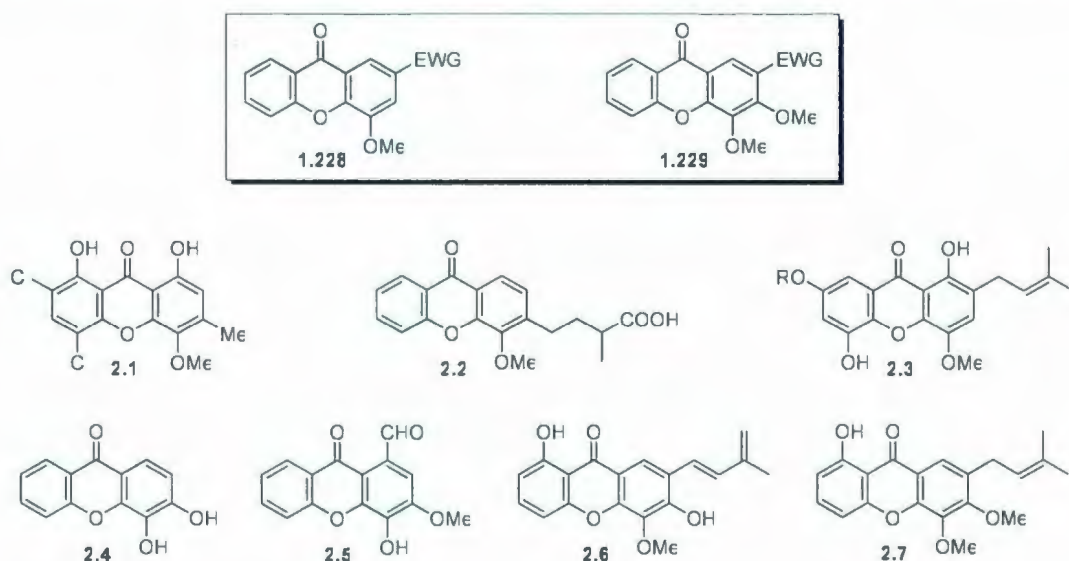
- 
- [82] Boudreault, P-L. T.; Wakim, S.; Blouin, N.; Simard, M.; Tessier, C.; Ye, T.; Leclerc, M. *J. Am. Chem. Soc.* **2007**, *127*, 9125–9136.
- [83] Shirota, Y.; Kageyama, H. *Chem. Rev.* **2007**, *107*, 953–1010.
- [84] Burden, R. S.; Kemp, M. S.; Willshire, C. W.; Owen, J. D. *J. Chem. Soc. Perkin Trans 1*, **1984**, *7*, 1445–1448.
- [85] (a) Lefemine, D. V.; Dann, M.; Barbatschi, F.; Hausmann, W. K.; Zbinovsky, V.; Monnikendam, P.; Adam, J.; Bohonos, N. *J. Am. Chem. Soc.* **1962**, *84*, 3184–3185.
- (b) Collins, J. F. *Brit. Med. Bull.* **1965**, *21*, 223–228.
- [86] Schach, V-W. M.; Els, H. *J. Am. Chem. Soc.* **1961**, *83*, 4678–4680.
- [87] Johnson, J. R.; Bruce, W. F.; Dutcher, J. D. *J. Am. Chem. Soc.* **1943**, *65*, 2005–2009.
- [88] Garattini, S.; Valzelli, L. *Serotonin*, Elsevier (Amsterdam), **1965**.
- [89] Kamel, M.; Allam, M. A.; El-Alfi, I. *Egypt. J. Chem.* **1973**, *16*, 91–100.
- [90] Ahluwalia, V. K.; Mallika, N.; Kumari, S.; Singh, R. P. *Indian J. Chem. Sec. B* **1989**, *28B*, 1021–1025.
- [91] Vandana, T.; Prasad, K. J. R. *Indian J. Chem. Sec. B* **2005**, *44B*, 815–818.
- [92] Liebermann, H.; Lewin, G.; Gruhn, A.; Gottesmann, E.; Lisser, D.; Schonda, K. *Justus Liebigs Ann. Chem.* **1934**, *513*, 156–179.
- [93] Singh, T.; Bedi, S. N. *Jour. Indian Chem. Soc.* **1957**, *34*, 321–323.
- [94] Sharghi, H.; Tamaddon, F.; Eshghi, H. *Iran. J. Chem. & Chem. Eng.* **2000**, *19*, 32–36.

## Chapter 2

# Synthesis and Physical Properties of 2-Substituted 4-Methoxyxanthenes and 3,4-Dimethoxyxanthenes

## 2.1 Introduction

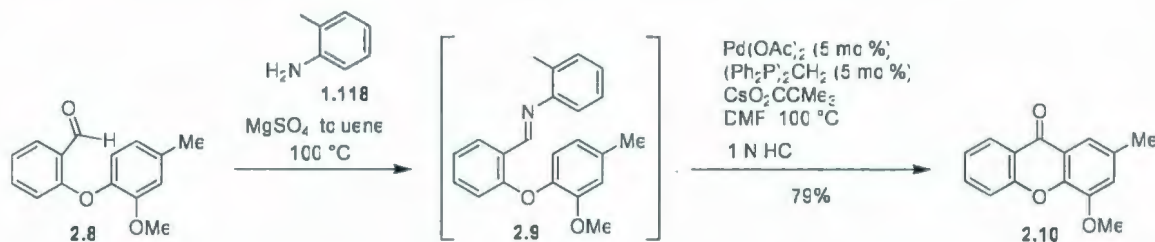
4-Methoxy- and 3,4-dimethoxyxanthone skeletons **1.228** and **1.229** are found in naturally-occurring xanthenes such as **2.1–2.3**<sup>1</sup> and **2.4–2.7**<sup>2</sup>, respectively (Figure 2.1).



**Figure 2.1** Examples of naturally-occurring 4-methoxy- and 3,4-dimethoxyxanthenes **2.1–2.7**.

However, only one synthetic approach to the 2-substituted 4-methoxyxanthone skeleton, *i.e.* **2.10**,<sup>3</sup> has been reported and this involves a palladium migration process<sup>4</sup> (Scheme 2.1). At the outset of the work described in this Chapter, no unnatural 3,4-dimethoxyxanthenes had been reported. The aim of this project was to develop IEDDA-based methodology for the synthesis of the target xanthenes (4-methoxy- and 3,4-dimethoxyxanthenes), which would be useful for further elaboration in later projects (see

Chapters 4 and 5). The physical properties of the newly-synthesized xanthenes **1.228** and **1.229** will also be discussed.



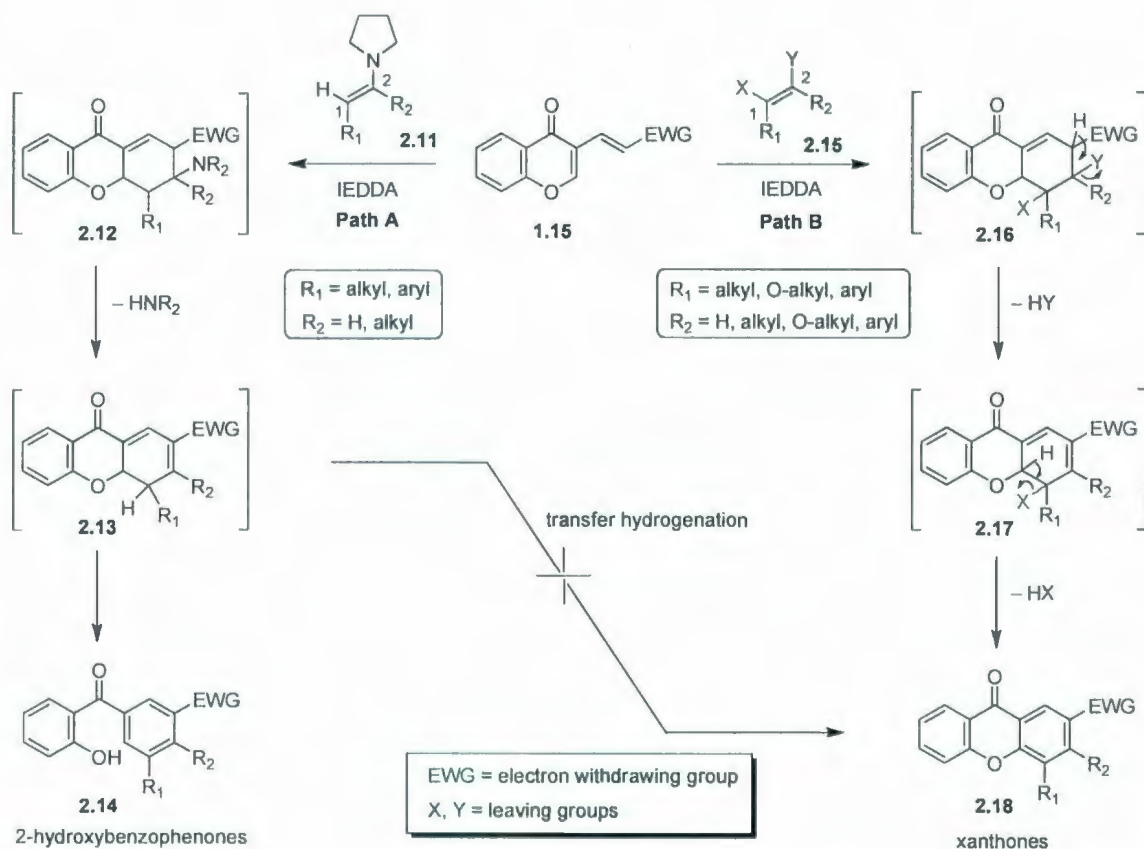
**Scheme 2.1** Synthesis of 2-methyl-4-methoxyxanthone **2.10** via a palladium migration process.

### 2.1.1 A Proposed Mechanism for the Synthesis of Xanthenes via the IEDDA Reaction

As described in Chapter 1, the reaction between diene **1.15** (EWG = CO<sub>2</sub>Et) and enamine **1.24** (Scheme 1.10, Chapter 1) was originally intended to afford xanthone **1.49**, but instead gave 2-hydroxybenzophenone **1.48**. The observed outcome was explained by the mechanism shown in Scheme 2.2, Path A.

Presumably, IEDDA reaction between dienes **1.15** with dienophiles **2.11** provided Diels-Alder adducts **2.12**, which underwent subsequent  $\beta$ -elimination of a pyrrolidine molecule to afford intermediates **2.13**. The observation that 2-hydroxybenzophenones **2.14** were obtained exclusively clearly indicated that internal elimination (to give 2-hydroxybenzophenones) is preferable to transfer hydrogenation (to give xanthenes).





**Scheme 2.2** Synthesis of 2-hydroxybenzophenones (path A) and the proposed synthesis of xanthenes (path B) via an IEDDA / elimination / elimination sequence.

To block the pathway leading to 2-hydroxybenzophenones **2.14**, and thus to enable the use of dienes **1.15** for xanthenes synthesis, two issues were identified: the carbon atom of the dienophile that reacts with the more electron-deficient terminus of the diene, *i.e.* C-1 of dienophile **2.15**, should (1) bear no hydrogen atom and (2) bear a leaving group. When these criteria are fulfilled, internal 1,2-elimination (**2.13**→**2.14**) cannot occur. Instead, an elimination of  $\text{HX}$  from **2.17** should furnish xanthenes **2.18**. Dienophiles such as enamine **1.225** and tetramethoxyethene (TME, **1.226**)<sup>5</sup> (Figure 2.2)

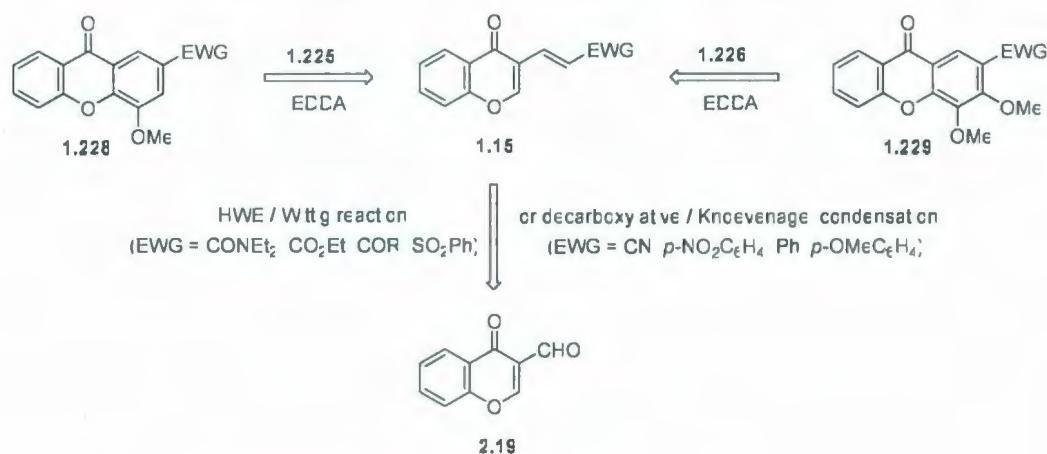
meet these requirements and were consequently employed for the synthesis of 2-substituted xanthenes and 3,4-dimethoxyxanthenes.



**Figure 2.2** Dienophiles used in the synthesis of 2-substituted xanthenes.

### 2.1.2 Retrosynthetic Analysis of 4-Methoxy- and 3,4-Dimethoxyxanthenes

Using the methodology described above, xanthenes **1.228** and **1.229** could conceivably be synthesized via IEDDA-driven domino reactions between dienes **1.15** and dienophiles such as **1.225** and **1.226** (Scheme 2.3). Dienes **1.15** should be accessible from commercially available 3-formylchromone (**2.19**) via Horner-Wadsworth-Emmons (HWE),<sup>6</sup> a Wittig<sup>7</sup> or a decarboxylative / Knoevenagel condensation<sup>8</sup> reaction. Using this methodology, it should be possible to adorn the diene system **1.15** with a range of EWGs, including  $\text{CONEt}_2$ ,  $\text{CO}_2\text{Et}$ ,  $\text{COPh}$ ,  $\text{COMe}$ ,  $\text{CN}$ ,  $\text{SO}_2\text{Ph}$ , and  $p\text{-NO}_2\text{C}_6\text{H}_4$ , or even an electron-neutral Ph group or an electron-donating  $p\text{-MeOC}_6\text{H}_4$  group.

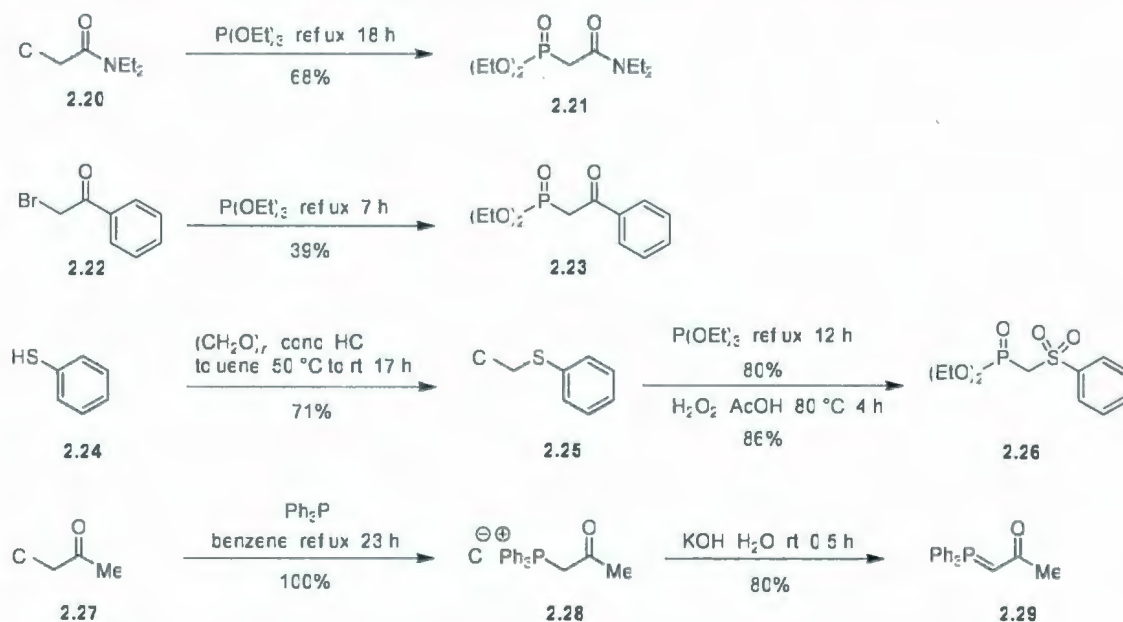


**Scheme 2.3** Retrosynthetic analysis of xanthenes **1.228** and **1.229**.

## 2.2 Results and Discussion

### 2.2.1 Synthesis of HWE Phosphonates and Wittig Reagent

The initial objective was the synthesis of the dienes and dienophiles that were required for the IEDDA-driven Diels-Alder reactions. Non-commercially available phosphonates for HWE reactions, *i.e.* **2.21**,<sup>9</sup> **2.23**,<sup>10</sup> **2.26**<sup>11</sup> (Scheme 2.4) were prepared from the corresponding halides **2.20**, **2.22**, and **2.24** via Arbuzov reactions. Wittig reagent **2.29** was obtained in good yield using a modified two-step literature procedure.<sup>12</sup>

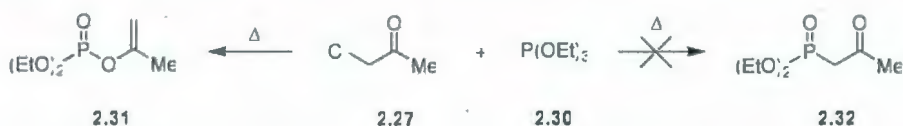


**Scheme 2.4** Synthesis of substrates for HWE and Wittig reactions.

The Wittig reagent **2.29** was chosen instead of the corresponding phosphonate **2.32** (Scheme 2.5) because of a synthetic problem. It was reported that the reaction of chloroacetone **2.27** with triethyl phosphite **2.30** gave only phosphonate ester **2.31**, but not the desired phosphonate **2.32**.<sup>13</sup> Although the desired phosphonate **2.32** could be



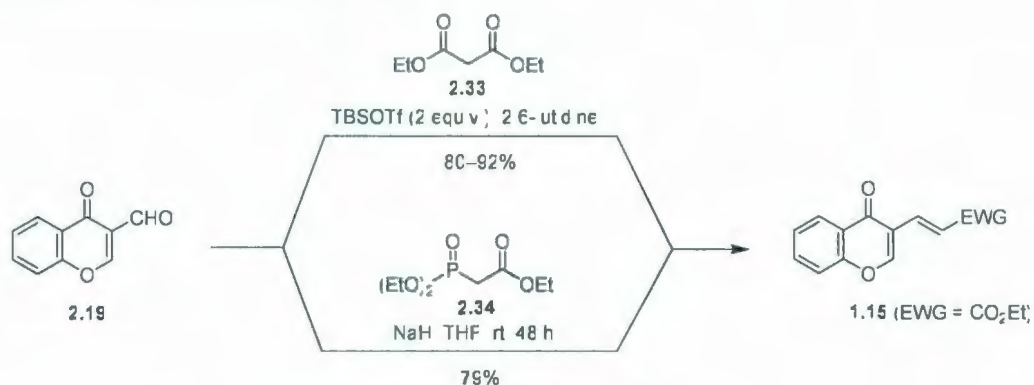
obtained by Arbuzov reaction with bromo- or iodoacetone,<sup>14</sup> this route was excluded as these haloacetones are not commercially available.



**Scheme 2.5** Attempted synthesis of phosphonate **2.32** from literature.

### 2.2.2 Synthesis of Chromone-fused Electron-deficient Dienes **1.15**

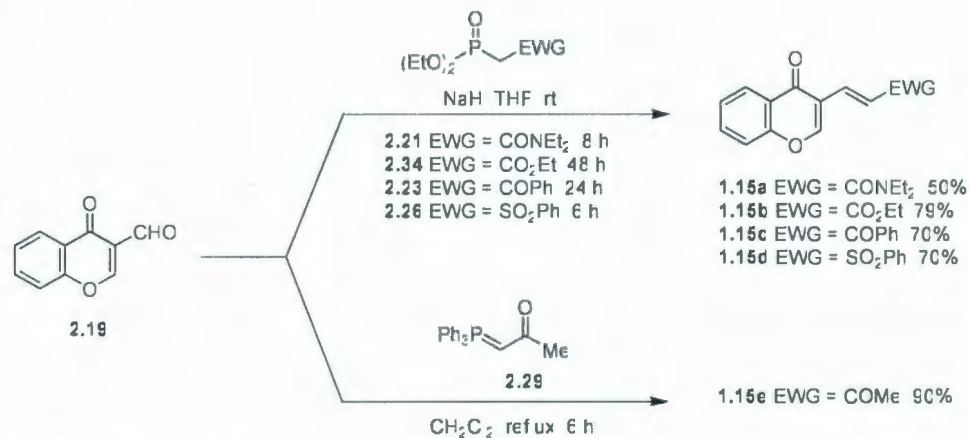
Diene **1.15** (EWG = CO<sub>2</sub>Et) was originally synthesized by Akiba *et al.* in 80–92% yield from 3-formylchromone (**2.19**) upon treatment with diethyl malonate (**2.33**) in the presence of *t*-butyldimethylsilyl triflate (TBSOTf) (Scheme 2.6).<sup>15</sup> Another synthesis of this diene (79%) was subsequently reported by Bodwell *et al.* using the HWE reaction with triethyl phosphonoacetate **2.34**.<sup>16</sup>



**Scheme 2.6** Reported syntheses of diene **1.15** (EWG = CO<sub>2</sub>Et).

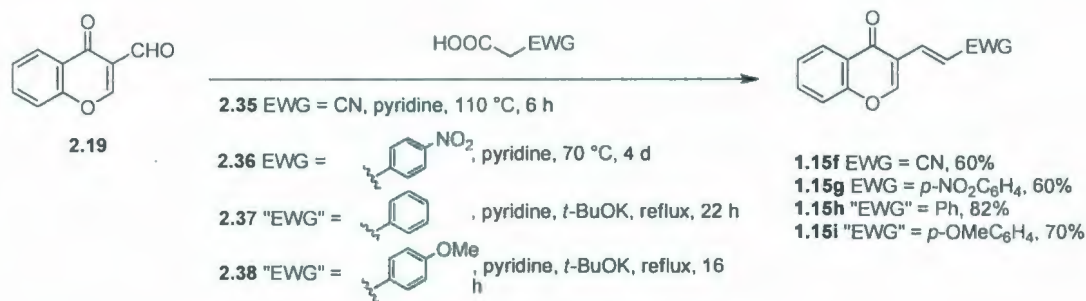
Using the same conditions for HWE reaction, a series of dienes **1.15a–d** (Scheme 2.7) was synthesized from 3-formylchromone (**2.19**) and the corresponding phosphonates in moderate to good yields (50–79%). Diene **1.15e** was obtained in 90% yield by reacting **2.19** with the Wittig reagent **2.29** in dichloromethane at reflux. For all of the

dienes **1.15a–e**, the (*E*) geometry of the newly-formed double bonds was clearly indicated by the magnitude of the  $^3J$  coupling constants (15.3–16.4 Hz) in their  $^1\text{H}$  NMR spectra.



**Scheme 2.7** Synthesis of dienes **1.15a–e**.

Dienes **1.15f–i** cannot be obtained in synthetically useful quantities via the Wittig reaction because the *Z*-isomers are typically the major products.<sup>17,18</sup> Alternatively, they were synthesized using decarboxylative Knoevenagel-type condensations. For example, dienes **1.15f**<sup>19</sup> and **1.15g–i**<sup>8</sup> were obtained in good yields from reactions between 3-formylchromone (**2.19**) and the corresponding phenylacetic acids **2.35–2.38** (Scheme 2.8).



**Scheme 2.8** Synthesis of dienes **1.15f–i**.

Specifically, carboxylic acids bearing EWGs such as CN (**2.35**) and 4-nitrophenyl (**2.36**) reacted with **2.19** in pyridine to give dienes **1.15f** and **1.15g**, respectively, in relatively good yields (60%). Surprisingly, diene **1.15g** was not obtained when the reaction mixture was heated at reflux in pyridine, either with, or without *t*-BuOK, according to literature procedures (pyridine, reflux, 24 h, 51% and pyridine, *t*-BuOK, reflux, 15 h, 47%).<sup>8</sup> In such cases, only recovered 3-formylchromone (**2.19**) was isolated. However, it was found that the desired reaction occurred under relatively mild conditions (pyridine, 70 °C, 4 d, 60%). Phenylacetic acids **2.37** and **2.38**, which bear electron-neutral or -donating groups, gave the best yields of the corresponding dienes **1.15h** (82%) and **1.15i** (70%), but it was necessary to conduct these reactions in the presence of *t*-BuOK. In all cases described above, the large coupling constant (16.3–17.1 Hz) across the newly-formed double bond was indicative of the (*E*) stereochemistry.

### 2.2.3 Synthesis of Dienophiles **1.225** and **1.226**

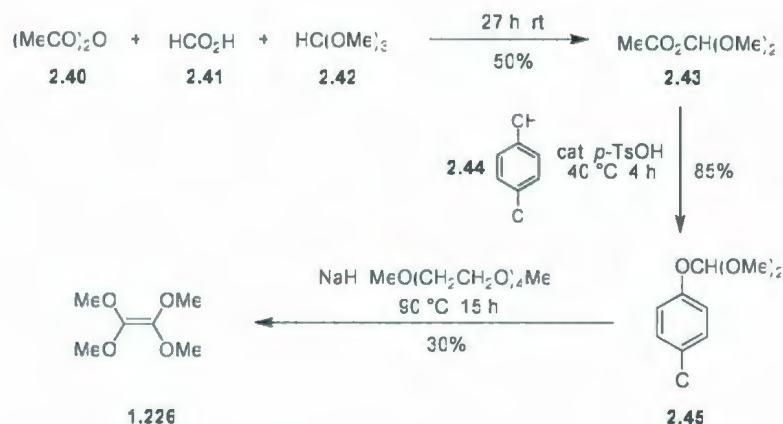


**Scheme 2.9** Synthesis of dienophile **1.225**.

Dienophile **1.225** was prepared upon reaction of dimethoxyacetaldehyde (**2.39**) with pyrrolidine in benzene at reflux (Scheme 2.9). Previous work in the Bodwell group had established that purification of this dienophile was very difficult;<sup>20</sup> therefore, the crude reaction mixture was used directly for each IEDDA reaction. Tetramethoxyethane



(**1.226**) was synthesized via a three-step synthesis according to published procedures (Scheme 2.10).<sup>21</sup>



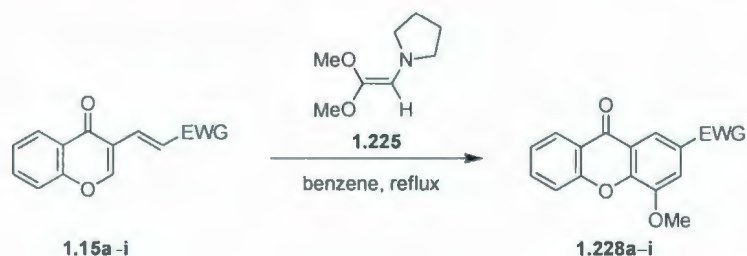
**Scheme 2.10** Synthesis of tetramethoxyethene (TME) **1.226**.

#### 2.2.4 Synthesis of 2-Substituted 4-Methoxyxanthenes

Reaction of dienes **1.15a–i** with freshly generated enamine **1.225** in benzene at reflux afforded the expected xanthenes **1.228a–i** in moderate to excellent yields (Table 2.1). Thin layer chromatography (tlc) analysis of these reactions showed essentially spot-to-spot conversions of the starting materials into the products. The yield and reaction rate tended to increase with the strength of the electron-withdrawing group on the diene and decrease with its steric demands. Among dienes **1.15a–f**, (Table 2.1, Entries 1–6), diene **1.15f**, which has a small and strongly electron-withdrawing substituent (EWG = CN), was the fastest to react and gave one of the best yields (**1.228f**, 84%). The lowest reactivity of this group was observed for dienes **1.15a** and **1.15d**, which have either a moderately electron-withdrawing substituent (EWG = CONEt<sub>2</sub>) or a strongly withdrawing, but bulky substituent (EWG = SO<sub>2</sub>Ph). The sensitivity of both the rate and yield of the reaction to electronic effects can be seen clearly in the behavior of the aryl

substituted dienes **1.15g–i** (Table 2.1, Entries 7–9). All of these observations are consistent with a rate-limiting, asynchronous IEDDA reaction,<sup>22</sup> followed by two fast eliminations (pyrrolidine and methanol, in either order) to give the observed 4-methoxyxanthenes **1.228a–i**.

**Table 2.1** Reactions of dienes **1.15a–i** with dienophile **1.225**.



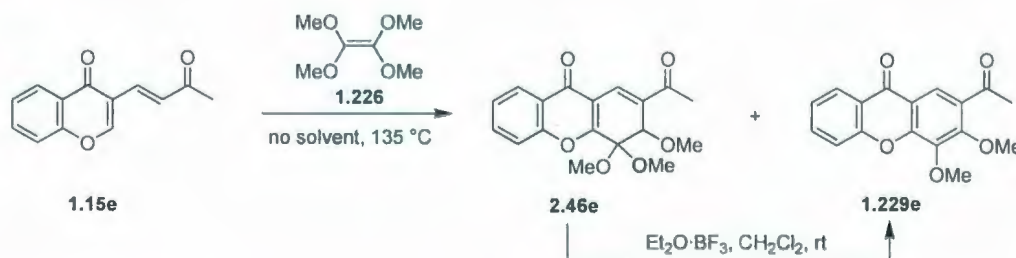
Entry	EWG	Xanthone	Time (h)	Yield (%)
1	CONEt <sub>2</sub>	<b>1.228a</b>	16	50
2	CO <sub>2</sub> Et	<b>1.228b</b>	2	71
3	COPh	<b>1.228c</b>	6.5	85
4	SO <sub>2</sub> Ph	<b>1.228d</b>	16	70
5	COMe	<b>1.228e</b>	6	90
6	CN	<b>1.228f</b>	2	84
7	<i>p</i> -NO <sub>2</sub> C <sub>6</sub> H <sub>4</sub>	<b>1.228g</b>	2	70
8	C <sub>6</sub> H <sub>5</sub>	<b>1.228h</b>	17	51
9	<i>p</i> -MeOC <sub>6</sub> H <sub>4</sub>	<b>1.228i</b>	44	39

### 2.2.5 Synthesis of 2-Substituted 3,4-Dimethoxyxanthenes

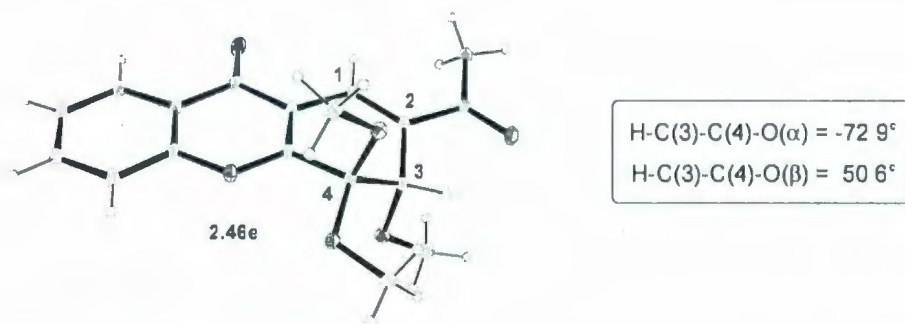
Attention was then turned to the use of tetramethoxyethene (TME, **1.226**), which was expected to afford 3,4-dimethoxyxanthenes **1.229** via an IEDDA / elimination

(MeOH) / elimination (MeOH) sequence. As anticipated for this less polar and more highly substituted dienophile, it proved to be a more reluctant reaction partner. In fact, under conditions similar to those successfully employed for the reactions of dienophile **1.225** with dienes **1.15a–i**, no reaction was observed between diene **1.15e** (*ca.* 0.2 M in benzene, reflux) and TME (5.0 equiv.). No further improvement was obtained when either toluene or xylenes were used as the solvent.

However, upon heating **1.15e** with only neat TME (b.p. = 140 °C) at 135 °C, the diene was consumed and xanthone **1.229e** (6%) was isolated along with an unaromatized product (Scheme 2.11), the spectroscopic data of which were consistent with one of the expected reaction intermediates, **2.48e** (Scheme 2.12). However, its identity as an isomer, **2.46e** (56%), was established by crystallographic methods (Figure 2.3). Prolonged heating of the reaction mixture at 135 °C or resubjection of **2.46e** to the original reaction conditions resulted in the slow formation of intractable material. However, in a tlc experiment, the addition of the Lewis acid Et<sub>2</sub>O·BF<sub>3</sub> to a pure sample of **2.46e** in dichloromethane at room temperature induced a rapid, spot-to-spot conversion to **1.229e**.



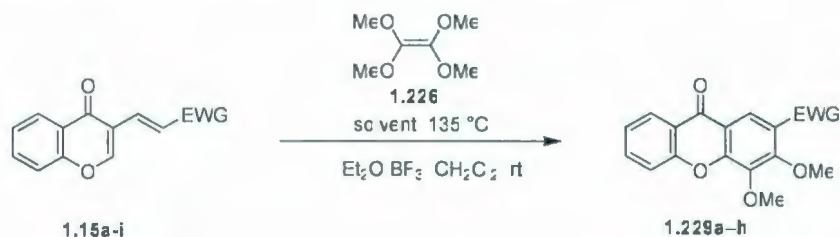




**Figure 2.3** ORTEP presentation of **2.46e**.

Subsequent reaction mixtures of dienes **1.15** with TME (**1.226**) were heated at 135 °C, cooled to room temperature after consumption of the diene or apparent reaction cessation (tlc analysis), diluted with dichloromethane and treated with  $\text{Et}_2\text{O} \cdot \text{BF}_3$  (4.0 equiv.) to give 3,4-dimethoxyxanthenes **1.229** (Table 2.2). Good yields were obtained for **1.229c** (84%) and **1.229e** (62%), while those for **1.229a–b** and **1.229d,f–g** were modest (25–36%). The least electron-deficient dienes **1.15h** and **1.15i** were unreactive, giving at best only traces of product. As an exception, **1.15f** gave a better yield of the product (**1.229f**, 53%) without treatment with  $\text{Et}_2\text{O} \cdot \text{BF}_3$ .

The use of high boiling solvents (xylenes, 1,1,2,2-tetrachloroethane and DMF), but with more concentrated solutions (*ca.* 1.0 M) than before, was then revisited. For dienes **1.15a** and **1.15b**, a steady improvement in the yield was observed in going from no solvent (28% and 36%) to xylenes (32% and 48%) and then 1,1,2,2-tetrachloroethane (40% and 70%). In changing to a much more polar solvent (DMF), the yield of **1.229a** dropped off considerably (12%) and DMF was consequently excluded from further studies. The use of 1,1,2,2-tetrachloroethane also resulted in significant yield enhancements for xanthenes **1.229b** (70%), **1.229c** (90%) and **1.229e** (98%).

**Table 2.2** Reactions of dienes **1.15a–i** with dienophile **1.226**.

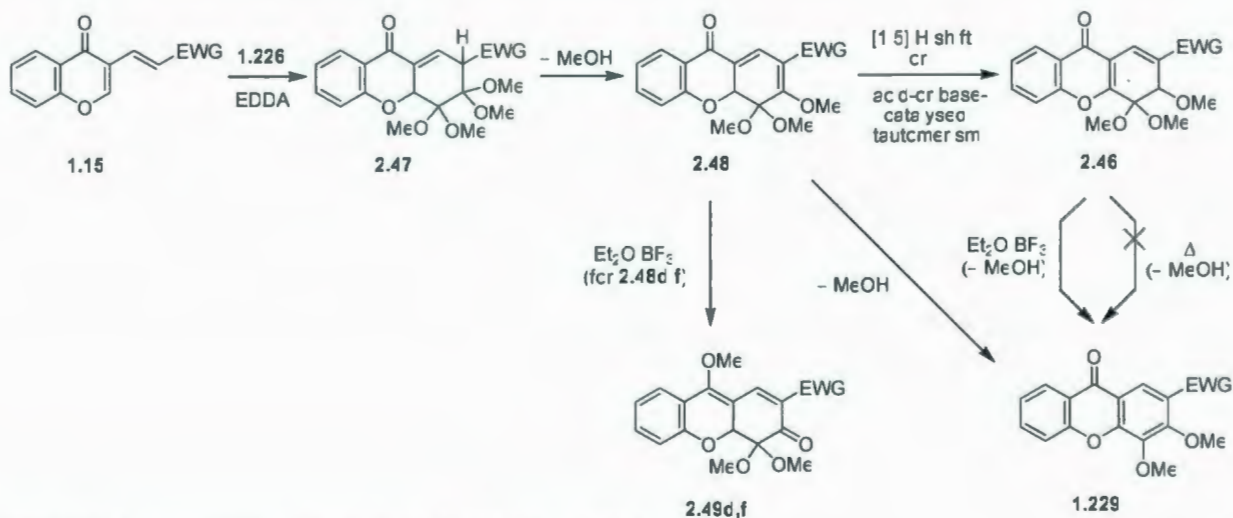
Entry	EWG	Xanthone	No solvent		Xylenes		$\text{C}_2\text{H}_2\text{Cl}_4$		DMF	
			h	%	h	%	h	%	h	%
1	CONEt <sub>2</sub>	<b>1.229a</b>	96	28	192	32	192	40	192	12
2	CO <sub>2</sub> Et	<b>1.229b</b>	24	36	144	48	48	70	-	
3	COPh	<b>1.229c</b>	24	84	-		26	90	-	
4	SO <sub>2</sub> Ph	<b>1.229d</b>	2	29	24	21	4	18	-	
5	COMe	<b>1.229e</b>	10	62	-		6	98	-	
6	CN	<b>1.229f</b>	2	27 <sup>a</sup>	-		24	38	-	
7	<i>p</i> -NO <sub>2</sub> C <sub>6</sub> H <sub>4</sub>	<b>1.229g</b>	23	25 <sup>b</sup>	-		48	trace <sup>e</sup>	-	
8	C <sub>6</sub> H <sub>5</sub>	<b>1.229h</b>	48	trace <sup>c</sup>	-		240	6	-	
9	<i>p</i> -MeOC <sub>6</sub> H <sub>4</sub>	<b>1.229i</b>	96	0 <sup>d</sup>	-		240	0	-	

*a*) 53% without Et<sub>2</sub>O·BF<sub>3</sub> treatment. *b*) 20% recovery of **1.15g**.

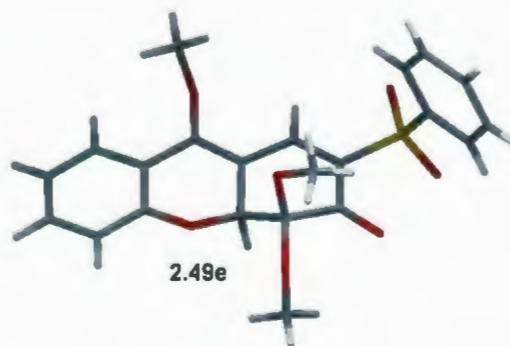
*c*) 60% recovery of **1.15h**. *d*) 60% recovery of **1.15i**. *e*) 59% recovery of **1.15g**.

Dienes **1.15d** and **1.15f** behaved somewhat differently from the others. Upon treatment of the crude mixtures with Et<sub>2</sub>O·BF<sub>3</sub>, a yellow byproduct, **2.49d** (10%) and **2.49f** (4%) (Scheme 2.12), formed alongside the desired xanthenes **1.229d** (18%) and **1.229f** (38%). The structure of **2.49d** was determined using single crystal X-ray analysis (Figure 2.4), and that of **2.49f** was assigned by analogy. The aryl substituted dienes

**1.15g–i** exhibited little or no reactivity toward TME (**1.226**). Slow, unproductive consumption of these dienes was observed under prolonged heating.



**Scheme 2.12** Proposed pathways to **1.229** and **2.49d,f**.



**Figure 2.4** X-ray structure of **2.49e**.

A proposed reaction landscape that is consistent with the observations is presented in Scheme 2.12. IEDDA reaction between **1.15** and **1.226** at 135 °C affords adducts **2.47**, which can undergo 1,2-elimination of methanol to afford dienes **2.48**. This elimination is proposed to occur first because the C(2) hydrogen atom should be the most acidic and, by inspection, an *antiperiplanar* orientation of the C–H bond and one of the



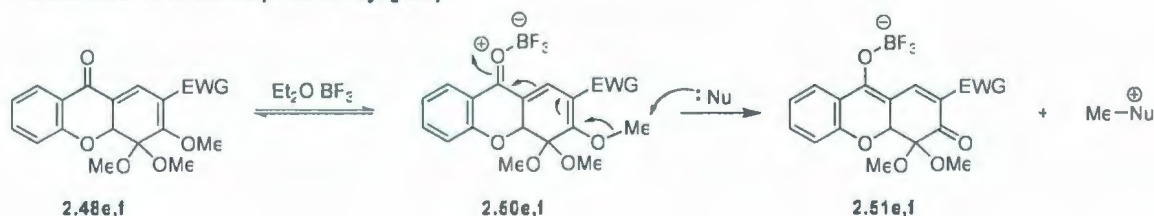
adjacent C–O bonds looks to be easily achievable. Dienes **2.48** then have two pathways available to them, namely the 1,2-elimination of a second molecule of methanol to afford xanthenes **1.229** and rearrangement to give dienes **2.46**. Rearrangement could conceivably occur either through a [1,5]-H shift<sup>23</sup> or an acid- or base-catalysed tautomerization. Regardless of which mechanism operates, the partial aromaticity of the 4-pyrone ring<sup>24</sup> in **2.46** may provide some incentive for rearrangement. Whatever the case, AM1 calculations<sup>25</sup> predict that the lowest energy conformer of **2.46e** is *ca.* 4 kcal / mol more stable than that of **2.48e**. The reluctance of the rearranged dienes **2.46** to undergo what must surely be a very exothermic elimination of methanol under quite forcing conditions (135 °C) is somewhat surprising, even considering that the C(3)-H bond of **2.46e** is oriented essentially *gauche* to both C(4)-O bonds (disfavoring E2-like elimination) in the crystal (Figure 2.3). Treatment of dienes **2.46** with Et<sub>2</sub>O·BF<sub>3</sub> proceeds smoothly under mild conditions, presumably because an E1-like mechanism becomes available. The formation of byproducts **2.49d,f** in the reactions of **1.15d,f** with **1.226** is difficult to explain without invoking the involvement of dienes **2.48d,f**. Whether these dienes are present at the end of the thermal stage of the reaction or they come from **2.46d,f** or **2.47d,f** upon treatment with Et<sub>2</sub>O·BF<sub>3</sub>, the conversion of **2.48d,f** to **2.49d,f** can be accounted for by a BF<sub>3</sub>-catalysed tautomerism involving the transfer of a methyl group from one end of a vinylogous ester to the other. The reason why the byproducts were formed only in the reactions of **1.15d,f** is unclear.

The proposed mechanism for the formation of **2.49e,f** (Scheme 2.13) involved in two processes: (1) generation of an electrophilic methyl group and (2) methyl transfer.

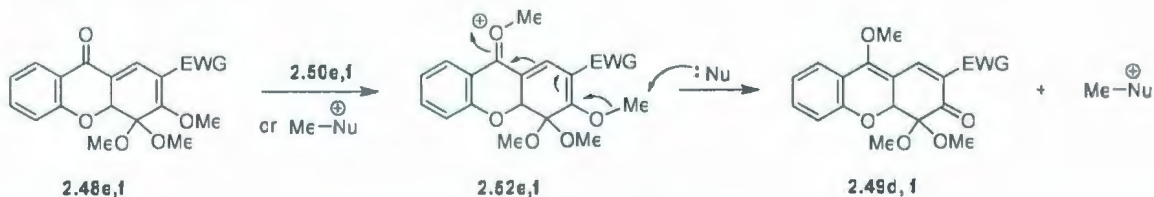
The nucleophile (Nu) could be a reaction partner, an intermediate, or a product. For example:

- if Nu is **2.48e,f** then  $\text{Me-Nu}^+$  is **2.52e,f** and the process repeats itself.
- if Nu is **2.46e,f** then  $\text{Me-Nu}^+$  will likely serve to propagate the methyl transfer because there is no electrophilic methyl group other than the one that was just attached.
- if Nu is **1.15e,f** or **2.47e,f**, they can either serve as  $\text{Me-Nu}^+$  or they can react via other reaction pathways leading to other products.
- if Nu is **1.229e,f** then  $\text{Me-Nu}^+$  will likely serve to propagate the methyl transfer because loss of the other electrophilic methyl group to form the C(3) ketone will involve the loss of some aromatic stabilization energy.

1. Generation of an electrophilic methyl group



2. Methyl transfer

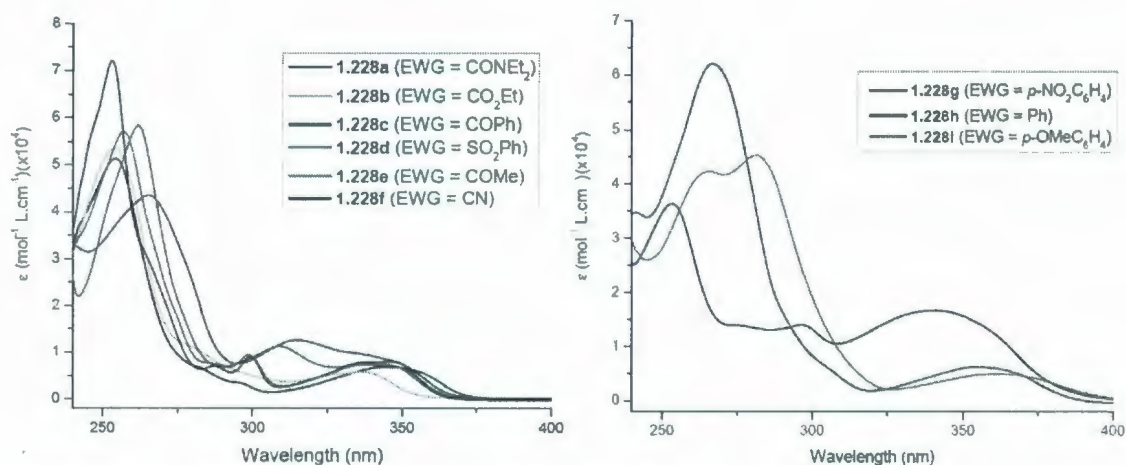


**Scheme 2.13** Proposed mechanism for the formation of **2.49d,f**.

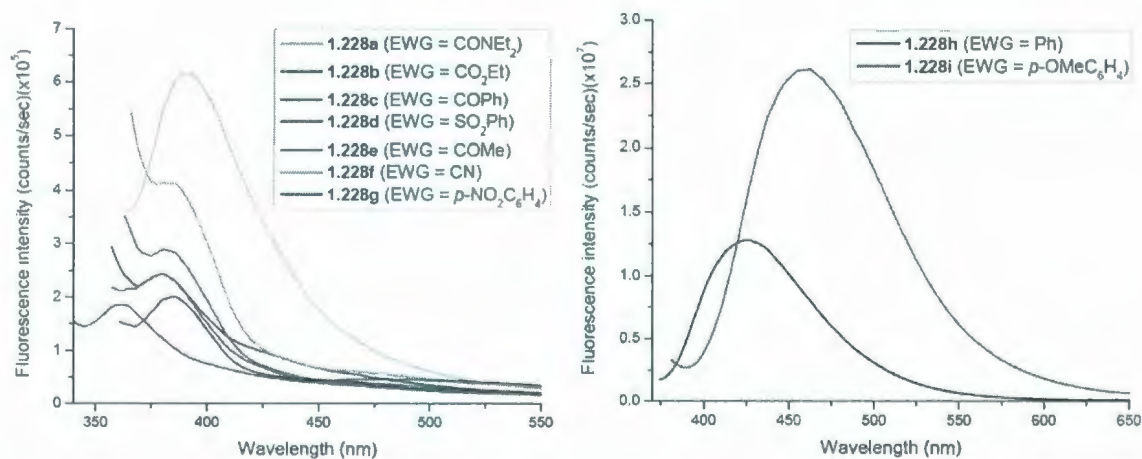
### 2.2.6 Physical Properties of 2-Substituted 4-Methoxy- and 3,4-Dimethoxyxanthenes

Xanthenes **1.228a–f** and **1.229a–f**, which bear an EWG, have similar broad absorption bands ranging from 315 to 346 nm. Xanthenes bearing a *p*-NO<sub>2</sub>C<sub>6</sub>H<sub>4</sub> substituent, *i.e.* **1.228g** and **1.229g**, have very broad absorption bands at shorter wavelengths than those of xanthenes bearing Ph or *p*-MeOC<sub>6</sub>H<sub>4</sub> (Figures 2.5–2.7 and Table 2.3, 2.4). The behavior of the 2-arylxanthenes **1.228g–i** was more interesting. As the electron-donating ability of the aryl substituent increased, the lowest energy absorption bands of **1.228g–i** moved to lower energy (longer wavelength) along with the emission bands with a concomitant increase in fluorescence intensity, which is inconsistent with the “energy gap law”.<sup>26</sup> Furthermore, the total reorganization energy ( $\lambda_t$ ) became larger ( $\lambda_t = 1680, 2340, 3030 \text{ cm}^{-1}$  for **1.228g–i**, respectively) as calculated from the increasing Stokes shifts (Table 2.3).<sup>27</sup> By comparison,  $\lambda_t$  ranges from 1420 to 2620  $\text{cm}^{-1}$  for **1.228a–f** and **1.229a–h**. Like xanthone itself,<sup>28</sup> xanthenes **1.228a–f** and **1.229a–h** exhibited very weak fluorescence ( $\Phi_{\text{em}} < 10^{-3}$ ). Quantum yields ( $\Phi_{\text{em}}$ ) for **1.229h**, **1.228h** and **1.228i** are 0.007, 0.07 and 0.13, respectively.<sup>29</sup> A tentative interpretation of this data is that charge transfer becomes more significant along the series **1.228g–i**, which increases the vibrational energy ( $\lambda_{\text{vib}}$ ) due to population of the  $\pi^*$  orbitals of the acceptor (the xanthone moiety) and solvent reorganization energy ( $\lambda_o$ )<sup>27</sup> due to changes in the dipole moment on formation of the charge transfer excited state.<sup>30</sup>





**Figure 2.5** Absorption spectra of 1.228a–f (*left*) and 1.228g–i (*right*) in  $\text{CHCl}_3$  ( $2 \times 10^{-5} \text{ M}$ ).



**Figure 2.6** Emission spectra of 1.228a–g (*left*) and 1.228h–i (*right*) in  $\text{CHCl}_3$  ( $2 \times 10^{-5} \text{ M}$ ).

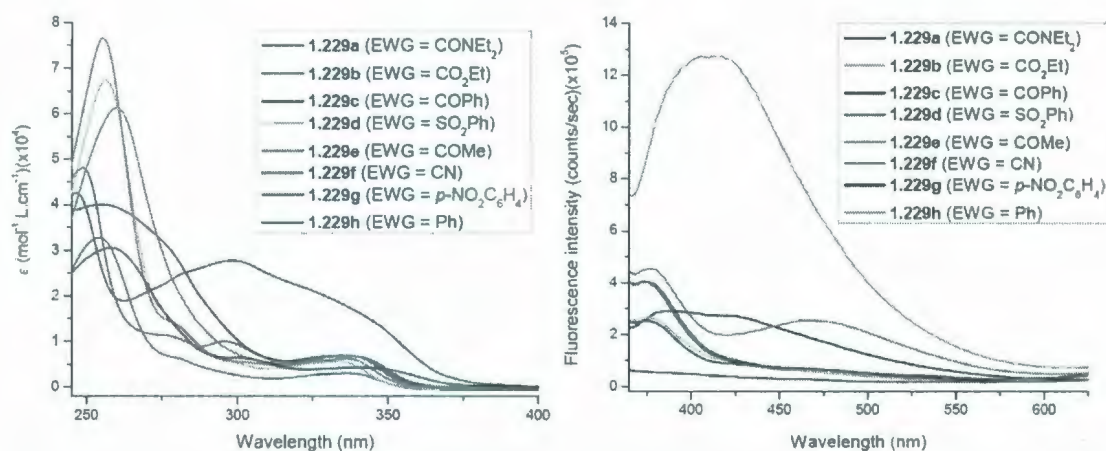


Figure 2.7 Absorption (*left*) and emission spectra (*right*) of **1.229a–h** in  $\text{CHCl}_3$  ( $2 \times 10^{-5}$  M).

Table 2.3 Physical data of 4-methoxyxanthenes **1.228a–i**.

EWG	$\lambda_{\text{max (abs)}}$ (nm)	$E_{\text{abs}} (\text{cm}^{-1})$ ( $= 1/\lambda \times 10^7$ )	$\lambda_{\text{max (em)}}$ (nm)	$E_{\text{em}} (\text{cm}^{-1})$ ( $= 1/\lambda \times 10^7$ )	Stokes shift ( $\text{cm}^{-1}$ ) ( $E_{\text{abs}} - E_{\text{em}}$ ) $= 2\lambda_t$	$\lambda_t$ ( $\text{cm}^{-1}$ )	$\Phi_{\text{em}}$
$\text{CONEt}_2$	344	29100	390	25500	3610	1800	-
$\text{CO}_2\text{Et}$	337	29700	380	26300	3360	1680	-
$\text{COPh}$	315	31700	362	27600	4120	2060	-
$\text{COMe}$	337	29700	380	26300	3360	1680	-
$\text{SO}_2\text{Ph}$	343	29200	380	26300	2840	1420	-
$\text{CN}$	346	28900	386	25900	2990	1500	-
$p\text{-NO}_2\text{C}_6\text{H}_4$	341	29300	385	26000	3350	1680	-
$\text{Ph}$	354	28200	426	23500	4770	2390	0.072
$p\text{-MeOC}_6\text{H}_4$	361	27700	462	21600	6060	3030	0.130

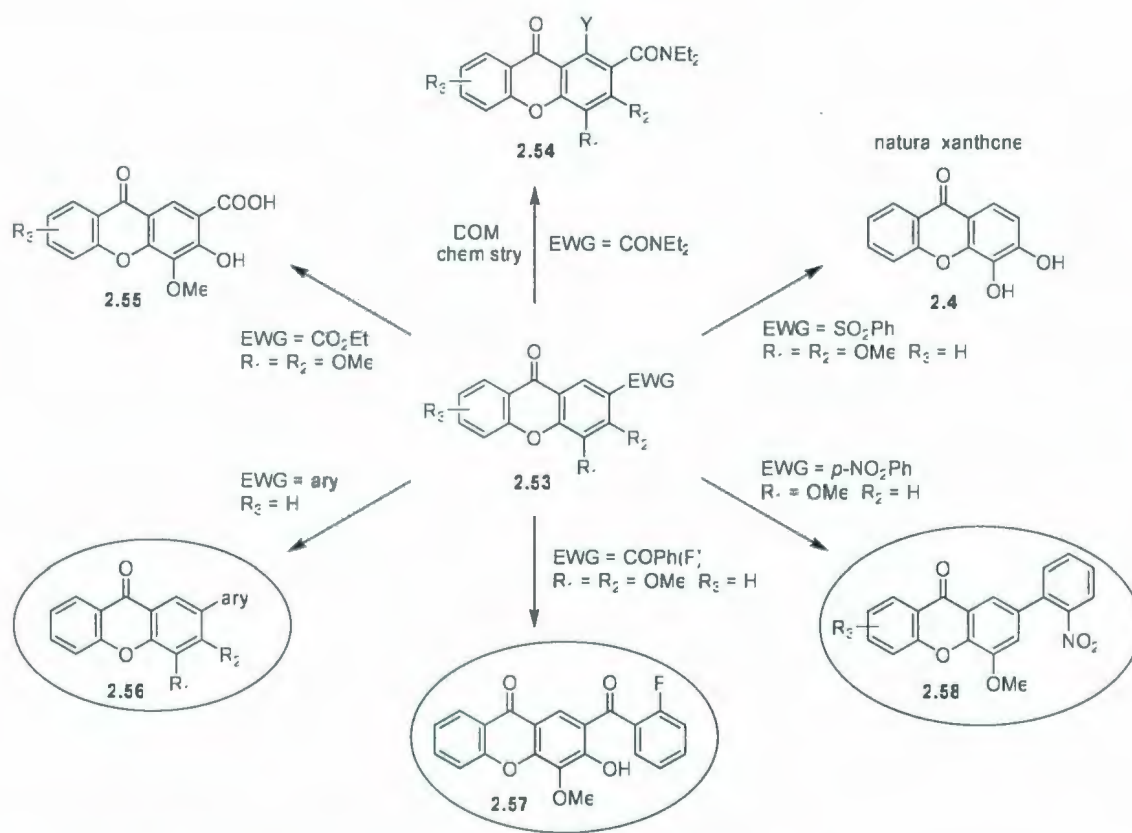
Table 2.4 Physical data of 3,4-dimethoxyxanthenes **1.229a–h**.

EWG	$\lambda_{\max}(\text{abs})$ (nm)	$E_{\text{abs}}(\text{cm}^{-1})$ ( $= 1/\lambda \times 10^7$ )	$\lambda_{\max}(\text{em})$ (nm)	$E_{\text{em}}(\text{cm}^{-1})$ ( $= 1/\lambda \times 10^7$ )	Stokes shift ( $\text{cm}^{-1}$ ) ( $E_{\text{abs}} - E_{\text{em}}$ ) $= 2\lambda_t$	$\lambda_t$ ( $\text{cm}^{-1}$ )	$\Phi_{\text{em}}$
CONEt <sub>2</sub>	337	29700	386	25900	3770	1880	-
CO <sub>2</sub> Et	336	29800	377	26500	3240	1620	-
COPh	336	29800	376	26600	3170	1580	-
COMe	337	29800	377	26500	3150	1570	-
SO <sub>2</sub> Ph	334	29900	373	26800	3130	1570	-
CN	336	29700	374	26700	2940	1470	-
<i>p</i> -NO <sub>2</sub> C <sub>6</sub> H <sub>4</sub>	298	33600	353	28300	5230	2620	-
Ph	341	29300	413	24200	5110	2560	0.0072

### 2.3 Conclusions

In summary, IEDDA reactions between dienes **1.15** with dienophiles **1.225** and **1.226** afforded a range of 4-methoxy- (**1.228a–i**) and 3,4-dimethoxyxanthenes (**1.229a–h**) with useful functionality at the 2 position. Particularly, compounds **2.54–2.58** and also the natural xanthone **2.4** can conceivably be approached from **2.53** bearing a suitable EWG (Scheme 2.14). Work aimed at the use of this methodology for the construction of new xanthone-based fluorophores such as **2.56** and more elaborate xanthonoid systems from key intermediates **2.57** and **2.58** will be introduced in the following sections.





**Scheme 2.14** Possible elaboration of the useful compound **2.53**.

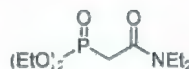
## 2.4 Experimental Section

### General Methods:

All experiments with moisture- or air-sensitive compounds were carried out under a N<sub>2</sub> atmosphere unless otherwise indicated. Commercially available chemicals purchased from Aldrich or Alfa Aesar were used without further purification. Solvents were dried and distilled according to standard procedures. Organic solvents were evaporated under reduced pressure using a rotary evaporator. Flash chromatography was performed using Silicycle silica gel 60, particle size 40–63 μm. Compounds on tlc plates were visualized under UV light (254 and 365 nm).

**Instrumentation:**

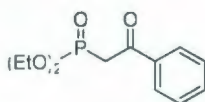
Melting points (mp) were determined on a Fisher-Johns apparatus and uncorrected. Infrared (IR) spectra were obtained using a Bruker TENSOR 27 instrument.  $^1\text{H}$  and  $^{13}\text{C}$  nuclear magnetic resonance (NMR) spectra were recorded on a Bruker AVANCE 500 MHz ( $\text{CDCl}_3$ , unless otherwise indicated) or a Bruker AVANCE II 600 MHz spectrometer (solid state). Chemical shifts are reported relative to internal standards:  $\text{Me}_4\text{Si}$  ( $\delta$  0.00 ppm) and  $\text{CDCl}_3$  ( $\delta$  77.23 ppm), respectively.  $^1\text{H}$  NMR data are presented as follows: chemical shift, multiplicity (s = singlet, d = doublet, t = triplet, q = quartet, m = multiplet), coupling constant ( $J$ , Hz), integration (# of H). Low-resolution mass spectra (MS) and high-resolution mass spectra (HRMS) of compounds were obtained using an Agilent 1100 Series LC/MSD and a Waters Micromass<sup>®</sup> GCT Premier<sup>™</sup> instruments, respectively. MS data are presented as follows:  $m/z$  (relative intensity), assignment (when appropriate), calculated mass for corresponding formula. UV-vis and fluorescence spectra were recorded using an Agilent 8453 spectrophotometer and a Photon Technology International fluoreometer.

**2.4.1 Experimental Procedures<sup>31</sup>****Diethyl 2-(diethylamino)-2-oxoethylphosphonate (2.21)<sup>9</sup>**

A mixture of *N,N*-diethylchloroacetamide (**2.20**) (3.60 g, 24.1 mmol) and triethyl phosphite (4.00 g, 24.1 mmol) was heated at 180 °C for 18 h. The volatile compounds were distilled off using a vacuum pump. The crude product was purified by column

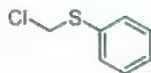
chromatography (EtOAc) to yield **2.21** (4.10 g, 68%) as a yellow oil:  $^1\text{H}$  NMR (500 MHz)  $\delta$  4.21–4.15 (m, 4H), 3.46–3.37 (m, 4H), 3.02 (d,  $J_{\text{P-H}} = 22$  Hz, 2H), 1.34 (t,  $J = 7.0$  Hz, 6H), 1.20 (t,  $J = 7.3$  Hz, 3H), 1.14 (t,  $J = 7.0$  Hz, 3H);  $^{13}\text{C}$  NMR (125 MHz)  $\delta$  164.2, 62.79, 62.75, 43.2, 40.7, 33.6 ( $J_{\text{CP}} = 134.3$  Hz), 16.6, 16.5, 14.4, 13.1; MS [APCI (+)]  $m/z$  (%) 252 ( $\text{M}^+$ , 100).

**Diethyl 2-oxo-2-phenylethylphosphonate (2.23)**<sup>10</sup>



A mixture of bromoacetophenone (**2.22**) (15.0 g, 75.4 mmol) and triethyl phosphite (12.1 g, 90.3 mmol) was heated at 120 °C for 6 h. After the volatile material was removed by vacuum distillation, the crude product was dissolved in  $\text{CH}_2\text{Cl}_2$  (200 mL), extracted with 1 M aqueous NaOH solution ( $4 \times 150$  mL), neutralized with 3 M HCl, and then extracted with  $\text{Et}_2\text{O}$  ( $4 \times 100$  mL). The organic layer was washed with brine dried, over  $\text{MgSO}_4$  and filtered. The solvent was removed under reduced pressure to yield **2.23** (7.51 g, 39%) as a colorless liquid:  $^1\text{H}$  NMR (500 MHz)  $\delta$  8.03–8.01 (m, 2H), 7.59 (t,  $J = 7.6$  Hz, 1H), 7.48 (t,  $J = 7.8$  Hz, 2H), 4.14 (m, 4H), 3.63 (d,  $J_{\text{P-H}} = 22$  Hz, 2H), 1.28 (t,  $J = 7.1$  Hz, 6H).

**Chloromethyl phenyl sulfide (2.25)**<sup>11</sup>

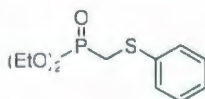


To a stirred mixture of paraformaldehyde (49.5 g, 1.65 mol) in toluene (200 mL) and concentrated HCl (500 mL) at 50 °C was added dropwise thiophenol (**2.24**) (139 g,



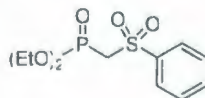
1.26 mol) over 30 min. The reaction mixture was cooled to room temperature and stirred for further 17 h. The organic layer was separated. The aqueous layer was extracted with toluene (4 x 150 mL). The combined organic layer was washed with brine, dried  $\text{MgSO}_4$ , and filtered. The solvent was removed under reduced pressure. The crude product was purified by vacuum distillation (b.p. 106–107 °C, 9–11 mmHg) to yield **2.25** (142.1 g, 71%) as a colorless liquid:  $^1\text{H}$  NMR (500 MHz)  $\delta$  7.53–7.51 (m, 2H), 7.39–7.25 (m, 3H), 4.97 (s, 2H);  $^{13}\text{C}$  NMR (125 MHz)  $\delta$  133.5, 131.2, 131.0, 129.4, 128.2.

### Diethyl (phenylthio)methylphosphonate (**2.59**)<sup>11</sup>



To stirred triethyl phosphite (238 g, 1.78 mol) at 120 °C was added dropwise chloromethyl phenyl sulfide (**2.25**) (216 g, 1.37 mol) over 40 min. The reaction mixture was stirred for further 18 h. Excess amount of  $\text{P}(\text{OEt})_3$  was removed by vacuum pump (b.p. 50 °C, 10 mmHg). The crude product was purified by vacuum distillation (b.p. 145–150 °C, 2 mmHg) to yield **2.59** (282 g, 80 %) as a colorless liquid:  $^1\text{H}$  NMR (500 MHz)  $\delta$  7.48 (d,  $J = 7.4$  Hz, 2H), 7.34 (t,  $J = 7.6$  Hz, 2H), 7.26 (t,  $J = 7.4$  Hz, 1H), 4.21–4.14 (m, 4H), 3.24 (d,  $J_{\text{P-H}} = 14$  Hz, 2H), 1.34 (t,  $J = 7.1$  Hz, 6H).

### Diethyl (phenylsulfonyl)methylphosphonate (**2.26**)<sup>11</sup>

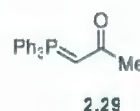
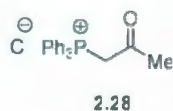


To a stirred solution of diethyl (phenylthio)methylphosphate (**2.59**) (10.4 g, 40.0 mmol) in AcOH (60 mL) at 50 °C was added dropwise  $\text{H}_2\text{O}_2$  (20 mL, 30% aqueous

solution) over 30 min. The reaction mixture was heated to 85 °C for a further 4 h and then allowed to cool to room temperature and poured into ice. 10 M aqueous NaOH solution was added until the pH reached 8 or 9. The layers were separated and the aqueous layer was extracted with CH<sub>2</sub>Cl<sub>2</sub> (4 x 50 mL). The combined organic layer was washed with 10% aqueous NaHSO<sub>3</sub> solution until no oxidizing agent remained. The solution was dried over MgSO<sub>4</sub> and filtered. The solvent was removed under reduced pressure. Column chromatography (20:80 EtOAc:hexanes) of the crude product yielded **2.26** (10.1 g, 86%) as a colorless liquid: <sup>1</sup>H NMR (500 MHz) δ 8.00 (d, *J* = 7.7 Hz, 2H), 7.68 (t, *J* = 7.4 Hz, 1H), 7.58 (t, *J* = 7.8 Hz, 2H), 4.19–4.12 (m, 4H), 3.76 (d, *J*<sub>P-H</sub> = 17 Hz, 2H), 1.30 (t, *J* = 7.1 Hz, 6H).

### 2-Oxopropyltriphenylphosphonium chloride (**2.28**)<sup>12</sup>

### 1-(Triphenylphosphoranylidene)-2-propanone (**2.29**)



To a clear solution of triphenylphosphine (15.7 g, 59.9 mmol) in benzene (50 mL) was added dropwise chloroacetone (4.61 g, 49.7 mmol) at room temperature. The reaction mixture was heated at reflux for 22 h. The white precipitate was collected by suction filtration, washed with benzene, and dried in air to yield **2.28** (17.7 g, 100%). This crude product was used for the next step.

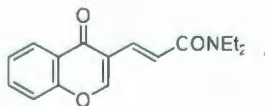
To a clear solution of ylide precursor **2.28** (5.01 g, 14.1 mmol) in water (50 mL) was added dropwise a solution of potassium hydroxide (800 mg, 14.3 mmol) in H<sub>2</sub>O (8 mL). The reaction mixture was stirred at room temperature for 30 min. The resulting

white precipitate was collected by suction filtration, washed with cold water, and dried in air to yield **2.29** (3.60 g, 80%) as a colorless solid:  $^1\text{H}$  NMR (500 MHz)  $\delta$  7.68–7.44 (m, 15H), 3.70 (d,  $J$  = 23.9 Hz, 1H), 2.10 (s, 3H).

**General procedure for the synthesis of dienes 1.15a–d.**

To a magnetically stirred, room temperature suspension of NaH (60% dispersion in mineral oil, 1.2 equiv.) in THF was slowly added the corresponding phosphonate (1.3 equiv.). The mixture was stirred at room temperature for 0.5 h and the resulting clear, yellow solution was added dropwise to a solution of 3-formylchromone (**2.19**) (1.0 equiv.) in THF. The resulting orange mixture was stirred at room temperature until the 3-formylchromone had been completely consumed (tlc analysis). The reaction mixture was quenched by the addition of saturated aqueous  $\text{NH}_4\text{Cl}$  solution (10–15 mL) and stirring was continued for 15 min. The solvent was removed under reduced pressure and  $\text{H}_2\text{O}$  and  $\text{CH}_2\text{Cl}_2$  were added to the residue. The layers were separated and the aqueous layer was extracted with  $\text{CH}_2\text{Cl}_2$ . The combined organic layers were washed with distilled water, washed with saturated aqueous  $\text{NaHSO}_3$  solution, washed with brine, dried over  $\text{MgSO}_4$  and filtered. The solvent was removed under reduced pressure and the residue was purified by column chromatography to yield pure dienes **1.15a–d**.

**(*E*)-*N,N*-Diethyl-3-(4-oxo-4*H*-chromen-3-yl)prop-2-enamide (1.15a)**

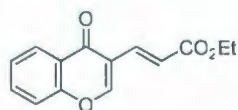


A solution derived from 60% NaH in mineral oil (1.38 g, 34.4 mmol) and *N,N*-diethyl diethyl phosphonoacetamide (**2.21**) (9.47 g, 37.7 mmol) in THF (60 mL) was



added dropwise to a solution of 3-formylchromone (**2.19**) (5.00 g, 28.7 mmol) in THF (60 mL). The resulting mixture was stirred at room temperature for 8 h and worked up according to the general procedure. Column chromatography (20:80 EtOAc:hexanes) of the crude product yielded diene **1.15a** (5.29 g, 68%) as a yellow solid:  $R_f$  = 0.35 (20:80 EtOAc:hexanes); mp 102–103 °C; IR  $\nu$  3057 (w), 2978 (w), 2936 (w), 1652 (s), 1610 (m), 1600 (s), 1464 (s), 1424 (s), 1396 (s), 1353 (s), 1287 (s), 1269 (s), 982 (s), 861 (s), 753 (s), 682 (s)  $\text{cm}^{-1}$ ;  $^1\text{H}$  NMR (500 MHz)  $\delta$  8.28 (dd,  $J$  = 7.8, 1.6 Hz, 1H), 8.10 (s, 1H), 8.04 (d,  $J$  = 14.6 Hz, 1H), 7.71–7.68 (m, 1H), 7.50–7.44 (m, 2H), 7.34 (d,  $J$  = 15.3 Hz, 1H), 3.54–3.49 (m, 4H), 1.29 (t,  $J$  = 7.0 Hz, 3H), 1.19 (t,  $J$  = 7.0 Hz, 3H);  $^{13}\text{C}$  NMR (125 MHz)  $\delta$  176.8, 166.4, 158.0, 155.7, 134.1, 133.2, 126.4, 125.9, 124.6, 122.7, 119.9, 118.4, 42.6, 41.3, 15.3, 13.4; MS [APCI (+)]  $m/z$  (%) 272 ( $M^+$ , 100); HRMS [CI (+)] calcd for  $\text{C}_{16}\text{H}_{17}\text{NO}_3 + \text{H}^+$  272.1287, found 272.1286.

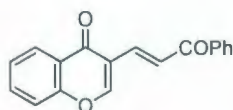
**(*E*)-Ethyl 3-(4-oxo-4*H*-chromen-3-yl)prop-2-enoate (**1.15b**)<sup>16</sup>**



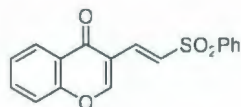
A solution derived from 60% NaH in mineral oil (550 mg, 13.8 mmol) and triethyl phosphonoacetate (**2.34**) (3.36 g, 15.0 mmol) in THF (30 mL) was added dropwise to a solution of 3-formylchromone (**2.19**) (2.00 g, 11.5 mmol) in THF (50 mL). The resulting mixture was stirred at room temperature for 48 h and worked up according to the general procedure. Column chromatography (10:90 EtOAc:hexanes) of the crude product yielded diene **1.15b** (2.22 g, 79%) as a light yellow solid. Alternatively, crystallization (95% ethanol) of the crude mixture yielded **1.15b** (1.68 g, 60%) as fine

yellow needles:  $R_f = 0.50$  (20:80 EtOAc:hexanes); mp 105–107 °C (ethanol);  $^1\text{H}$  NMR (500 MHz)  $\delta$  8.29 (dd,  $J = 7.3, 1.2$  Hz, 1H), 8.12 (s, 1H), 7.72–7.69 (m, 1H), 7.49–7.44 (m, 2H), 7.42 (d,  $J = 16.0$  Hz, 1H), 7.29 (d,  $J = 16.3$  Hz, 1H), 4.26 (q,  $J = 6.9$  Hz, 2H), 1.33 (t,  $J = 7.5$  Hz, 3H);  $^{13}\text{C}$  NMR (125 MHz)  $\delta$  176.1, 167.5, 157.5, 155.7, 135.5, 134.2, 126.5, 126.0, 124.4, 122.4, 119.6, 118.3, 60.7, 14.5; MS [APCI (+)]  $m/z$  (%) 245 ( $\text{M}^+$ , 100), 199 ( $\text{M}^+ - \text{OEt}$ , 58).

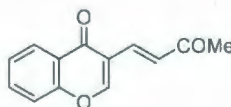
**(*E*)-3-(3-Oxo-3-phenylprop-1-enyl)-4*H*-chromen-4-one (1.15c)**<sup>32</sup>



A solution derived from 60% NaH in mineral oil (0.550 g, 13.8 mmol) and diethyl (2-oxo-2-phenylethyl)phosphonate (**2.23**) (3.84 g, 15.0 mmol) in THF (30 mL) was added dropwise to a solution of 3-formylchromone (**2.19**) (2.00 g, 11.5 mmol) in THF (30 mL). The resulting mixture was stirred at room temperature for 24 h and worked up according to the general procedure. Column chromatography (10:90 EtOAc:hexanes) of the crude product yielded diene **1.15c** (2.22 g, 70%) as a light yellow solid:  $R_f = 0.45$  (20:80 EtOAc:hexanes); mp 168–169 °C (lit. mp<sup>33</sup> 170 °C);  $^1\text{H}$  NMR (500 MHz)  $\delta$  8.70 (d,  $J = 16.4$  Hz, 1H), 8.32 (d,  $J = 7.9$  Hz, 1H), 8.21 (s, 1H), 8.11 (d,  $J = 7.4$  Hz, 2H), 7.72 (t,  $J = 7.4$  Hz, 1H), 7.59 (t,  $J = 7.0$  Hz, 1H), 7.52–7.47 (m, 5H);  $^{13}\text{C}$  NMR (125 MHz)  $\delta$  190.8, 176.5, 159.1, 155.7, 138.1, 135.5, 134.3, 133.2, 128.9, 128.8, 126.5, 126.2, 126.0, 124.5, 119.9, 118.4; MS [APCI (+)]  $m/z$  (%) 277 ( $\text{M}^+$ , 100).

**(*E*)-3-(2-(Phenylsulfonyl)vinyl)-4*H*-chromen-4-one (1.15d)**<sup>32</sup>

A solution derived from 60% NaH in mineral oil (0.550 g, 13.8 mmol) and diethyl (2-sulfonyl-2-phenylethyl)phosphonate (**2.26**) (4.38 g, 15.0 mmol) in THF (30 mL) was added dropwise to a solution of 3-formylchromone (**2.19**) (2.01 g, 11.5 mmol) in THF (30 mL). The resulting mixture was stirred at room temperature for 6 h and worked up according to the general procedure. Column chromatography (10:90 EtOAc:hexanes) of the crude product yielded diene **1.15d** (2.51 g, 70%) as a colorless solid:  $R_f$  = 0.35 (20:80 EtOAc:hexanes); mp 194–195 °C (lit. mp<sup>34</sup> 207 °C, recrystallized from acetic acid); <sup>1</sup>H NMR (500 MHz)  $\delta$  8.23 (dd,  $J$  = 8.2, 1.6 Hz, 1H), 8.17 (s, 1H), 8.09 (d,  $J$  = 14.8 Hz, 1H), 7.95–7.94 (m, 2H), 7.74–7.70 (m, 1H), 7.63–7.60 (m, 1H), 7.56–7.45 (m, 4H), 7.33 (d,  $J$  = 14.8 Hz, 1H); <sup>13</sup>C NMR (125 MHz)  $\delta$  175.9, 159.4, 155.7, 140.8, 134.6, 133.6, 133.2, 131.9, 129.5, 128.0, 126.5, 126.5, 124.3, 118.4, 117.9; MS [APCI (+)]  $m/z$  (%) 313 ( $M^+$ , 100).

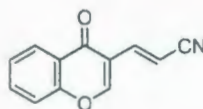
**(*E*)-3-(3-Oxobut-1-enyl)-4*H*-chromen-4-one (1.15e)**

To solution of 3-formylchromone (**2.19**) (1.01 g, 5.74 mmol) in CH<sub>2</sub>Cl<sub>2</sub> (20 mL) was added 1-(triphenylphosphoranylidene)-2-propanone (**2.29**) (3.66 g, 11.5 mmol) in one portion at room temperature. The yellow resulting mixture was heated at reflux for 6 h. The solvent was removed under reduced pressure and the crude product was purified



by chromatography (40:60 EtOAc:hexanes) to yield diene **1.15e** (1.11 g, 90%) as a yellow solid:  $R_f$  = 0.35 (40:60 EtOAc:hexanes); mp 173–174 °C; IR  $\nu$  3079 (w), 1684 (s), 1639 (s), 1596 (s), 1559 (s), 1465 (s), 1413 (s), 1285 (s), 1264 (s), 985 (s), 854 (s), 765 (s) ( $\text{cm}^{-1}$ );  $^1\text{H}$  NMR (500 MHz)  $\delta$  8.30 (dd,  $J$  = 7.7, 2.0 Hz, 1H), 8.17 (s, 1H), 7.73–7.70 (m, 1H), 7.52–7.46 (m, 3H), 7.35 (d,  $J$  = 16.1 Hz, 1H), 2.38 (s, 3H);  $^{13}\text{C}$  NMR (125 MHz)  $\delta$  198.8, 176.2, 157.6, 155.8, 134.3, 133.8, 129.7, 126.6, 126.2, 124.3, 119.6, 118.4, 28.9; MS [APCI (+)]  $m/z$  (%) 215 ( $\text{M}^+$ , 100); HRMS [CI (+)] calcd for  $\text{C}_{13}\text{H}_{10}\text{O}_3 + \text{H}^+$  215.0708, found 215.0708.

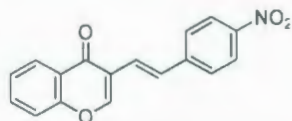
**(*E*)-3-(4-Oxo-4*H*-chromen-3-yl)prop-2-enenitrile (1.15f)<sup>19</sup>**



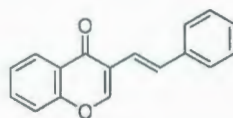
A mixture of 3-formylchromone (**2.19**) (8.01 g, 46.0 mmol) and cyanoacetic acid (**2.35**) (4.01 g, 47.1 mmol) preheated to 110 °C (melting occurred) and pyridine (15 mL) was added quickly. The resulting dark reaction mixture was then cooled to room temperature and stirred for 6 h. The reaction was worked up using either of the following procedures: (1) the yellow precipitate was collected by suction filtration and washed with cold methanol to yield diene **1.15f** (4.08 g, 45%) as yellow crystals, or (2) the reaction mixture was poured into ice-water (150 mL) and the yellow precipitate was collected by suction filtration, washed several times with water, washed quickly with cold methanol and dried in air to yield diene **1.15f** (5.44 g, 60%) as a yellow solid:  $R_f$  = 0.45 (50:50 EtOAc:hexanes); mp 190–191 °C ( $\text{CH}_3\text{CN}$ ) (lit. mp<sup>19b</sup> 193–195 °C);  $^1\text{H}$  NMR (500 MHz)  $\delta$  8.27 (dd,  $J$  = 8.3, 1.7 Hz, 1H), 8.07 (s, 1H), 7.75–7.72 (m, 1H), 7.52–7.48 (m, 2H), 7.13

(d,  $J = 17.1$  Hz, 1H), 7.01 (d,  $J = 15.7$  Hz, 1H);  $^{13}\text{C}$  NMR (125 MHz)  $\delta$  176.1, 158.1, 155.6, 141.7, 134.7, 126.54, 126.48, 124.3, 118.6, 118.6, 118.4, 101.7; MS [APCI (+)]  $m/z$  (%) 198 ( $\text{M}^+$ , 100).

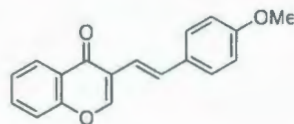
**(*E*)-3-(4-Nitrostyryl)-4*H*-chromen-4-one (1.15g)<sup>8</sup>**



A mixture of 4-nitrophenylacetic acid (**2.36**) (7.80 g, 43.1 mmol) and 3-formylchromone (**2.19**) (5.00 g, 28.7 mmol) in pyridine (50 mL) was heated with stirring at 70–80 °C for 4 d. The reaction mixture was cooled to room temperature, poured into ice-water (400 mL) and acidified with aqueous 6 M HCl solution until the pH reached 1–2. The yellow precipitate was collected by suction filtration, washed several times with deionized water and dried in air. Column chromatography (50:50 petroleum ether: $\text{CH}_2\text{Cl}_2$ ) of the crude product yielded diene **1.15g** (5.04 g, 60%) as a yellow solid:  $R_f = 0.65$  ( $\text{CH}_2\text{Cl}_2$ ); mp 233–234 °C (lit. mp<sup>17</sup> 225–226 °C);  $^1\text{H}$  NMR (500 MHz)  $\delta$  8.32 (dd,  $J = 8.8, 1.7$  Hz, 1H), 8.22 (d,  $J = 8.6$  Hz, 2H), 8.16 (s, 1H), 7.88 (d,  $J = 16.1$  Hz, 1H), 7.73–7.69 (m, 1H), 7.64 (d,  $J = 8.6$  Hz, 2H), 7.51–7.45 (m, 2H), 7.08 (d,  $J = 16.2$  Hz, 1H);  $^{13}\text{C}$  NMR (125 MHz)  $\delta$  176.6, 155.9, 154.9, 147.2, 144.2, 134.1, 129.9, 127.2, 126.5, 125.8, 124.3, 124.1, 121.1, 118.3; MS [APCI (+)]  $m/z$  (%) 294 ( $\text{M}^+$ , 100).

**(*E*)-3-Styryl-4*H*-chromen-4-one (1.15h)**<sup>8</sup>

A mixture of phenylacetic acid (**2.37**) (19.5 g, 144 mmol), *t*-BuOK (5.08 g, 43.1 mmol) and 3-formylchromone (**2.19**) (5.00 g, 28.7 mmol) in pyridine (80 mL) was heated at reflux for 22 h. The reaction mixture was cooled to room temperature, poured into ice-water (400 mL) and acidified with aqueous 6 M HCl solution until the pH reached 1–2. The yellow precipitate was collected by suction filtration, washed several time with deinionized water and dried in air. Recrystallization (95% ethanol) yielded **1.15h** (5.84 g, 82%) as a yellow solid:  $R_f$  = 0.60 (35:65 EtOAc:hexanes); mp 170–171 °C (ethanol) (lit. mp<sup>17</sup> 168–169 °C); <sup>1</sup>H NMR (500 MHz)  $\delta$  8.31 (dd,  $J$  = 8.0, 1.4 Hz, 1H), 8.12 (s, 1H), 7.69–7.66 (m, 1H), 7.64 (d,  $J$  = 16.5 Hz, 1H), 7.54–7.42 (m, 4H), 7.37–7.26 (m, 3H), 6.99 (d,  $J$  = 16.3 Hz, 1H); <sup>13</sup>C NMR (125 MHz)  $\delta$  176.8, 156.1, 153.2, 137.6, 133.7, 132.0, 128.9, 128.1, 126.8, 126.5, 125.5, 124.4, 122.1, 119.3, 118.3; MS [APCI (+)]  $m/z$  (%) 249 ( $M^+$ , 100).

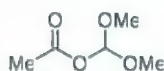
**(*E*)-3-(4-Methoxystyryl)-4*H*-chromen-4-one (1.15i)**<sup>35</sup>

A mixture of 4-methoxyphenylacetic acid (**2.38**) (9.54 g, 57.4 mmol), *t*-BuOK (5.08 g, 43.0 mmol), and 3-formylchromone (**2.19**) (5.00 g, 28.7 mmol) in pyridine (100 mL) was heated at reflux for 16 h. The reaction mixture was cooled to room temperature, poured into ice-water (400 mL) and acidified with aqueous 6 M HCl solution until the pH

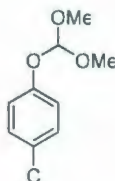


reached 1–2. The yellow precipitate was collected by suction filtration, washed several times with deionized water and dried in air. Column chromatography (20:80 EtOAc:hexanes) of crude the product yielded **1.15i** (5.58 g, 70%) as a yellow solid:  $R_f$  = 0.45 (35:65 EtOAc:hexanes); mp 123–124 °C; IR  $\nu$  2959 (s), 2927 (s), 2871 (w), 1642 (s), 1622 (m), 1600 (s), 1561 (m), 1509 (s), 1464 (s), 1251 (s), 1211 (s), 1028 (s), 973 (s), 819 (s), 749 (s), 694 (s)  $\text{cm}^{-1}$ ;  $^1\text{H}$  NMR (500 MHz)  $\delta$  8.30 (dd,  $J$  = 7.7, 1.7 Hz, 1H), 8.10 (s, 1H), 7.68–7.65 (m, 1H), 7.56 (d,  $J$  = 16.3 Hz, 1H), 7.46 (d,  $J$  = 8.0 Hz, 2H), 7.42 (t,  $J$  = 7.7 Hz, 1H), 6.90 (d,  $J$  = 8.2 Hz, 2H), 6.87 (d,  $J$  = 16.4 Hz, 1H);  $^{13}\text{C}$  NMR (125 MHz)  $\delta$  177.1, 159.7, 156.3, 152.9, 133.8, 131.6, 130.6, 128.3, 126.7, 125.6, 124.3, 122.6, 118.5, 117.2, 114.5, 55.7; MS [APCI (+)]  $m/z$  (%) 279.0 ( $\text{M}^+$ , 100); HRMS [EI (+)] calcd for  $\text{C}_{18}\text{H}_{14}\text{O}_3$  278.0943, found 278.0946.

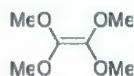
#### Dimethoxymethyl acetate (**2.43**)<sup>21a</sup>



To a mixture of acetic anhydride (**2.40**) (104 mL, 1.10 mol) and formic acid (**2.41**) (51.0 mL, 1.20 mol) was added trimethyl orthoformate (**2.42**) (110 mL, 1.00 mol). The colorless reaction mixture was stirred at room temperature for 24 h, followed by slow distillation under reduced pressures to remove all volatile side-products. The desired product **2.43** (59.1 g, 44%) was collected at 65–67 °C, 20 mmHg (lit. bp<sup>21a</sup> 69 °C, 35 mmHg) as a colorless liquid:  $^1\text{H}$  NMR (500 MHz)  $\delta$  6.20 (s, 1H), 3.42 (s, 6H), 2.11 (s, 3H);  $^{13}\text{C}$  NMR (125 MHz)  $\delta$  169.6, 109.4, 52.3, 21.2.

**Dimethoxy-4-chlorophenoxymethane (2.45)<sup>21b</sup>**

A mixture of dimethoxy methyl acetate (**2.43**) (37.2 g, 0.28 mol), 4-chlorophenol (**2.44**) (27.0 g, 0.21 mol), and *p*-toluenesulfonic acid (40.1 mg, 0.29 mmol) was heated with stirring at 40 °C for 4 h. After the side-product was removed under reduced pressure, the desired product **2.45** (36.1 g, 85%) was collected at 122–123 °C, 15 mmHg (lit.<sup>21b</sup> 122 °C, 13 mmHg) as a colorless liquid: <sup>1</sup>H NMR (500 MHz) δ 7.26–7.24 (m, 2H), 7.00–6.98 (m, 2H), 5.56 (s, 1H), 3.44 (s, 6H); <sup>13</sup>C NMR (125 MHz) δ 153.5, 129.6, 127.9, 119, 113.1, 51.5.

**Tetramethoxyethane (1.226)<sup>21c</sup>**

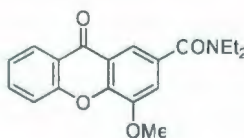
To a suspension of sodium hydride (15.2 g, 60% dispersion in mineral oil, 380 mmol) in tetraethyleneglycol dimethyl ether (120 mL) was added dropwise dimethoxy-4-chlorophenoxymethane (**2.45**) (65.0 g, 0.32 mol) over 1 h at room temperature. The resulting brown mixture was then heated with stirring at 95 °C for a further 19 h. The reaction mixture was cooled to room temperature and let to stand for 24 h. The precipitates were filtered off by suction filtration and washed with pentane (3 x 20 mL). The desired product **1.226** (14.2 g, 30%) was collected at 50–51 °C, 12 mm Hg (lit.<sup>21c</sup>

46–49 °C, 12 mmHg) as a colorless liquid:  $^1\text{H}$  NMR (500 MHz)  $\delta$  3.60 (s, 12H);  $^{13}\text{C}$  NMR (125 MHz)  $\delta$  140.9, 58.2; GCMS  $m/z$  (%) 149 ( $\text{M}^+$ , 30), 105 (90), 75 (100).

#### General procedure for synthesis of 4-methoxyxanthenes (1.228a–i)

A mixture of aqueous 60% dimethoxyacetaldehyde (**2.41**) (3.02 mL, 20.0 mmol) and pyrrolidine (1.65 mL, 20.0 mmol) in benzene (40 mL) was heated at reflux with a Barrett apparatus for 3 h. The freshly prepared 1-(2,2-dimethoxyvinyl)pyrrolidine (**1.225**) in benzene (20–25 mL) was cooled to room temperature, and the diene **1.15a–i** (1.1–2.5 mmol) was added in one portion. The resulting orange mixture was heated at reflux until the diene was consumed completely (tlc analysis). The reaction mixture was cooled to room temperature and the solvent was removed under reduced pressure. The residue was dissolved in  $\text{CH}_2\text{Cl}_2$ , washed with aqueous 1 M HCl solution (2 x 20 mL), dried over  $\text{MgSO}_4$ , and filtered. The solvent was removed under reduced pressure and the residue was purified by chromatography to yield the desired xanthenes **1.228a–i**.

#### *N,N*-Diethyl-4-methoxy-9-oxo-9*H*-xanthene-2-carboxamide (**1.228a**)

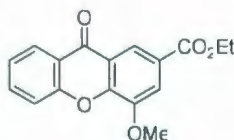


A mixture of enamine **1.225** and diene **1.15a** (499 mg, 1.84 mmol) was heated at reflux for 16 h and worked up according to the general procedure. Column chromatography (10:90 EtOAc: $\text{CH}_2\text{Cl}_2$ ) yielded xanthone **1.228a** (299 mg, 50%) as a yellow solid:  $R_f$  = 0.50 (50:50 EtOAc:  $\text{CH}_2\text{Cl}_2$ ); mp 105–106 °C; IR  $\nu$  2965 (w), 2934 (w), 2842 (w), 1653 (s), 1628 (s), 1598 (s), 1573 (m), 1468 (s), 1459 (s), 1434 (s), 1314

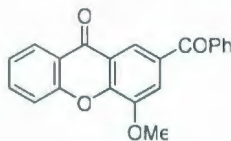


(m), 1287 (s), 1264 (s), 1165 (s), 1091 (s), 981 (m), 867 (m), 830 (m), 755 (s), 723 (m) ( $\text{cm}^{-1}$ );  $^1\text{H}$  NMR (500 MHz)  $\delta$  8.34 (dd,  $J = 8.3, 1.6$  Hz, 1H), 7.92 (d,  $J = 1.1$  Hz, 1H), 7.78–7.75 (m, 1H), 7.63 (d,  $J = 9.1$  Hz, 1H), 7.42 (t,  $J = 7.3$  Hz, 1H), 7.35 (d,  $J = 2.4$  Hz, 1H), 4.07 (s, 3H), 3.58 (br s, 2H), 3.38 (br s, 2H), 1.26–1.22 (br m, 6H);  $^{13}\text{C}$  NMR (125 MHz)  $\delta$  177.0, 170.1, 156.1, 149.4, 147.2, 135.3, 132.5, 126.9, 124.7, 122.1, 121.8, 118.6, 115.4, 114.5, 56.8, 43.9, 39.9, 14.5, 13.1; MS [APCI (+)]  $m/z$  (%) 326 ( $\text{M}^+$ , 100); HRMS [EI (+)] calcd for  $\text{C}_{19}\text{H}_{19}\text{NO}_4$  325.1314, found 325.1318.

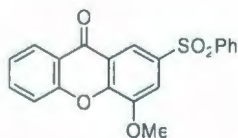
**Ethyl-4-methoxy-9-oxo-9H-xanthene-2-carboxylate (1.228b)**



A mixture of enamine **1.225** and diene **1.15b** (488 mg, 2.00 mmol) was heated at reflux for 2 h and worked up according to the general procedure. Column chromatography (10:90 EtOAc:hexanes) yielded xanthone **1.228b** (423 mg, 71%) as a yellow solid:  $R_f = 0.50$  (35:65 EtOAc:hexanes); mp 184–186 °C (methanol); IR  $\nu$  2986 (w), 2838 (w), 1715 (s), 1669 (s), 1600 (s), 1575 (s), 1493 (s), 1465 (s), 1290 (s), 1226 (s), 1187 (s), 1088 (s), 990 (s), 941 (s), 758 (s) ( $\text{cm}^{-1}$ );  $^1\text{H}$  NMR (500 MHz)  $\delta$  8.63 (s, 1H), 8.36 (d,  $J = 8.2$  Hz, 1H), 7.89 (s, 1H), 7.77 (t,  $J = 7.7$  Hz, 1H), 7.63 (d,  $J = 8.4$  Hz, 1H), 7.43 (t,  $J = 7.5$  Hz, 1H), 4.44 (q,  $J = 7.0$  Hz, 2H), 4.10 (s, 3H), 1.45 (t,  $J = 7.1$  Hz, 3H);  $^{13}\text{C}$  NMR (125 MHz)  $\delta$  176.6, 165.7, 155.8, 149.3, 148.8, 135.2, 126.8, 125.9, 124.7, 122.1, 121.7, 120.1, 118.4, 115.2, 61.5, 56.6, 14.4; MS [APCI (+)]  $m/z$  (%) 299 ( $\text{M}^+$ , 100); HRMS [EI (+)] calcd for  $\text{C}_{17}\text{H}_{14}\text{O}$  298.0841, found 298.0845.

**2-Benzoyl-4-methoxy-9H-xanthen-9-one (1.228c)**

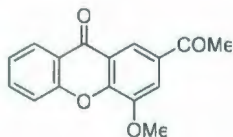
A mixture of enamine **1.225** and diene **1.15c** (552 mg, 2.00 mmol) was heated at reflux for 6.5 h and worked up according to the general procedure. Column chromatography (15:85 EtOAc:hexanes) yielded xanthone **1.228c** (562 mg, 85%) as a yellow solid:  $R_f$  = 0.30 (35:65 EtOAc:hexanes); mp 224–225 °C (CH<sub>3</sub>CN-acetone); IR  $\nu$  2976 (w), 2938 (w), 1656 (s), 1596 (s), 1571 (s), 1493 (s), 1466 (s), 1384 (s), 1327 (s), 1283 (s), 1231 (s), 1121 (s), 1090 (s), 973 (s), 878 (s), 832 (s), 752 (s), 726 (s), 685 (s) (cm<sup>-1</sup>); <sup>1</sup>H NMR (500 MHz)  $\delta$  8.34 (dd,  $J$  = 7.6, 1.3 Hz, 1H), 8.27 (d,  $J$  = 2.1 Hz, 1H), 7.86–7.83 (m, 3H), 7.80–7.77 (m, 1H), 7.67–7.62 (m, 2H), 7.53 (t,  $J$  = 7.7 Hz, 2H), 7.44 (t,  $J$  = 8.2 Hz, 1H), 4.13 (s, 3H); <sup>13</sup>C NMR (125 MHz)  $\delta$  195.4, 176.8, 156.0, 149.6, 149.5, 137.5, 135.4, 132.9, 132.8, 130.2, 128.7, 126.9, 125.0, 121.9, 121.8, 121.7, 118.6, 115.2, 56.9; MS [APCI (+)]  $m/z$  (%) 331 (M<sup>+</sup>, 100); HRMS [EI (+)] calcd for C<sub>21</sub>H<sub>14</sub>O<sub>4</sub> 330.0892, found 330.0895.

**4-Methoxy-2-(phenylsulfonyl)-9H-xanthen-9-one (1.228d)**

A mixture of enamine **1.225** and diene **1.15d** (0.310 g, 1.00 mmol) was heated at reflux for 16 h and worked up according to the general procedure. Column chromatography (20:80 EtOAc:hexanes) yielded xanthone **1.228d** (256 mg, 70%) as a

yellow solid:  $R_f = 0.45$  (50:50 EtOAc:hexanes); mp 242–243 °C (CHCl<sub>3</sub>-acetone); IR  $\nu$  3069 (w), 2945 (w), 2843 (w), 1656 (s), 1589 (m), 1570 (m), 1489 (m), 1466 (s), 1443 (s), 1324 (s), 1309 (s), 1270 (s), 1145 (s), 1099 (s), 1085 (s), 981 (s), 913 (s), 859 (s), 767 (s), 759 (s), 737 (s), 713 (s), 692 (s) (cm<sup>-1</sup>); <sup>1</sup>H NMR (500 MHz)  $\delta$  8.48 (d,  $J = 2.0$  Hz, 1H), 8.31 (dd,  $J = 7.9, 1.5$  Hz, 1H), 8.01 (d,  $J = 7.2$  Hz, 2H), 7.79–7.75 (m, 1H), 7.72 (d,  $J = 2.1$  Hz, 1H), 7.59 (t,  $J = 8.6$  Hz, 2H), 7.53 (t,  $J = 7.6$  Hz, 2H), 7.43 (t,  $J = 7.5$  Hz, 1H), 4.09 (s, 3H); <sup>13</sup>C NMR (125 MHz)  $\delta$  176.1, 155.9, 149.9, 149.4, 141.4, 137.2, 135.7, 133.7, 129.7, 128.0, 127.0, 125.3, 122.8, 121.7, 118.9, 118.6, 112.6, 57.1; MS [APCI (+)]  $m/z$  (%) 367 (M<sup>+</sup>, 100); HRMS [EI (+)] calcd for C<sub>20</sub>H<sub>14</sub>O<sub>5</sub>S 366.0562, found 366.0571.

#### 2-Ethanoyl-4-methoxy-9H-xanthen-9-one (1.228e)

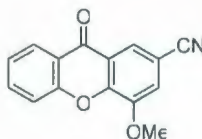


A mixture of enamine **1.225** and diene **1.15c** (428 mg, 2.00 mmol) was heated at reflux for 6 h and worked up according to the general procedure. Column chromatography (15:85 EtOAc:hexanes) yielded xanthone **1.228e** (483 mg, 90%) as a yellow solid:  $R_f = 0.40$  (50:50 EtOAc:hexanes); mp 207–208 °C (acetone-hexanes); IR  $\nu$  2964 (m), 1686 (m), 1662 (m), 1590 (m), 1570 (m), 1488 (m), 1464 (s), 1261 (s), 1220 (s), 1087 (s), 1021 (s), 982 (m), 881 (s), 803 (s), 757 (s), 668 (s) (cm<sup>-1</sup>); <sup>1</sup>H NMR (500 MHz)  $\delta$  8.51 (d,  $J = 1.8$  Hz, 1H), 8.37 (dd,  $J = 7.9, 1.5$  Hz, 1H), 7.88 (d,  $J = 2.0$  Hz, 1H), 7.81–7.77 (m, 1H), 7.66 (d,  $J = 8.3$  Hz, 1H), 7.46 (t,  $J = 7.5$  Hz, 1H), 4.10 (s, 3H), 2.73 (s, 3H); <sup>13</sup>C NMR (125 MHz)  $\delta$  197.0, 176.9, 156.0, 149.9, 149.5, 135.5, 132.7, 127.0,

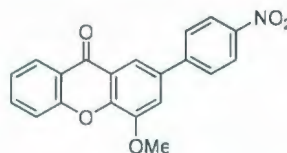


125.0, 122.1, 121.8, 119.9, 118.7, 113.1, 56.8, 26.6; MS [APCI (+)]  $m/z$  (%) 269 ( $M^+$ , 100); HRMS [EI (+)] calcd for  $C_{16}H_{12}O_4$  268.0736, found 268.0747.

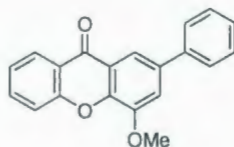
**4-Methoxy-9-oxo-9H-xanthene-2-carbonitrile (1.228f)**



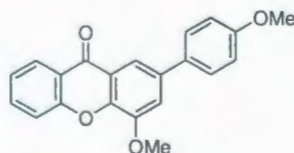
A mixture of enamine **1.225** and diene **1.15f** (493 mg, 2.50 mmol) was heated at reflux for 2 h and worked up according to the general procedure. Column chromatography (20:80 EtOAc:hexanes) yielded xanthone **1.228f** (528 mg, 84%) as a light yellow solid:  $R_f$  = 0.50 (50:50 EtOAc:hexanes); mp 278–279 °C ( $CH_3CN$ ); IR  $\nu$  3083 (w), 2945 (w), 2230 (s), 1669 (s), 1593 (s), 1570 (s), 1490 (s), 1463 (s), 1375 (s), 1323 (s), 1289 (s), 1230 (s), 1137 (s), 1085 (s), 997 (s), 939 (s), 883 (s), 873 (s), 866 (s), 760 (s), 687 (m) ( $cm^{-1}$ );  $^1H$  NMR (500 MHz)  $\delta$  8.34 (dd,  $J$  = 7.8, 1.6 Hz, 1H), 8.26 (d,  $J$  = 2.4 Hz, 1H), 7.82–7.78 (m, 1H), 7.64 (d,  $J$  = 8.0 Hz, 1H), 7.47 (t,  $J$  = 8.1 Hz, 1H), 7.37 (d,  $J$  = 1.2 Hz, 1H), 4.08 (s, 3H);  $^{13}C$  NMR (125 MHz)  $\delta$  175.7, 156.0, 149.8, 149.3, 135.9, 127.1, 125.4, 123.7, 123.1, 121.8, 118.7, 118.2, 116.6, 107.7, 57.0; MS [APCI (+)]  $m/z$  (%) 252 ( $M^+$ , 100); HRMS [EI (+)]  $m/z$  (%) calcd for  $C_{15}H_9NO_3$  251.0582, found 251.0587.

**4-Methoxy-2-(4-nitrophenyl)-9H-xanthen-9-one (1.228g)**

A mixture of enamine **1.225** and diene **1.15g** (498 mg, 1.70 mmol) was heated at reflux for 2 h and worked up according to the general procedure. Column chromatography (80:20 CH<sub>2</sub>Cl<sub>2</sub>:hexanes) yielded xanthone **1.228g** (413 mg, 70%) as a yellow solid:  $R_f$  = 0.35 (70:30 CH<sub>2</sub>Cl<sub>2</sub>:hexanes); mp > 300 °C; IR  $\nu$  2925 (w), 2851 (w), 1665 (s), 1594 (m), 1573 (s), 1512 (s), 1467 (s), 1341 (s), 1289 (s), 1222 (s), 1143 (s), 1094 (s), 1064 (m), 979 (s), 850 (s), 845 (s), 759 (s) (cm<sup>-1</sup>); <sup>1</sup>H NMR (500 MHz)  $\delta$  8.39–8.37 (m, 1H), 8.35 (d,  $J$  = 8.5 Hz, 2H), 8.19 (d,  $J$  = 2.6 Hz, 1H), 7.85 (d,  $J$  = 8.8 Hz, 2H), 7.79–7.77 (m, 1H), 7.66 (d,  $J$  = 7.9 Hz, 1H), 7.47 (d,  $J$  = 1.6 Hz, 1H), 7.43 (d,  $J$  = 7.7 Hz, 1H), 4.15 (s, 3H); <sup>13</sup>C NMR (150 MHz) {<sup>1</sup>H} CPMAS (cross-polarization under magic angle spinning), using 100 kHz of <sup>1</sup>H decoupling and 62.5 kHz for the Hartmann-Hahn matching condition. The spectrum was collected at room temperature (298 K) with a spinning rate  $\nu$  = 20 kHz and 10240 scans:  $\delta$  173.9, 153.3, 148.2, 145.5, 144.3, 132.8, 131.9, 131.4, 125.5, 124.3, 121.3, 121.0, 119.6, 116.4, 110.0, 55.6 (two signals fewer than expected); MS [APCI (+)]  $m/z$  (%) 348 (M<sup>+</sup>, 100); HRMS [EI (+)] calcd for C<sub>20</sub>H<sub>13</sub>NO<sub>5</sub> 347.0794, found 347.0793.

**4-Methoxy-2-phenyl-9H-xanthen-9-one (1.228h)**

A mixture of enamine **1.225** and diene **1.15h** (496 mg, 2.00 mmol) was heated at reflux for 17 h and worked up according to the general procedure. Column chromatography (2:98 CH<sub>2</sub>Cl<sub>2</sub>:hexanes) yielded xanthone **1.228h** (308 mg, 51%) as a yellow solid:  $R_f$  = 0.55 (35:65 EtOAc:hexanes); mp 162–163 °C; IR  $\nu$  2923 (w), 2873 (w), 1656 (s), 1598 (s), 1571 (m), 1465 (s), 1325 (s), 1288 (s), 1218 (s), 1095 (s), 917 (s), 867 (s), 753 (s), 696 (s) (cm<sup>-1</sup>); <sup>1</sup>H NMR (500 MHz)  $\delta$  8.37 (dd,  $J$  = 8.0, 1.6 Hz, 1H), 8.14 (d,  $J$  = 2.3 Hz, 1H), 7.77–7.73 (m, 1H), 7.68 (d,  $J$  = 8.0 Hz, 2H), 7.64 (d,  $J$  = 8.3 Hz, 1H), 7.50–7.47 (m, 3H), 7.42–7.38 (m, 2H), 4.11 (s, 3H); <sup>13</sup>C NMR (125 MHz)  $\delta$  177.4, 156.2, 149.2, 146.3, 140.1, 137.1, 135.0, 129.2, 128.0, 127.4, 127.0, 124.4, 123.0, 121.9, 118.5, 115.9, 114.8, 56.8; MS [APCI (+)]  $m/z$  (%) 303 ( $M^+$ , 100); HRMS [EI (+)] calcd for C<sub>20</sub>H<sub>14</sub>O<sub>3</sub> 302.0943, found 302.0959.

**4-Methoxy-2-(4-methoxyphenyl)-9H-xanthen-9-one (1.228i)**

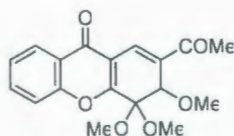
A mixture of enamine **1.225** and diene **1.15i** (301 mg, 1.08 mmol) was heated at reflux for 44 h and worked up according to the general procedure. Column chromatography (10:90 EtOAc:hexanes) yielded xanthone **1.228i** (140 mg, 39%) as a yellow solid:  $R_f$  = 0.50 (35:65 EtOAc:hexanes); mp 186–187 °C (CHCl<sub>3</sub>-hexanes); IR  $\nu$



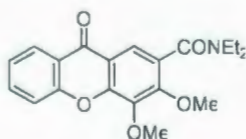
2942 (w), 2825 (w), 1653 (s), 1598 (s), 1578 (m), 1558 (m), 1490 (s), 1465 (s), 1366 (s), 1286 (s), 1219 (s), 1179 (s), 1028 (s), 979 (s), 820 (s), 793 (s), 751 (s), 683 (s) ( $\text{cm}^{-1}$ );  $^1\text{H}$  NMR (500 MHz)  $\delta$  8.36 (dd,  $J = 7.9, 1.8$  Hz, 1H), 8.08 (d,  $J = 2.6$  Hz, 1H), 7.76–7.73 (m, 1H), 7.64–7.60 (m, 3H), 7.43 (d,  $J = 2.8$  Hz, 1H), 7.40 (t,  $J = 7.6$  Hz, 1H), 7.03–7.00 (m, 2H), 4.10 (s, 3H), 3.87 (s, 3H);  $^{13}\text{C}$  NMR (125 MHz)  $\delta$  177.4, 159.7, 156.2, 149.1, 145.9, 136.7, 134.9, 132.6, 128.4, 126.9, 124.3, 123.0, 121.9, 118.5, 115.2, 114.6, 114.5, 56.8, 55.6; MS [APCI (+)]  $m/z$  (%) 333 ( $[\text{M}+\text{H}^+]$ , 100); HRMS [EI (+)] calcd for  $\text{C}_{21}\text{H}_{16}\text{O}_4$  332.1049, found 332.1063.

#### General procedure for synthesis of 3,4-dimethoxyxanthenes (1.229a–i)

To a clear, preheated (135 °C) solution of diene **1.15a–i** (1.00 mmol) in 1,1,2,2-tetrachloroethane (1 mL) was added tetramethoxyethane (**1.226**) (740 mg, 5.00 mmol). The reaction mixture was heated with stirring at 135 °C until the diene was completely consumed (tlc analysis). The reaction mixture was cooled to room temperature and diluted with  $\text{CH}_2\text{Cl}_2$  (10 mL). Boron trifluoride diethyl etherate ( $\text{BF}_3\cdot\text{Et}_2\text{O}$ ) (500  $\mu\text{L}$ , 4.00 mmol) was added and the resulting mixture was stirred at room temperature until the conversion was completed (tlc analysis). The reaction mixture was quenched by the addition of 10% aqueous  $\text{NaHCO}_3$  solution (15 mL). The layers were separated and the aqueous layer was extracted with  $\text{CH}_2\text{Cl}_2$  (3 x 15 mL). The combined organic layers were washed with brine (2 x 15 mL), dried over anhydrous  $\text{MgSO}_4$  and filtered. The solvent was removed under reduced pressure and the resulting residue was purified by column chromatography to yield xanthenes **1.229a–h**.

**2-Ethanoyl-3,4,4-trimethoxy-3H-xanthen-9(4H)-one (2.46c)**

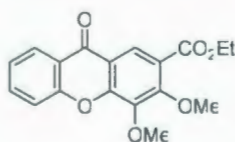
A mixture of TME (**1.226**) and diene **1.15e** (428 mg, 2.00 mmol) was heated at 135 °C without solvent for 10 h. The reaction mixture was cooled to room temperature, diluted with CH<sub>2</sub>Cl<sub>2</sub> (20 mL) and washed with 1 N HCl solution (2 x 10 mL). Column chromatography (20:80 EtOAc:hexanes) yielded **2.46c** (185 mg, 56%) as a colorless solid: *R<sub>f</sub>* = 0.50 (35:65 EtOAc:hexanes) or colorless crystal (148 mg, 45%, acetone-hexanes); mp 216–217 °C (acetone-hexanes); IR  $\nu$  2917 (w), 2837 (w), 1653 (s), 1610 (s), 1565 (s), 1466 (s), 1420 (s), 1262 (s), 1225 (s), 1198 (s), 1146 (s), 1100 (s), 1071 (s), 921 (s), 899 (s), 762 (s), 698 (s) (cm<sup>-1</sup>); <sup>1</sup>H NMR (500 MHz)  $\delta$  8.27 (dd, *J* = 7.5, 1.7 Hz, 1H), 7.88 (s, 1H), 7.74–7.71 (m, 1H), 7.63 (d, *J* = 7.8 Hz, 1H), 7.48 (t, *J* = 7.6 Hz, 1H), 4.73 (s, 1H), 3.60 (s, 3H), 3.33 (s, 3H), 3.23 (s, 3H), 2.53 (s, 3H); <sup>13</sup>C NMR (125 MHz)  $\delta$  197.7, 174.9, 163.4, 155.8, 135.0, 134.5, 131.1, 126.4, 123.7, 119.1, 115.3, 99.2, 70.2, 57.8, 51.2, 49.8, 25.4 (one signal fewer than expected); MS [APCI (+)] *m/z* (%) 331 (M<sup>+</sup>, 100); HRMS [EI (+)] calcd for C<sub>18</sub>H<sub>18</sub>O<sub>6</sub> 330.1103, found 330.1113.

***N,N*-Diethyl-3,4-dimethoxy-9-oxo-9H-xanthene-2-carboxamide (1.229a)**

Diene **1.15a** (271 mg, 1.00 mmol) was subjected to the general procedure (8 d heating). Column chromatography (20:80 EtOAc:CH<sub>2</sub>Cl<sub>2</sub>) of the crude product yielded

xanthone **1.229a** (142 mg, 40% (48% borsm: 17% recovery of diene **1.15a**)) as a yellow solid:  $R_f = 0.55$  (EtOAc); mp 97–98 °C; IR  $\nu$  2971 (w), 2935 (w), 1660 (s), 1633 (s), 1600 (s), 1463 (s), 1417 (s), 1348 (s), 1312 (s), 1289 (s), 1220 (s), 1147 (s), 1058 (s), 886 (s), 756 (s) ( $\text{cm}^{-1}$ );  $^1\text{H}$  NMR (500 MHz)  $\delta$  8.33 (dd,  $J = 8.05, 1.35$  Hz, 1H), 7.95 (s, 1H), 7.77–7.73 (m, 1H), 7.58 (d,  $J = 7.8$  Hz, 1H), 7.41 (t,  $J = 7.6$  Hz, 1H), 4.10 (s, 3H), 4.09 (s, 3H), 3.59–3.56 (m, 2H), 3.21–3.17 (m, 2H), 1.28 (t,  $J = 7.0$  Hz, 3H), 1.08 (t,  $J = 6.8$  Hz, 3H);  $^{13}\text{C}$  NMR (125 MHz)  $\delta$  176.2, 167.2, 156.2, 154.3, 151.4, 140.8, 135.0, 128.4, 126.9, 124.6, 121.7, 119.6, 118.6, 118.2, 62.1, 61.9, 43.3, 39.3, 14.2, 13.0; MS [APCI (+)]  $m/z$  (%) 356 ( $\text{M}^+$ , 100); HRMS [EI (+)] calcd for  $\text{C}_{20}\text{H}_{21}\text{NO}_5$  355.1420 found 355.1412.

**Ethyl 3,4-dimethoxy-9-oxo-9H-xanthene-2-carboxylate (1.229b)**

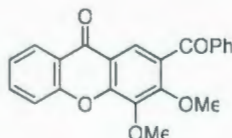


Diene **1.15b** (244 mg, 1.00 mmol) was subjected to the general procedure (2 d heating). Column chromatography (10:90 EtOAc:hexanes) of the crude product yielded xanthone **1.229b** (230 mg, 70%) as a yellow solid:  $R_f = 0.55$  (35:65 EtOAc:hexanes); mp 125–126 °C; IR  $\nu$  2988 (w), 2840 (w), 1714 (s), 1671 (s), 1600 (s), 1456 (s), 1438 (s), 1340 (s), 1285 (s), 1218 (s), 1058 (s), 889 (s), 749 (s), 700 (m) ( $\text{cm}^{-1}$ );  $^1\text{H}$  NMR (500 MHz)  $\delta$  8.55 (s, 1H), 8.34 (dd,  $J = 7.9, 1.9$  Hz, 1H), 7.78–7.75 (m, 1H), 7.59 (d,  $J = 7.9$  Hz, 1H), 7.43 (t,  $J = 7.6$  Hz, 1H), 4.42 (q,  $J = 7.1$  Hz, 2H), 4.10 (s, 3H), 4.01 (s, 3H), 1.43 (t,  $J = 7.1$  Hz, 3H);  $^{13}\text{C}$  NMR (125 MHz)  $\delta$  176.3, 165.0, 158.0, 156.2, 153.1, 142.2,



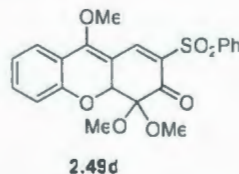
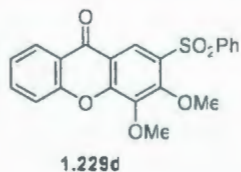
135.3, 127.1, 124.9, 124.7, 122.7, 121.8, 118.4, 62.4, 62.1, 61.6, 14.5 (one signal fewer than expected); MS [APCI (+)]  $m/z$  (%) 329 ( $M^+$ , 100); HRMS [EI (+)] calcd for  $C_{18}H_{16}O_6$  328.0947, found 328.0952.

**2-Benzoyl-3,4-dimethoxy-9H-xanthen-9-one (1.229c)**



Diene **1.15c** (276 mg, 1.00 mmol) was subjected to the general procedure (26 h heating). Column chromatography (10:90 EtOAc:hexanes) of the crude product yielded xanthone **1.229c** (324 mg, 90%) as a yellow solid:  $R_f$  = 0.55 (35:65 EtOAc:hexanes); mp 156–157 °C; IR  $\nu$  2943 (w), 2844 (w), 1654 (s), 1596 (s), 1464 (m), 1416 (s), 1318 (s), 1286 (s), 1250 (m), 1223 (m), 1115 (s), 1072 (s), 759 (s), 729 (s), 704 (s), 668 (s) ( $cm^{-1}$ );  $^1H$  NMR (500 MHz)  $\delta$  8.33 (dd,  $J$  = 8.2, 2.0 Hz, 1H), 8.11 (s, 1H), 7.85–7.83 (m, 2H), 7.79–7.76 (m, 1H), 7.62–7.59 (m, 2H), 7.48 (t,  $J$  = 7.7 Hz, 2H), 7.43 (t,  $J$  = 7.6 Hz, 1H), 4.11 (s, 3H), 3.96 (s, 3H);  $^{13}C$  NMR (125 MHz)  $\delta$  194.5, 176.3, 156.4, 156.2, 152.5, 141.0, 137.5, 135.2, 133.7, 130.14, 130.08, 128.7, 127.0, 124.8, 122.4, 121.8, 118.4, 118.2, 62.2, 62.1; MS [APCI (+)]  $m/z$  (%) 361 ( $M^+$ , 100); HRMS [EI (+)] calcd for  $C_{22}H_{16}O_5$  360.0998, found 360.1007.

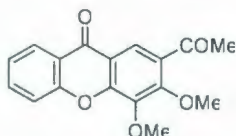
**3,4-Dimethoxy-2-(phenylsulfonyl)-9H-xanthen-9-one (1.229d) and 4,4,9-trimethoxy-2-(phenylsulfonyl)-4,4a-dihydro-3H-xanthen-3-one (2.49d)**



Diene **1.15d** (312 mg, 1.00 mmol) was subjected to the general procedure (4 h heating). Column chromatography (2:98 EtOAc:CH<sub>2</sub>Cl<sub>2</sub>) of the crude product yielded xanthone **1.229d** (71.4 mg, 18%) as a yellow solid:  $R_f$  = 0.55 (2:98 EtOAc:CH<sub>2</sub>Cl<sub>2</sub>); mp 186–188 °C; IR  $\nu$  3089 (w), 2951 (w), 2846 (w), 1665 (s), 1582 (s), 1560 (s), 1483 (s), 1412 (s), 1316 (s), 1263 (s), 1147 (s), 1090 (s), 1041 (s), 951 (s), 768 (s), 753 (s), 743 (s), 686 (s) (cm<sup>-1</sup>); <sup>1</sup>H NMR (500 MHz)  $\delta$  8.91 (s, 1H), 8.35 (dd,  $J$  = 7.9, 1.7 Hz, 1H), 8.01–8.00 (m, 2H), 7.79–7.75 (m, 1H), 7.62–7.51 (m, 4H), 7.47–7.44 (m, 1H), 4.01 (s, 3H), 3.95 (s, 3H); <sup>13</sup>C NMR (125 MHz)  $\delta$  175.6, 156.0, 155.3, 154.7, 141.9, 141.5, 135.5, 133.5, 131.4, 129.1, 128.6, 127.2, 125.3, 123.7, 121.8, 118.3, 118.1, 62.1, 61.9; MS [APCI (+)]  $m/z$  (%) 397 (M<sup>+</sup>, 100); HRMS [EI (+)] calcd for C<sub>21</sub>H<sub>16</sub>O<sub>6</sub> 396.0668, found 396.0668; and a byproduct **2.49d** (42.9 mg, 10%) as a yellow solid:  $R_f$  = 0.52 (2:98 EtOAc:CH<sub>2</sub>Cl<sub>2</sub>); mp 234–235 °C; IR  $\nu$  3047 (w), 2990 (w), 2839 (w), 1695 (s), 1612 (s), 1545 (s), 1449 (s), 1368 (s), 1311 (s), 1275 (s), 1158 (s), 1111 (s), 1081 (s), 964 (s), 862 (s), 767 (s), 748 (s), 688 (s) (cm<sup>-1</sup>); <sup>1</sup>H NMR (500 MHz)  $\delta$  8.65 (s, 1H), 8.09 (d,  $J$  = 7.6 Hz, 2H), 7.59 (t,  $J$  = 7.6 Hz, 2H), 7.52–7.48 (m, 3H), 7.40–7.37 (m, 1H), 7.08 (t,  $J$  = 7.6 Hz, 1H), 7.02 (d,  $J$  = 7.6 Hz, 1H), 5.18 (s, 1H), 4.08 (s, 3H), 3.63 (s, 3H), 3.08 (s, 3H); <sup>13</sup>C NMR (125 MHz)  $\delta$  185.1, 161.5, 157.1, 141.7, 140.4, 134.0, 133.8, 131.9, 129.3,

129.0, 124.9, 123.0, 118.4, 118.1, 111.9, 97.0, 63.7, 52.9, 52.0 (one signal fewer than expected); MS [APCI (+)]  $m/z$  (%) 429 ( $M^+$ , 2), 397 ( $M^+ - \text{OMe}$ , 100); HRMS [EI (+)] calcd 428.0930 for  $\text{C}_{22}\text{H}_{20}\text{O}_7$  found 428.0930.

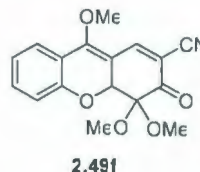
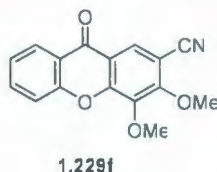
**2-Ethanoyl-3,4-dimethoxy-9H-xanthen-9-one (1.229e)**



Diene **1.15c** (214 mg, 1.00 mmol) was subjected to the general procedure (6 h heating). Column chromatography (20:80 EtOAc:hexanes) of the crude product yielded xanthone **1.229e** (292 mg, 98%) as a yellow solid:  $R_f$  = 0.55 (35:65 EtOAc:hexanes); mp 145–146 °C; IR  $\nu$  2947 (w), 2843 (w), 1676 (s), 1660 (s), 1593 (s), 1465 (s), 1414 (s), 1356 (s), 1330 (s), 1290 (s), 1086 (s), 1047 (s), 951 (s), 749 (s), 680 (m) ( $\text{cm}^{-1}$ );  $^1\text{H}$  NMR (500 MHz)  $\delta$  8.43 (s, 1H), 8.33 (dd,  $J$  = 8.1, 1.6 Hz, 1H), 7.78–7.74 (m, 1H), 7.58 (d,  $J$  = 9.0 Hz, 1H), 7.43 (t,  $J$  = 7.6 Hz, 1H), 4.13 (s, 3H), 4.08 (s, 3H), 2.66 (s, 3H);  $^{13}\text{C}$  NMR (125 MHz)  $\delta$  198.2, 176.3, 157.1, 156.2, 153.3, 141.3, 135.3, 130.0, 127.1, 124.9, 123.4, 121.8, 118.4, 118.3, 62.0 (2C), 31.1; MS [APCI (+)]  $m/z$  (%) 299 ( $M^+$ , 100); HRMS [EI (+)] calcd for  $\text{C}_{17}\text{H}_{14}\text{O}_5$  298.0841, found 298.0842.



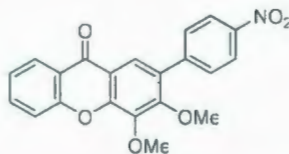
**3,4-Dimethoxy-9-oxo-9*H*-xanthene-2-carbonitrile (1.229f) and 4,4,9-trimethoxy-3-oxo-4,4a-dihydro-3*H*-xanthene-2-carbonitrile (2.49f)**



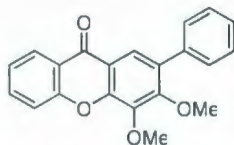
Diene **1.15f** (197 mg, 1.00 mmol) was subjected to the general procedure (24 h heating). Column chromatography (20:80 EtOAc:hexanes) of the crude product yielded xanthone **1.229f** (107 mg, 38%) as a yellow solid:  $R_f$  = 0.50 (20:80 EtOAc:hexanes); mp 187–188 °C; IR  $\nu$  2942 (w), 2841 (w), 2233 (s), 1672 (s), 1596 (s), 1562 (m), 1487 (m), 1453 (s), 1417 (s), 1352 (s), 1312 (s), 1214 (s), 1115 (s), 1069 (s), 865 (s), 754 (s), 668 (s) ( $\text{cm}^{-1}$ );  $^1\text{H}$  NMR (500 MHz)  $\delta$  8.35 (s, 1H), 8.33 (dd,  $J$  = 7.5, 1.9 Hz, 1H), 7.81–7.77 (m, 1H), 7.59 (d,  $J$  = 8.4 Hz, 1H), 7.47–7.44 (m, 1H), 4.26 (s, 3H), 4.09 (s, 3H);  $^{13}\text{C}$  NMR (125 MHz)  $\delta$  175.2, 158.4, 156.0, 154.1, 140.6, 135.7, 127.8, 127.1, 125.3, 121.6, 118.7, 118.4, 115.4, 103.3, 62.4, 62.2; MS [APCI (+)]  $m/z$  (%) 282 ( $\text{M}^+$ , 100); HRMS [CI (+)] calcd for  $\text{C}_{16}\text{H}_{11}\text{NO}_4 + \text{H}^+$  281.0766, found 282.0768; and a byproduct **2.49f** (12.5 mg, 4%) as a yellow solid:  $R_f$  = 0.47 (20:80 EtOAc:hexanes); mp 202–203 °C; IR  $\nu$  2942 (w), 2841 (w), 2225 (s), 1682 (s), 1598 (s), 1556 (m), 1478 (m), 1456 (m), 1332 (s), 1294 (s), 1117 (s), 1094 (s), 1080 (s), 1045 (s), 967 (s), 898 (s), 778 (s) ( $\text{cm}^{-1}$ );  $^1\text{H}$  NMR (500 MHz)  $\delta$  8.13 (s, 1H), 7.47 (d,  $J$  = 8.40 Hz, 1H), 7.41 (t,  $J$  = 8.05 Hz, 1H), 7.09 (t,  $J$  = 7.55 Hz, 1H), 7.05 (d,  $J$  = 8.2 Hz, 1H), 5.31 (s, 1H), 4.03 (s, 3H), 3.72 (s, 3H), 3.33 (s, 3H);  $^{13}\text{C}$  NMR (125 MHz)  $\delta$  185.8, 160.4, 157.0, 145.5, 134.2, 125.0, 123.1, 118.2, 118.0, 115.2, 113.4, 106.8, 96.7, 63.8, 53.0, 52.3 (one signal fewer than expected); MS

[APCI (+)]  $m/z$  (%)  $M^+$  not observed, 282 ( $M^+ - \text{OMe}$ , 100); HRMS [EI (+)] calcd for  $\text{C}_{17}\text{H}_{15}\text{NO}_5$  313.0950, found 313.0950.

**3,4-Dimethoxy-2-(4-nitrophenyl)-9H-xanthen-9-one (1.229g)**



A mixture of TME (**1.226**) and diene **1.15g** (190 mg, 0.64 mmol) was heated at 135 °C without solvent for 23 h. The reaction was cooled to room temperature and diluted with  $\text{CH}_2\text{Cl}_2$  (10 mL).  $\text{BF}_3 \cdot \text{Et}_2\text{O}$  (4.0 equiv.) was added and the mixture was stirred at room temperature for 5 h and worked up according to the general procedure. Column chromatography (2:98 EtOAc: $\text{CH}_2\text{Cl}_2$ ) of the crude product yielded xanthone **1.229g** (60.4 mg, 25% (31% borsm: 20% recovery of diene **1.15g**)) as a yellow solid:  $R_f$  = 0.55 (2:98 EtOAc: $\text{CH}_2\text{Cl}_2$ ); mp 214–215 °C (acetone); IR  $\nu$  2951 (w), 2843 (w), 1665 (s), 1600 (s), 1514 (s), 1456 (s), 1343 (s), 1312 (s), 1292 (s), 1227 (s), 1089 (s), 1039 (s), 980 (s), 844 (s), 760 (s), 753 (s), 748 (s), 705 (s) ( $\text{cm}^{-1}$ );  $^1\text{H}$  NMR (500 MHz)  $\delta$  8.36 (dd,  $J$  = 7.7, 1.7 Hz, 1H), 8.33–8.30 (m, 2H), 8.12 (s, 1H), 7.79–7.75 (m, 3H), 7.61 (d,  $J$  = 8.0 Hz, 1H), 7.45–7.42 (m, 1H), 4.14 (s, 3H), 3.91 (s, 3H);  $^{13}\text{C}$  NMR (125 MHz)  $\delta$  176.5, 156.3, 155.7, 151.4, 147.4, 143.9, 141.5, 135.2, 130.5, 130.0, 127.1, 124.7, 123.7, 122.8, 121.8, 118.9, 118.4, 62.2, 61.7; MS [APCI (+)]  $m/z$  (%) 378 ( $M^+$ , 100); HRMS [EI (+)] calcd for  $\text{C}_{21}\text{H}_{15}\text{NO}_6$  377.0899, found 377.0896.

**3,4-Dimethoxy-2-phenyl-9H-xanthene-9-one (1.229h)**

Diene **1.15h** (248 mg, 1.00 mmol) was subjected to the general procedure (10 h heating). Column chromatography (80:20 CH<sub>2</sub>Cl<sub>2</sub>:hexanes) of the crude product yielded xanthone **1.229h** (19.3 mg, 6%) as a yellow solid: *R<sub>f</sub>* = 0.40 (80:20 CH<sub>2</sub>Cl<sub>2</sub>:hexanes); mp 115–117 °C; IR  $\nu$  2933 (w), 2847 (w), 1662 (s), 1600 (s), 1465 (s), 1453 (s), 1413 (s), 1354 (s), 1291 (s), 1226 (s), 1086 (s), 1039 (s), 1021 (s), 952 (s), 895 (s), 756 (s), 710 (s) (cm<sup>-1</sup>); <sup>1</sup>H NMR (500 MHz)  $\delta$  8.35 (d, *J* = 7.9 Hz, 1H), 8.09 (s, 1H), 7.75 (t, *J* = 8.0 Hz, 1H), 7.61–7.57 (m, 3H), 7.50–7.37 (m, 4H), 4.12 (s, 3H), 3.85 (s, 3H); <sup>13</sup>C NMR (125 MHz)  $\delta$  156.3, 156.1, 150.6, 141.4, 137.2, 134.9, 132.6, 129.6, 128.5, 127.8, 127.0, 124.4, 122.7, 121.9, 118.8, 118.3, 62.1, 61.5 (one signal fewer than expected); MS [APCI (+)] *m/z* (%) 333 (*M*<sup>+</sup>, 100); HRMS [EI (+)] calcd for C<sub>21</sub>H<sub>16</sub>O 332.1049, found 332.1055.

**2.4.2 UV and Fluorescence Measurements**

Solutions of xanthenes **1.228a–i** and **1.229a–h** in CHCl<sub>3</sub> were prepared with concentration around 2 × 10<sup>-5</sup> M. As absorption and emission spectra of de-aerated solutions (5 min by a vigorous N<sub>2</sub> purge) and non-deaerated solutions were identical, the deaeration was excluded from the experiments for simplification. UV and fluorescence of all samples were measured in the same range of absorbance (0.9 < *A* < 1.2).



Concentrations of all samples were normalized. Extinction coefficients ( $\epsilon$ ) were calculated by using equation (1).

$$A = \epsilon lc \quad (1)$$

( $A$  is absorbance;  $l$  is the optical path length;  $c$  is concentration)

The excitation wavelengths ( $\lambda_{\text{ex}} = \lambda_{\text{max}}^{\text{asb}} + 20$ ) were applied for all compounds. Emission data were corrected (multiple with the correction factors of the instrument). Emission quantum yields ( $\Phi_{\text{em}}$ ) were measured in optically dilute ( $A < 0.1$  at 350 nm) solutions ( $\text{CHCl}_3$  for sample and aqueous 0.1 M  $\text{H}_2\text{SO}_4$  for quinine bisulfate, a standard). The emission quantum yields were calculated by using equation (2).<sup>36</sup>

$$\Phi_{\text{em}}^{\text{u}} = \Phi_{\text{em}}^{\text{std}} \left( \frac{A^{\text{std}}}{A^{\text{u}}} \right) \left( \frac{I^{\text{u}}}{I^{\text{std}}} \right) \left( \frac{n_{\text{D}}^{\text{u}}}{n_{\text{D}}^{\text{std}}} \right)^2 \quad (2)$$

$A$  is the absorbance of the sample at excitation wavelength (depending on absorbance of standard, 350 nm for quinine bisulfate).  $I$  is the integrated intensity of the emission band.  $n_{\text{D}}$  is the refractive index of the solvent (1.443 for  $\text{CHCl}_3$  and 1.333 for 0.1 M  $\text{H}_2\text{SO}_4$ , assumed equal to that of  $\text{H}_2\text{O}$ ). The superscripts u and std refer to the unknown sample and standard, respectively. The emission quantum yield ( $\Phi_{\text{em}}$ ) of quinine bisulfate is 0.54.

All measurements were carried out in the same cuvette (quartz) at room temperature. Spectra were plotted using Origin 7.5 software.

## UV/Vis and Fluorescence data of 1.228a-i

EWG	UV		Fluorescence		Quantum yield
	$\lambda_{\max}$ (nm)	$\epsilon$ (mol <sup>-1</sup> .L.cm <sup>-1</sup> )	$\lambda_{\max}$ (nm)	Intensity	
CONEt <sub>2</sub>	344	6,814	390	615,897	
	254	51,439	299	66,078	
CO <sub>2</sub> Et	337	5,674	380	244,287	
	254	53,376	300	46,553	
COPh	315	12,545	362	185,313	
	265	43,504	294	37,345	
COMe	337	1,415	380	245,287	
	309	11,238	363	133,872	
	262	58,563	295	38,487	
SO <sub>2</sub> Ph	343	7,328	380	288,977	
	299	9,452	357	148,035	
	257	57,238	301	62,257	
CN	346	7,936	386	413,502	
	299	9,068	357	239,171	
	253	72,410	299	86,600	
<i>p</i> -C <sub>6</sub> H <sub>4</sub> NO <sub>2</sub>	341	16,659	385	200,710	
	296	14,015	NA	NA	
	253	36,407	300	34,635	
Ph	354	6,222	426	12,829,500	0.072
	267	62,088	426	8,516,661	
<i>p</i> -C <sub>6</sub> H <sub>4</sub> OMe	361	4,928	462	29,399,386	0.130
	281	45,407	462	26,191,601	
	265	42,335	462	20,797,729	

## UV/Vis and Fluorescence data of 1.229a–h

EWG	UV		F		Quantum yield
	$\lambda_{\max}$ (nm)	$\epsilon$ (mol <sup>-1</sup> .L.cm <sup>-1</sup> )	$\lambda_{\max}$ (nm)	Intensity	
CONEt <sub>2</sub>	337	6,757	386	292,084	
	296	10,010	416	166,144	
	249	48,182	293	22,883	
CO <sub>2</sub> Et	336	3,027	377	263,474	
	254	32,780	297	72,717	
COPh	336	6,910	376	253,818	
	255	39,951	300	42,196	
COMe	337	6,849	377	455,026	
	260	61,348	300	128,435	
SO <sub>2</sub> Ph	334	5,559	373	406,415	
	256	67,401	295	113,976	
CN	336	6,193	374	403,819	
	255	76,622	298	101,770	
<i>p</i> -C <sub>6</sub> H <sub>4</sub> NO <sub>2</sub>	298	27,773	353	69,625	
	247	42,631	292	10,738	
Ph	341	4,317	413	1,272,229	0.0072
	258	30,505	298	216,598	

## 2.4.3 Crystallographic Data for 2.46e and 2.49d

X-ray crystallographic analysis for compounds **2.46e** and **2.49d** was performed by Dr. Louise N. Dawe, Memorial University. The text and data given below were taken from the reports provided by Dr. Dawe.



**2-Ethanoyl-3,4,4-trimethoxy-3*H*-xanthen-9(4*H*)-one (2.46e)**

A colorless prism, monoclinic crystal of  $C_{18}H_{18}O_6$  (formula weight 330.34) having approximate dimensions of 0.38 x 0.38 x 0.35 mm was mounted on a glass fiber. All measurements were made on a Rigaku Saturn CCD area detector with graphite monochromated Mo-K $\alpha$  radiation ( $\lambda = 0.71070$  Å). Indexing was performed from 360 images that were exposed for 13 seconds. The crystal-to-detector distance was 40.02 mm.

Cell constants and an orientation matrix for data collection corresponded to a primitive monoclinic cell with dimensions:  $a = 8.4566(7)$  Å,  $b = 10.6306(9)$  Å,  $\beta = 96.6446(16)^\circ$ ,  $c = 17.7943(16)$  Å,  $V = 1588.9(2)$  Å<sup>3</sup>. For  $Z = 4$  and F.W. = 330.34, the calculated density is 1.381 g/cm<sup>3</sup>. The systematic absences of:  $h0l: l \pm 2n$ ,  $0k0: k \pm 2n$  uniquely determine the space group to be:  $P2_1/c$  (#14).

The data were collected at a temperature of  $-120 \pm 1$  °C to a maximum  $2\theta$  value of  $61.6^\circ$ . A total of 720 oscillation images were collected. A sweep of data was done using  $\omega$  scans from  $-75.0$  to  $105.0^\circ$  in  $0.5^\circ$  step, at  $\chi = 0.0^\circ$  and  $\Phi = 0.0^\circ$ . The exposure rate was 26.0 [sec/°]. The detector swing angle was  $15.06^\circ$ . The crystal-to-detector distance was 40.02 mm. Readout was performed in the 0.137 mm pixel mode.

The final cycle of full-matrix least-squares refinement on  $F$  was based on 3628 observed reflections and 219 variable parameters and converged (largest parameter shift was 0.00 times its esd) with unweighted and weighted agreement factors of:  $R_1 = 0.0427$  and  $wR_2 = 0.1143$ . The standard deviation of an observation of unit weight was 1.064.

Unit weights were used. The maximum and minimum peaks on the final difference Fourier map corresponded to 0.29 and -0.21 e<sup>-</sup>/Å<sup>3</sup>, respectively.

**4,4,9-Trimethoxy-2-(phenylsulfonyl)-4,4a-dihydro-3H-xanthen-3-one (2.49d)**

A yellow prism crystal of C<sub>22</sub>H<sub>20</sub>O<sub>7</sub>S having approximate dimensions of 0.58 x 0.49 x 0.10 mm was mounted on a glass fiber. All measurements were made on a Rigaku Saturn CCD area detector with graphite monochromated Mo-Kα radiation. Indexing was performed from 360 images that were exposed for 20 seconds. The crystal-to-detector distance was 40.02 mm.

Cell constants and an orientation matrix for data collection corresponded to a primitive triclinic cell with dimensions:  $a = 9.2279(17)$  Å,  $\alpha = 87.802(9)^\circ$ ;  $b = 9.907(2)$  Å,  $\beta = 71.462(8)^\circ$ ;  $c = 11.199(2)$  Å,  $\gamma = 86.140(10)^\circ$ ;  $V = 968.4(3)$  Å<sup>3</sup>. For  $Z = 2$  and F.W. = 428.46, the calculated density is 1.469 g/cm<sup>3</sup>. Based on a statistical analysis of intensity distribution, and the successful solution and refinement of the structure, the space group was determined to be P-1 (#2).

The data were collected at a temperature of -160 ± 1 °C to a maximum 2θ value of 61.7°. A sweep of data was done using ω scans from -75.0 to 105.0° in 0.5° step, at  $\chi = 0.0^\circ$  and  $\theta = 0.0^\circ$ . The exposure rate was 40.0 [sec/°]. The detector swing angle was 15.22°. The detector swing angle was 15.22°. The crystal-to-detector distance was 40.02 mm. Readout was performed in the 0.137 mm pixel mode.

The final cycle of full-matrix least-squares refinement on F was based on 4433 observed reflections and 273 variable parameters and converged (largest parameter shift was 0.00 times its esd) with unweighted and weighted agreement factors of  $R_1 = 0.0505$

and  $wR_2 = 0.1192$ . The standard deviation of an observation of unit weight was 1.11. Unit weights were used. The maximum and minimum peaks on the final difference Fourier map corresponded to 0.32 and  $-0.48 \text{ e}/\text{\AA}^3$ , respectively.

## 2.5 References and Notes

- 
- [1] (a) Dembitsky, V. M.; Tolstikov, G. A. *Chemistry for Sustainable Development* **2004**, 12, 13–18. (b) Kijjoa, A.; Gonzalez, M.J.; Afonso, C. M.; Pinto, M. M. M.; Anantachoke, C.; Herz, W. *Phytochemistry* **2000**, 53, 1021–1024.
- [2] (a) Saraiva, L.; Fresco, P.; Pinto, E.; Sousa, E.; Pinto, M.; Gonçalves, J. *Bioorg. Med. Chem.* **2003**, 11, 1215–1225. (b) Nkengfack, A. E.; Mkounga, P.; Fomum, Z. T.; Meyer, M.; Bodo, B. *J. Nat. Prod.* **2002**, 65, 734–736. (c) Chen, J.-J.; Chen, I.-S.; Duh, C.-Y. *Planta Med.* **2004**, 70, 1195–1200.
- [3] Zhao, J.; Yue, D.; Campo, M. A.; Larock, R. C. *J. Am. Chem. Soc.* **2007**, 129, 5288–5295.
- [4] Methodology was discussed in Chapter 1, Scheme 22, p.23–25.
- [5] Bellus, D.; Fischer, H.; Greuter, H.; Martin, P. *Helv. Chim. Acta.* **1978**, 61, 1784–1840.
- [6] Wadsworth, W. S. *Org. React. (N.Y.)* **1977**, 25, 73.
- [7] Maryanoff, B. E.; Reitz, A. B. *Chem. Rev.* **1989**, 89, 863–927.
- [8] Silva, V. L. M., Silva, A. M. S., Pinto, D. C. G. A., Cavaleiro, J. A. S., Patonay, T. *Synlett* **2004**, 2717–2720.
- [9] Watanabe, M.; Hisamatsu, S.; Hotokezaka, H.; Furukawa, S. *Chem. Pharm. Bull.* **1986**, 34, 2810–2820.



- 
- [10] Mathey, F.; Savignac, P. *Tetrahedron* **1978**, *34*, 649–654.
- [11] Bell, T. W.; Sondheimer, F. *J. Org. Chem.* **1981**, *46*, 217–219.
- [12] Enders, D.; von Berg, S.; Jandeleit, B. *Org. Synth.* **2002**, *78*, 169–176.
- [13] (a) Allen, J. F.; Johnson, O. H. *J. Am. Chem. Soc.* **1955**, *77*, 2871–2875. (b) Pottie, I. R. *Ph.D. Thesis* **2002**, Memorial Univeristy.
- [14] (a) Pudovic, A. N.; Aver'yanova, V. P. *Zhur. Obshchei. Khim.* **1956**, *26*, 1426–1231.  
(b) Hudson, R. F. *Structure and Mechanism in Organo-Phosphorus Chemistry*, Wiberg, K. B. Ed., London, **1965**, Vol. 5, pp. 131–163.
- [15] Iwasaki, H.; Kum, T.; Yamaoto, Y.; Akiba, K. *Heterocycles* **1988**, *27*, 1599–1606.
- [16] Bodwell, G. J.; Hawco, K. M.; da Silva, R. P. *Synlett* **2003**, 179–182.
- [17] Sandulache, A. S., Silva, A. M. S., Pinto, D. C. G. A., Almeida, L. M. P. M., Cavaleiro, J. A. S. *New. J. Chem.* **2003**, *27*, 1592–1598.
- [18] Jorge, H. M.; Karsten, K.; Ulrich, F.; Hernan, P. M.; Boris, W. L.; Ana, E. B.; Ramiro, A. M. *Heterocycles*, **2007**, *71*, 1327–1345.
- [19] (a) Nohara, A.; Umetani, T.; Sanno, Y. *Jpn. Kokai Tokyo Koho* **1975**, JP50052067.  
(b) Akira, N.; Hisashi, K.; Taketoshi, S.; Hirosada, S.; Morio, K.; Yasushi, S. *J. Med. Chem.* **1977**, *20*, 141–145.
- [20] Pottie, I. R. *Ph.D. Thesis* **2002**, Memorial Univeristy.
- [21] (a) Scheeren, J. W.; Stevens, W. *Rec. Trav. Chim. Pays-Bas* **1966**, *85*, 793–799; (b) Scheeren, J. W.; Staps, R. J. F. M.; Nivard, R. J. F. *Rec. Trav. Chim. Pays-Bas* **1973**, *92*, 11–19; (c) Reference 5.

- [22] A stepwise reaction (Michael / Mannich) cannot be ruled out at this time, but we currently favor the asynchronous IEDDA pathway. More conclusive commentary on this subject will have to wait a detailed computational investigation.
- [23] Hess, A. B., Jr.; Baldwin, J. E. *J. Org. Chem.* **2002**, *67*, 6025–6033.
- [24] (a) Zborowski, K.; Ryszard, G.; Proniewicz, L. M. *J. Phys. Org. Chem.* **2005**, *18*, 250–254. (b) Lumbroso, H.; Cure, J.; Evers, M.; *Z. Naturforsch. A* **1986**, *41*, 1250–1257.
- [25] Chem3D, Version 5.0.
- [26] The “energy gap law” states that the non-radiative decay rate increase exponentially as the energy gap or emission energy decrease. The non-radiative decay rate ( $k_{nr}$ ) increase leading to decreasing of fluorescence quantum yield  $\Phi_{em}$  (see the below equation, assumed radiative rate  $k_r$  is a constant).

$$\Phi_{em} = \frac{k_r}{k_r + k_{nr}}$$

Therefore, the “energy gap law” can be stated that the energy gap decrease, fluorescence quantum yield decrease. See: Caspar, J.; Mayer, T. J. *J. Phys. Chem.* **1983**, *87*, 952–957.

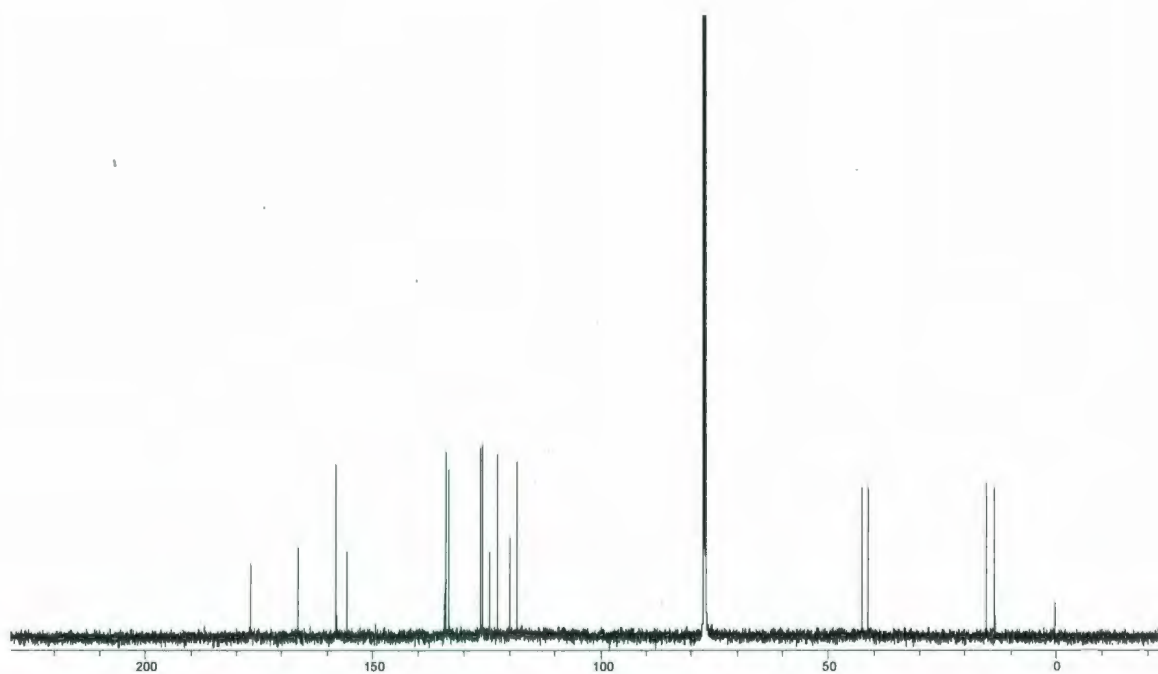
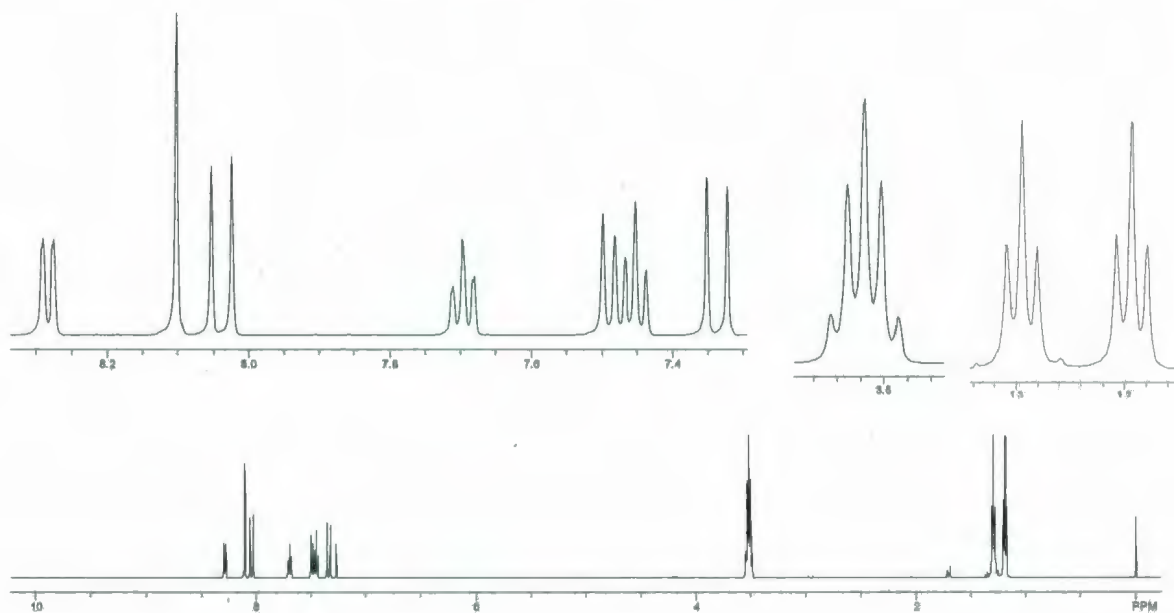
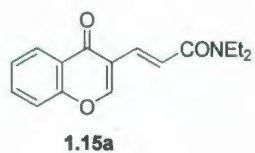
- [27] Stokes shifts are given by  $E_{abs} - E_{em} = 2\lambda_t$ , where  $\lambda_t$  is the total reorganization energy, which is a linear combination of the vibrational ( $\lambda_{vib}$ ) and solvent reorganization ( $\lambda_o$ ) energies, respectively.
- [28] (a) Heinz, B.; Schmidt, B.; Root, C.; Satzger, H.; Milota, F.; Fierz, B.; Kiefhaber, T.; Zinth, W.; Gilch, P. *Phys. Chem. Chem. Phys.* **2006**, *8*, 3432–3439. (b) Murov, S.

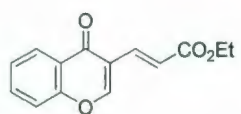
- 
- L.; Carmichael, I.; Hug, G. L. *Handbook of Photochemistry*, Marcel Dekker: New York, **1993**.
- [29] The intensity changes indicate that there are other (yet to be identified) non-radiative pathways that lower  $\Phi_{em}$ .
- [30] Chen, P.; Meyer, T. J. *Chem. Rev.* **1998**, *98*, 1439–1477.
- [31] For all known compounds, a literature citation is given after the compound name. In all cases, the spectroscopic data is consistent with published data.
- [32] Hawco, K. M. *B.Sc. Thesis* **2002**, Memorial University.
- [33] Polyakov, V. K. *Ukr. Khim. Zh.* **1982**, *48*, 772–775.
- [34] Chen, Y. S.; Khan, M.; Rao, S. N.; Krishnaiah, M.; Raju, K. V. N. *Acta Cryst.* **1996**, *52*, 1847–1849.
- [35] This new compound was synthesized following the literature procedure in reference 8.
- [36] Coe, B. J.; Friesen, D. A.; Thompson, D. W.; Meyer, T. J. *Inorg. Chem.* **1996**, *35*, 4575–4584.



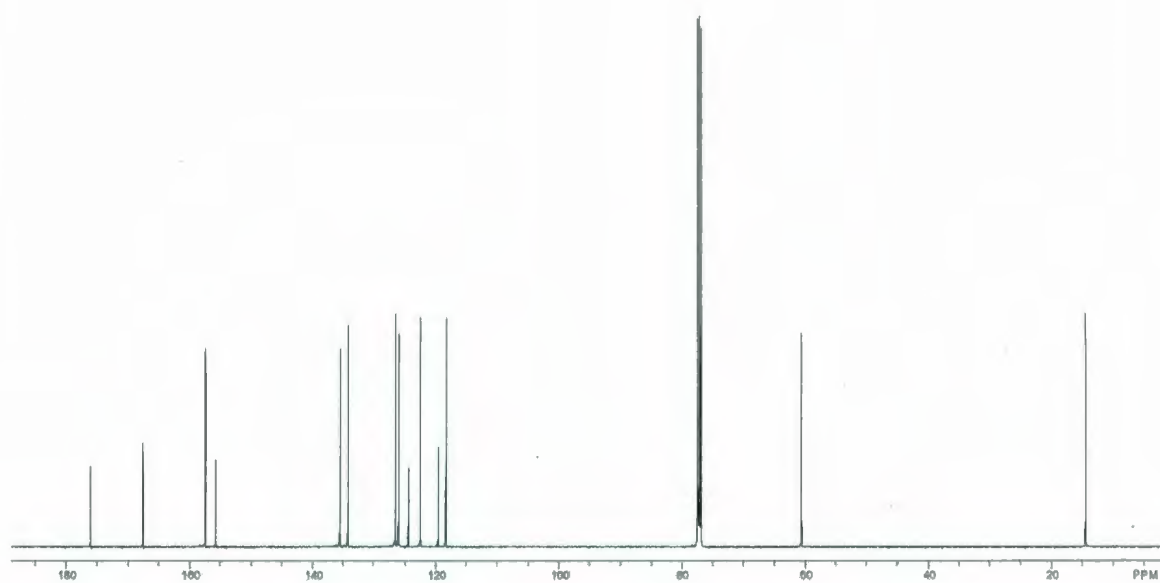
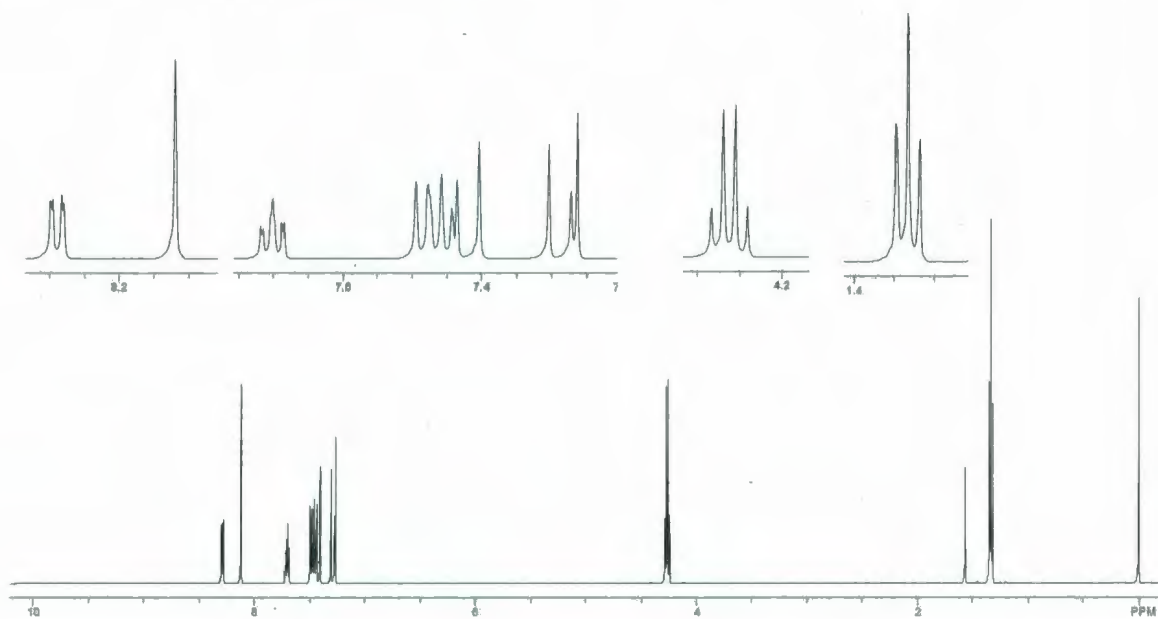
## **Appendix**

### **Selected NMR Spectra of Synthesized Compounds**

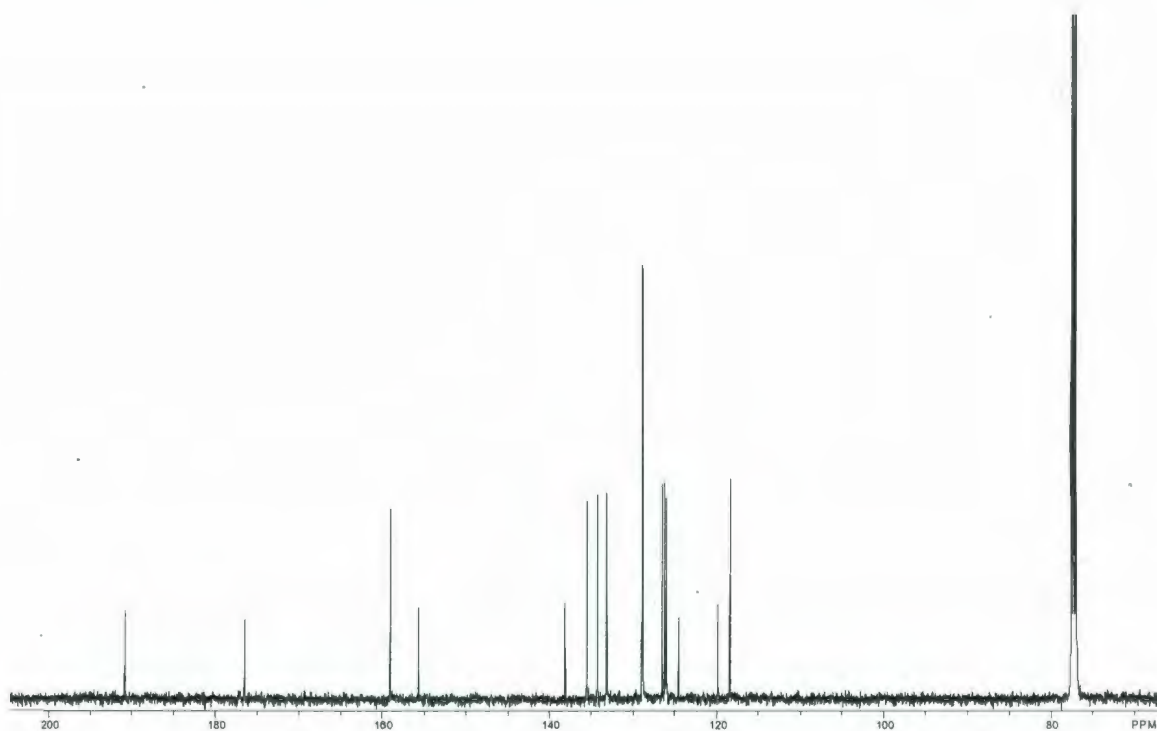
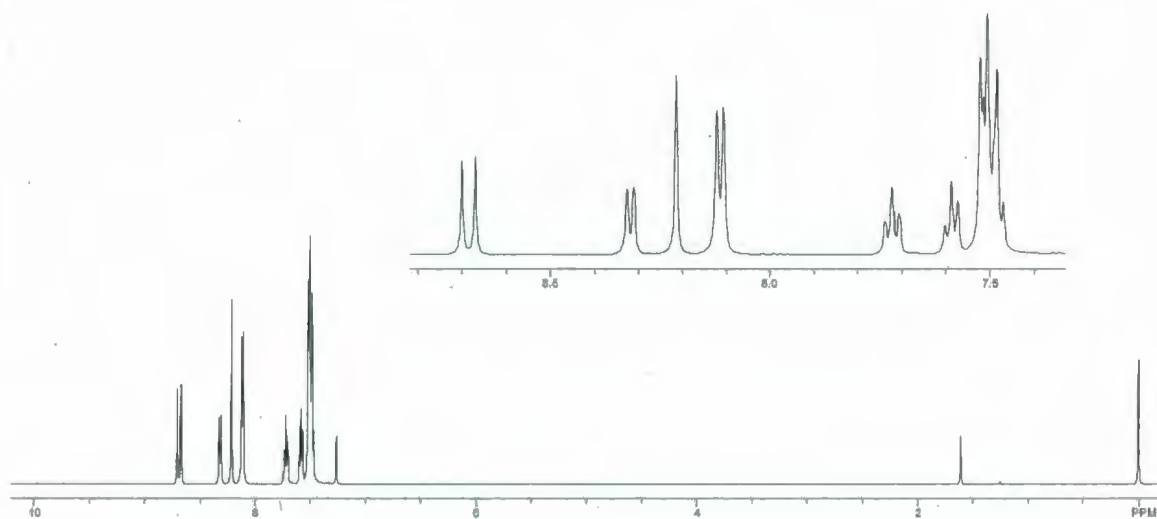
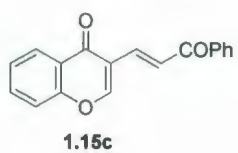


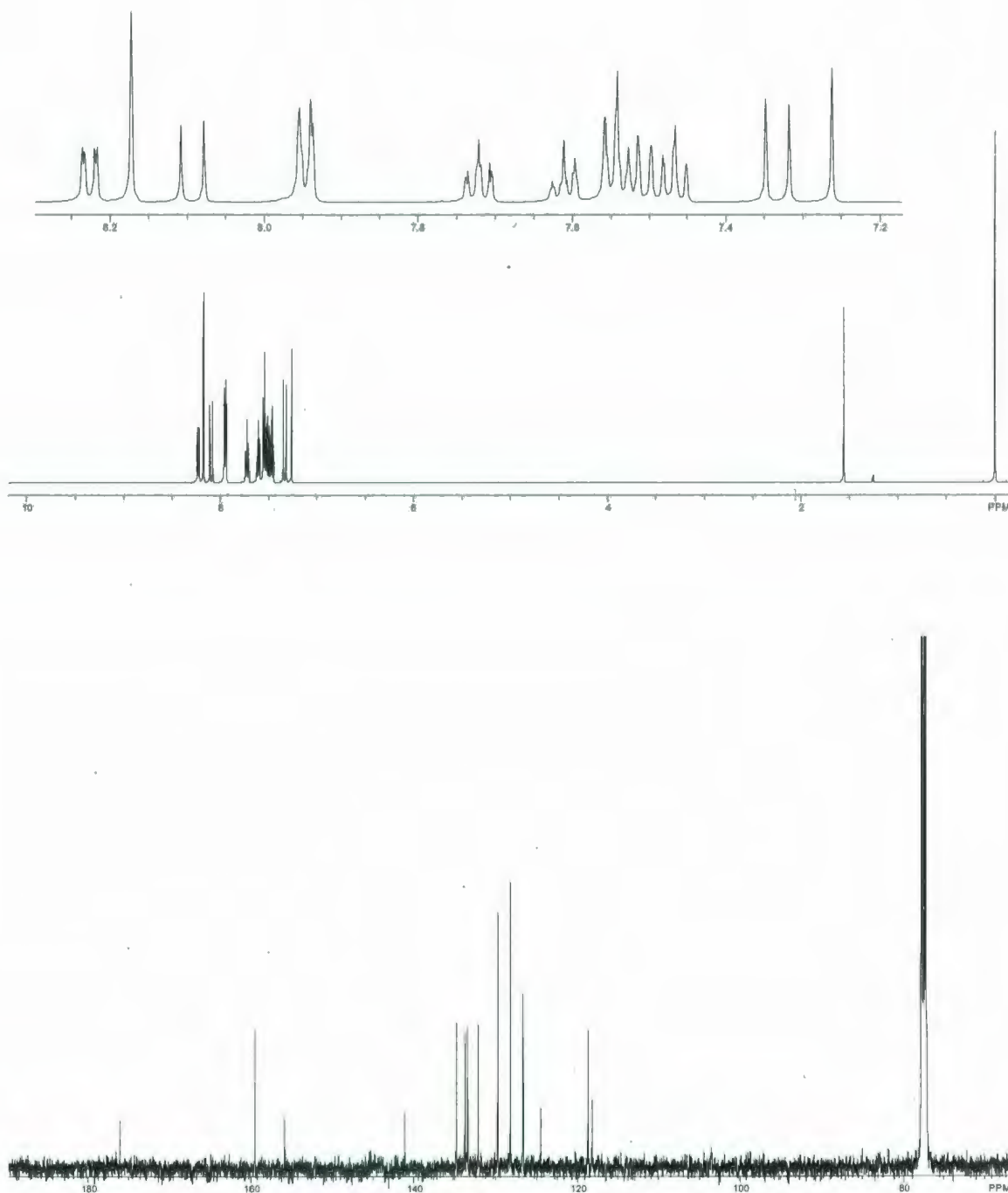
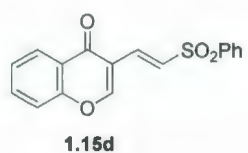


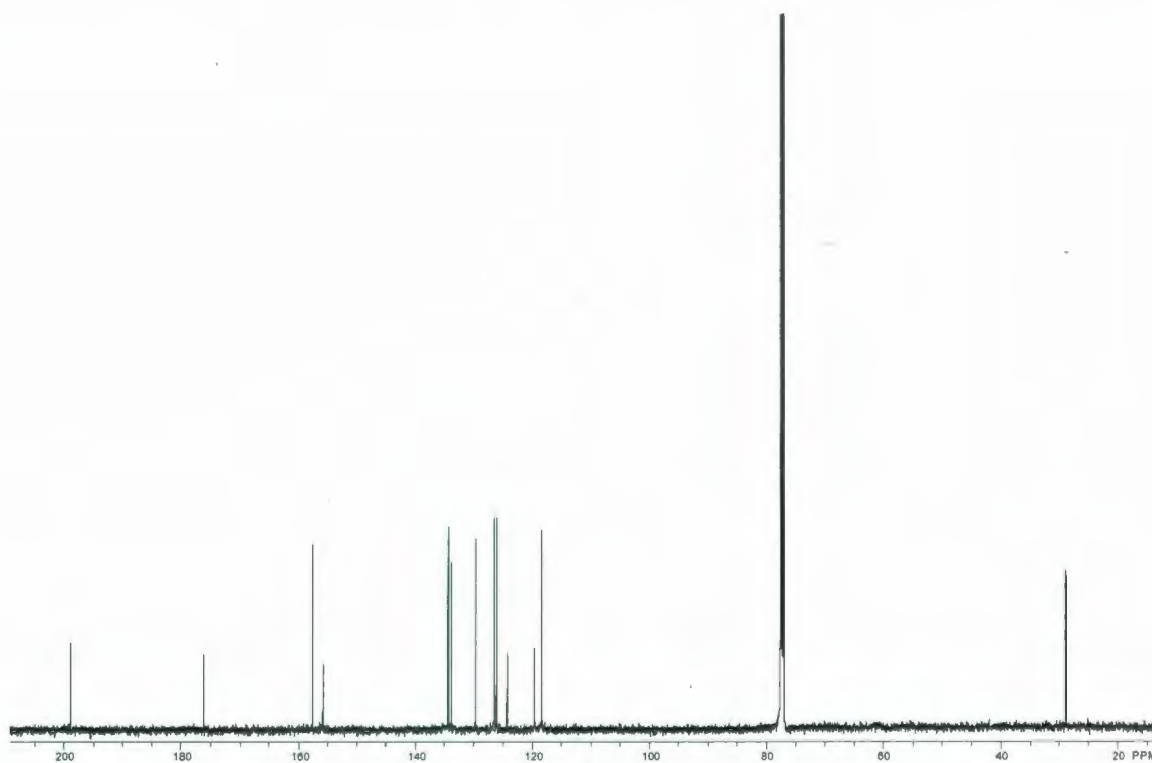
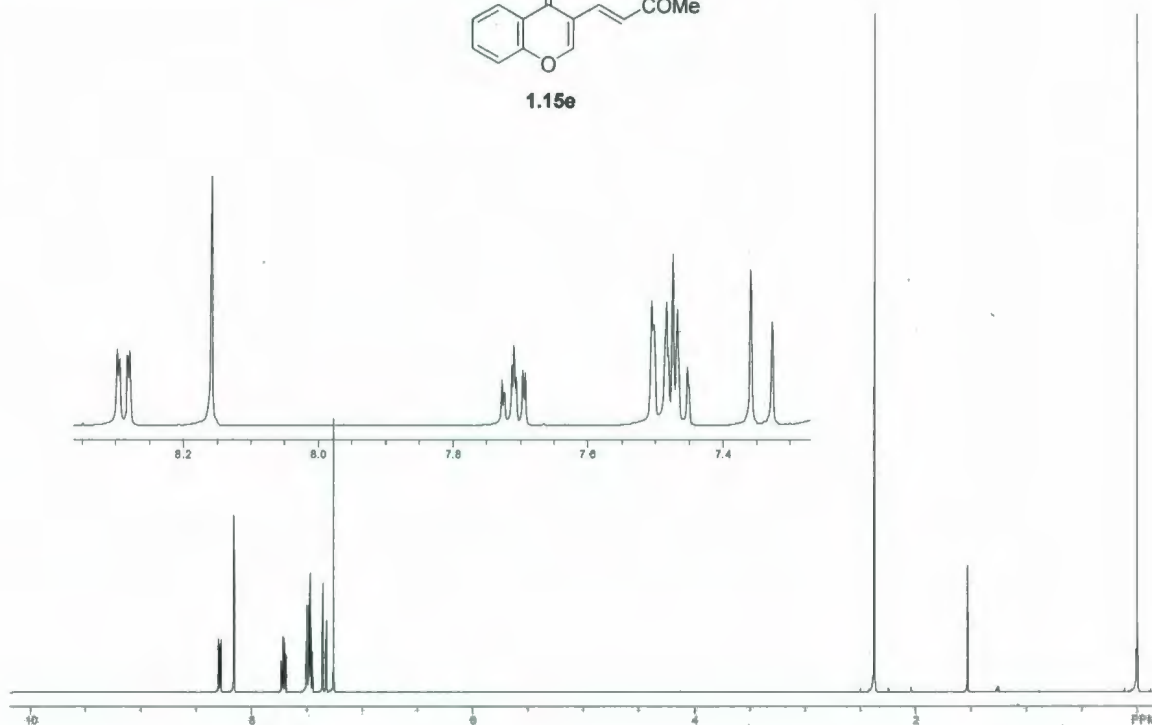
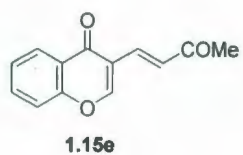
1.15b



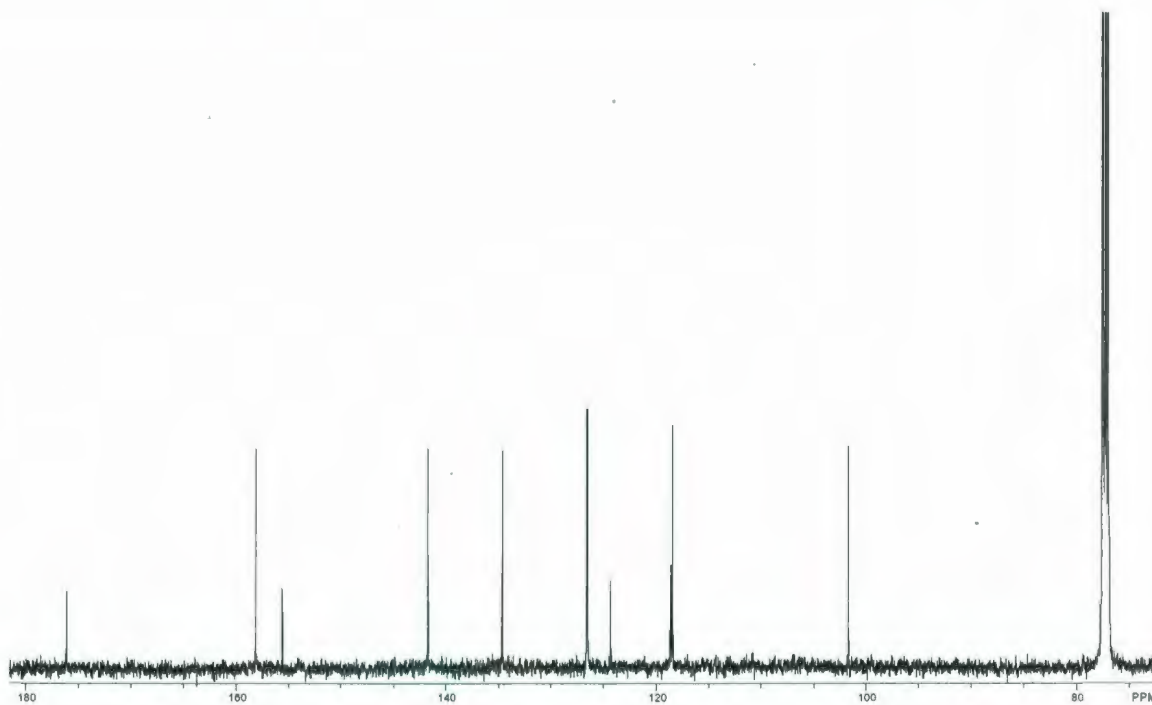


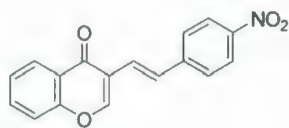




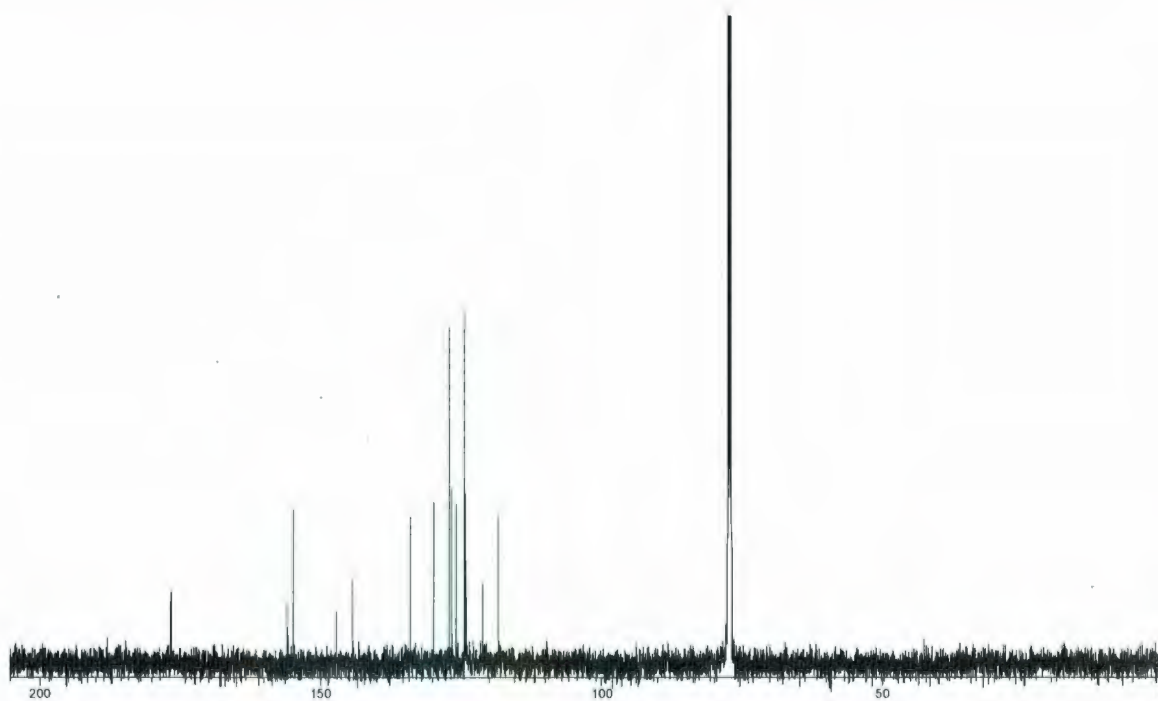
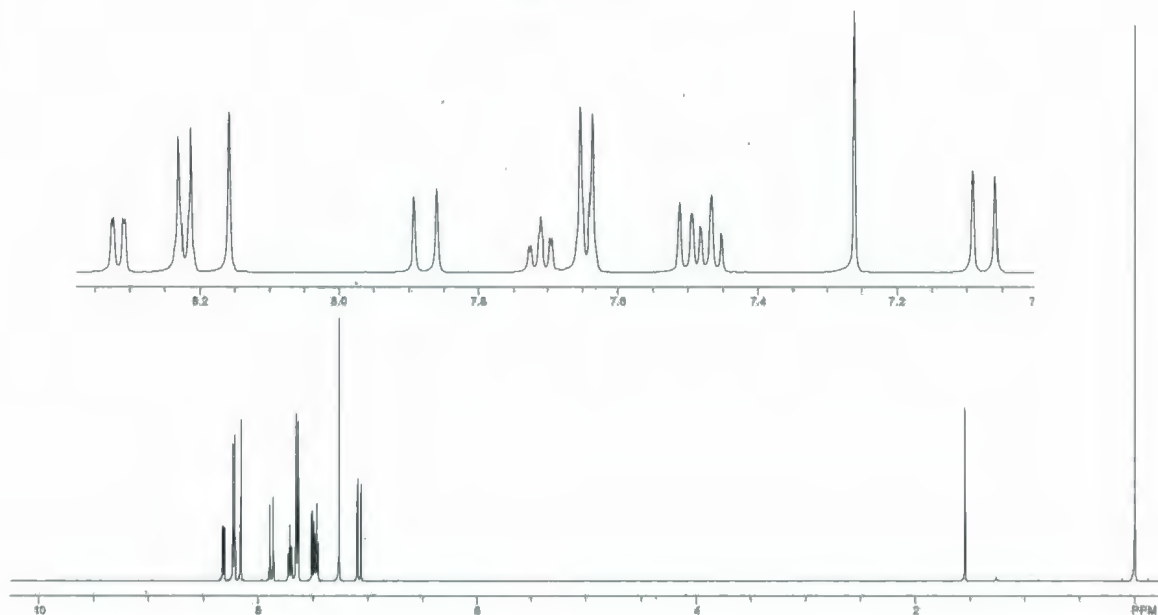


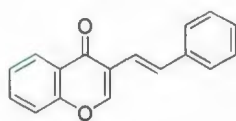




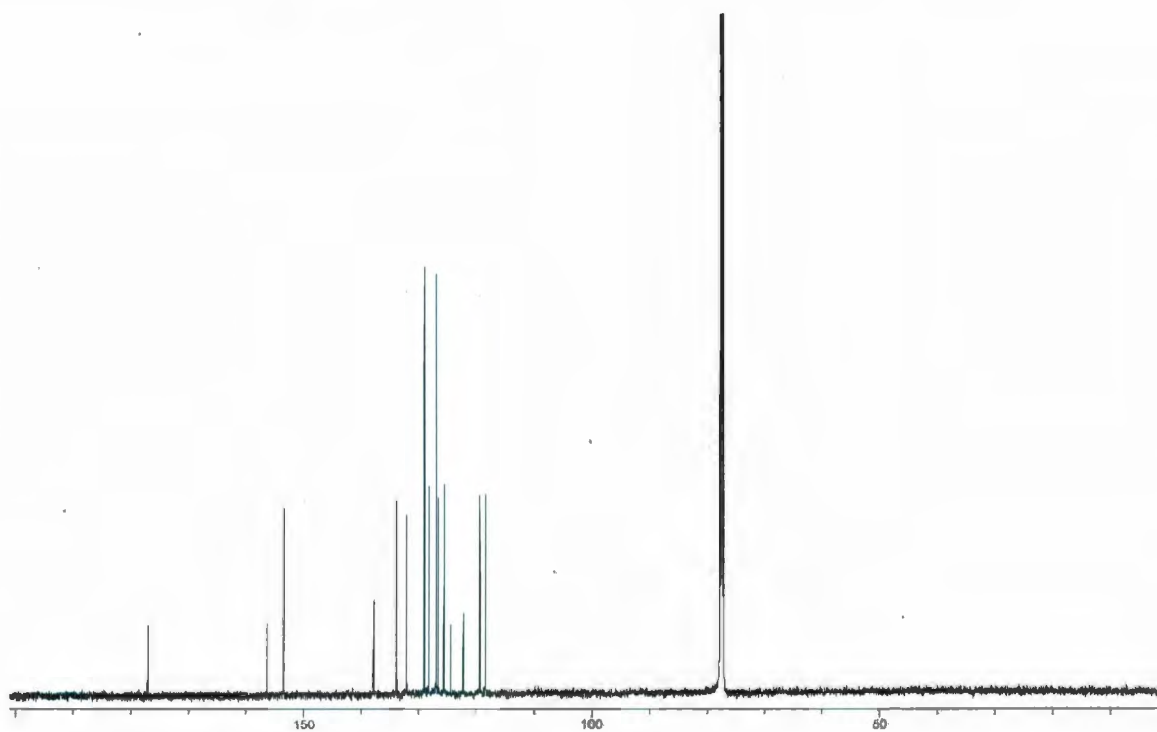
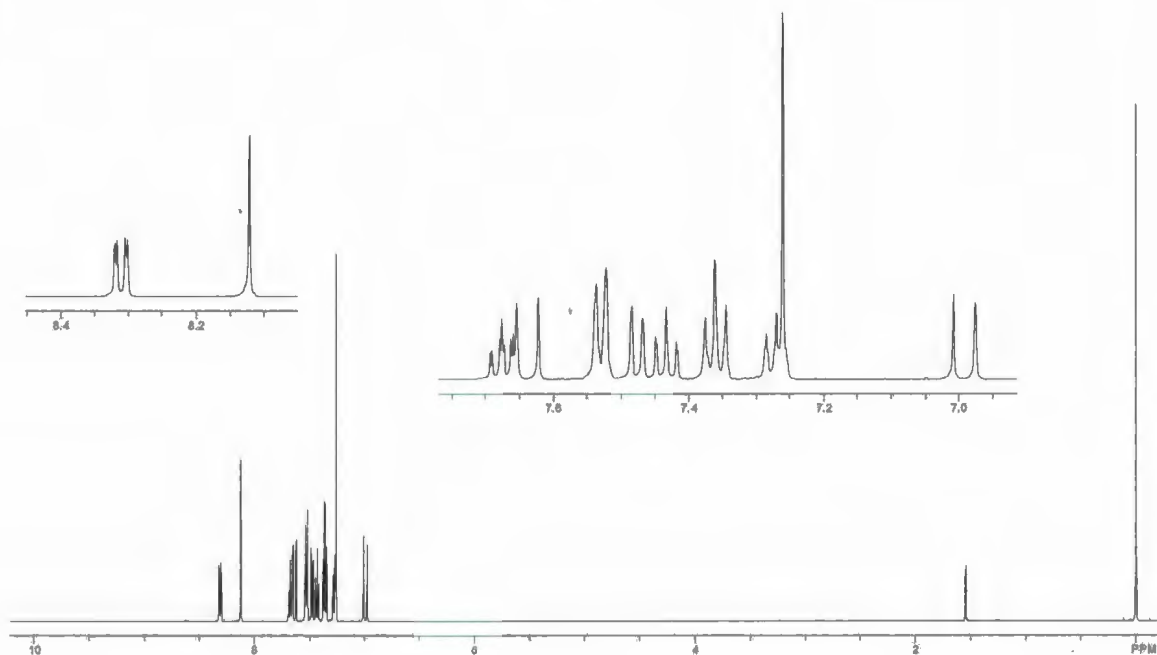


1.15g

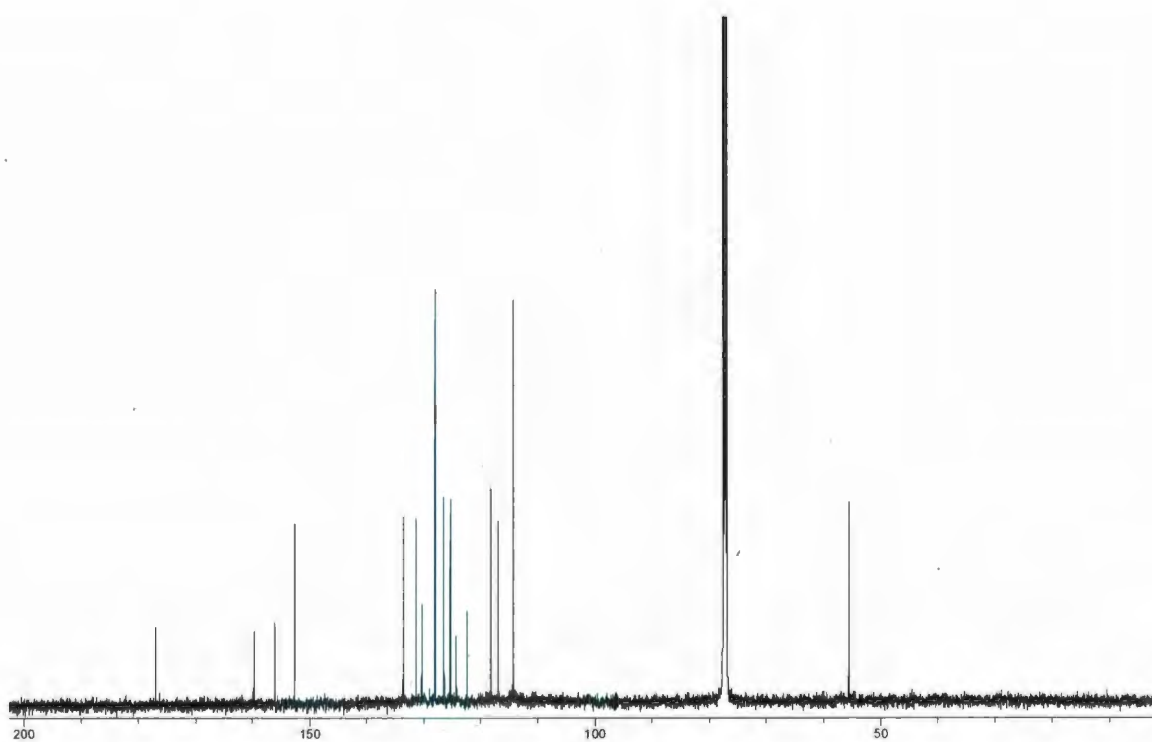
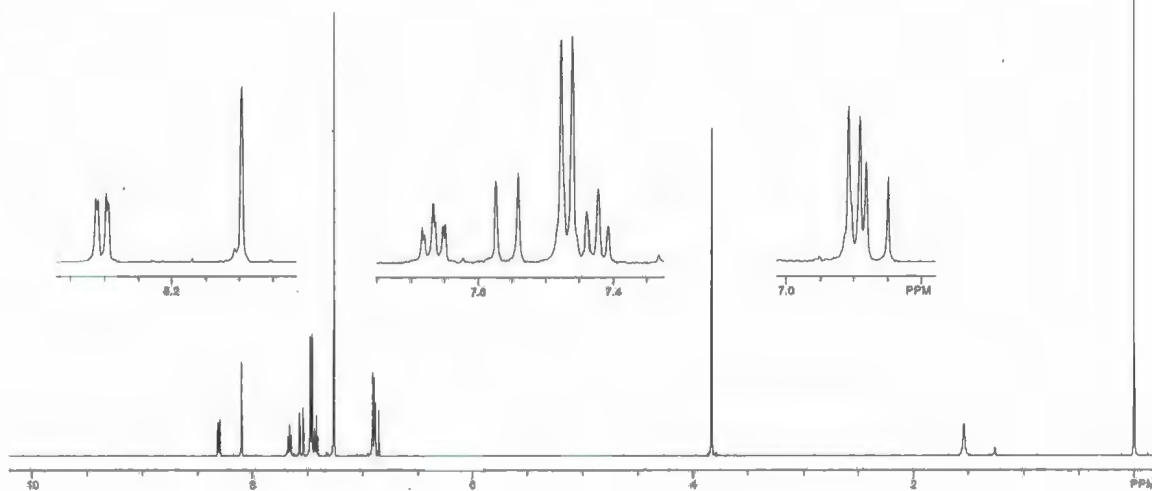
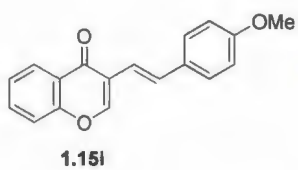


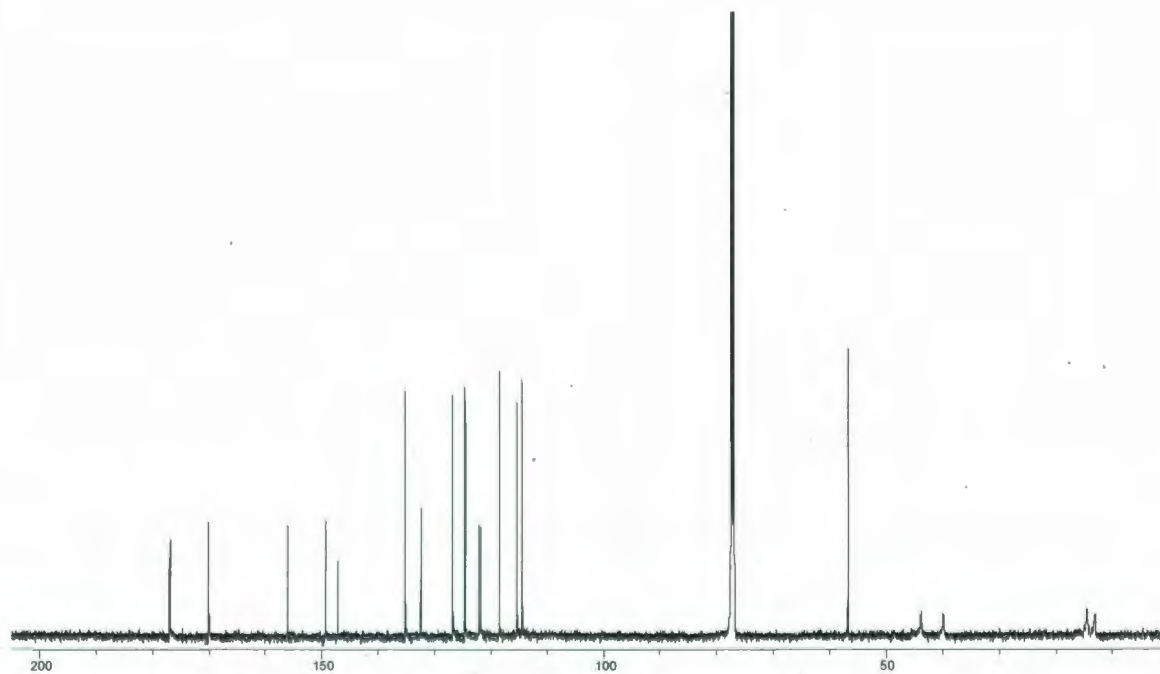
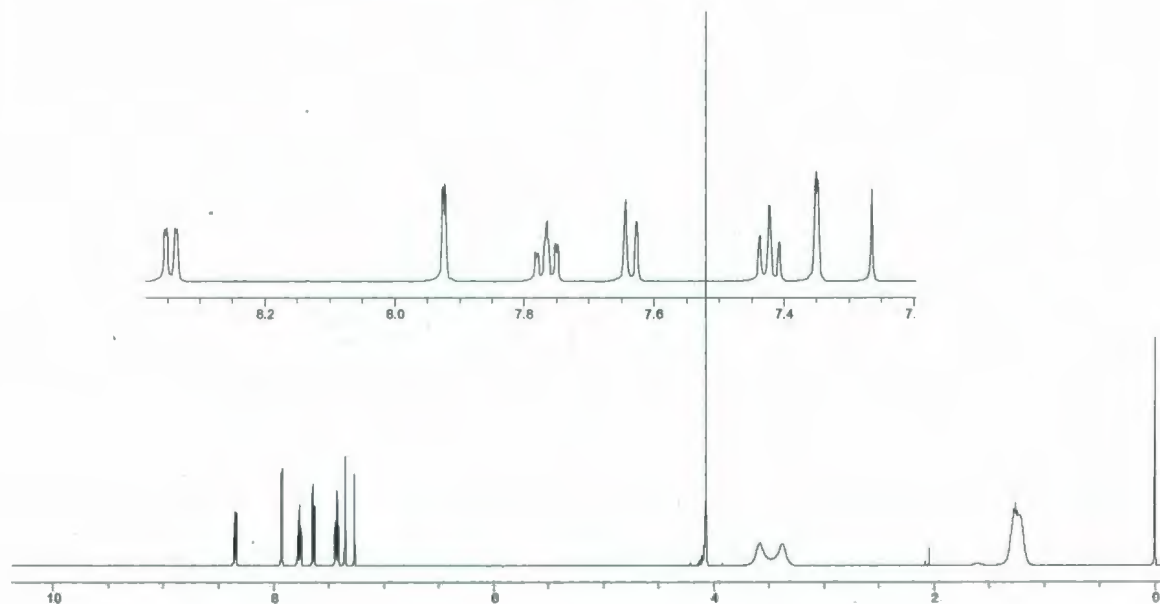
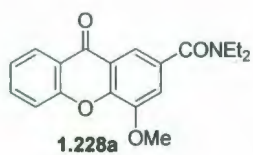


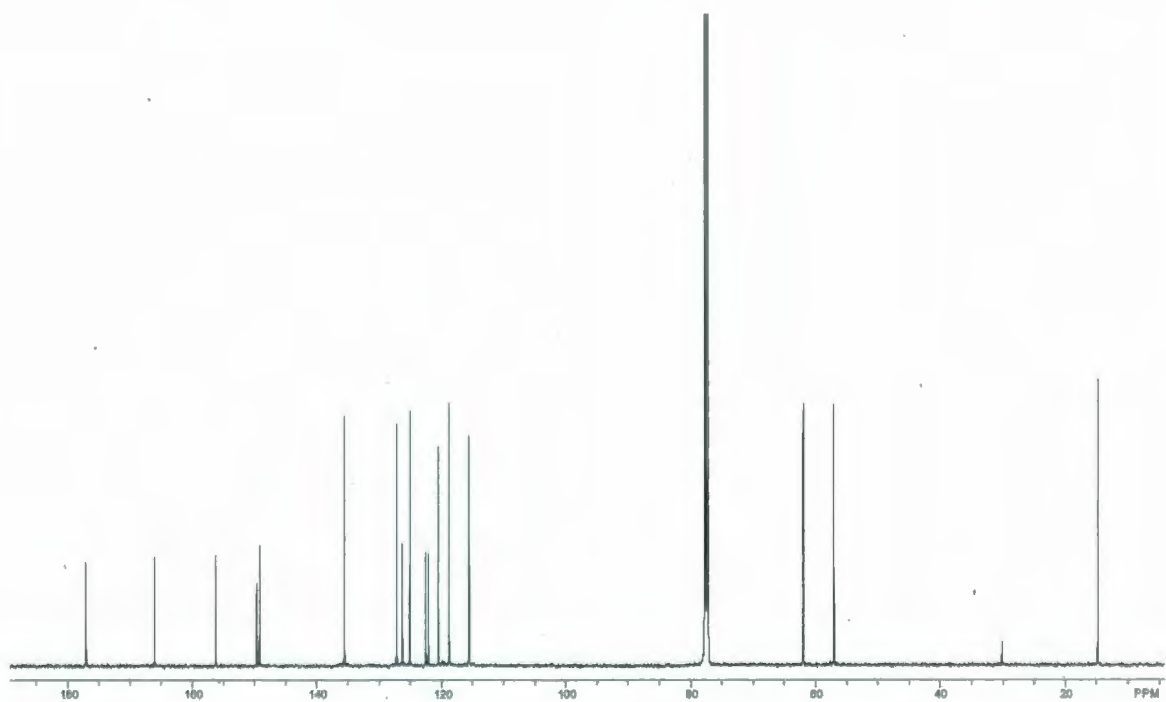
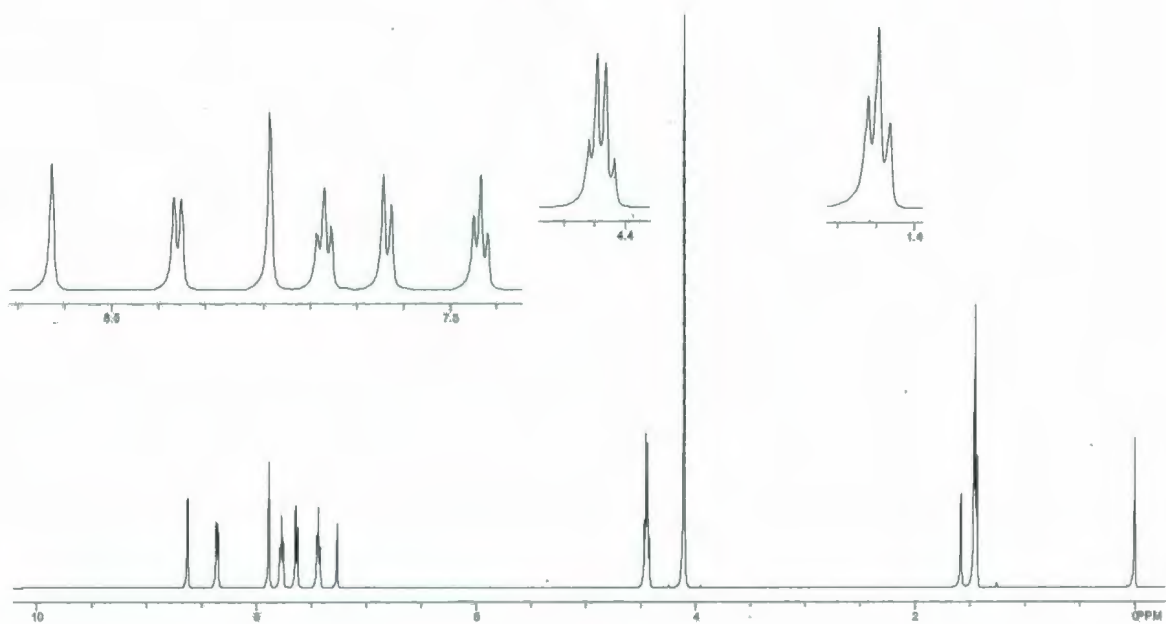
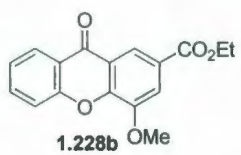
1.15h



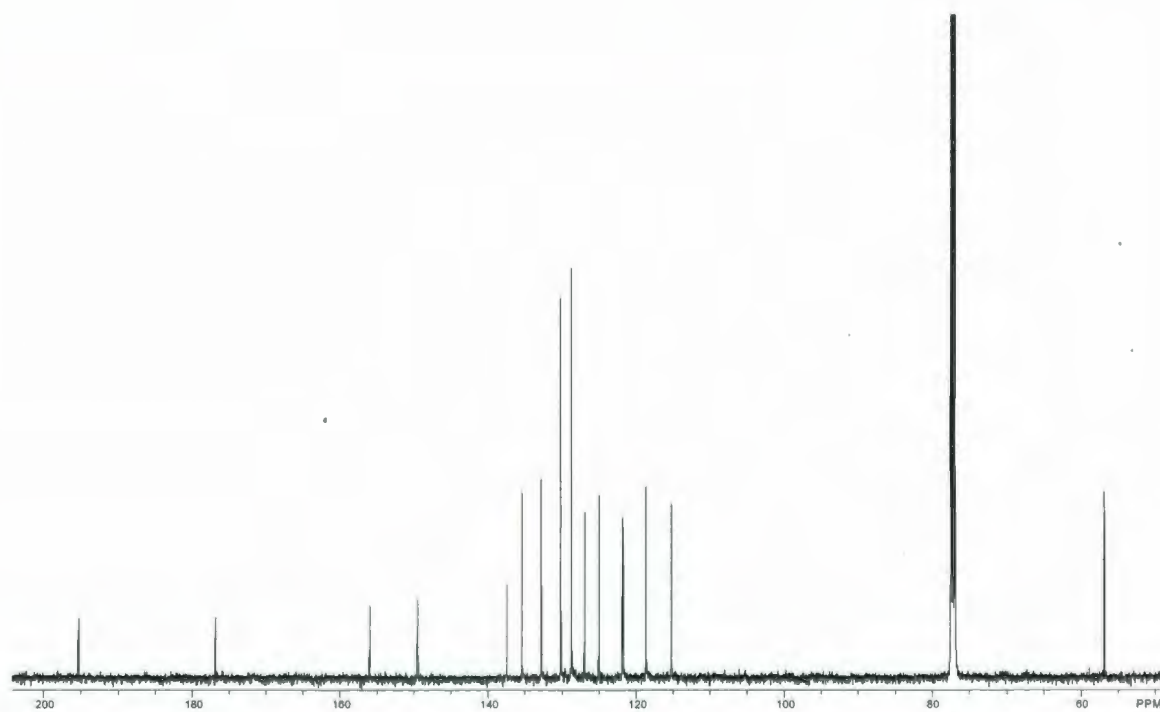
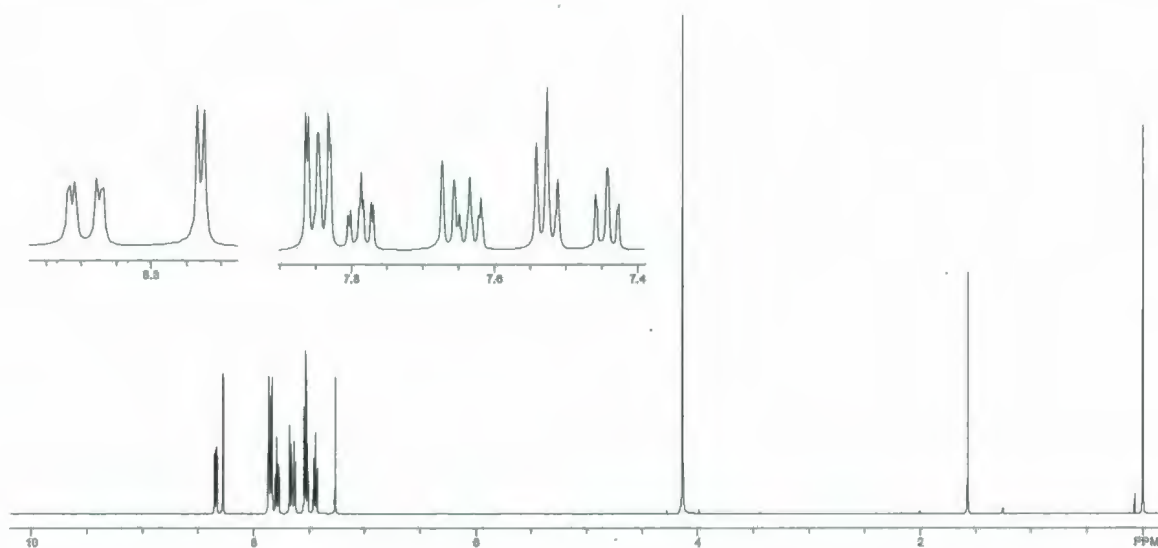
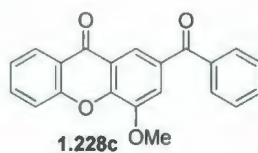


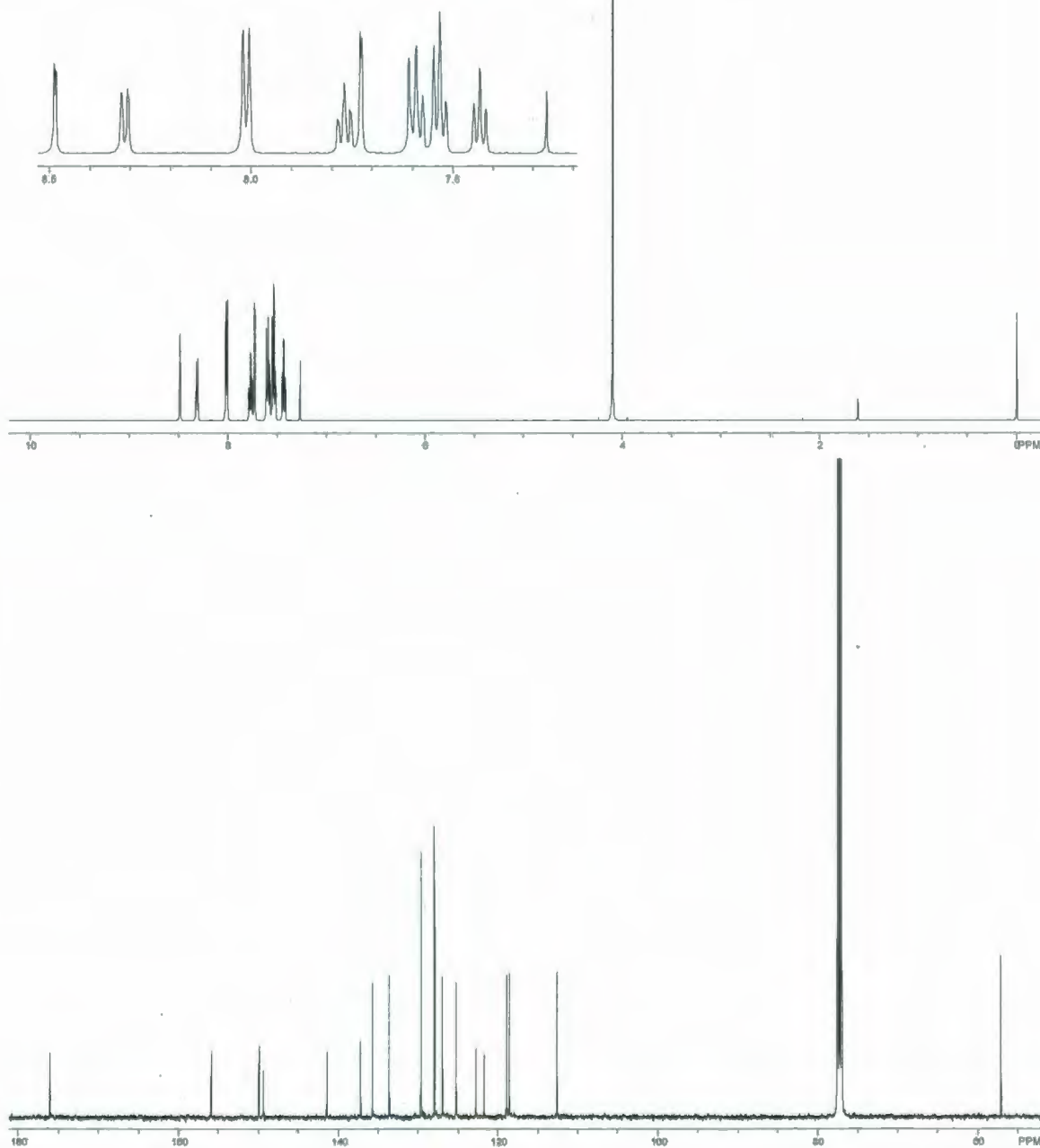
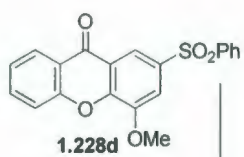


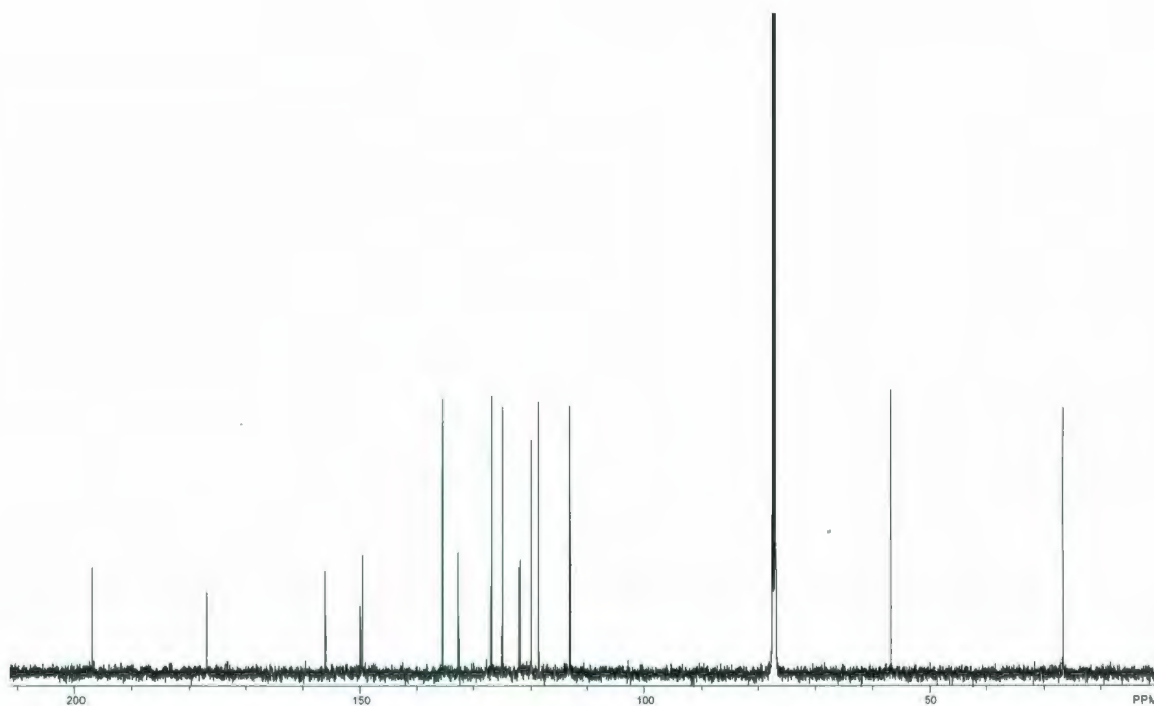
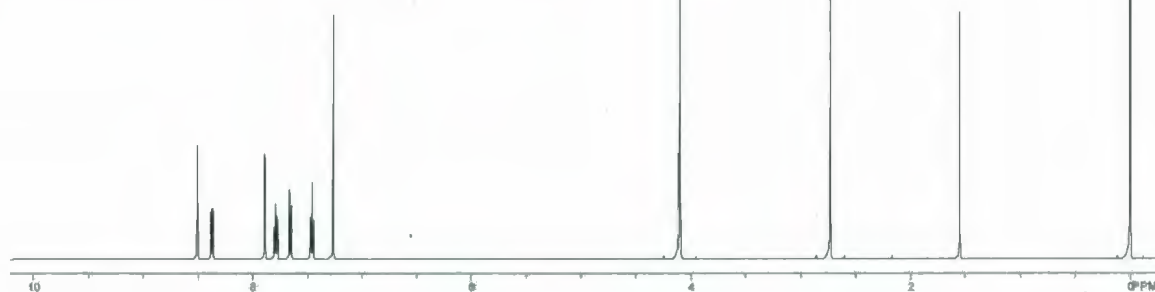
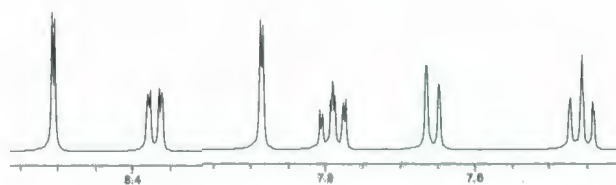
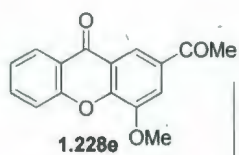




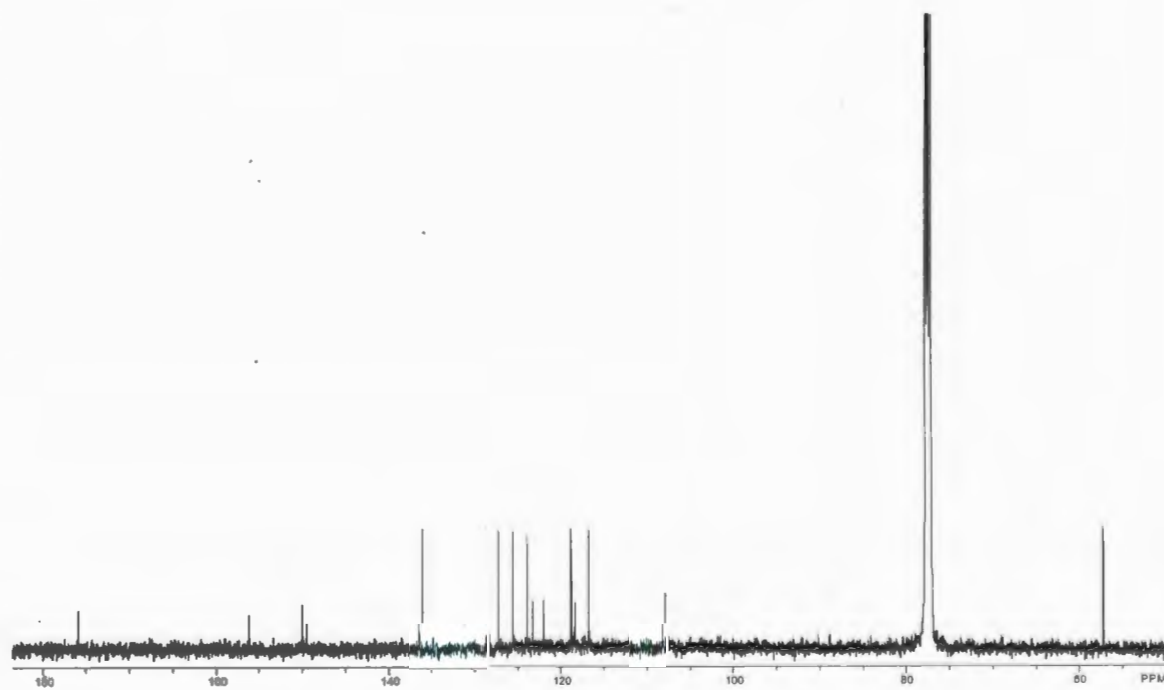
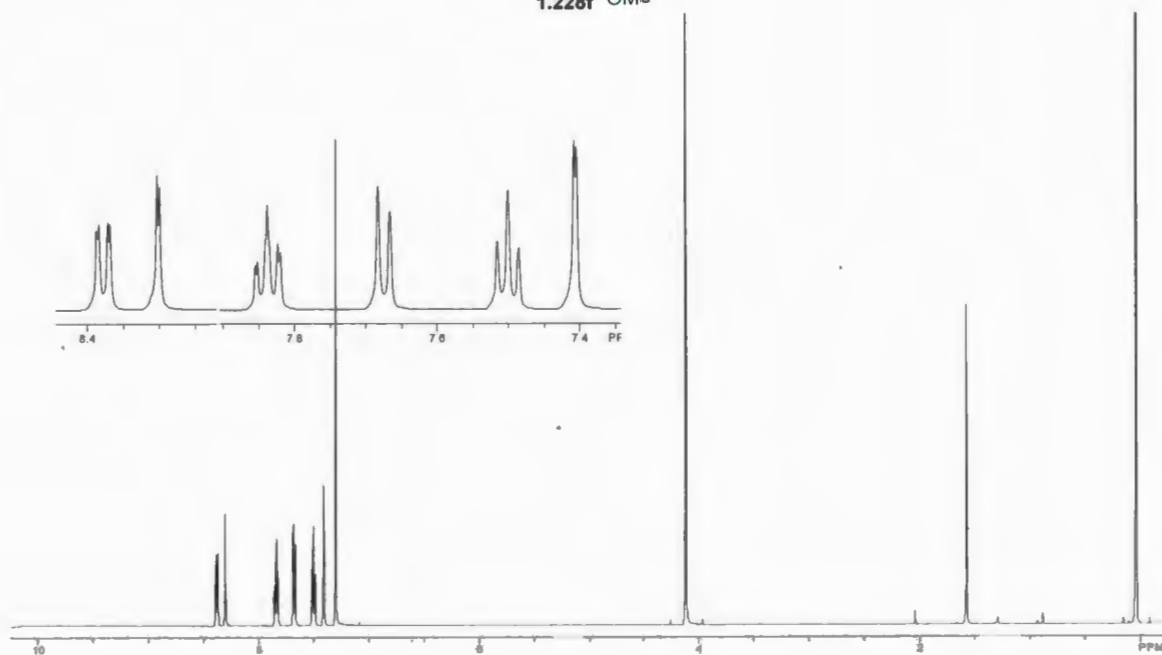
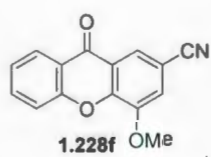


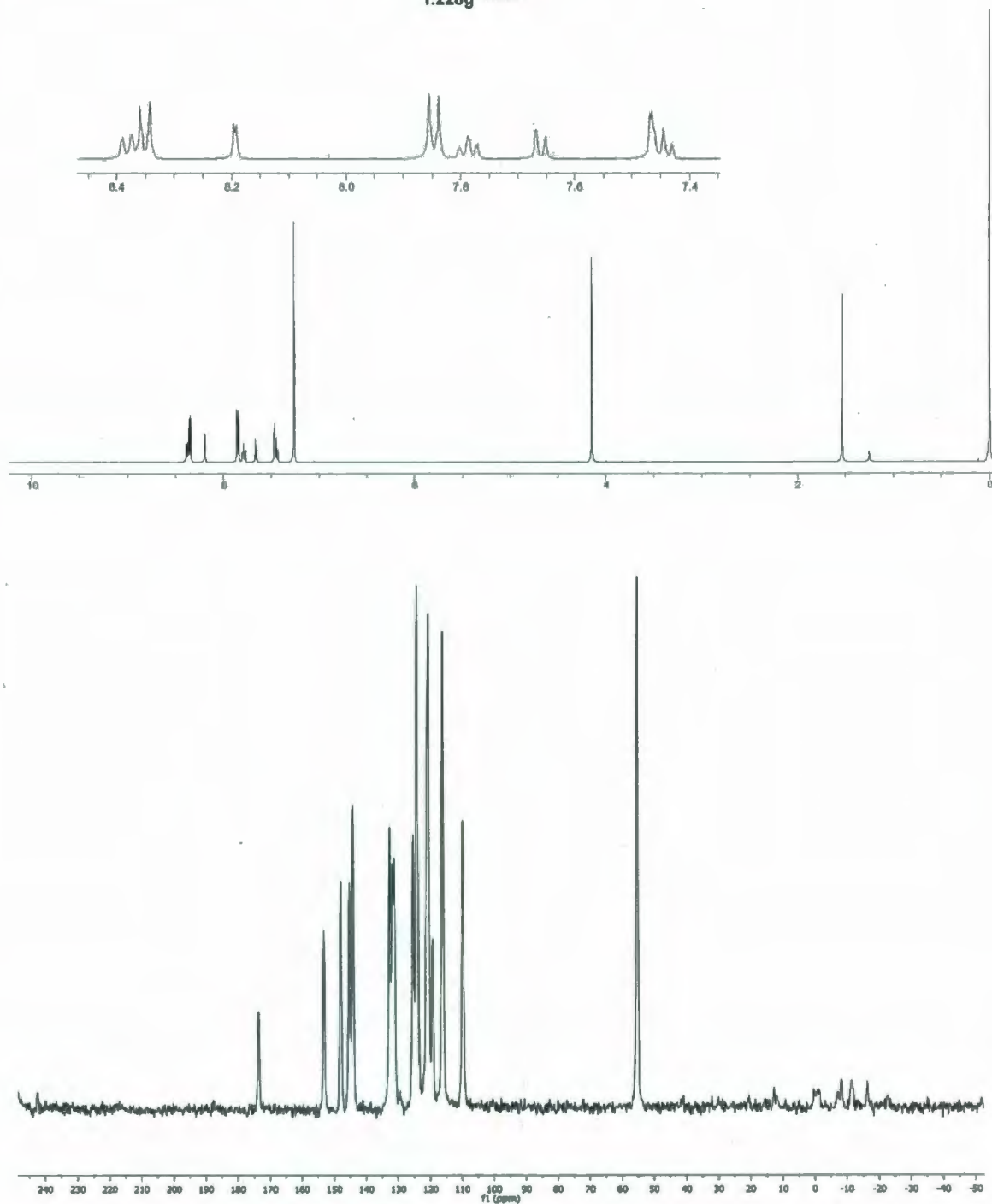
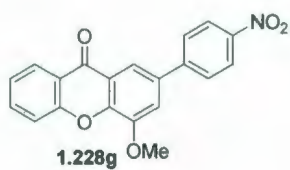


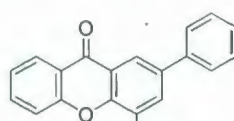




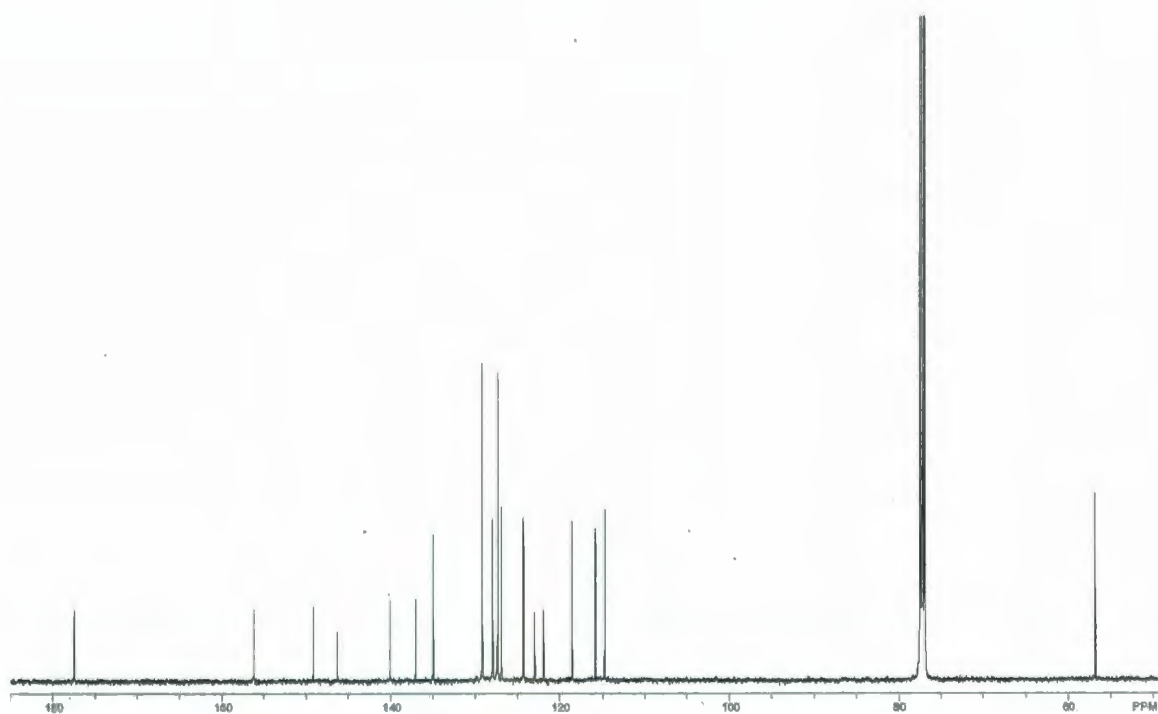
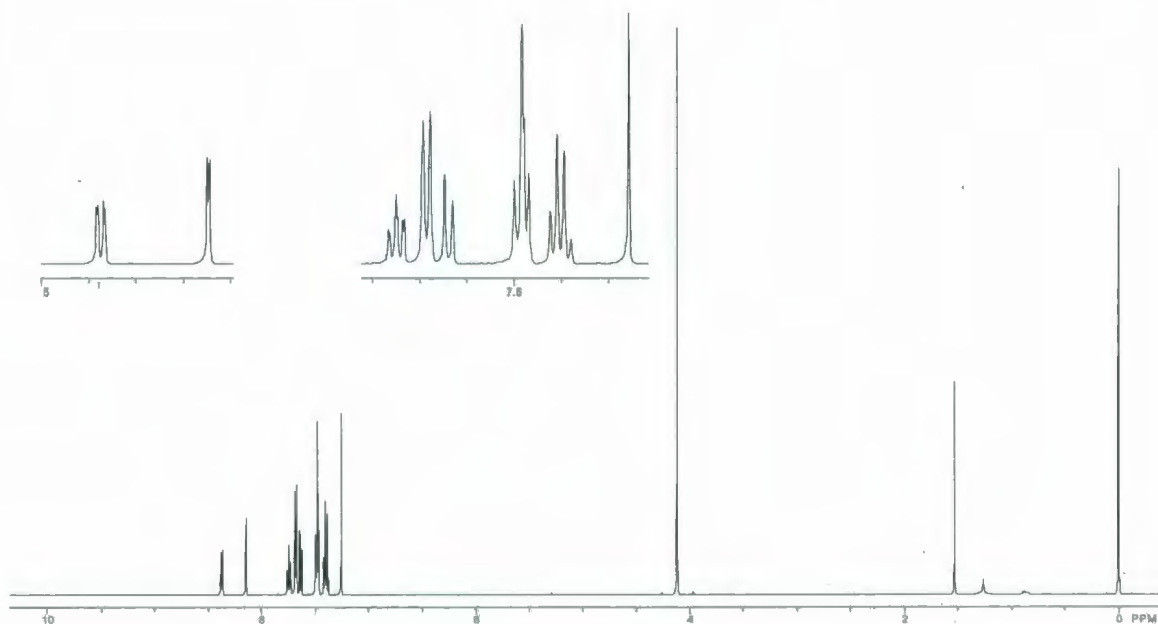




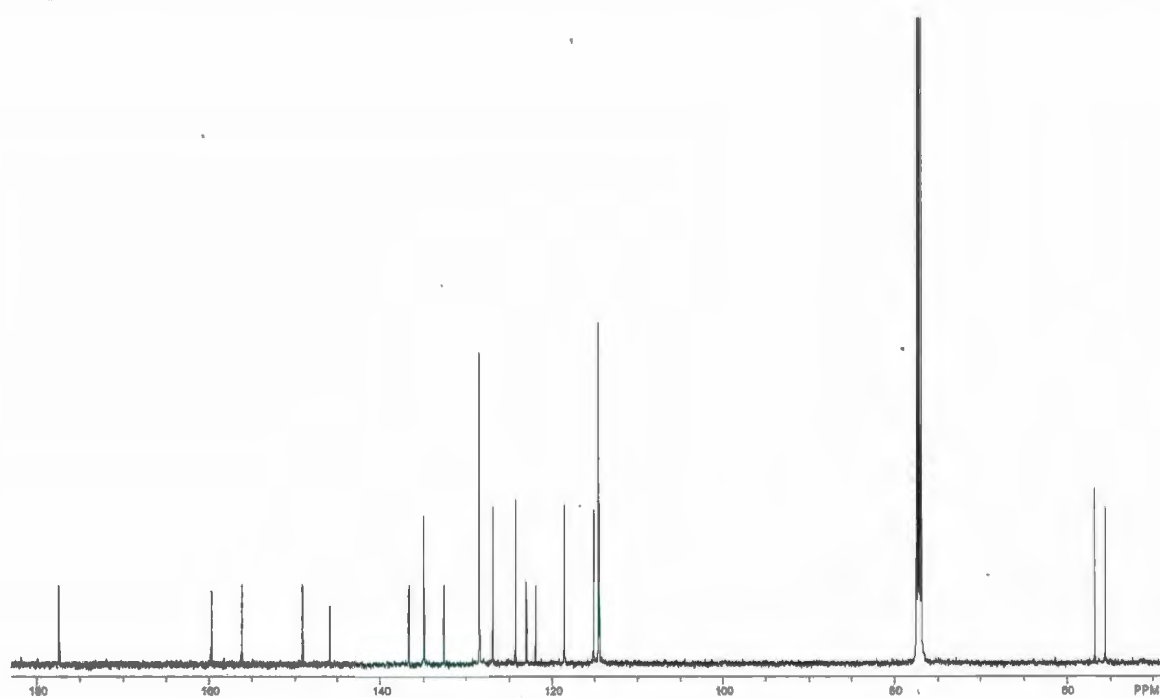
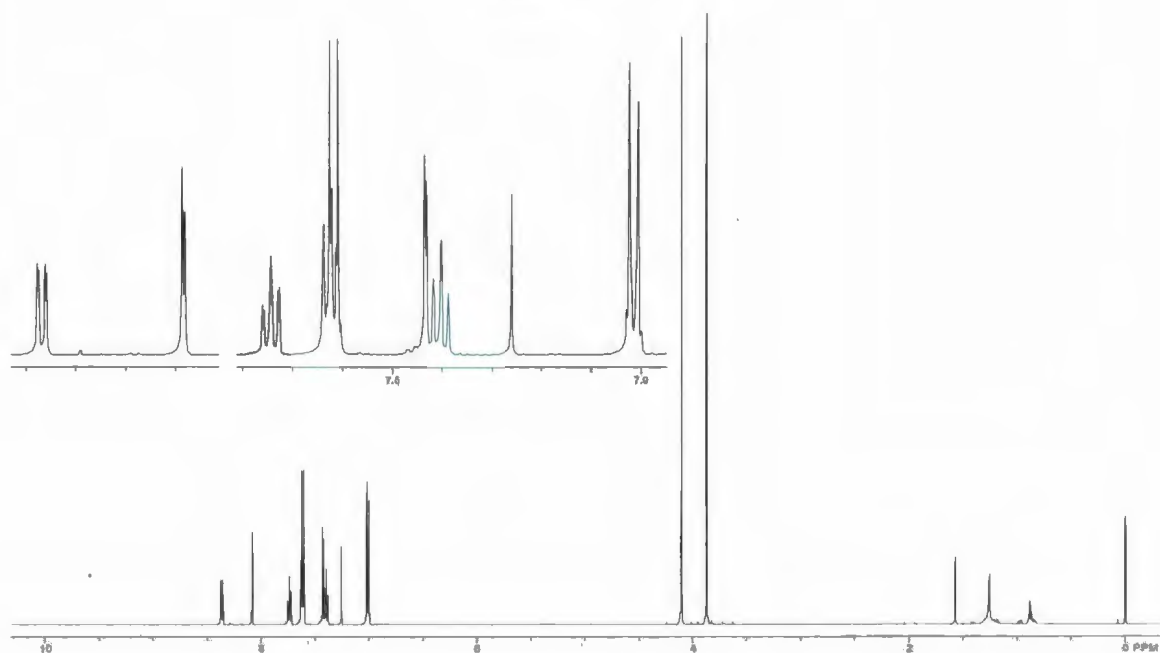
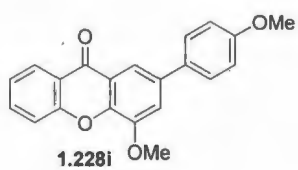


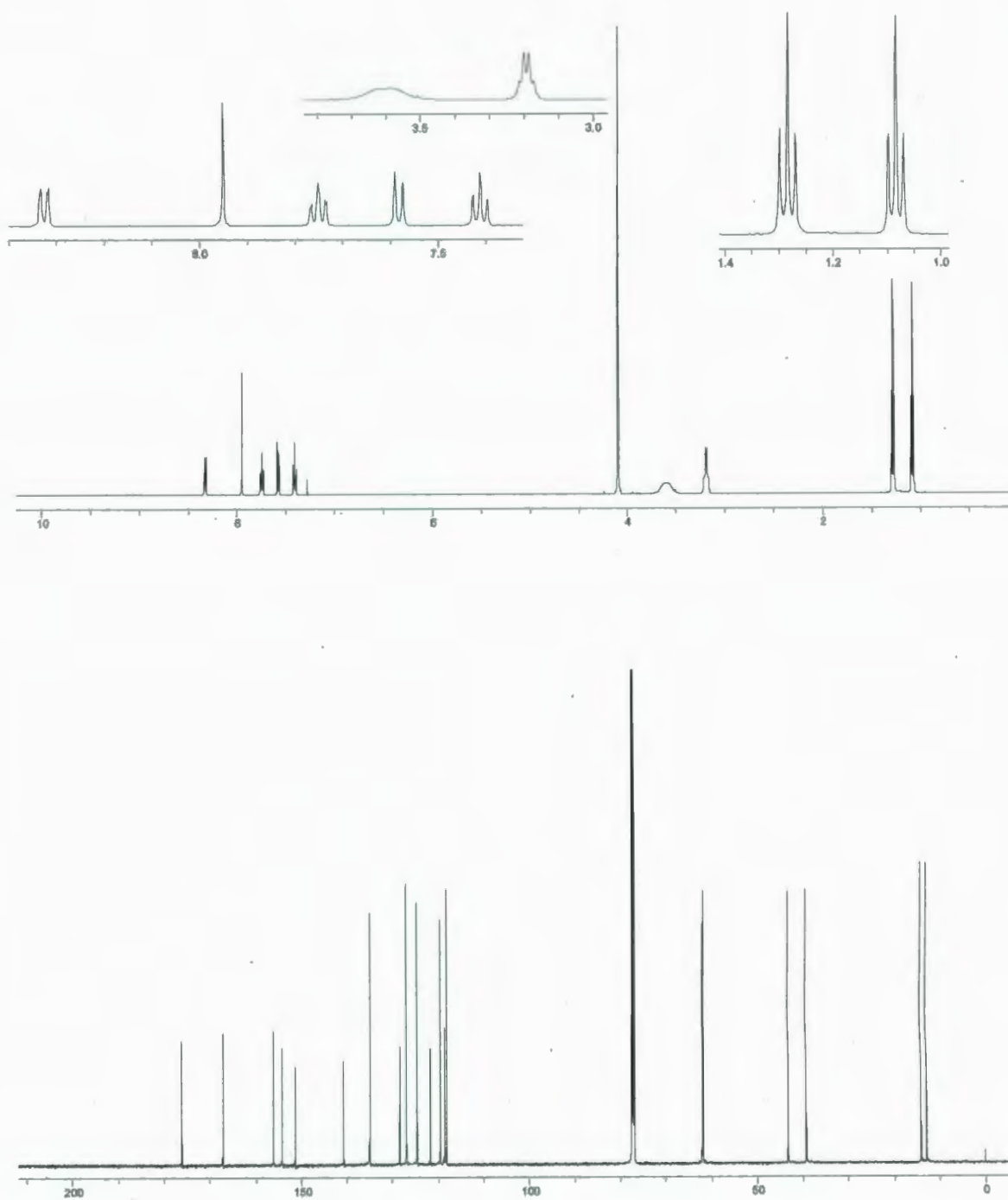
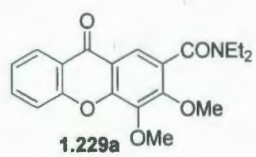


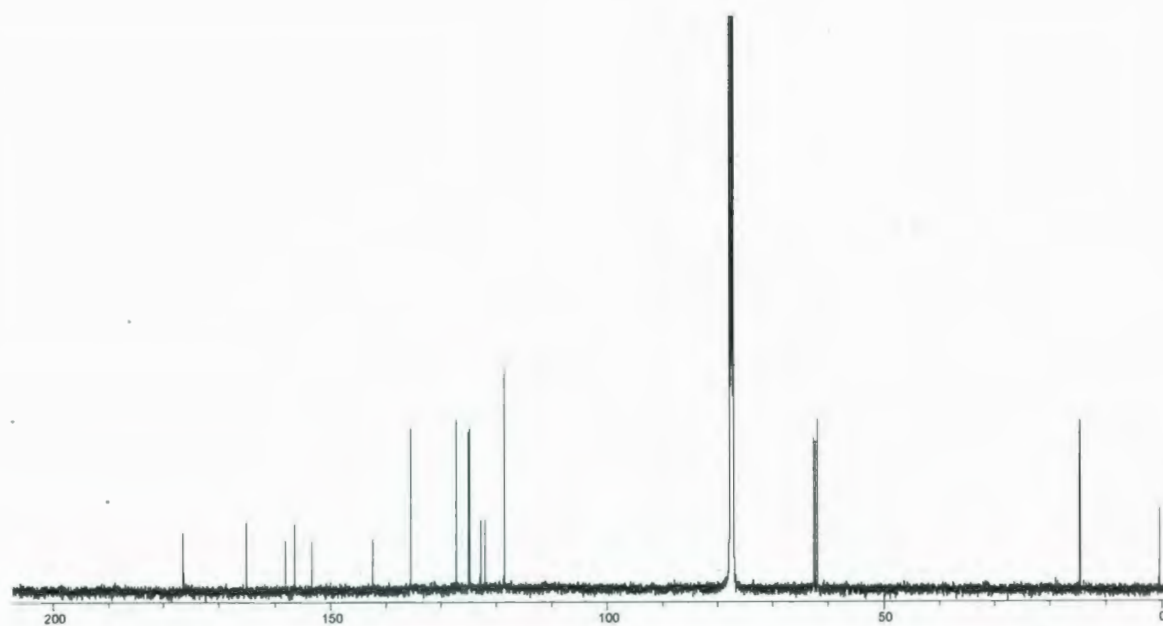
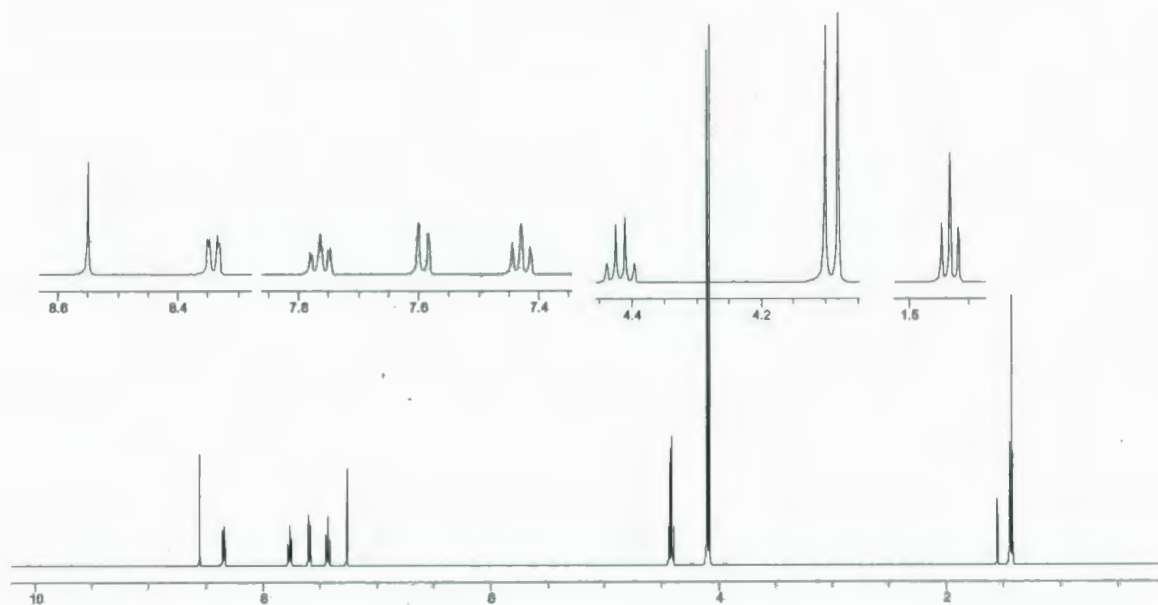
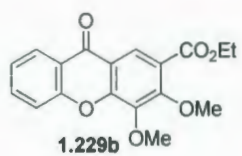
1.228h OMe



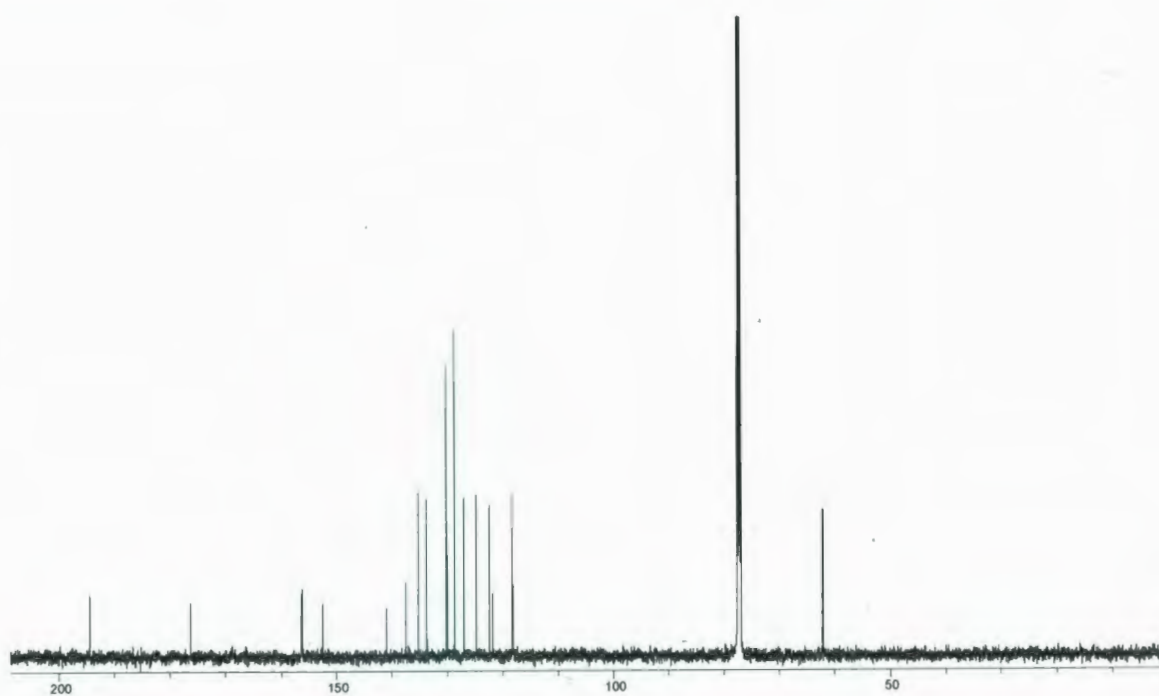
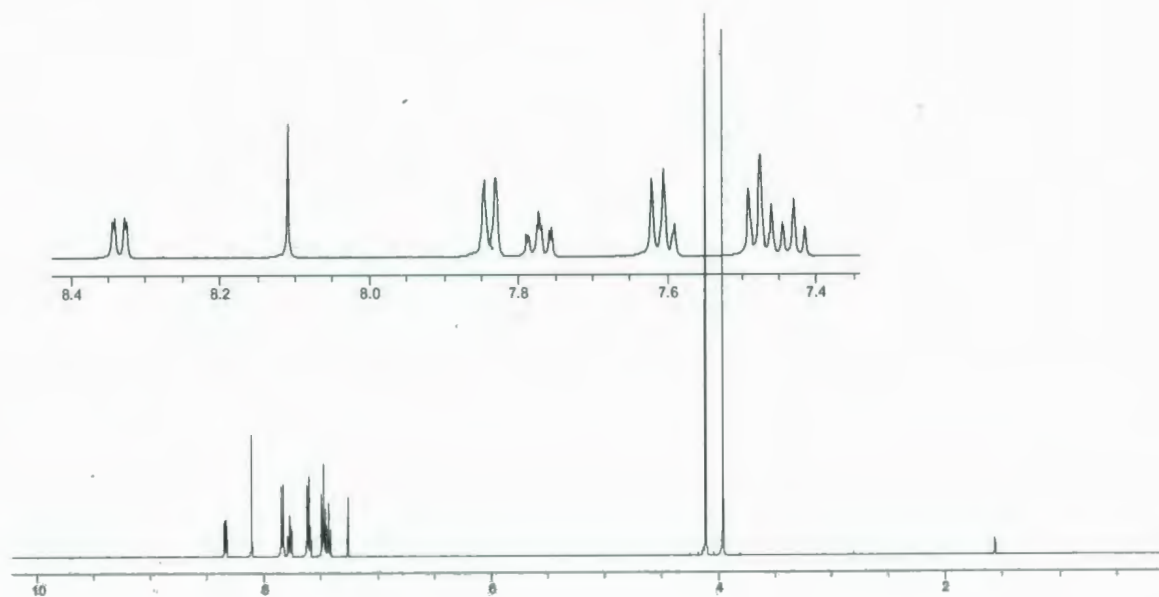
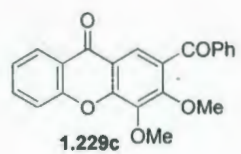


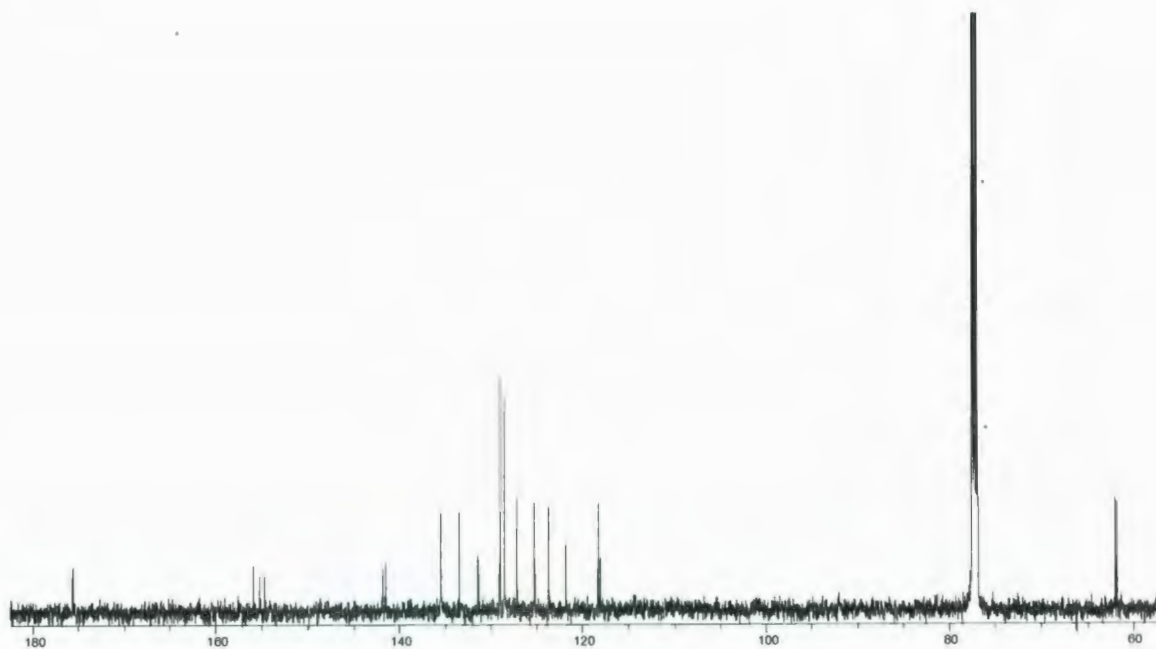
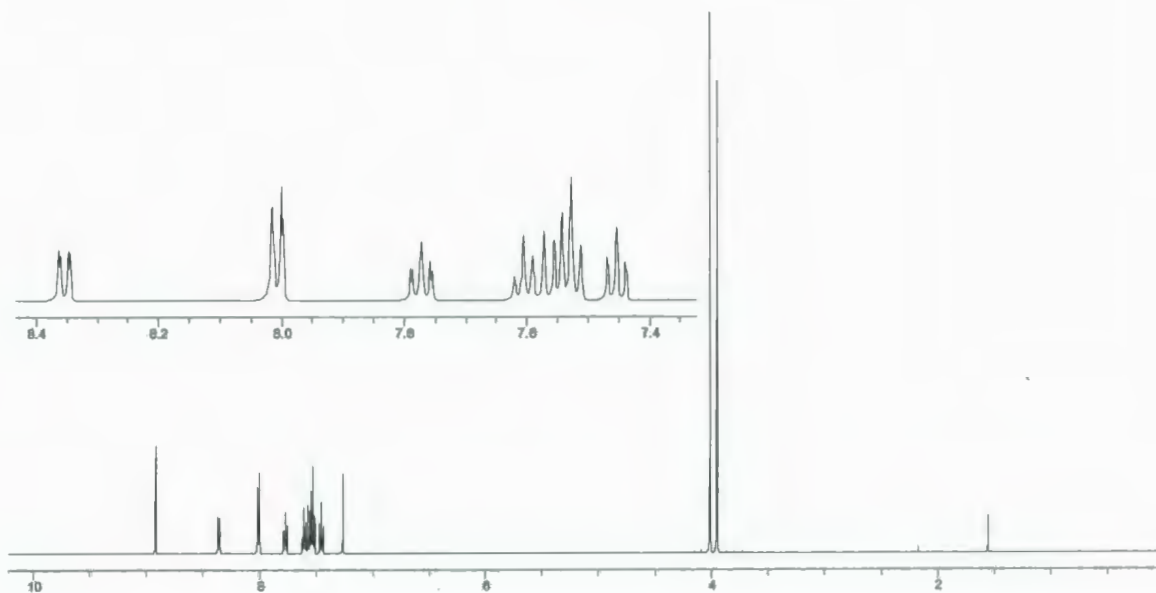
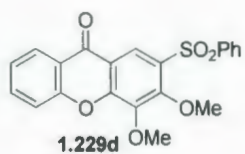


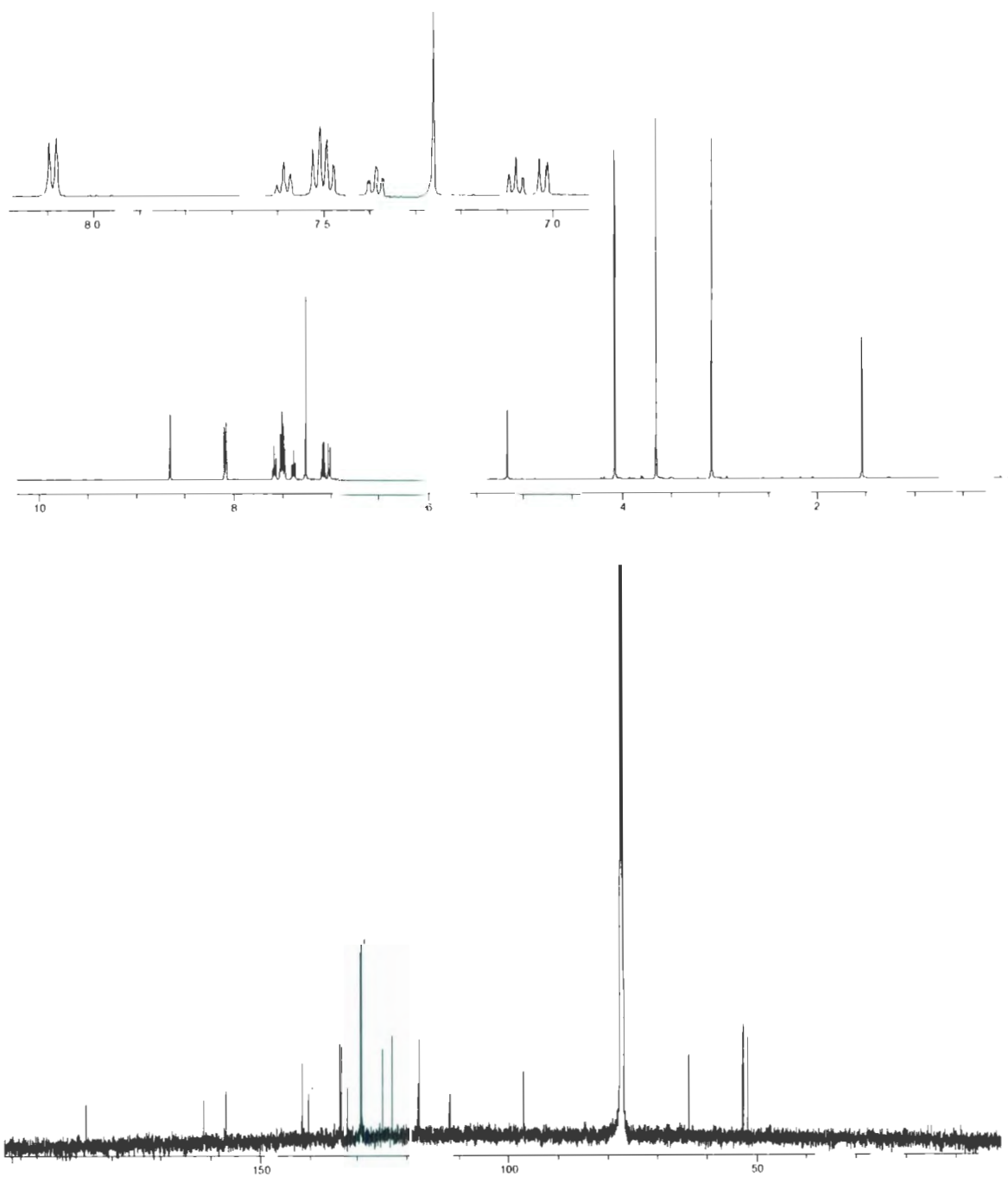
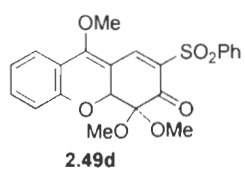




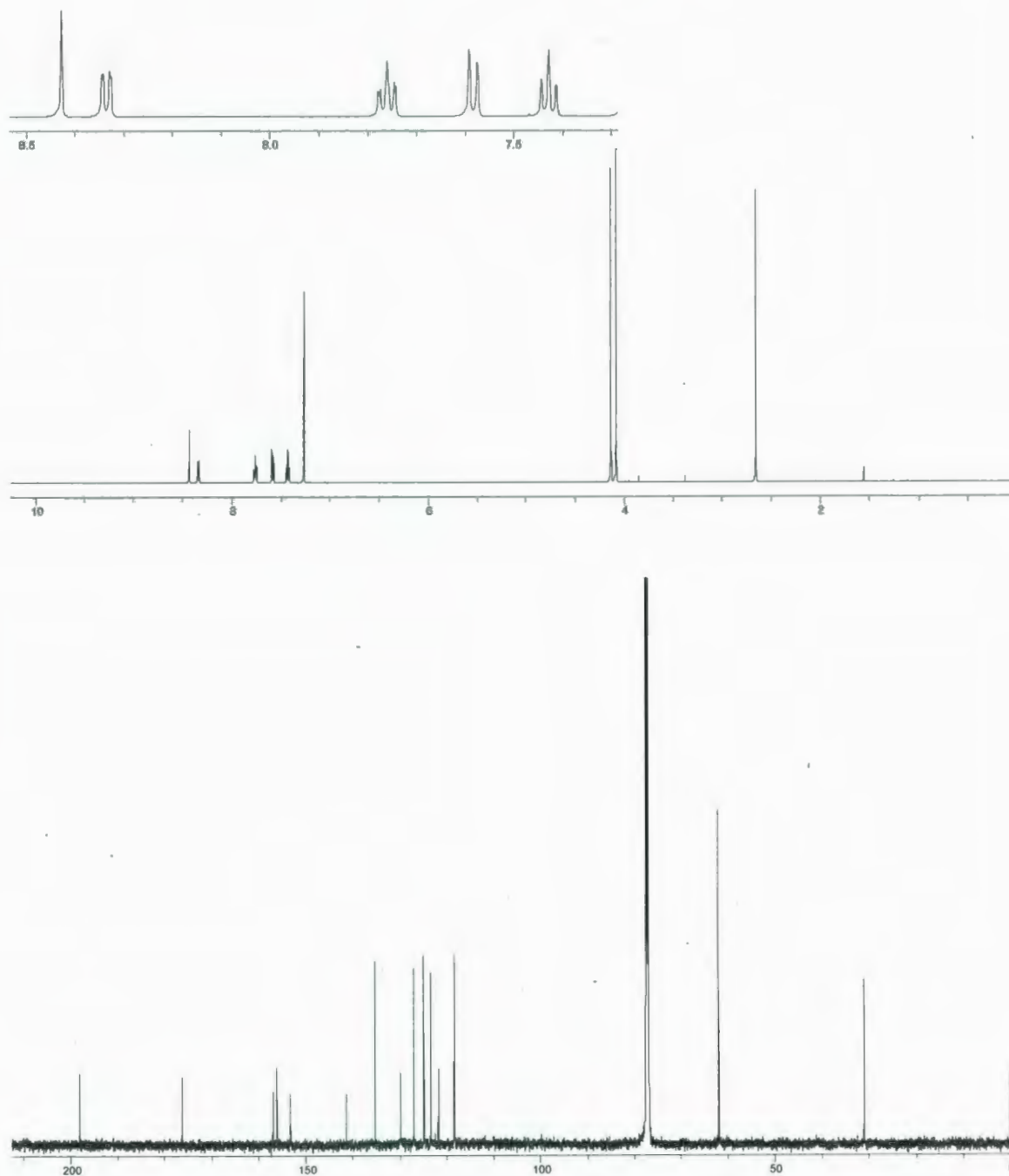
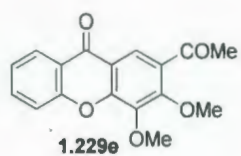


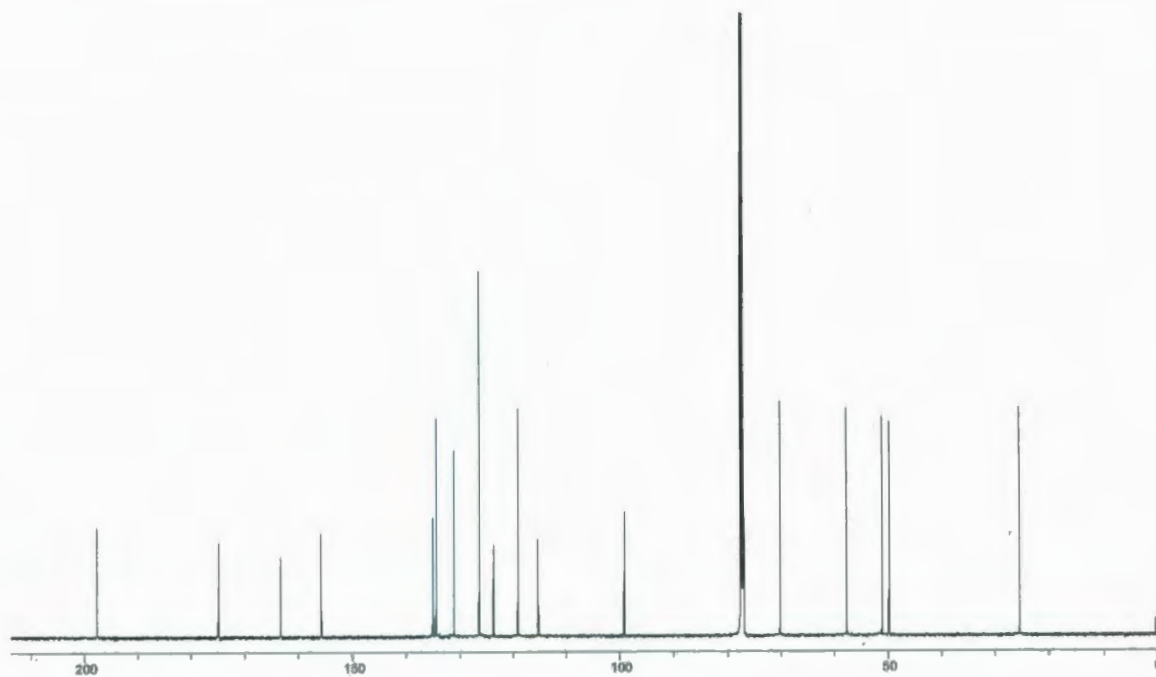
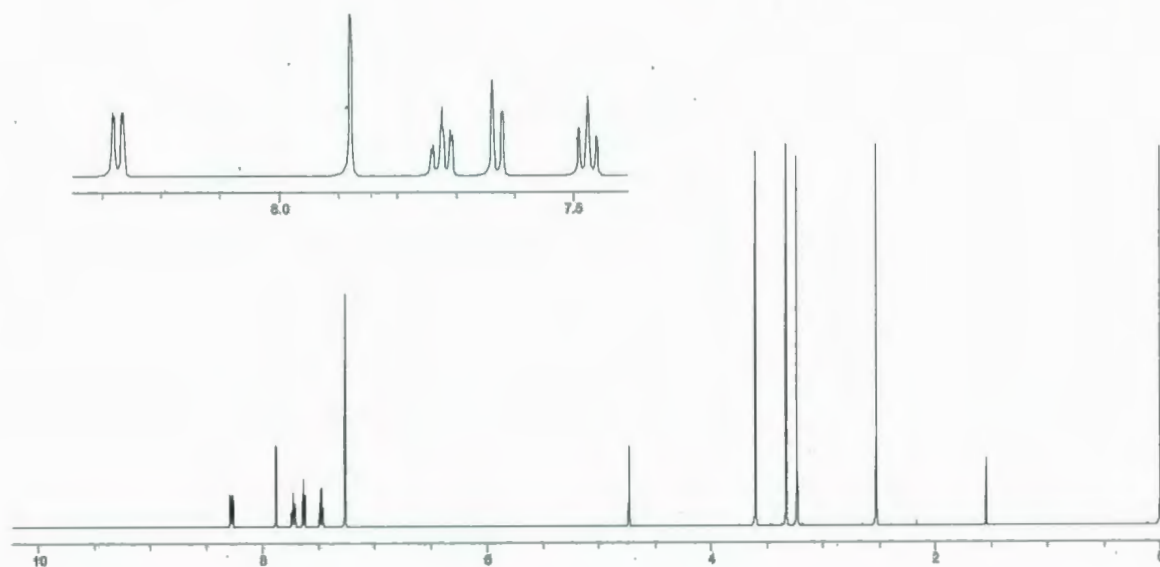
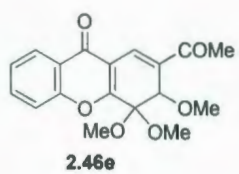


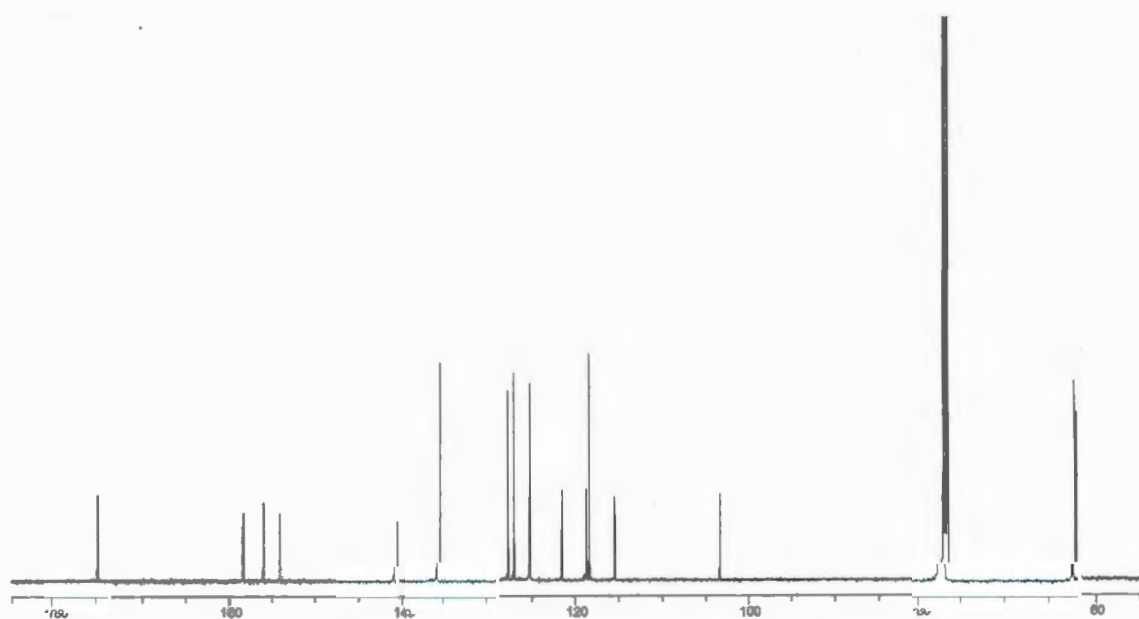
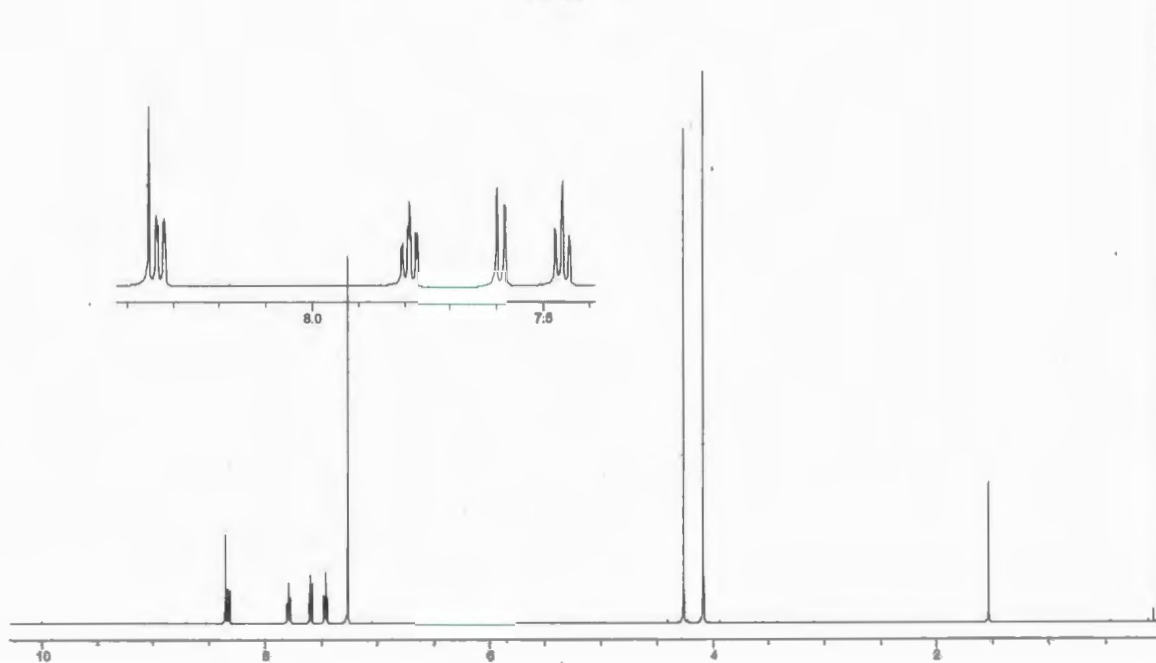
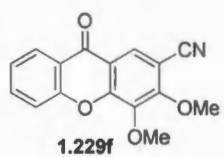




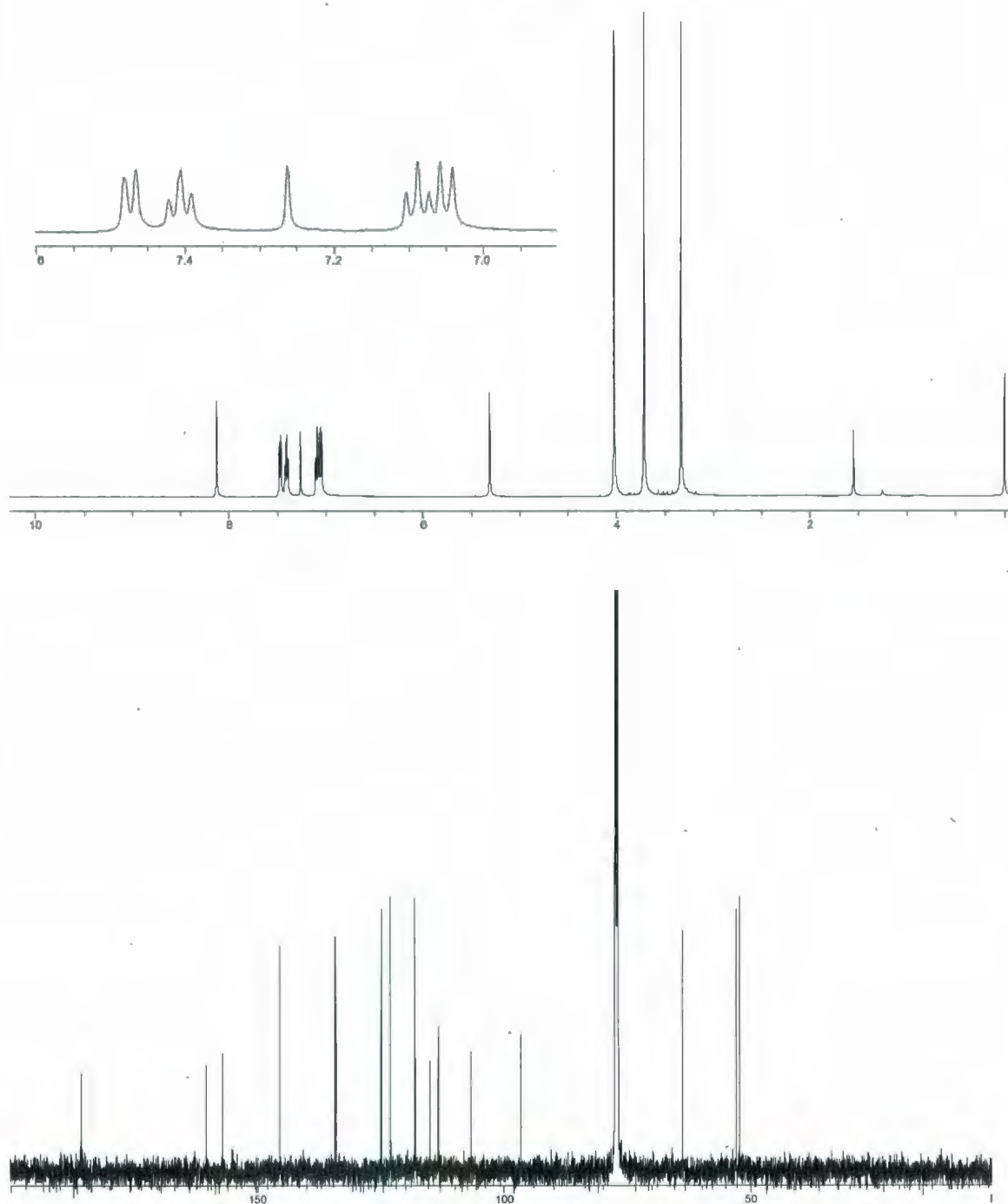
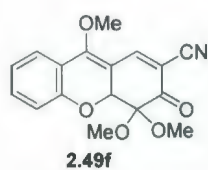


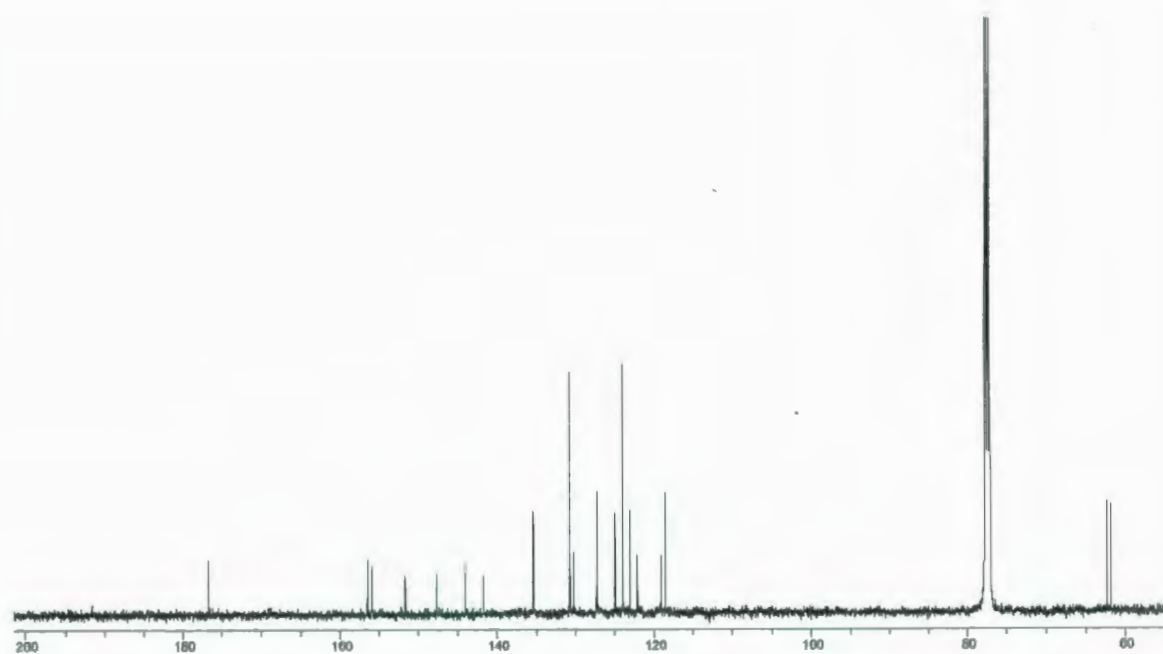
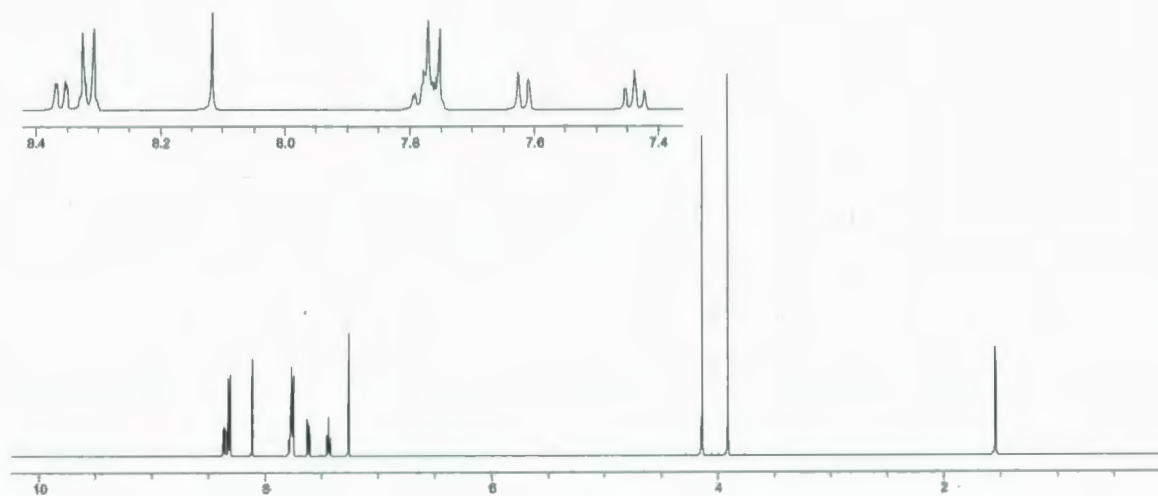
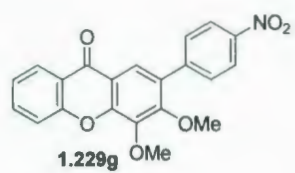


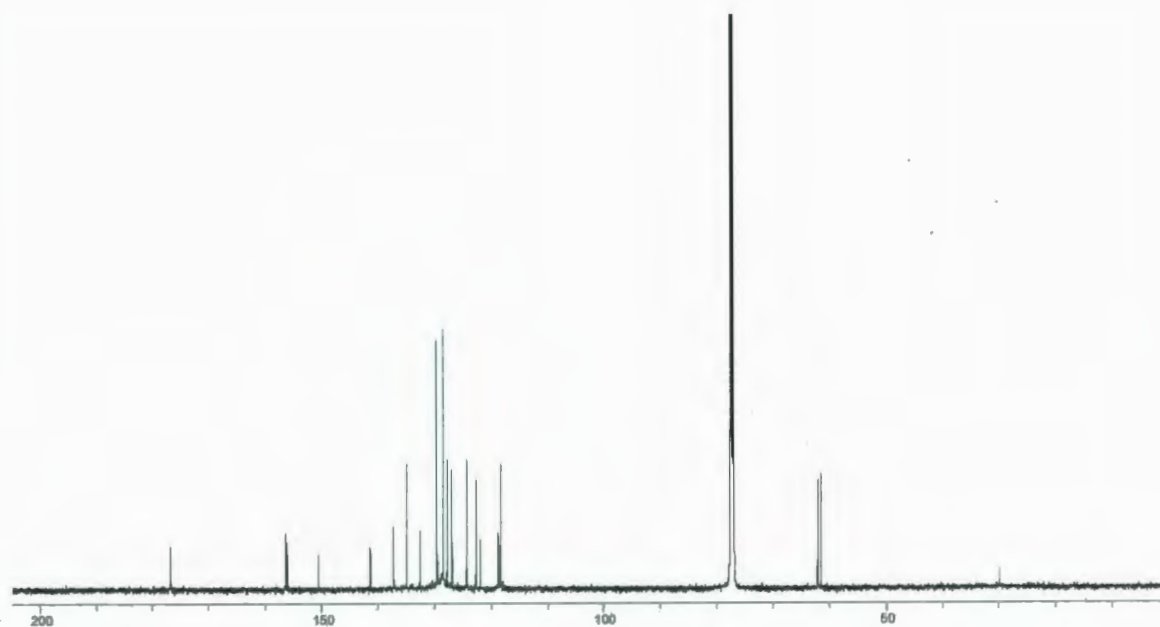
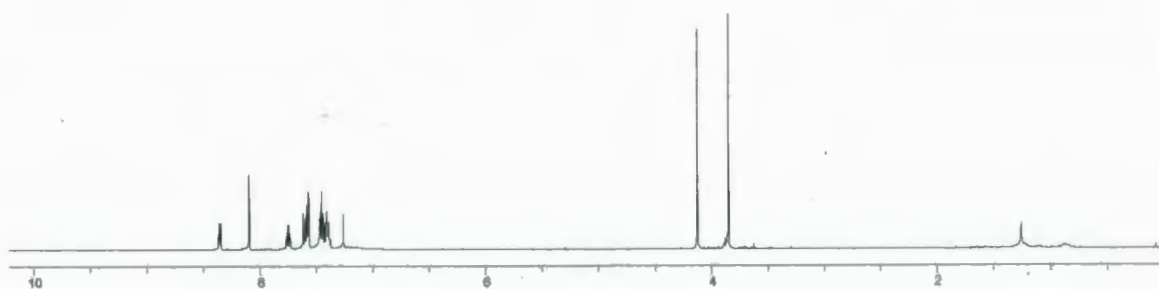
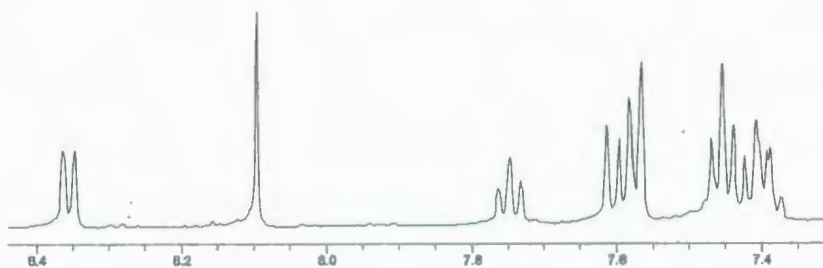
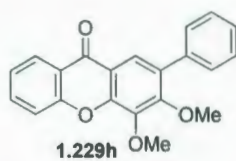












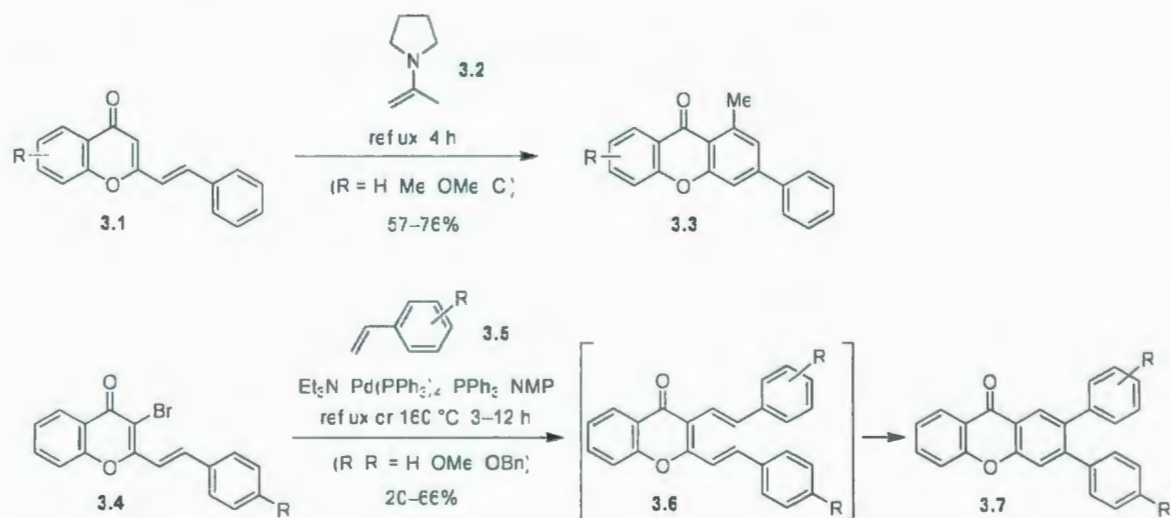


## Chapter 3

# Synthesis and Physical Properties of 2-Aryl-4-methoxyxanthenes and the Attempted Synthesis of 2,4-Diarylxanthenes

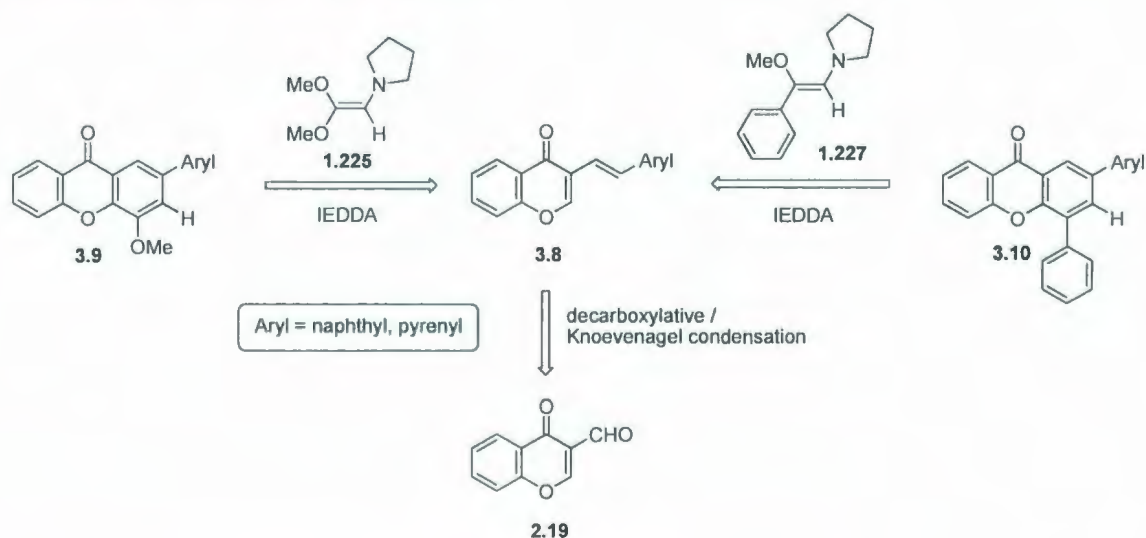
## 3.1 Introduction

Xanthenes possessing aryl substituents have not been found in nature, but some of them have been synthesized during the course of methodological studies. For example, 3-phenylxanthenes **3.3**<sup>1</sup> were obtained from the Diels-Alder reactions between 2-styrylchromones **3.1** and enamines **3.2**, while 2,3-diarylxanthenes **3.7**<sup>2</sup> were synthesized from 3-bromo-2-styrylchromones **3.4** with styrenes **3.5** via Heck coupling, followed by electrocyclic ring closure and oxidation (Scheme 3.1). However, the physical properties of these synthetic xanthenes were not studied.



Scheme 3.1 Synthesis of arylxanthenes **3.3** and **3.7**.

Among the newly synthesized 4-methoxy- and 3,4-dimethoxyxanthenes **1.228** and **1.229** (Chapter 2), xanthenes **1.228h,i**, which have a phenyl and 4-methoxyphenyl group at the 2 position, respectively, gave the highest fluorescence quantum yields ( $\Phi_{\text{em}} = 0.07$  and  $0.13$ , respectively). As such, xanthenes **3.9** and **3.10** (Scheme 3.2) which bear larger arenyl substituents (naphthyl and pyrenyl) are postulated to exhibit higher fluorescence quantum yields than those of **1.228h,i**. The aims of this project were to synthesize mono- and diarylxanthenes employing the methodology developed in Chapter 2 and to study their physical properties. Specifically, 2-aryl-4-methoxyxanthenes **3.9** and 2-aryl-4-phenylxanthenes **3.10** could be obtained from the reactions of the corresponding dienes **3.8** with enamines **1.225** and **1.227**, respectively (Scheme 3.2). The new dienes **3.8**, in turn, should be accessible from 3-formylchromone (**2.19**) via a decarboxylative / Knoevenagel condensation. Thus, the aryl substituents in the target systems originate from both the diene and the dienophile.

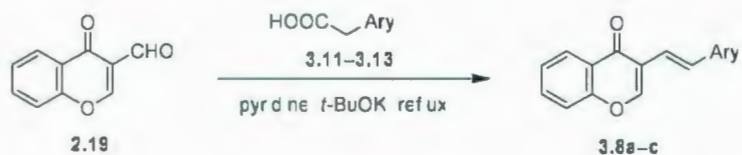


**Scheme 3.2** Retrosynthetic analysis of target arylxanthenes **3.9** and **3.10**.

## 3.2 Results and Discussion

### 3.2.1 Synthesis of Dienes 3.8

Dienes **3.8a–c** were prepared according to the procedure for diene **1.15h** (Chapter 2). Specifically, the reaction of 3-formylchromone (**2.19**) with the corresponding arylacetic acids **3.11–3.13** (2–3 equiv.) in pyridine at reflux in the presence of *t*-BuOK gave dienes **3.8a–c** in moderate yields (Table 3.1). In comparison to diene **1.15h**, which was formed in good yield (82%) after reacting for 22 h, the yields of **3.8a–c** (37–50%) were lower and the reaction times were longer (47–240 h). The greater steric demands of the naphthalenyl and pyrenyl substituents (compared to phenyl) and the differences in the acidity of the benzylic protons are likely to be important factors here. The *trans* geometries of the double bonds in the newly synthesized dienes **3.8a–c** were confirmed by proton NMR spectroscopy ( $J \approx 16$  Hz).

**Table 3.1** Synthesis of dienes **3.8a–c**.

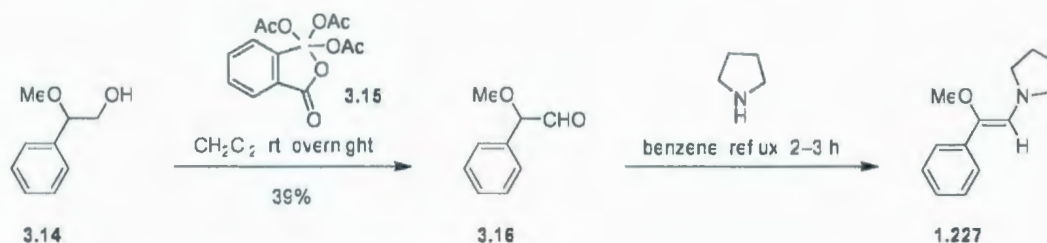
Entry	HOOC-Ary	Dienes 1.15h and 3.8a–c		
		Structure	Time (h)	Yield (%)
1	<p>2.37</p>	<p>1.15h</p>	22	82
2	<p>3.11</p>	<p>3.8a</p>	51	42
3	<p>3.12</p>	<p>3.8b</p>	240	37
4	<p>3.13</p>	<p>3.8c</p>	47	50

### 3.2.2 Synthesis of Dienophile 1.227

Dienophile **1.227**, an enamine, was prepared from the reaction of pyrrolidine with methoxyphenylacetaldehyde (**3.16**),<sup>3</sup> which was obtained from 2-methoxy-2-phenylethanol (**3.14**) via a Dess-Martin oxidation (Scheme 3.3). Although the oxidation of **3.14** was carried out under mild conditions, the major product **3.16** (39%) was formed



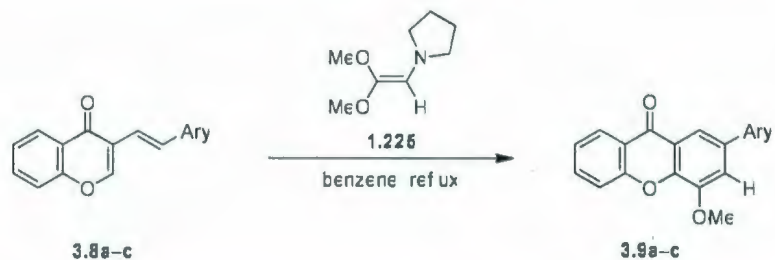
along with a minor product, benzaldehyde, which has been reported to be the major product in the oxidation of phenylallylic alcohols with PCC.<sup>4</sup> The low yield of the desired aldehyde **3.16** can, to some extent, be attributed to the use of vacuum distillation for purification.



**Scheme 3.3** Synthesis of dienophile **1.227**.

### 3.2.3 Synthesis of 2-Aryl-4-methoxyxanthenes

The IEDDA-driven domino reactions between dienes **3.8a–c** and enamine **1.225** (generated from dimethoxyacetaldehyde and pyrrolidine) successfully gave 2-aryl-4-methoxyxanthenes **3.9a–c** (Table 3.2). Similar to xanthenes **1.228h** (50%, Chapter 2), **3.9a** was obtained in moderate yield (44%). An attempt to improve the reaction yields of **1.228h** and **3.9a** by increasing the amount of enamine **1.225** from 10 to 18 equiv. was unsuccessful. Surprisingly, xanthenes **3.9b** and **3.9c** were obtained in high yields, 81% and 90%, respectively. The reason why the yields for these compounds were so high is unclear.

**Table 3.2** Synthesis of 2-aryl-4-methoxyxanthenes **3.9a–c**.

Entry	Diene	Arylxanthone		
		Structure	Time (h)	Yield (%)
1	<b>1.15h</b>	 <b>1.228h</b>	17	51 <sup>a</sup> 50 <sup>b</sup>
2	<b>3.8a</b>	 <b>3.9a</b>	29	44 <sup>a</sup> 53 <sup>b</sup>
3	<b>3.8b</b>	 <b>3.9b</b>	29	81 <sup>c</sup>
4	<b>3.8c</b>	 <b>3.9c</b>	29	90 <sup>b</sup>

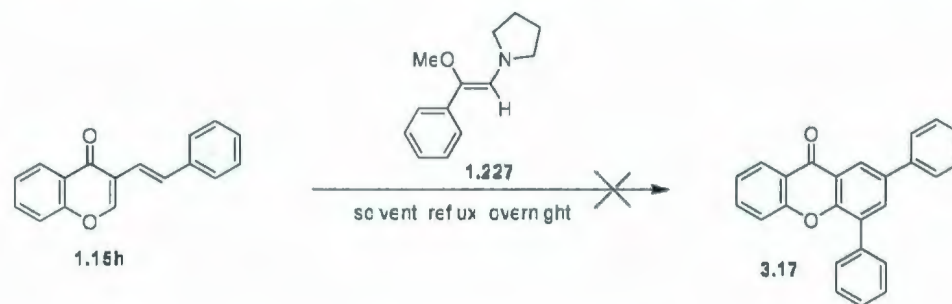
a) 10 equiv. of dienophile

b) 18 equiv. of dienophile

c) 13 equiv. of dienophile

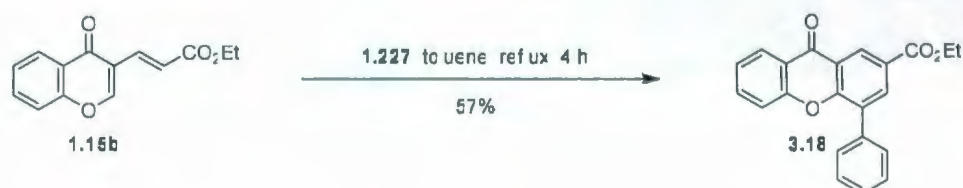
### 3.2.4 Attempted Synthesis of 2,4-Diarylxanthenes

The IEDDA reaction between diene **1.15h** and enamine **1.227** was attempted first. When conditions similar to those employed successfully for dienes **1.15** (*ca.* 0.2 M in benzene, reflux) and enamine **1.225** were used, no reaction was observed (Scheme 3.4).



**Scheme 3.4** Attempted synthesis of 2,4-diphenylxanthenes **3.17**.

The reaction was then performed with higher concentration of diene **1.15h** (*ca.* 1.0 M) in toluene, a higher boiling solvent. Although diene **1.15h** was consumed completely after 2 h (tlc analysis), no major new spots were observed by tlc analysis and no trace of the desired diarylxanthone **3.17** was detected by mass spectrometric analysis of the crude reaction mixture. To probe whether the diene / dienophile combination was not reactive enough, a more electron-deficient diene, **1.15b** (EWG = CO<sub>2</sub>Et), was reacted with enamine **1.227**. Indeed, the desired xanthone **3.18** was obtained in 57% yield from this reaction (Scheme 3.5).

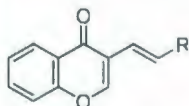
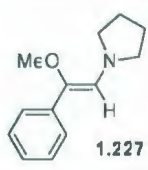
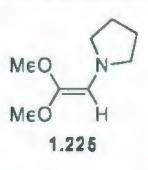
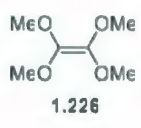


**Scheme 3.5** Synthesis of aylixanthenes **3.18**.



To understand more about the relative reactivity of dienophiles **1.227**, **1.225** and **1.226**, their HOMO energies were calculated (RHF/3-21G\*\*//AM1/toluene)<sup>5</sup> along with the LUMO energies of dienes **1.15b**, **1.15h**, and **3.8a–c** (Table 3.3).

**Table 3.3** HOMO–LUMO gap calculations.

Entry	Dienophiles HOMO (eV)					
				 1.227	 1.225	 1.226
				–6.99	–7.41	–8.18
	dienes	R	LUMO (eV)	HOMO–LUMO (eV)		
1	<b>1.15b</b>	CO <sub>2</sub> Et	1.99	8.98	9.4	10.17
2	<b>1.15h</b>	Ph	2.17	9.16	9.58	10.35
3	<b>1.15g</b>	<i>p</i> -NO <sub>2</sub> C <sub>6</sub> H <sub>4</sub>	1.38	8.37	8.79	–
4	<b>3.8a</b>	1-naphthyl	2.16	9.15	9.57	–
5	<b>3.8b</b>	2-naphthyl	2.16	9.15	9.57	–
6	<b>3.8c</b>	1-pyrenyl	1.53	8.52	8.94	–

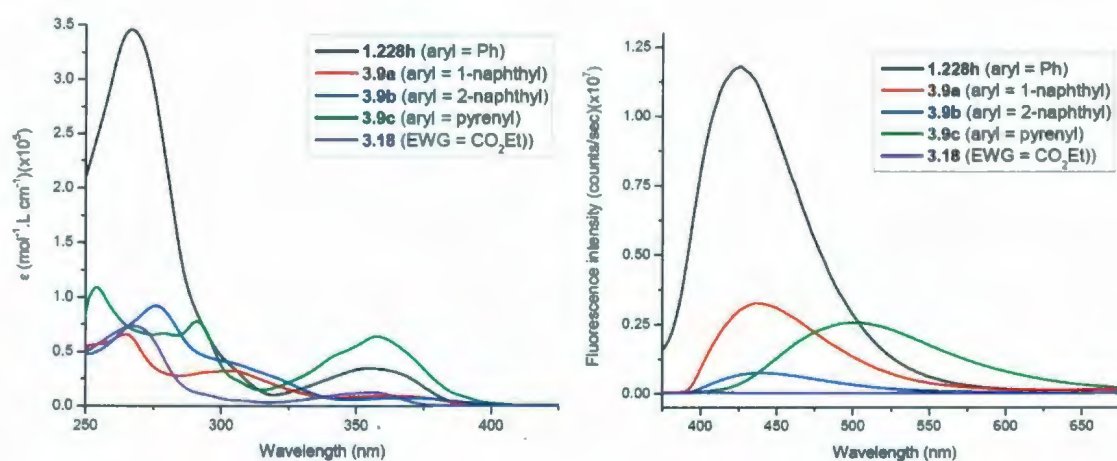
The HOMO energy levels of dienophiles **1.227**, **1.225**, and **1.226** are respectively –6.99, –7.41, and –8.18 eV, which suggest that enamine **1.227** should be the most reactive of the three dienophiles. However, the observation of lower reactivity than **1.225** suggests that the steric demands of the phenyl group in dienophile **1.227** destabilize the IEDDA<sup>6</sup> transition state. This may also be the reason that a different reaction pathway



appears to have been taken in the reaction with diene **1.15h**. Therefore, no further attempt was made to employ dienes bearing electron-neutral groups, *e.g.* **3.8a** and **3.8b**. However, dienes **1.15g** and **3.8c** (Table 3.3), which have lower-lying LUMOs than **1.15b**, may be good substrates for future investigation.

### 3.2.5 Physical Properties of Arylxanthoness **3.9a–c** and **3.18**

The positions of the lowest energy absorption bands of arylxanthoness **3.9a–c** and **3.18** (356–366 nm) are similar to that of xanthone **1.228h** (354 nm), but much lower in intensity, except for **3.9c** (Figure 3.1, Table 3.4). The anomalous behaviour of **3.9c** was also observed in its fluorescence, in which it emitted at a longer wavelength (504 nm) than those of **1.228h** (426 nm), **3.9a** (436 nm), and **3.9b** (438 nm). As a result, xanthone **3.9c** has the largest reorganization energy ( $\lambda_t = 4050 \text{ cm}^{-1}$ ) among the series of xanthoness, while those of xanthoness **3.18** and **3.9a–b** range from 1639 to  $2345 \text{ cm}^{-1}$ . As expected, the fluorescence quantum yields of arylxanthoness **3.9a–c** ( $\Phi_{\text{em}} = 0.11\text{--}0.14$ ) are higher than that of **1.228h** ( $\Phi_{\text{em}} = 0.072$ ), but not by very much. Similar to the 4-methoxyxanthoness **1.228a–g**, 4-phenylxanthone **3.18** exhibits much weaker fluorescence than the 2-aryl-4-methoxyxanthoness **3.9a–c**. It thus appears as though a phenyl group at the 2-position enhances the fluorescence more than a phenyl group at the 4-position.



**Figure 3.1** Absorption and emission spectra of arylxanthenes **1.228h**, **3.9a–c** and **3.18** in  $\text{CHCl}_3$  ( $3 \times 10^{-5} \text{ M}$ ).

**Table 3.4** Physical data of xanthenes **3.9a–c** and **3.18** in comparison with **1.228h**.

Comp.	$\lambda_{\text{max (abs)}}$ (nm)	$E_{\text{abs}} (\text{cm}^{-1})$ ( $= 1/\lambda \times 10^7$ )	$\lambda_{\text{max (em)}}$ (nm)	$E_{\text{em}} (\text{cm}^{-1})$ ( $= 1/\lambda \times 10^7$ )	Stokes shift ( $\text{cm}^{-1}$ ) ( $E_{\text{abs}} - E_{\text{em}} = 2\lambda_t$ )	$\lambda_t$ ( $\text{cm}^{-1}$ )	$\Phi_{\text{em}}$
<b>1.228h</b>	354	28200	426	23500	4770	2390	0.072
<b>3.9a</b>	362	27600	436	22900	4690	2350	0.11
<b>3.9b</b>	366	27300	438	22800	4490	2250	0.14
<b>3.9c</b>	358	27900	504	19800	8090	4050	0.12
<b>3.18</b>	356	28100	403	24800	3280	1640	-

### 3.3 Conclusions

2-Aryl-4-methoxyxanthenes **3.9a–c** were successfully synthesized employing the IEDDA-driven domino reactions between the corresponding aryl dienes **3.8a–c** and dienophile **1.225**. However, the reaction of diene **3h** with dienophile **1.227** failed to

afford 2,4-diphenylxanthone **3.17**. Although it was not a suitable approach for formation of 2,4-diarylxanthenes **3.10**, the 4-arylxanthenes such as **3.18** were obtained. The fluorescence quantum yields of xanthenes **3.9a–c**, which bear naphthyl and pyrenyl groups, are slightly higher than that of xanthenes **1.228h**, which bear a phenyl group. Overall, this work contributed the development of new methodology for the synthesis of 4-arylxanthenes as well as enriched a rare category of compounds through the synthesis of some new aryloxanthenes.

### 3.4 Experimental Section

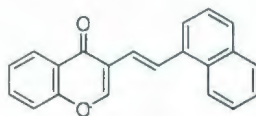
General methods and instrumentation used are identical to those described in Chapter 2 (see page 76–77).

#### 3.4.1 Experimental Procedures<sup>7</sup>

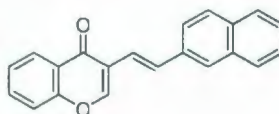
##### General procedure for the synthesis of dienes **3.8a–c**

A mixture of arylacetic acid (2–3 equiv.), *t*-BuOK (1–1.5 equiv.) and 3-formylchromone (1 equiv.) in pyridine was heated at reflux until 3-formylchromone was consumed (tlc analysis). The reaction mixture was cooled to room temperature, poured into ice-water (300 mL) and acidified with aqueous 6 N HCl solution until the pH reached  $\approx 5$ . The yellow precipitate was collected by suction filtration, washed several times with deionized water and dried in air. Purification of the crude product by column chromatography yielded dienes **3.8a–c** as yellow solids.



**(*E*)-3-(1-Naphthyl)-4*H*-chromen-4-one (3.8a)**

A mixture of 1-naphthaleneacetic acid (**3.12**) (3.18 g, 17.1 mmol), *t*-BuOK (1.02 g, 8.60 mmol) and 3-formylchromone (**2.19**) (993 mg, 5.70 mmol) in pyridine (35 mL) was heated at reflux for 51 h and worked up according to the general procedure. Column chromatography (20:80 EtOAc:hexanes) yielded diene **3.8a** (709 mg, 42%) as a yellow solid:  $R_f$  = 0.35 (20:80 EtOAc:hexanes); mp 117–118 °C; IR  $\nu$  3059 (w), 1640 (m), 1612 (m), 1643 (s), 1404 (m), 1358 (m), 1289 (m), 1196 (m), 1156 (m), 973 (m), 857 (m), 787 (s), 775 (s), 757 (s), 695 (m) ( $\text{cm}^{-1}$ );  $^1\text{H}$  NMR (500 MHz)  $\delta$  8.58 (d,  $J$  = 16.0 Hz, 1H), 8.34 (dd,  $J$  = 8.0, 1.3 Hz, 1H), 8.28 (d,  $J$  = 8.3 Hz, 1H), 8.15 (s, 1H), 7.85 (d,  $J$  = 8.0 Hz, 1H), 7.79 (d,  $J$  = 8.0 Hz, 1H), 7.73 (d,  $J$  = 7.1 Hz, 1H), 7.67 (t,  $J$  = 7.5 Hz, 1H), 7.56–7.40 (m, 5H), 6.96 (d,  $J$  = 15.9 Hz, 1H);  $^{13}\text{C}$  NMR (125 MHz)  $\delta$  176.9, 155.9, 153.9, 135.4, 133.9, 133.7, 131.5, 129.6, 128.7, 128.4, 126.4, 126.35, 126.0, 125.8, 125.5, 124.5, 124.2, 123.5, 122.2, 122.1, 118.26; MS [APCI (+)]  $m/z$  (%) 299 ( $\text{M}^+$ , 100); HRMS [EI (+)] calcd for  $\text{C}_{21}\text{H}_{14}\text{O}_2$  298.0994, found 298.0988.

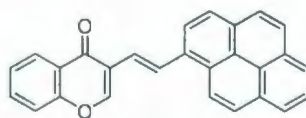
**(*E*)-3-(2-Naphthyl)-4*H*-chromen-4-one (3.8b)**

A mixture of 2-naphthaleneacetic acid (**3.13**) (3.18 g, 17.1 mmol), *t*-BuOK (673 mg, 5.70 mmol) and 3-formylchromone (**2.19**) (0.993 g, 5.70 mmol) in pyridine (35 mL) was heated at reflux for 10 d and worked up according to the general procedure. Column



chromatography (10:90 EtOAc:hexanes) yielded diene **3.8b** (635 mg, 37%) as a yellow solid:  $R_f$  = 0.39 (20:80 EtOAc:hexanes); mp 160–161 °C; IR  $\nu$  3086 (w), 1635 (s), 1614 (m), 1570 (m), 1466 (s), 1401 (w), 1385 (w), 1350 (m), 1218 (m), 1188 (m), 1166 (m), 974 (m), 850 (m), 818 (m), 803 (m), 754 (s), 695 (m) ( $\text{cm}^{-1}$ );  $^1\text{H}$  NMR (500 MHz)  $\delta$  8.32 (dd,  $J$  = 7.8, 1.8 Hz, 1H), 8.15 (s, 1H), 7.87–7.77 (m, 5H), 7.74 (dd,  $J$  = 8.7, 1.4 Hz, 1H), 7.69–7.65 (m, 1H), 7.48–7.41 (m, 4H), 7.11 (d,  $J$  = 16.5 Hz, 1H);  $^{13}\text{C}$  NMR (125 MHz)  $\delta$  176.8, 156.1, 153.2, 135.1, 133.9, 133.7, 133.4, 131.9, 128.5, 128.3, 127.9, 127.1, 126.5, 126.2, 125.5, 124.4, 123.7, 122.1, 119.6, 118.3 (one signal fewer than expected); MS [APCI (+)]  $m/z$  (%) 299 ( $\text{M}^+$ , 100); HRMS [EI (+)] calcd for  $\text{C}_{21}\text{H}_{14}\text{O}_2$  298.0994, found 298.0991.

**(*E*)-3-(1-Pyrenyl)-4*H*-chromen-4-one (3.8c)**



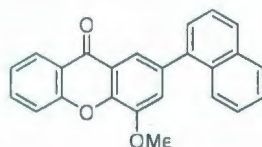
A mixture of 1-pyreneacetic acid (**3.14**) (500 mg, 1.92 mmol), *t*-BuOK (108 mg, 962  $\mu\text{mol}$ ) and 3-formylchromone (**2.19**) (167 mg, 959  $\mu\text{mol}$ ) in pyridine (18 mL) was heated at reflux for 47 h and worked up according to the general procedure. Column chromatography (20:80 EtOAc:hexanes) yielded diene **3.8c** (179 mg, 50%) as a yellow solid:  $R_f$  = 0.32 (20:80 EtOAc:hexanes); mp 185–186 °C; IR  $\nu$  3054 (w), 1636 (s), 1574 (w), 1556 (w), 1466 (s), 1400 (m), 1358 (m), 1220 (m), 1193 (m), 1173 (m), 968 (m), 841 (s), 824 (m), 753 (s), 716 (s), 693 (s) ( $\text{cm}^{-1}$ );  $^1\text{H}$  NMR (500 MHz)  $\delta$  8.90 (d,  $J$  = 16.6, 1H), 8.54 (d,  $J$  = 8.3, 1H), 8.35 (d,  $J$  = 8.0, 1H), 8.28 (d,  $J$  = 7.4 Hz, 1H), 8.17–8.11 (m, 5H), 8.03 (s, 2H), 8.00–7.97 (t,  $J$  = 7.6, 1H), 7.68–7.65 (t,  $J$  = 7.0, 1H), 7.47–7.43 (m,

2H), 7.11 (d,  $J = 16.3$  Hz, 1H);  $^{13}\text{C}$  NMR (125 MHz)  $\delta$  177.0, 155.9, 154.0, 133.7, 132.3, 131.7, 131.2, 129.4, 128.7, 127.9, 127.7, 127.6, 126.5, 126.2, 125.53, 125.5, 125.3, 125.2, 125.1, 124.5, 123.5, 122.3, 122.2, 118.3 (three signals fewer than expected); MS [APCI (+)]  $m/z$  (%) 373 ( $\text{M}^+$ , 100); HRMS [EI (+)] calcd for  $\text{C}_{27}\text{H}_{16}\text{O}_2$  372.1150, found 372.1145.

### General procedure for synthesis of 2-aryl-4-methoxyxanthenes 3.9a–c

See the general procedure for synthesis of 4-methoxyxanthenes **1.228** in Chapter 2 (page 90).

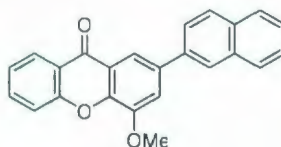
#### 4-Methoxy-2-(1-naphthyl)-9H-xanthen-9-one (3.9a)



A mixture of enamine **1.225** (5.40 mmol) and diene **3.8a** (90.1 mg, 302  $\mu\text{mol}$ ) was heated at reflux for 29 h and worked up according to the general procedure. Column chromatography (10:90 EtOAc:hexanes) yielded xanthone **3.9a** (56.4 mg, 53%) as a yellow solid:  $R_f = 0.50$  (35:65 EtOAc:hexanes); mp 158–159  $^{\circ}\text{C}$ ; IR  $\nu$  3053 (w), 2945 (w), 1657 (s), 1610 (m), 1596 (m), 1570 (w), 1489 (s), 1467 (s), 1397 (m), 1363 (m), 1340 (m), 1313 (s), 1293 (s), 1258 (m), 1224 (s), 1189 (m), 1169 (m), 1149 (m), 1113 (m), 1091 (m), 973 (m), 871 (m), 777 (s), 757 (s), 690 (m), 662 (m) ( $\text{cm}^{-1}$ );  $^1\text{H}$  NMR (500 MHz)  $\delta$  8.39 (dd,  $J = 8.0, 1.6$  Hz, 1H), 8.27 (d,  $J = 2.7$  Hz, 1H), 8.14 (s, 1H), 7.97–7.93 (m, 2H), 7.89 (d,  $J = 7.8$  Hz, 1H), 7.84 (dd,  $J = 8.0, 2.1$  Hz, 1H), 7.78–7.75 (m, 1H), 7.65 (d,  $J = 7.7$  Hz, 1H), 7.61 (d,  $J = 1.9$  Hz, 1H), 7.56–7.50 (m, 2H), 7.42 (t,  $J = 7.9$  Hz, 1H),

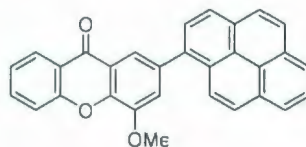
4.16 (s, 3H);  $^{13}\text{C}$  NMR (125 MHz)  $\delta$  177.4, 156.3, 148.7, 146.2, 139.1, 136.6, 135.1, 134.1, 131.7, 128.7, 128.4, 127.5, 127.0, 126.6, 126.2, 125.8, 125.6, 124.4, 122.8, 122.1, 118.8, 118.6, 117.8, 56.8; MS [APCI (+)]  $m/z$  (%) 353 ( $\text{M}^+$ , 100); HRMS [EI (+)] calcd for  $\text{C}_{24}\text{H}_{16}\text{O}_3$  352.1099, found 352.1094.

#### 4-Methoxy-2-(2-naphthyl)-9H-xanthen-9-one (3.9b)

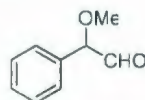


A mixture of enamine **1.225** (4.42 mmol) and diene **3.8b** (99.9 mg, 335  $\mu\text{mol}$ ) was heated at reflux for 29 h and worked up according to the general procedure. Column chromatography (10:90 EtOAc:hexanes) yielded xanthone **3.9b** (95.2 mg, 81%) as a yellow solid:  $R_f$  = 0.32 (20:80 EtOAc:hexanes); mp 210–211  $^{\circ}\text{C}$ ; IR  $\nu$  3052(w), 3002 (w), 2961 (w), 1654 (s), 1599 (s), 1570 (w), 1494 (s), 1467 (s), 1445 (m), 1380 (m), 1360 (m), 1337 (m), 1312 (s), 1294 (s), 1276 (m), 1217 (m), 1198 (m), 1180 (m), 1165 (s), 1151 (m), 1094 (m), 1062 (m), 984 (m), 869 (m), 850 (m), 813 (s), 758 (s), 742 (m), 687 (m), 662 (m) ( $\text{cm}^{-1}$ );  $^1\text{H}$  NMR (500 MHz)  $\delta$  8.39 (dd,  $J$  = 8.0, 1.6 Hz, 1H), 8.26 (d,  $J$  = 2.6 Hz, 1H), 8.13 (s, 1H), 7.96–7.92 (m, 2H), 7.88 (d,  $J$  = 7.5 Hz, 1H), 7.83 (dd,  $J$  = 8.6, 2.0 Hz, 1H), 7.78–7.74 (m, 1H), 7.65 (d,  $J$  = 8.4 Hz, 1H), 7.60 (d,  $J$  = 1.7 Hz, 1H), 7.55–7.49 (m, 2H), 7.42 (t,  $J$  = 7.7 Hz, 1H), 4.15 (s, 3H);  $^{13}\text{C}$  NMR (125 MHz)  $\delta$  177.4, 156.2, 149.3, 146.4, 137.4, 136.9, 135.0, 133.9, 133.0, 128.9, 128.5, 127.9, 127.0, 126.8, 126.5, 126.2, 125.5, 124.4, 123.1, 122.0, 118.6, 116.1, 114.9, 56.9; MS [APCI (+)]  $m/z$  (%) 353 ( $\text{M}^+$ , 100); HRMS [EI (+)] calcd for  $\text{C}_{24}\text{H}_{16}\text{O}_3$  352.1099, found 352.1099.



**4-Methoxy-2-(1-pyrenyl)-9H-xanthen-9-one (3.9c)**

A mixture of enamine **1.225** (4.32 mmol) and diene **3.8c** (90.0 mg, 242  $\mu\text{mol}$ ) was heated at reflux for 29 h and worked up according to the general procedure. Column chromatography (35:65 EtOAc:hexanes) yielded xanthone **3.9c** (91.8 mg, 90%) as a yellow solid:  $R_f$  = 0.30 (20:80 EtOAc:hexanes); mp 257–258 °C (decomposed, melted at 261–262 °C); IR  $\nu$  3043 (w), 2941 (w), 2843 (w), 1657 (s), 1595 (s), 1570 (m), 1486 (s), 1466 (s), 1443 (s), 1374 (m), 1352 (m), 1338 (m), 1316 (s), 1282 (s), 1220 (s), 1176 (s), 1090 (w), 983 (m), 847 (s), 758 (s), 752 (m), 687 (m), 662 (m) ( $\text{cm}^{-1}$ );  $^1\text{H}$  NMR (500 MHz)  $\delta$  8.40 (d,  $J$  = 7.6 Hz, 1H), 8.26–8.17 (m, 5H), 8.12 (s, 2H), 8.06–8.02 (m, 3H), 7.80–7.77 (m, 1H), 7.70 (d,  $J$  = 8.1 Hz, 1H), 7.52 (d,  $J$  = 1.0 Hz, 1H), 7.44 (t,  $J$  = 7.4 Hz, 1H), 4.10 (s, 3H);  $^{13}\text{C}$  NMR (125 MHz)  $\delta$  177.4, 156.3, 148.8, 146.2, 137.0, 136.4, 135.1, 131.7, 131.18, 131.14, 128.8, 128.2, 127.94, 127.86, 127.6, 127.0, 126.4, 125.6, 125.3, 125.2, 125.1, 125.0, 124.9, 124.4, 122.9, 122.1, 119.3, 118.6, 118.2, 56.9; MS [APCI (+)]  $m/z$  (%) 427 ( $\text{M}^+$ , 100); HRMS [EI (+)] calcd for  $\text{C}_{30}\text{H}_{18}\text{O}_3$  426.1256, found 426.1250.

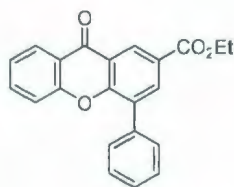
**( $\pm$ )-Methoxyphenylacetaldehyde (3.16)<sup>3</sup>**

To a solution of 2-methoxy-2-phenylethanol (**3.14**) (2.72 g, 17.9 mmol) in  $\text{CH}_2\text{Cl}_2$  (50 mL) was added saturated aqueous sodium bicarbonate solution (18 drops), followed



by Dess-Martin periodinane<sup>8</sup> (18.2 g, 42.9 mmol). The reaction mixture was stirred at room temperature overnight. Saturated aqueous NaHCO<sub>3</sub> solution (30 mL), saturated aqueous Na<sub>2</sub>S<sub>2</sub>O<sub>3</sub> solution (30 mL) and Et<sub>2</sub>O (30 mL) were added into reaction mixture. After stirring for 10 min, the solids were removed by suction filtration and the layers were separated. The aqueous layer was extracted with Et<sub>2</sub>O (3 x 30 mL). The combined organic layers were washed with saturated aqueous NaHCO<sub>3</sub> solution (30 mL), washed with brine, dried over MgSO<sub>4</sub> and then filtered. The solvent was removed under reduced pressure. The crude product was purified by vacuum distillation (4–5 mmHg, 93–95 °C), yielding **3.16** (1.04 g, 39%) as yellow liquid: *R*<sub>f</sub> = 0.65 (35:65 EtOAc:Hexanes), <sup>1</sup>H NMR (500 MHz) δ 9.60 (d, *J* = 1.6 Hz, 1H), 7.44–7.34 (m, 5H), 4.64 (d, *J* = 1.3 Hz, 1H), 3.45 (s, 3H); <sup>13</sup>C NMR (125 MHz) δ 198.5, 134.0, 129.3, 127.7, 88.5, 57.5; MS [APCI (+)] *m/z* (%) 151 (*M*<sup>+</sup>, 12).

#### Ethyl-4-phenyl-9-oxo-9*H*-xanthene-2-carboxylate (**3.18**)



A mixture of enamine **1.227** (1.24 mmol) and diene **1.15b** (68.6 mg, 28.1 μmol) was heated at reflux in toluene for 4 h and worked up according to the general procedure for xanthenes **1.228** (Chapter 2, page 90). Column chromatography (20:80 EtOAc:hexanes) of the crude product yielded xanthone **3.18** (54.9 mg, 57%) as a yellow solid: *R*<sub>f</sub> = 0.32 (20:80 EtOAc:hexanes); mp 205–206 °C; IR ν 3087 (w), 1716 (s), 1670 (s), 1614 (m), 1597 (s), 1465 (s), 1443 (s), 1400 (m), 1372 (m), 1338 (m), 1288 (s), 1227

(s), 1123 (m), 1190 (m), 1026 (s), 994 (w), 883 (w), 769 (m), 757 (s), 738 (m), 700 (m), 685 (m) ( $\text{cm}^{-1}$ );  $^1\text{H}$  NMR (500 MHz)  $\delta$  9.05 (d,  $J = 2.2$  Hz, 1H), 8.43 (d,  $J = 2.2$  Hz, 1H), 8.37 (dd,  $J = 8.1, 1.4$  Hz, 1H), 7.76–7.70 (m, 1H), 7.68 (d,  $J = 7.5$  Hz, 2H), 7.55 (t,  $J = 7.5$  Hz, 2H), 7.49–7.41 (m, 3H), 4.45 (q,  $J = 7.1$  Hz, 2H), 1.45 (t,  $J = 7.1$  Hz, 3H);  $^{13}\text{C}$  NMR (125 MHz)  $\delta$  177.1, 165.7, 156.1, 155.8, 136.5, 135.8, 135.4, 132.2, 129.9, 128.8, 128.53, 128.50, 127.1, 126.5, 124.9, 122.2, 121.7, 118.5, 61.7, 14.6; MS [APCI (+)]  $m/z$  (%) 345 ( $\text{M}^+$ , 100); HRMS [EI (+)] calcd for  $\text{C}_{22}\text{H}_{16}\text{O}_4$  344.1049, found 344.1042.

### 3.4.2 UV and Fluorescence Measurements

Methods are identical to those described in Chapter 2, page 105–106. Solutions of all xanthenes in  $\text{CHCl}_3$  were prepared with concentration around  $2\text{--}3 \times 10^{-5}$  M.

*Table of UV data of dienes 3.8a–c, xanthenes 3.9a–c and 3.18.*

	Compounds	$\lambda_{\text{max}}$ ( $\epsilon$ )
Dienes	3.8a	252 (41700), 333 (30000)
	3.8b	283 (51200), 293 (48100), 327 (48100)
	3.8c	253 (49000), 299 (46700), 386 (62000)
Xanthenes	3.9a	265 (65300), 304 (31600), 362 (9100)
	3.9b	276 (91500), 366 (7050)
	3.9c	254 (109000), 291 (77400), 358 (63800)
	3.18	267 (72949), 356 (12067)

### 3.5 References and Notes

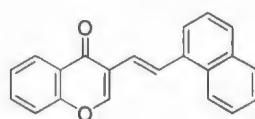
---

- [1] Kelkar, A. S.; Letcher, R. M.; Cheung, K.-K.; Chiu, K.-F.; Brown, G. D. *J. Chem. Soc. Perkin Trans. 1* **2000**, 3732–3741.
- [2] (a) Santos, C. M. M.; Silva, A. M. S.; Cavaleiro, J. A. S. *Synlett* **2005**, 3095–3098.  
(b) Santos, C. M. M.; Silva, A. M. S.; Cavaleiro, J. A. S. *Synlett* **2007**, 3113–3116.
- [3] Trost, B. M.; Ball, Z. T.; Laemmerhold, K. M. *J. Am. Chem. Soc.* **2005**, *127*, 10028–10038.
- [4] Fernandes, R. A.; Kumar, P. *Tetrahedron Lett.* **2003**, *44*, 1275–1278.
- [5] SPARTAN '08 software from Wavefunction, Inc. Irvine, CA, USA.
- [6] Both an asynchronous IEDDA and a stepwise reaction (Michael / Mannich) pathway may have the same effect caused by steric demands.
- [7] For all known compounds, a literature citation is given after the compound name. In all cases, the spectroscopic data is consistent with published data.
- [8] Dess, D. B.; Martin, J. C. *J. Org. Chem.* **1983**, *48*, 4155–4156.

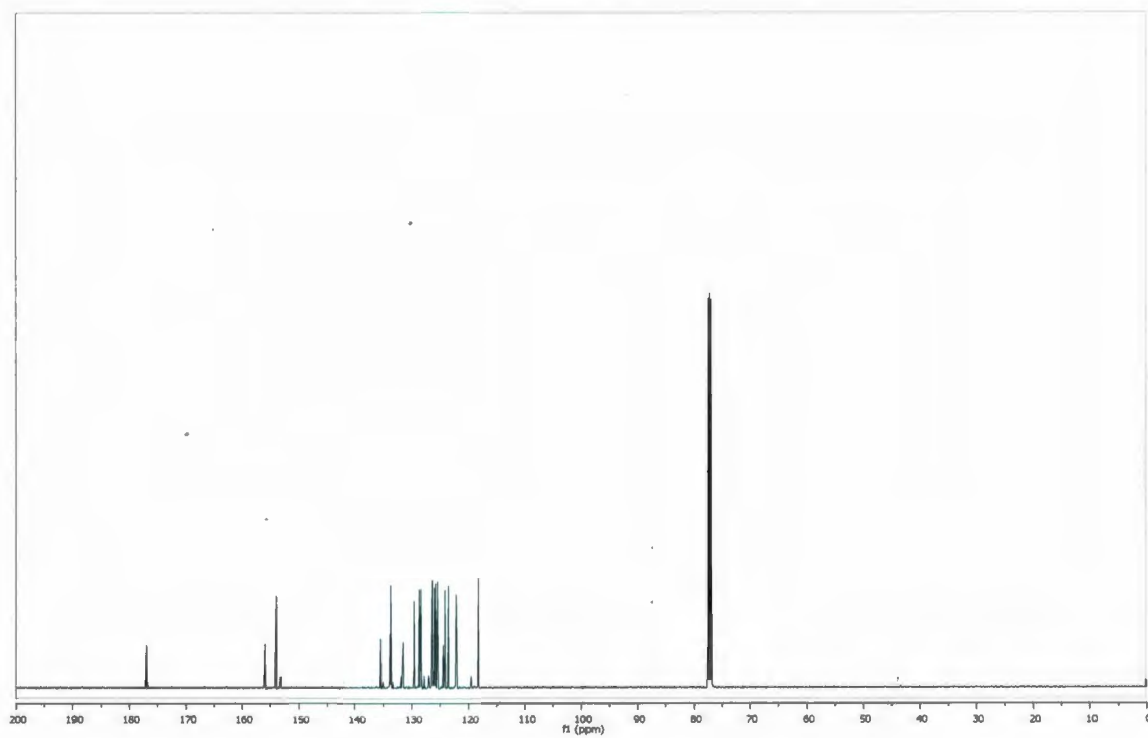
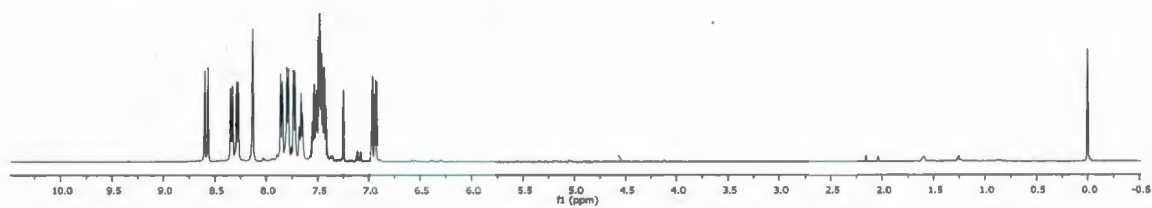
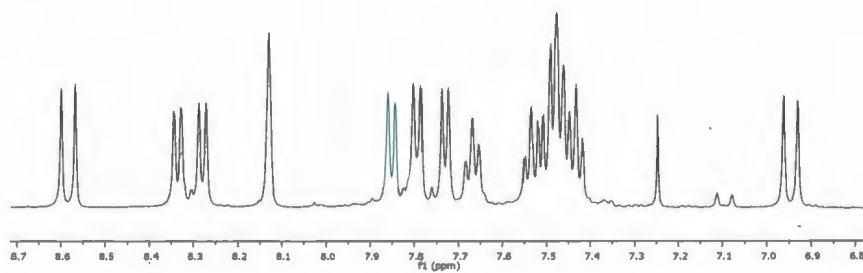
## **Appendix**

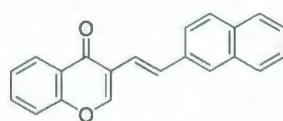
### **Selected NMR Spectra of Synthesized Compounds**



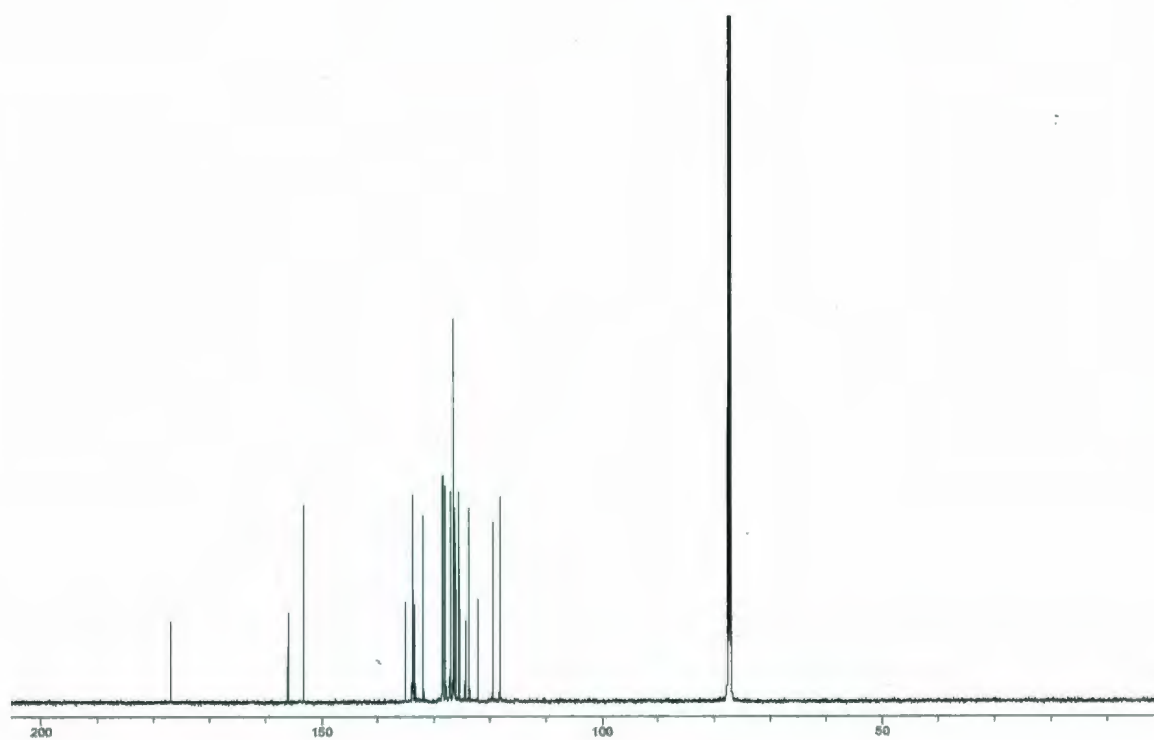
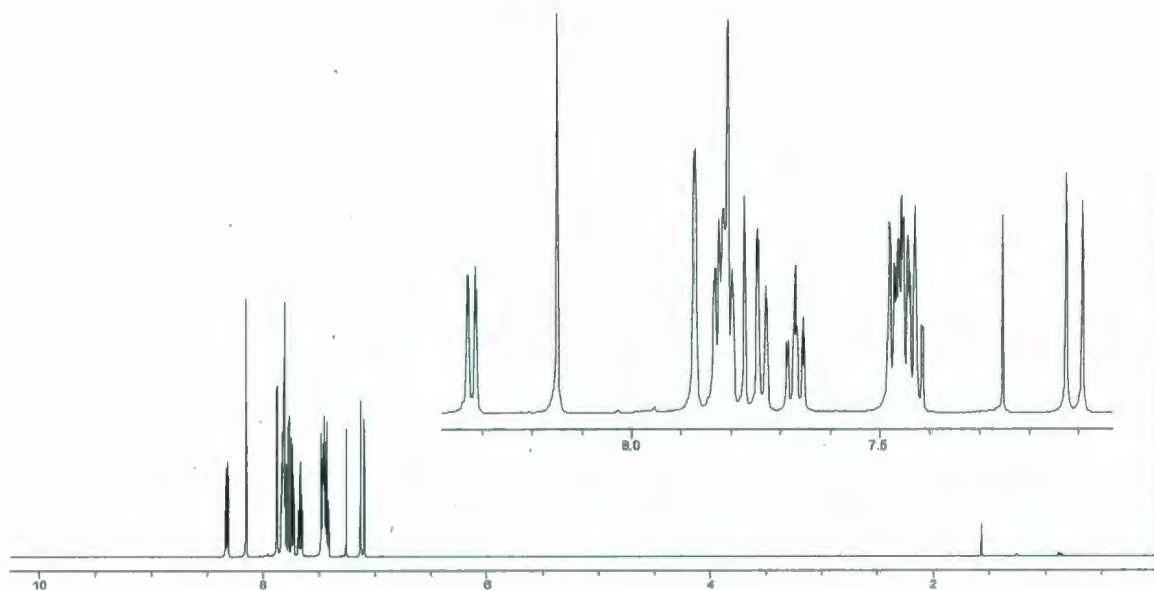


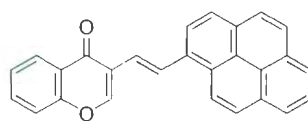
3.8a



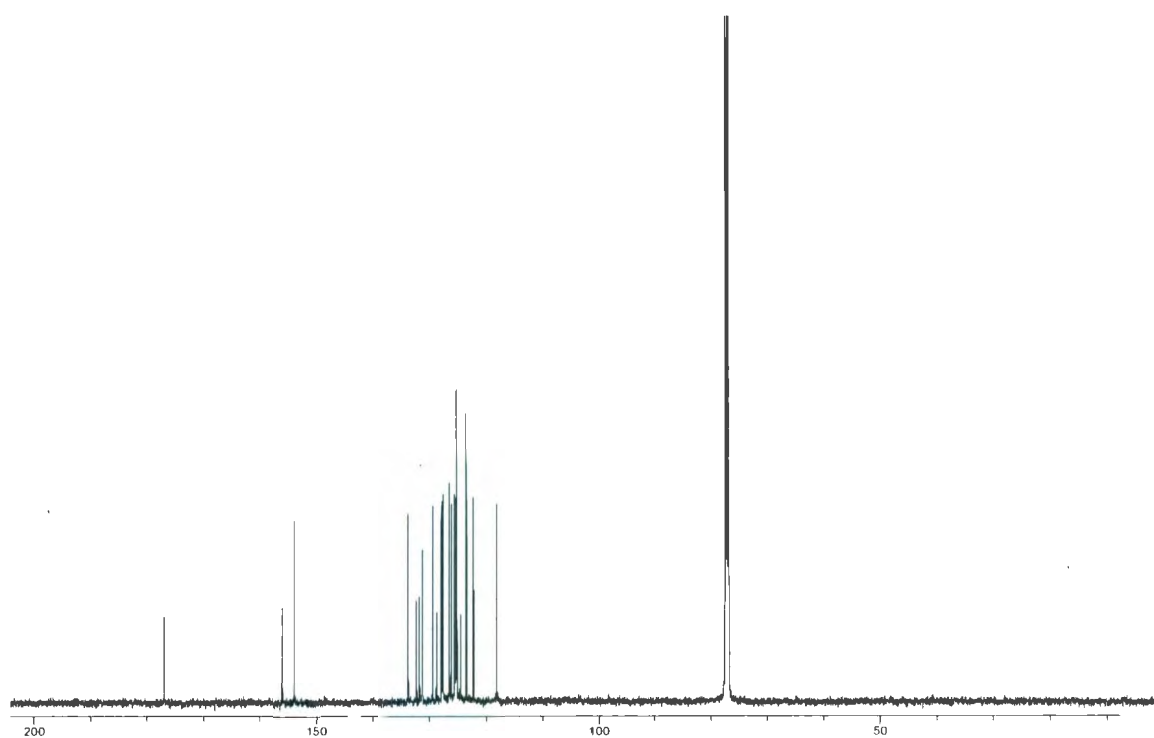
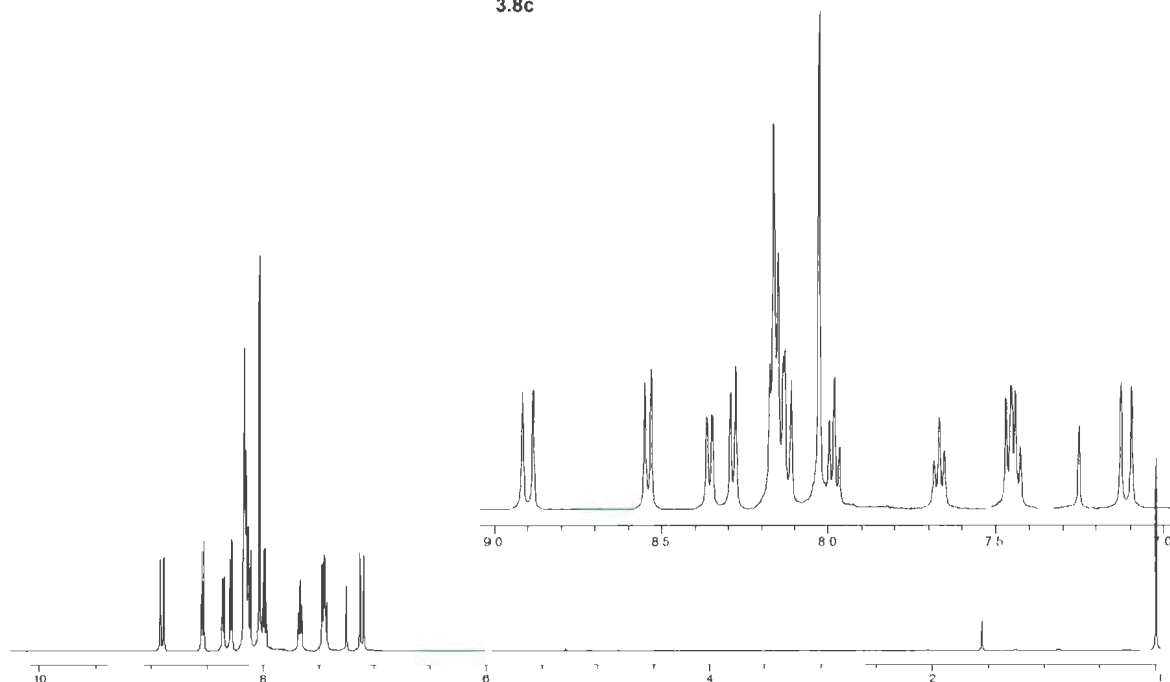


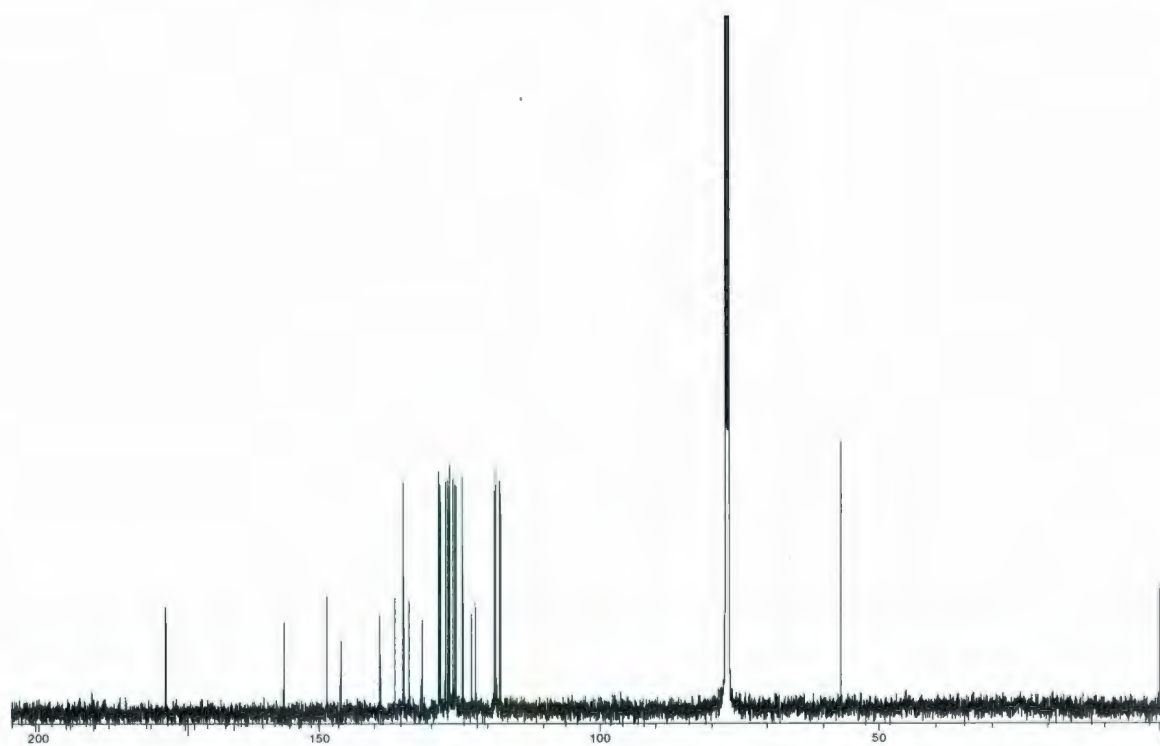
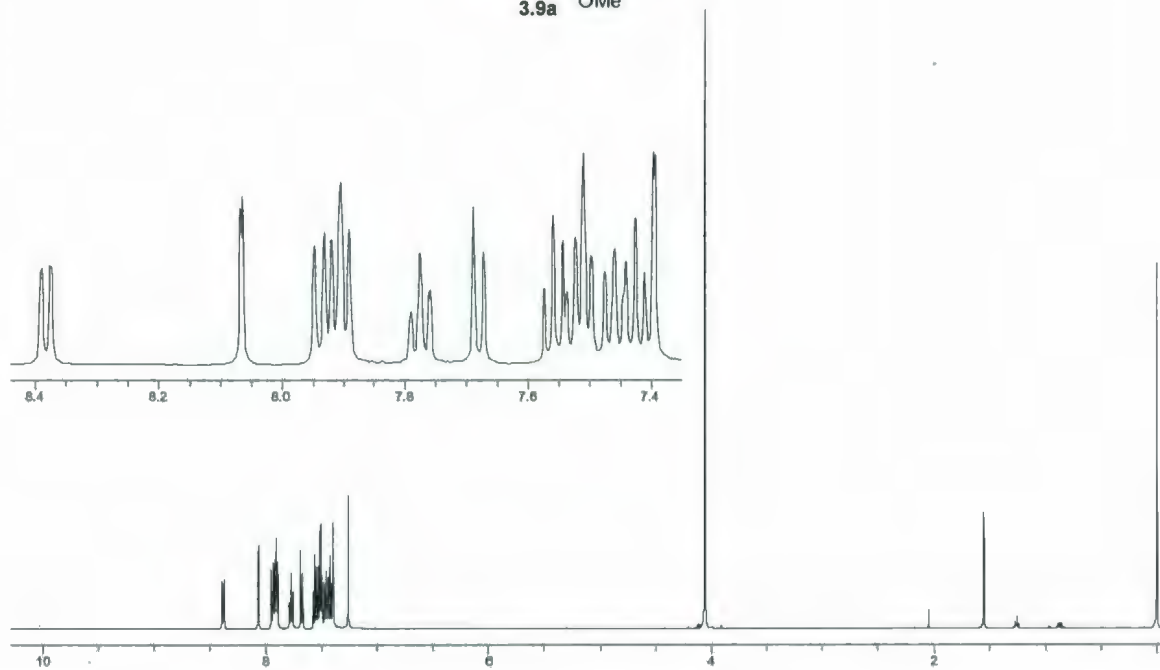
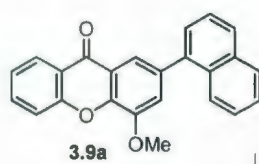
3.8b



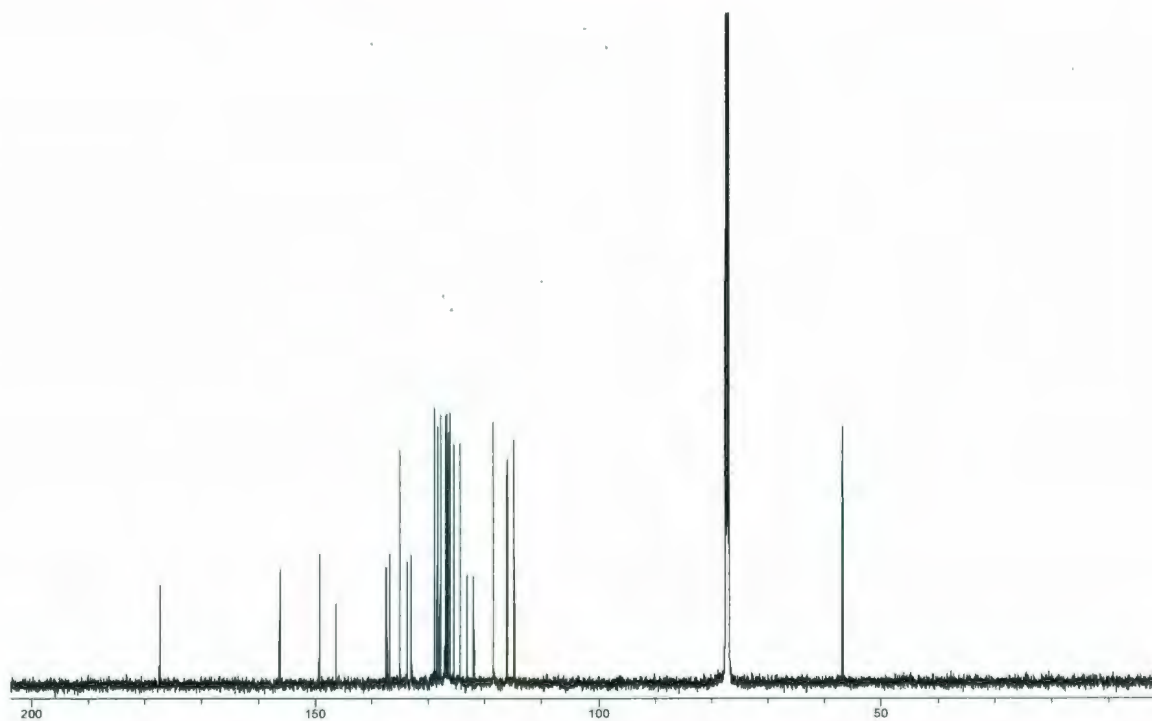
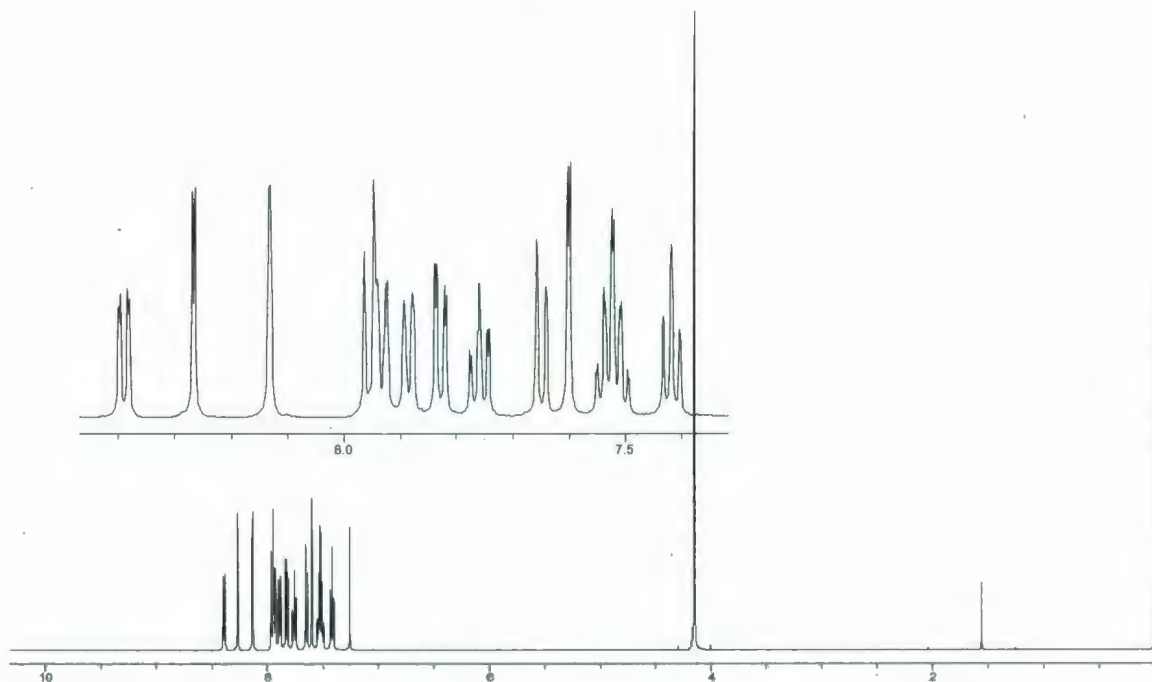
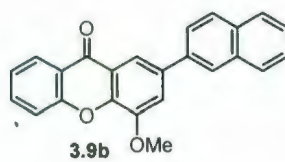


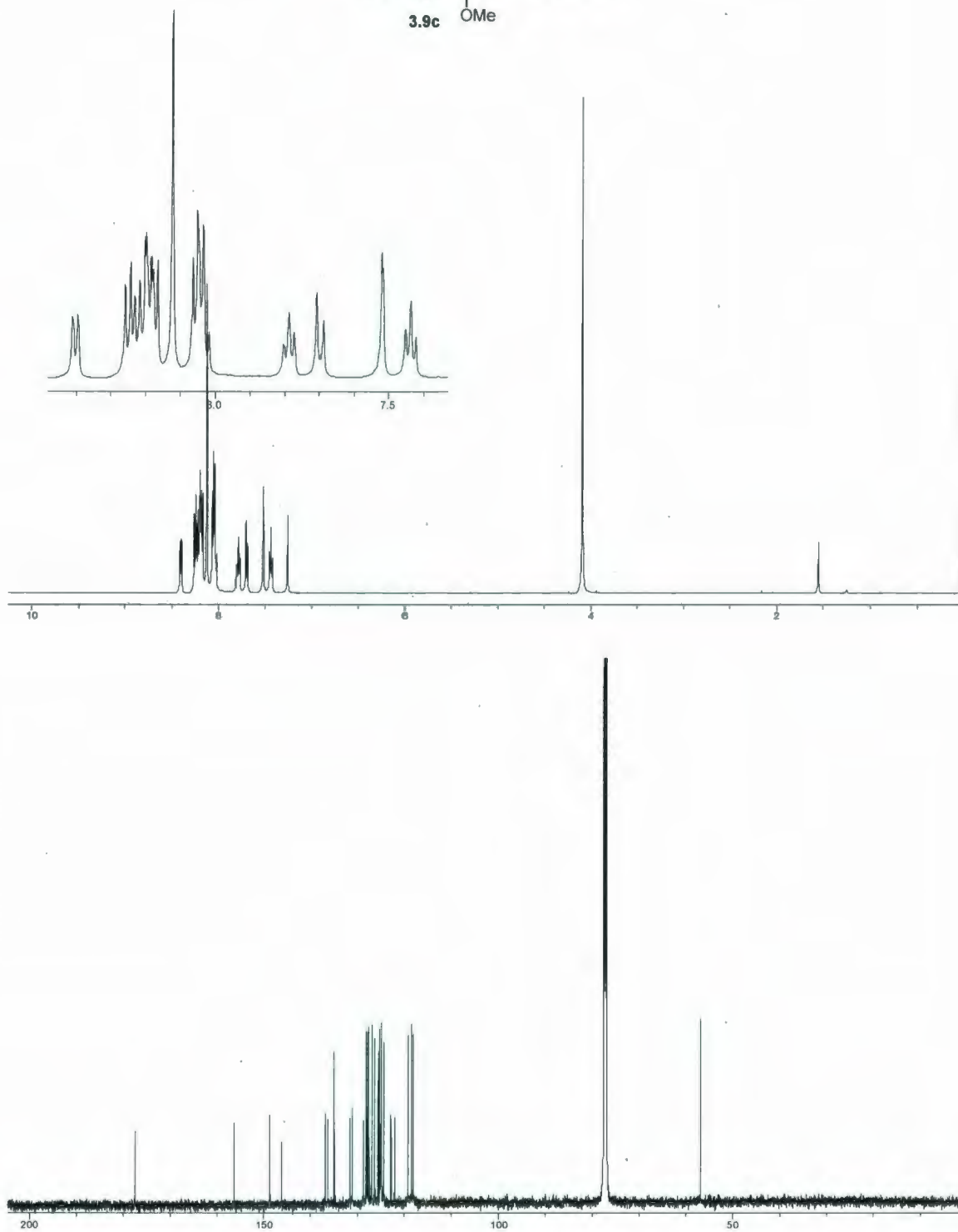
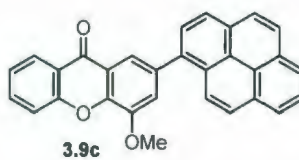
3.8c

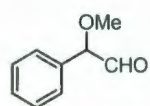




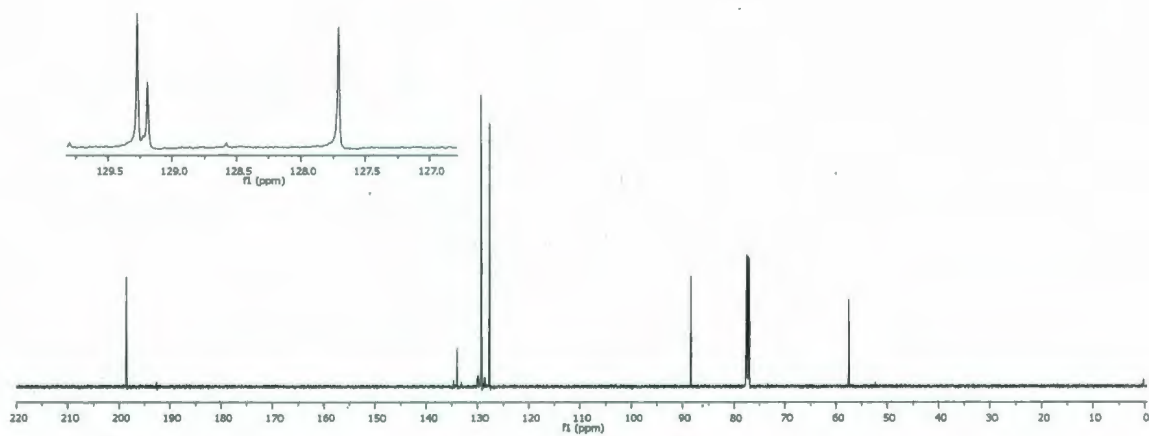
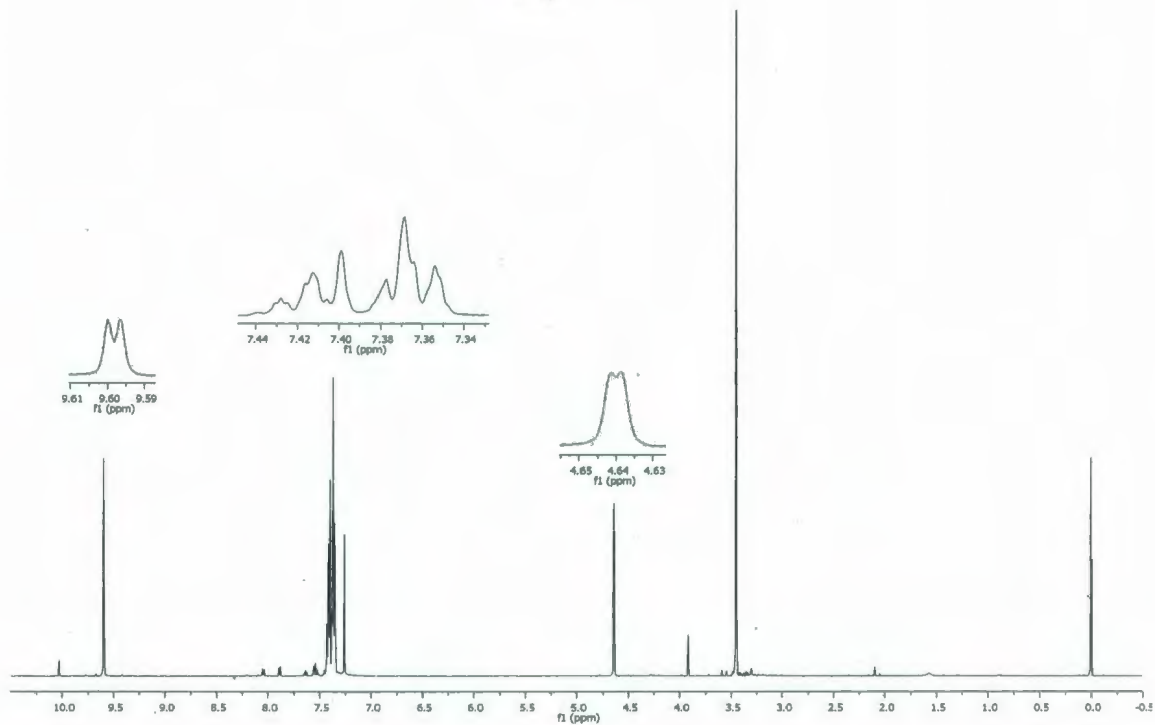


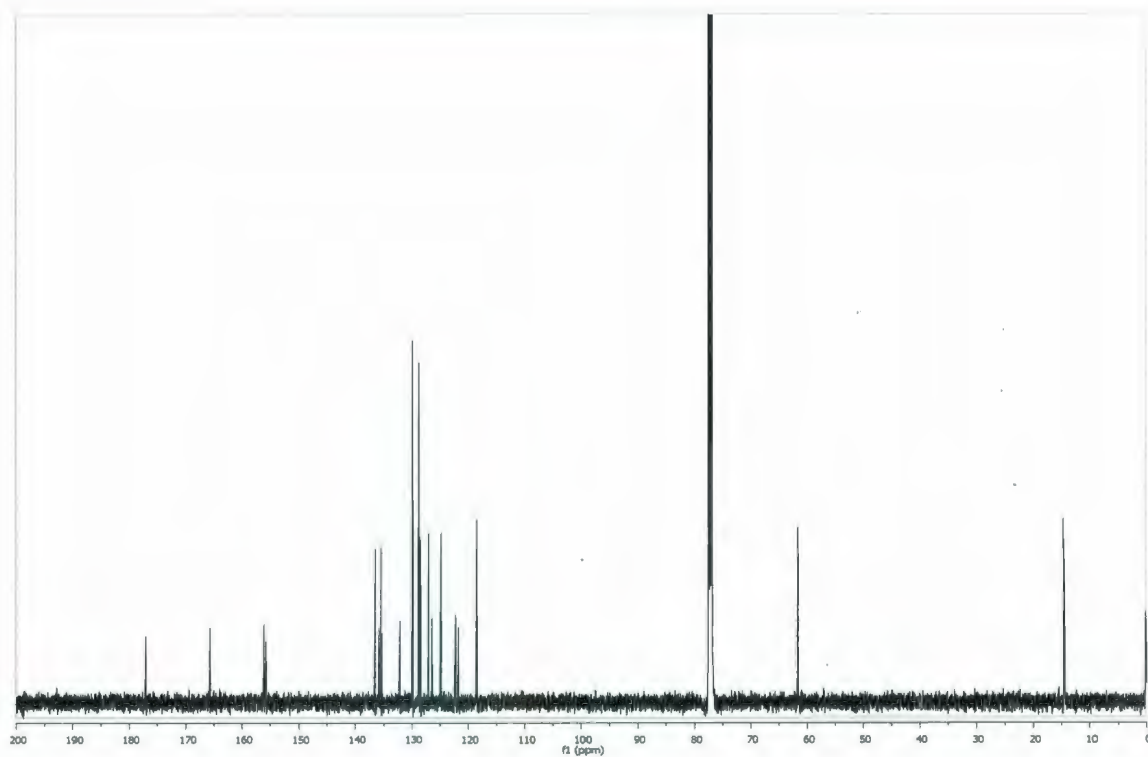
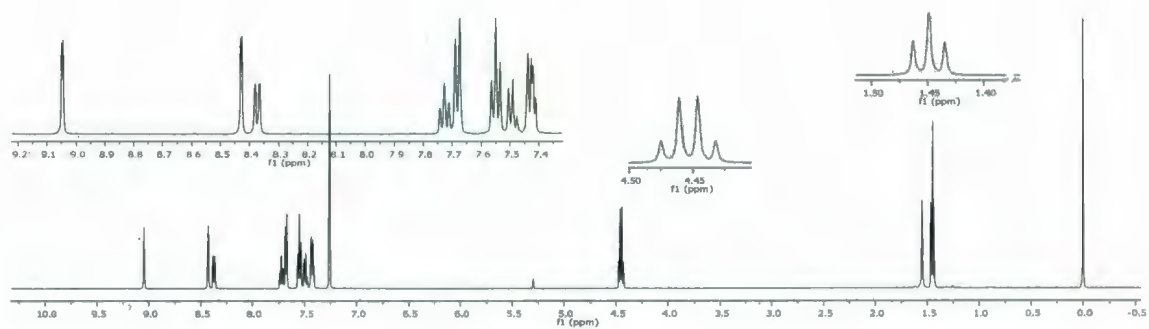
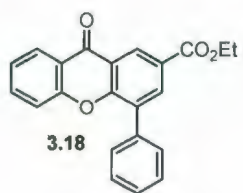






3.16





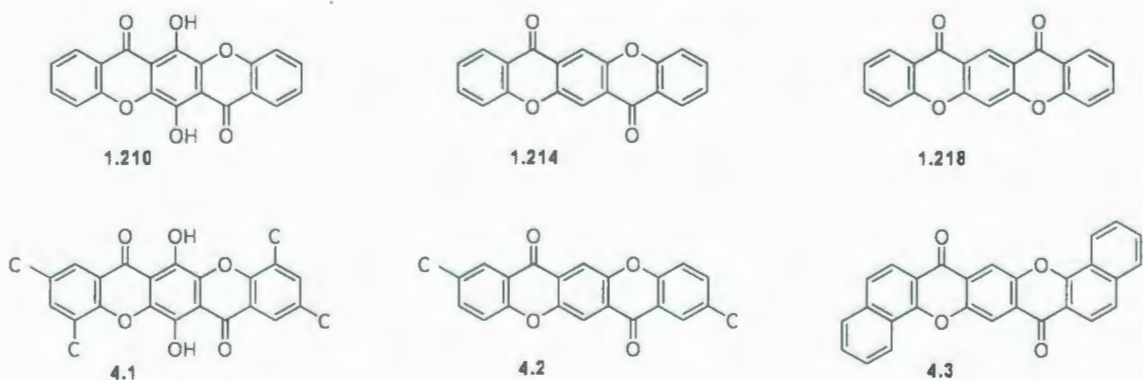


## Chapter 4

### Synthesis and Physical Properties of *syn*-Xanthonoid Hetero[5]acenes and an Attempted Synthesis of Xanthonoid Hetero[*n*]acenes (*n* = 5, 9) via a Two-directional Approach

#### 4.1 Introduction

Only a handful of hetero[5]acenes consisting of alternating benzene and 4-pyranone units are known (Figure 4.1), and no such compounds have been found in nature. Compound **1.210** was first prepared in 1934 via a multi-step synthesis.<sup>1</sup> The remaining compounds **1.214**, **1.218**, **4.1–4.3** were reported (including three patents) during the period of 1957–2000.<sup>2,3,4</sup> The key steps of all of these syntheses were a double-nucleophilic substitution and a double-cyclization, via diaryl ether or bis(benzophenone) intermediates (see examples in Schemes 1.36–1.39, Chapter 1). Although potentially useful applications in pigment dyes<sup>2</sup> (**4.1**, **4.2**) and organic electroluminescent devices<sup>3</sup> (**1.214**, **4.3**) were found, this linear heteroacene skeleton does not appear to have received any interest since the year 2000.



**Figure 4.1** Known xanthone-based heteroacenes.

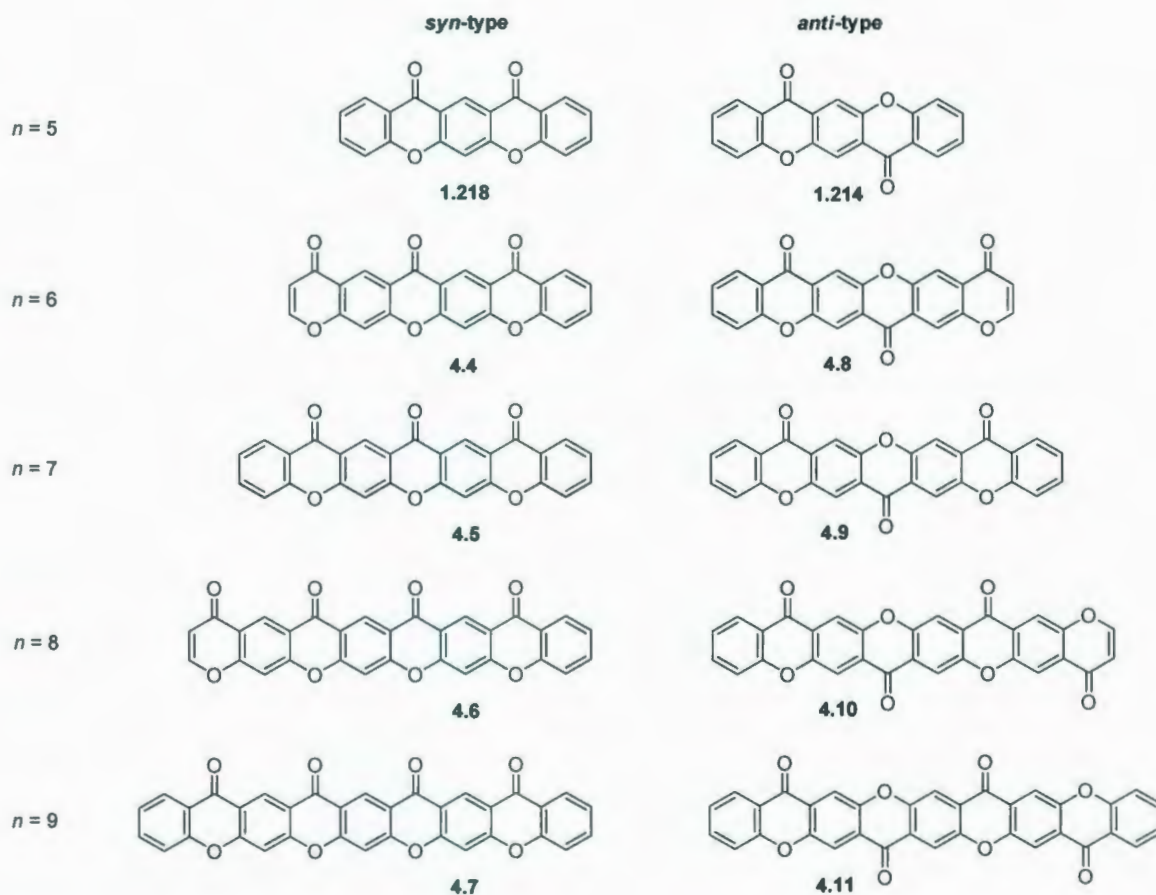
Like other heteroacene systems, the nomenclature of these xanthone-based heteroacenes is not consistent. For example, the names “chromonoxanthone”<sup>5</sup> and “dixanthone”<sup>4</sup> were given to **1.214** and **1.218**, respectively, in which the difference between them is the orientation of their carbonyl groups. However, these two frameworks can be distinguished by their IUPAC names, which was established based on the main xanthene skeleton and the benzene-pyranone fused rings (Figure 4.2).



**Figure 4.2** IUPAC names of compounds **1.214** and **1.218**.

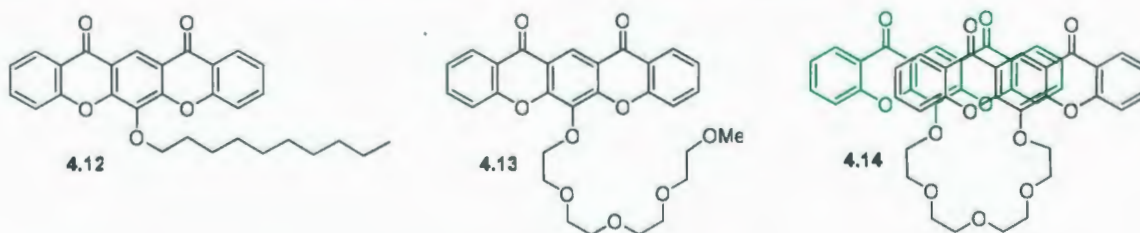
In this chapter, the term “xanthonoid hetero[*n*]acenes” ( $n \geq 3$ ) will be applied to compounds having skeletons such as **1.218**, **1.214**, and **4.4–4.11** (Figure 4.3). The prefixes *syn* (same orientation of the carbonyl groups) and *anti* (opposite / alternating orientation of the carbonyl groups) will be used where appropriate to distinguish these two frameworks.

The synthesis of a xanthonoid hetero[*n*]acene ( $n > 5$ ) has not been reported, although the structure of xanthonoid hetero[9]acene **4.11** was published in a Japanese patent.<sup>3</sup> Therefore, the aim of this research was to develop new methodologies, involving the IEDDA reaction, to construct xanthonoid hetero[*n*]acenes (Figure 4.3). Specifically, *syn*- and *anti*-xanthonoid hetero[5]acenes **1.218**, **1.214** and *syn*-xanthonoid hetero[9]acenes **4.7** were chosen as primary target structures.



**Figure 4.3** Xanthonoid hetero[ $n$ ]acenes.

In addition, new xanthonoid hetero[5]acene derivatives, which contain an alkoxy (**4.12**) or oligo(ethylene oxide) side chain (**4.13**) (Figure 4.4), were also of interest, as was **4.14**, which was thought to have potential application as an organic chemosensor.<sup>6</sup>



**Figure 4.4** New xanthonoid hetero[5]acene derivatives **4.12**–**4.14**.



An organic chemosensor is a system containing two parts: a sensing (receptor) part and a signaling (reporter) part. In system 4.14, the crown ether-like unit was expected to exhibit selective binding with metal ions and thus function as an ionophore<sup>7</sup> (sensing unit), whereas the aromatic chromophores were expected to provide the signal. There are three kinds of organic chemosensors. The first one is *chromogenic* sensors, so-called colorimetric or “naked eye” chemosensors. Upon sensing a substrate, a significant shift of absorption bands takes place in the visible region of the spectrum, which leads to visual change in color of the solution. The second type is *fluorescent* chemosensors, which are based both on the change in fluorescence intensity and on the shift of the emission band of a compound as a result of interaction with a substrate. The third category is *photoswitchable* chemosensors, which exhibit reversible “switching on-switching off” behavior under the influence of light. Various chemosensors consisting of crown ethers and aromatic chromophores have been designed. A variety of metal ions, including alkali ions, rare earth ions and some transition-metal ions, can be selectively detected depending on the cavity dimension and heteroatom types, *i.e.* oxa- (O), thia- (S), or aza- (N), of the crown ether units. Some examples are shown in Table 4.1.<sup>8</sup> Determination of these ions by chemosensors are very important because ions are involved in various biological process ( $\text{Na}^+$ ,  $\text{K}^+$ ,  $\text{Mg}^{2+}$ ,  $\text{Ca}^{2+}$ ), are used in treatment of various illness ( $\text{Li}^+$ ,  $\text{Ca}^{2+}$ ), and also could cause serious harm to the environment and to human health ( $\text{Ba}^{2+}$ ,  $\text{Pb}^{2+}$ ,  $\text{Tl}^+$ ,  $\text{Ag}^+$ ,  $\text{Hg}^{2+}$ ,  $\text{Cd}^{2+}$ ). Although a large number of chemosensors are available for this purpose, research aimed at the discovery of new



compounds that provide optimal levels of safety, accessibility, sensitivity, and selectivity is still being conducted.

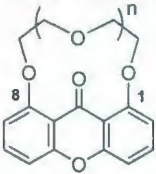
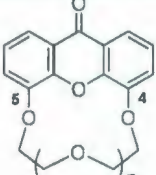
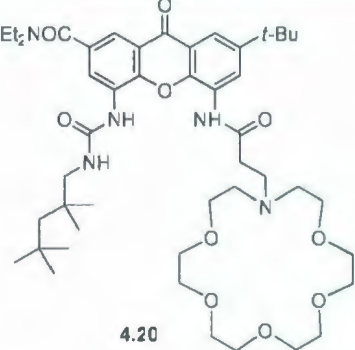
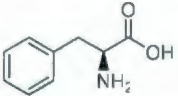
**Table 4.1** Examples of chromophore-based crown ethers.

Chromophore-based crown ethers	Selective binding to ions
<p style="text-align: center;">4.15</p>	$\text{Na}^+$ ( $n = 1$ ) $\text{K}^+$ ( $n = 2$ ) $\text{Cs}^+$ ( $n = 3$ )
<p style="text-align: center;">4.16</p>	$\text{Pb}^{2+}$
<p style="text-align: center;">4.17</p>	$\text{Hg}^{2+}$

The xanthone core has also been employed in chemosensors (Table 4.2). Interestingly, each of the two oxygen atoms of the xanthone core has been incorporated into the crown ether unit (4.18, 4.19).<sup>9</sup> Another structural characteristic of these systems is that there is no linker between ionophore and chromophore. Besides complexation with ions, some chemosensors have shown selective binding with particular molecules.<sup>6</sup> For example, xanthone-based crown ether 4.20<sup>10</sup> (Table 4.2) was used as a receptor for extracting L-phenylalanine 4.21 from water. It was proposed that the ammonium cation and carboxylate anion of L-phenylalanine associated with the crown ether unit and the

amine side chain, respectively, while the benzene ring of L-phenylalanine had a  $\pi$ - $\pi$  interaction with the xanthone moiety.

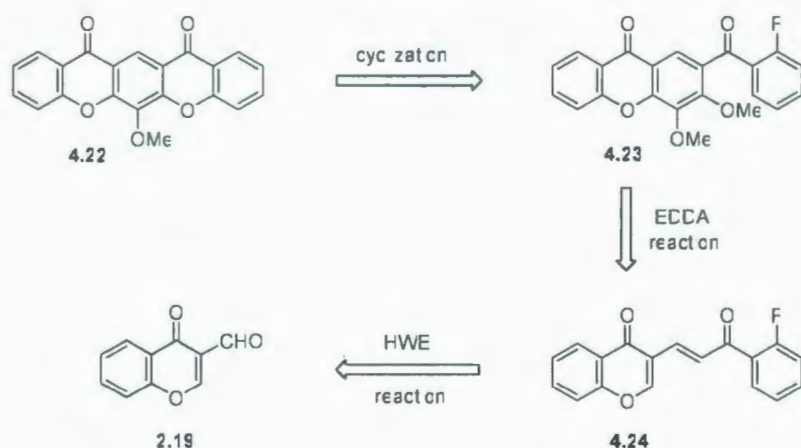
**Table 4.2** Examples of xanthone-based crown ethers.

Xanthone-based crown ethers	Selective binding to ions / molecule
 <p style="text-align: center;">4.18</p>	<p style="text-align: center;"><math>\text{Ba}^{2+}</math> (<math>n = 5</math>)</p>
 <p style="text-align: center;">4.19</p>	<p style="text-align: center;"><math>\text{Na}^+</math>, <math>\text{K}^+</math> (<math>n = 3</math>)  <math>\text{K}^+</math>, <math>\text{Cs}^+</math> (<math>n = 4</math>)  <math>\text{Cs}^+</math> (<math>n = 5</math>)</p>
 <p style="text-align: center;">4.20</p>	 <p style="text-align: center;">4.21 L-phenylalanine</p>

## 4.2 Retrosynthetic Analysis of Xanthonoid Hetero[n]acenes

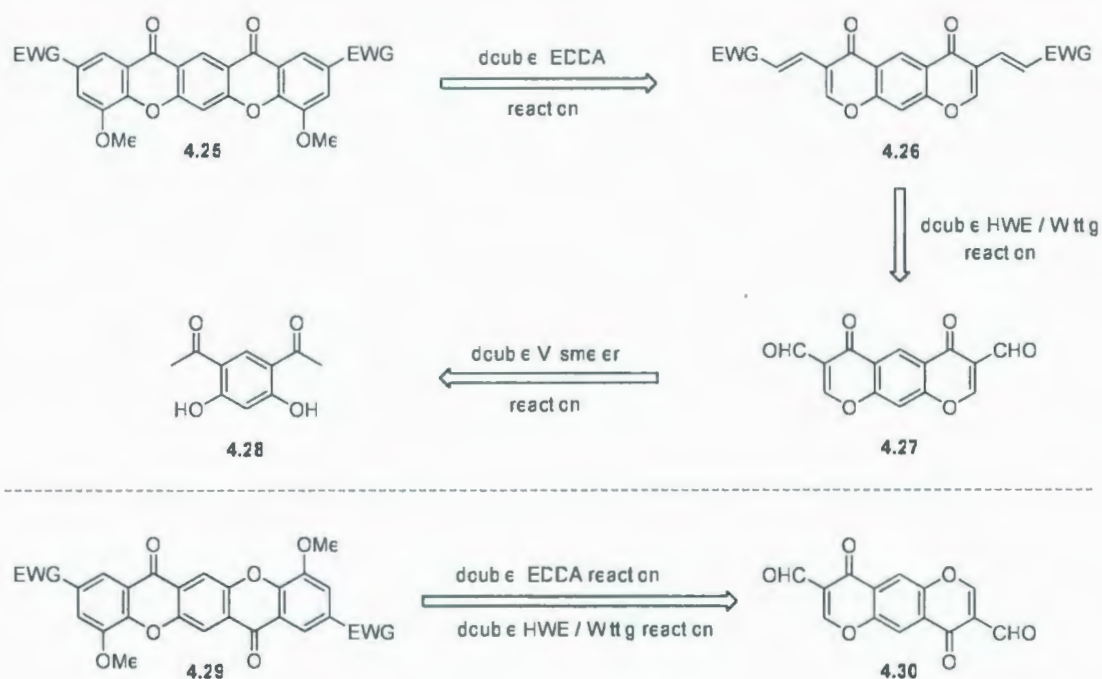
The general strategy to build xanthonoid hetero[n]acene frameworks was to employ the IEDDA reaction for the construction of the benzene rings, followed by an intramolecular nucleophilic aromatic substitution to form the pyranone rings. Retrosynthetic analysis of the first target structure, xanthonoid hetero[5]acene **4.22** (Scheme 4.1), led back to 3,4-dimethoxyxanthone **4.23** via an intramolecular nucleophilic

aromatic substitution and a selective demethylation. As described in Chapter 2, the 3,4-dimethoxyxanthone such as **4.23** could be synthesized from diene **4.24** using the IEDDA reaction with TME.<sup>11</sup> A HWE transform then brought the analysis back to a commercially available material, 3-formylchromone (**2.19**). This synthetic route is a “one-directional approach” as the new rings in the target structure **4.22** are installed consecutively from one side of the starting material **2.19**.



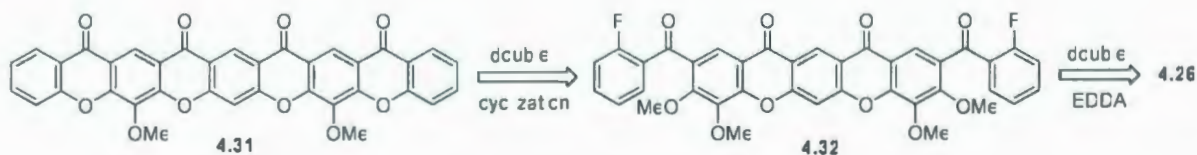
**Scheme 4.1** Retrosynthetic analysis of *syn* xanthonoid hetero[5]acene **4.22** via a one-directional approach.

Another approach, which might be applicable to both *syn*- and *anti*-xanthonoid hetero[5]acenes, involved a “two-directional” strategy. For instance, *syn*-xanthonoid hetero[5]acenes **4.25** (Scheme 4.2) might be obtained from *syn*-dialdehyde **4.27** via a double-HWE (or Wittig) reaction and a double-IEDDA reaction. Intermediate **4.27** could be prepared from dihydroxyacetophenone **4.28** via a double-Vilsmeier reaction. Similarly, *anti*-xanthonoid hetero[5]acenes **4.29** might be obtained from the key intermediate **4.30**.



**Scheme 4.2** Retrosynthetic analysis of *syn*- and *anti*-xanthonoid hetero[5]acenes **4.25** and **4.29** via a two-directional approach.

Also using a two-directional approach, the *syn*-xanthonoid hetero[9]acene **4.31** (Scheme 4.3) was envisioned as coming from *syn*-bis(diene) **4.26** (EWG = 2-fluorobenzoyl) via a double-IEDDA reaction and a double-intramolecular nucleophilic aromatic substitution.



**Scheme 4.3** Retrosynthetic analysis of *syn*-xanthonoid hetero[9]acene **4.31** via a two-directional approach.

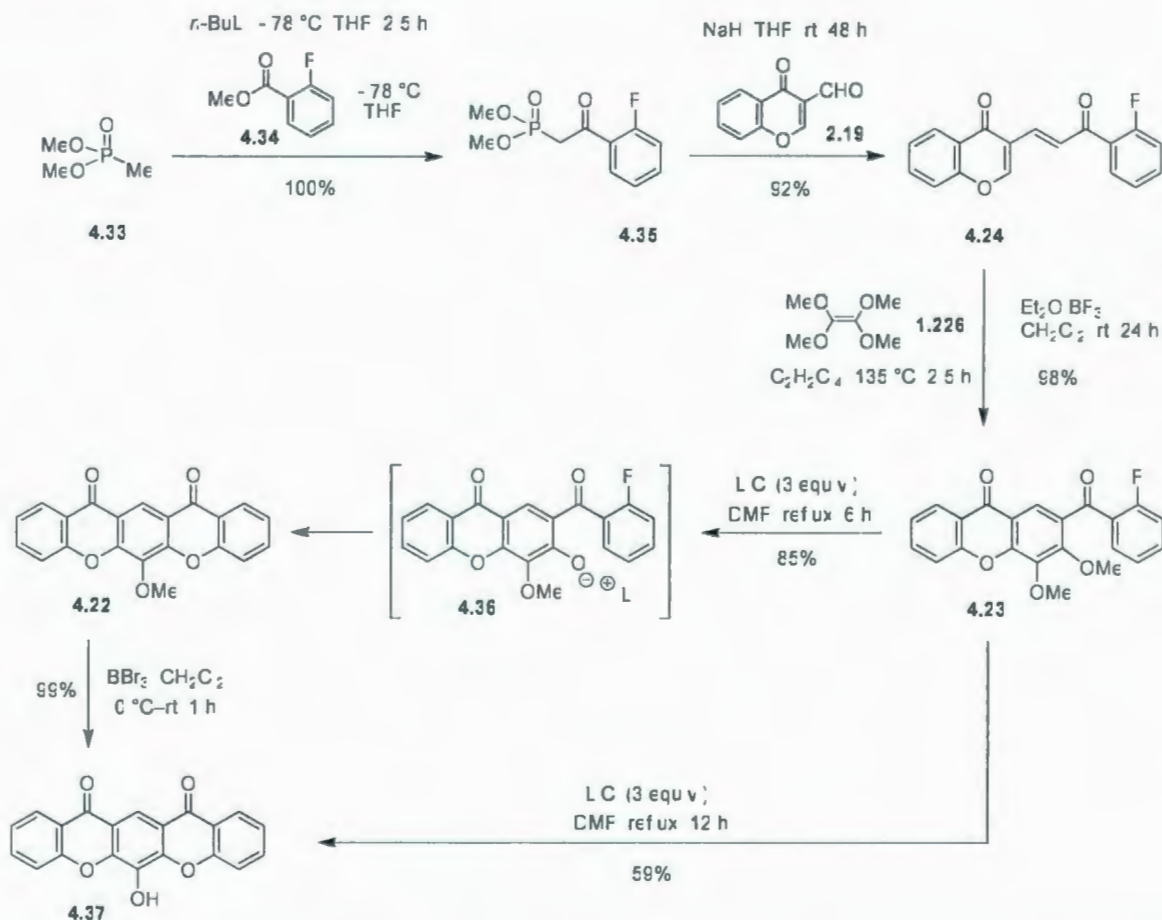


### 4.3 Results and Discussions

#### 4.3.1 Synthesis of *syn*-Xanthonoid Hetero[5]acenes via a One-directional Approach

The synthesis of xanthonoid hetero[5]acene **4.22** (Scheme 4.4) commenced with an acylation of the anion derived from dimethyl methylphosphate (**4.33**) to afford phosphonate **4.35** in quantitative yield.<sup>12</sup> Treatment of phosphonate **4.35** with sodium hydride formed an ylide, which was reacted with 3-formylchromone (**2.19**) to furnish diene **4.24** (92%). The IEDDA-driven domino reaction between diene **4.24** and TME (**1.226**) smoothly afforded 3,4-dimethoxyxanthone **4.23** in a very impressive yield (98%). This yield was consistent with the results presented in Chapter 2, *i.e.* the IEDDA reactions of dienes **1.15** where the EWG was a ketone with TME (**1.226**) gave 3,4-dimethoxyxanthenes in very good yields (90–98%). When xanthone **4.23** was heated with LiCl (3 equiv.) in DMF,<sup>13</sup> the cyclization occurred smoothly to form xanthonoid hetero[5]acene **4.22** (85%, 6 h) or hydroxyl xanthonoid hetero[5]acene **4.37** (59%, 12 h). As predicted, selective demethylation took place at the 3-methoxy group. This is the more electrophilic methyl group because the developing negative charge on the oxygen atom can be resonance stabilized by both of the carbonyl groups. In contrast, the phenoxide ion resulting from nucleophilic attack at the 4-methoxy group receives no resonance stabilization. Phenoxide ion **4.36** is perfectly situated to undergo cyclization via an intramolecular nucleophilic aromatic substitution. As LiCl was used in excess (3 equiv.), demethylation eventually occurred at the 4-methoxy group when the reaction time was prolonged. Alternatively, the hydroxyl compound **4.37** could be obtained in 99% yield via demethylation of **4.22** using BBr<sub>3</sub>. The syntheses of xanthonoid

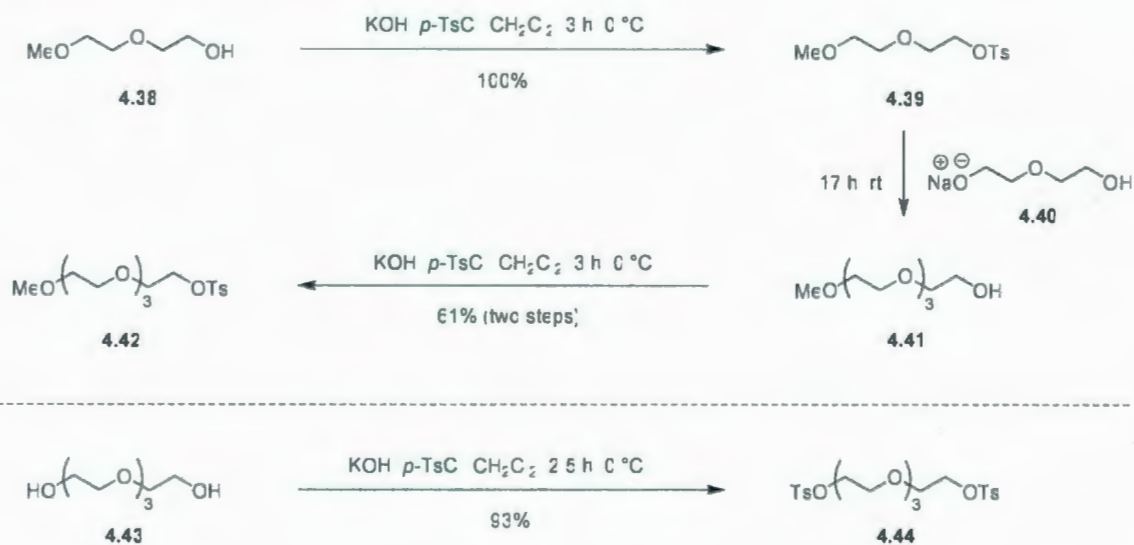
hetero[5]acenes **4.22** and **4.37** were achieved in excellent overall yields (77% and 76%, respectively) in four or five steps from the commercially available starting materials **4.33** and **4.34**.



**Scheme 4.4** Synthesis of xanthonoid hetero[5]acenes **4.22** and **4.37** via a one-directional approach.

The next objectives were the syntheses of three xanthonoid hetero[5]acene derivatives **4.12–4.14** (Figure 4.4) and the study of some their physical properties, such as electronic absorption, fluorescence and modeling studies.

First, polyethylene glycol mono- and ditosylate **4.42** and **4.44** were synthesized in good yields following literature procedures (Scheme 4.5).<sup>14</sup> The three-step synthesis of compound **4.42** commenced with a tosylation of **4.38** to give **4.39** in quantitative yield. Compound **4.41**<sup>15</sup> was obtained by chain extension of **4.39** via  $S_N2$  reaction with alkoxide **4.40**, which was formed from diethylene glycol and sodium metal upon heating at 70 °C. The crude product **4.41** was subjected to another tosylation to afford **4.42** (61% from **4.39**). Similarly, ditosylation of tetra(ethylene glycol) (**4.43**) smoothly gave **4.44** in 93% yield under similar tosylation conditions.

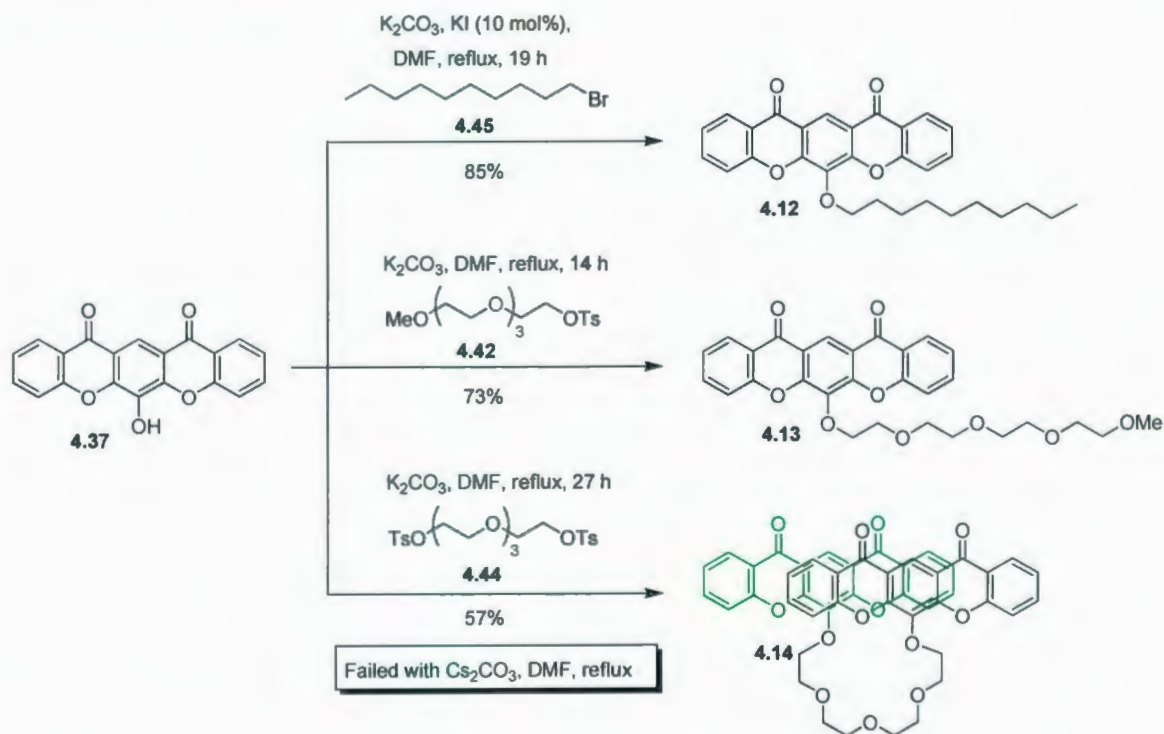


**Scheme 4.5** Synthesis of tosylated polyethylene oxide chains **4.42** and **4.44**.

Alkylation reactions of hydroxyl xanthonoid hetero[5]acene **4.37** with 1-bromodecane (**4.45**), 1-methoxy-11-tosyl-3,6,9-trioxaundecane (**4.42**) and 1,11-ditosyl-3,6,9-trioxaundecane (**4.44**) were carried out under similar conditions to give xanthonoid hetero[5]acenes **4.12** (85%), **4.13** (63%), and **4.14** (57%), respectively (Scheme 4.6). By comparison, the crown-ether xanthenes **4.18** and **4.19** ( $n = 3-5$ ) (Scheme 4.7) were

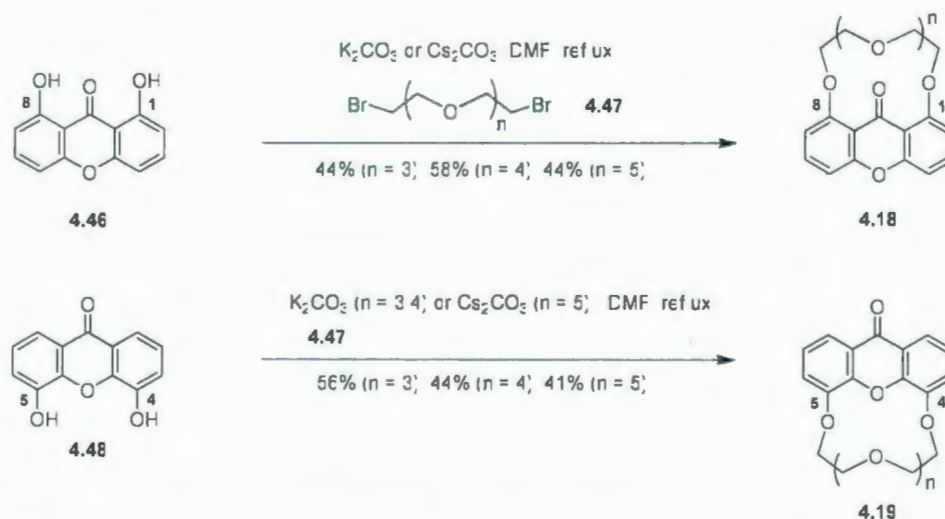


obtained in moderate yields (40–57%) from dialkylation of the corresponding dihydroxyxanthenes **4.46** and **4.48**, respectively, with appropriate polyethylene glycol dibromides **4.47**.<sup>16,17</sup> Thus, it can be said that the desired compound **4.14** was obtained in relatively good yield (57%).



**Scheme 4.6** Synthesis of xanthonoid hetero[5]acene derivatives **4.12–4.14**.



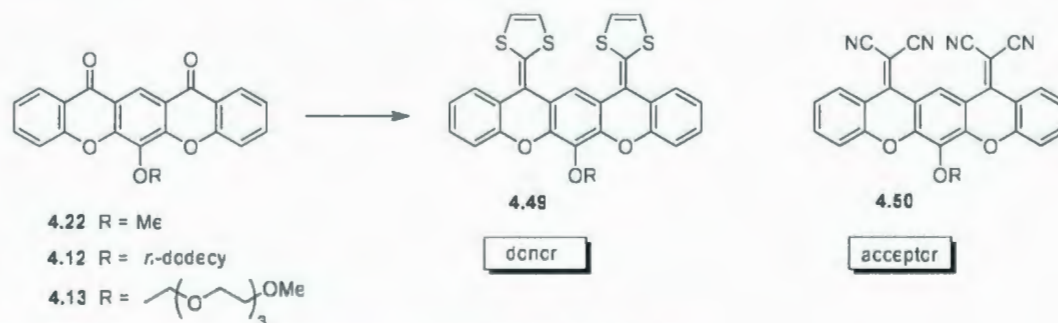


**Scheme 4.7** Synthesis of xanthenes-based **4.18** and **4.19** via dialkylation.

It was also reported that using either  $\text{Cs}_2\text{CO}_3$  or  $\text{K}_2\text{CO}_3$  in alkylation reactions of compound **4.46** did not cause dramatic changes in reaction rates and yields of xanthone-based crown ethers **4.18**.<sup>16</sup> In contrast, xanthone-based crown ether **4.19** ( $n = 5$ ) was not obtained when using  $\text{K}_2\text{CO}_3$ , but it was formed in 41% yield with  $\text{Cs}_2\text{CO}_3$ . The other congeners of **4.19** ( $n = 3, 4$ ) were obtained in 56% and 44% yield, respectively, using  $\text{K}_2\text{CO}_3$ .<sup>17</sup> Clearly, the nature of the base played an important role in the latter case. Presumably, after the first alkylation of 4,5-dihydroxyxanthone **4.48** took place, the polyethylene oxide chain could bind to the alkali ion. With an appropriately-sized cation, the two reaction sites are brought close enough for the second alkylation to occur, but when an inappropriately-sized cation is present, the two reaction sites cannot easily come close enough to undergo reaction. This kind of reaction is called a “host-guest template reaction”. This is likely the reason why the dialkylation of **4.37** with ditosylate **4.44** did not occur when  $\text{K}_2\text{CO}_3$  was replaced with  $\text{Cs}_2\text{CO}_3$ . In this case, although xanthonoid

hetero[5]acene **4.14** is not a cyclic compound like xanthone-based crown ethers **4.19**,  $\pi$ - $\pi$  interactions between two aromatic moieties may make it behave in the same fashion as crown ethers. As such, the polyethylene oxide tether might show selective binding with  $K^+$  over  $Cs^+$ . Hence, complexation studies of **4.14** with alkali ions will be worth pursuing in the future.

The carbonyl groups on *syn*-xanthonoid hetero[5]acenes **4.22**, **4.12** and **4.13** can conceivably be modified to form new donor and acceptor systems such as **4.49** and **4.50**, respectively (Scheme 4.8). The synthesis of these systems is being carried out in collaboration with Dr. Zhao's group at Memorial University.

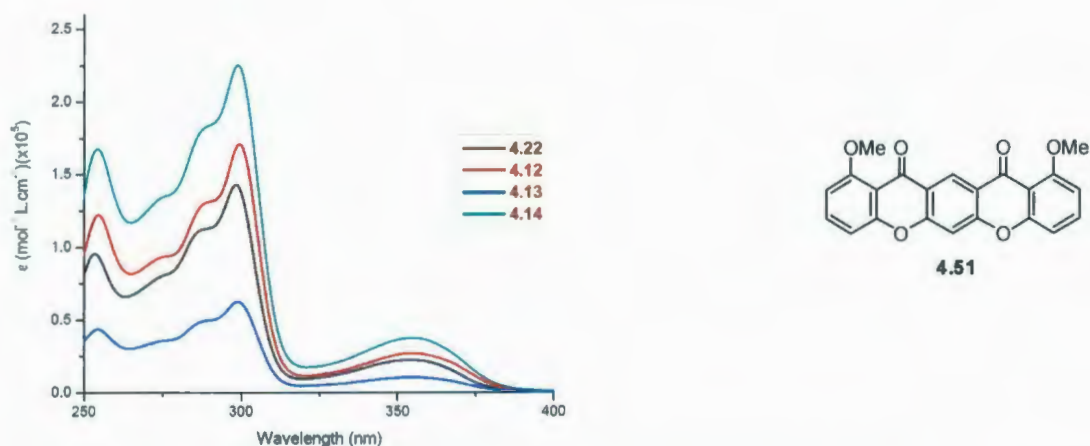


Scheme 4.8 New donor and acceptor systems **4.49** and **4.50**.

### 4.3.2 Physical Properties of *syn*-Xanthonoid Hetero[5]acenes **4.22** and **4.12–4.14**

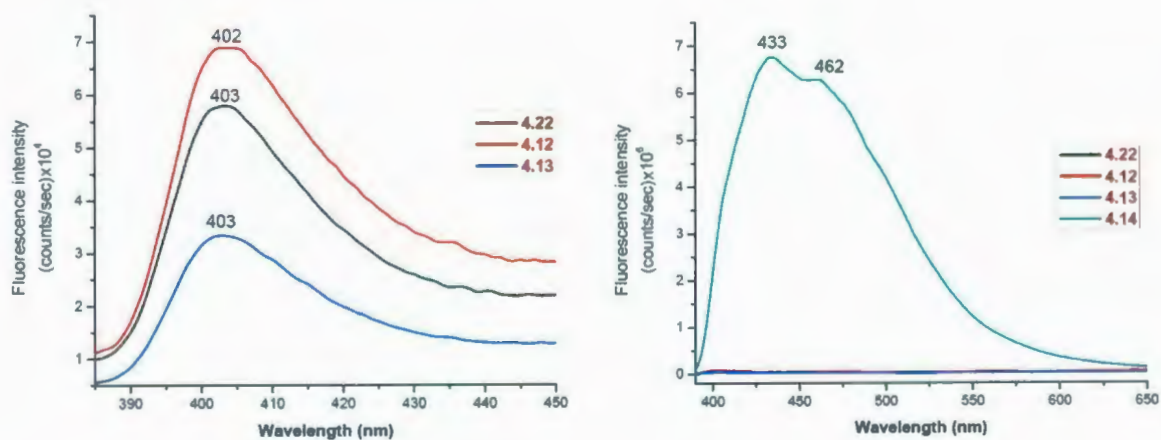
#### 4.3.2.1 UV-Vis, Fluorescence, and Quantum Yield Studies

The absorption spectra of **4.22** and **4.12–4.14** are very similar and have their lowest energy absorbance maximum at 355 nm (Figure 4.5), which is similar to that of the known *syn*-xanthonoid hetero[5]acene **4.51** ( $\lambda_{\text{max}}$  (MeOH) = 224, 272, 359 nm).<sup>5b</sup>



**Figure 4.5** Absorption spectra of **4.12**–**4.14** and **4.22** in  $\text{CHCl}_3$  ( $2 \times 10^{-5} \text{ M}$ ).

As no alteration of the chromophore absorption property was observed for bis(xanthonoid hetero[5]acene) **4.14**, except for the intensity of the longest wavelength absorption, it was assumed that almost no interaction between two hetero[5]acene moieties occurs in the ground state.



**Figure 4.6** Emission spectra of **4.12**–**4.14** and **4.22** in  $\text{CHCl}_3$  ( $2 \times 10^{-5} \text{ M}$ ).

In contrast, the fluorescence spectrum of **4.14** differed greatly from those of **4.22**, **4.12** and **4.13** (Figure 4.6). Whereas **4.22**, **4.12** and **4.13** showed very weak blue

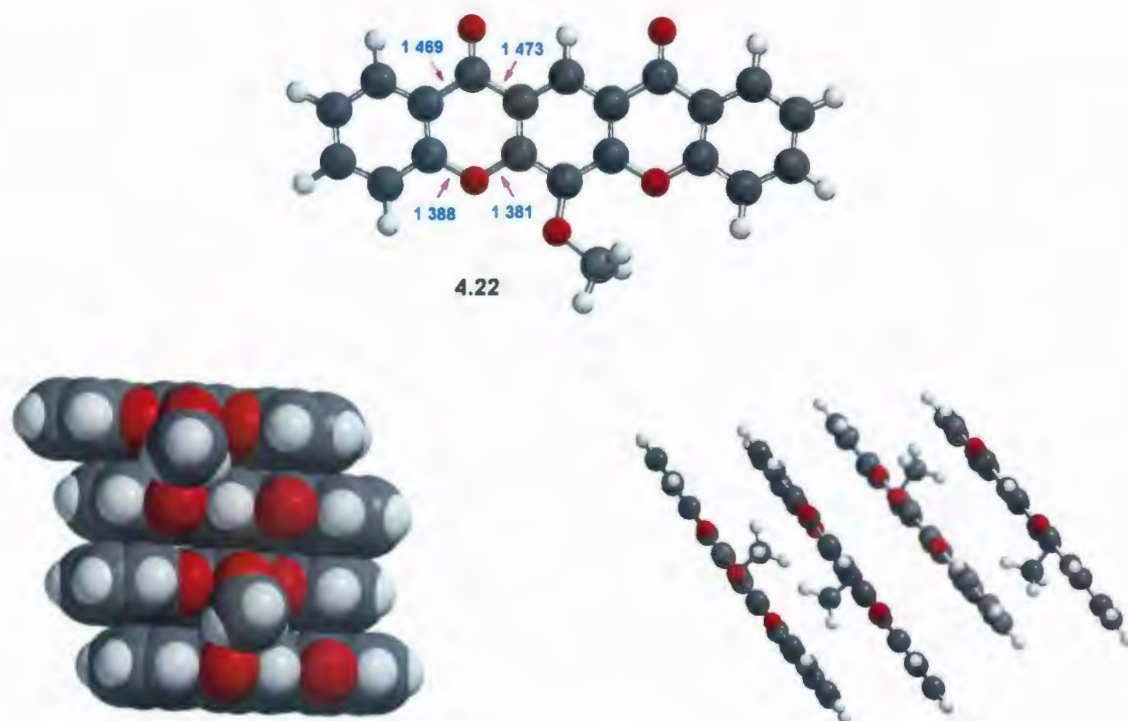


fluorescence at 402–403 nm, the fluorescence spectrum of **4.14** consisted of a broad and much more intense red-shifted band with two maxima (433 and 462 nm). Double emission appears to be typical vibronic progression bands, while the red-shift and broadness are presumably caused by the formation of an intramolecular excimer between the two hetero[5]acene moieties. The Stokes shifts of **4.22**, **4.12** and **4.13** ( $\Delta = 3430 \text{ cm}^{-1}$ ) is smaller than that of **4.14** ( $\Delta = 5150 \text{ cm}^{-1}$ ) due to their more rigid structures. Although compound **4.14** exhibited the strongest fluorescence among its analogues, its fluorescence quantum yield was still very weak ( $\Phi_{\text{em}} = 2 \times 10^{-3}$ ).

#### 4.3.2.2 Modeling Studies

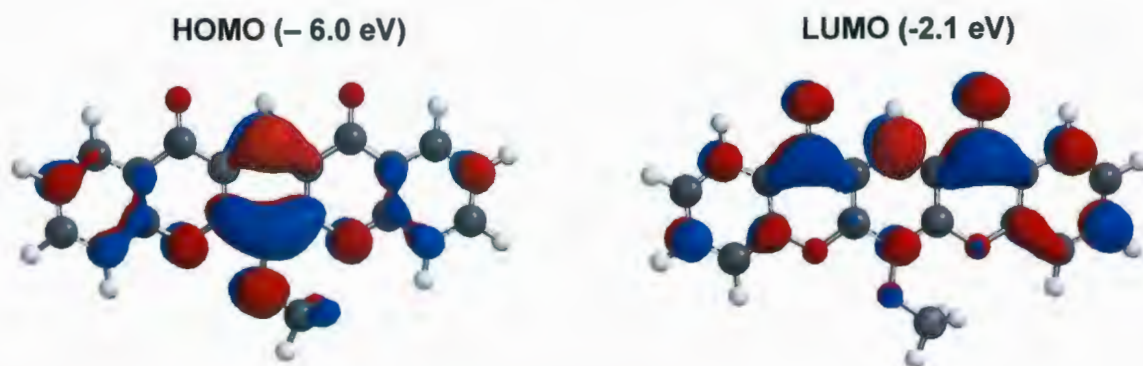
Density functional theory (DFT) calculations of *syn*-xanthonoid hetero[5]acene **4.22** was carried out at B3LYP/6-31G(d)//AM1 level.<sup>18</sup> The computed structure of **4.22** has an essentially planar framework with a slight arc in the pentacyclic system due to the shorter length of the C–O single bonds (1.381–1.388 Å) in comparison to the C<sub>aryl</sub>–C<sub>carbonyl</sub> bonds (1.469–1.473 Å) in the pyranone ring (Figure 4.7, *top*). The predicted packing motif (MMFF94)<sup>18</sup> of **4.22** showed antiparallel cofacial  $\pi$ -stacking arrangements (opposite orientations of methoxy groups) between adjacent molecules to minimize steric and dipolar effects. The average calculated interplanar distance is 3.8 Å.





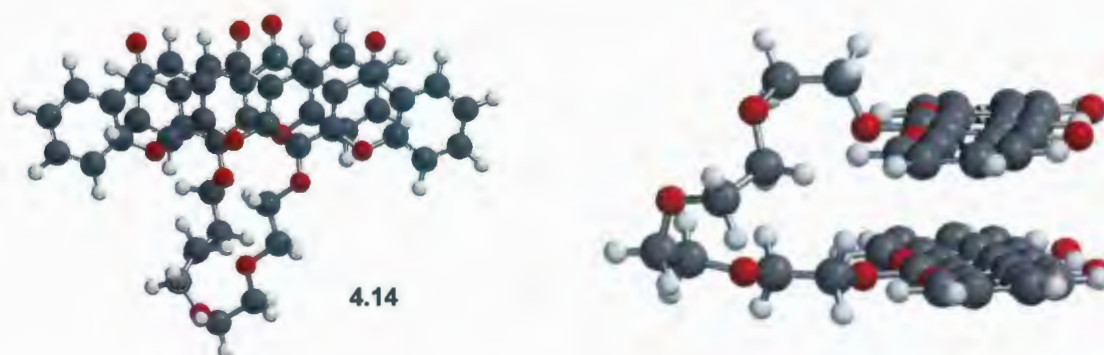
**Figure 4.7** Modeling structure of **4.22** (*top*) and its predicted packing motif (*bottom*).

Compound **4.22** has a LUMO energy level of  $-2.1$  eV and a HOMO energy level at  $-6.0$  eV. The calculated HOMO-LUMO energy gap is thus  $3.9$  eV, while the experimental HOMO-LUMO energy gap, which was evaluated from the absorption edge ( $\lambda = 371$  nm), is  $3.3$  eV. The experimental energy gap ( $3.3$  eV) is in the range of HOMO-LUMO gaps ( $3.0$ – $3.5$  eV) of hetero[5]acenes containing at least one oxygen atom.<sup>19</sup> HOMO and LUMO maps are shown in Figure 4.8.



**Figure 4.8** Representations of the HOMO and LUMO of **4.22**.

The computed structure (MMFF94)<sup>18</sup> of **4.14** (Figure 4.9) showed  $\pi$ - $\pi$  interactions between the two hetero[5]acene moieties in the molecule with an average interplanar distance of 3.8 Å. The predicted  $\pi$ - $\pi$  stacking can provide some support for the hypothesis that this compound may behave like a 15-crown-5 ether system, which usually has some selectivity for Na<sup>+</sup> and K<sup>+</sup> ions. For Cs<sup>+</sup>, a larger cavity such as 18-crown-6 or 21-crown-7 is required. Again, there appears to be cause for optimism that systems such as **4.14** may show some selectivity in its complexation with alkali ions.

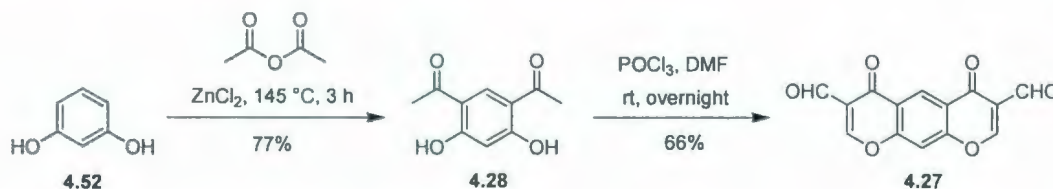


**Figure 4.9** Modeling structure of **4.14**: front view (*left*) and side view (*right*).

### 4.3.3 Attempted Synthesis of Xanthonoid Hetero[n]acenes ( $n = 5, 9$ ) via a Two-directional Approach

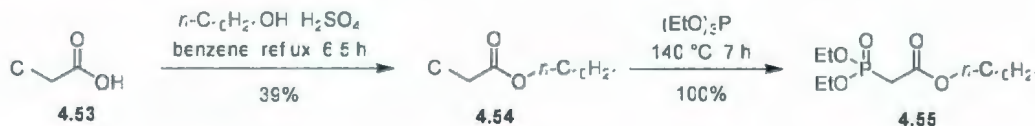
#### 4.3.3.1 Attempted Synthesis of Bis(dienes) 4.26

To reach the target *syn*-xanthonoid hetero[n]acenes **4.25** ( $n = 5$ ) (Scheme 4.2) and **4.31** ( $n = 9$ ) (Scheme 4.3) via a two-directional approach, bis(diene) **4.26** was a required intermediate. First, the known dialdehyde **4.27** was prepared in two steps with synthetically useful yields from commercially available *m*-cresol **4.52** via a double-acylation reaction and a double-Vilsmeier reaction (Scheme 4.9).<sup>20,21</sup>



Scheme 4.9 Synthesis of dialdehyde **4.27**.

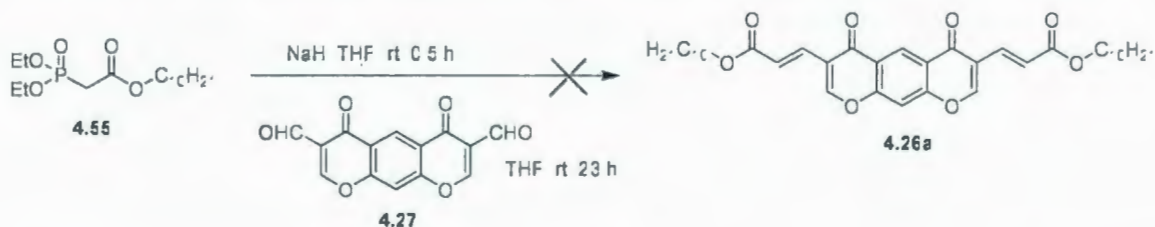
Anticipating that bis(diene) **4.26** would have low solubility in common organic solvents, phosphonate **4.55**, which bears a long alkyl chain, was prepared for the subsequent HWE reaction. The two-step synthesis consisted of an esterification and an Arbuzov reaction to afford phosphonate **4.55** in 39% overall yield from chloroacetic acid (**4.53**) (Scheme 4.10).<sup>22</sup>



Scheme 4.10 Synthesis of phosphonate **4.55**.

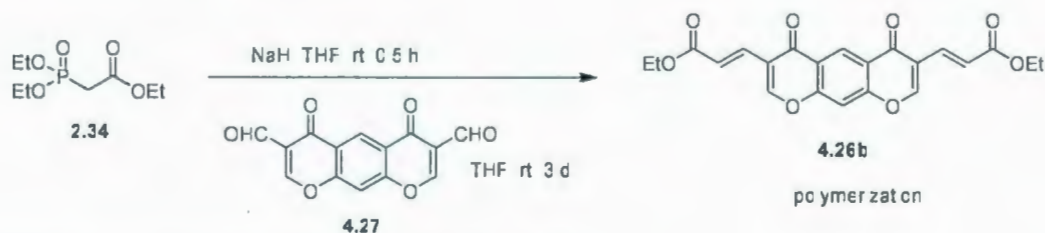


The stage was set for the double-HWE reaction between dialdehyde **4.27** and phosphonate **4.55** to form bis(diene) **4.26a** (Scheme 4.11). When the ylide derived from **4.55** was added to a suspension of dialdehyde **4.27**, a clear, red solution was obtained by the time dialdehyde **4.27** had been completely consumed. Workup afforded a thick red oil, from which none of the desired bis(diene) could be detected by mass spectrometry.



**Scheme 4.11** Attempted synthesis of bis(diene) **4.26a**.

The HWE reaction was then attempted with phosphonate **2.34** to afford bis(diene) **4.26b** (Scheme 4.12).

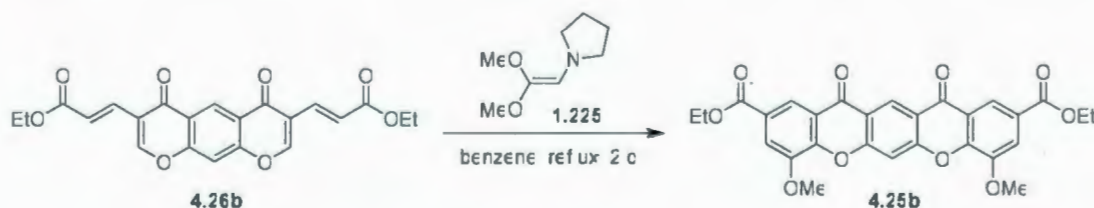


**Scheme 4.12** Attempted synthesis of bis(diene) **4.26b**.

After dialdehyde **4.27** had been completely consumed (tlc analysis), the newly-formed yellow precipitate was collected by suction filtration. Unexpectedly, this precipitate, which appeared normal in solution, “melted” within one or two minutes on the filter paper and became sticky with a concomitant color change from yellow to orange to dark red. The sticky, dark red product was poorly soluble in common organic solvents, and whatever material could be dissolved showed a very complex  $^1\text{H}$  NMR spectrum.

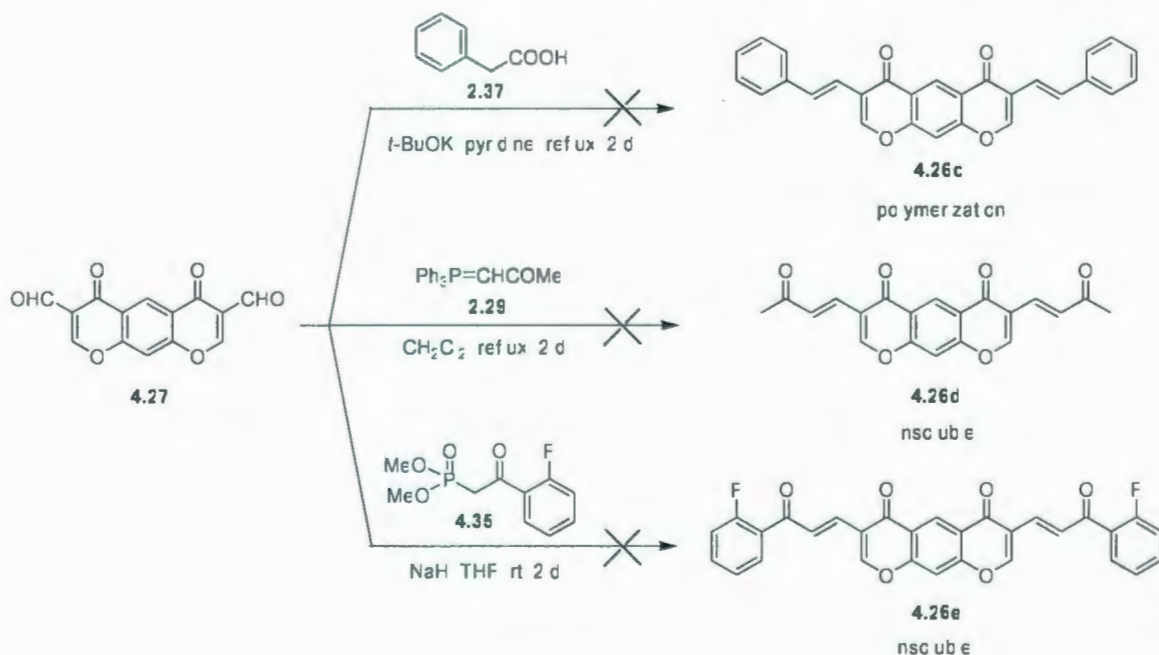


Mass spectrometric analysis ([APCI (+)]) showed a small peak corresponding to the mass of the desired diene **4.26b** ( $m/z$  411 ( $M^+$ )). Assuming that the HWE reaction did occur to form bis(diene) **4.26b** (the yellow precipitate), it can be concluded that it self-reacted (*i.e.* polymerized) upon isolation. Hence, another attempt was made to use the crude product **4.26b** for the next step without isolation. The HWE reaction between dialdehyde **4.27** and phosphonate **2.34** was repeated on the same scale under the above conditions, but the resulting yellow precipitate (the assumed bis(diene) **4.26b**) was kept in THF when the reaction had reached completion (tlc analysis). The THF was removed by decantation, and the yellow precipitate was washed with petroleum ether several times to remove unreacted phosphonate. A benzene solution of freshly prepared enamine **1.225** (20 equiv.) was then added, and the reaction mixture was then heated at reflux for 2 d. Workup gave a sticky red product, which was slightly soluble in  $CDCl_3$ . However, NMR and MS analysis did not show any signals attributable to the desired xanthone **4.25b**. Interestingly, during the washing of the flask containing the sticky red product with acetone, a small amount of a yellow solid stuck to the round bottomed flask was revealed. Although this yellow solid was very poorly soluble in common organic solvents, the correct mass of xanthone **4.25b** (Scheme 4.13) was obtained ([APCI (+)]  $m/z$  (%) 519 ( $M^+$ , 36)).



**Scheme 4.13** Synthesis of *syn*-xanthonoid hetero[5]acene **4.25b** via a two-directional approach.

To ascertain whether other bis(dienes) bearing phenyl or ketone groups would behave in the same manner as **4.26a–b**, the syntheses of bis(dienes) **4.26c–e** were attempted (Scheme 4.14). First, the double-decarboxylative / Knoevenagel condensation between dialdehyde **4.27** and phenyl acetic acid (**2.37**) gave a yellow precipitate, which turned to red and then dark red during suction filtration. In this case, the tiny particles aggregated to form a granular solid instead of a sticky one. This solid was insoluble in common organic solvents, and no evidence for the desired product was observed by mass spectrometry. Thus, it is probable that diene **4.26c** was formed, but it also tended to polymerize in the solid state like diene **4.26b**, but with a different appearance.



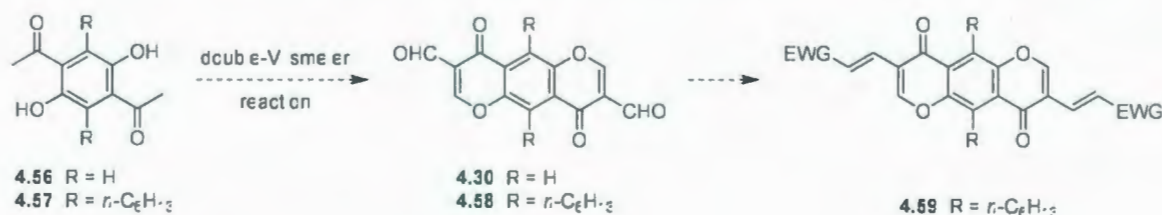
Scheme 4.14 Attempted synthesis of dienes **4.26c–e**.

The double-Wittig or double-HWE reactions of dialdehyde **4.27** and **2.29** or phosphonate **4.35**, respectively, produced yellow solids, which were stable, but insoluble in several solvents. Thus, no mass spectra could be obtained. It was thought that if a

long alkyl chain could be installed on dialdehyde **4.27**, the solubility of products would increase. However, no concise synthetic route to such systems could be identified, so this idea was applied to the synthesis of *anti*-dialdehydes, such as **4.56**.

#### 4.3.3.2 Toward the Synthesis of *anti*-Dialdehyde **4.56**<sup>23</sup>

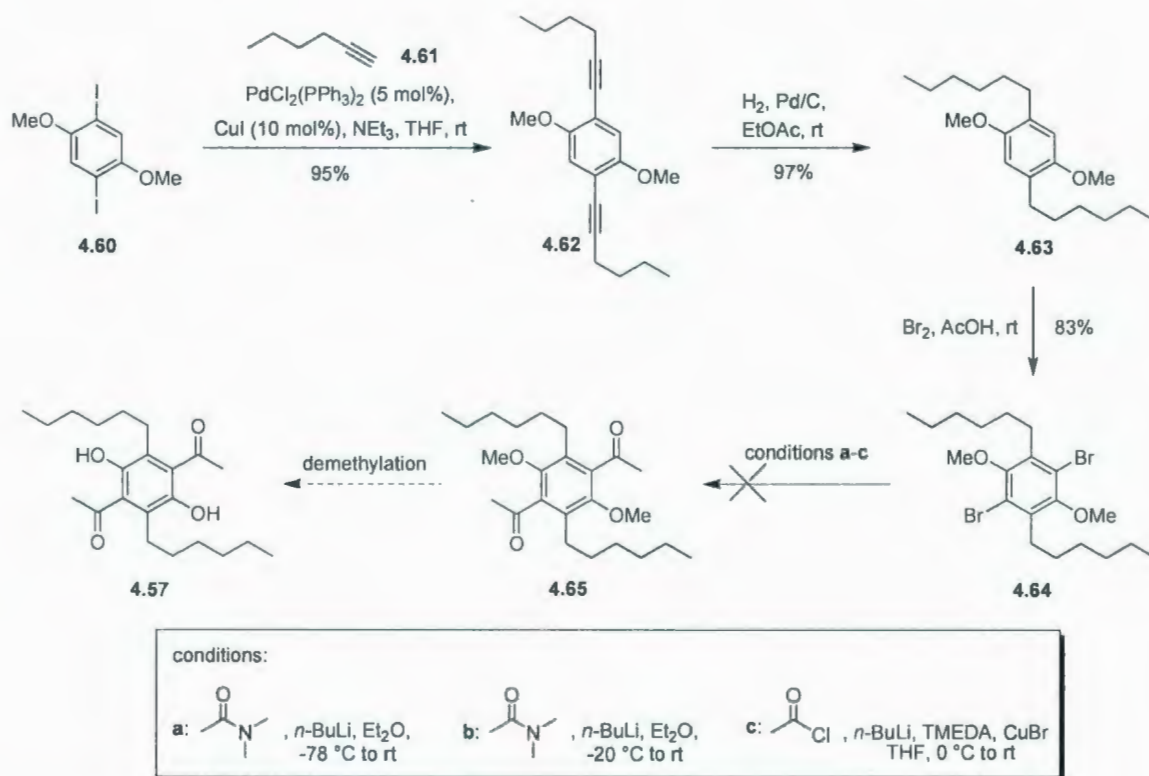
The key intermediate in the synthesis of the parent *anti*-dialdehyde **4.30** would be **4.56** (Scheme 4.15). However, in order to maintain solubility through further synthetic steps leading to bis(diene) **4.59**, the hexasubstituted benzene **4.57** was the first target.



**Scheme 4.15** Synthesis route toward diene **4.59**.

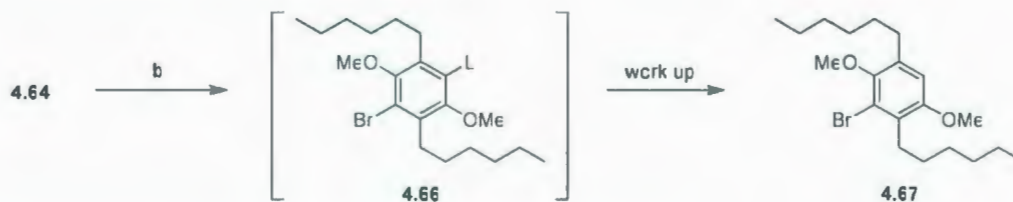
The attempted synthesis of hexasubstituted benzene **4.57** (Scheme 4.16) commenced with a double-Sonogashira reaction of diiodide **4.60**<sup>24</sup> with 1-hexyne (**4.61**), followed by catalytic hydrogenation and electrophilic dibromination of the resulting intermediate **4.63** to afford hexasubstituted benzene **4.64** in a very good yield. Unfortunately, the attempted conversion of the bromo substituents into acetyl groups under several sets of conditions failed to afford **4.65**. The hindered environment may be the cause of the failure.





**Scheme 4.16** Toward the synthesis of hexasubstituted benzene **4.57**.

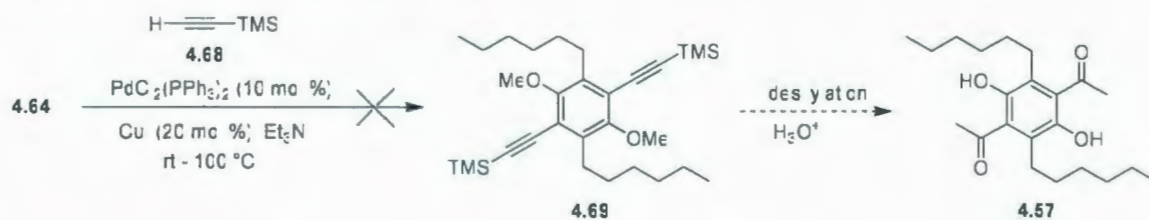
Although unidentified products were obtained using the above conditions **a** and **c**, product **4.67** was obtained from the attempted double-acylation reactions using conditions **b**. This product was presumably formed via a protonation of the monolithiated compounds **4.66** upon work up (Scheme 4.17).



**Scheme 4.17** Product of the double-acylation reaction of **4.64**.



Alternatively, the target **4.57** could be obtained from intermediate **4.69** via desilylation, followed by acid-catalysed hydration of the alkynes (Scheme 4.18). However, compound **4.69** was not formed in an attempted double-Sonogashira reaction of dibromo **4.64**. The use of modified Sonogashira conditions and / or the corresponding diiodide is suggested for future work.



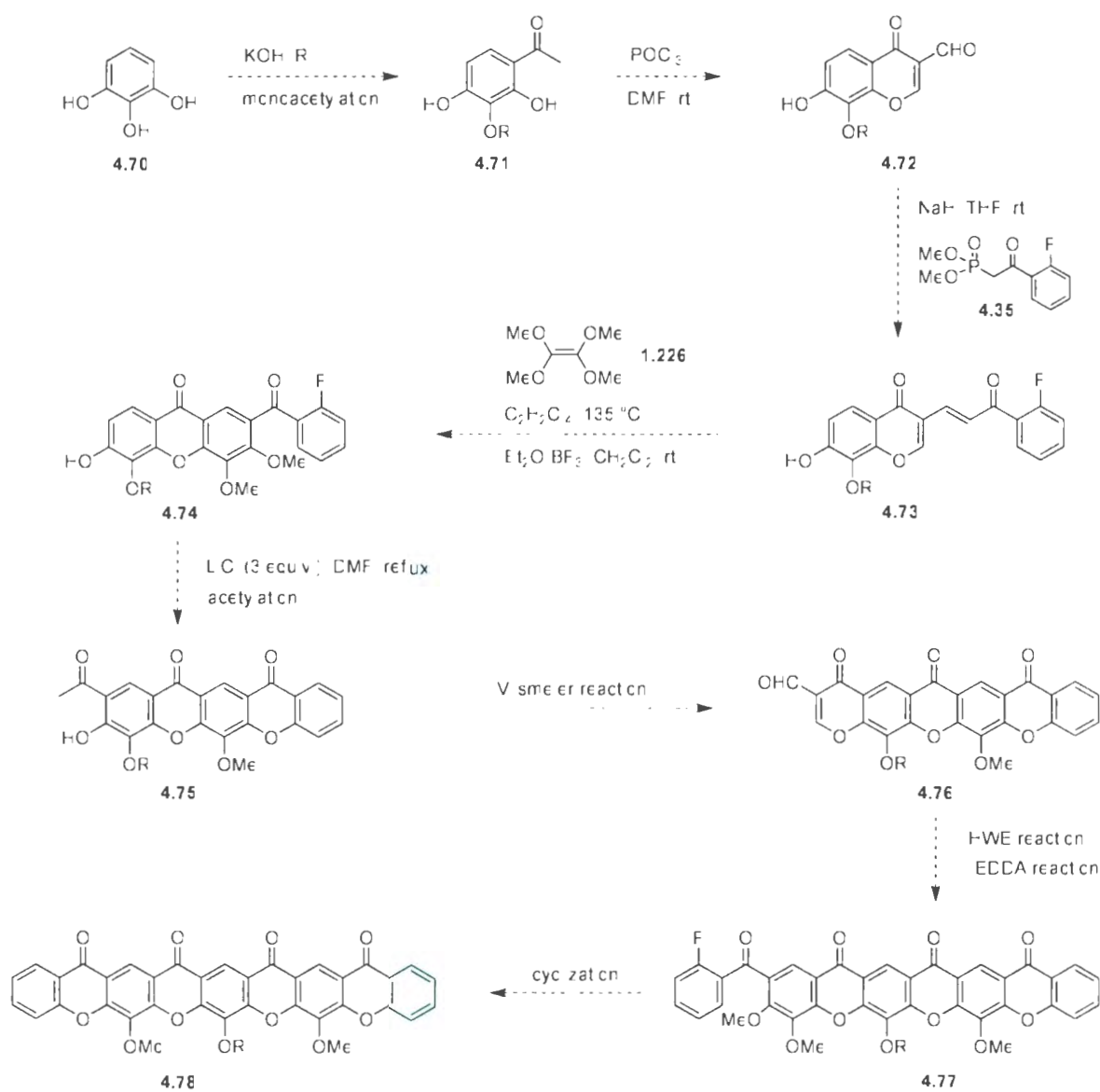
**Scheme 4.18** Alternative approach to the target **4.57**.

#### 4.4 Conclusions and Proposal for Future Work

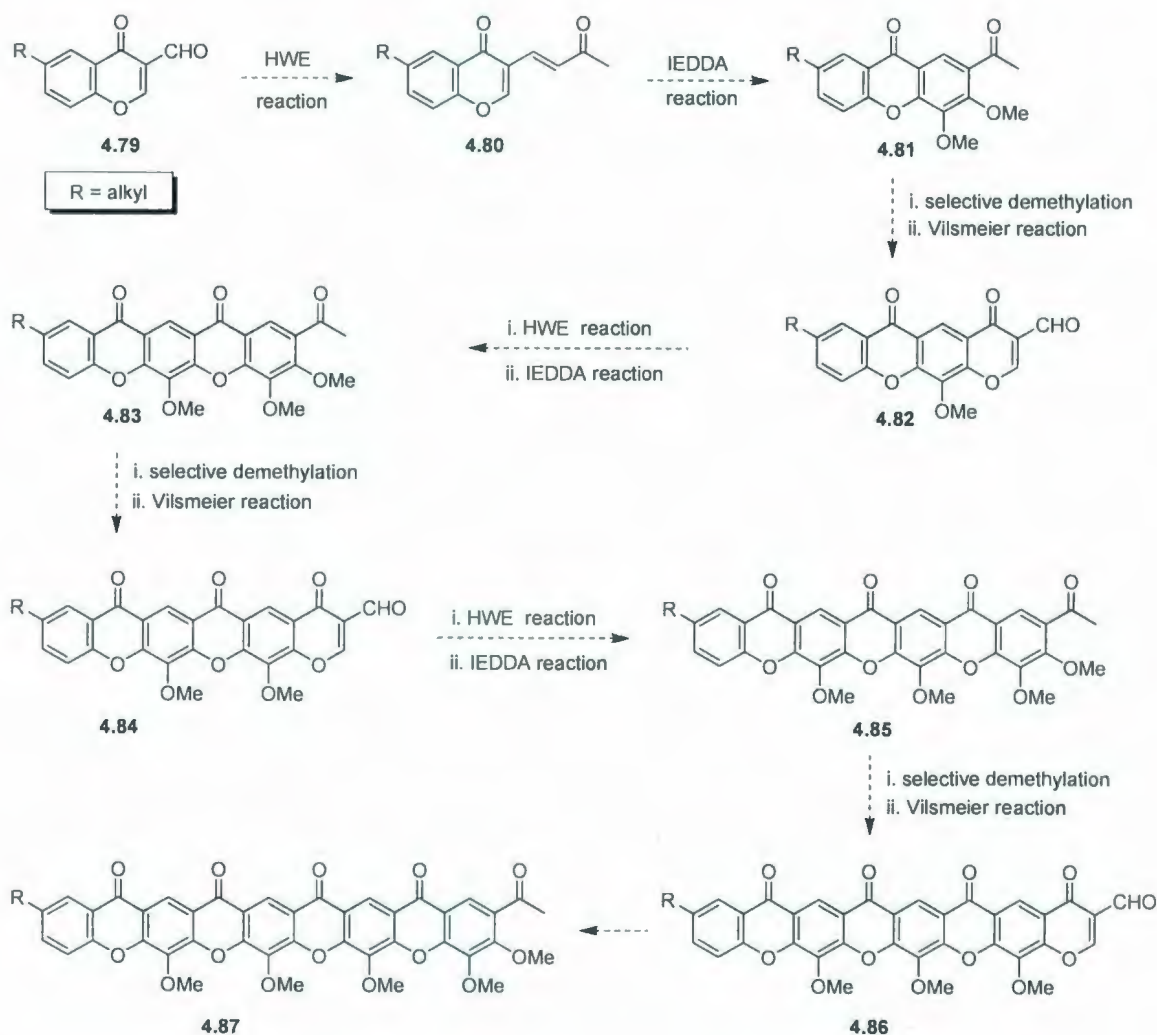
The new xanthone-forming methodology described in Chapter 2, which involves IEDDA-driven domino reactions, was successfully employed for the synthesis of the first targets, *syn*-xanthonoid hetero[5]acenes **4.22**, **4.37** and their derivatives **4.12–4.14**. The key points of the synthetic route are: (1) it employed 3,4-dimethoxyxanthone **4.23**, which was synthesized using the methodology described in Chapter 2, as the key intermediate; (2) it led to the desired products in just four or five steps from commercially available starting materials; (3) good yields were obtained in every single step. Physical properties including absorption and emission spectroscopy of the synthesized *syn*-xanthonoid hetero[5]acenes, **4.22**, **4.12–4.14**, were studied. These compounds were also submitted for further elaboration to form new donor and acceptor systems such as **4.49–4.50** (collaborative work) and show promise as potential chemosensors (future work).

Although ultimately unsuccessful yet, a two-directional approach to the *syn*-xanthonoid hetero[*n*]acenes ( $n = 5, 9$ ) **4.25**, **4.31** and the *anti*-xanthonoid hetero[5]acene **4.29** was investigated. The two-directional approach failed to deliver the desired bis(dienes) **4.26**, which appear to have polymerized upon isolation by suction filtration in air. The attempted synthesis of dialdehyde **4.59** could not be completed because of the problems involved with the preparation of the key intermediate **4.57**. However, some alternative routes are proposed below for future work.

Future work should focus on complexation studies of compound **4.14** and preparation of key intermediate **4.57** for further synthesis of *anti*-bis(dienes) **4.59**. In case these dienes exhibit the same behavior as *syn*-bis(dienes) **4.26**, *i.e.* polymerization occurs, the two-directional approach will be excluded from the synthesis of these target structures. Alternatively, the stepwise approaches shown below can be proposed for the synthesis of *syn*-xanthonoid hetero[*n*]acenes ( $n = 5, 6, 7, 9$ ) (Scheme 4.19) or *syn*-xanthonoid hetero[*n*]acenes ( $n = 4-9$ ) (Scheme 4.20) using the same chemistry.



**Scheme 4.19** Proposed stepwise approach to *syn*-xanthonoid hetero[n]acenes ( $n = 5, 6, 7, 9$ ).



**Scheme 4.20** Proposed stepwise approach to *syn*-xanthonoid hetero[n]acenes ( $n = 4-9$ ).

#### 4.4 Experimental Section

General methods and instrumentation used are identical to those described in Chapter 2 (see page 76–77). Compounds **4.62–4.64** were characterized (mp,  $^1\text{H}$  and  $^{13}\text{C}$  NMR, MS) at the University of Mainz, except for HRMS, which was done at Memorial University.

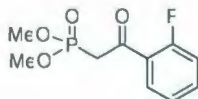


### Instrumentation at the University of Mainz, Germany:

Melting points (mp) were determined on a Büchi HWS SG 2000 apparatus and are uncorrected. Infrared (IR) spectra were obtained using a FT/IR-4100 Fourier Transform Infrared Spectrometer (JASCO).  $^1\text{H}$  and  $^{13}\text{C}$  nuclear magnetic resonance (NMR) spectra were recorded on a Bruker AC300, Bruker ARX 400, Bruker AV 400 ( $\text{CDCl}_3$ , unless otherwise indicated). Chemical shifts are reported relative to internal standards:  $\text{Me}_4\text{Si}$  ( $\delta$  0.00 ppm) and  $\text{CDCl}_3$  ( $\delta$  77.0 ppm), respectively. Low-resolution mass spectra (MS) of compounds were obtained using a Finnigan MAT 90.

#### 4.4.1 Experimental Procedures<sup>25</sup>

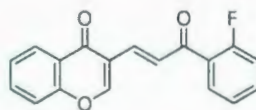
##### Dimethyl 2-fluorophenyl-2-oxoethylphosphonate (**4.35**)<sup>12</sup>



To a solution of dimethyl methylphosphonate (**4.33**) (4.01 g, 32.3 mmol) in THF (40 mL) was slowly added 0.78 M *n*-BuLi in hexane (20.5 mL, 16.0 mmol) at  $-78\text{ }^{\circ}\text{C}$  over 0.5 h. The resulting cloudy solution was stirred at  $-50\text{ }^{\circ}\text{C}$  for a further 1.5 h, then it was cooled to  $-78\text{ }^{\circ}\text{C}$ , and a solution of methyl-2-fluorobenzoate (**4.34**) (1.23 g, 7.98 mmol) in THF (60 mL) was slowly added. The reaction mixture was stirred at  $-78\text{ }^{\circ}\text{C}$  for a further 2.5 h and quenched with saturated solution of  $\text{NH}_4\text{Cl}$  (30 mL). The organic layer was separated, and the aqueous layer was extracted with EtOAc (3 x 50 mL). The combined organic layers were dried over  $\text{MgSO}_4$  and filtered. After the solvents were removed under reduced pressure, the crude product was purified by column chromatography (80:20 EtOAc:hexanes) to yield **4.35** (1.96 g, 100%) as a colourless oil:

$R_f = 0.35$  (EtOAc); IR (neat)  $\nu$  2955 (w), 2923 (m), 2853 (w), 1681 (m), 1609 (m), 1577 (w), 1481 (w), 1452 (m), 1291 (w), 1258 (m), 1209 (w), 1021 (s), 1001 (s), 830 (w), 803 (m), 773 (m)  $\text{cm}^{-1}$ ;  $^1\text{H}$  NMR (500 MHz)  $\delta$  7.89 (td,  $J = 8.1, 1.4$  Hz, 1H), 7.58–7.54 (m, 1H), 7.27–7.24 (m, 1H), 7.18–7.14 (m, 1H), 3.78 (d,  $J_{\text{P-H}} = 11.6$  Hz, 6H), 3.74 (dd,  $J = 22.1, 1.5$  Hz, 2H);  $^{13}\text{C}$  NMR (125 MHz)  $\delta$  189.8, 162.0 (d,  $J_{\text{C-F}} = 254.9$  Hz), 135.6, 131.3, 125.4, 124.8, 116.9 (d,  $J_{\text{C-C-F}} = 23.9$  Hz), 53.27, 53.21, 41.7 (d,  $J_{\text{C-P}} = 132.1$  Hz); MS [APCI (+)]  $m/z$  (%) 246.9 ( $[\text{M}+\text{H}]^+$ , 100); HRMS [EI (+)] calcd for  $\text{C}_{10}\text{H}_{12}\text{FO}_4\text{P}$  246.0457, found 246.0461.

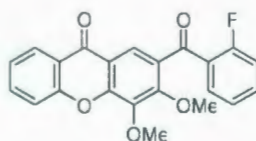
**(*E*)-3-(3-Oxo-3-(2-fluorophenyl)prop-1-enyl)-4*H*-chromen-4-one (4.24)**



To a suspension of NaH (60% dispersion in mineral oil, 368 mg, 9.20 mmol) in THF (15 mL) was slowly added dimethyl 2-fluorophenyl-2-oxoethylphosphonate **4.35** (2.80 g, 11.4 mmol) in THF (10 mL). The mixture was stirred at room temperature for 30 min and the freshly prepared ylide was added dropwise into a solution of 3-formylchromone (1.32 g, 7.57 mmol) in THF (20 mL). The resulting orange mixture was stirred at room temperature for 2 d and worked up according to the general procedure for dienes **1.15a–d** (Chapter 2, page 81). Column chromatography (2:98 EtOAc: $\text{CH}_2\text{Cl}_2$ ) of the crude product yielded diene **4.24** (2.05 g, 92%) as a yellow solid:  $R_f = 0.45$  (2:98 EtOAc: $\text{CH}_2\text{Cl}_2$ ); mp 135–136 °C, IR  $\nu$  3063 (w), 1678 (m), 1653 (m), 1615 (m), 1601 (m), 1561 (w), 1488 (w), 1466 (m), 1449 (m), 1408 (m), 1292 (m), 1266 (m), 1163 (w), 1024 (w), 985 (w), 875 (w), 846 (w), 755 (s), 749 (s), 677 (w) ( $\text{cm}^{-1}$ );  $^1\text{H}$  NMR (500

MHz, DMSO- $d_6$ )  $\delta$  9.00 (s, 1H), 8.18–8.14 (m, 2H), 7.88–7.85 (m, 1H), 7.78–7.73 (m, 2H), 7.71–7.67 (m, 1H), 7.57 (t,  $J = 7.3$  Hz, 1H), 7.50 (d,  $J = 15.9$  Hz, 1H), 7.42–7.37 (m, 2H);  $^{13}\text{C}$  NMR (125 MHz, DMSO- $d_6$ )  $\delta$  189.1, 175.3, 161.5, 160.3 (d,  $J_{\text{C-F}} = 251.5$  Hz), 155.1, 136.9, 134.7, 134.4 (d,  $J_{\text{C-F}} = 8.9$  Hz), 130.5, 127.6, 126.7 (d,  $J_{\text{C-F}} = 54.3$  Hz), 126.3, 125.5, 125.0, 123.5, 118.6, 118.2, 116.7 (d,  $J_{\text{C-F}} = 22.4$  Hz); MS [APCI (+)]  $m/z$  (%) 295.0 ( $[\text{M}+\text{H}]^+$ , 100); HRMS [EI (+)] calcd for  $\text{C}_{18}\text{H}_{11}\text{FO}_3$  294.0692, found 294.0686.

### 3,4-Dimethoxy-2-(2-fluorobenzoyl)-9H-xanthene-9-one (4.23)

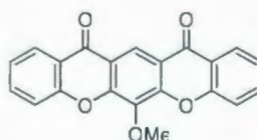


To a clear, preheated (135 °C) solution of diene **4.24** (1.0 g, 3.4 mmol) in 1,1,2,2-tetrachloroethane (1 mL) was added tetramethoxyethane **1.226** (2.5 g, 17 mmol). The reaction mixture was heated with stirring at 135 °C for 2.5 h, then it was cooled to room temperature and diluted with  $\text{CH}_2\text{Cl}_2$  (10 mL). Boron trifluoride diethyl etherate ( $\text{BF}_3 \cdot \text{Et}_2\text{O}$ ) (2.5 mL, 17 mmol) was added and the resulting mixture was stirred at room temperature for 1 d and worked up according to the general procedure for 3,4-dimethoxyxanthenes **1.229a–i** (Chapter 2, page 97). Column chromatography (2:98 EtOAc: $\text{CH}_2\text{Cl}_2$ ) of the crude product yielded xanthone **4.23** (1.26 g, 98%) as a yellow solid:  $R_f = 0.60$  (2:98 EtOAc: $\text{CH}_2\text{Cl}_2$ ); mp 130–131 °C; IR  $\nu$  2946 (s), 2845 (s), 1652 (s), 1597 (s), 1465 (s), 1450 (s), 1352 (s), 1295 (s), 1270 (m), 1203 (m), 1152 (m), 1115 (m), 1077 (s), 778 (m), 755 (s), 674 (m) ( $\text{cm}^{-1}$ );  $^1\text{H}$  NMR (500 MHz)  $\delta$  8.34 (dd,  $J = 8.0, 1.7$



Hz, 1H), 8.24 (s, 1H), 7.79–7.75 (m, 2H), 7.60 (d,  $J = 8.9$  Hz, 1H), 7.58–7.54 (m, 1H), 7.43 (t,  $J = 7.6$  Hz, 1H), 7.29 (t,  $J = 7.6$  Hz, 1H), 7.11 (t,  $J = 9.4$  Hz, 1H), 4.08 (s, 3H), 3.92 (s, 3H);  $^{13}\text{C}$  NMR (125 MHz)  $\delta$  191.0, 176.2, 161.3 (d,  $J_{\text{C-F}} = 254.1$  Hz), 156.6, 156.1, 153.2, 140.7, 135.2, 134.5 (d,  $J = 8.8$  Hz), 131.1, 131.0, 127.6 (d,  $J = 11.7$  Hz), 127.0, 124.8, 124.6, 124.58, 123.1, 121.8, 118.3, 116.6 (d,  $J_{\text{C-F}} = 22.0$  Hz), 62.03, 62.00; MS [APCI (+)]  $m/z$  (%) 379.0 ( $[\text{M}+\text{H}]^+$ , 100); HRMS [EI (+)] calcd for  $\text{C}_{22}\text{H}_{15}\text{FO}_5$  378.0903, found 378.0900.

#### 6-Methoxy-benzopyrano[3,2-*b*]xanthene-12,14-dione (4.22)

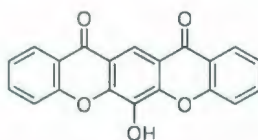


To a clear solution of 3,4-dimethoxyxanthone **4.23** (501 mg, 1.32 mmol) in anhydrous DMF (25 mL) was added lithium chloride (167 mg, 3.96 mmol). The reaction mixture was heated at reflux for 6 h. Solvent was removed, and the residue was washed with 10% citric acid aqueous solution (25 mL). The precipitate was isolated by suction filtration, washed several times with deionized water, and dried in air. Column chromatography (2:98 EtOAc: $\text{CH}_2\text{Cl}_2$ ) of the crude product yielded **4.22** (386 mg, 85%) as a colorless solid:  $R_f = 0.30$  (2:98 EtOAc: $\text{CH}_2\text{Cl}_2$ ); mp > 300 °C; IR  $\nu$  3079 (w), 2951 (w), 2849 (w), 1675 (s), 1602 (s), 1561 (w), 1466 (s), 1435 (s), 1343 (m), 1316 (s), 1293 (m), 1221 (s), 1144 (m), 1123 (m), 1081 (m), 947 (m), 769 (s), 752 (s), 685 (m) ( $\text{cm}^{-1}$ );  $^1\text{H}$  NMR (500 MHz)  $\delta$  9.14 (s, 1H), 8.38 (dd,  $J = 8.1, 1.6$  Hz, 2H), 7.81–7.78 (m, 2H), 7.63 (d,  $J = 8.9$  Hz, 2H), 7.45 (t,  $J = 7.6$  Hz, 2H), 4.27 (s, 3H);  $^{13}\text{C}$  NMR (150 MHz)



{ $^1\text{H}$ } CPMAS (cross-polarization under magic angle spinning), using 100 kHz of  $^1\text{H}$  decoupling and 62.5 kHz for the Hartmann-Hahn matching condition. The spectrum was collected at room temperature (298 K) with a spinning rate  $\nu = 20$  kHz and 10240 scans: 174.4, 173.1, 155.4, 154.2, 151.4, 138.0, 135.3, 133.48, 124.7, 122.6, 120.3, 118.6, 116.9, 63.0; MS [APCI (+)]  $m/z$  (%) 345.0 ( $[\text{M}+\text{H}]^+$ , 100); HRMS [CI (+)] calcd for  $\text{C}_{21}\text{H}_{12}\text{O}_5+\text{H}^+$  345.0763, found 345.0769.

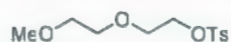
**6-Hydroxy-benzopyrano[3,2-*b*]xanthene-12,14-dione (4.37)**



Compound **4.37** was synthesized by two procedures: (1) to a clear solution of 3,4-dimethoxyxanthone **4.23** (141 mg, 373  $\mu\text{mol}$ ) in anhydrous DMF (10 mL) was added lithium chloride (47.0 mg, 1.11 mmol). The reaction mixture was heated at reflux with stirring for 12 h. Solvent was removed, and the residue was washed with 10% citric acid aqueous solution (25 mL). The precipitate was isolated by suction filtration, washed several times with deionized water, acetone (3 x 3 mL) and dried in air to yield **4.37** (72.1 mg, 59%) as a colorless solid; (2) to a suspension of methoxy hetero[5]acene **4.22** (427 mg, 1.24 mmol) in  $\text{CH}_2\text{Cl}_2$  (20 mL) was added  $\text{BBr}_3$  (0.23 mL, 2.48 mmol) at 0  $^\circ\text{C}$ . The orange resulting solution was stirred at 0  $^\circ\text{C}$  for 15 min then warmed up to room temperature and stirred at this temperature for further 1 h. The reaction mixture was quenched by addition of ice-cold  $\text{H}_2\text{O}$  (100 mL) and aqueous saturated  $\text{NH}_4\text{Cl}$  (10 mL). Solvent was removed under reduced pressure, and the precipitates were collected by

suction filtration, washed with H<sub>2</sub>O (10 mL) and acetone (3 mL) to yield **4.37** (406 mg, 99%) as light grey solid:  $R_f = 0.23$  (2:98 EtOAc:CH<sub>2</sub>Cl<sub>2</sub>); mp > 300 °C; IR  $\nu$  3182 (w), 1662 (s), 1622 (w), 1606 (s), 1597 (s), 1567 (w), 1465 (m), 1451 (s), 1396 (w), 1369 (m), 1318 (s), 1283 (s), 1219 (s), 1183 (m), 1160 (m), 1127 (m), 1072 (m), 986 (w), 755 (s), 679 (m) (cm<sup>-1</sup>); <sup>1</sup>H NMR (500 MHz, DMF d<sub>7</sub>)  $\delta$  8.80 (s, 1H), 8.47 (dd,  $J = 7.8, 1.4$  Hz, 2H), 8.17–8.11 (m, 2H), 7.90 (d,  $J = 8.3$  Hz, 2H), 7.74 (t,  $J = 7.4$  Hz, 2H) (OH was not observed); MS [APCI (+)]  $m/z$  (%) 331 ([M+H]<sup>+</sup>, 100); HRMS [EI (+)] calcd for C<sub>20</sub>H<sub>10</sub>O<sub>5</sub> 330.0528, found 330.0527.

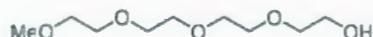
**2-(2-Methoxyethoxy)ethyl *p*-toluenesulfonate (4.39)**<sup>14</sup>



To a cold mixture of diethyl glycol monomethyl ether **4.38** (7.61 g, 100 mmol) and *p*-toluenesulfonyl chloride (19.1 g, 100 mmol) in CH<sub>2</sub>Cl<sub>2</sub> (100 mL) was added potassium hydroxide (11.1 g, 198 mmol) in portions (the internal temperature must be below 5 °C). The reaction mixture was stirred at 0 °C for further 2.5 h, then CH<sub>2</sub>Cl<sub>2</sub> (40 mL) and ice cold H<sub>2</sub>O (100 mL) were added. The layers were separated, and the aqueous layer was extracted with CH<sub>2</sub>Cl<sub>2</sub> (3 x 20 mL). The combined organic layer was washed with H<sub>2</sub>O (2 x 20 mL), dried over MgSO<sub>4</sub>, and filtered to yield (after removal of the solvent under reduced pressure) **4.38** (27.4 g, 100%) as colorless liquid (used for next step without any purification):  $R_f = 0.72$  (EtOAc); <sup>1</sup>H NMR (500 MHz)  $\delta$  7.80 (d,  $J = 8.2$  Hz, 2H), 7.34 (d,  $J = 8.3$  Hz, 2H), 4.17 (t,  $J = 5.0$  Hz, 2H), 3.69 (t,  $J = 4.6$  Hz, 2H), 3.59–3.57 (m, 2H), 3.49–3.47 (m, 2H), 3.35 (s, 3H), 2.45 (s, 3H); <sup>13</sup>C NMR (125 MHz) 145.0,

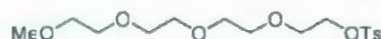
133.2, 130.0, 128.2, 72.0, 70.9, 69.4, 68.9, 59.2, 21.8; MS [APCI (+)]  $m/z$  (%) 275 ( $[M+H]^+$ , 100).

**Tetra(ethylene glycol) monomethyl ether (4.41)**<sup>15</sup>



To diethylene glycol (7.10 g, 66.9 mmol) was added sodium metal (0.46 g, 20.0 mmol) in portions at room temperature. The reaction mixture was stirred for 45 min and then warmed up to 70 °C for further 30 min to give a clear yellow solution. The resulting solution (**4.40**) was cooled to room temperature and 1-methoxy-5-tosyl-3-oxapentane **4.39** (2.74 g, 9.99 mmol) was added dropwise. The reaction mixture was stirred at room temperature for 17 h, quenched with H<sub>2</sub>O (50 mL), extracted with CH<sub>2</sub>Cl<sub>2</sub> (5 x 30 mL), dried over MgSO<sub>4</sub>, and filtered. The solvent was removed under reduced pressure to yield crude **4.41** as clear yellow liquid (used directly for the next step):  $R_f$  = 0.05 (EtOAc, I<sub>2</sub> dip).

**2-(2-(2-(2-methoxyethoxy)ethoxy)ethoxy)ethyl *p*-toluenesulfonate (4.42)**<sup>14</sup>

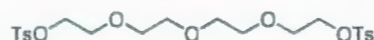


To a cold mixture of tetra(ethylene glycol) monomethyl ether **4.41** (2.08 g, 9.99 mmol) and *p*-toluenesulfonyl chloride (1.90 g, 9.97 mmol) in CH<sub>2</sub>Cl<sub>2</sub> (50 mL) was added potassium hydroxide (112 mg, 2.00 mmol) in portions (the internal temperature must be below 5 °C). The reaction mixture was stirred at 0 °C for further 2.5 h, then CH<sub>2</sub>Cl<sub>2</sub> (30 mL) and ice cold H<sub>2</sub>O (100 mL) were added. The layers were separated, and the aqueous layer was extracted with CH<sub>2</sub>Cl<sub>2</sub> (3 x 30 mL). The combined organic layer was washed with H<sub>2</sub>O (2 x 20 mL), dried over MgSO<sub>4</sub>, and filtered. After the solvent was removed



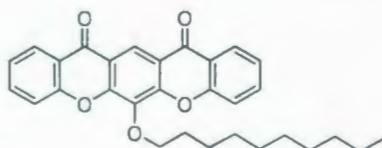
under reduced pressure, the crude product was purified by column chromatography (EtOAc) to yield **4.42** (2.2 g, 61% from **4.39**) as colorless liquid:  $R_f = 0.11$  (EtOAc);  $^1\text{H}$  NMR (500 MHz)  $\delta$  7.80 (d,  $J = 8.6$  Hz, 2H), 7.34 (d,  $J = 8.1$  Hz, 2H), 4.16 (t,  $J = 5.3$  Hz, 2H), 3.69 (t,  $J = 4.8$  Hz, 2H), 3.65–3.63 (m, 7H), 3.58 (s, 3H), 3.55–3.53 (m, 2H), 3.37 (s, 3H), 2.45 (s, 3H);  $^{13}\text{C}$  NMR (125 MHz) 145.0, 133.3, 130.0, 128.2, 72.2, 70.96, 70.81, 70.74, 69.4, 68.9, 59.2, 21.8; MS [APCI (+)]  $m/z$  (%) 363 ( $[\text{M}+\text{H}]^+$ , 41), 380 ( $[\text{M}+\text{H}_2\text{O}]^+$ , 100).

**2-(2-(2-(2-hydroxyethoxy)ethoxy)ethoxy)ethyl di-*p*-toluenesulfonate (4.44)**<sup>14</sup>



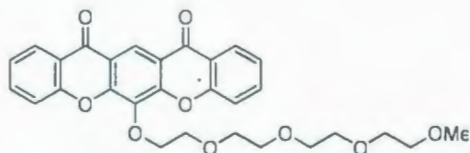
To a cold mixture of tetra(ethylene glycol) **4.43** (1.94 g, 9.99 mmol) and *p*-toluenesulfonyl chloride (3.80 g, 19.9 mmol) in  $\text{CH}_2\text{Cl}_2$  (50 mL) was added potassium hydroxide (4.48 g, 79.8 mmol) in portions (the internal temperature must be below 5 °C). The reaction mixture was stirred at 0 °C for further 2 h, then  $\text{CH}_2\text{Cl}_2$  (40 mL) and ice cold  $\text{H}_2\text{O}$  (100 mL) were added. The layers were separated, and the aqueous layer was extracted with  $\text{CH}_2\text{Cl}_2$  (3 x 20 mL). The combined organic layer was washed with  $\text{H}_2\text{O}$  (2 x 20 mL), dried over  $\text{MgSO}_4$ , and filtered. The solvent was removed under reduced pressure to yield crude product **4.44** (4.66 g, 93%) (used directly for the next steps without any purification) as colorless liquid:  $R_f = 0.55$  (70:30 EtOAc:hexanes);  $^1\text{H}$  NMR (500 MHz)  $\delta$  7.79 (d,  $J = 8.2$  Hz, 4H), 7.34 (d,  $J = 8.0$  Hz, 4H), 4.15 (t,  $J = 5.0$  Hz, 4H), 3.73–3.54 (m, 12H), 2.44 (s, 6H);  $^{13}\text{C}$  NMR (125 MHz)  $\delta$  144.9, 133.1, 129.9, 128.05, 128.03, 70.81, 70.63, 69.4, 68.8, 61.82, 61.78, 21.7; MS [APCI (+)]  $m/z$  (%) 503 ( $[\text{M}+\text{H}]^+$ , 39), 520 ( $[\text{M}+\text{H}_2\text{O}]^+$ , 100).



**6-Decoxy-benzopyrano[3,2-*b*]xanthene-12,14-dione (4.12)**

To a suspension of hydroxyl hetero[5]acence **4.37** (50.1 mg, 152  $\mu\text{mol}$ ) in anhydrous DMF (5 mL) was added portionwise potassium carbonate (41.5 mg, 300  $\mu\text{mol}$ ). The resulting red solution was stirred for 10 min, then potassium iodide (10 mol %) and 1-bromodecane (**4.45**) (33.2 mg, 150  $\mu\text{mol}$ ) were added. The reaction mixture was heated at reflux for 19 h. Solvent was removed under reduced pressure and the crude product was purified by column chromatography (2:98 EtOAc:CH<sub>2</sub>Cl<sub>2</sub>) to yield **4.12** (60 mg, 85%) as a colorless solid:  $R_f$  = 0.55 (2:98 EtOAc:CH<sub>2</sub>Cl<sub>2</sub>); mp 128–129 °C; IR  $\nu$  2922 (w), 2850 (w), 1682 (s), 1599 (s), 1561 (w), 1541 (w), 1466 (s), 1435 (s), 1339 (m), 1311 (s), 1294 (w), 1220 (s), 1128 (s), 1079 (m), 760 (s), 746 (s), 682 (s) (cm<sup>-1</sup>); <sup>1</sup>H NMR (500 MHz)  $\delta$  9.1 (s, 1H), 8.36 (dd,  $J$  = 8.1, 1.6 Hz, 2H), 7.80–7.76 (m, 2H), 7.58 (d,  $J$  = 8.2 Hz, 2H), 7.44 (t,  $J$  = 7.3 Hz, 2H), 4.39 (t,  $J$  = 6.5 Hz, 2H), 2.01–1.95 (m, 2H), 1.74–1.68 (m, 2H), 1.49–1.28 (m, 12H), 0.89 (t,  $J$  = 7.1 Hz, 3H); <sup>13</sup>C NMR (125 MHz) 176.5, 156.2, 153.3, 136.0, 135.5, 127.3, 124.9, 121.7, 121.6, 119.2, 118.3, 75.7, 32.1, 30.5, 29.95, 29.90, 29.7, 29.6, 26.3, 22.9, 14.3; MS [APCI (+)]  $m/z$  (%) 471 ([M+H]<sup>+</sup>, 100); HRMS [EI (+)] calcd for C<sub>30</sub>H<sub>30</sub>O<sub>5</sub> 470.2093, found 470.2100.

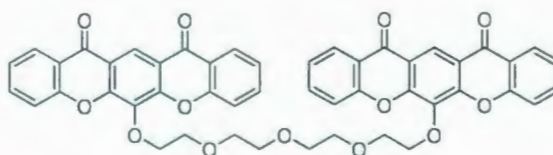
**6-(2-(2-(2-(2-methoxyethoxy)ethoxy)ethoxy)ethoxy)benzopyrano[3,2-*b*]xanthene-12,14-dione (4.13)**



To a suspension of hydroxyl hetero[5]acene **4.37** (101 mg, 306  $\mu\text{mol}$ ) in anhydrous DMF (10 mL) was added potassium carbonate (83.2 mg, 602  $\mu\text{mol}$ ) in portions. The resulting orange solution was stirred for 15 min then **4.42** (245 mg, 676  $\mu\text{mol}$ ) was added. The reaction mixture was heated at reflux for 14 h. DMF was then removed under reduced pressure and  $\text{CH}_2\text{Cl}_2$  (100 mL) and  $\text{H}_2\text{O}$  (20 mL) were added to the residue to give a suspension. The solids were collected by suction filtration to recover starting material hydroxyl hetero[5]acene **4.37** (15 mg, 15%) and the layers of the filtrate were separated. The aqueous layer was extracted with  $\text{CH}_2\text{Cl}_2$  (3 x 30 mL), washed with aqueous saturated  $\text{NH}_4\text{Cl}$  (1 x 10 mL), washed with  $\text{H}_2\text{O}$  (1 x 20 mL), washed with brine, dried over  $\text{MgSO}_4$ , and filtered. After the solvent was removed, the crude product was purified by column chromatography (20:80 petroleum ether:EtOAc) to yield **4.13** (98.4 mg, 62%, 73% brsm) as a colorless solid:  $R_f = 0.23$  (20:80 petroleum ether:EtOAc); mp 118–120  $^\circ\text{C}$ ; IR  $\nu$  2926 (m, br), 2875 (m), 1738 (m), 1674 (s), 1597 (s), 1562 (w), 1466 (s), 1436 (s), 1341 (s), 1312 (s), 1219 (s), 1122 (s), 1076 (s), 764 (s), 750 (s), 685 (s) ( $\text{cm}^{-1}$ );  $^1\text{H}$  NMR (500 MHz)  $\delta$  9.10 (s, 1H), 8.34 (dd,  $J = 6.5, 1.0$  Hz, 2H), 7.78 (t,  $J = 7.8$  Hz, 2H), 7.61 (d,  $J = 8.3$  Hz, 2H), 7.43 (t,  $J = 7.7$  Hz, 2H), 4.59 (t,  $J = 4.6$  Hz, 2H), 4.05 (t,  $J = 4.5$  Hz, 2H), 3.80–3.78 (m, 2H), 3.66–3.61 (m, 8H), 3.53–3.51 (m,

2H), 3.36 (s, 3H);  $^{13}\text{C}$  NMR (125 MHz)  $\delta$  176.4, 156.2, 153.0, 135.77, 135.59, 127.2, 125.0, 121.7, 121.6, 119.1, 118.4, 74.4, 72.1, 71.1, 71.0, 70.9, 70.8, 70.7 (2C), 59.2; MS [APCI (+)]  $m/z$  (%) 521 ( $[\text{M}+\text{H}]^+$ , 100); HRMS [EI (+)] calcd for  $\text{C}_{29}\text{H}_{28}\text{O}_9$  520.1733, found 520.1729.

**6,6'-(2,2'-(2,2'-Oxybis(ethane-2,1-diyl)bis(oxy))bis(ethane-2,1-diyl))bis(oxy)-dibenzoparano[3,2-*b*]xanthene-12,14-dione (4.14)**

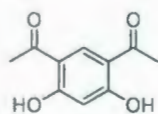


To a suspension of hydroxyl hetero[5]acence **4.37** (99.8 mg, 302  $\mu\text{mol}$ ) in anhydrous DMF (10 mL) was added potassium carbonate (83.5 mg, 604  $\mu\text{mol}$ ) in portions. The resulting orange solution was stirred for 15 min then **4.44** (184 mg, 366  $\mu\text{mol}$ ) was added. The reaction mixture was heated at reflux for 27 h. After DMF was removed under reduced pressure,  $\text{CH}_2\text{Cl}_2$  (30 mL) and  $\text{H}_2\text{O}$  (20 mL) were added to the residue. The layers were separated and the aqueous layer was extracted with  $\text{CH}_2\text{Cl}_2$  (3 x 30 mL), washed with aqueous saturated  $\text{NH}_4\text{Cl}$  (1 x 10 mL), washed with  $\text{H}_2\text{O}$  (1 x 20 mL), washed with brine, dried over  $\text{MgSO}_4$ , and filtered. After the solvent was removed, the crude product was purified by column chromatography (50:50 EtOAc: $\text{CH}_2\text{Cl}_2$ ) to yield **4.14** (69.4 mg, 57%) as a colorless solid:  $R_f$  = 0.30 (50:50 EtOAc: $\text{CH}_2\text{Cl}_2$ ); mp 264–265  $^\circ\text{C}$ ; IR  $\nu$  3073 (w), 2871 (w), 1677 (s), 1599 (s), 1467 (s), 1437 (s), 1340 (m), 1312 (s), 1220 (s), 1124 (s), 1074 (m), 763 (s), 750 (s), 685 (s) ( $\text{cm}^{-1}$ );  $^1\text{H}$  NMR (500 MHz)  $\delta$  9.02 (s, 2H), 8.28 (dd,  $J$  = 7.3, 1.4 Hz, 4H), 7.73–7.70 (m, 4H), 7.53 (d,  $J$  = 8.7



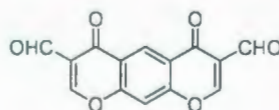
Hz, 4H), 7.37 (t,  $J = 7.5$  Hz, 4H), 4.55 (t,  $J = 4.5$  Hz, 4H), 4.01 (t,  $J = 5.0$  Hz, 4H), 3.73 (t,  $J = 5.0$  Hz, 4H), 3.59 (t,  $J = 4.8$  Hz, 4H);  $^{13}\text{C}$  NMR (125 MHz)  $\delta$  176.2, 156.1, 152.9, 135.69, 135.49, 127.2, 124.9, 121.65, 121.55, 119.1, 118.2, 74.3, 71.04, 71.0 (one peak missing due to overlap); MS [APCI (+)]  $m/z$  (%) 819 ( $[\text{M}+\text{H}]^+$ , 100); HRMS could not be obtained either by [EI (+)] or [CI (+)].

#### 5-Acetyl-2,4-dihydroxyacetophenone (**4.28**)<sup>20</sup>



To a vigorously stirred mixture of acetic anhydride (9.18 g, 89.9 mmol) and zinc chloride (12.3 g, 90.2 mmol) was added resorcinol (**4.52**) (5.01 g, 45.5 mmol) in a portion. The reaction mixture was slowly heated up to 150 °C for 3 h, then was cooled to room temperature and cold aqueous 1 M HCl (500 mL) was added. The precipitates were collected by suction filtration. Column chromatography (35:65 EtOAc:Hexanes) of the crude product yielded **4.28** (6.76 g, 77%) as a yellow solid:  $R_f = 0.31$  (35:65 EtOAc:Hexanes); mp 186–187 °C (lit. mp<sup>20</sup> 178–179 °C);  $^1\text{H}$  NMR (500 MHz)  $\delta$  12.94 (s, 2H), 8.21 (s, 1H), 6.43 (s, 1H), 2.63 (s, 6H); MS [APCI (+)]  $m/z$  (%) 195 ( $[\text{M}+\text{H}]^+$ , 100).

#### 4,6-Dioxo-4*H*,6*H*-benzo[1,2-*b*:5,4-*b'*]dipyran-3,7-dicarboxylaldehyde (**4.27**)<sup>21</sup>

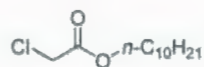


To a solution of 4,6-diacetylresorcinol (**4.28**) (5.53 g, 28.5 mmol) in DMF (75 mL) was added dropwise  $\text{POCl}_3$  (17.5 g, 114 mmol) at 0 °C. The resulting reaction



mixture was stirred at room temperature for 27 h. The reaction mixture was poured into ice-cold water (600 mL) and stirred vigorously for 30 min. The yellow precipitate was collected by suction filtration, washed several times with H<sub>2</sub>O, and dried in air. The crude product was purified by recrystallization (CH<sub>2</sub>Cl<sub>2</sub>) to yield **4.27** (5.09 g, 66%) as yellow crystals:  $R_f = 0.28$  (2:98 EtOAc:CH<sub>2</sub>Cl<sub>2</sub>); mp 275 °C (decomposed) (same as lit.<sup>21</sup>); <sup>1</sup>H NMR (500 MHz)  $\delta$  10.39 (s, 2H), 9.26 (s, 1H), 8.56 (s, 2H), 7.68 (s, 2H); <sup>13</sup>C NMR (125 MHz)  $\delta$  187.8, 174.8, 161.1, 158.8, 127.7, 123.9, 120.7, 108.7; MS [APCI (+)]  $m/z$  (%) 271 ([M+H]<sup>+</sup>, 100).

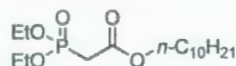
**Decyl chloroacetate (4.54)<sup>22a</sup>**



1-Decanol (3.37 g, 21.3 mmol) was added dropwise to the suspension of K<sub>2</sub>CO<sub>3</sub> (4.58 g, 27.7 mmol) in CH<sub>2</sub>Cl<sub>2</sub> (10 mL). The reaction mixture was stirred at room temperature for 30 min and cooled in ice bath for 10 min before dropwise addition of chloroacetyl chloride (**4.53**) (2.40 g, 21.3 mmol). The resulting reaction mixture was stirred at room temperature for 1.5 h. The reaction mixture was filtered and the solids were washed with CH<sub>2</sub>Cl<sub>2</sub>. The filtrate was washed with aqueous 20% NaHCO<sub>3</sub> (2 x 20 mL), washed with H<sub>2</sub>O (2 x 30 mL), washed with brine, dried over MgSO<sub>4</sub>, and filtered. The solvent was removed under reduced pressure. Pure product **4.54** (1.93 g, 39%) was collected by distillation at 150–152 °C, 8 mmHg (lit.<sup>22a</sup> b.p. 148–150 °C, 10 mmHg) as colorless liquid: <sup>1</sup>H NMR (500 MHz)  $\delta$  4.19 (t,  $J = 6.6$  Hz, 2H), 4.06 (s, 2H), 1.66 (q,  $J =$

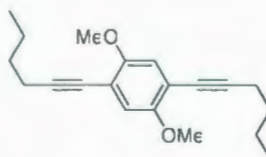
7.0 Hz, 2H), 1.36–1.27 (m, 14H), 0.88 (t,  $J = 7.0$  Hz, 3H);  $^{13}\text{C}$  NMR (125 MHz)  $\delta$  167.6, 66.7, 41.2, 32.1, 29.72, 29.7, 29.5, 29.4, 28.7, 26.0, 22.9, 14.3.

**Decyl diethyl phosphoacetate (4.55)<sup>22b</sup>**



A mixture of decyl chloroacetate (**4.54**) (3.94 g, 16.8 mmol) and triethyl phosphite (5.71 g, 34.4 mmol) was heated at 140 °C for 7 h. The excess amount of  $\text{P}(\text{OEt})_3$  and volatile by-products were removed by vacuum distillation to yield crude product **4.55** (5.65 g, 100%) as a colorless liquid (used for the HWE reaction without any purification):  $^1\text{H}$  NMR (500 MHz)  $\delta$  4.20–4.10 (m, 6H), 2.96 (d,  $J_{\text{P-H}} = 22$  Hz, 2H), 1.64 (q,  $J = 7.0$  Hz, 2H), 1.35 (t,  $J = 7.1$  Hz, 6H), 1.31–1.22 (m, 14 H), 0.88 (t,  $J = 6.9$  Hz, 3H);  $^{13}\text{C}$  NMR (125 MHz)  $\delta$  166.1, 66.0, 62.9, 62.8, 34.6 ( $J_{\text{C-P}} = 134.2$  Hz), 32.1, 29.72, 29.71, 29.49, 29.42, 28.7, 28.6, 26.0, 22.9, 16.6, 16.5, 14.3.

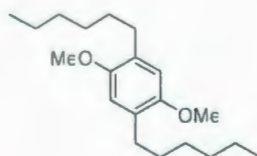
**2,5-Bis(1-hexynyl)-1,4-dimethoxybenzene (4.62)**



To a stirred mixture of 2,5-diiodo-1,4-dimethoxybenzene (**4.60**) (1.95 g, 5.00 mmol),  $\text{PdCl}_2(\text{PPh}_3)_2$  (175 mg, 250  $\mu\text{mol}$ ) and 1-hexyne (**4.61**) (1.15 g, 14.0 mmol) in  $\text{Et}_3\text{N}$  (8.0 mL) was added  $\text{CuI}$  (95.2 mg, 500  $\mu\text{mol}$ ) in one portion at room temperature. The reaction mixture was stirred at room temperature for 27 h. Water (20 mL) and  $\text{CH}_2\text{Cl}_2$  (20 mL) were added to the reaction mixture. The organic layer was separated,

and the aqueous layer was extracted with  $\text{CH}_2\text{Cl}_2$  (4 x 20 mL). The combined organic layer was washed with brine (2 x 10 mL), dried over anhydrous  $\text{MgSO}_4$  and filtered through Celite<sup>®</sup>. The solvent was removed under reduced pressure. Column chromatography (5:95 EtOAc:petroleum ether) of the crude product yielded **4.62** (1.44 g, 95%) as a light yellow solid:  $R_f = 0.50$  (5:95 EtOAc:petroleum ether); mp 72 °C; IR  $\nu$  2956 (m), 2869 (w), 2227 (w), 1498 (s), 1457 (s), 1390 (s), 1322 (w), 1204 (s), 1036 (s), 860 (s), 781 (s), 736 (s) ( $\text{cm}^{-1}$ );  $^1\text{H}$  NMR (400 MHz),  $\delta$  6.79 (s, 2H), 3.75 (s, 6H), 2.40 (t,  $J = 7.0$  Hz, 4H), 1.59–1.37 (m, 8H), 0.88 (t,  $J = 7.4$  Hz, 6H);  $^{13}\text{C}$  NMR (75 MHz)  $\delta$  153.7, 115.8, 113.2, 96.0, 77.2, 56.4, 30.9, 22.1, 19.5, 13.7; MS (FD)  $m/z$  (%) 298 (M, 100).

#### 1,4-Dimethoxy-2,5-di-*n*-hexylbenzene (4.63)

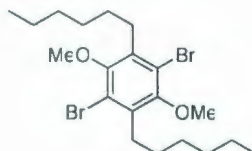


A mixture of 2,5-bis(1-hexynyl)-1,4-dimethoxybenzene (**4.62**) (1.31 g, 4.39 mmol) and Pd/C (0.13 g) in EtOAc (50 mL) was stirred under a hydrogen atmosphere at room temperature for 2.5 d. The reaction mixture was filtered through Celite<sup>®</sup>. The solvent was removed under reduced pressure to yield crude product **4.63** (1.31 g, 97%) as a colourless solid:  $R_f = 0.65$  (5:95 EtOAc:petroleum ether); mp 43–44 °C; IR  $\nu$  2951 (s), 2921 (s), 2852 (s), 1697 (w), 1505 (s), 1463 (s), 1402 (s), 1318 (m), 1206 (s), 1045 (s), 855 (s), 838 (m), 725 (s), 711 (s) ( $\text{cm}^{-1}$ );  $^1\text{H}$  NMR (300 MHz)  $\delta$  6.58 (s, 2H), 3.70 (s, 6H), 2.49 (t,  $J = 7.0$  Hz, 4H), 1.54–1.44 (m, 4H), 1.33–1.26 (m, 12H), 0.84 (t,  $J = 7.0$  Hz, 6H);



$^{13}\text{C}$  NMR (75 MHz)  $\delta$  151.2, 129.3, 113.0, 56.2, 31.8, 30.22, 30.18, 29.4, 22.7, 14.1; MS (FD)  $m/z$  (%) 306 (M, 100); HRMS [EI (+)] calcd for  $\text{C}_{20}\text{H}_{34}\text{O}_2$  306.2559, found 306.2556.

**2,5-Dibromo-1,4-dimethoxy-3,6-di-*n*-hexylbenzene (4.64)**



To a stirred solution of 1,4-dimethoxy-2,5-di-*n*-hexylbenzene (**4.63**) (1.31 g, 4.27 mmol) in glacial AcOH (20.0 mL) at room temperature was added dropwise a solution of bromine (1.36 g, 8.54 mmol) in glacial AcOH (2.0 mL). The reaction mixture was stirred at room temperature for 2 d. After the addition of water (50 mL), the reaction mixture was extracted with  $\text{CHCl}_3$  (3 x 30 mL). The combined organic layer was washed with distilled water (1 x 30 mL), washed with aqueous 10%  $\text{NaHCO}_3$  (3 x 30 mL), washed with brine (2 x 20 mL), dried over anhydrous  $\text{MgSO}_4$  and filtered. The solvent was removed under reduced pressure. Column chromatography (petroleum ether) of the crude product yielded **4.64** (1.64 g, 83%) as an off-white solid:  $R_f$  = 0.80 (5:95 EtOAc:petroleum ether); mp 48–49 °C; IR  $\nu$  2954 (s), 2920 (s), 2852 (s), 1597 (w), 1559 (w), 1451 (s), 1381 (s), 1299 (w), 1198 (m), 1084 (m), 1018 (s), 891 (w), 791 (w), 726 (m) ( $\text{cm}^{-1}$ );  $^1\text{H}$  NMR (400 MHz)  $\delta$  3.84 (s, 6H), 2.84–2.80 (m, 4H), 1.62–1.54 (m, 4H), 1.49–1.42 (m, 4H), 1.38–1.35 (m, 8H), 0.94 (t,  $J$  = 7.1 Hz, 6H);  $^{13}\text{C}$  NMR (75 MHz)  $\delta$  152.2, 136.0, 119.6, 61.2, 31.5, 31.46, 29.6, 29.5, 22.6, 14.1; MS (FD)  $m/z$  (%) 464 (M, 100); HRMS [EI (+)] calcd for  $\text{C}_{20}\text{H}_{32}\text{Br}_2\text{O}_2$  462.0769, found 462.0776.



#### 4.4.2 UV and Fluorescence Measurements

Methods are identical to those described in Chapter 2, page 105–106. Solutions of all xanthenes in  $\text{CHCl}_3$  were prepared with concentration around  $2\text{--}3 \times 10^{-5}$  M.

*Table of UV and Fluorescence data*

	Compounds	$\lambda_{\text{abs}} (\epsilon, \text{cm}^{-1} \text{M}^{-1})$	$\lambda_{\text{em}} (\text{nm})$
Diene	4.24	289 (19300), 320 (26100)	-
Xanthone	4.23	280 (43000), 346 (7640)	-
Hetero[5]acenes	4.22	254 (95500), 299 (143000), 354 (22200)	403
	4.12	255 (123000), 300 (171000), 355 (26500)	402
	4.13	255 (43400), 299 (62300), 354 (10300)	403
	4.14	254 (16800), 299 (22600), 354 (37200)	433, 462

#### 4.5 References and Notes

- [1] Liebermann, H.; Lewin, G.; Gruhn, A.; Gottesmann, E.; Lissner, D.; Schonda, K. *Justus Liebigs Ann. Chem.* **1934**, 513, 156–179.
- [2] (a) Rohlad, W.; Wuest, H.; Sasse, H. J. (Badische Anilin- & Soda-Fabrik A.-G.), **1963**, GB920851. (b) Bohler, H.; Kehrer, F. (Sandoz Ltd.) **1965**, CH386029.
- [3] Wakimoto, T. (Pioneer Electronic Corp., Japan) *Jpn. Kokai Tokkyo Koho* **1999**, JP11054279.
- [4] Sharghi, H.; Tamaddon, F.; Eshghi, H. *Iran. J. Chem. & Chem. Eng.* **2000**, 19, 32–36.
- [5] (a) Ref 1. (b) Singh, T.; Bedi, S. N. *J. Indian Chem. Soc.* **1957**, 34, 321–323.

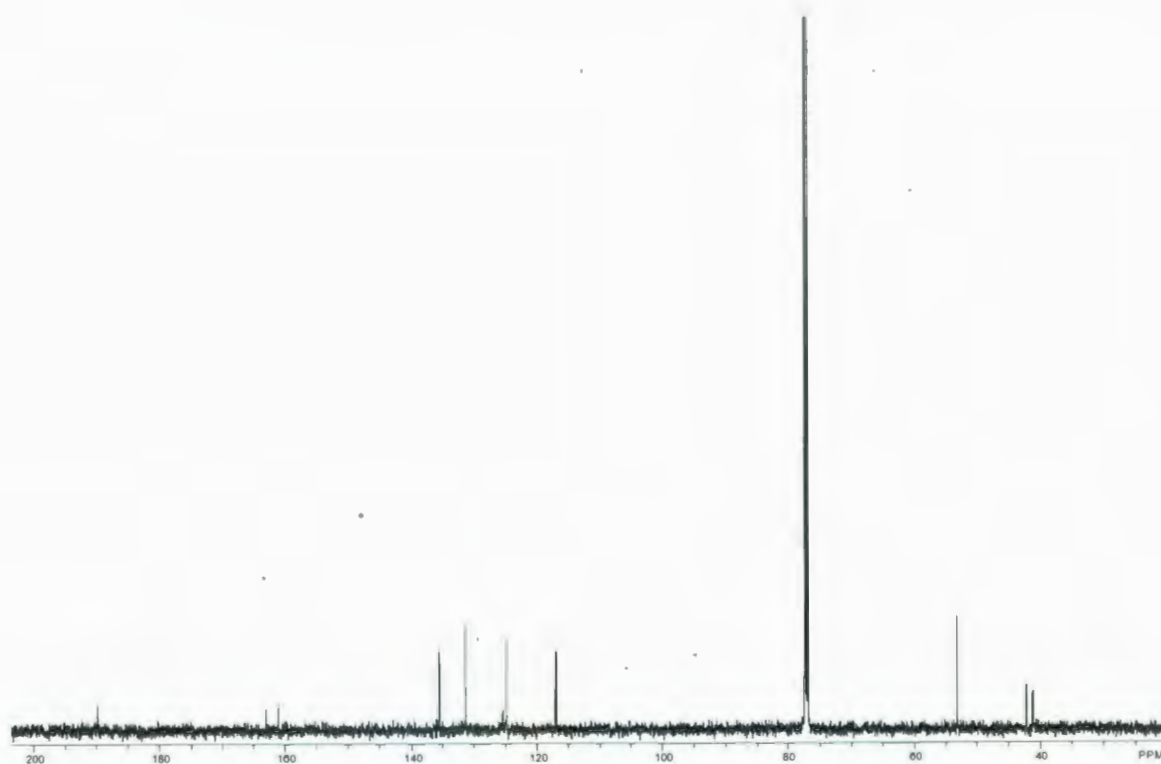
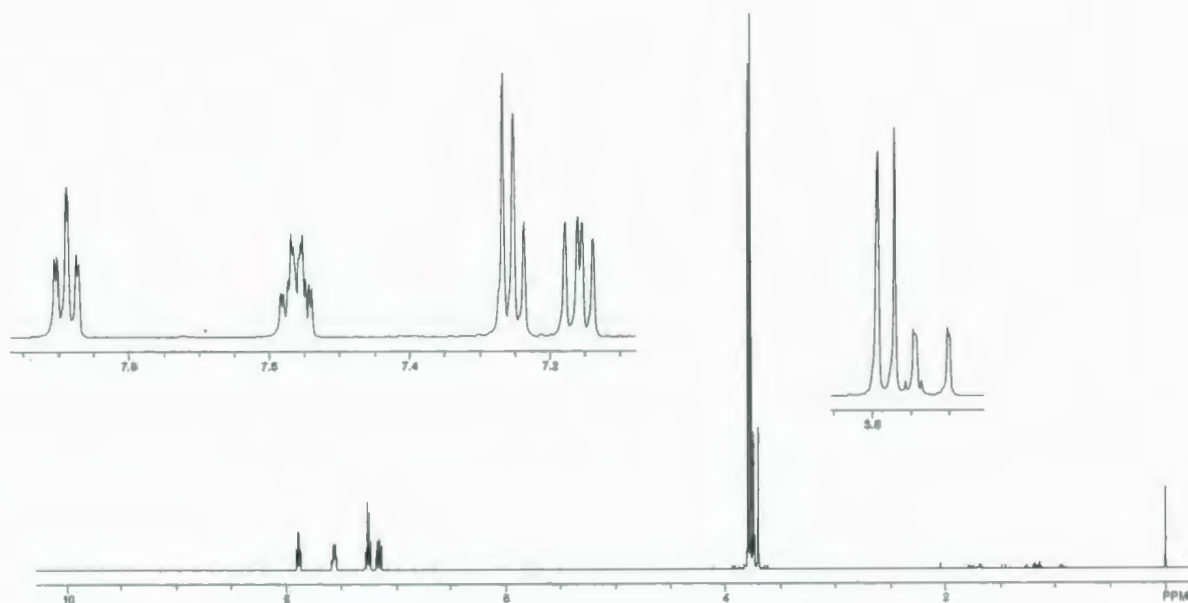
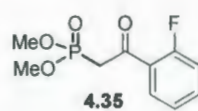
- 
- [6] A review: Tsukanov, A. V.; Dubonosov, A. D.; Bren, V. A.; Minkin, V. I. *Chem. Heterocycl. Compd.* **2008**, *44*, 899–923.
- [7] “Ionophore is any of a group of organic compounds that form a complex with an ion and transport it across a membrane” (definition from Medicinal dictionary).
- [8] (a) For **4.15**, see: Xia, W.-S.; Schmehl, R. H.; Li, C.-J.; Mague, J. T.; Luo, C.-P.; Guldi, D. M. *J. Phys. Chem. B* **2002**, *106*, 833–843. (b) For **4.16**, see: Chen, C.-T.; Huang, W.-P. *J. Am. Chem. Soc.* **2002**, *124*, 6246–6247. (c) For **4.17**, see: Yoon, S.; Albers, A.; Wong, A. P.; Chang, C. J. *J. Am. Chem. Soc.* **2005**, *127*, 16030–16031.
- [9] Montalti, M.; Prodi, L.; Zaccheroni, N. *J. Fluores.* **2000**, *10*, 71–76.
- [10] Hernández, J.V.; Muñiz, F. M.; Oliva, A. I.; Simón, L.; Pérez, E.; Morán, J. R. *Tetrahedron Lett.* **2003**, *44*, 6983–6985.
- [11] Dang, A.-T.; Miller, D. O.; Dawe, L. N.; Bodwell, G. J. *Org. Lett.* **2008**, *10*, 233–236.
- [12] Procedure was modified from literature: González-Morales, A.; Díaz-Coutiño, D.; Fernández-Zertuche, M.; García-Barradas, O.; Ordóñez, M. *Tetrahedron: Asymmetry* **2004**, *15*, 457–463.
- [13] (a) Wuts, P. G. M.; Greene, T. W. *Greene’s Protective Group in Organic Synthesis*, Fourth Edition, John Wiley & Sons, Inc., Hoboken, New Jersey, 2007, pp. 374. (b) Bernard, A. M.; Ghiani, M. R.; Piras, P. P.; Rivoldini, A. *Synthesis* **1989**, 287–289.
- [14] Bongers, K. M.; van den Berg, R. J. B. H. N.; Heitman, L. H.; IJzerman, A. P.; Oosterom, J.; Timmers, C. M.; Overkleeft, H. S.; van der Marel, G. A. *Bioorg. Med. Chem.* **2007**, *15*, 4841–4856.

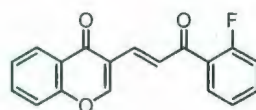
- 
- [15] Tang, D. H.; Fan, Q. H. *J. Chem. Res. (S)*, **2003**, 698–699.
- [16] Mills, O. S.; Mooney, N. J.; Robinson, P. M.; Watt, C. I. F.; Co, B. G. *J. Chem. Soc. Perkin Trans 2*, **1995**, 4, 697–706.
- [17] Cox, B. G.; Hurwood, T. V.; Prodi, L.; Montalti, M.; Bolletta, F.; Watt, C. I. F. *J. Chem. Soc. Perkin Trans 2*, **1999**, 2, 289–296.
- [18] SPARTAN '08 software from Wavefunction, Inc. Irvine, CA, USA.
- [19] (a) Kawaguchi, K.; Nakano, K.; Nozaki, K. *J. Org. Chem.* **2007**, 72, 5119–5128. (b) Kawaguchi, K.; Nakano, K.; Nozaki, K. *Org. Lett.* **2008**, 10, 1199–1202.
- [20] Anjaneyulu, A. S. R.; Mallavadhani, U. V.; Venkateswarlu, Y.; Prasad, A. V. R. *Indian J. Chem. Sec. B* **1987**, 26B, 823–826.
- [21] Mallaiah, B. V.; Srimannarayana, G. *Indian J. Chem. Sec. B* **1982**, 21B, 975–976.
- [22] (a) For **4.54**, see: Zofia, D. S.; Dulewicz, E.; Brycki, B.; *ARKIVOC* **2007**, (vi) 90–102. (b) For **4.55**: following the standard procedure for preparing HWE phosphonates in Chapter 2.
- [23] The work described in this section was carried out by the author at the University of Mainz in the laboratory of Prof. B. Witulski.
- [24] Wariishi, K.; Morishima, S.; Inagaki, Y. *Org. Proc. Res. Develp.* **2003**, 7, 98–100
- [25] For all known compounds, a literature citation is given after the compound name. In all cases, the spectroscopic data is consistent with published data.

## **Appendix**

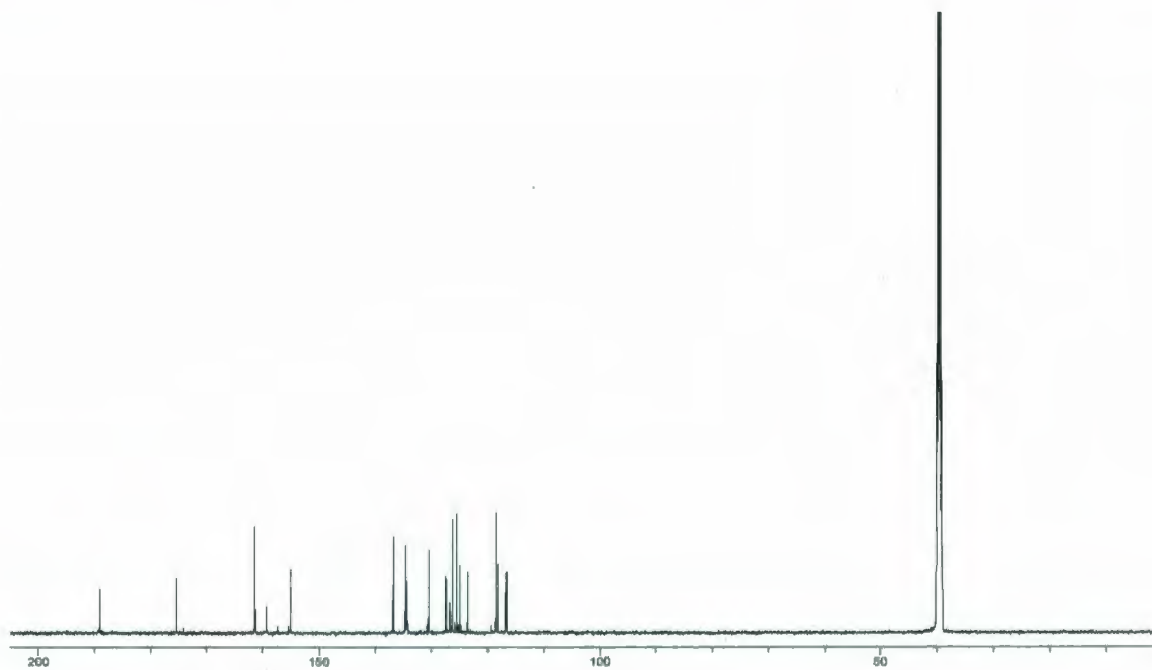
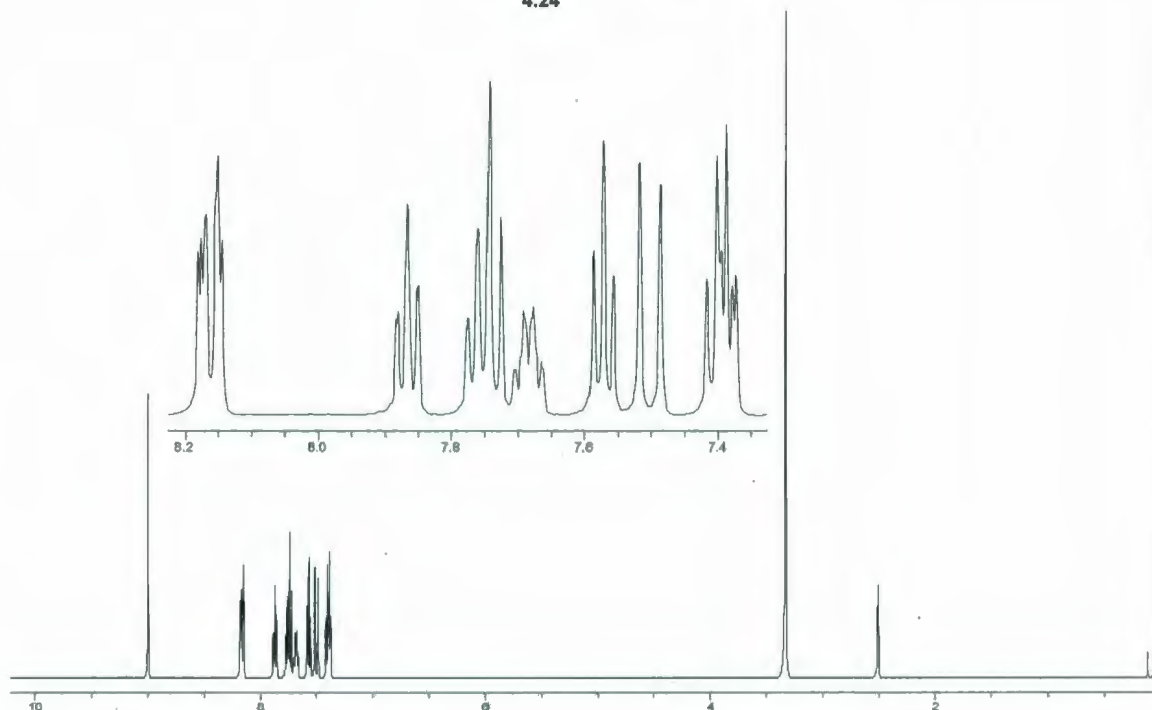
Selected NMR spectra for synthesized compounds

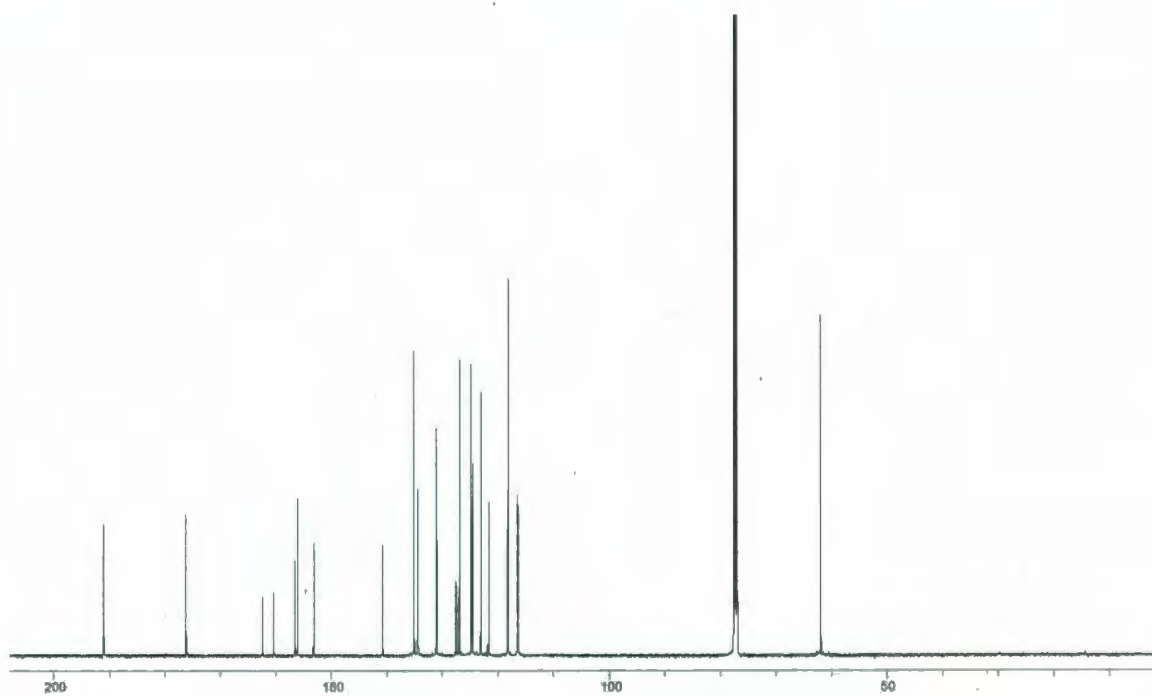
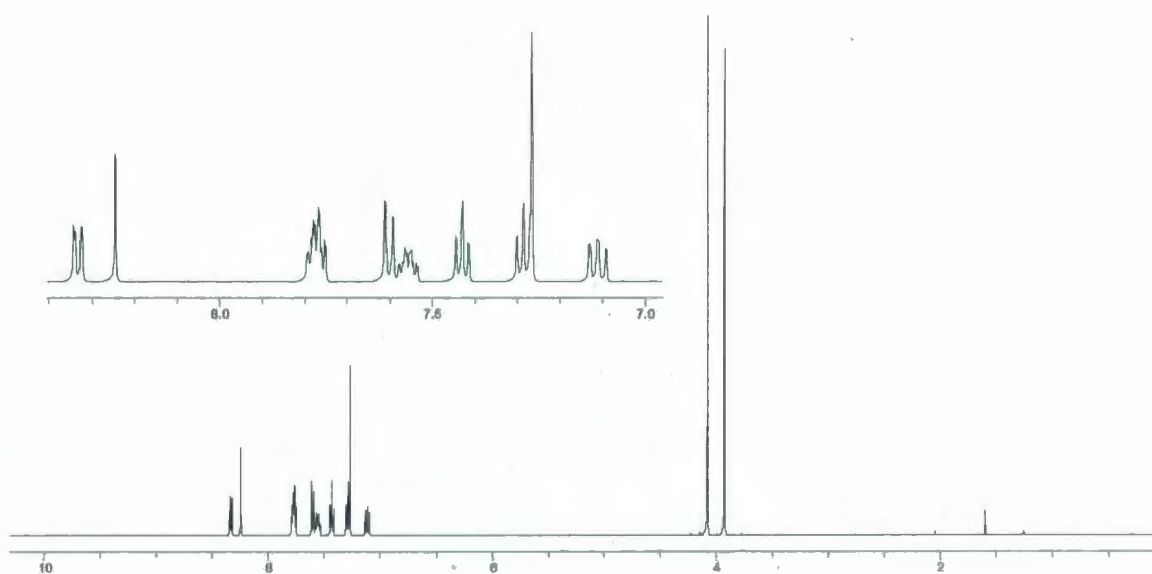
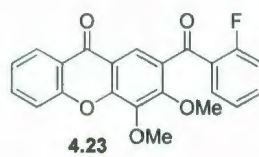


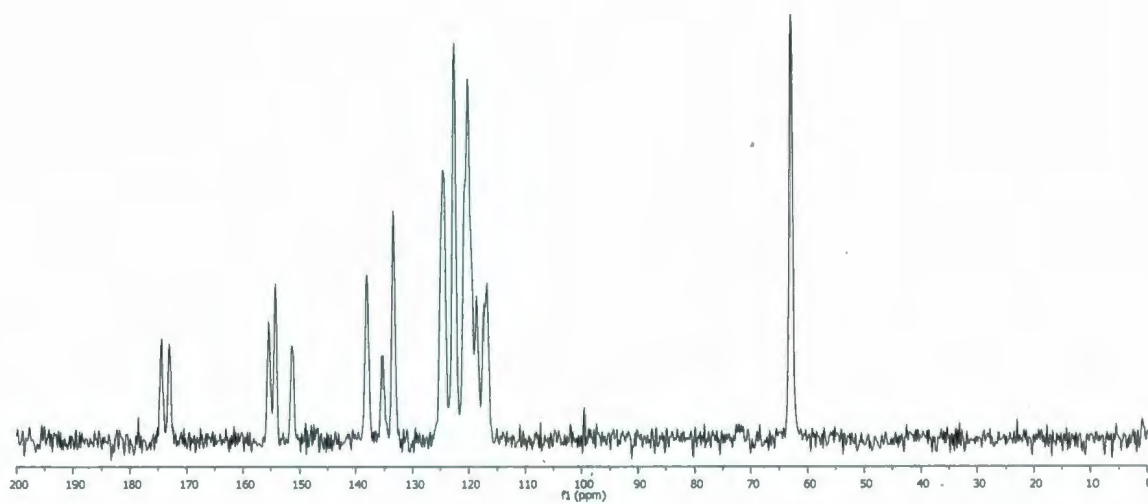
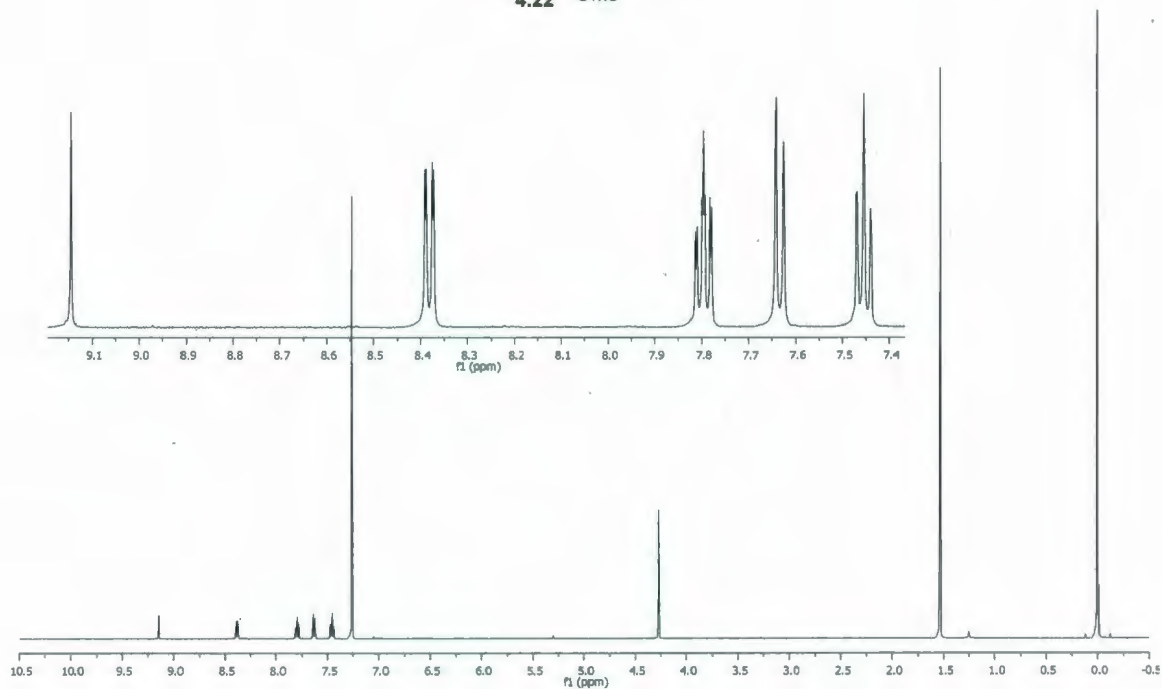
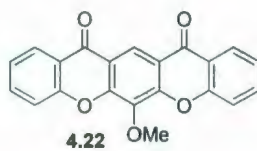




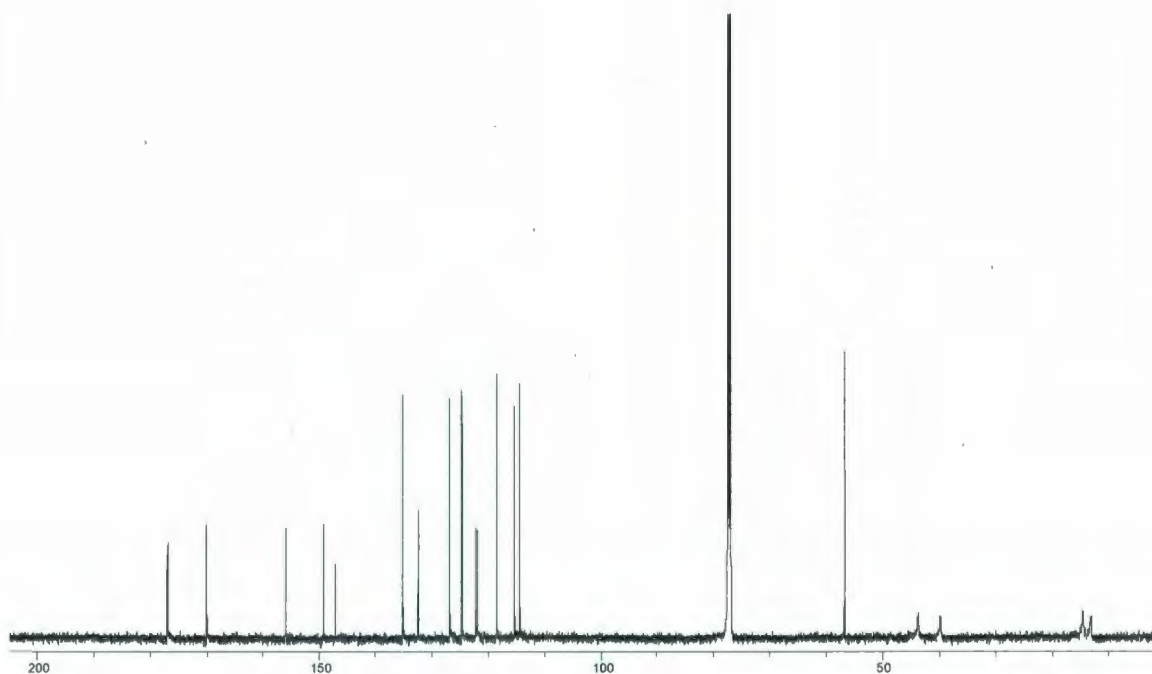
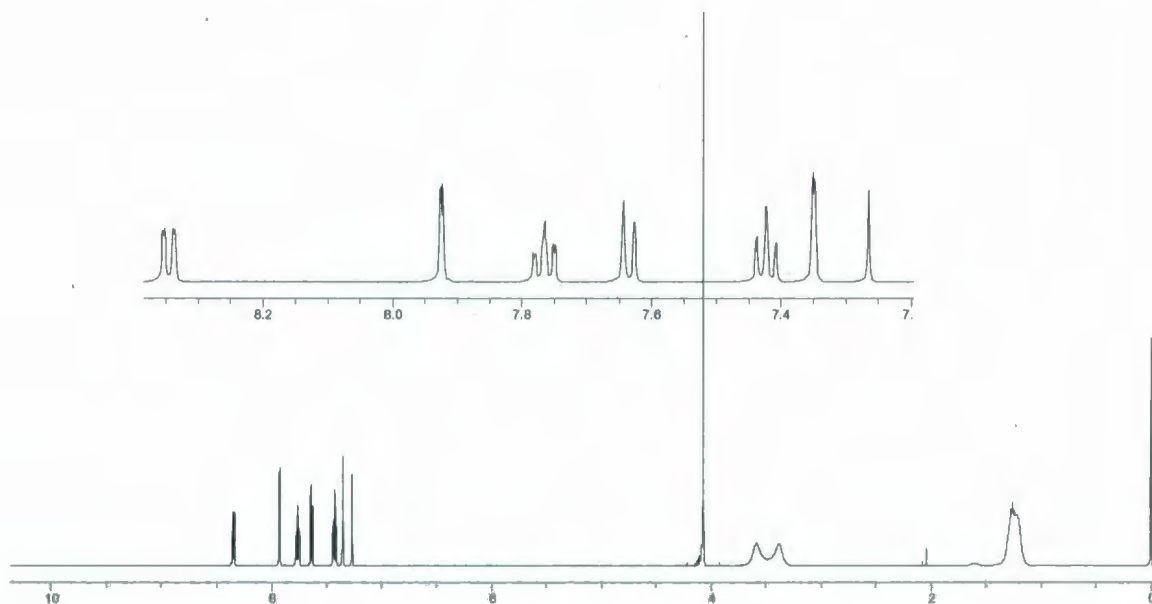
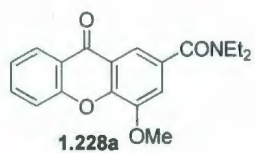
4.24

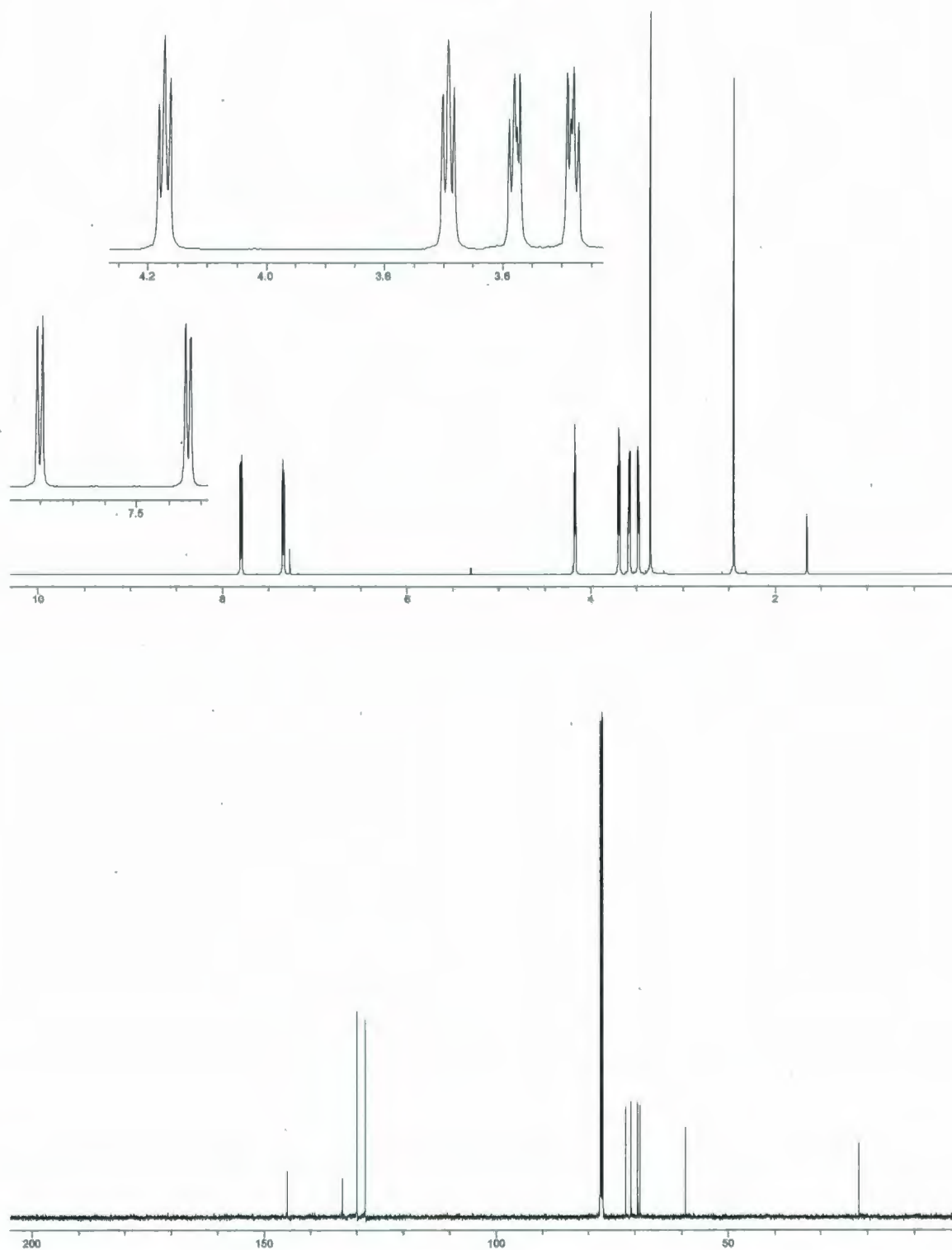
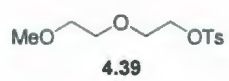




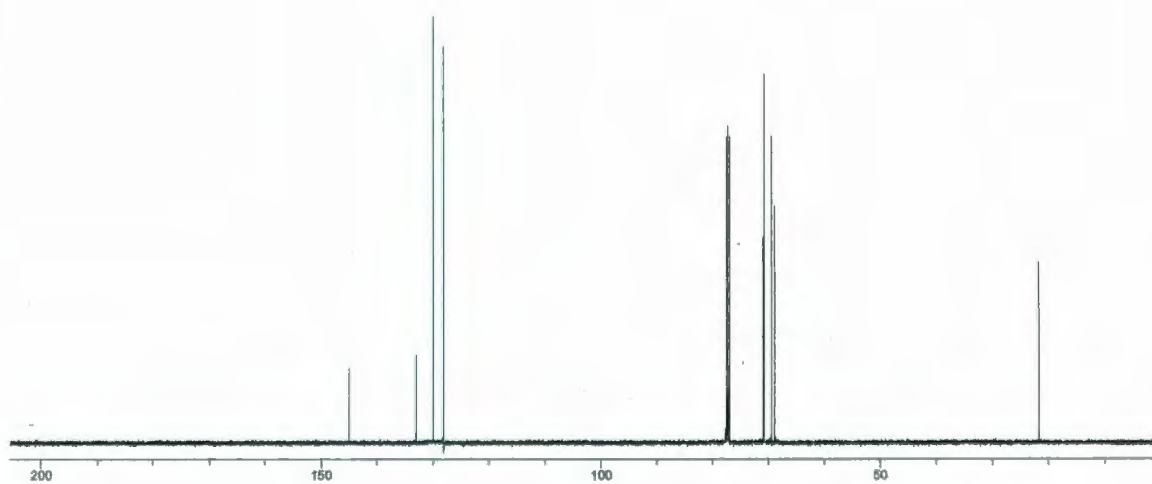
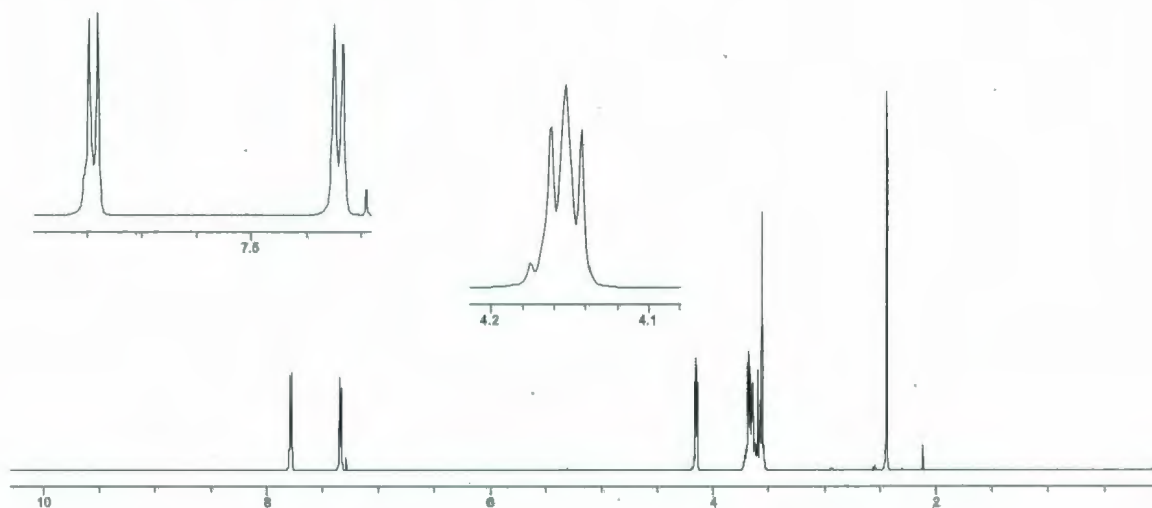
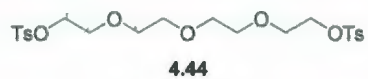




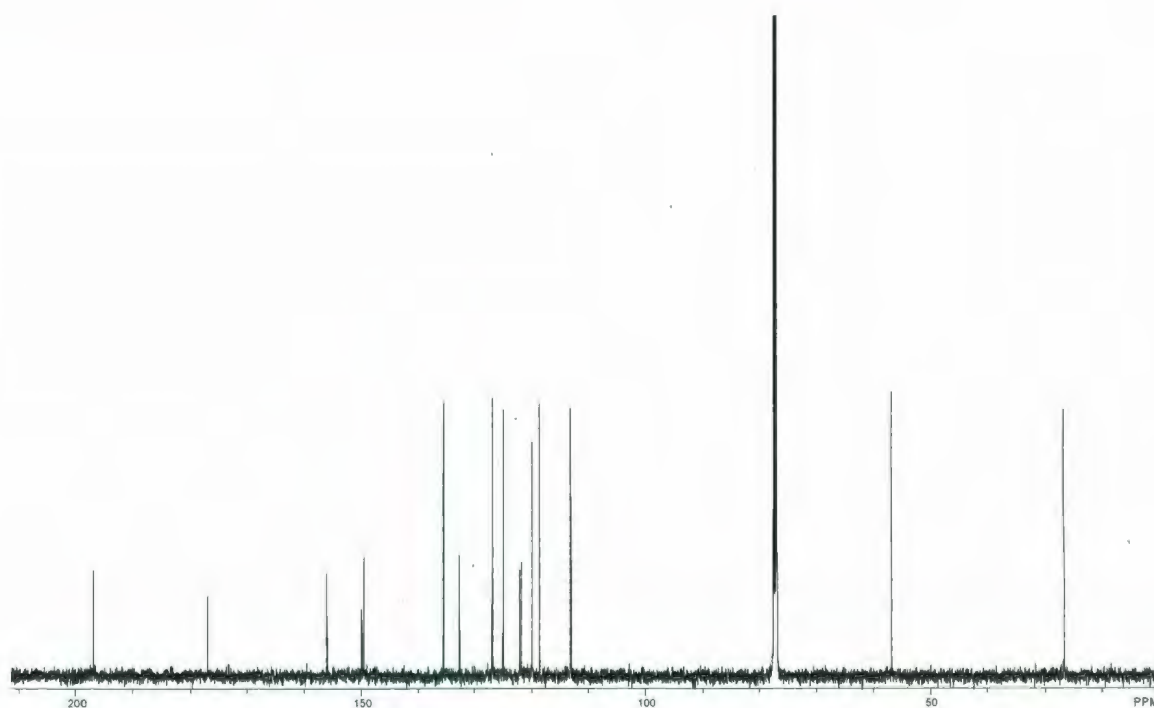
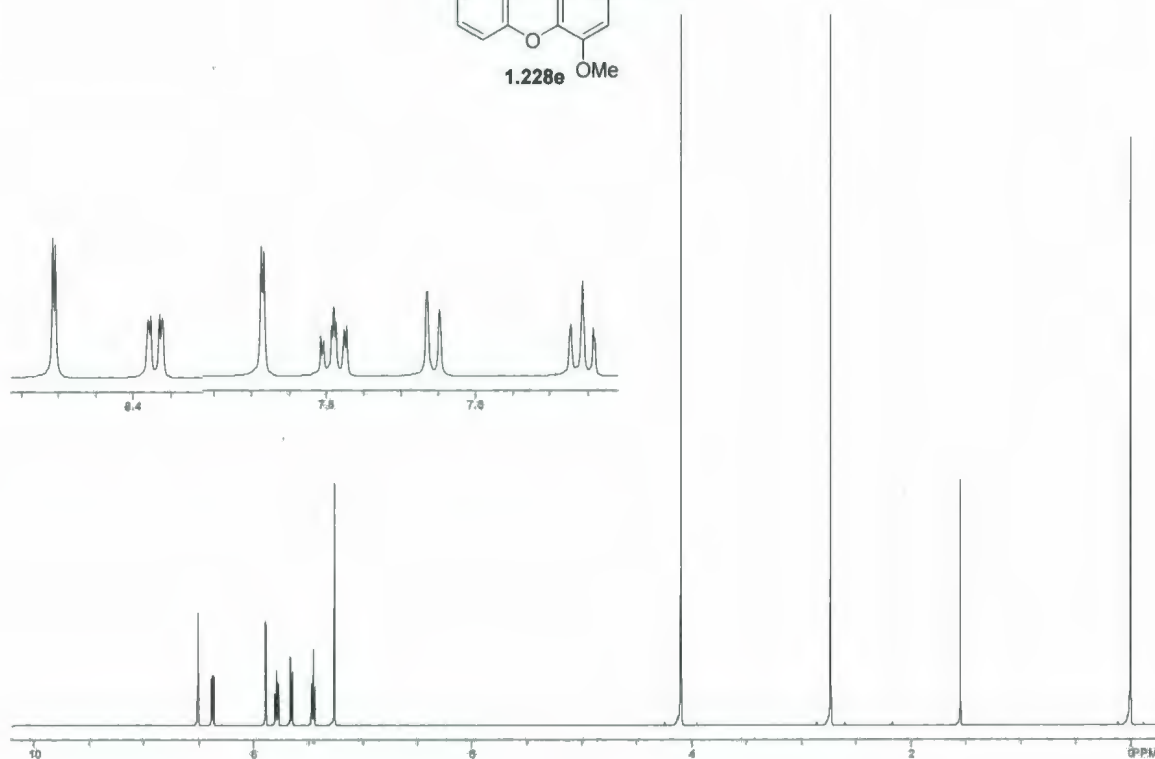
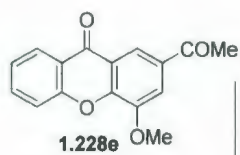


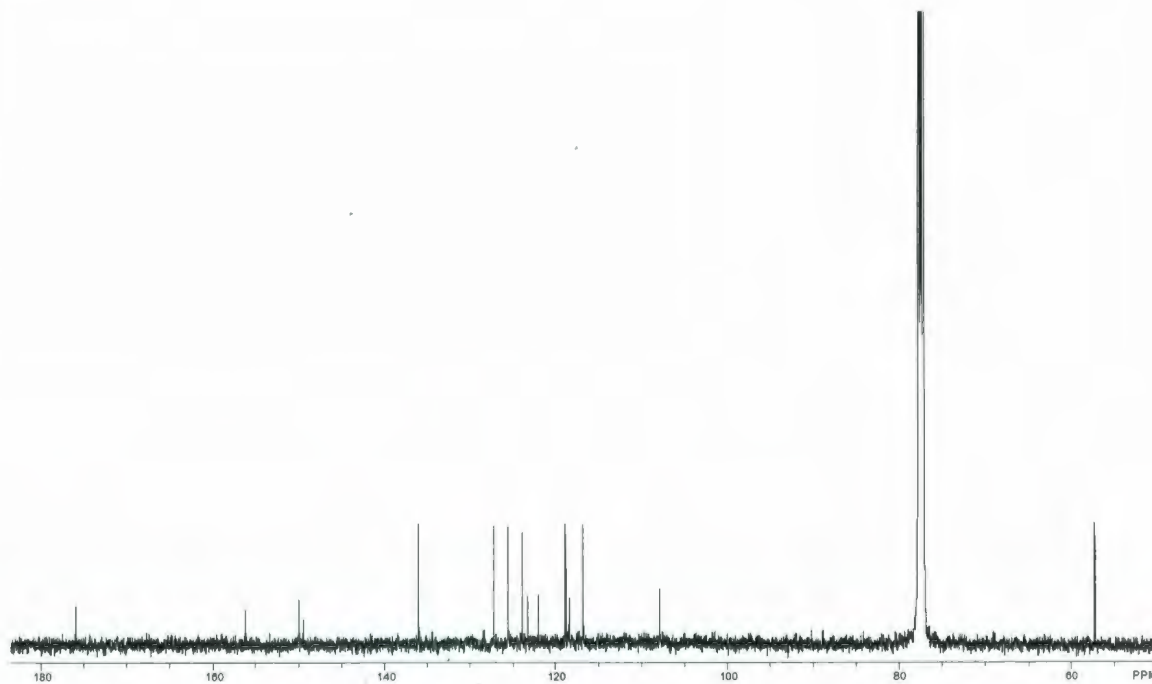
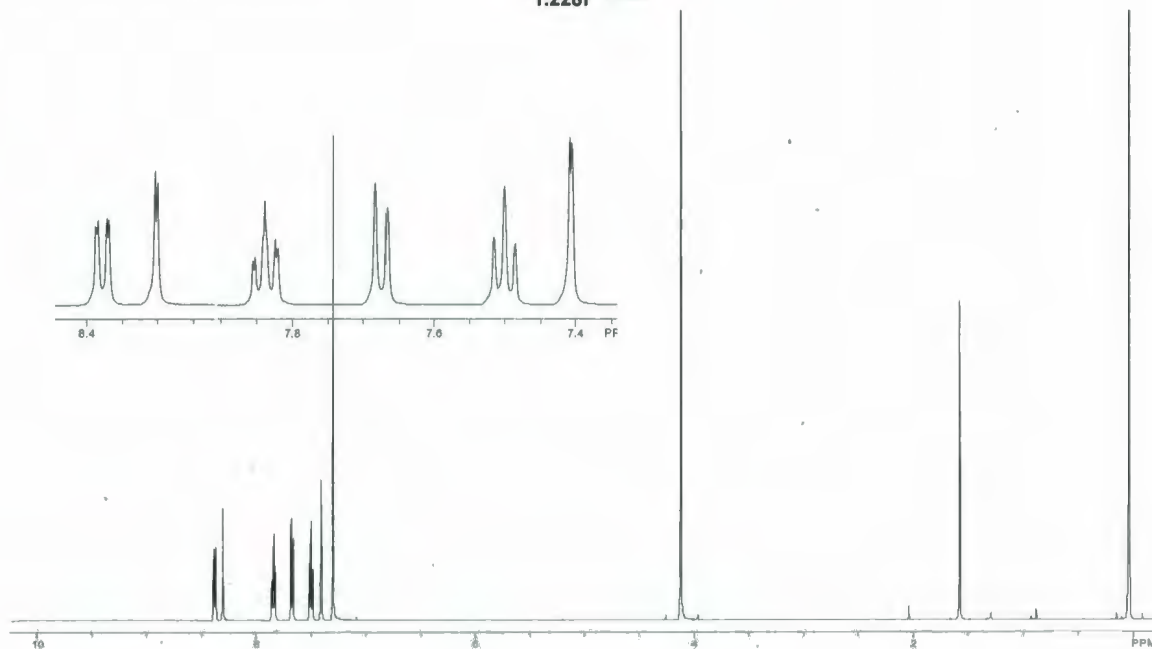
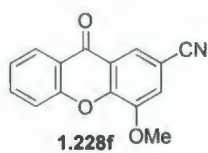


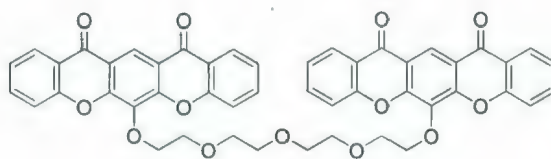




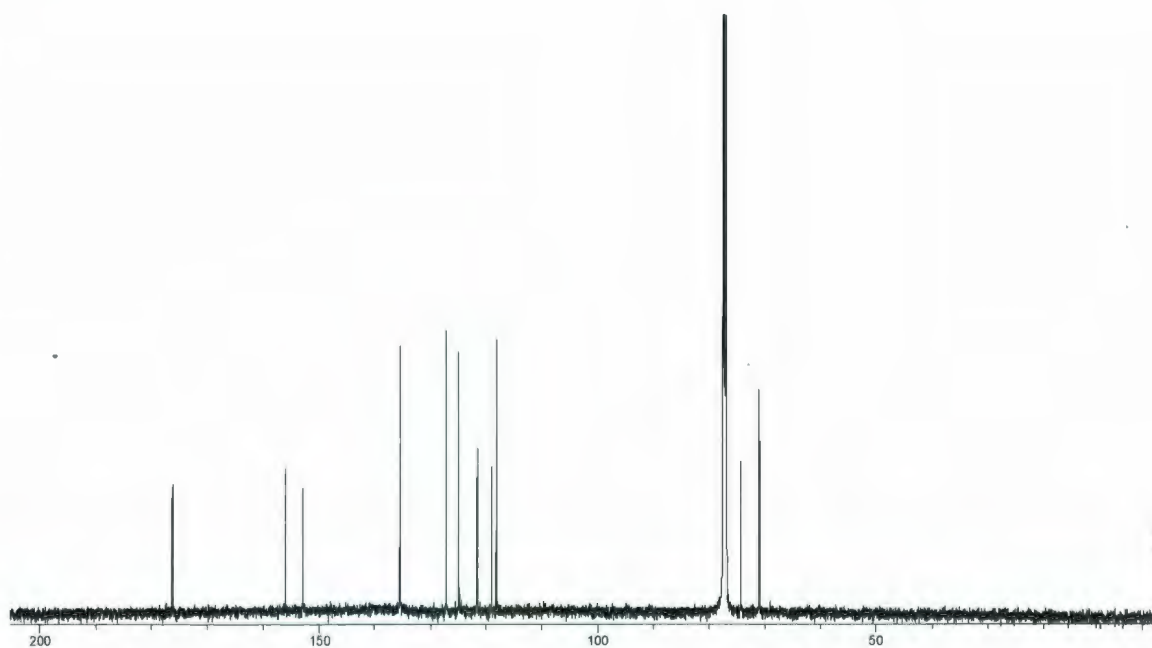
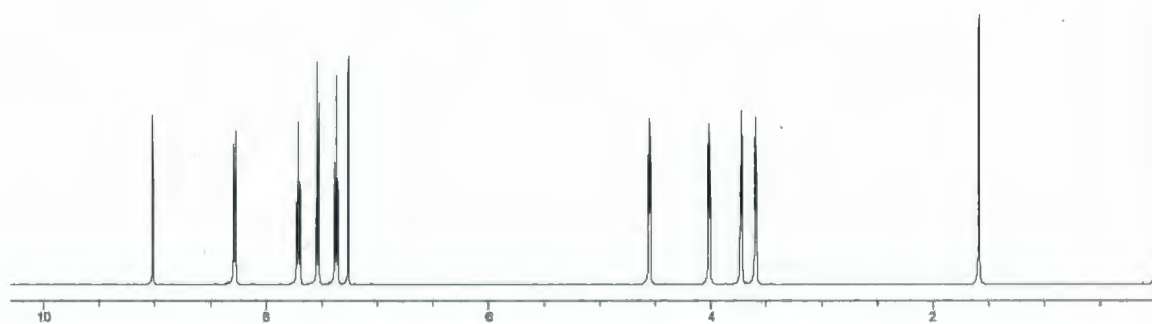
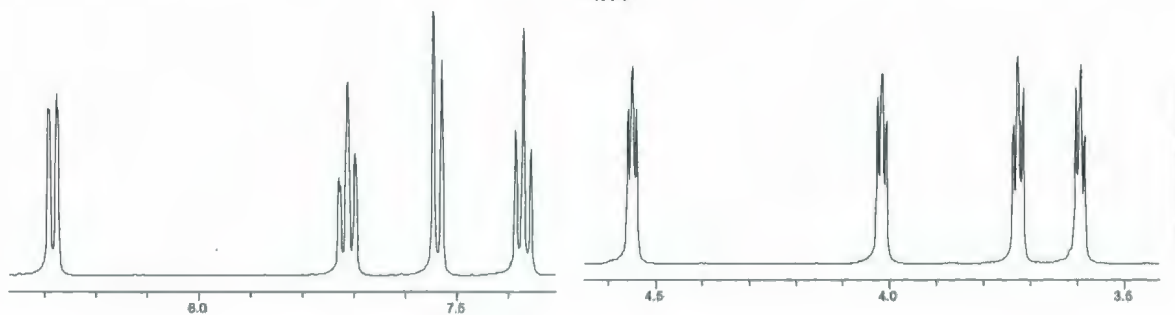


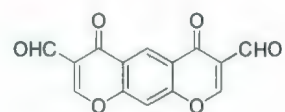




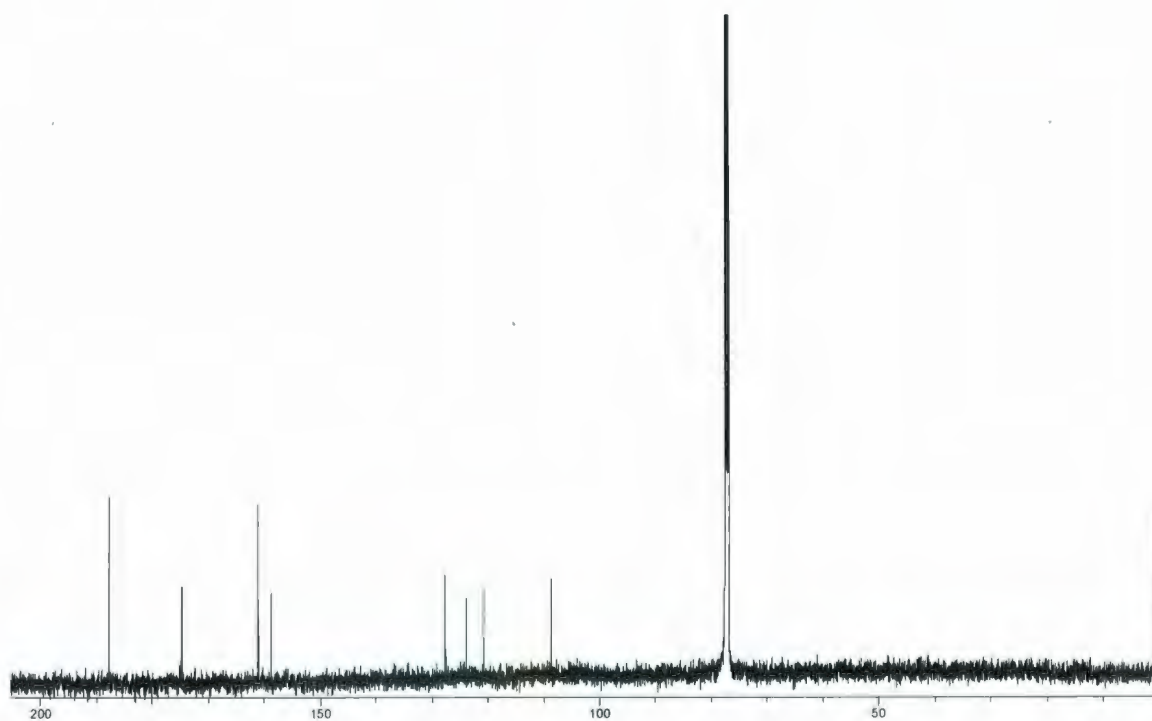
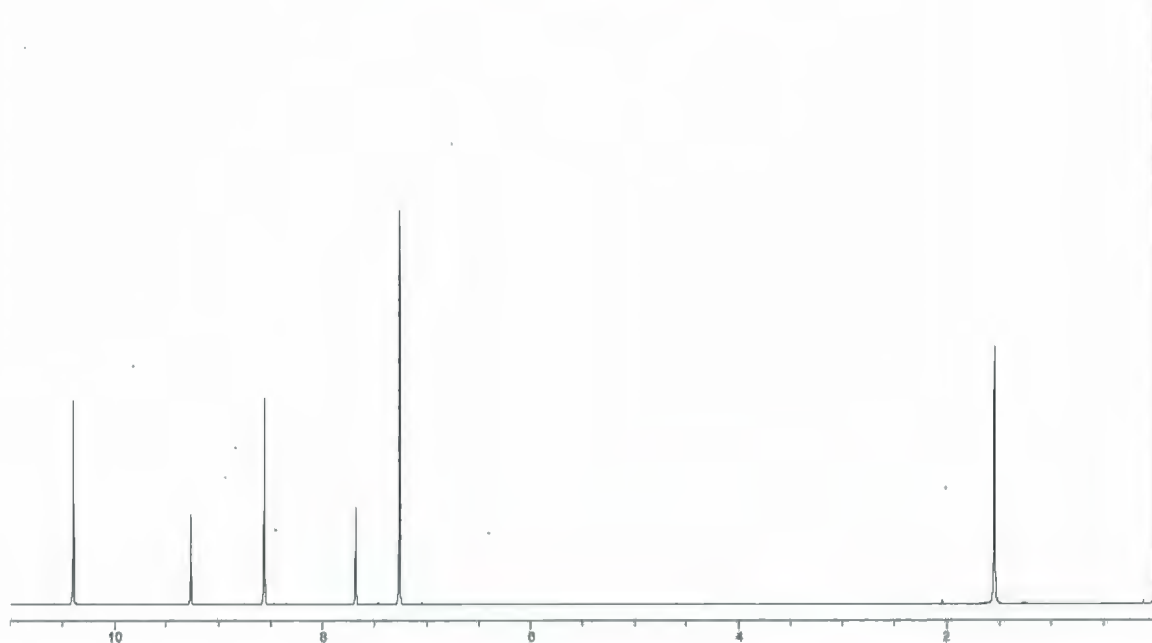


4.14

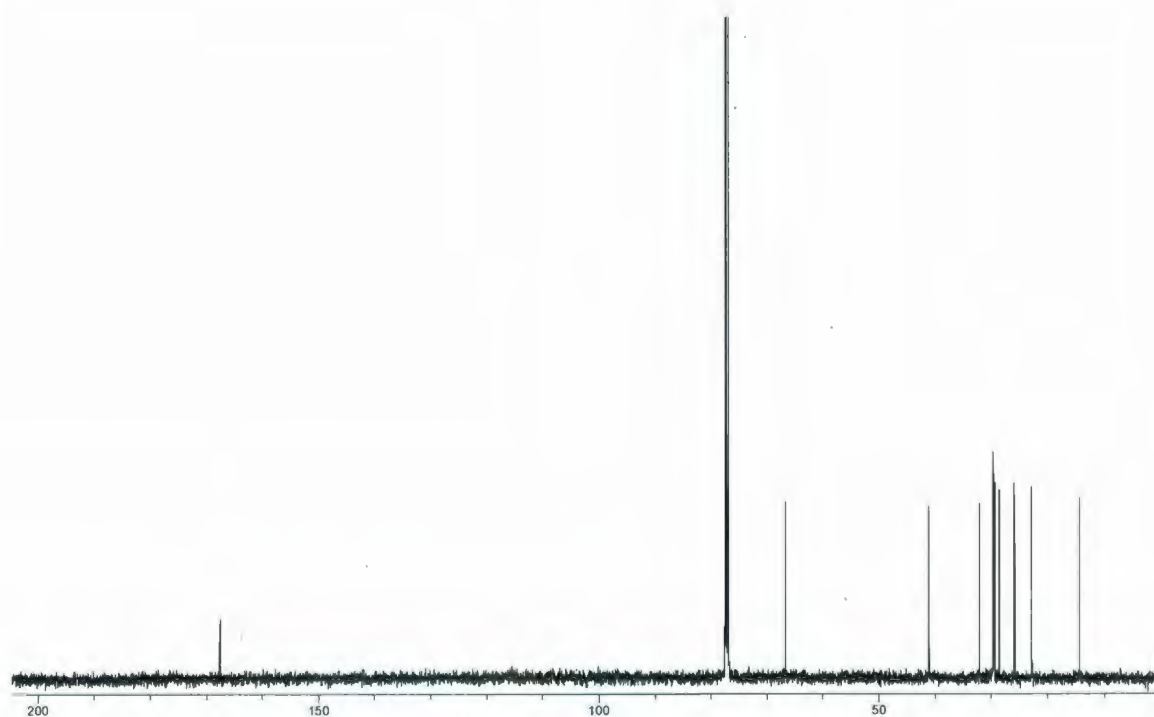
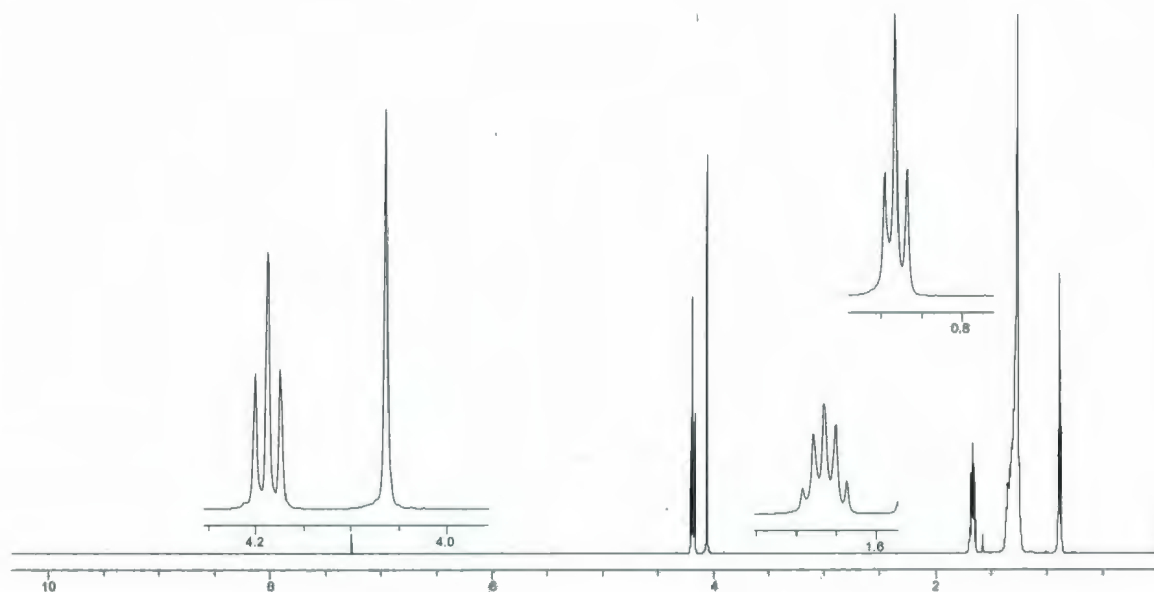
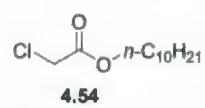


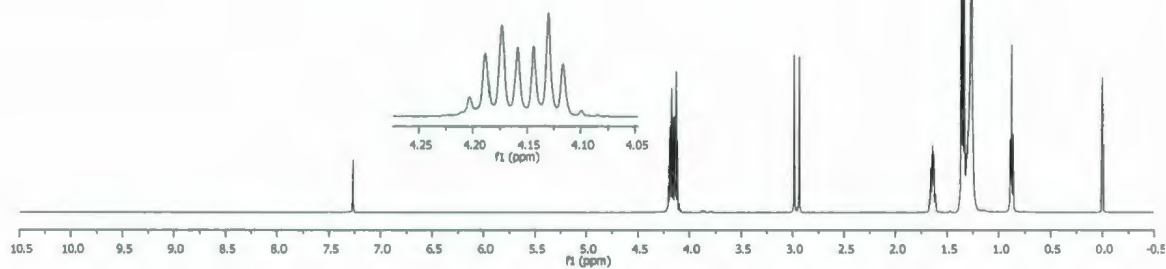
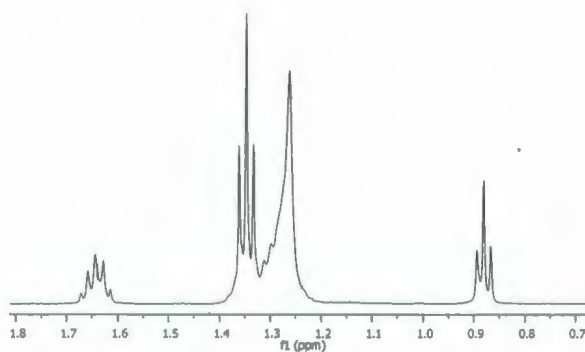


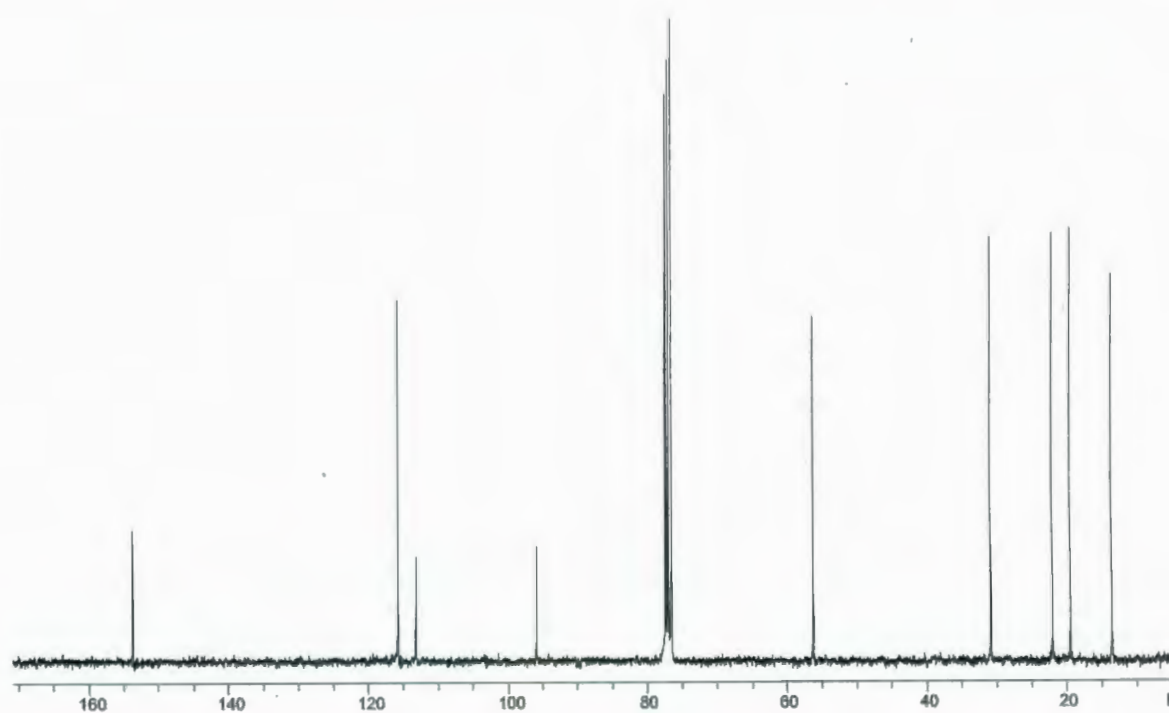
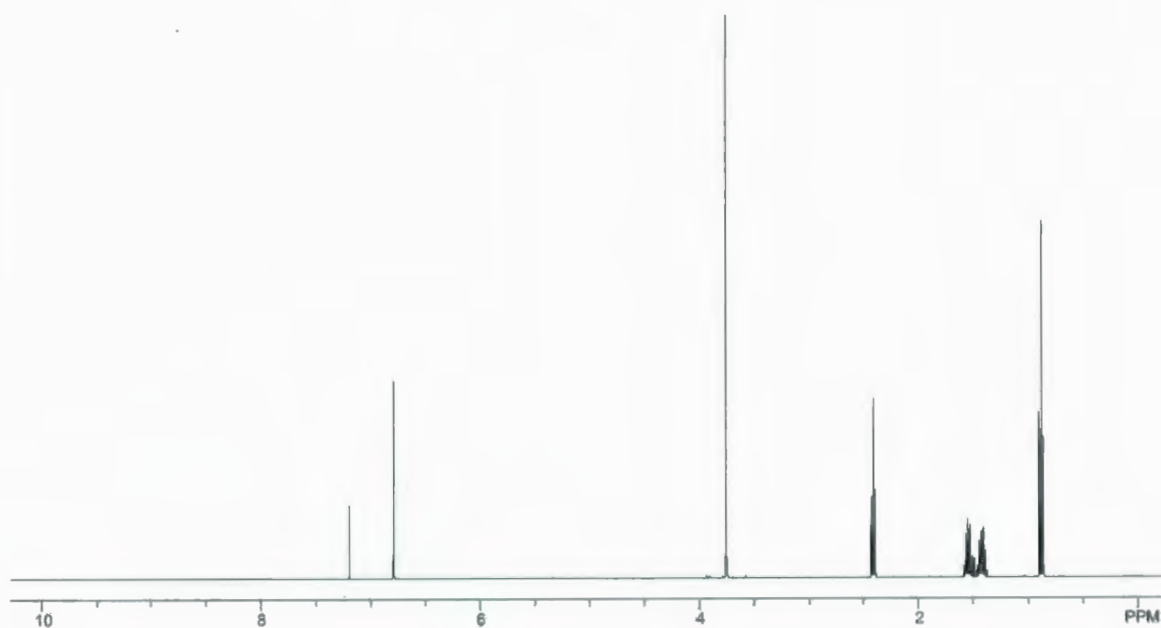
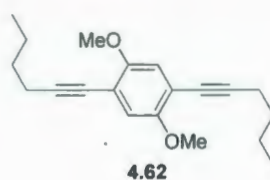
4.27

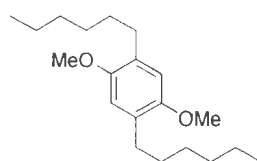




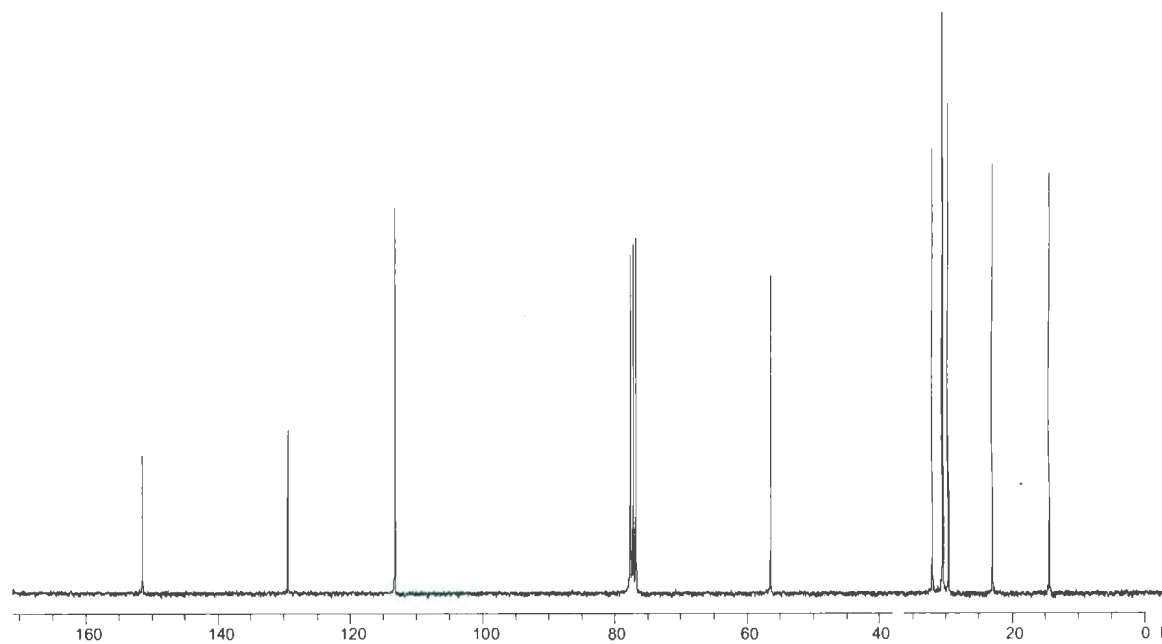
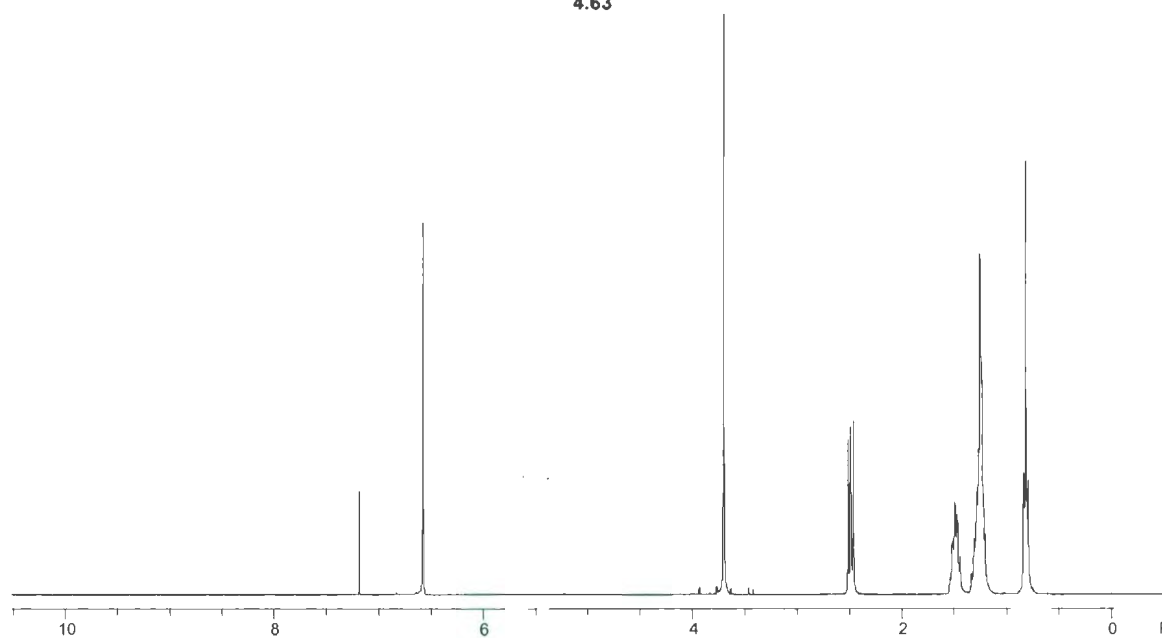




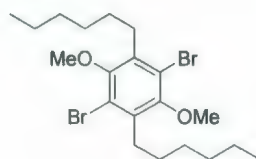




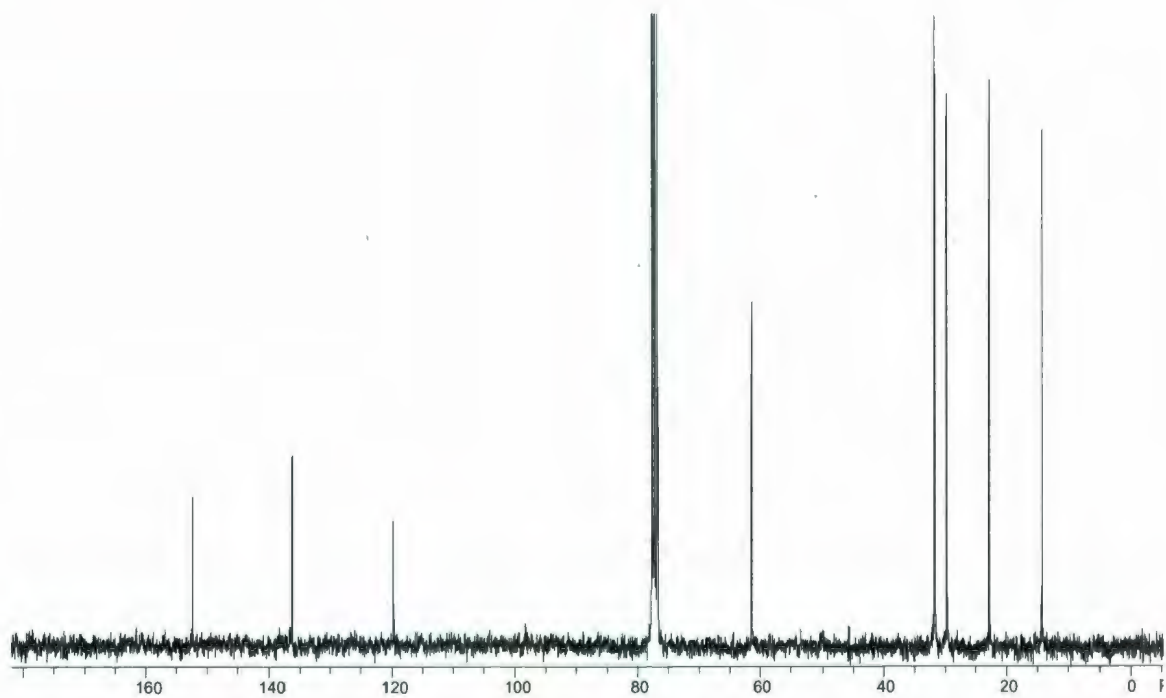
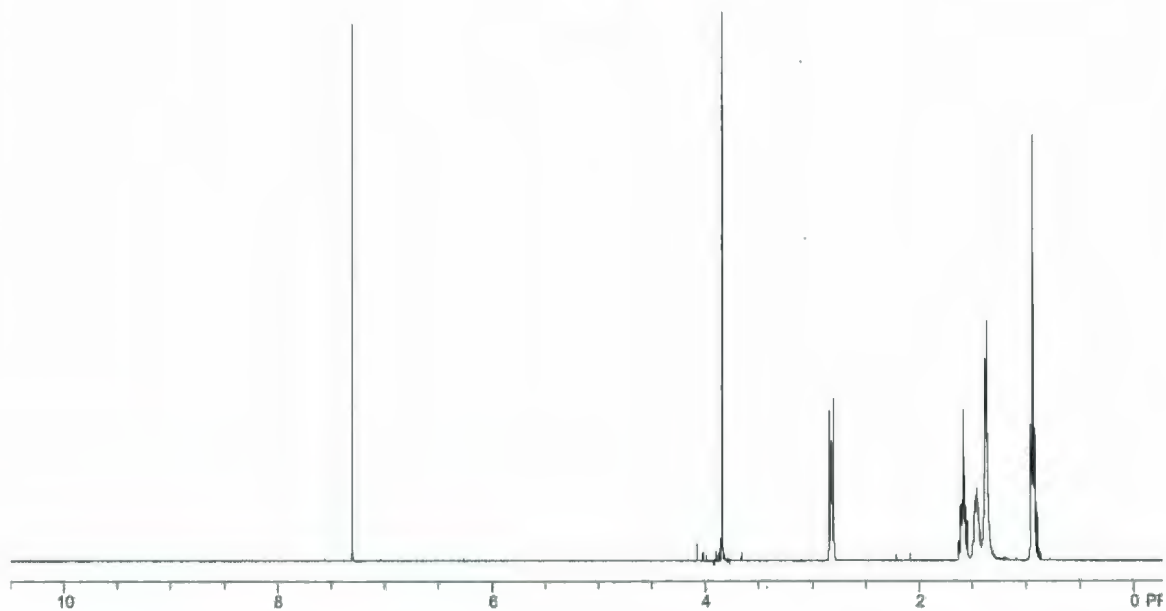
4.63







4.64



## Chapter 5

### Synthesis and Physical Properties of New Donor-Acceptor Xanthone-Carbazole Hybrid Systems

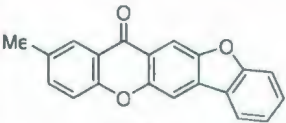
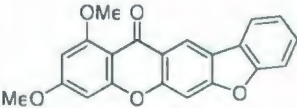
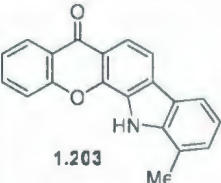
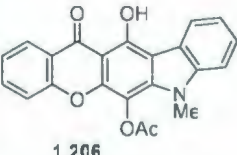
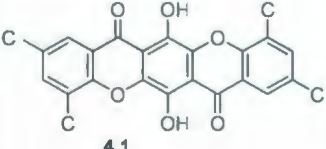
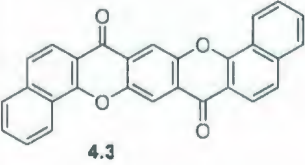
#### 5.1 Introduction

Xanthone-based compounds such as benzofuroxanthenes **1.192**, **1.198** (Entry 1, Table 5.1),<sup>1</sup> indoloxanthenes **1.203**, **1.206** (Entry 2, Table 5.1),<sup>2</sup> or chromonoxanthenes **4.1**, **4.3** (Entry 3, Table 5.1)<sup>3</sup> were synthesized by others for the study of their pharmaceutical properties (see Chapter 1, pages 40–45). A few studies on the physical properties of the latter two classes of xanthone-based compounds were carried out,<sup>4</sup> in which only the chromonoxanthenes, were reported to have potential applications as pigment dyes and in organic electroluminescent devices.<sup>5</sup> Although these xanthone-based compounds fall under the heading category of heteroacenes, which are currently a hotbed for the discovery of new compounds with potential applications in electronic and optoelectronic devices,<sup>6</sup> they have not been revisited, even just for methodology development, since the year 2001.

On the other hand, carbazole-based compounds have been explored to a much greater extent and continue to garner interest because of their interesting physical properties. There are three known types of carbazole-based compounds: (1) carbazole-fused heteroaromatic systems such as **1.186**,<sup>7</sup> **5.1**,<sup>8</sup> **5.2**<sup>9</sup> (Entry 1, Table 5.2); (2) carbazole-linked  $\pi$ -systems such as **5.3**<sup>10</sup> (Entry 2, Table 5.2); and (3) carbazole-linked acceptor units such as **5.4**,<sup>11</sup> **5.5**<sup>12</sup> (Entry 3, Table 5.2). Carbazole itself is known for its

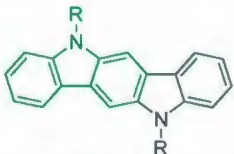
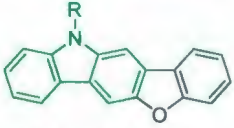
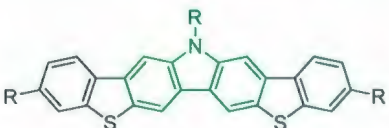
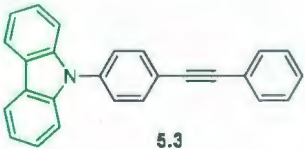
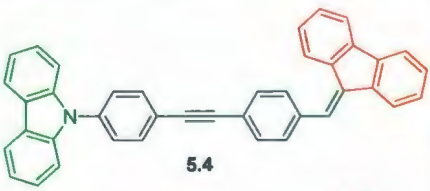
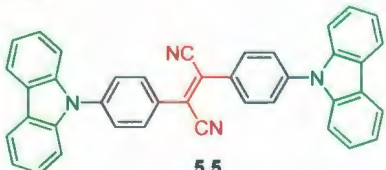
intense luminescence<sup>13</sup> and electron-donor properties.<sup>11,12</sup> As such, the combination of the carbazole moiety with any of the three above-mentioned partners, *i.e.* heteroaromatic systems,  $\pi$ -systems, and acceptor units affords frameworks that may have applications in the following fields: organic light-emitting diodes (OLEDs), field-effect transistors (FETs), and organic photovoltaic cells (OPVs, so-called organic solar cells). In general, carbazole-based heteroacenes possesses planar and relatively rigid frameworks, which promise to enhance  $\pi$ -conjugation leading to intense luminescence and high charge carrier mobility. Therefore, they have potential applications in OLEDs and FETs. Carbazole-linked  $\pi$ -system compounds have been used mainly in OLEDs as blue, white, green, and red emitters.<sup>10</sup> Furthermore, carbazole-linked acceptor compounds, which are classified as donor-acceptor systems (so-called “push-pull” systems), have potential applications in both OLEDs and OPVs, as they exhibit high fluorescence quantum yields and good electron transport.

**Table 5.1** Xanthone-based compounds.

Entry	Compounds	Class	Potential properties	Potential applications
1	<p><b>Benzofuroxanthones</b></p>  <p>1.192</p>  <p>1.198</p>	heteroacenes	biological activity	therapeutics
2	<p><b>Indoloxanthones</b></p>  <p>1.203</p>  <p>1.206</p>	heteroacenes	biological activity	therapeutics
3	<p><b>Chromonoxanthones</b></p>  <p>4.1</p>  <p>4.3</p>	heteroacenes	biological activity luminescence	pigment dyes electroluminescent devices



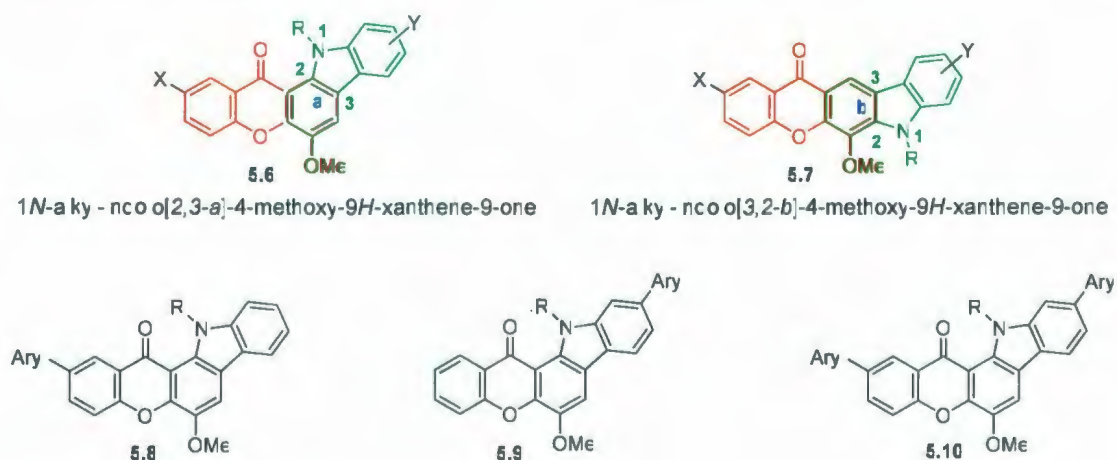
**Table 5.2** Carbazole-based compounds.

Entry	Compounds	Class	Potential properties	Potential applications
1	<p>Carbazole-fused heteroaromatics</p>  <p>1.186: R = <i>p</i>-octylphenyl</p>  <p>5.1: R = <i>p</i>-phenyl</p>  <p>5.2: R = <i>n</i>-C<sub>4</sub>H<sub>9</sub></p>	heteroacenes	luminescence, charge carrier ability	OLEDs FETs
2	<p>Carbazole-linked <math>\pi</math>-system</p>  <p>5.3</p>	light-emitting organic compounds	luminescence	OLEDs
3	<p>Carbazole-linked acceptor</p> <p><b>donor</b> — <b>linker</b> — <b>acceptor</b></p>  <p>5.4</p>  <p>5.5</p>	donor-acceptor system	luminescence electron transfer	OLEDs organic solar cells

From this brief overview of the properties of xanthone- and carbazole-based compounds, indoloxanthenes (from here on also referred to as xanthone-carbazole hybrid systems) may possess distinct properties and structural characteristics because they contain both xanthone and carbazole moieties. First, xanthone-carbazole hybrid compounds are expected to inherit properties from their “parents”, xanthone and carbazole, which may endow them with properties that are desirable both for pharmaceuticals and in electronic or optoelectronic devices. Second, xanthone-carbazole hybrid compounds are not only heteroacenes, but they are also unusual donor-acceptor systems, in which the carbazole donor is *fused* to the xanthone acceptor. This contrasts typical donor-acceptor systems, where the donor and acceptor units are connected via a linker, usually a  $\pi$ -system. The structures and physical properties of the very few known xanthone-carbazole hybrid systems (**1.203**, **1.206**) have not been studied with an eye toward applications in OLEDs, FETs, or OPVs. Thus, these promising systems were chosen as target structures.

Only two approaches for the synthesis of xanthone-carbazole systems have been reported.<sup>2</sup> In both cases, the xanthone moiety was introduced via “ring B construction” or “ring C construction”, while the carbazole or indole moieties were present in the starting materials (Chapter 1, page 43). As such, the development of new approaches to xanthone-carbazole hybrid systems would be advantageous, not just for the sake of methodology development, but also to allow for broader scope in the synthesis of this class of compounds.

Thus, the aims of this research were (1) to synthesize new xanthone-carbazole hybrid systems such as **5.6**, **5.7** (Figure 5.1) employing the IEDDA-based methodology described in Chapter 2; (2) to study their physical properties (absorption, emission, aggregation and electrochemistry) and (3) to extend the molecular framework to aryl-substituted xanthone-carbazole systems such as **5.8–5.10** and study their physical properties.



**Figure 5.1** Target structures and IUPAC names.

The IUPAC names of these compounds based on an indole moiety fused to a xanthone skeleton are shown in Figure 5.1. However, to highlight the unique features and properties of the systems containing fused xanthone and carbazole units, a common name for the target structures, *i.e.* “xanthone-carbazole hybrid systems”, is used in this Chapter.

## 5.2 Synthetic Approach to Xanthone-Carbazole Hybrid Systems

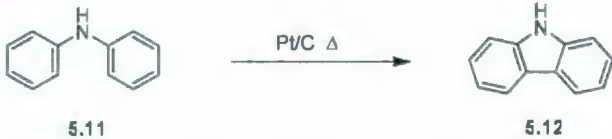
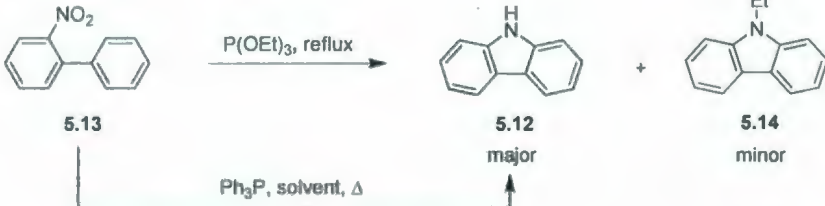
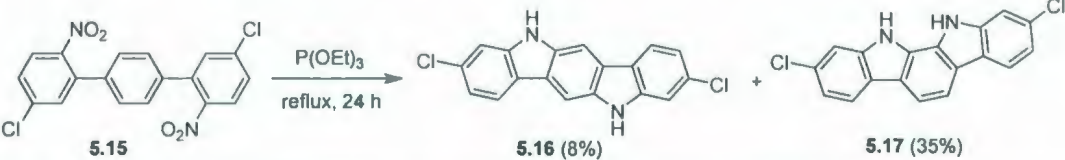
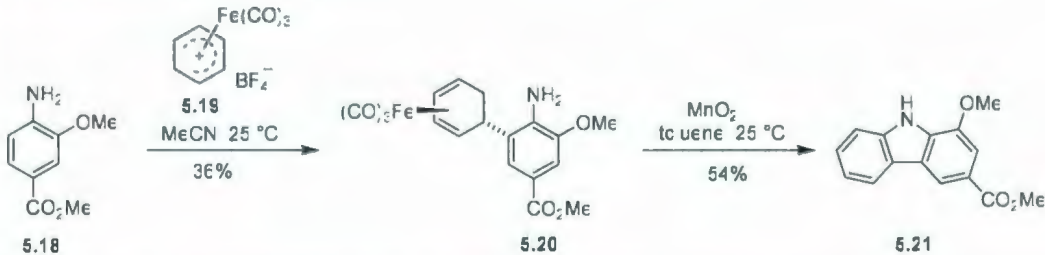
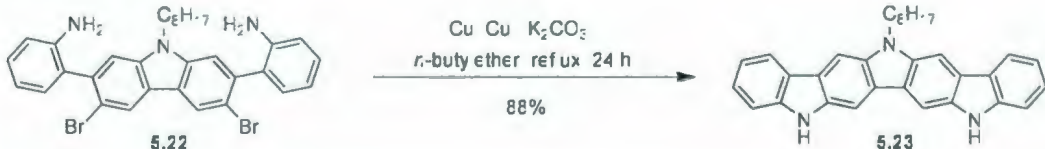
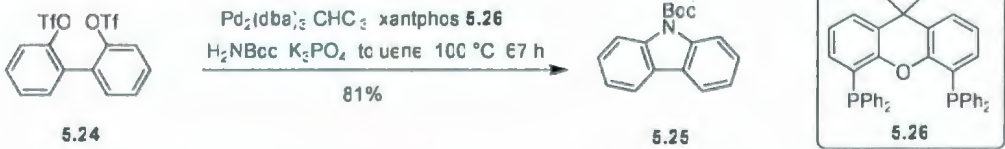
The synthetic approach to xanthone-carbazole hybrid systems revolved around the construction of the two key parts: the xanthone system and the carbazole system. For



xanthone construction, the IEDDA strategy, the development of which was described in Chapter 2, was employed. Several approaches to the carbazole framework have been reported. One of the earliest syntheses of carbazole (**5.12**), which was published in 1926, involved a cyclodehydrogenation of diphenylamine (**5.11**) in the vapor phase over a Pt/C catalyst (Entry 1, Table 5.3).<sup>14</sup> The improvement of this method was realised by changing the catalyst to platinum supported on silica or alumina,<sup>15</sup> or on magnesium oxide.<sup>16</sup> However, the highest yield of carbazole (**5.12**) was only 10% for the Pt/MgO catalyst. Cadogan *et al.* discovered that *o*-nitrobiaryl compounds reacted with triphenylphosphite at reflux (this reaction was later named the Cadogan reaction) to give carbazole (**5.12**) in good yield (83%) (Entry 2, Table 5.3).<sup>17</sup> However, later investigations in this reaction found that the desired carbazole was often contaminated with an *N*-ethylated product **5.14**, which resulted from an alkyl transfer to the product either directly from P(OEt)<sub>3</sub> or, more likely, from the triethyl phosphate byproduct of the reaction.<sup>18</sup> To prevent the formation of this unwanted product, a modification of the Cadogan reaction that employs triphenylphosphite instead of triethylphosphite was developed.<sup>18a</sup> Optimal yields of carbazoles were obtained in the range of 67–99%, depending on what substituents were present. The disadvantages of this modification are the choice of a suitable solvent for the reaction and the difficulty in separating the byproduct P(O)(OPh)<sub>3</sub> from the polar carbazole products. Therefore, the original Cadogan reaction is still employed for the synthesis of larger carbazole systems.<sup>19</sup> However, this reaction is not very regioselective and, where possible, gives mixtures of products, *e.g.* **5.16** and **5.17** (Entry 2, Table 5.3).

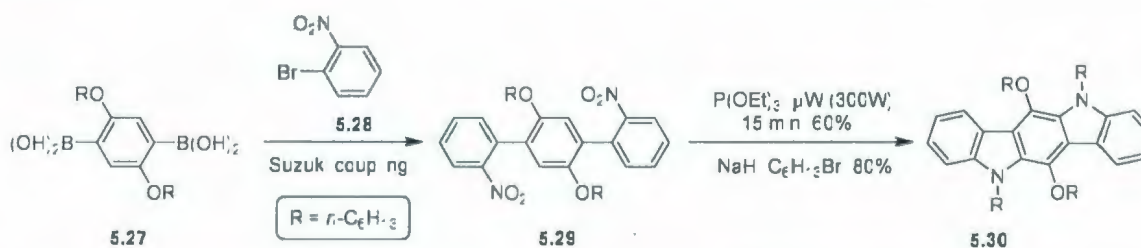


Table 5.3 Methodologies for the synthesis of carbazole framework.

Entry	Methodologies for synthesis of the carbazole framework
1	<p>Cyclodehydrogenation</p>  <p>5.11 <math>\xrightarrow{\text{Pt/C } \Delta}</math> 5.12</p>
2	<p>Cadogan reaction</p>  <p>5.13 <math>\xrightarrow{\text{P(OEt)}_3, \text{ reflux}}</math> 5.12 (major) + 5.14 (minor)</p> <p>5.13 <math>\xrightarrow{\text{Ph}_3\text{P, solvent, } \Delta}</math> 5.12</p>  <p>5.15 <math>\xrightarrow[\text{reflux, 24 h}]{\text{P(OEt)}_3}</math> 5.16 (8%) + 5.17 (35%)</p>
3	<p>Iron-mediated arylamine cyclization</p>  <p>5.18 <math>\xrightarrow[\text{MeCN, 25 } ^\circ\text{C}]{\text{5.19, } \text{Fe(CO)}_5, \text{BF}_4^-}</math> 5.20 (36%) <math>\xrightarrow[\text{toluene, 25 } ^\circ\text{C}]{\text{MnO}_2}</math> 5.21 (54%)</p>
4	<p>Ullmann coupling</p>  <p>5.22 <math>\xrightarrow[\text{n-butyl ether, reflux, 24 h}]{\text{Cu, Cu, K}_2\text{CO}_3}</math> 5.23 (88%)</p>
5	<p>Double <i>N</i>-arylation</p>  <p>5.24 <math>\xrightarrow[\text{H}_2\text{NBoc, K}_3\text{PO}_4, \text{ toluene, 100 } ^\circ\text{C, 67 h}]{\text{Pd}_2(\text{dba})_3, \text{CHCl}_3, \text{xantphos, 5.26}}</math> 5.25 (81%)</p> <p>5.24 <math>\rightarrow</math> 5.26</p>

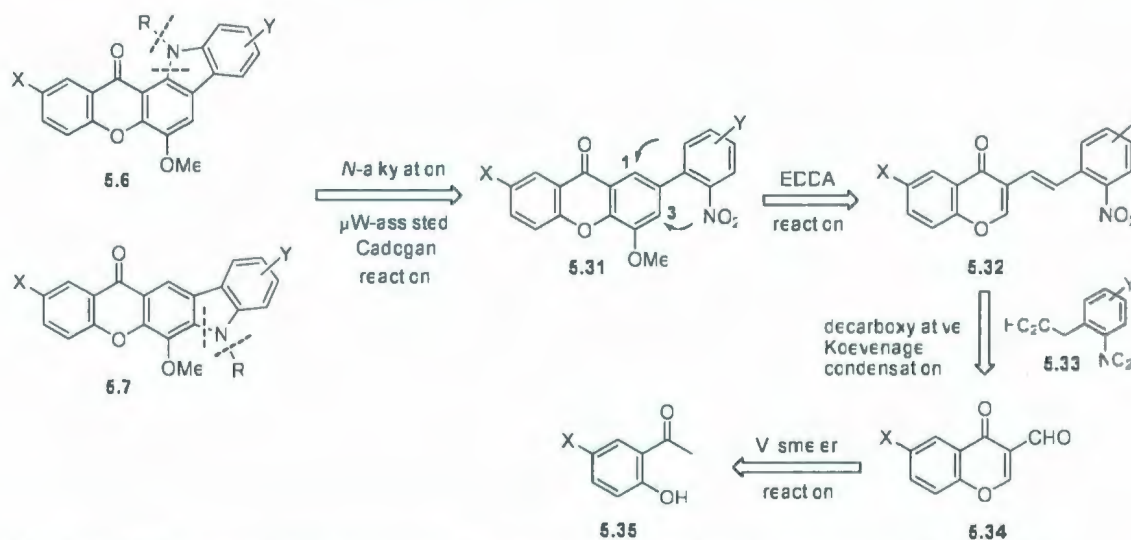
The synthesis of carbazole compounds via iron-mediated arylamine cyclization was investigated starting in the 1980s.<sup>20</sup> For example, carbazole **5.21** (Entry 3, Table 5.3) was obtained in a two-step procedure involving *ortho*-selective electrophilic substitution of an arylamine **5.18** by a tricarbonyliron-complexed cyclohexadienyl cation **5.19**, followed by oxidative cyclization of the resulting complex **5.20** with concomitant aromatization.<sup>21</sup> However, the yields of the carbazoles obtained using this method were moderate at best. Intramolecular Ullmann coupling of **5.22** (Entry 4, Table 5.3)<sup>22</sup> and double *N*-arylation of ditriflate **5.24** (Entry 5, Table 5.3)<sup>23</sup> gave carbazoles **5.23** and **5.25**, respectively. Although these reactions proceed in good yield and do not have regioselectivity issues, finding appropriate conditions is an issue.

Among the aboved-mentioned methods for the synthesis of carbazoles, the Cadogan reaction is among the simplest ones, both in terms of reagents and conditions. Indeed, this reaction has been widely used for the synthesis of carbazoles and even for the synthesis of indolocarbazoles.<sup>17–19</sup> In unpublished work, Witulski *et al.*<sup>24</sup> successfully synthesized indolocarbazole **5.30** using a microwave-assisted double-Cadogan reaction<sup>25</sup> (Scheme 5.1). In this Chapter, the use of this microwave-assisted Cadogan reaction to establish the carbazole moiety in the target xanthone-carbazole hybrid systems is described.



**Scheme 5.1** Synthesis of indolocarbazole **5.30** via microwave-assisted Cadogan reaction.

The retrosynthetic cleavage of the indicated bonds in xanthone-carbazole hybrid systems **5.6** and **5.7** according to a Cadogan transform revealed xanthenes **5.31** as precursors (Scheme 5.2). As mentioned earlier, the Cadogan reaction is known to occur with relatively low regioselectivity when more than one position for ring closure is available. Consequently, nitrophenylxanthenes **5.31** were expected to undergo ring closures at both the 1 and 3 positions due to the free rotation around the biaryl bond connecting the xanthone system and the nitrophenyl group. The subsequent *N*-alkylation of the resulting products would give constitutional isomers **5.6** and **5.7**, respectively. The key intermediate xanthenes **5.31** could be taken back to hydroxyacetophenones **5.35** via three steps: an IEDDA-driven domino reaction (see Chapter 2), a decarboxylative Knoevenagel condensation and a Vilsmeier reaction. The required nitro group for the Cadogan reaction step originates from nitrophenyl acetic acids **5.33**, which should be available in up to two steps from commercial starting materials following literature procedures.<sup>26</sup>



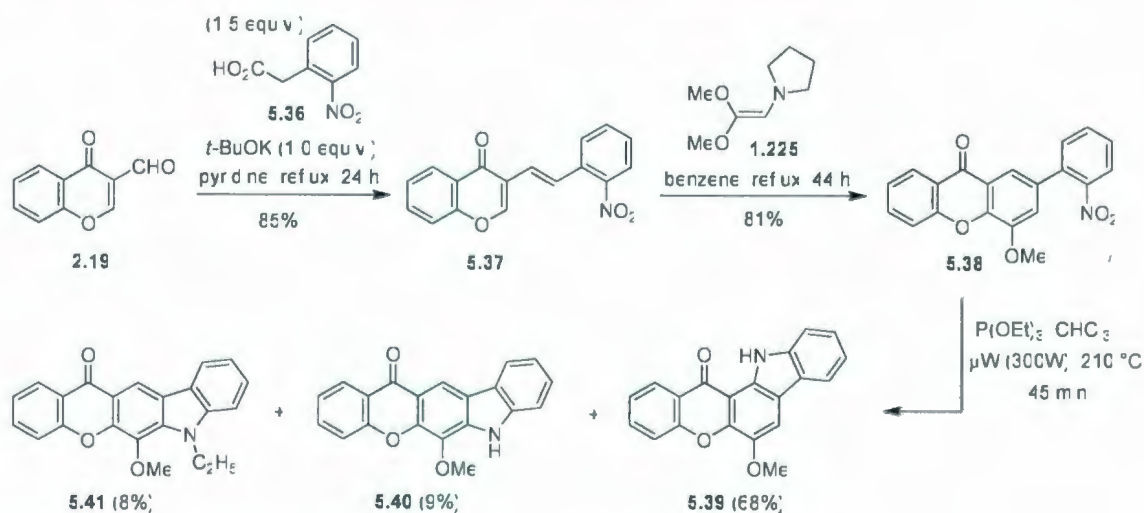
**Scheme 5.2** Retrosynthetic analysis of target xanthone-carbazole compounds **5.6** and **5.7**.



## 5.3 Results and Discussion

### 5.3.1 Synthesis of the Parent Xanthone-Carbazole Hybrid Systems

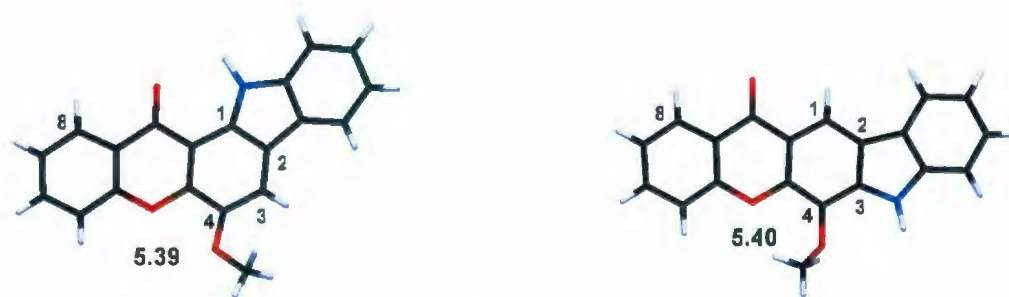
The synthesis of the parent xanthone-carbazole compounds **5.39–5.41** (Scheme 5.3) commenced with the preparation of diene **5.37** via a decarboxylative Knoevenagel condensation of 3-formylchromone (**2.19**) and 2-nitrophenylacetic acid (**5.36**) (1.5 equiv.). Employment of the conditions (pyridine, 70–80 °C) successfully used for *p*-nitrophenyl diene **1.15g** (see Chapter 2, page 62) gave only 7% of the desired diene **5.37** along with 52% recovery of starting material **2.19** after 3 d of heating. The yield of diene **5.37** was significantly improved upon modifying the conditions (pyridine, reflux, 4 d, 56%) and (*t*-BuOK, pyridine, reflux, 24 h, 85%). Obviously, the use of a stronger base (*t*-BuOK) accelerated the reaction and improved the reaction yield. The (*E*) geometry of the newly-formed C-C double bonds of diene **5.37** was confirmed by the magnitude of the  $^3J$  coupling constants (16.1–16.7 Hz) in its  $^1\text{H}$  NMR spectrum.



Scheme 5.3 Synthesis of the parent xanthone-carbazole compounds **5.39–5.41**.



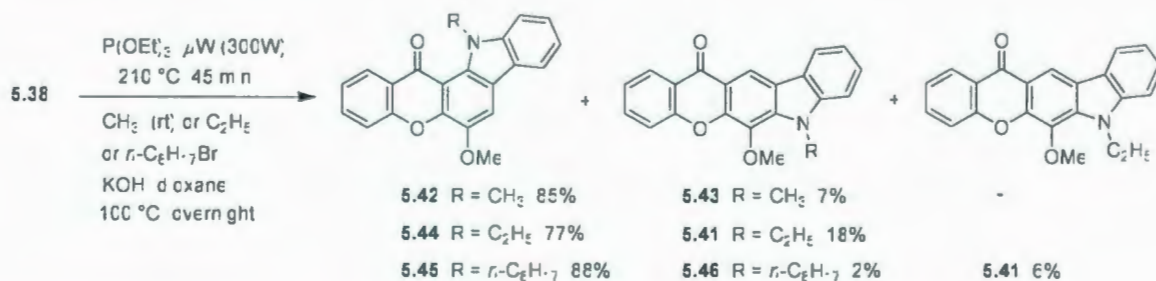
Xanthone **5.38** was smoothly generated in 81% yield from the IEDDA-driven domino reaction between diene **5.37** and enamine **1.225**. A Cadogan reaction was then carried out under microwave irradiation (300 W, 210 °C) for 45 min (three 15-min periods).<sup>27</sup> It was found that the reaction mixture could be stirred more easily when  $\text{CHCl}_3$  or  $\text{CH}_2\text{Cl}_2$  (1 mL) was added as a cosolvent, due to the enhancement of solubility. As expected, both the “angular” isomer **5.39** (68%) and “linear” isomer **5.40** (9%) were formed along with byproduct **5.41** (8%). The total yield was relatively high (85%), and the angular isomer **5.39** was the major product. The structures of **5.39** and **5.40** were confirmed using single crystal X-ray analysis (Figure 5.2)<sup>28</sup> as well as by their  $^1\text{H}$  NMR spectra. In particular, H-8 (dd, 8.40 ppm) in the angular isomer **5.39** and H-1 (s, 8.85 ppm) in the linear isomer **5.40** are the lowest-field signals among the aryl hydrogens in the molecules. The N-H signals were easily recognized by  $\text{D}_2\text{O}$  exchange experiments.



**Figure 5.2** X-ray structures of **5.39** and **5.40**.

The non-*N*-alkylated xanthone-carbazoles **5.39** and **5.40** have low solubility in common organic solvents. They also appeared as very close spots on tlc. To improve the prospects of separating and adequately characterizing the two isomers, the crude Cadogan products were subjected to *N*-alkylation reactions to form more soluble products. Three

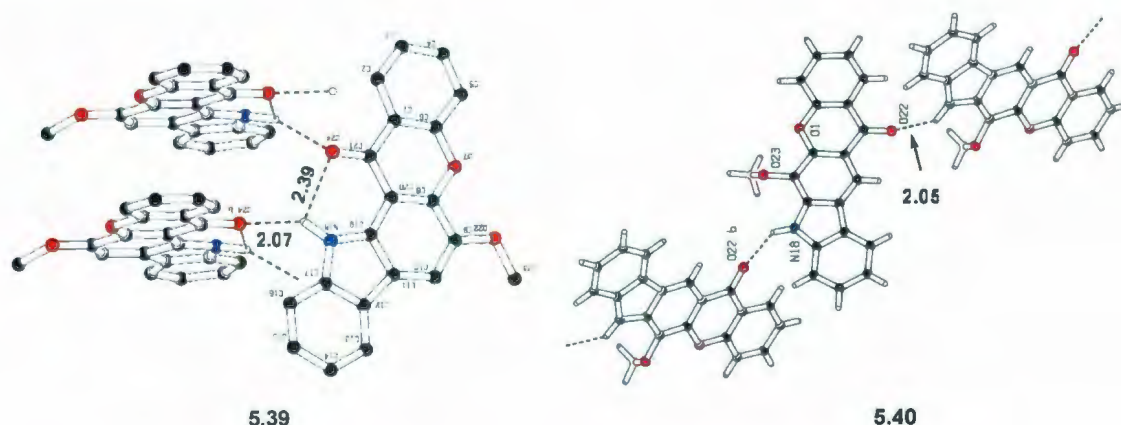
different alkyl groups, namely methyl, ethyl, and *n*-octyl were employed. Attempted *N*-methylation of the product mixture obtained from the Cadogan reaction of xanthone **5.38** using conditions (MeI, NaH, THF, rt) that had been used successfully for indolocarbazole **5.30** (Scheme 5.1) was unsuccessful. However, using new conditions (KOH, dioxane, rt), the *N*-methylated products **5.42** (major, 85%) and **5.43** (minor, 7%) were formed in excellent combined yield (92%) (Scheme 5.4). No *N*-ethylated byproducts were isolated or observed in this reaction. The *N*-alkylation of the Cadogan products with ethyl iodide or octyl bromide did not occur at room temperature using KOH in dioxane, but the reactions were successful upon heating at 100 °C. Similarly, excellent combined yields (95–96%) were obtained in these alkylations, and the angular isomers **5.44** and **5.45** were the most abundant isomers. The yield ratios between the angular isomers and the linear isomers in these cases were 12:1 (*R* = CH<sub>3</sub>), 4:1 (*R* = C<sub>2</sub>H<sub>5</sub>), and 11:1 (*R* = *n*-C<sub>8</sub>H<sub>17</sub>), respectively.



**Scheme 5.4** Synthesis of *N*-alkylated xanthone-carbazole compounds **5.41**–**5.46**.

In theory, products **5.39** and **5.40** could both undergo an ethyl transfer from the phosphorus species P(OEt)<sub>3</sub> or P(O)(OEt)<sub>3</sub> in the Cadogan reaction step. However, in practise, byproduct **5.41** was the only one observed. This result indicated that the linear isomer more easily reacted with ethylating agents (triethyl phosphite or triethyl

phosphate) than the angular one. Hydrogen bonding can be used to explain this result. From the X-ray structures (Figure 5.3), the angular isomer **5.39** showed both intramolecular (2.39 Å) and intermolecular (2.07 Å) hydrogen bonds while the linear isomer **5.40** showed only the intermolecular hydrogen bond (2.05 Å). In other words, the absence of intramolecular hydrogen bonding in the linear isomer presumably makes it more reactive toward the alkylation (the N–H group is more easily deprotonated) than the angular one (the N–H group is harder to deprotonate). The lower product ratio for the *N*-ethylated compounds **5.44** and **5.41** is presumably because the *N*-alkylation product of the linear isomer and the byproduct obtained from ethyl transfer to the linear isomer are one and the same (**5.41**).



**Figure 5.3** Hydrogen bonds of in X-ray structures of **5.39** (*left*) and **4.40** (*right*).

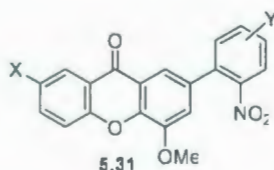
In brief, the parent xanthone-carbazole hybrid systems (**5.39–5.46**) were successfully synthesized in only four steps from readily-available starting materials. High yields (>80%) were obtained in every single step. The microwave-assisted Cadogan reactions, followed by an *N*-alkylation gave consistent results and high



combined yields (92–96%) with the angular isomers **5.42**, **5.44**, **5.45** (77–88%) as the major products in all cases. Further examples of the microwave-assisted Cadogan reaction are described in the following Section.

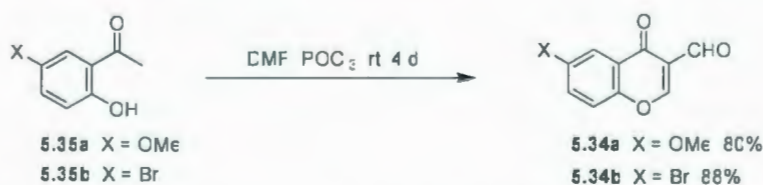
### 5.3.2 Synthesis of Substituted Xanthone-Carbazole Hybrid Systems

With the parent xanthone-carbazole hybrid systems in hand, the research was broadened to include the microwave-assisted Cadogan reactions of *o*-nitrophenylxanthenes bearing substituents on the chromone and / or the nitrophenyl moieties (Figure 5.4). Methoxy- and bromo- groups were chosen because they could conceivably serve as handles for further elaboration. The synthesis of some substituted xanthenes **5.31** commenced with the preparation of some non-commercially-available starting materials, *i.e.* 3-formylchromones **5.34a** and **5.34b**, *o*-nitrophenylacetic acids **5.33a** and **5.33b** as well as intermediate dienes **5.32a–f** (Table 5.4).



**Figure 5.4** Xanthenes bearing substituents **5.31**.

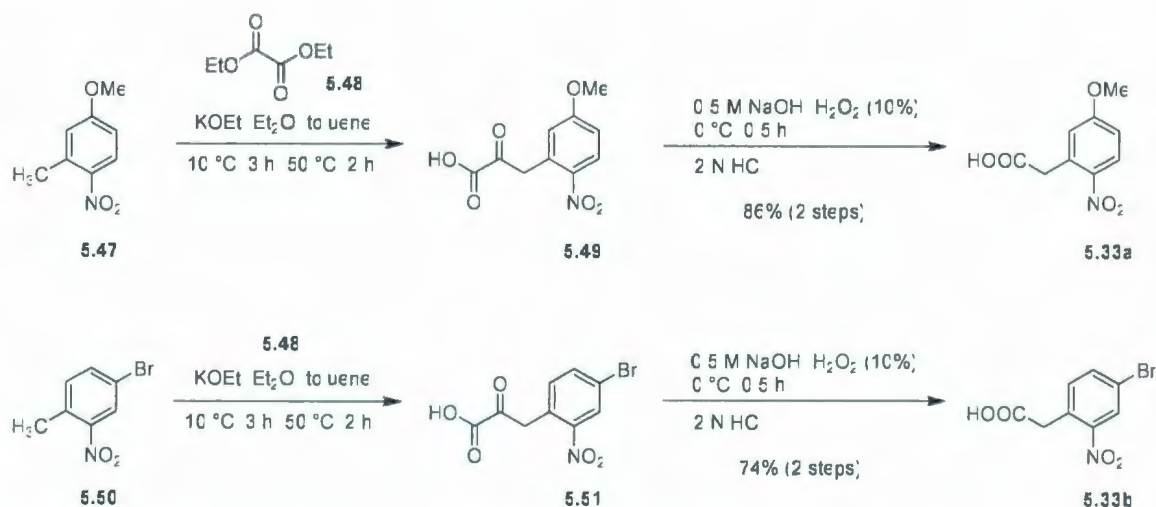
First, the 6-methoxy- and 6-bromo-3-formylchromones **5.34a** and **5.34b** were prepared from the corresponding hydroxyacetophenones **5.35a** and **5.35b**, respectively, via Vilsmeier reactions<sup>29</sup> in good yields (Scheme 5.5).



**Scheme 5.5** Synthesis of 3-formylchromone derivatives **5.34a** and **5.34b**.

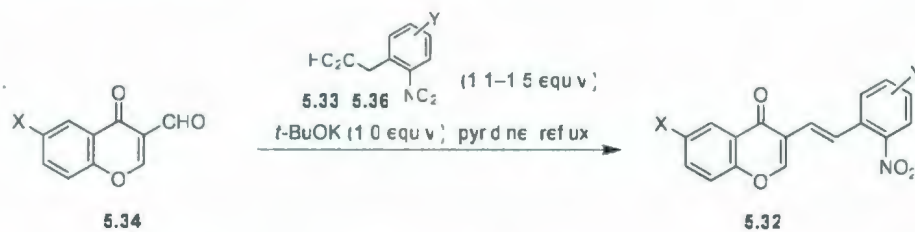


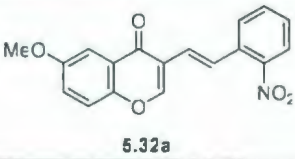
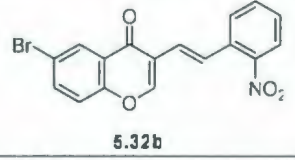
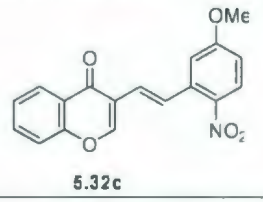
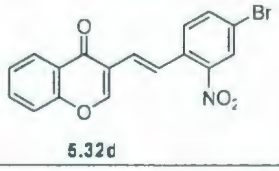
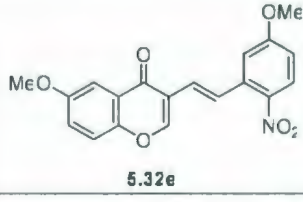
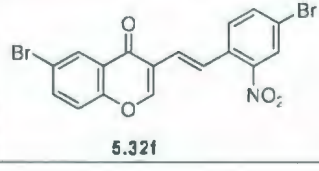
Second, *o*-nitrophenylacetic acid derivatives **5.33a** and **5.33b** were obtained in good yields via a two-step synthesis, which followed the literature procedures for **5.33b**<sup>26</sup> (Scheme 5.6).



**Scheme 5.6** Synthesis of *o*-nitrophenylacetic acid derivatives **5.33a** and **5.33b**.

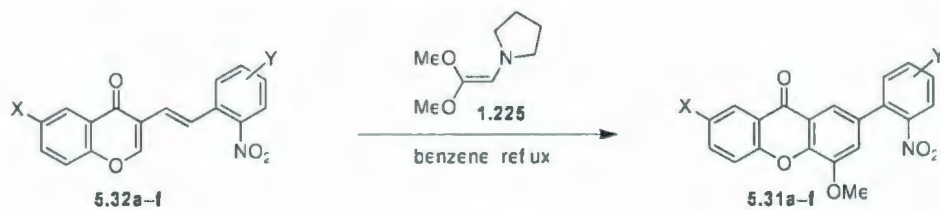
Third, a series of dienes **5.32a–f** (Table 5.4) was synthesized from 3-formylchromones **5.34a–b** and nitrophenylacetic acids **5.33a–b** and **5.36** via decarboxylative Knoevenagel condensation under the conditions used previously for diene **5.37** (Scheme 5.3). However, the reaction times (1–3 h) to form the substituted dienes **5.32a–f** were much shorter than that of diene **5.37** (24 h), which bears no substituent. Similarly, dienes **5.32a–f** were obtained in good yields (78–88%), and dienes bearing a bromo substituent were obtained in slightly lower yields than those bearing a methoxy group. The *E* geometry of the newly formed C–C double bonds was again confirmed by <sup>1</sup>H NMR (<sup>3</sup>*J* ≈ 16 Hz).

Table 5.4 Synthesis of *o*-nitrophenyl dienes 5.32a–f.

Entry	Chromone	Nitrophenylacetic acid	Diene 5.32	Time (h)	Yield (%)
a	5.34a	5.36		1.75	83
b	5.34b	5.36		3.0	79
c	2.19	5.33a		3.0	88
d	2.19	5.33b		1.5	78
e	5.34a	5.33a		2.5	86
f	5.34b	5.33b		1.0	78

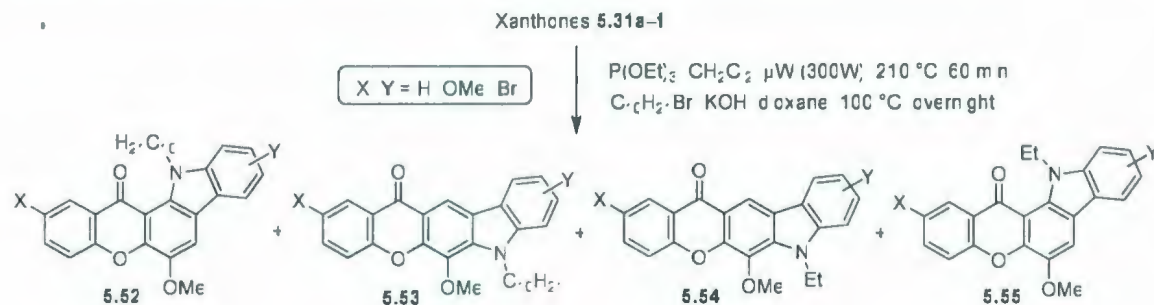
Finally, the IEDDA-driven domino reactions between dienes **5.32a–f** and enamine **1.225** smoothly afforded *o*-nitrophenylxanthenes **5.31a–f** (Table 5.5). Excellent yields were obtained for **5.31b** (98%) and **5.31c** (96%). The yields of the other xanthenes were in the range of 74–86%, except for **5.31f** (56%), which may have suffered losses during purification by chromatography due to its lower solubility.

At this point, the stage was set for the synthesis of substituted xanthone-carbazole hybrid systems from xanthenes **5.31a–f** via microwave-assisted Cadogan reactions,<sup>30</sup> followed by *N*-alkylations. Using the same conditions (300 W, 210 °C) that were successfully used for xanthenes **5.38**, the Cadogan reactions of xanthenes **5.31a–e** were irradiated for a total of 60 min (3 x 20 min periods), by which time the starting materials were consumed completely (tlc analysis). Slightly different behaviour was exhibited by xanthone **5.31f**, which was consumed a little faster, *i.e.* in only 40 min (2 x 20 min periods). After workup, the crude Cadogan products were subjected to *N*-alkylations with 1-bromodecane employing the established conditions (KOH, dioxane, 100 °C, overnight). In most cases, a mixture of products including angular isomer **5.52**, linear isomer **5.53**, and linear byproduct **5.54** were obtained (Table 5.6). However, the angular byproduct **5.55a** (trace) was also isolated. Its appearance, albeit in very small amounts, indicated that the angular isomer could undergo ethyl transfer during the Cadogan reaction, but its reaction rate must be much slower than that of the linear isomer.

**Table 5.5** Synthesis of *o*-nitrophenyl xanthenes **5.31a–f**.

Entry	Diene	Xanthone	Time (h)	Yield (%)
<b>a</b>	<b>5.32a</b>	 <b>5.31a</b>	20	74
<b>b</b>	<b>5.32b</b>	 <b>5.31b</b>	20	98
<b>c</b>	<b>5.32c</b>	 <b>5.31c</b>	2.5	96
<b>d</b>	<b>5.32d</b>	 <b>5.31d</b>	2.0	86
<b>e</b>	<b>5.32e</b>	 <b>5.31e</b>	3.5	82
<b>f</b>	<b>5.32f</b>	 <b>5.31f</b>	2.0	56



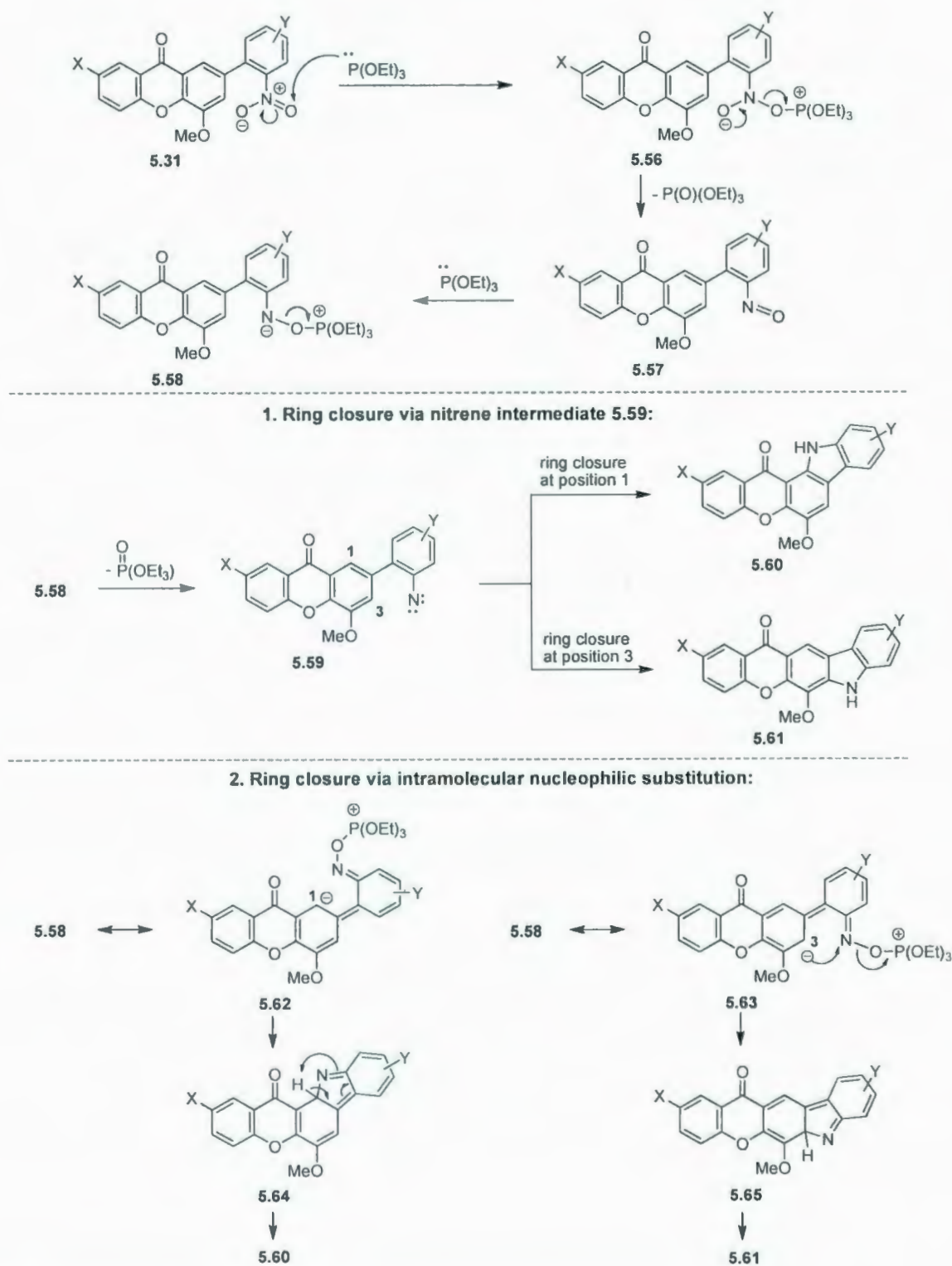
**Table 5.6** Synthesis of substituted xanthone-carbazole hybrid systems.

Entry	Xanthenes	Xanthone-carbazoles (%)				Total yield (%)	Ratio 5.52: (5.53 + 5.54)
		5.52	5.53	5.54	5.55		
<b>a</b>		79	0	14	trace	<b>93</b>	6:1
<b>b</b>		70	11	7	0	<b>88</b>	4:1
<b>c</b>		48	15	12	0	<b>75</b>	2:1
<b>d</b>		52	4	5	0	<b>61</b>	6:1
<b>e</b>		64	0	15	0	<b>79</b>	4:1
<b>f<sup>31</sup></b>		64	9	0	0	<b>74</b>	7:1

Substituted xanthone-carbazole systems **5.52a-f** – **5.55a-f** were obtained in good total yields (61–93%), but slightly lower than the unsubstituted ones (92–96%) (Scheme 5.4). The angular isomers **5.52a-f** were major products in all cases and the linear isomers **5.53a** and **5.53c** were not observed. The angular / linear ratios in these cases ranged from 4:1 to 7:1, except when a methoxy group was attached on the nitrophenyl moiety (Entry c), the ratio dropped to 2:1.

Although the Cadogan reaction has been widely applied in the synthesis of the carbazole framework, its mechanism has not been well-studied. Cadogan himself proposed two possible reaction pathways, one of them involving a nitrene intermediate<sup>32</sup> and the other one an intramolecular nucleophilic substitution<sup>17</sup> (Scheme 5.7). Using compound **5.31** as an example, the nitro group first undergoes reduction to afford a nitroso compound **5.57**, which can react further with  $\text{P}(\text{OEt})_3$  to form intermediate **5.58**. In the first proposed mechanism, the ring closure of nitrene **5.59**, which can be formed from intermediate **5.58**, can occur at positions 1 and 3 via C-H insertion to give angular isomer **5.60** and linear isomer **5.61**, respectively. In the second mechanism, intermediates **5.62** and **5.63**, which are resonance structures of intermediate **5.58**, can undergo cyclization via intramolecular nucleophilic substitution, followed by a 1,5-H shift to form angular isomer **5.60**, via **5.64** and linear isomer **5.61**, via **5.65**, respectively. However, both mechanisms cannot explain why the angular isomer is formed favourably over the linear one. A possible explanation for this phenomenon is that the intramolecular hydrogen bond may be developing at the transition state leading to the angular isomer, which makes it more stable than that of the linear one.

In brief, substituted xanthone-carbazole hybrid systems **5.52** and **5.53** (X, Y = H, OMe, Br) were synthesized in good total yields (61–93%) via a microwave-assisted Cadogan reaction of nitrophenylxanthenes **5.31a–f**, which were obtained in three steps using the same synthetic route for the non-substituted xanthone **5.38**. The angular isomers **5.52** (42–79%) were the major products in all cases.



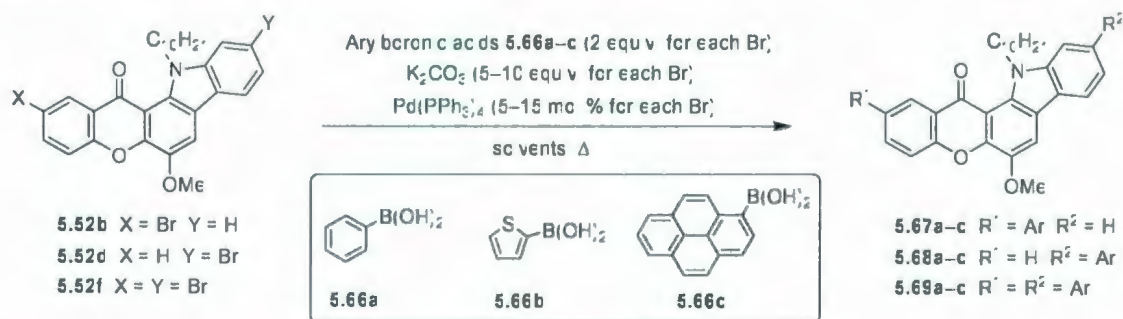
Scheme 5.7 Mechanisms of the Cadogan reaction proposed by Cadogan.<sup>17,32</sup>



### 5.3.3 Synthesis of Aryl-substituted Xanthone-Carbazole Hybrid Systems

A series of aryl-substituted xanthone-carbazole hybrid systems **5.67a–c**, **5.68a–c**, and **5.69a–c** (aryl = phenyl, 2-thienyl, 1-pyrenyl) (Table 5.7) was successfully synthesized from the newly-synthesized bromo-substituted xanthone-carbazoles<sup>33</sup> **5.52b**, **5.52d**, and **5.52f** using Suzuki couplings. These biaryl systems were expected to exhibit higher fluorescence quantum yields than those of the non-substituted, bromo- or methoxy-substituted xanthone-carbazole hybrid systems. The designed structures were aimed for potential applications in OLEDs or EFTs.

**Table 5.7** Synthesis of aryl-substituted xanthone-carbazole hybrid systems.



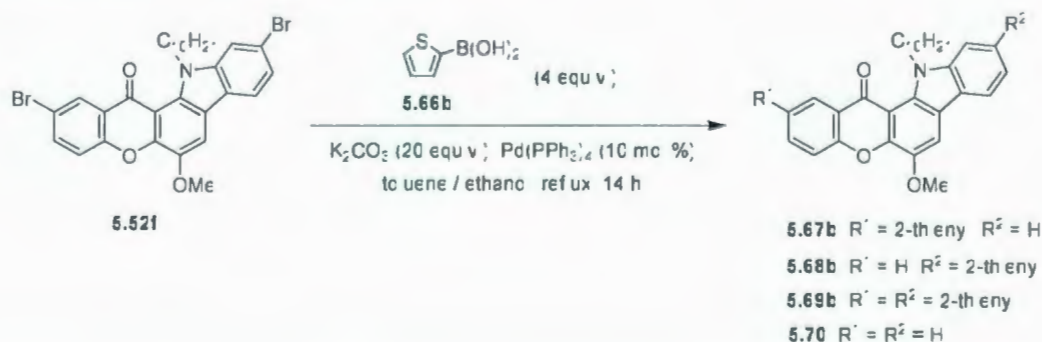
Entry	Boronic acids	Conditions	Suzuki coupling products: yield (%)		
			<b>5.67a–c</b>	<b>5.68a–c</b>	<b>5.69a–c</b>
1	<b>5.66a*</b>	toluene-ethanol (1.5:1) 80 °C, 2 h	<b>5.67a</b> : 100%	<b>5.68a</b> : 93%	<b>5.69a</b> : 86%
2	<b>5.66b</b>	DMF 100–120 °C, 24–26 h	<b>5.67b</b> : 71% <sup>a</sup>	<b>5.68b</b> : 71% <sup>b</sup>	<b>5.69b</b> : 80% <sup>c</sup>
3	<b>5.66c**</b>	dioxane-H <sub>2</sub> O (2:1) 100 °C, 2 h	<b>5.67c</b> : 100%	<b>5.68c</b> : 93%	<b>5.69c</b> : 92% <sup>d</sup>

(\*):  $K_2CO_3$  (10 equiv. for each Br);  $Pd(PPh_3)_4$  (5 mol% for each Br)

(\*\*):  $K_2CO_3$  (10 equiv. for each Br);  $Pd(PPh_3)_4$  (10 mol% for each Br)

- (a):  $K_2CO_3$  (5 equiv.);  $Pd(PPh_3)_4$  (10 mol%), DMF, 100 °C, 24 h, 26% recovery of SM (or 95% borsm)  
 (b):  $K_2CO_3$  (10 equiv.);  $Pd(PPh_3)_4$  (15 mol%), dioxane- $H_2O$  (2:1), 120 °C, 2 h  
 (c):  $K_2CO_3$  (20 equiv.);  $Pd(PPh_3)_4$  (30 mol%), DMF, 120 °C, 26 h  
 (d): 18 h

The initial coupling reactions of **5.52b**, **5.52d**, **5.52f** with phenylboronic acid **5.66a** occurred smoothly to give phenyl-substituted xanthone-carbazole systems **5.67a**–**5.69a**, respectively, in good-to-excellent yields (86–100%) (Entry 1, Table 5.7). However, when the same conditions were applied for the Suzuki coupling of the dibromo substrate **5.52f** and 2-thienylboronic acid **5.66b**, a mixture of products, including monocoupling products **5.67b**, **5.68b**, the desired dicoupling product **5.69b**, and the debromination product **5.70**, were obtained ( $^1H$  NMR and mass spectroscopic analysis) (Scheme 5.8). Yields of products could not be determined due to unsuccessful column chromatographic attempts at purification.



Scheme 5.8 Suzuki coupling of **5.52f** with 2-thienylboronic acid **5.66b**.

Besides the co-solvent system toluene-ethanol,<sup>34</sup> DMF<sup>35</sup> and dioxane- $H_2O$ <sup>36</sup> are also used in Suzuki couplings. Therefore, these solvent systems were employed for the

couplings with 2-thienylboronic acids **5.66b** with the same base and catalyst. The monocoupling products **5.67b** and **5.68b** were formed in similar yields (71%), but the reaction time was much shorter in dioxane-H<sub>2</sub>O (120 °C, 2 h) than in DMF (100 °C, 24 h) (Entry 2, Table 5.7). However, the amount of protodebromination product **5.70** increased during the course of reaction (tlc observation) when dioxane-H<sub>2</sub>O was used as a co-solvent system. Di-2-thienyl substituted xanthone-carbazole **5.69b** was obtained in 80% yield in DMF and none of the byproduct **5.70** was produced. It is worth noting that the catalyst loading was increased to 15 mol% (per bromo group) in the couplings of **5.52d** or **5.52f** with **5.66b**. This may well have contributed to the enhancement of the reaction rates and reaction yields in these cases. Although the Suzuki coupling of **5.52f** with 1-pyrenylboronic acid **5.66c** failed with toluene-ethanol (1.5:1) as the solvent, a series of 1-pyrenyl substituted xanthone-carbazole systems **5.67c** (100%), **5.68c** (93%) and **5.69c** (92%) was formed in excellent yields in dioxane-H<sub>2</sub>O (2:1).

In brief, a new series of the phenyl-, 2-thienyl-, and 1-pyrenyl- substituted xanthone-carbazole hybrid systems **5.67a–c**, **5.68a–c**, and **5.69a–c** was synthesized in good-to-excellent yields (71–100%) from the corresponding bromo-substituted xanthone-carbazoles via Suzuki coupling reactions. Three different solvent systems were used (toluene-ethanol, DMF, and dioxane-H<sub>2</sub>O), each one being most suitable for a particular arylboronic acid.

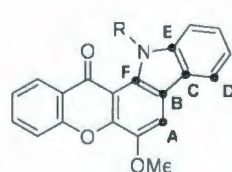
#### 5.3.4 Structures and X-ray Packing Motifs of Xanthone-Carbazole Hybrid Systems

One of the characteristics of acenes and hetero[5]acenes that makes them of interest with regard to charge transport is their planar frameworks. The planar structure



provides an opportunity for intermolecular  $\pi$ - $\pi$  interactions to favor stacking in the packing motif of the molecule and this type of long-range order often leads to high charge carrier mobility of the molecule.<sup>37</sup>

X-ray crystal structure determinations of xanthone-carbazole hybrid systems **5.39**–**5.42** (Figure 5.5) revealed that they have essentially coplanar frameworks. Similar to the xanthone moiety ( $\Phi = 2.85^\circ$ , see Chapter 1, page 13), the carbazole units also have only slight deviations from planarity. The relative average torsion angles ( $\Phi$ , Figure 5.5) are in the range of  $2.05$ – $2.37^\circ$ . Such slight distortions could easily be accounted for by crystal packing forces and, as such, are not necessarily innate structural features of the molecules. The alkylated compounds **4.42** ( $R = \text{CH}_3$ ) and **4.41** ( $R = \text{C}_2\text{H}_5$ ) have even smaller relative average torsion angles ( $\Phi = 0.98$ – $1.00^\circ$ ) than those of the non-alkylated ones, *i.e.* **5.39** and **5.40** ( $R = \text{H}$ ).



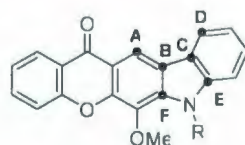
angular isomer

**5.39**  $R = \text{H}$ 

ABCD  $2.76^\circ$   
 FBCE  $1.58^\circ$   
 ABCE  $178.67^\circ$  ( $1.33^\circ$ )  
 FBCE  $177.49^\circ$  ( $2.51^\circ$ )  
 $\Phi_{\text{CEC}} : 2.05^\circ$

**5.42**  $R = \text{Me}$ 

ABCD  $0.21^\circ$   
 FBCE  $0.05^\circ$   
 ABCE  $178.26^\circ$  ( $1.74^\circ$ )  
 FBCE  $178.10^\circ$  ( $1.90^\circ$ )  
 $\Phi_{\text{CEC}} : 0.98^\circ$



near isomer

**5.40**  $R = \text{H}$ 

ABCD  $3.61^\circ$   
 FBCE  $1.13^\circ$   
 ABCE  $177.53^\circ$  ( $3.47^\circ$ )  
 FBCE  $177.73^\circ$  ( $2.27^\circ$ )  
 $\Phi_{\text{CEC}} : 2.37^\circ$

**5.41**  $R = \text{Et}$ 

ABCD  $1.27^\circ$   
 FBCE  $0.08^\circ$   
 ABCE  $178.80^\circ$  ( $1.20^\circ$ )  
 FBCE  $179.26^\circ$  ( $0.74^\circ$ )  
 $\Phi_{\text{CEC}} : 1.00^\circ$

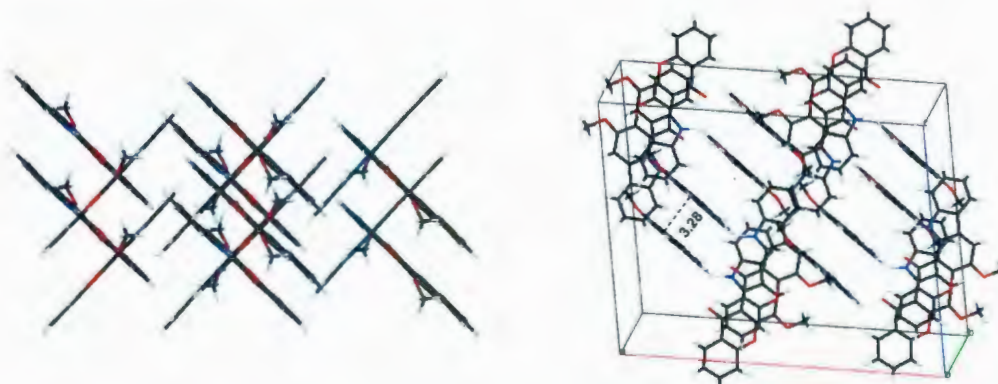
$\Phi_{\text{CEC}}$  is the relative average torsion angle of indicated carbon atoms

**Figure 5.5** The relative average torsion angles of **5.39**–**5.41** (X-ray calculations).

The virtually planar structures of these compounds do indeed result in some  $\pi$  stacking in the crystal. X-ray crystallographic analysis of angular isomer **5.39** (Figure

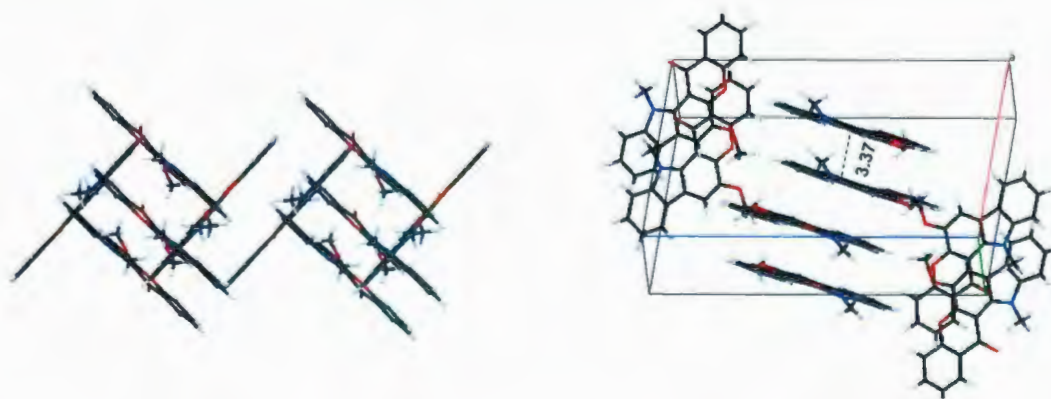


5.6) shows that the molecules stack cofacially in the solid state (face-to-face interaction) with a minimal intermolecular distance of 3.28 Å. The molecules also adopt a 90°-herringbone arrangement, in which the adjacent xanthone-carbazole units show minimal edge-to-face contact of 3.80 Å (C-to-C).



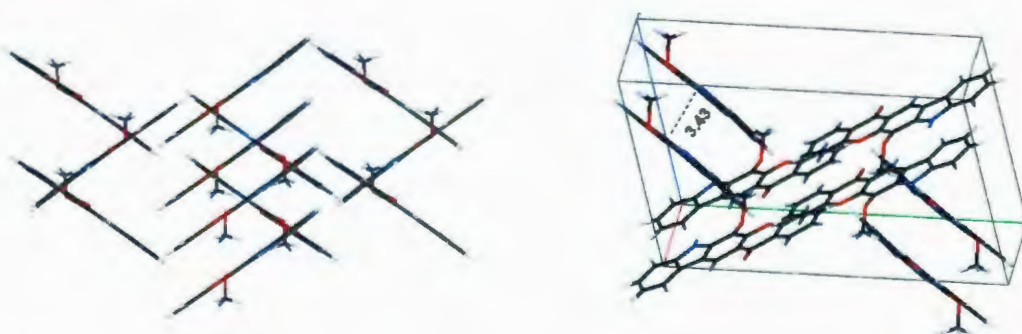
**Figure 5.6** X-ray packing motif of angular isomer **5.39** ( $R = H$ ).

Similarly, the angular isomer **4.42** ( $R = CH_3$ ) displays both parallel and 90°-herringbone packing motifs with a minimal interplanar distance of 3.37 Å and edge-to-face contacts of 4.10 Å (C-to-C) from the adjacent stacks (Figure 5.7).



**Figure 5.7** X-ray packing motif of angular isomer **5.42** ( $R = CH_3$ ).

The packing motif of linear isomer **5.40** ( $R = H$ ) is slightly different (Figure 5.8). Face-to-face and edge-to-face arrangements are also observed for this compound. However, the herringbone angle is  $71^\circ$ , instead of  $90^\circ$  as for the angular isomers **5.39** (Figure 5.6) and **5.42** (Figure 5.7). The minimal interplanar distance of  $3.43 \text{ \AA}$  and edge-to-face contacts of  $3.88 \text{ \AA}$  (C-to-C) were measured between two molecules and from the neighbouring stacks, respectively.



**Figure 5.8** X-ray packing motif of linear isomer **5.40** ( $R = H$ ).

The linear isomer **5.41** ( $R = C_2H_5$ ) adopts  $\pi$ - $\pi$  stacking with a minimal interplanar distance of  $3.40 \text{ \AA}$  and a herringbone arrangement with an angle of  $135^\circ$  (Figure 5.9). The closest edge-to-face contact of  $3.64 \text{ \AA}$  (C-to-C) is the shortest distance in comparison to those of **5.39**, **5.40**, and **5.42** ( $3.8$ – $4.1 \text{ \AA}$ ).



**Figure 5.9** X-ray packing motif of linear isomer **5.41** ( $R = C_2H_5$ ).

In summary, xanthone-carbazole hybrid systems **5.39–5.42** exhibit both  $\pi$ – $\pi$  stacking and herringbone arrangements in the crystal, which is a commonly-observed packing motif of heteroacenes. The edge-to-face angles changed from  $90^\circ$  in the angular isomers (**5.39**, **5.42**) to  $71^\circ$  and  $135^\circ$  in linear isomers (**5.40** and **5.41**, respectively). The planar structures of these compounds enable strong  $\pi$ – $\pi$  stacking with minimal interplanar distance range from 3.28 to 3.43 Å. These figures easily fall within the  $\pi$ – $\pi$  stacking distance ( $\approx 3.5$  Å) required for producing high charge carrier mobilities by intermolecular hopping.<sup>38</sup> In fact, the known hetero[5]acenes **1.183–1.186** (Chapter 1, Table 1.2, page 39), which have interplanar distances range from 3.44 to 3.52 Å, exhibit high charge carrier mobilities. Thus, xanthone-carbazoles **5.39–5.42** are good candidates to have similar charge transport properties, provided their HOMO-LUMO energy gaps are similar to those of hetero[5]acenes **1.183–1.186**.

### 5.3.5 Physical properties of Xanthone-Carbazole Hybrid Systems

#### 5.3.5.1 Non-substituted Xanthone-Carbazole Hybrid Systems

In this section, the results of UV/Vis absorption, fluorescence, cyclic voltammetry, aggregation, and modeling studies of the non-substituted xanthone-carbazole hybrid systems are presented along with a discussion of the results and a comparison of these results to pentacene and other known hetero[5]acenes.

#### Optical properties.

In general, mixture of a molecule bearing electron-donor and a molecule bearing electron-acceptor exhibits a “charge transfer absorption band” due to the formation of a charge-transfer complex. Normally, the “charge transfer absorption band”, the lowest

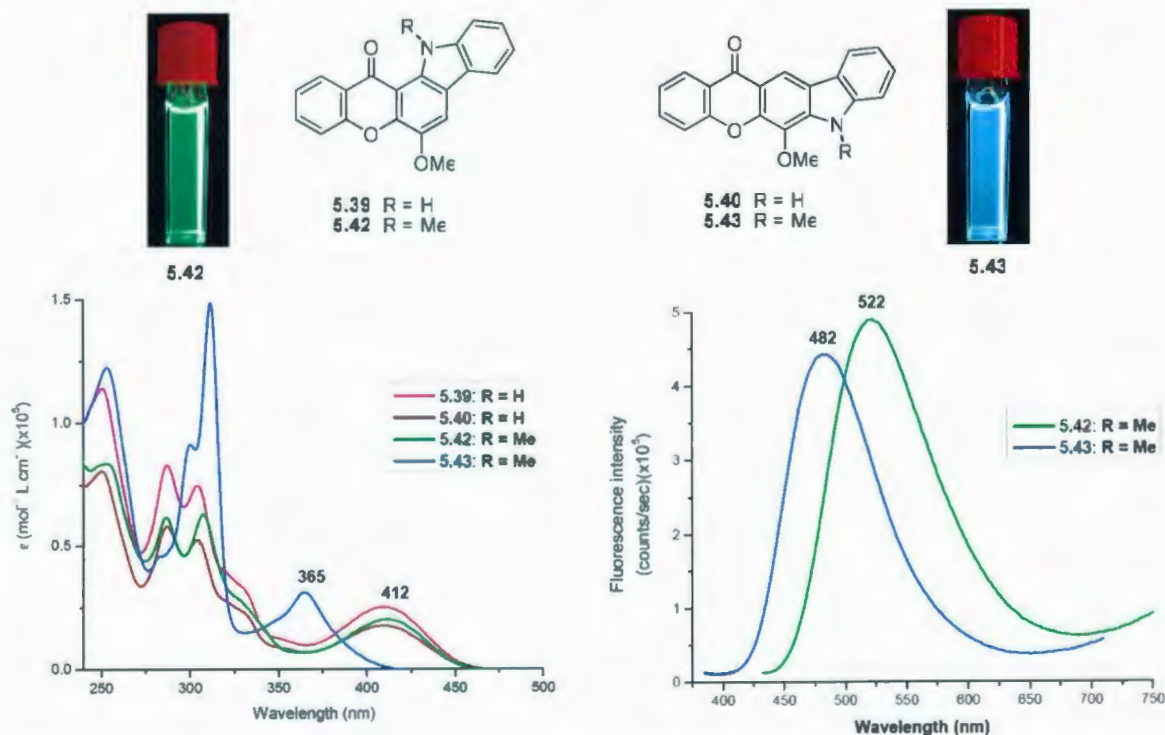


energy band, is broad and sensitive to solvent polarity. In particular, the absorption energy decreases (longer wavelength, or red-shift) as the solvent polarity increases.<sup>39</sup> These features may be expected to manifest themselves in a molecule containing both an electron-donor and electron acceptor unit in its structure, such as xanthone-carbazole hybrid system.

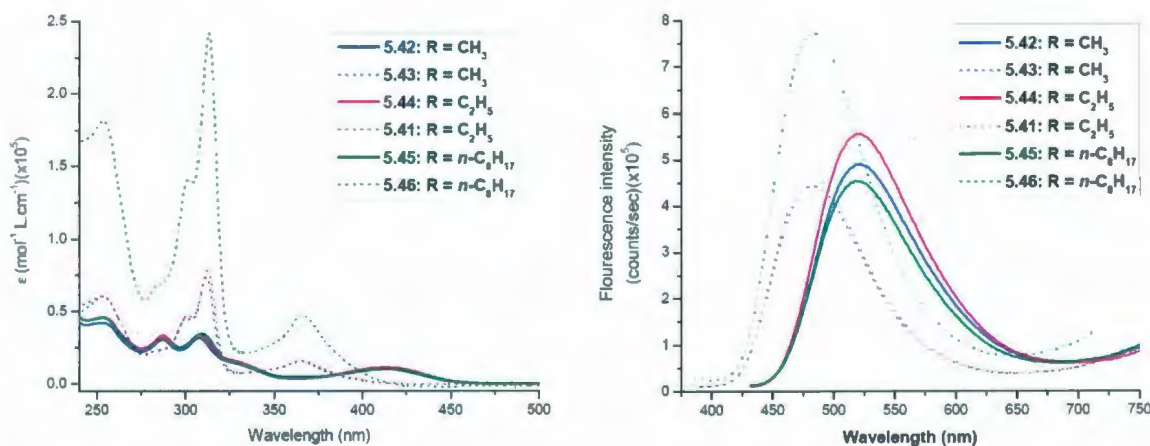
The UV/Vis spectra of the non-*N*-alkylated angular and linear isomers **5.39**, **5.40** ( $R = H$ ) have the same shape, and their longest wavelength absorption maxima are both at 412 nm (Figure 5.10). Interestingly, when hydrogen was replaced by a methyl group, the spectrum of the angular isomer **5.42** maintains the same appearance, *i.e.* broader absorption bands, while the linear isomer **5.43** exhibits a rather different spectrum in terms of its shape and the position of the longest wavelength maximum (365 nm). In the fluorescence spectra, almost no fluorescence was observed for the non-*N*-alkylated xanthone-carbazoles **5.39** and **5.40**. Presumably, non-radiative processes may occur at the excited states, which suppresses the emission (or decrease the fluorescence quantum yield). In contrast, distinct emissions, *i.e.* green fluorescence ( $\lambda_{\text{max}} = 522$  nm) and blue fluorescence ( $\lambda_{\text{max}} = 482$  nm) were observed for the angular isomer **5.42** and the linear isomer **5.43**, respectively. Replacing the methyl group with longer alkyl chains such as ethyl or *n*-octyl groups did not affect the absorption and emission properties of this series of compounds. For example, the angular isomers **5.44** ( $R = C_2H_5$ ) and **5.45** ( $R = n\text{-}C_8H_{17}$ ) have similar absorption / emission maxima ( $\lambda_{\text{max}} = 412 / 519$  nm for **5.45** and 522 nm for **5.44**) to those of **5.42** ( $R = CH_3$ ). The linear isomers **5.41** ( $R = C_2H_5$ ), **5.46** ( $R = n\text{-}C_8H_{17}$ ) also have similar absorption / emission maxima ( $\lambda_{\text{max}} = 366 / 485$  nm for **5.41**



and 486 nm for **5.46**) to those of **5.43** ( $\lambda_{\text{max}} = 365 / 482$  nm) (Figure 5.11, Table 5.8). The 36–40 nm red-shift in emission in going from linear to angular isomers indicates that the angular isomers tend to have stronger  $\pi$ – $\pi$  interactions than the linear ones. This feature is consistent with the shorter interplanar distances in the X-rays structure of the linear **5.40** and **5.41** ( $d = 3.28$ – $3.37$  Å) in comparison with the angular **5.39** and **5.42** ( $d = 3.40$ – $3.43$  Å) (Figures 5.6–5.9). The anomalously high intensity in both absorption and emission spectra of the linear isomer **5.46** may be due to a stronger transitory induced dipole moment (or charge separation) in comparison to those of the other compounds.



**Figure 5.10** Absorption spectra (*left*) and emission spectra (*right*) of xanthone-carbazoles **5.39**, **5.40**, **5.42** and **5.43** in  $\text{CHCl}_3$  ( $2 \times 10^{-5}$  M).



**Figure 5.11** Absorption spectra (*left*) and emission spectra (*right*) of the angular **5.42**, **5.44**, **5.45** (solid lines) and the linear **5.43**, **5.41**, **5.46** (dotted lines) in CHCl<sub>3</sub> ( $2 \times 10^{-5}$  M).

The reorganization energies ( $\lambda_t$ ) of the linear isomers **5.43**, **5.41**, **5.46** ( $\lambda_t = 3330$ – $3370$  cm<sup>-1</sup>) are larger than those of the angular ones **5.42**, **5.44**, **5.45** ( $\lambda_t = 2500$ – $2560$  cm<sup>-1</sup>) as calculated from the Stokes shifts<sup>40</sup> (Table 5.8). A tentative interpretation of this data is that charge transfer becomes more significant in the linear isomers than in the angular ones.<sup>41</sup> The HOMO-LUMO energy gaps ( $E_g$ ) of xanthone-carbazoles **5.39**–**5.46** vary from 2.66 to 3.04 eV. These values are larger than that of pentacene (1.85 eV),<sup>42</sup> but within the range (2.65–3.30 eV) of compounds that exhibit relatively high charge carrier mobility (see Chapter 1, page 39, Table 1.2). Unlike methoxyxanthenes **1.228** and **1.229** (Chapter 2) and xanthonoid hetero[5]acenes **4.12**–**4.14** (Chapter 4), which have weak fluorescence ( $\Phi_{em} \approx 10^{-3}$ ) (2-phenyl-4-methoxyxanthone **1.228i** is an exception:  $\Phi_{em} = 0.13$ ), xanthone-carbazole hybrid systems **5.39**–**5.46** exhibit moderate fluorescence quantum yields ( $\Phi_{em} = 0.18$ – $0.30$ ).

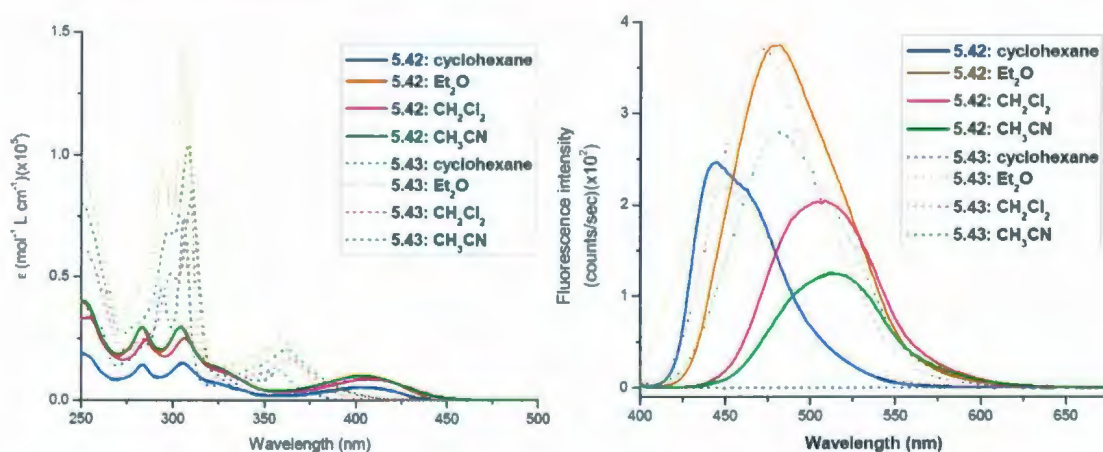
Table 5.8 Photophysical data of compounds 5.39–5.46.

Comp.	$\lambda_{\text{(abs)}}$ (nm) peak / edge	$\lambda_{\text{max (em)}}$ (nm)	$\lambda_{\text{t}}$ (cm <sup>-1</sup> )	$E_{\text{g}}$ (eV) ( = 1240 / $\lambda_{\text{edge}}$ )	$\Phi_{\text{em}}$
5.39	412 / 453	no fluorescence	-	2.74	-
5.40	412 / 453	no fluorescence	-	2.74	-
5.42	412 / 453	522	2560	2.74	0.18
5.43	365 / 421	482	3330	2.95	0.26
5.44	412 / 467	522	2560	2.66	0.30
5.41	366 / 421	486	3370	2.95	0.25
5.45	412 / 467	519	2500	2.66	0.26
5.46	366 / 408	485	3350	3.04	0.27

The absorption and emission spectra of the parent xanthone-carbazole systems **5.42** and **5.43** ( $R = \text{CH}_3$ ) were recorded in four different solvents, *i.e.* cyclohexane, diethyl ether, dichloromethane, and acetonitrile (Figure 5.12).<sup>43</sup> For the angular isomer **5.42**, the positions of the absorption maxima are almost the same in all four solvents ( $\lambda_{\text{max}} = 404\text{--}408\text{ nm}$ ). However, in the fluorescence spectra, red-shifts (36 nm, 28 nm, 3 nm) were observed along with the increase of solvent polarity from cyclohexane to diethyl ether, dichloromethane and acetonitrile, respectively. For the linear isomer **5.43**, the absorption maxima also spanned a small range ( $\lambda_{\text{max}} = 357\text{--}363\text{ nm}$ ): with cyclohexane and diethyl ether clustered at one end of the range ( $\lambda_{\text{max}} = 357\text{ nm}$ ), and dichloromethane and acetonitrile clustered at the other ( $\lambda_{\text{max}} = 362\text{--}363\text{ nm}$ ). Although linear isomer **5.43** exhibited no fluorescence in cyclohexane, it was fluorescent in the other three solvents,



whereupon solvatochromic red-shifts of 25 nm (from ether to dichloromethane) and 10 nm (from dichloromethane to acetonitrile) were observed (Figure 5.12, Table 5.9). The similarity of the magnitude of the red-shifts in the emission maxima observed for both angular and linear isomers in the same series of solvents did not support the notion of stronger charge transfer in the linear isomer that was suggested by the reorganization energies ( $\lambda_t$ ). However, the experiment confirmed that xanthone-carbazole hybrid systems do have charge transfer absorption bands.



**Figure 5.12** Absorption spectra (*left*) and emission spectra (*right*) of angular **5.42** (solid lines) and linear **5.43** (dotted lines) in cyclohexane, diethyl ether, dichloromethane, and acetonitrile ( $4 \times 10^{-5}$  M).

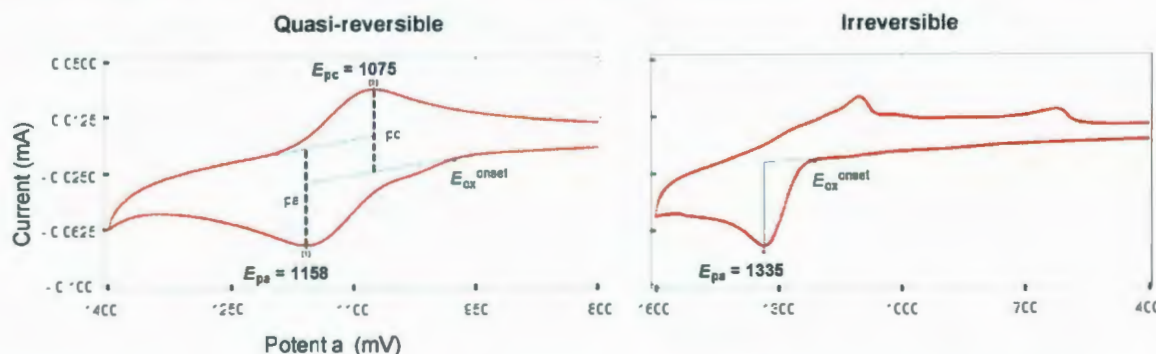
**Table 5.9** UV/Vis absorption and emission data for **5.42** and **5.43** in different solvents.

Comp.	Cyclohexane		Et <sub>2</sub> O		CH <sub>2</sub> Cl <sub>2</sub>		CH <sub>3</sub> CN	
	$\lambda_{\text{max}}$ (abs)	$\lambda_{\text{max}}$ (em)	$\lambda_{\text{max}}$ (abs)	$\lambda_{\text{max}}$ (em)	$\lambda_{\text{max}}$ (abs)	$\lambda_{\text{max}}$ (em)	$\lambda_{\text{max}}$ (abs)	$\lambda_{\text{max}}$ (em)
<b>5.42</b>	404	444	404	480	408	508	404	511
<b>5.43</b>	357	-	357	446	363	471	362	481



### Electrochemical properties.

The redox behaviour of the newly-synthesized xanthone-carbazole hybrid systems was also of interest. Cyclic voltammetry experiments of the angular and linear xanthone-carbazoles **5.42** and **5.43** ( $R = \text{CH}_3$ ) provided some interesting results (Figure 5.13).<sup>44</sup>



**Figure 5.13** Cyclic voltammograms of angular isomer **5.42** (left) and linear isomer **5.43** (right).

Solution of  $\text{Bu}_4\text{NBF}_4$  (0.1 M) in  $\text{CH}_2\text{Cl}_2:\text{CH}_3\text{CN}$  (4:1, v/v) was used as the supporting electrolyte. Pt wire was used as the counter electrode, glassy carbon as the working electrode, and Ag / AgCl as the reference.  $E_{\text{HOMO}} = -(4.4 + E_{\text{ox}}^{\text{onset}})$  eV.<sup>46</sup> Scan rate:  $500 \text{ V s}^{-1}$  (rt).

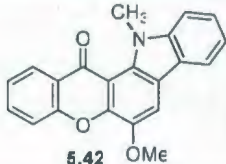
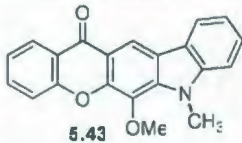
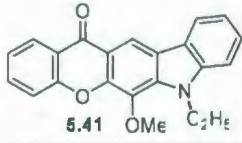
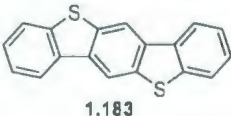
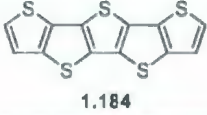
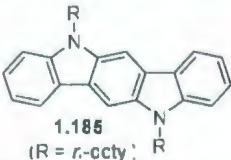
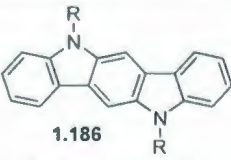
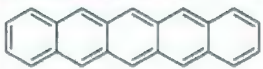
For the angular isomer **5.42**, one-electron oxidation ( $E_{\text{pa}}$ ) and one-electron reduction ( $E_{\text{pc}}$ ) peaks were observed at 1158 and 1075 mV, respectively. No other redox processes were observed within the scan range of 0–1400 mV. The separation between oxidation and reduction peaks of 83 mV (1158 – 1075 mV) and the ratio of peak currents ( $i_{\text{pa}} / i_{\text{pc}}$ ) of 1.36 mA ( $= 0.0420 / 0.0308 \text{ mA}$ ) are significantly larger than those for an ideal reversible one-electron process (59 mV and 1, respectively).<sup>45</sup> In other words, the angular isomer **5.42** exhibits quasi-reversible redox behaviour. On the other hand, the voltammogram of the linear isomer **5.43** contained only a one-electron oxidation peak

( $E_{pa}$ ) at 1335 mV in the scan range of 0–1600 mV. Thus, this compound has irreversible redox behaviour.

The HOMO energy levels ( $E_{HOMO}$ ) of **5.42** and **5.43**, as evaluated from the oxidation onset ( $E_{ox}^{onset}$ ),<sup>46</sup> are –5.37 and –5.60 eV, respectively (Table 5.10). These HOMO levels are lower than that of pentacene (–4.60 eV)<sup>47</sup>, pentathiophene **1.184** (–5.33 eV)<sup>35</sup> and of indolocarbazole **1.186** (–5.12 eV),<sup>48</sup> indicating a better oxidation stability for the xanthone-carbazole hybrid systems.

As discussed in Chapter 1, three important quantities that typically have an influence on the charge carrier mobility of an organic compound are the  $\pi$ – $\pi$  stacking distance ( $d$ ), the HOMO-LUMO energy gap ( $E_g$ ), and the HOMO energy levels ( $E_{HOMO}$ ). In the preceding sections, relevant data obtained for the xanthone-carbazole systems (X-ray packing motifs, optical properties (UV/Vis and fluorescence), and electrochemical properties (cyclic voltammetry) have been discussed and compared to data for pentacene and some hetero[5]acenes having relatively high charge carrier mobility. A full picture of the photophysical and electrochemical data of xanthone-carbazole hybrid systems **5.41–5.43**, pentacene **1.166** and selected hetero[5]acenes **1.183–1.186** is presented in Table 5.10.

**Table 5.10** Photophysical and electrochemical data for 5.41–5.43, selected hetero[5]acenes and pentacene.

Hetero[5]acenes	$E_{ox}$ (V) peak / onset	$\lambda_{(abs)}$ (nm) peak / edge	$E_{HOMO}$ (eV)	$E_g$ (eV)	$E_{LUMO}$ (eV)	$d$ (Å)	Mobility (cm <sup>2</sup> V <sup>-1</sup> s <sup>-1</sup> )
 5.42	1.16 / 0.97	412 / 453	-5.37	2.74	-2.63	3.37	-
 5.43	1.34 / 1.20	365 / 421	-5.60	2.95	-2.65	-	-
 5.41	-	366 / 421	-	2.95	-	3.40	-
 1.183	1.15 / 0.96	369 / 380	-5.8	3.3	-2.5	3.52	1 x 10 <sup>-2</sup>
 1.184	- / 1.12	358 / 388	-5.33	3.2	-2.04	3.50	4.5 x 10 <sup>-2</sup>
 1.185 (R = <i>n</i> -octyl)	-	428 / 468	-	2.65 (thin film)	-	3.49	0.3 x 10 <sup>-2</sup>
 1.186 (R = <i>p</i> -octylphenyl)	- / 0.75	415 / 442	-5.12	2.80 (thin film)	2.3	3.44	12 x 10 <sup>-2</sup>
 1.166	- / 0.64	- / 670	-4.60	1.85	-2.75	6.27	500 x 10 <sup>-2</sup>



In general, the xanthone-carbazole hybrid systems **5.41–5.43** fulfill the three “requirements” for high charge carrier mobility. Specifically, the interplanar distances in the crystal (3.37–3.40 Å) are less than 3.5 Å and both the HOMO-LUMO energy gaps (2.74–2.95 eV) and HOMO energy levels (–5.37, –5.60 eV) are similar to those of the indicated hetero[5]acenes. Moreover, compounds **5.41–5.43** are soluble in common solvents, which should facilitate processing and device fabrication. Further studies of these compounds in thin films and measurement of their charge carrier mobilities will be conducted in collaboration with other groups.

#### Aggregation studies.

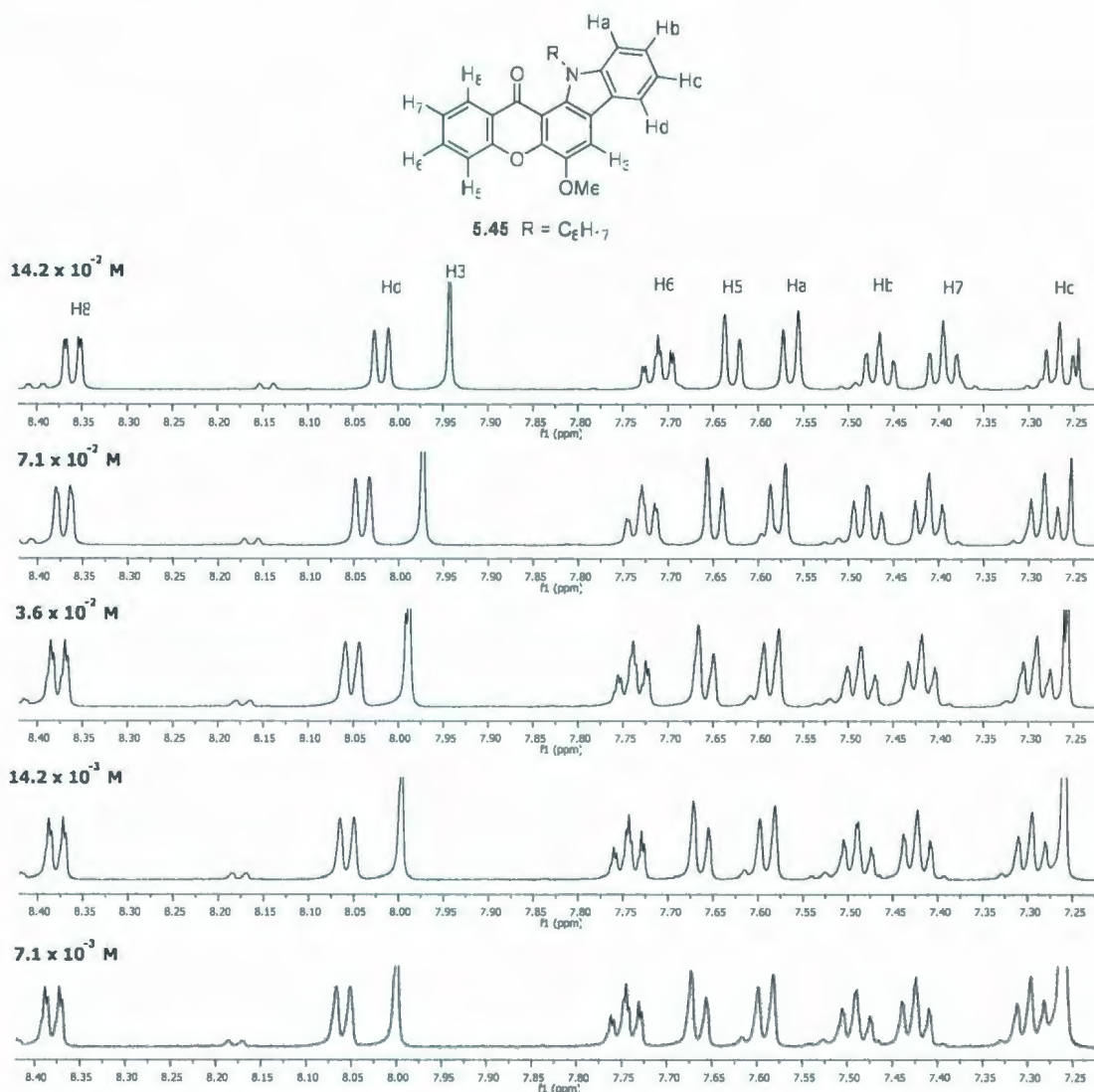
In general, the aggregation of a compound, if it occurs, depends on at least one of the following conditions: concentration, solvent, and temperature. Thus, to ascertain whether or not the xanthone-carbazole systems aggregate in solution, a concentration-dependent  $^1\text{H}$  NMR ( $\text{CDCl}_3$  as solvent) experiment was performed using the angular isomer **5.45** ( $\text{R} = \text{C}_8\text{H}_{17}$ ). Temperature- and solvent-dependent experiments were not performed, but would be worth including in future investigations.

A series of spectra were recorded over the concentration range  $7.1 \times 10^{-3}$  M to  $1.4 \times 10^{-1}$  M. The data show that the aromatic proton signals (Figure 5.14) and the protons of the methoxy group (Figure 5.15) in **5.45** were almost unchanged at concentrations of  $7.1 \times 10^{-3}$  M and  $1.4 \times 10^{-2}$  M, but they shifted progressively upfield at higher concentrations. The largest total upfield-shifts (from  $7.1 \times 10^{-3}$  M to  $7.1 \times 10^{-2}$  M) were observed for the protons on the bottom edge of the molecule, *i.e.*  $\text{H}_d$  (0.040 ppm),  $\text{H}_3$  (0.056 ppm),  $\text{H}_6$  (0.034 ppm),  $\text{H}_5$  (0.036 ppm),  $\text{H}_c$  (0.030 ppm) and  $\text{H}(\text{Me})$  (0.040 ppm)

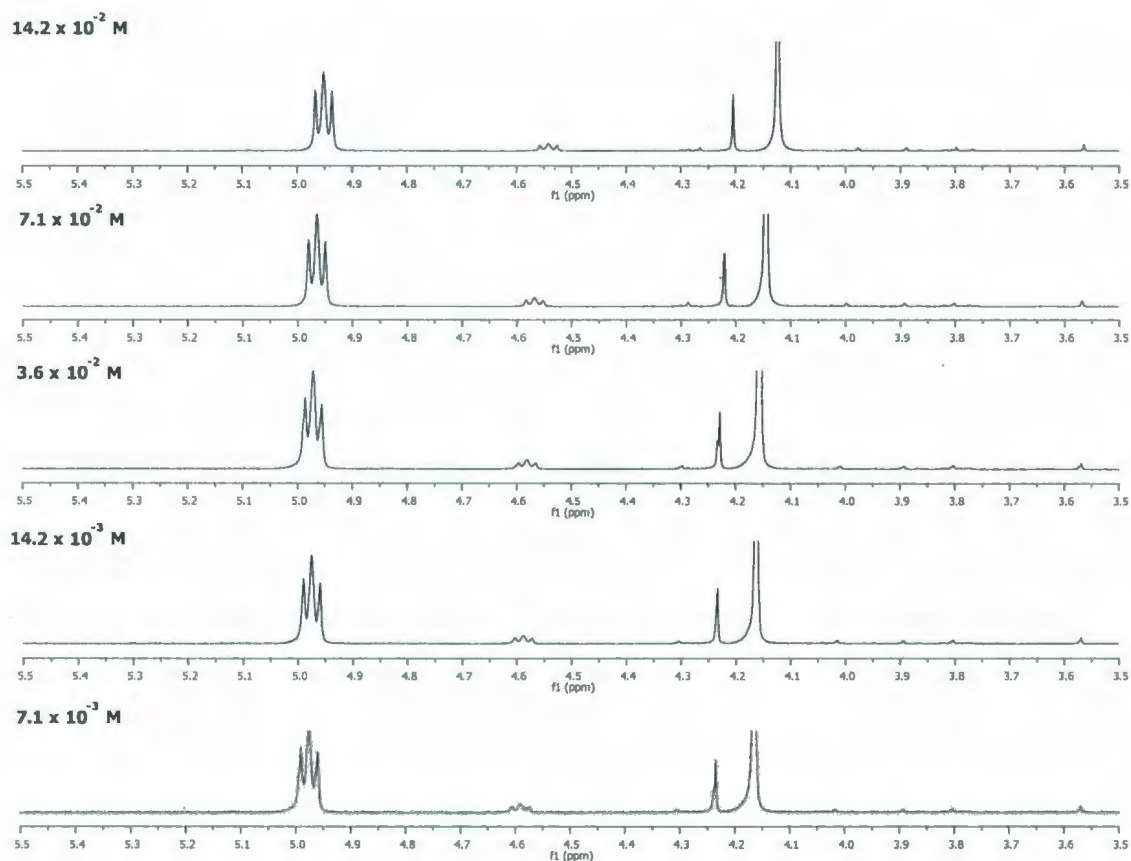


(see the experimental section for  $\Delta\delta$  shifts over whole concentration range, page 367).

The upfield shifts are consistent with aggregation by  $\pi$ -stacking (mutual shielding of aggregated molecules), but the small magnitude of the shifts and the relatively high concentration at which an upfield shift is observed suggest that the degree of aggregation is low.

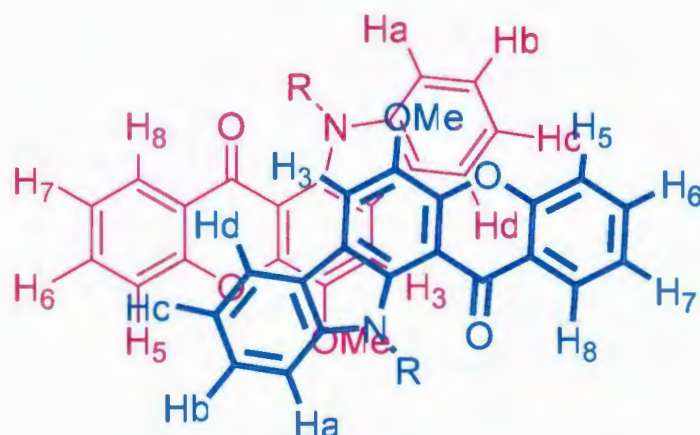


**Figure 5.14** Aromatic proton shifts in  $^1\text{H}$  NMR spectra of compound **5.45**.



**Figure 5.15** Proton shifts of methoxy group in  $^1\text{H}$  NMR spectra of compound 5.45.

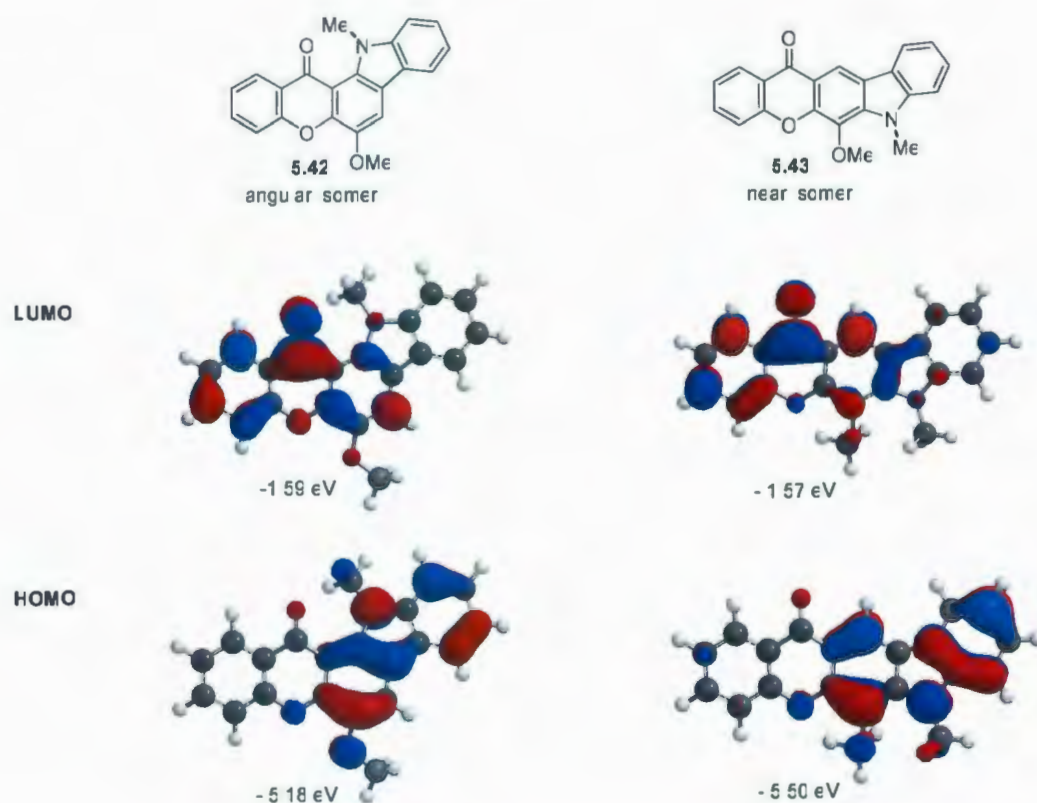
The observation that the upfield shifts are more pronounced for the protons on the bottom edge of the molecule indicates that the aggregation motif in solution might resemble the  $\pi$ -stacking motif observed in the crystal structure of the angular isomer 5.42 ( $\text{R} = \text{CH}_3$ ) (Figure 5.7 (the X-ray structure)). The offset *anti* relationship between neighbouring molecules (Figure 5.16) places the bottom edge protons of a molecule deeper in the shielding zone of a neighbouring molecule than the upper edge protons.



**Figure 5.16** Representative stacking of **5.45** based on aggregation studies.

#### Modeling studies.

One of key characteristics of the xanthone-carbazole hybrid system is its donor-acceptor nature. This feature is revealed in the HOMO and LUMO maps of **5.42** and **5.43** (Figure 5.17), which were obtained from DFT calculations (B3LYP/6-31G(d)//MMFF).<sup>49</sup> For the angular isomer **5.42**, the LUMO is completely localized on the xanthone unit, whereas for the linear isomer **5.43**, it extends slightly to the pyrrole ring. For both isomers, the HOMO is localized to the carbazole units. Interestingly, the central benzene ring has components in both the HOMO and the LUMO.



**Figure 5.17** HOMO and LUMO maps of **5.42** (*left*) and linear isomer **5.43** (*right*).

In summary, the physical properties of non-substituted xanthone-carbazole hybrid systems were studied via UV/Vis absorption, emission, fluorescence quantum yield, cyclic voltammetry, aggregation, and DFT calculations. All experiments provided useful information about the nature of these new hetero[5]acene frameworks. Based upon a comparison of the properties of the xanthone-carbazole systems with those of pentacene and other hetero[5]acenes that exhibit high charge carrier mobility, these compounds are expected to be good candidates for solid studies on their suitability for application in OLEDs or OFETs.

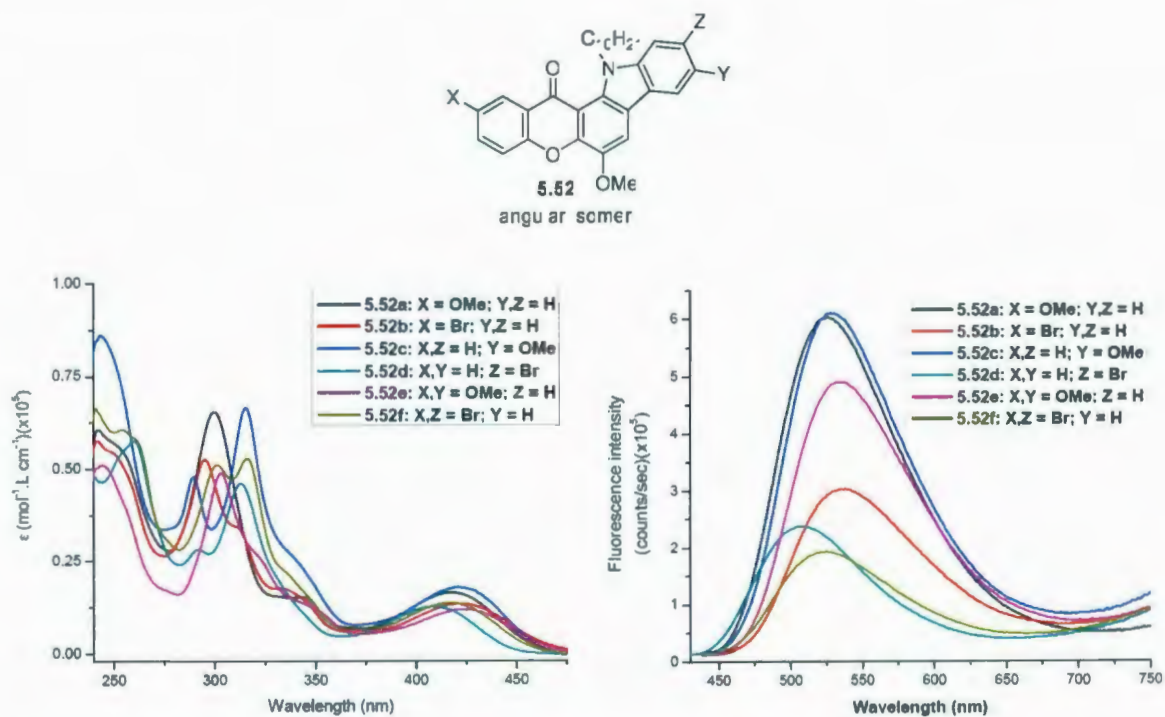


### 5.3.5.2 Physical Properties of Substituted Xanthone-Carbazole Hybrid Systems

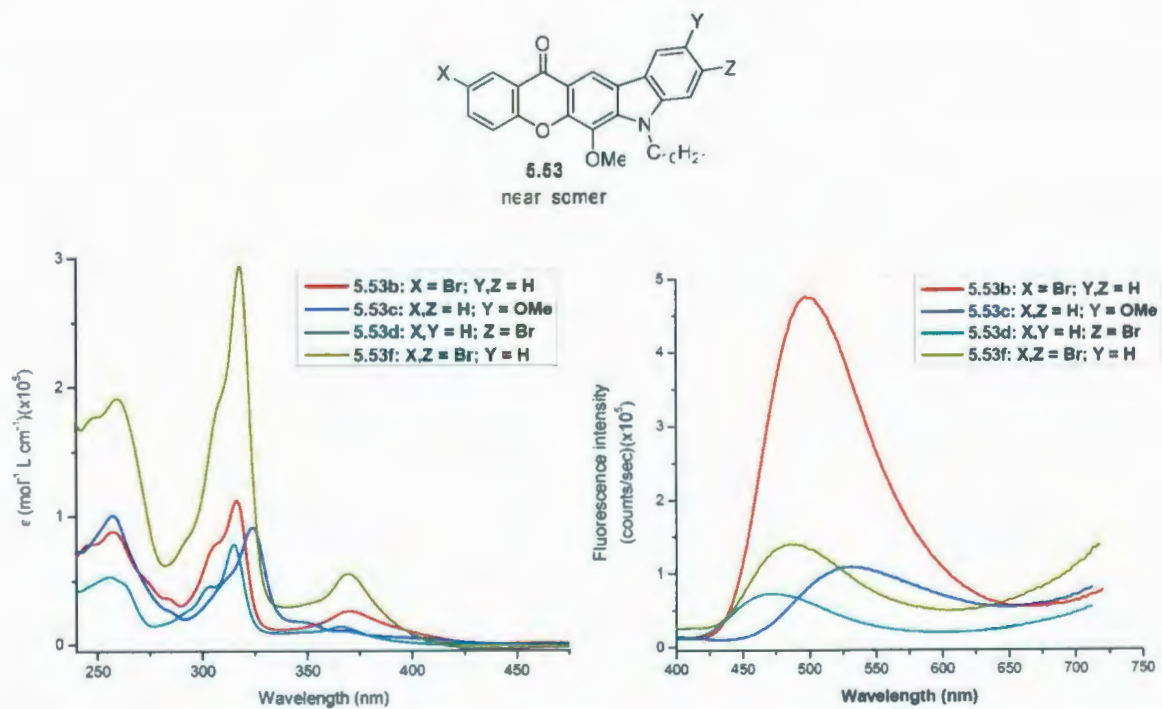
The optical properties of the substituted xanthone-carbazole hybrid systems, including the angular isomers **5.52a–f** and the linear isomers **5.53b–d,f**, were also studied. Their properties were compared with those of the non-substituted xanthone-carbazoles (parent systems), which were represented by the angular compound **5.70** ( $R = n\text{-C}_{10}\text{H}_{21}$ ) and the linear compound **5.56** ( $R = n\text{-C}_8\text{H}_{17}$ ).

All of the substituted angular derivatives **5.52a–f** have absorption maxima ( $\lambda_{\text{abs}} = 409\text{--}421\text{ nm}$ ) and emissions ( $\lambda_{\text{em}} = 508\text{--}538\text{ nm}$ ) that are similar to those of the parent compound **5.70** ( $\lambda_{\text{abs}} = 421\text{ nm}$ ,  $\lambda_{\text{em}} = 519\text{ nm}$ ) (Figure 5.18 and Table 5.11, Entry 1–7). In comparison to **5.70**, substituted compounds **5.52a–f** show very small red-shifts (6–19 nm) in fluorescence, but compound **5.52d**, which bears a bromo group on the carbazole moiety has blue-shift (11 nm) in both its absorption and emission spectra. It can be said that the substituents (OMe, Br) did not have any major effect on the optical properties of the angular xanthone-carbazole framework.

The substituted linear isomers **5.53b–d,f** behave similarly to the parent compound **5.56**, except for **5.53c**, which bear a methoxy group on carbazole moiety. In particular, compound **5.53c**, despite having an identical absorption maximum to the parent compound **5.56** ( $\lambda_{\text{abs}} = 366\text{ nm}$ ), exhibits emission at 532 nm, which is 46 nm red-shifted in comparison to **5.56** ( $\lambda_{\text{em}} = 485\text{ nm}$ ) (Figure 5.19 and Table 5.11, Entries 8–12).



**Figure 5.18** Absorption (*left*) and emission (*right*) spectra of angular isomers **5.52a–f**.



**Figure 5.19** Absorption (*left*) and emission (*right*) spectra of linear isomers **5.53b–d,f**.

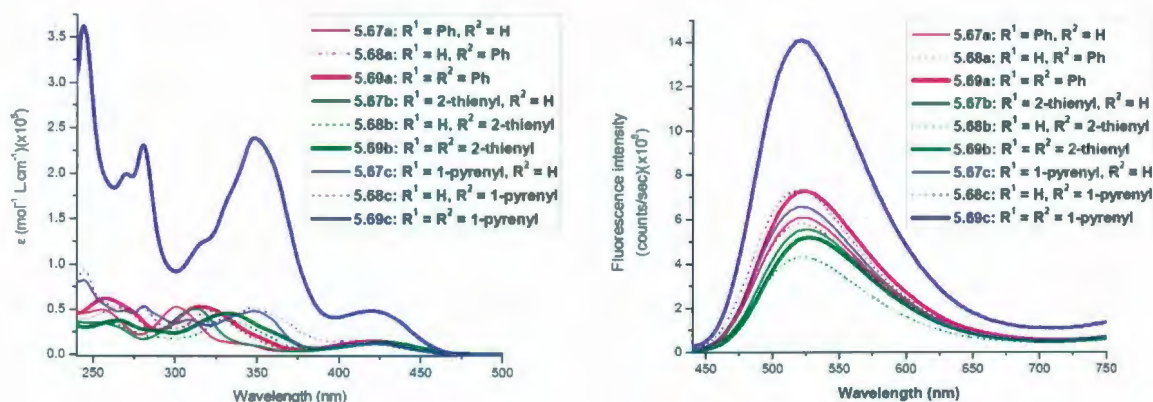
**Table 5.11** Photophysical data of substituted compounds **5.52** and **5.53** in comparison with their parent compound **5.70** and **5.46**, respectively.

Entry	Comp.	$\lambda_{\text{(abs)}} \text{ (nm)}$ peak / edge	$\lambda_{\text{max (em)}} \text{ (nm)}$	$\lambda_{\text{t}}$	$E_{\text{g}} \text{ (eV)}$ (= 1240 / $\lambda_{\text{edge}}$ )	$\Phi_{\text{em}}$
1	<b>5.70</b>	421 / 460	519	2240	2.70	0.32
2	<b>5.52a</b>	418 / 463	525	2440	2.68	0.25
3	<b>5.52b</b>	421 / 475	538	2580	2.61	0.16
4	<b>5.52c</b>	421 / 466	528	2410	2.66	0.32
5	<b>5.52d</b>	409 / 452	508	2380	2.74	0.18
6	<b>5.52e</b>	421 / 481	535	2530	2.56	0.16
7	<b>5.52f</b>	418 / 466	525	2440	2.66	0.05
8	<b>5.46</b>	366 / 408	485	3350	3.04	0.27
9	<b>5.53b</b>	370 / 432	497	3450	2.87	0.29
10	<b>5.53c</b>	366 / 410	532	4260	3.02	0.11
11	<b>5.53d</b>	366 / 410	474	3110	3.02	0.04
12	<b>5.53f</b>	369 / 402	486	3260	3.08	0.01

The reorganization energies ( $\lambda_{\text{t}}$ ) and the HOMO-LUMO energy gaps ( $E_{\text{g}}$ ) of the angular isomers **5.52** are smaller ( $\lambda_{\text{t}} = 2410\text{--}2580 \text{ cm}^{-1}$ ;  $E_{\text{g}} = 2.56\text{--}2.74 \text{ eV}$ ) than those of the linear ones **5.53** ( $\lambda_{\text{t}} = 3110\text{--}4260 \text{ cm}^{-1}$ ;  $E_{\text{g}} = 2.87\text{--}3.08 \text{ eV}$ ) (Table 5.11). These values are similar to those of the unsubstituted xanthone-carbazoles for both isomers. Moderate fluorescence quantum yields ( $\Phi_{\text{em}} = 0.16\text{--}0.32$ ) were observed for most of substituted xanthone-carbazoles. Compounds **5.53d**, **5.52f**, and **5.53f** which all have  $Z = \text{Br}$ , exhibit weak fluorescence quantum yields ( $\Phi_{\text{em}} = 1\text{--}5 \times 10^{-2}$ ).



The introduction of an electron-neutral phenyl group or electron-rich 2-thienyl and 1-pyrenyl groups into the xanthone-carbazole frameworks did not affect the properties of the systems significantly. For example, these aryl substituted compounds, *i.e.* **5.67–5.69**, have absorption maxima (415–427 nm) and emission maxima (519–528 nm) similar to those of the parent compound **5.70** ( $\lambda_{\text{abs}} = 421$  nm,  $\lambda_{\text{em}} = 519$  nm). In addition, both their reorganization energies ( $\lambda_t = 2150$ – $2470$ ) and HOMO-LUMO energy gaps ( $E_g = 2.61$ – $2.70$  eV) remain virtually the same as those of **5.70**. Moderate quantum yields ( $\Phi_{\text{em}} = 0.24$ – $0.37$ ) were measured for the series of aryl substituted compounds. The dipyrenyl substituted compound **5.69c** exhibits the strongest intensity in both its absorption and emission ( $\Phi_{\text{em}} = 0.37$ ) among the xanthone-carbazole systems, with or without substituents (Figure 5.20 and Table 5.12).



**Figure 5.20** Absorption (*left*) and emission (*right*) spectra of aryl substituted xanthone-carbazole hybrid systems **5.67–5.69**.



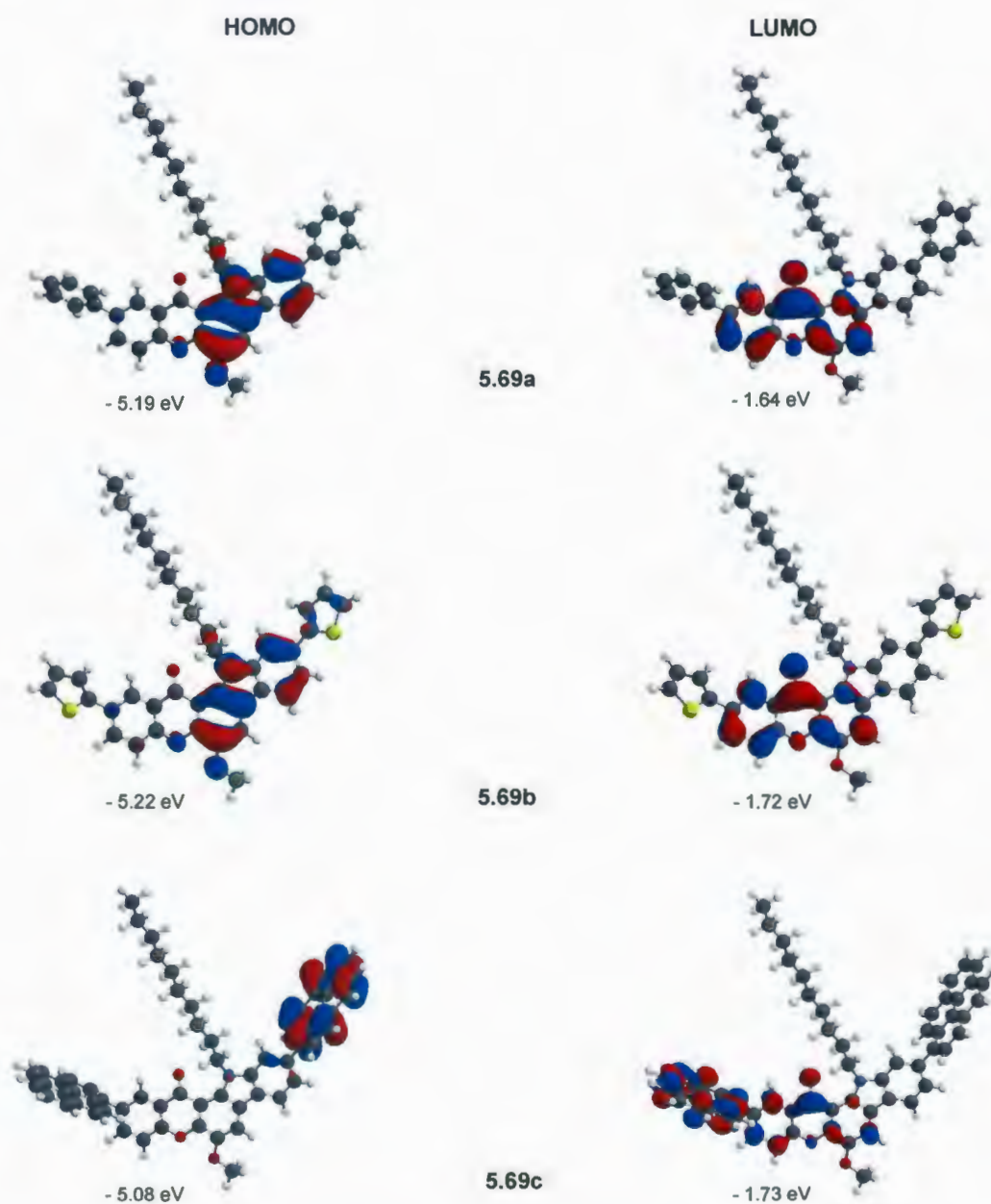
Table 5.12 Photophysical data of parent **5.70** and aryl-substituted compounds **5.67–5.69**.

Comp.	$\lambda_{\text{(abs)}} \text{ (nm)}$ peak / edge	$\lambda_{\text{max (em)}} \text{ (nm)}$	$\lambda_{\text{t}} \text{ (cm}^{-1}\text{)}$	$E_{\text{g}} \text{ (eV)}$ ( = 1240 / $\lambda_{\text{edge}}$ )	$\Phi_{\text{em}}$
<b>5.70</b>	421 / 460	519	2240	2.70	0.32
<b>5.67a</b>	419 / 468	522	2300	2.70	0.33
<b>5.68a</b>	416 / 469	521	2440	2.65	0.34
<b>5.69a</b>	421 / 475	526	2280	2.64	0.34
<b>5.67b</b>	421 / 470	528	2370	2.61	0.28
<b>5.68b</b>	419 / 466	523	2460	2.64	0.24
<b>5.69b</b>	427 / 476	528	2150	2.66	0.27
<b>5.67c</b>	420 / 468	522	2440	2.61	0.30
<b>5.68c</b>	415 / 470	519	2470	2.65	0.35
<b>5.69c</b>	420 / 460	521	2270	2.64	0.37

Density functional theory (DFT) calculations of all of the substituted xanthone-carbazole hybrid systems were carried out at the B3LYP/6-31G(d)//MMFF level.<sup>42</sup> The aryl-substituted compounds **5.67–5.69** have HOMO energy levels (–5.08 to –5.22 eV) that are slightly higher than those of the non-substituted ones (–5.18 to –5.48 eV). By comparison, the HOMO energy levels of methoxy- or bromo-substituted xanthone-carbazoles vary from –5.07 to –5.73 eV. In all of the xanthone-carbazole compounds, with or without substituents, their HOMOs are localized on the carbazole moiety while the LUMOs are limited to the xanthone moiety. Therefore, the substituents seem to have little or no influence on the core properties of the xanthone-carbazole framework. It thus appears that there is little interaction between the different  $\pi$  systems. One exception is

the dipyrenyl substituted compound **5.69c**, the HOMO of which is only on the pyrenyl group attached to the carbazole unit, and the LUMO of which is spread over the xanthone moiety and the pyrenyl group bonded to it (Figure 5.21). This suggests that the pyrenyl group can act as either a donor or acceptor in the molecule, depending on the part of the molecule to which it is attached. However, compound **5.69c** also has similar optical properties to the other members of its family.

In brief, UV/Vis absorption, fluorescence, and modeling studies were carried out for xanthone-carbazole hybrid systems bearing methoxy, bromo, phenyl, 2-thienyl, and 1-pyrenyl substituents. The studies show most of the substituted angular and linear isomers have physical properties similar to those of their corresponding parent compounds **5.70** and **5.56**, respectively. Only the linear isomer **5.53c**, which bears a methoxy group on carbazole moiety, has green fluorescence ( $\lambda_{em} = 532$  nm) while its analogs have blue fluorescence ( $\lambda_{em} = 474\text{--}486$  nm). Among the xanthone-carbazole systems, angular isomer **5.52e** has smallest energy gap ( $E_g = 2.56$  eV) and the dipyrenyl substituted compound **5.69c** has the greatest fluorescence quantum yield ( $\Phi_{em} = 0.37$ ). A full picture of the quantum yields of all of xanthone-carbazoles is presented in Figure 5.22.



**Figure 5.21** HOMO (*left*) and LUMO (*right*) maps of 5.69a–c.



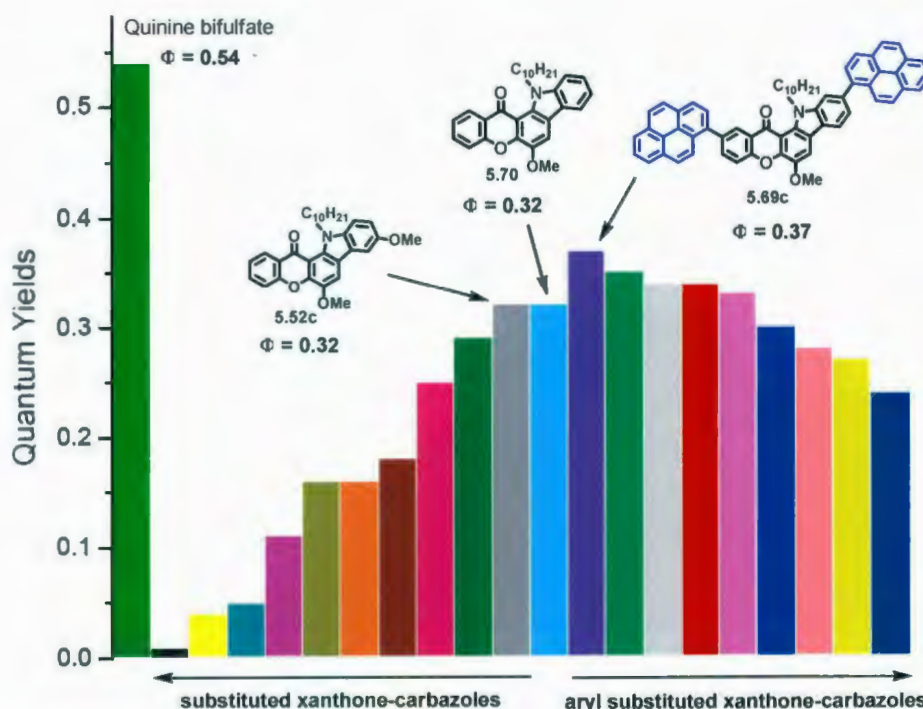


Figure 5.22 Quantum yields of substituted xanthone-carbazoles and the parent compound 5.70.

#### 5.4 Conclusions and Proposal for Future Work

All objectives / targets of this research, namely the design, synthesis, and study of the physical properties a new class of hetero[5]acenes (xanthone-carbazole hybrid systems) were accomplished.

First, the approach to the new xanthone-carbazole systems was designed to proceed through a 4-methoxyxanthone using the new methodology described in Chapter 2, which involves an IEDDA-driven domino reaction. The *o*-nitrophenyl group on the xanthone system was the utilized (without the need for any synthetic manipulation) to form carbazole unit via a microwave-assisted Cadogan reaction.

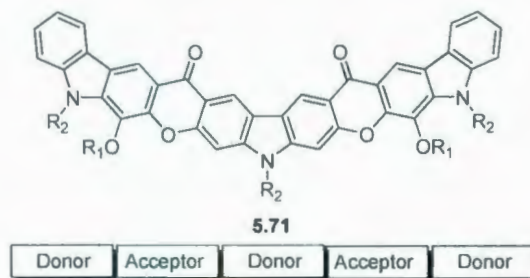
Second, the target structures, including non-substituted xanthone-carbazoles and substituted ones, were successfully synthesized in good-to-excellent yields via four or



five step sequences. Seven nitrophenylxanthenes were used to produce a family of 24 new donor-acceptor xanthone-carbazole hybrid systems. As predicted, two constitutional isomers, dubbed angular and linear, were obtained from the Cadogan reactions, in which the angular isomers are the major products in all cases. In addition, a series of 9 new aryl-substituted xanthone-carbazole systems (aryl = phenyl-, 2-thienyl-, and 1-pyrenyl) was also obtained in good-to-excellent yields via Suzuki coupling from the corresponding bromo-substituted xanthone-carbazole compounds.

Third, the physical properties of all of the newly-synthesized xanthone-carbazole compounds were studied using UV/Vis spectroscopy, fluorescence spectroscopy, cyclic voltammetry,  $^1\text{H}$  NMR spectroscopy, and computational methods. On the basis of the results, the following conclusions about the new hetero[5]acene frameworks could be drawn: (1) all angular isomers have green fluorescence while most of the linear ones have blue fluorescence; (2) all xanthone-carbazoles have relatively small energy gaps (2.56–3.08 eV); (3) the parent compounds **5.52** and **5.53** ( $\text{R} = \text{CH}_3$ ) have low-lying HOMO levels (–5.37 to –5.60 eV), and the others are expected to be similar; (4) most of the xanthone-carbazoles exhibit moderate quantum yields ( $\Phi_{\text{em}} = 0.16\text{--}0.37$ ); (5) all substituents investigated little or no influence on the optical properties of the xanthone-carbazole systems. In addition, X-ray crystallographic analysis showed a small interplanar distance (3.28–3.43 Å) for the parent compounds. In comparison to pentacene and hetero[5]acenes that are known to possess high charge carrier mobilities, the properties of the new xanthone-carbazole hybrid systems render them good candidates for the investigation of their suitability for applications in OLEDs and FETs.

Future work will focus on the study of the parent compounds in the solid state. This will require collaboration with another group and will include the measurement of charge carrier mobilities. If good results are obtained, the larger donor-acceptor system such as **5.71** (Figure 5.23) will be the next target.



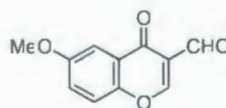
**Figure 5.23** Future target structure **5.71**.

## 5.5 Experimental Section

General methods and instrumentation are identical to those described in Chapter 2 (Memorial University) and in Chapter 4 (University of Mainz). In addition, a Shimadzu UV-2501PC instrument and a Perkin-Elmer LS50B Luminescence Spectrometer were used for UV/Vis and fluorescence measurements, respectively, at the University of Mainz.

### 5.5.1 Experiment Procedures<sup>50</sup>

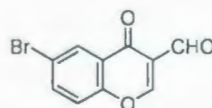
#### 6-Methoxy-3-formylchromone (**5.34a**)<sup>51</sup>



To a clear solution of 2'-hydroxy-5'-methoxyacetophenone (**5.35**) (4.01 g, 24.1 mmol) in DMF (19 mL) was added dropwise phosphorus(V) oxychloride (14.7 g, 95.9 mmol) at 0 °C. The resulting solution was stirred at room temperature for 4 d. The

reaction mixture was poured into ice-cold water (400 mL) and vigorously stirred for 30 min. The yellow precipitate was collected by suction filtration, washed several times with H<sub>2</sub>O and dried in air. The crude product was purified by recrystallization (EtOAc) or column chromatography (2:98 EtOAc:CH<sub>2</sub>Cl<sub>2</sub>) to yield **5.34a** (2.82 g, 58%) or (3.91 g, 80%), respectively, as a yellow solid:  $R_f$  = 0.41 (35:65 EtOAc:hexanes); mp 164–165 °C (lit. mp<sup>52</sup> 163–165 °C); <sup>1</sup>H NMR (500 MHz)  $\delta$  10.41 (s, 1H), 8.53 (s, 1H), 7.65 (d,  $J$  = 3.1 Hz, 1H), 7.48 (d,  $J$  = 9.8 Hz, 1H), 7.33 (dd,  $J$  = 8.8, 3.1 Hz, 1H), 3.93 (s, 1H); <sup>13</sup>C NMR (125 MHz)  $\delta$  189.0, 176.1, 160.4, 158.2, 151.2, 126.4, 124.7, 120.2, 119.9, 105.7, 56.3; MS [APCI (+)]  $m/z$  (%) 205 ([M+H]<sup>+</sup>, 100).

#### 6-Bromo-3-formylchromone (**5.34b**)<sup>51</sup>



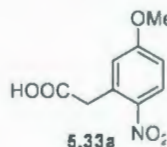
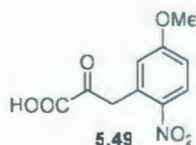
To a clear solution of 5'-bromo-2'-hydroxyacetophenone (**5.35b**) (7.53 g, 35.2 mmol) in DMF (28 mL) was added dropwise phosphorus(V) oxychloride (21.5 g, 140 mmol) at 0 °C. The resulting solution was stirred at room temperature for 4 d. The reaction mixture was poured into ice-cold water (400 mL) and vigorously stirred for 30 min. The yellow precipitate was collected by suction filtration, washed several times with H<sub>2</sub>O and dried in air. The crude product was purified by recrystallization (EtOH) or column chromatography (2:98 EtOAc:CH<sub>2</sub>Cl<sub>2</sub>) to yield diene **5.34b** (5.84 g, 66%) or (7.77 g, 88%), respectively, as a yellow solid:  $R_f$  = 0.39 (35:65 EtOAc:hexanes); mp 191–192 °C (lit. mp<sup>53</sup> 190–193 °C); <sup>1</sup>H NMR (500 MHz)  $\delta$  10.37 (s, 1H), 8.54 (s, 1H), 8.42 (d,  $J$  = 2.3 Hz, 1H), 7.84 (dd,  $J$  = 8.8, 2.7 Hz, 1H), 7.45 (d,  $J$  = 8.8 Hz, 1H); <sup>13</sup>C NMR



(125 MHz)  $\delta$  188.3, 174.9, 160.8, 155.2, 138.0, 129.1, 126.9, 120.7, 120.6, 120.57; MS [APCI (+)]  $m/z$  (%) 255 ( $^{81}\text{Br}$ ,  $[\text{M}+\text{H}]^+$ , 100), 253 ( $^{79}\text{Br}$ ,  $[\text{M}+\text{H}]^+$ , 85).

**3-(5-Methoxy-2-nitrophenyl)-2-oxopropanoic acid (**5.49**)**<sup>26,54</sup>

**2-(5-Methoxy-2-nitrophenyl)acetic acid (**5.33a**)**<sup>26,54</sup>



To a clear solution of 3-methyl-4-nitroanisole **5.47** (3.02 g, 18.1 mmol) and diethyl oxalate **5.48** (5.26 g, 36.0 mmol) in toluene (5 mL), at 0 °C, was added dropwise a potassium ethoxide solution prepared from potassium (1.41 g, 36.1 mmol) and EtOH (6 mL) in Et<sub>2</sub>O (20 mL). The resulting red solution was stirred at below 10 °C for 3 h, then heated at 40–50 °C for a further 2 h. The dark purple precipitate was collected by suction filtration and washed with Et<sub>2</sub>O. The solids were dissolved in water (100 mL), and aqueous 2 M NaOH (10 mL) was added to give a red solution, which was washed again with Et<sub>2</sub>O. The solution was acidified with aqueous 6 M HCl (pH = 1–2) and extracted with CH<sub>2</sub>Cl<sub>2</sub>. The organic layer was dried over MgSO<sub>4</sub> and filtered. The solvent was removed under reduced pressure to afford crude **5.49** (4.24 g) as a yellow solid, which was used in the next step without further purification.

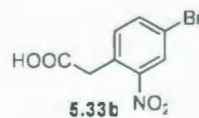
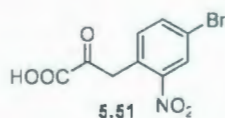
To a red solution of crude **5.49** (4.24 g) in 0.5 M NaOH (40 mL) was added H<sub>2</sub>O<sub>2</sub> (10%) at 0 °C until a persistent yellow color was obtained. The resulting yellow mixture was stirred at 0 °C for 30 min and acidified with 6 M HCl solution. The precipitates were collected by suction filtration, washed with H<sub>2</sub>O, and dried in air. The crude product was



purified by recrystallization (EtOAc) to yield **5.33a** (3.28 g, 86%) as light yellow crystals: mp 177–178 °C (EtOAc) (Lit. mp<sup>54</sup> 177 °C (EtOH / H<sub>2</sub>O)) ; <sup>1</sup>H NMR (500 MHz, DMSO)  $\delta$  12.50 (s, 1H), 8.15 (d,  $J$  = 8.6 Hz, 1H), 7.12 (d,  $J$  = 3.2 Hz, 1H), 7.07 (dd,  $J$  = 9.1, 2.3 Hz, 1H), 3.99 (s, 2H), 3.88 (s, 3H); <sup>13</sup>C NMR (125 MHz, DMSO)  $\delta$  171.2, 163.1, 141.4, 133.8, 127.6, 118.8, 113.2, 56.1 (CH<sub>2</sub> signal is overlap with solvent peaks); MS [APCI (-)]  $m/z$  (%) 166 ([M – COOH]<sup>+</sup>, 100).

**3-(4-Bromo-2-nitrophenyl)-2-oxopropanoic acid (5.51)**<sup>26,54</sup>

**2-(4-Bromo-2-nitrophenyl)acetic acid (5.33b)**<sup>26,54</sup>

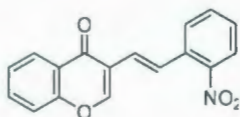


To a clear solution of 4-bromo-1-methyl-2-nitrobenzene (**5.50**) (1.01 g, 4.67 mmol) and diethyl oxalate (1.35 g, 9.26 mmol) in toluene (5 mL) at 0 °C was added dropwise a potassium ethoxide solution prepared from potassium (360 mg, 9.26 mmol) and EtOH (3 mL) in Et<sub>2</sub>O (15 mL). The resulting red solution was stirred at below 10 °C for 3 h and then heated at 40–50 °C for a further 2 h. The resulting dark purple precipitate was collected by suction filtration and washed with Et<sub>2</sub>O. The solids were dissolved in water (100 mL), and aqueous 2 M NaOH (10 mL) was added to give a red solution, which was washed again with Et<sub>2</sub>O. The solution was acidified with aqueous 6 M HCl (pH = 1–2) and extracted with CH<sub>2</sub>Cl<sub>2</sub>. The organic layer was dried over MgSO<sub>4</sub> and filtered. The solvent was removed under reduced pressure to afford crude **5.51** (1.11 g) as a yellow solid, which was used in the next step without further purification.

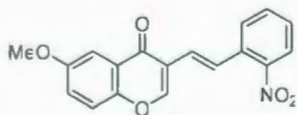
To a red solution of crude **5.51** (1.11 g) in aqueous 0.5 M NaOH (20 mL) was added H<sub>2</sub>O<sub>2</sub> (10%) at 0 °C until a yellow color persisted. The resulting yellow mixture was stirred at 0 °C for 30 min and acidified with aqueous 6 M HCl. The precipitate was collected by suction filtration, washed with H<sub>2</sub>O, and dried in air. The crude product was purified by column chromatography (50:50 EtOAc:CH<sub>2</sub>Cl<sub>2</sub>) to yield **5.33b** (870 mg, 74% for two steps) as a light yellow solid: mp 167–168 °C (Lit. mp<sup>26a</sup>: not reported); <sup>1</sup>H NMR (500 MHz, DMSO)  $\delta$  12.63 (s, 1H), 8.26 (d,  $J$  = 2.6 Hz, 1H), 7.94 (dd,  $J$  = 8.2, 2.1 Hz, 1H), 7.52 (d,  $J$  = 8.3 Hz, 1H), 3.98 (s, 2H); <sup>13</sup>C NMR (125 MHz, DMSO)  $\delta$  170.9, 149.3, 136.4, 135.3, 129.8, 127.2, 120.3, 38.3; MS [APCI (-)]  $m/z$  (%) 214 ([M–COOH]<sup>–</sup>, 100).

#### General procedure for synthesis of dienes (**5.32a–f**)

A mixture of the 3-formylchromone derivatives (1.0 equiv.), the *o*-nitrophenylacetic acid derivative (1.1–1.5 equiv.), and potassium *tert*-butoxide (95%, 1.0 equiv.) in anhydrous pyridine (20 mL) was heated at reflux until the 3-formylchromone was consumed completely (tlc analysis). The reaction mixture was cooled to room temperature, poured into ice-cold water, and acidified with aqueous 6 M HCl (pH = 1–2). The precipitate was collected by suction filtration, washed several times with H<sub>2</sub>O, and dried in air. In case the particles were very small, the aqueous solution was extracted with EtOAc, dried over MgSO<sub>4</sub>, filtered, and concentrated. The crude product was purified by column chromatography to yield the desired dienes **5.32a–f** as yellow solids.

**(E)-3-(2-Nitrostyryl)-4H-chromen-4-one (5.37)**

A mixture of 3-formylchromone **2.19** (383 mg, 2.20 mmol), *o*-nitrophenylacetic acid (**5.36**) (597 mg, 3.30 mmol), and potassium *tert*-butoxide (246 mg, 2.19 mmol) in anhydrous pyridine (20 mL) was heated at reflux for 24 h and worked up according to the general procedure. Column chromatography (2:98 EtOAc:CH<sub>2</sub>Cl<sub>2</sub>) of the crude product yielded **5.37** (551 mg, 85%) as a yellow solid: *R*<sub>f</sub> = 0.55 (2:98 EtOAc:CH<sub>2</sub>Cl<sub>2</sub>); mp 188–189 °C (lit. mp<sup>55</sup> 194–195 °C); <sup>1</sup>H NMR (500 MHz) δ 8.30 (dd, *J* = 8.1, 1.5 Hz, 1H), 8.21 (s, 1H), 7.97 (dd, *J* = 8.3, 1.2 Hz, 1H), 7.90 (d, *J* = 16.1 Hz, 1H), 7.78 (d, *J* = 7.5 Hz, 1H), 7.70 (td, *J* = 6.9, 1.6 Hz, 1H), 7.62 (t, *J* = 7.5 Hz, 1H), 7.49 (d, *J* = 8.0 Hz, 1H), 7.46–7.41 (m, 2H), 7.07 (d, *J* = 16.7 Hz, 1H); <sup>13</sup>C NMR (125 MHz) δ 176.5, 156.2, 153.6, 148.2, 134.0, 133.4, 133.3, 128.7, 128.4, 126.5, 126.2, 125.7, 124.9, 124.2, 121.8, 118.4 (one signal fewer than expected); MS [APCI (+)] *m/z* (%) 294 (*M*<sup>+</sup>, 100).

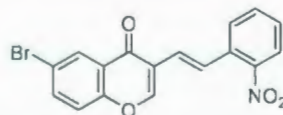
**(E)-6-Methoxy-3-(2-nitrostyryl)-4H-chromen-4-one (5.32a)**

A mixture of 6-methoxy-3-formylchromone **5.34a** (257 mg, 1.26 mmol), *o*-nitrophenylacetic acid (342 mg, 1.89 mmol), and potassium *tert*-butoxide (149 mg, 1.26 mmol) in anhydrous pyridine (20 mL) was heated at reflux for 1.75 h and worked up according to the general procedure. Column chromatography (20:80 EtOAc:hexanes) yielded **5.32a** (336 mg, 83%) as a yellow solid: *R*<sub>f</sub> = 0.44 (35:65 EtOAc:hexanes); mp



152–153 °C; IR  $\nu$  3069 (w), 2929 (w), 2845 (w), 1647 (s), 1624 (s), 1600 (s), 1572 (m), 1512 (s), 1484 (s), 1450 (s), 1356 (s), 1321 (s), 1279 (s), 1192 (s), 1142 (s), 1029 (s), 954 (s), 811 (s), 777 (s), 733 (s), 711 (s) ( $\text{cm}^{-1}$ );  $^1\text{H}$  NMR (500 MHz)  $\delta$  8.19 (s, 1H), 7.97 (dd,  $J = 8.3, 0.8$  Hz, 1H), 7.93 (d,  $J = 16.8$  Hz, 1H), 7.79 (d,  $J = 8.4$  Hz, 1H), 7.65 (d,  $J = 3.0$  Hz, 1H), 7.62 (t,  $J = 7.4$  Hz, 1H), 7.44–7.40 (m, 2H), 7.28 (dd,  $J = 8.9, 3.2$  Hz, 1H), 7.07 (d, 16.6 Hz, 1H), 3.92 (s, 3H);  $^{13}\text{C}$  NMR (125 MHz)  $\delta$  176.3, 157.4, 153.5, 151.1, 148.2, 133.35, 133.31, 128.7, 128.4, 126.0, 124.9, 124.88, 124.4, 124.1, 120.9, 119.8, 105.5, 56.2; MS [APCI (+)]  $m/z$  (%) 324 ( $\text{M}^+$ , 100); HRMS [EI (+)] calcd for  $\text{C}_{18}\text{H}_{13}\text{NO}_5$  323.0794, found 323.0797.

**(*E*)-6-Bromo-3-(2-nitrostyryl)-4*H*-chromen-4-one (5.32b)**

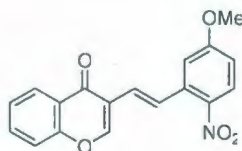


A mixture of 6-bromo-3-formylchromone **5.34b** (557 mg, 2.20 mmol), *o*-nitrophenylacetic acid (598 mg, 3.30 mmol), and potassium *tert*-butoxide (260 mg, 2.19 mmol) in anhydrous pyridine (20 mL) was heated at reflux for 3 h and worked up according to the general procedure. Column chromatography (10:90 EtOAc:hexanes) yielded **5.32b** (647 mg, 79%) as a yellow solid:  $R_f = 0.65$  (35:65 EtOAc:hexanes); mp 232–233 °C; IR  $\nu$  3000 (w), 2943 (m), 2863 (m), 1627 (s), 1596 (s), 1475 (m), 1463 (m), 1450 (s), 1436 (s), 1390 (m), 1358 (m), 1269 (s), 1217 (m), 1166 (s), 1038 (s), 1010 (s), 976 (m), 878 (s), 804 (s), 774 (s), 763 (s), 752 (s), 703 (s) ( $\text{cm}^{-1}$ );  $^1\text{H}$  NMR (500 MHz)  $\delta$  8.42 (d,  $J = 1.8$  Hz, 1H), 8.20 (s, 1H), 7.99 (dd,  $J = 8.2, 1.1$  Hz, 1H), 7.88 (d,  $J = 16.0$  Hz, 1H), 7.77 (dd,  $J = 9.0$  Hz, 1H), 7.62 (t,  $J = 7.3$  Hz, 1H), 7.45–7.42 (m, 1H), 7.39 (d,  $J$

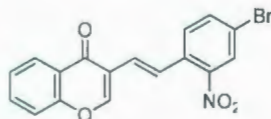


= 8.5 Hz, 1H), 7.04 (d,  $J$  = 15.9 Hz, 1H);  $^{13}\text{C}$  NMR (125 MHz)  $\delta$  175.2, 155.0, 153.5, 148.2, 137.0, 133.5, 133.1, 129.1, 128.8, 128.6, 126.8, 125.5, 125.0, 123.7, 122.0, 120.3, 119.2; MS [APCI (+)]  $m/z$  (%) 374 ( $^{81}\text{Br}$ ,  $\text{M}^+$ , 100), 372 ( $^{79}\text{Br}$ ,  $\text{M}^+$ , 97); HRMS [EI (+)] calcd for  $\text{C}_{17}\text{H}_{10}\text{BrNO}_4$  370.9793, found 372.9785 ( $^{81}\text{Br}$ , 98), 370.9798 ( $^{79}\text{Br}$ , 100).

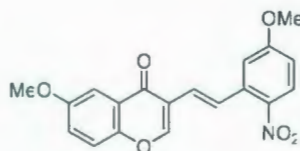
**(*E*)-3-(5-methoxy-2-nitrostyryl)-4*H*-chromen-4-one (5.32c)**



A mixture of 3-formylchromone (**2.19**) (221 mg, 1.27 mmol), 5-methoxy-2-nitrophenylacetic acid (**5.33a**) (304 mg, 1.44 mmol), and potassium *tert*-butoxide (150 mg, 1.27 mmol) in anhydrous pyridine (20 mL) was heated at reflux for 3 h and worked up according to the general procedure. Column chromatography (1:99 EtOAc:CH<sub>2</sub>Cl<sub>2</sub>) yielded **5.32c** (361 mg, 88%) as a yellow solid:  $R_f$  = 0.39 (1:99 EtOAc:CH<sub>2</sub>Cl<sub>2</sub>); mp 158–159 °C; IR  $\nu$  3087 (w), 3050 (w), 2947 (w), 2842 (w), 1649 (s), 1634 (s), 1606 (s), 1574 (s), 1562 (s), 1505 (s), 1463 (s), 1349 (s), 1319 (s), 1296 (s), 1198 (s), 1165 (s), 1033 (s), 964 (m), 815 (m), 752 (s) (cm<sup>-1</sup>);  $^1\text{H}$  NMR (500 MHz)  $\delta$  8.30 (dd,  $J$  = 8.3, 1.5 Hz, 1H), 8.24 (s, 1H), 8.09 (d,  $J$  = 9.4 Hz, 1H), 7.97 (d,  $J$  = 16.0 Hz, 1H), 7.72–7.68 (m, 1H), 7.50 (d,  $J$  = 8.8 Hz, 1H), 7.45 (t,  $J$  = 7.6 Hz, 1H), 7.16 (d,  $J$  = 3.4 Hz, 1H), 7.04 (d,  $J$  = 15.7 Hz, 1H), 6.89 (dd,  $J$  = 9.6, 2.5 Hz, 1H), 3.95 (s, 3H);  $^{13}\text{C}$  NMR (125 MHz)  $\delta$  176.5, 163.5, 156.3, 153.4, 141.2, 136.5, 134.0, 127.8, 127.4, 126.5, 125.7, 124.3, 123.9, 121.9, 118.4, 113.9, 113.3, 56.2; MS [APCI (+)]  $m/z$  (%) 324 ( $\text{M}^+$ , 100); HRMS [CI (+)] calcd for  $\text{C}_{18}\text{H}_{13}\text{NO}_5 + \text{H}^+$  324.0872, found 324.0864.

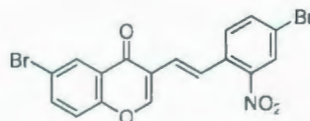
**(E)-3-(4-bromo-2-nitrostyryl)-4H-chromen-4-one (5.32d)**

A mixture of 3-formylchromone **2.19** (221 mg, 1.27 mmol), 4-bromo-2-nitrophenylacetic acid (**5.33a**) (354 mg, 1.44 mmol), and potassium *tert*-butoxide (150 mg, 1.27 mmol) in anhydrous pyridine (20 mL) was heated at reflux for 1.5 h and worked up according to the general procedure. Column chromatography (1:99 EtOAc:CH<sub>2</sub>Cl<sub>2</sub>) yielded **5.32d** (365 mg, 78%) as a yellow solid: *R*<sub>f</sub> = 0.56 (1:99 EtOAc:CH<sub>2</sub>Cl<sub>2</sub>); mp 173–174 °C; IR  $\nu$  3092 (w), 3031 (w), 2970 (w), 2848 (w), 1738 (s), 1726 (m), 1653 (s), 1627 (w), 1614 (m), 1573 (w), 1550 (m), 1516 (s), 1463 (s), 1341 (s), 1217 (s), 1180 (m), 1141 (m), 1031 (w), 965 (m), 848 (m), 771 (s), 755 (s), 693 (s) (cm<sup>-1</sup>); <sup>1</sup>H NMR (500 MHz)  $\delta$  8.30 (dd, *J* = 8.2, 1.6 Hz, 1H), 8.20 (s, 1H), 8.12 (d, *J* = 2.0 Hz, 1H), 7.88 (d, *J* = 16.8 Hz, 1H), 7.74–7.68 (m, 2H), 7.65 (d, *J* = 7.7 Hz, 1H), 7.49 (d, *J* = 9.1 Hz, 1H), 7.47–7.43 (m, 1H), 7.05 (d, *J* = 15.6 Hz, 1H); <sup>13</sup>C NMR (125 MHz)  $\delta$  176.4, 156.1, 153.9, 148.3, 136.4, 134.1, 132.2, 129.9, 127.9, 126.6, 125.8, 125.3, 125.0, 124.2, 121.5, 118.4 (one signal fewer than expected); MS [APCI (+)] *m/z* (%) 374 (<sup>81</sup>Br, M<sup>+</sup>, 100), 372 (<sup>79</sup>Br, M<sup>+</sup>, 88); HRMS [EI (+)] calcd for C<sub>17</sub>H<sub>10</sub><sup>79</sup>BrNO<sub>2</sub> 370.9793, found 372.9780 (<sup>81</sup>Br, 98), 370.9800 (<sup>79</sup>Br, 100).

**(E)-6-Methoxy-3-(5-methoxy-2-nitrostyryl)-4H-chromen-4-one (5.32e)**

A mixture of 6-methoxy-3-formylchromone (**5.34a**) (259 mg, 1.27 mmol), 4-methoxy-2-nitrophenylacetic acid (**5.33a**) (304 mg, 1.44 mmol), and potassium *tert*-butoxide (150 mg, 1.27 mmol) in anhydrous pyridine (20 mL) was heated at reflux for 2.5 h and worked up according to the general procedure. Column chromatography (1:99 EtOAc:CH<sub>2</sub>Cl<sub>2</sub>) yielded **5.32e** (384 mg, 86%) as a yellow solid: *R<sub>f</sub>* = 0.39 (2:98 EtOAc:CH<sub>2</sub>Cl<sub>2</sub>); mp 184–185 °C; IR  $\nu$  2960 (w), 2841 (w), 1651 (s), 1614 (m), 1606 (m), 1572 (s), 1503 (s), 1482 (s), 1442 (s), 1346 (s), 1331 (s), 1297 (s), 1281 (s), 1204 (s), 1189 (m), 1146 (m), 1084 (s), 1028 (s), 955 (m), 870 (m), 818 (s), 751 (m), 708 (s) (cm<sup>-1</sup>); <sup>1</sup>H NMR (500 MHz)  $\delta$  8.21 (s, 1H), 8.08 (d, *J* = 8.5 Hz, 1H), 8.00 (d, *J* = 16.3 Hz, 1H), 7.64 (d, *J* = 2.6 Hz, 1H), 7.43 (d, *J* = 9.2 Hz, 1H), 7.28 (dd, *J* = 8.9, 3.7 Hz, 1H), 7.15 (d, *J* = 3.3 Hz, 1H), 7.03 (d, *J* = 16.2 Hz, 1H), 6.89 (dd, *J* = 8.9, 2.8 Hz, 1H), 3.94 (s, 3H), 3.92 (s, 3H); <sup>13</sup>C NMR (125 MHz)  $\delta$  176.3, 163.5, 157.4, 153.4, 151.0, 141.1, 136.5, 127.8, 127.2, 124.8, 124.1 (2C), 120.9, 119.8, 113.8, 113.2, 105.4, 56.2, 56.17; MS [APCI (+)] *m/z* (%) 354 (M<sup>+</sup>, 100); HRMS [EI (+)] calcd for C<sub>19</sub>H<sub>15</sub>NO<sub>6</sub> 353.0899, found 353.0897.



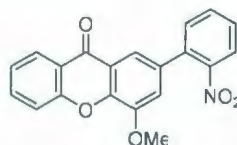
**(E)-6-Bromo-3-(4-bromo-2-nitrostyryl)-4H-chromen-4-one (5.32f)**

A mixture of 6-bromo-3-formylchromone (**5.34b**) (321 mg, 1.27 mmol), 4-bromo-2-nitrophenylacetic acid (**5.33b**) (354 mg, 1.44 mmol), and potassium *tert*-butoxide (150 mg, 1.27 mmol) in anhydrous pyridine (20 mL) was heated at reflux for 1.0 h and worked up according to the general procedure. Column chromatography (2:98 EtOAc:CH<sub>2</sub>Cl<sub>2</sub>) yielded **5.32f** (448 mg, 78%) as a yellow solid:  $R_f = 0.57$  (2:98 EtOAc:CH<sub>2</sub>Cl<sub>2</sub>); mp 273–274 °C; IR  $\nu$  3086 (w), 3053 (w), 2848 (w), 1645 (s), 1620 (m), 1605 (m), 1558 (m), 1547 (s), 1516 (s), 1463 (s), 1437 (s), 1337 (s), 1252 (s), 1163 (s), 1127 (s), 1062 (m), 977 (s), 837 (s), 787 (s), 758 (s), 723 (s) (cm<sup>-1</sup>); <sup>1</sup>H NMR (500 MHz)  $\delta$  8.42 (d,  $J = 2.8$  Hz, 1H), 8.19 (s, 1H), 8.13 (d,  $J = 1.9$  Hz, 1H), 7.86 (d,  $J = 16.0$  Hz, 1H), 7.78 (dd,  $J = 8.7, 2.7$  Hz, 1H), 7.74 (dd,  $J = 8.4, 1.9$  Hz, 1H), 7.64 (d,  $J = 7.8$  Hz, 1H), 7.39 (d,  $J = 8.7$  Hz, 1H), 7.02 (d,  $J = 16.1$  Hz, 1H); <sup>13</sup>C NMR (150 MHz, {<sup>1</sup>H} CPMAS (cross-polarization under magic angle spinning), using 100 kHz of <sup>1</sup>H decoupling and 62.5 kHz for the Hartmann-Hahn matching condition. The spectrum was collected at room temperature (298 K) with a spinning rate  $\nu = 20$  kHz and 10240 scans)  $\delta$  174.4, 157.7, 153.8, 146.6, 138.0, 136.9, 135.4, 134.2, 131.0, 127.2, 126.3, 122.1, 119.1 (four signals fewer than expected); MS [APCI (+)]  $m/z$  (%) 454 (<sup>81</sup>Br<sub>2</sub>, M<sup>+</sup>, 48%), 452 (<sup>79</sup>Br<sup>81</sup>Br, M<sup>+</sup>, 100), 450 (<sup>79</sup>Br<sub>2</sub>, M<sup>+</sup>, 51%); HRMS [CI (+)] calcd for C<sub>17</sub>H<sub>9</sub>Br<sub>2</sub>NO<sub>4</sub>+H<sup>+</sup> 449.8877, found 449.8978.



**General procedure for synthesis of 4-methoxy-2-*o*-nitrophenylxanthenes (5.31a–f)**

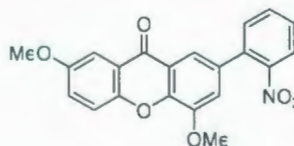
A mixture of aqueous 60% dimethoxyacetaldehyde (0.90 mL, 10 mmol) and pyrrolidine (0.83 mL, 10 mmol) in benzene (30 mL) was heated at reflux with a Barrett apparatus for 3 h. The freshly prepared solution of 1-(2,2-dimethoxyvinyl)pyrrolidine (*ca.* 0.2 M, 10 equiv.) was cooled to room temperature and the diene (1.0 equiv.) was added in one portion as a solid. The resulting orange mixture was heated at reflux until the diene was consumed completely (tlc analysis). The reaction mixture was cooled to room temperature and the solvent was removed under reduced pressure. The residue was dissolved in CH<sub>2</sub>Cl<sub>2</sub>, washed with aqueous 1M HCl (2 x 20 mL), dried over MgSO<sub>4</sub>, and filtered. The solvent was removed under reduced pressure and the residue was purified by column chromatography to yield the desired xanthenes **5.31a–f**.

**4-Methoxy-2-(2-nitrophenyl)-9H-xanthene-9-one (5.38)**

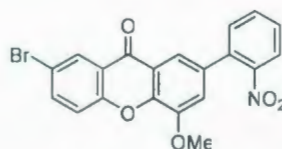
A mixture of freshly prepared enamine **1.225** (*ca.* 80.0 mmol) and diene **5.37** (2.55 g, 8.69 mmol) was heated at reflux for 44 h and worked up according to the general procedure. Column chromatography (CH<sub>2</sub>Cl<sub>2</sub>) yielded xanthone **5.38** (2.44 g, 81%) as a yellow solid: *R<sub>f</sub>* = 0.45 (CH<sub>2</sub>Cl<sub>2</sub>); mp 184–185 °C; IR  $\nu$  1656 (s), 1569 (s), 1514 (s), 1465 (s), 1374 (s), 1342 (s), 1322 (s), 1217 (s), 1092 (s), 887 (m), 784 (m), 765 (s) (cm<sup>-1</sup>); <sup>1</sup>H NMR (500 MHz),  $\delta$  8.35 (dd, *J* = 7.6, 1.8 Hz, 1H), 7.95 (d, *J* = 8.5 Hz, 1H), 7.90 (d, *J* = 18 Hz, 1H), 7.87–7.75 (m, 1H), 7.69–7.64 (m, 2H), 7.55 (t, *J* = 7.4 Hz, 2H), 7.42

(t,  $J = 7.5$  Hz, 1H); 7.14 (d,  $J = 2.0$  Hz, 1H), 4.03 (s, 3H);  $^{13}\text{C}$  NMR (125 MHz)  $\delta$  177.0, 156.2, 149.0, 146.8, 135.5, 135.2, 133.3, 132.9, 132.5, 129.0, 126.9, 124.6, 123.0, 122.0, 118.6, 117.2, 115.3, 56.8; MS [APCI (+)]  $m/z$  (%) 348 ( $\text{M}^+$ , 100); HRMS [EI (+)] calcd for  $\text{C}_{20}\text{H}_{13}\text{NO}_5$  347.0794, found 347.0787.

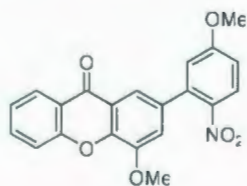
#### 4,7-Dimethoxy-2-(2-nitrophenyl)-9H-xanthene-9-one (5.31a)



A mixture of freshly prepared enamine **1.225** (ca. 10.0 mmol) and diene **5.32a** (323 mg, 1.00 mmol) was heated at reflux for 20 h and worked up according to the general procedure. Column chromatography (30:70 EtOAc:hexanes) yielded xanthone **5.31a** (280 mg, 74%) as a yellow solid:  $R_f = 0.21$  (35:65 EtOAc:hexanes); mp 219–220 °C; IR  $\nu$  3069 (w), 3019 (w), 2928 (w), 2851 (w), 1644 (s), 1617 (m), 1601 (m), 1569 (m), 1520 (s), 1477 (s), 1437 (s), 1355 (s), 1289 (s), 1206 (s), 1157 (s), 1017 (s), 997 (s), 866 (s), 834 (s), 785 (s), 751 (s) ( $\text{cm}^{-1}$ );  $^1\text{H}$  NMR (500 MHz),  $\delta$  7.95 (d,  $J = 8.3$  Hz, 1H), 7.90 (d,  $J = 1.1$  Hz, 1H), 7.71 (d,  $J = 3.3$  Hz, 1H), 7.67 (t,  $J = 7.5$  Hz, 1H), 7.59 (d,  $J = 8.3$  Hz, 1H), 7.56–7.53 (m, 2H), 7.36 (dd,  $J = 9.6$  Hz, 3.1 Hz, 1H); 7.12 (d,  $J = 1.2$  Hz, 1H), 4.02 (s, 3H), 3.93 (s, 3H);  $^{13}\text{C}$  NMR (125 MHz)  $\delta$  176.9, 156.5, 151.0, 149.3, 149.0, 146.7, 135.6, 133.1, 132.8, 132.5, 128.9, 125.3, 124.5, 122.29, 122.26, 120.0, 117.2, 115.0, 105.9, 56.8, 56.2; MS [APCI (+)]  $m/z$  (%) 378 ( $\text{M}^+$ , 100); HRMS [EI (+)] calcd for  $\text{C}_{21}\text{H}_{15}\text{NO}_6$  377.0899, found 377.0923.

**7-Bromo-4-methoxy-2-(2-nitrophenyl)-9H-xanthene-9-one (5.31b)**

A mixture of freshly prepared enamine **1.225** (*ca.* 9.60 mmol) and diene **5.32b** (357 mg, 960  $\mu$ mol) was heated at reflux for 20 h and worked up according to the general procedure. Column chromatography (20:80 EtOAc:hexanes) yielded xanthone **5.31b** (402 mg, 98%) as a yellow solid:  $R_f$  = 0.65 (35:65 EtOAc:hexanes); mp 262–263 °C; IR  $\nu$  3086 (w), 2943 (w), 1663 (s), 1618 (m), 1595 (m), 1567 (m), 1514 (s), 1495 (s), 1464 (s), 1446 (s), 1350 (s), 1312 (s), 1279 (s), 1262 (s), 1214 (s), 1092 (s), 869 (m), 826 (s), 785 (s), 766 (s) ( $\text{cm}^{-1}$ );  $^1\text{H}$  NMR (500 MHz),  $\delta$  8.47 (d,  $J$  = 2.1 Hz, 1H), 7.97 (d,  $J$  = 8.2 Hz, 1H), 7.88 (d,  $J$  = 2.0 Hz, 1H), 7.84 (dd,  $J$  = 8.7 Hz, 2.7 Hz, 1H), 7.69 (t,  $J$  = 7.5 Hz, 1H), 7.58–7.53 (m, 3H), 7.15 (d,  $J$  = 2.2 Hz, 1H); 4.02 (s, 3H);  $^{13}\text{C}$  NMR (125 MHz)  $\delta$  175.8, 155.0, 149.2, 149.0, 146.6, 138.1, 135.4, 133.8, 132.9, 132.4, 129.4, 129.1, 124.6, 123.2, 122.6, 120.6, 117.8, 117.2, 115.6, 56.8; MS [APCI (+)]  $m/z$  (%) 426 ( $^{79}\text{Br}$ ,  $\text{M}^+$ , 100), 428 ( $^{81}\text{Br}$ ,  $\text{M}^+$ , 89); HRMS [EI (+)] calcd for  $\text{C}_{20}\text{H}_{12}^{79}\text{BrNO}_5$  424.9899, found 424.9897.

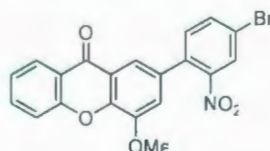
**4-Methoxy-2-(5-methoxy-2-nitrophenyl)-9H-xanthene-9-one (5.32c)**

A mixture of freshly prepared enamine **1.225** (*ca.* 10.0 mmol) and diene **5.31c** (291 mg, 900  $\mu$ mol) was heated at reflux for 2.5 h and worked up according to the



general procedure. Column chromatography ( $\text{CH}_2\text{Cl}_2$ ) yielded xanthone **5.32c** (327 mg, 96%) as a yellow solid:  $R_f = 0.41$  (1:99 EtOAc:  $\text{CH}_2\text{Cl}_2$ ); mp 222–223 °C; IR  $\nu$  3086 (w), 2944 (w), 2841 (w), 1667 (m), 1657 (s), 1608 (s), 1597 (s), 1582 (s), 1572 (s), 1496 (s), 1468 (s), 1327 (s), 1268 (s), 1253 (s), 1102 (m), 1091 (m), 1018 (m), 984 (s), 865 (s), 762 (s) ( $\text{cm}^{-1}$ );  $^1\text{H}$  NMR (500 MHz),  $\delta$  8.36 (dd,  $J = 8.1$  Hz, 1.6 Hz, 1H), 8.08 (d,  $J = 8.4$  Hz, 1H), 7.88 (d,  $J = 2.4$  Hz, 1H), 7.78–7.75 (m, 1H), 7.65 (d,  $J = 8.4$  Hz, 1H), 7.42 (t,  $J = 7.5$  Hz, 1H), 7.12 (d,  $J = 1.9$  Hz, 1H); 6.99 (dd,  $J = 9.3$  Hz, 3.0 Hz, 1H), 6.93 (d,  $J = 2.2$  Hz, 1H), 4.02 (s, 3H), 3.94 (s, 3H);  $^{13}\text{C}$  NMR (125 MHz)  $\delta$  177.1, 163.0, 156.2, 148.8, 146.7, 141.9, 138.6, 135.2, 134.2, 127.6, 126.9, 124.6, 122.9, 122.0, 118.6, 117.4, 116.9, 115.5, 114.0, 56.9, 56.3; MS [APCI (+)]  $m/z$  (%) 378 ( $\text{M}^+$ , 100); HRMS [EI (+)] calcd for  $\text{C}_{21}\text{H}_{15}\text{NO}_6$  377.0899, found 377.0896.

#### 4-Methoxy-2-(4-bromo-2-nitrophenyl)-9H-xanthene-9-one (**5.31d**)

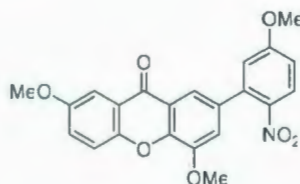


A mixture of freshly prepared enamine **1.225** (ca. 10.0 mmol) and diene **5.32d** (335 mg, 900  $\mu\text{mol}$ ) was heated at reflux for 2 h and worked up according to the general procedure. Column chromatography ( $\text{CH}_2\text{Cl}_2$ ) yielded xanthone **5.31d** (329 mg, 86%) as a yellow solid:  $R_f = 0.30$  ( $\text{CH}_2\text{Cl}_2$ ); mp 254–255 °C; IR  $\nu$  3095 (w), 2997 (w), 2942 (w), 2840 (w), 1657 (s), 1612 (s), 1594 (s), 1572 (w), 1553 (m), 1521 (s), 1495 (s), 1464 (s), 1440 (s), 1372 (s), 1340 (s), 1322 (s), 1296 (s), 1273 (s), 1216 (s), 1182 (s), 1146 (s), 1093 (s), 983 (s), 875 (s), 839 (s), 758 (s) ( $\text{cm}^{-1}$ );  $^1\text{H}$  NMR (500 MHz),  $\delta$  8.35 (dd,  $J = 8.3$



Hz, 1.7 Hz, 1H), 8.09 (d,  $J = 2.1$  Hz, 1H), 7.87 (d,  $J = 2.1$  Hz, 1H), 7.81–7.75 (m, 2H), 7.64 (d,  $J = 8.5$  Hz, 1H), 7.43–7.41 (m, 2H), 7.09 (d,  $J = 2.0$  Hz, 1H); 4.02 (s, 3H);  $^{13}\text{C}$  NMR (125 MHz)  $\delta$  176.9, 156.1, 149.5, 149.1, 146.9, 135.9, 135.3, 134.4, 133.7, 132.2, 127.5, 126.9, 124.7, 123.0, 122.2, 121.9, 118.6, 117.2, 115.0, 56.9; MS [APCI (+)]  $m/z$  (%) 428 ( $^{81}\text{Br}$ ,  $\text{M}^+$ , 85), 426 ( $^{79}\text{Br}$ ,  $\text{M}^+$ , 100); HRMS [EI (+)] calcd for  $\text{C}_{20}\text{H}_{12}^{79}\text{BrNO}_5$  424.9899, found 424.9904.

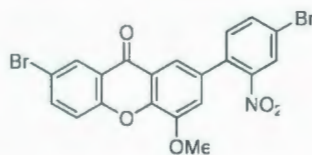
#### 4,7-Dimethoxy-2-(5-methoxy-2-nitrophenyl)-9H-xanthene-9-one (5.32e)



A mixture of freshly prepared enamine **1.225** (ca. 10.0 mmol) and diene **5.31e** (353 mg, 1.00 mmol) was heated at reflux for 3.5 h and worked up according to the general procedure. Column chromatography (1:99 EtOAc: $\text{CH}_2\text{Cl}_2$ ) yielded xanthone **5.32e** (333 mg, 82%) as a yellow solid:  $R_f = 0.47$  (2:98 EtOAc: $\text{CH}_2\text{Cl}_2$ ); mp 272–273 °C; IR  $\nu$  3068 (w), 2996 (w), 2955 (w), 2839 (w), 1652 (s), 1615 (s), 1570 (s), 1509 (s), 1477 (s), 1449 (s), 1336 (s), 1311 (s), 1294 (s), 1273 (s), 1243 (s), 1208 (s), 1154 (s), 1106 (s), 1026 (s), 936 (m), 868 (s), 818 (s), 787 (s), 732 (s) ( $\text{cm}^{-1}$ );  $^1\text{H}$  NMR (500 MHz),  $\delta$  8.08 (d,  $J = 9.6$  Hz, 1H), 7.99 (s, 1H), 7.71 (d,  $J = 2.5$  Hz, 1H), 7.59 (d,  $J = 9.6$  Hz, 1H), 7.37 (dd,  $J = 9.1, 2.8$  Hz, 1H), 7.01 (s, 1H), 6.99 (d,  $J = 8.9$  Hz, 1H); 6.94 (d,  $J = 1.9$  Hz, 1H), 4.02 (s, 3H), 3.94 (s, 6H);  $^{13}\text{C}$  NMR (125 MHz)  $\delta$  176.9, 162.9, 156.5, 151.0, 148.8, 146.7, 141.9, 138.7, 134.0, 127.5, 125.3, 122.3, 122.2, 120.0, 117.4, 116.8, 115.1, 114.0,

106.0, 56.8, 56.3, 56.2; MS [APCI (+)]  $m/z$  (%) 408 ( $M^+$ , 100); HRMS [EI (+)] calcd for  $C_{22}H_{17}NO_7$  407.1005, found 407.1003.

**7-Bromo-4-methoxy-2-(4-bromo-2-nitrophenyl)-9H-xanthene-9-one (5.32f)**

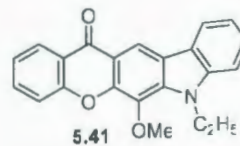
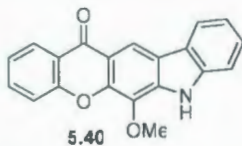
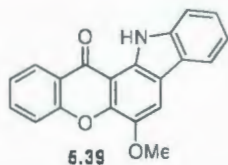


A mixture of freshly prepared enamine **1.225** (*ca.* 10.0 mmol) and diene **5.31f** (451 mg, 1.00 mmol) was heated at reflux for 2 h and worked up according to the general procedure. Column chromatography ( $CH_2Cl_2$ ) yielded xanthone **5.32f** (285 mg, 56%) as a yellow solid:  $R_f$  = 0.55 ( $CH_2Cl_2$ ); mp 283–284 °C; IR  $\nu$  3086 (w), 2936 (w), 2845 (w), 1647 (s), 1604 (s), 1558 (m), 1530 (s), 1465 (s), 1441 (s), 1417 (s), 1358 (s), 1338 (s), 1311 (s), 1287 (s), 1272 (s), 1213 (s), 1173 (s), 1047 (s), 826 (s), 788 (s), 708 (s) ( $cm^{-1}$ );  $^1H$  NMR (500 MHz)  $\delta$  8.46 (d,  $J$  = 1.9 Hz, 1H), 8.10 (d,  $J$  = 1.7 Hz, 1H), 7.85 (d,  $J$  = 1.9 Hz, 1H), 7.81 (td,  $J$  = 9.1, 2.1 Hz, 2H), 7.54 (d,  $J$  = 9.0 Hz, 1H), 7.41 (d,  $J$  = 8.2 Hz, 1H), 7.10 (d,  $J$  = 2.1 Hz, 1H), 4.02 (s, 3H);  $^{13}C$  NMR (125 MHz)  $\delta$  175.7, 154.9, 146.5, 149.1, 138.2, 136.0, 134.2, 133.6, 132.7, 129.4, 127.6, 123.2, 122.68, 122.4, 120.6, 117.9, 117.1, 115.3, 56.9; MS [APCI (+)]  $m/z$  (%) 508 ( $^{81}Br_2$ ,  $M^+$ , 43), 506 ( $^{79}Br^{81}Br$ ,  $M^+$ , 100), 504 ( $^{79}Br_2$ ,  $M^+$ , 53); HRMS [EI (+)] calcd for  $C_{20}H_{11}Br_2NO_5$  504.8909, found 504.8908.

**1'-H-Indole[2',3'-a]-4-methoxy-9H-xanthene-9-one (5.39)**<sup>56</sup>

**1'-H-Indole[3',2'-b]-4-methoxy-9H-xanthene-9-one (5.40)**

**1'-Ethyl-1'-H-indole[3',2'-b]-4-methoxy-9H-xanthene-9-one (5.41)**



4-Methoxy-2-(2-nitrophenyl)-9H-xanthene-9-one (**5.38**) (100.4 mg, 0.289 mmol) was suspended in triethyl phosphite (6 mL) and chloroform (2 mL) in a microwave reaction tube. The solution was heated three times for 15 minutes up to 210 °C with a maximum irradiation power of 300 W. Excess triethyl phosphite and the byproduct, triethyl phosphate, were removed by bulb-to-bulb vacuum distillation at 140 °C. A mixture of products **5.39** (61.9 mg, 68%), **5.40** (8.7 mg, 9%), and **5.41** (8.4 mg, 8%) were isolated through repeated column chromatography (petroleum ether:EtOAc:CH<sub>2</sub>Cl<sub>2</sub> 8:1:2 and petroleum ether:CH<sub>2</sub>Cl<sub>2</sub> 1:1) as yellow solids.

**5.39:**  $R_f$  = 0.52 (petroleum ether:EtOAc:CH<sub>2</sub>Cl<sub>2</sub> 8:1:2); mp 265–270 °C; IR (ATR)  $\nu$  3430 (w), 3360 (w), 3061 (w), 3036 (w), 2943 (w), 2845 (w), 2362 (w), 2351 (w), 1645 (s), 1598 (s), 1573 (m), 1497 (s), 1466 (s), 1444 (m), 1391 (m), 1332 (s), 1317 (s), 1275 (s), 1234 (s), 1220 (m), 1211 (s), 1198 (m), 1167 (m), 1156 (m), 1113 (m), 976 (m), 901 (m), 877 (m), 862 (m), 760 (s), 729(s), 687(s) (cm<sup>-1</sup>); <sup>1</sup>H NMR (400 MHz)  $\delta$  10.59 (s, 1H), 8.40 (dd,  $J$  = 8.0, 1.6 Hz, 1H), 8.05 (dd,  $J$  = 7.8, 0.8 Hz, 1H), 7.99 (s, 1H), 7.76 (ddd,  $J$  = 8.4, 6.9, 1.6 Hz, 1H), 7.69 (dd,  $J$  = 8.4, 0.8 Hz, 1H), 7.58 (td,  $J$  = 8.1, 0.8 Hz, 1H), 7.41–7.34 (m, 2H), 7.28 (ddd,  $J$  = 7.8, 7.1, 0.8 Hz, 1H), 4.16 (s, 3H); <sup>13</sup>C NMR (100



MHz)  $\delta$  178.5, 156.0, 146.2, 142.0, 139.4, 134.4, 131.5, 125.9, 125.3, 124.0, 122.0, 121.9, 119.8, 119.4, 118.3, 116.6, 111.5, 110.2, 108.0, 57.6; MS (FD)  $m/z$  315 ( $M^+$ ).

**5.40:**  $R_f$  = 0.28 (petroleum ether:EtOAc:CH<sub>2</sub>Cl<sub>2</sub> 8:1:2); mp 296–297 °C; IR (ATR)  $\nu$  3355 (br, m), 3060 (w), 3037 (w), 3006 (w), 2955 (w), 2918 (w), 2850 (w), 2356 (w), 2344 (w), 1652 (m), 1599 (s), 1509 (m), 1489 (m), 1467 (s), 1456 (m), 1422 (s), 1396 (m), 1338 (s), 1305 (m), 1281 (m), 1249 (m), 1234 (m), 1145 (m), 1089 (m), 968 (m), 891 (m), 758 (m), 736 (m), 697 (m) (cm<sup>-1</sup>); <sup>1</sup>H NMR (400 MHz)  $\delta$  8.85 (s, 1H), 8.50 (s, 1H), 8.43 (dd,  $J$  = 7.9, 1.6 Hz, 1H), 8.17 (dd,  $J$  = 7.7, 0.8 Hz, 1H), 7.75 (ddd,  $J$  = 8.5, 7.0, 1.6 Hz, 1H), 7.61 (dd,  $J$  = 8.4, 0.7 Hz, 1H), 7.50–7.48 (m, 2H), 7.41 (ddd,  $J$  = 8.0, 7.0, 1.1 Hz, 1H), 7.36–7.29 (m, 1H), 4.27 (s, 3H); <sup>13</sup>C NMR (100 MHz)  $\delta$  177.5, 155.9, 147.1, 140.6, 137.4, 134.4, 131.5, 127.0, 126.9, 123.8, 122.1, 121.7, 121.3, 121.2, 120.9, 117.8, 116.7, 114.0, 110.9, 61.9; MS (FD)  $m/z$  315 ( $M^+$ ).

**5.41:**  $R_f$  = 0.57 (petroleum ether:EtOAc:CH<sub>2</sub>Cl<sub>2</sub> 8:1:2); mp 175–178 °C; IR (ATR)  $\nu$  3048 (w), 2956 (s), 2854 (s), 2727 (w), 2359 (w), 2340 (w), 1907 (w), 1727 (s), 1645 (m), 1625 (s), 1599 (s), 1585 (s), 1504 (m), 1487 (w), 1463 (s), 1453 (s), 1416 (m), 1331 (m), 1264 (s), 1240 (m), 1124 (m), 1074 (m), 966 (m), 760 (m), 743 (m), 732 (s), 697 (m) (cm<sup>-1</sup>); <sup>1</sup>H NMR (400 MHz)  $\delta$  8.55 (s, 1H), 8.42 (dd,  $J$  = 7.9, 1.6 Hz, 1H), 8.18 (d,  $J$  = 7.7 Hz, 1H), 7.75 (ddd,  $J$  = 8.4, 7.0, 1.6 Hz, 1H), 7.61 (dd,  $J$  = 8.4, 0.6 Hz, 1H), 7.54 (ddd,  $J$  = 8.2, 7.2, 1.1 Hz, 1H), 7.46–7.39 (m, 2H), 7.32 (ddd,  $J$  = 7.9, 7.0, 0.6 Hz, 1H), 4.69 (q,  $J$  = 7.1 Hz, 2H), 4.25 (s, 3H), 1.52 (t,  $J$  = 7.1 Hz, 3H); <sup>13</sup>C NMR (75 MHz)  $\delta$  177.3, 155.9, 148.1, 142.0, 136.4, 134.3, 130.9, 128.8, 126.8, 123.7, 123.4, 122.6, 121.3, 120.9, 120.4, 117.7, 116.0, 113.8, 108.8, 62.5, 39.7, 14.9; MS (FD)  $m/z$  343 ( $M^+$ ).



**General procedure for Cadogan reactions, followed by *N*-alkylations***Procedure for Cadogan reactions:*

A mixture of the xanthone **5.31**, triethyl phosphite (4 mL) and dichloromethane (1 mL) was microwave irradiated at the set conditions (210 °C, 300 W) for 60 min (3 x 20 min periods) unless otherwise indicated. Excess P(OEt)<sub>3</sub> and triethyl phosphate were destroyed by heating the resulting mixture with aqueous 6 M HCl (12 mL) at 70 °C in EtOAc (20 mL) for 12 h. After cooling to room temperature, distilled water (30 mL) and CH<sub>2</sub>Cl<sub>2</sub> (30 mL) were added into the reaction mixture. The organic layer was separated and the aqueous layer was extracted with CH<sub>2</sub>Cl<sub>2</sub> or EtOAc (3 x 30 mL). The combined organic layer was washed with distilled water (2 x 40 mL), washed with aqueous 10% NaHCO<sub>3</sub> (2 x 30 mL), washed with brine (2 x 30 mL), dried over MgSO<sub>4</sub>, and filtered. The solvent was removed under reduced pressure to yield a mixture of Cadogan products as a yellow solid, which was used in the subsequent *N*-alkylation reaction without further purification.

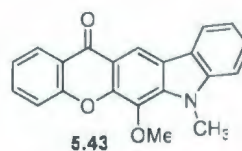
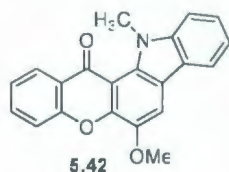
*Procedure for *N*-alkylation reactions:*

To a suspension of the Cadogan reaction product in dioxane (15 mL) was added potassium hydroxide (4 equiv.) in dioxane (2 mL) in several portions. The resulting red mixture was stirred at room temperature for 30 min, followed by the addition of an excess amount of alkyl bromide or alkyl iodide (1.0 mL). The reaction mixture was stirred at room temperature or heated at reflux overnight. Dichloromethane (15 mL) and distilled water (20 mL) were added to the reaction mixture. The layers were separated and the aqueous layer was extracted with CH<sub>2</sub>Cl<sub>2</sub> (3 x 15 mL). The combined organic layers

were washed with water, washed with brine, dried over  $\text{MgSO}_4$  and filtered. The crude product was purified by column chromatography to afford xanthone-carbazole products.

**1'-Methyl-1'H-indole[2',3'-a]-4-methoxy-9H-xanthene-9-one (5.42)**

**1'-Methyl-1'H-indole[3',2'-b]-4-methoxy-9H-xanthene-9-one (5.43)**



A mixture of xanthone **5.38** (173.6 mg, 500  $\mu\text{mol}$ ), triethyl phosphite (4 mL) and dichloromethane (1 mL) was microwave irradiated for 45 min and worked up according to the general procedure. The crude Cadogan product (157.6 mg, 500  $\mu\text{mol}$ ), potassium hydroxide (112 mg, 2.00 mmol), and methyl iodide (1.0 mL) in dioxane was stirred at room temperature overnight and worked up according to the general procedure. Column chromatography (50:50  $\text{CH}_2\text{Cl}_2$ :petroleum ether) of the crude product yielded **5.42** (138.3 mg, 85%) and **5.43** (11.6 mg, 7%) as yellow solids.

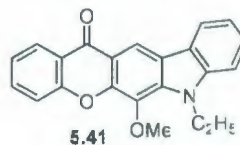
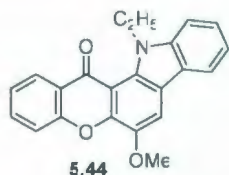
**5.42:**  $R_f$  = 0.45 (50:50  $\text{CH}_2\text{Cl}_2$ :petroleum ether); mp 199–200  $^\circ\text{C}$ ; IR (ATR)  $\nu$  3022 (w), 2936 (w), 2830 (w), 1643 (s), 1607 (s), 1585 (m), 1567 (m), 1464 (s), 1419 (m), 1362 (m), 1324 (s), 1270 (s), 1203 (s), 1178 (m), 1063 (m), 953 (s), 763 (s), 741 (s) ( $\text{cm}^{-1}$ );  $^1\text{H}$  NMR (300 MHz)  $\delta$  8.29 (dd,  $J$  = 7.9, 1.7 Hz, 1H), 7.98–7.95 (m, 1H), 7.88 (s, 1H), 7.70–7.64 (m, 1H), 7.57 (dd,  $J$  = 8.5, 1.2 Hz, 1H), 7.50–7.40 (m, 2 H), 7.37–7.32 (m, 1 H), 7.25–7.20 (m, 1 H), 4.15 (3 H), 4.07 (s, 3 H);  $^{13}\text{C}$  NMR (75 MHz)  $\delta$  177.0, 155.1, 147.7, 143.6, 142.6, 134.3, 133.4, 126.6, 125.7, 124.2, 123.1, 122.7, 120.1, 119.2, 118.7, 117.9,

110.6, 109.0, 57.5, 36.6; [APCI (+)]  $m/z$  (%) 330 ( $M^+$ , 100); HRMS [EI (+)] calcd for  $C_{21}H_{15}NO_3$  329.1052, found 329.1050.

**5.43:**  $R_f$  = 0.44 (50:50  $CH_2Cl_2$ :petroleum ether); mp 207–208 °C; IR (ATR)  $\nu$  3055 (w), 2935 (w), 2825 (w), 1654 (m), 1626 (s), 1599 (s), 1469 (s), 1439 (s), 1403 (s), 1325 (s), 1286 (s), 1246 (s), 1151 (m), 1079 (s), 991 (m), 959 (m), 757 (s), 737 (s) ( $cm^{-1}$ );  $^1H$  NMR (300 MHz)  $\delta$  8.77 (s, 1H), 8.35 (dd,  $J$  = 8.0, 2.8 Hz, 1H), 8.1 (d,  $J$  = 7.7 Hz, 1H), 7.70–7.64 (m, 1H), 7.54 (dd,  $J$  = 8.5, 1.0 Hz, 1H), 7.50–7.44 (m, 1H), 7.36–7.23 (m, 3H), 4.14 (s, 3H), 4.13 (s, 3H);  $^{13}C$  NMR (75 MHz)  $\delta$  177.6, 156.2, 148.4, 143.3, 137.6, 134.5, 132.6, 127.1, 127.0, 123.9, 123.4, 122.6, 121.5, 121.0, 120.8, 118.0, 116.2, 114.0, 109.0, 62.9, 31.5; [APCI (+)]  $m/z$  (%) 330 ( $M^+$ , 100); HRMS [EI (+)] calcd for  $C_{21}H_{15}NO_3$  329.1052, found 329.1058.

**1'-Ethyl-1'-H-indole[2',3'-a]-4-methoxy-9H-xanthene-9-one (5.44)**

**1'-Ethyl-1'-H-indole[3',2'-b]-4-methoxy-9H-xanthene-9-one (5.41)**



A mixture of xanthone **5.38** (69.5 mg, 200  $\mu$ mol), triethyl phosphite (4 mL) and dichloromethane (1 mL) was microwave irradiated for 45 min and worked up according to the general procedure. The crude Cadogan product (63.0 mg, 200  $\mu$ mol), potassium hydroxide (44.8 mg, 0.80 mmol), and ethyl iodide (1.0 mL) in dioxane was heated at 100 °C overnight and worked up according to the general procedure. Column



chromatography (50:50 CH<sub>2</sub>Cl<sub>2</sub>:petroleum ether) of the crude product yielded **5.44** (53.0 mg, 77%) and **5.41** (12.7 mg, 18%) as yellow solids.

**5.44:**  $R_f$  = 0.65 (CH<sub>2</sub>Cl<sub>2</sub>); mp 211–212 °C; IR 3053 (w), 3000 (w), 2985 (w), 2954 (w), 2859 (w), 2830 (w), 1729 (m), 1660 (s), 1612 (m), 1588 (m), 1567 (m), 1491 (m), 1466 (s), 1428 (s), 1323 (s), 1285 (s), 1269 (s), 1204 (s), 1179 (s), 1093 (s), 1065 (s), 963 (s), 932 (s), 869 (m), 848 (m), 791 (s), 760 (s), 741 (s), 728 (s), 683 (s) (cm<sup>-1</sup>); <sup>1</sup>H NMR (300 MHz)  $\delta$  8.33–8.30 (m, 1H), 8.01–7.98 (m, 1H), 7.93 (s, 1H), 7.71–7.65 (m, 1H), 7.61–7.53 (m, 2H), 7.46–7.41 (m, 1H), 7.39–7.33 (m, 1H), 7.27–7.21 (m, 1H), 4.92 (q,  $J$  = 7.0 Hz, 2H), 4.01 (s, 3H), 1.34 (t,  $J$  = 7.0 Hz, 3H); <sup>13</sup>C NMR (75 MHz)  $\delta$  177.2, 154.9, 147.8, 142.7, 142.5, 134.3, 132.0, 126.8, 125.7, 124.2, 123.1, 123.06, 120.1, 119.3, 119.1, 117.9, 111.2, 111.0, 109.1, 57.5, 43.2, 15.2; [APCI (+)]  $m/z$  (%) 344 (M<sup>+</sup>, 100); HRMS [EI (+)] calcd for C<sub>22</sub>H<sub>17</sub>NO<sub>3</sub> 343.1208, found 343.1201.

**5.41:**  $R_f$  = 0.55 (CH<sub>2</sub>Cl<sub>2</sub>); mp 201–202 °C; IR 3050 (w), 3004 (w), 2969 (w), 2944 (w), 2874 (w), 2846 (w), 1730 (m), 1645 (m), 1625 (s), 1611 (m), 1599 (s), 1586 (s), 1504 (m), 1487 (w), 1466 (s), 1452 (s), 1417 (s), 1338 (s), 1330 (s), 1300 (s), 1264 (s), 1239 (s), 1194 (m), 1175 (m), 1082 (s), 1001 (m), 967 (s), 905 (m), 891 (m), 760 (s), 732 (s), 697 (s) (cm<sup>-1</sup>); <sup>1</sup>H NMR (300 MHz)  $\delta$  8.77 (s, 1H), 8.35 (dd,  $J$  = 7.9, 1.6 Hz, 1H), 8.12–8.10 (m, 1H), 7.70–7.65 (m, 1H), 7.54 (dd,  $J$  = 8.5, 1.0 Hz, 1H), 7.49–7.44 (m, 1H), 7.38–7.31 (m, 2H), 7.27–7.22 (m, 1H), 4.63 (q,  $J$  = 7.0 Hz, 2H), 4.18 (s, 3H), 1.44 (t,  $J$  = 7.0 Hz, 3H); <sup>13</sup>C NMR (125 MHz)  $\delta$  177.6, 156.2, 148.3, 142.2, 136.7, 134.5, 132.6, 127.08, 127.07, 123.9, 123.7, 122.8, 121.5, 121.1, 120.7, 118.0, 116.2, 114.0, 109.1, 62.8,

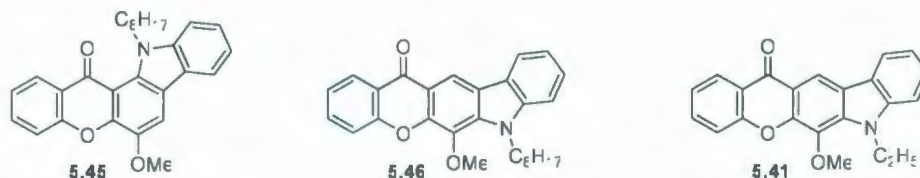


39.9, 15.1; [APCI (+)]  $m/z$  (%) 344 ( $M^+$ , 100); HRMS [EI (+)] calcd for  $C_{22}H_{17}NO_3$  343.1208, found 343.1203.

**1'-Octyl-1'-H-indole[2',3'-a]-4-methoxy-9H-xanthene-9-one (5.45)**

**1'-Otyl-1'-H-indole[3',2'-b]-4-methoxy-9H-xanthene-9-one (5.46)**

**1'-Ethyl-1'-H-indole[3',2'-b]-4-methoxy-9H-xanthene-9-one (5.41)**



A mixture of xanthone **5.38** (69.5 mg, 200  $\mu$ mol), triethyl phosphite (4 mL) and dichloromethane (1 mL) was microwave irradiated for 45 min and worked up according to the general procedure. The crude Cadogan product (63.0 mg, 200  $\mu$ mol), potassium hydroxide (44.8 mg, 0.80 mmol), and octyl iodide (1.0 mL) in dioxane was heated at 100  $^{\circ}$ C overnight and worked up according to the general procedure. Column chromatography (50:50  $CH_2Cl_2$ :petroleum ether) of the crude product yielded **5.45** (75.0 mg, 88%), **5.46** (1.7 mg, 2%) and **5.41** (4.1 mg, 6%) as yellow solids.

**5.45:**  $R_f$  = 0.65 (5:95 EtOAc-petroleum ether); mp 111–113  $^{\circ}$ C; IR (ATR)  $\nu$  3066 (w), 3034 (w), 2922 (m), 2853 (m), 1729 (m), 1659 (s), 1610 (m), 1586 (m), 1464 (s), 1426 (s), 1380 (s), 1322 (s), 1267 (s), 1202 (s), 1171 (s), 1089 (m), 1069 (m), 756 (s), 738 (s), 724 (s) ( $cm^{-1}$ );  $^1H$  NMR (300 MHz)  $\delta$  8.31 (dd,  $J$  = 8.1, 1.7 Hz, 1H), 7.98 (d,  $J$  = 7.9 Hz, 1H), 7.92 (s, 1H), 7.70–7.65 (m, 1H), 7.59 (dd,  $J$  = 8.5, 1.2 Hz, 1H), 7.53–7.50 (m, 1 H), 7.44–7.32 (m, 2 H), 7.25–7.19 (m, 1 H), 4.92 (m, 2H), 4.09 (s, 3 H), 1.64–1.50 (m, 2 H), 1.11–1.07 (m, 10H), 0.73 (t,  $J$  = 6.8 Hz, 3H);  $^{13}C$  NMR (75 MHz)  $\delta$  177.1, 155.0, 147.8,

142.8, 142.6, 134.3, 132.1, 126.8, 125.6, 124.2, 123.2, 123.0, 120.0, 119.3, 119.1, 117.9, 111.3, 111.2, 109.1, 57.5, 47.8, 32.0, 29.4, 29.4, 27.0, 22.8, 14.3; [APCI (+)]  $m/z$  (%) 428 ( $M^+$ , 100); HRMS [EI (+)] calcd for  $C_{28}H_{29}NO_3$  427.2147, found 427.2139.

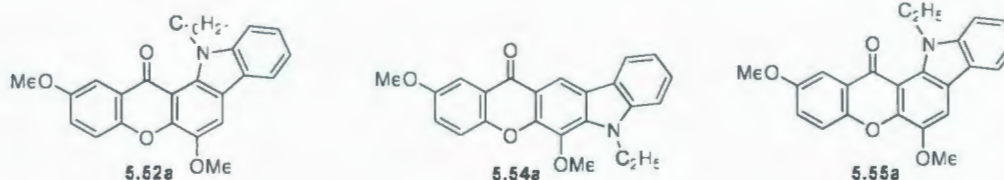
**5.46**  $R_f$  = 0.60 (5:95 EtOAc-petroleum ether); mp 102–103 °C; IR (ATR)  $\nu$  3055 (w), 3019 (w), 2952 (w), 2916 (m), 2849 (m), 1648 (m), 1624 (s), 1597 (s), 1503 (m), 1465 (s), 1448 (s), 1416 (s), 1362 (m), 1337 (s), 1271 (m), 1091 (s), 754 (s), 729 (s), 695 (s), ( $cm^{-1}$ );  $^1H$  NMR (300 MHz)  $\delta$  8.78 (s, 1H), 8.36 (dd,  $J$  = 7.8, 1.8 Hz, 1H), 8.12–8.10 (m, 1H), 7.70–7.65 (m, 1H), 7.54 (dd,  $J$  = 8.5, 1.2 Hz, 1H), 7.49–7.44 (m, 1 H), 7.38–7.31 (m, 2H), 7.27–7.22 (m, 1H), 4.55–4.50 (m, 2H), 4.17 (s, 3 H), 1.90–1.80 (m, 2H), 1.25–1.17 (m, 10H), 0.80 (t,  $J$  = 6.8 Hz, 3H);  $^{13}C$  NMR (75 MHz)  $\delta$  177.4, 156.0, 148.1, 142.4, 136.7, 134.3, 132.2, 126.9, 126.8, 123.7, 123.3, 122.6, 121.3, 120.9, 120.4, 117.8, 116.0, 113.8, 109.1, 62.6, 45.1, 31.8, 30.0, 29.4, 29.3, 27.1, 22.6, 14.1; [APCI (+)]  $m/z$  (%) 428 ( $M^+$ , 100); HRMS [EI (+)] calcd for  $C_{28}H_{29}NO_3$  427.2147, found 427.2139.

**5.41**: characterization data was given previously.

**1'-Decyl-1'H-indole[2',3'-a]-4,7-dimethoxy-9H-xanthene-9-one (5.52a)**

**1'-Ethyl-1'H-indole[3',2'-b]-4,7-dimethoxy-9H-xanthene-9-one (5.54a)**

**1'-Ethyl-1'H-indole[2',3'-a]-4,7-dimethoxy-9H-xanthene-9-one (5.55a)**



A mixture of xanthone **5.31a** (151.5 mg, 401  $\mu$ mol), triethyl phosphite (4 mL) and dichloromethane (1 mL) was microwave irradiated for 60 min and worked up according

to the general procedure. The crude Cadogan product (86.3 mg, 250  $\mu\text{mol}$ ), potassium hydroxide (56.2 mg, 1.00 mmol), and decyl bromide (1.0 mL) in dioxane was heated at 100 °C overnight and worked up according to the general procedure. Column chromatography (70:30 petroleum ether:EtOAc) of the crude product yielded **5.52a** (95.5 mg, 79%), **5.54a** (12.9 mg, 14%) and **5.55a** (trace) as yellow solids.

**5.52a**:  $R_f$  = 0.68 (70:30 petroleum ether:EtOAc); mp 125–126 °C; IR  $\nu$  3027 (w), 2924 (m), 2852 (m), 1648 (s), 1614 (s), 1569 (m), 1427 (s), 1468 (s), 1452 (s), 1436 (s), 1372 (m), 1326 (s), 1266 (s), 1217 (s), 1195 (s), 1160 (s), 1067 (s), 1029 (s), 1019 (s), 918 (w), 813 (s), 758 (s), 737 (s), 722 (s) ( $\text{cm}^{-1}$ );  $^1\text{H}$  NMR (500 MHz),  $\delta$  8.05 (d,  $J$  = 8.4 Hz, 1H), 8.00 (s, 1H), 7.75 (d,  $J$  = 2.9 Hz, 1H), 7.60 (t,  $J$  = 8.2 Hz, 2H), 7.48 (t,  $J$  = 8.0 Hz, 1H), 7.35 (dd,  $J$  = 9.5, 2.7 Hz, 1H), 7.29 (t,  $J$  = 8.1 Hz, 1H), 4.99 (t,  $J$  = 7.3 Hz, 2H), 4.15 (s, 3H), 3.97 (s, 3H), 1.69–1.63 (m, 2H), 1.25–1.14 (m, 14H), 0.84 (t,  $J$  = 7.1 Hz, 3H);  $^{13}\text{C}$  NMR (125 MHz)  $\delta$  176.9, 156.4, 149.8, 147.9, 142.8, 142.7, 132.0, 125.4, 124.3, 123.4, 123.1, 120.0, 119.3, 119.2, 118.8, 111.2, 110.9, 108.8, 106.1, 57.5, 56.2, 47.8, 32.1, 29.7 (2C), 29.48, 29.47, 29.44, 27.0, 22.9, 14.3; MS [APCI (+)]  $m/z$  (%) 486 ( $\text{M}^+$ , 100); HRMS [EI (+)] calcd for  $\text{C}_{31}\text{H}_{35}\text{NO}_4$  485.2566, found 485.2563.

**5.54a**:  $R_f$  = 0.46 (70:30 petroleum ether:EtOAc); mp 201–202 °C; IR  $\nu$  3055 (w), 2939 (w), 2841 (w), 1649 (s), 1620 (s), 1598 (s), 1591 (s), 1489 (s), 1451 (s), 1417 (s), 1331 (s), 1289 (s), 1197 (s), 1160 (s), 1145 (s), 1082 (m), 1033 (s), 821 (s), 785 (s), 735 (s), 730 (s) ( $\text{cm}^{-1}$ );  $^1\text{H}$  NMR (500 MHz),  $\delta$  8.84 (s, 1H), 8.19 (d,  $J$  = 8.3 Hz, 1H), 7.80 (d,  $J$  = 3.0 Hz, 1H), 7.55 (d,  $J$  = 8.5 Hz, 1H), 7.53 (t,  $J$  = 6.8 Hz, 1H), 7.43 (d,  $J$  = 8.2 Hz, 1H), 7.35 (dd,  $J$  = 9.7, 2.8 Hz, 1H), 7.31 (t,  $J$  = 8.0 Hz, 1H), 4.69 (q,  $J$  = 7.2 Hz, 2H), 4.24 (s,



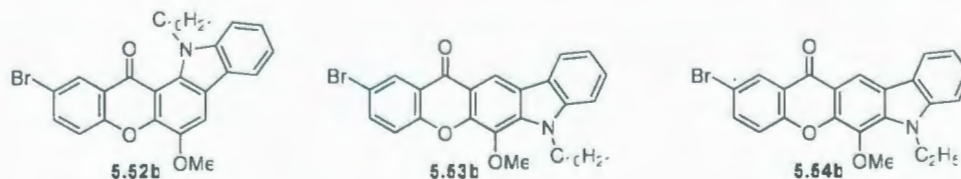
3H), 3.96 (s, 3H), 1.51 (t,  $J = 7.0$  Hz, 3H);  $^{13}\text{C}$  NMR (125 MHz)  $\delta$  177.5, 156.1, 151.0, 148.4, 142.3, 136.6, 132.4, 127.1, 124.4, 123.7, 122.8, 121.7, 121.1, 120.6, 119.4, 115.8, 113.9, 109.0, 106.4, 62.7, 56.2, 39.9, 15.1; MS [APCI (+)]  $m/z$  (%) 374 ( $\text{M}^+$ , 100); HRMS [EI (+)] calcd for  $\text{C}_{23}\text{H}_{19}\text{NO}_4$  373.1314, found 373.1310.

**5.55a:**  $R_f = 0.45$  (70:30 petroleum ether:EtOAc); mp (not measured due to impure sample);  $^1\text{H}$  NMR (500 MHz) (unclean spectrum, peaks attributable to the product are listed),  $\delta$  8.06 (d,  $J = 7.7$  Hz, 1H), 7.98 (s, 1H), 7.76 (d,  $J = 3.1$  Hz, 1H), 7.61 (d,  $J = 9.1$  Hz, 2H), 7.51-7.47 (m, 1H), 7.35 (dd,  $J = 9.1, 3.1$  Hz, 1H), 7.32-7.28 (m, 1H), 5.00 (q,  $J = 7.1$  Hz, 2H), 4.16 (s, 3H), 3.97 (s, 3H), 0.88 (t,  $J = 6.9$  Hz, 3H); MS [APCI (+)]  $m/z$  (%) 374 ( $\text{M}^+$ , 100); HRMS [EI (+)] calcd for  $\text{C}_{23}\text{H}_{19}\text{NO}_4$  373.1314, found 373.1311.

**1'-Decyl-1'-H-indole[2',3'-a]-7-bromo-4-methoxy-9H-xanthene-9-one (5.52b)**

**1'-Decyl-1'-H-indole[3',2'-b]-7-bromo-4-methoxy-9H-xanthene-9-one (5.53b)**

**1'-Ethyl-1'-H-indole[3',2'-b]-7-bromo-4-methoxy-9H-xanthene-9-one (5.54b)**



A mixture of xanthone **5.31b** (200.1 mg, 469  $\mu\text{mol}$ ), triethyl phosphite (4 mL) and dichloromethane (1 mL) was microwave irradiated for 60 min and worked up according to the general procedure. The crude Cadogan product (99.1 mg, 251  $\mu\text{mol}$ ), potassium hydroxide (56.2 mg, 1.00 mmol), and decyl bromide (1.0 mL) in dioxane was heated at 100  $^{\circ}\text{C}$  overnight and worked up according to the general procedure. Column



chromatography (70:30 petroleum ether:EtOAc) of the crude product yielded **5.52b** (93.9 mg, 70%), **5.53b** (14.8 mg, 11%) and **5.54b** (7.4 mg, 7%) as yellow solids.

**5.52b**:  $R_f$  = 0.63 (70:30 petroleum ether:EtOAc); mp 106–107 °C; IR  $\nu$  3053 (w), 2918 (m), 2850 (m), 1654 (s), 1623 (w), 1600 (m), 1564 (m), 1491 (m), 1465 (s), 1436 (s), 1323 (s), 1267 (s), 1221 (s), 1207 (s), 1193 (s), 1173 (s), 1128 (m), 1095 (m), 1066 (s), 1022 (s), 959 (m), 906 (m), 859 (m), 809 (s), 737 (s), 724 (s) ( $\text{cm}^{-1}$ );  $^1\text{H}$  NMR (500 MHz),  $\delta$  8.46 (d,  $J$  = 2.3 Hz, 1H), 8.00 (d,  $J$  = 7.4 Hz, 1H), 7.93 (s, 1H), 7.76 (dd,  $J$  = 8.8, 2.3 Hz, 1H), 7.56 (d,  $J$  = 8.4 Hz, 1H), 7.51–7.46 (m, 2H), 7.29–7.25 (m, 1H), 4.90 (t,  $J$  = 5.6 Hz, 2H), 4.11 (s, 3H), 1.70–1.64 (m, 2H), 1.25–1.16 (m, 14H), 0.85 (t,  $J$  = 7.3 Hz, 3H);  $^{13}\text{C}$  NMR (125 MHz)  $\delta$  175.7, 153.6, 147.5, 142.8, 142.5, 137.0, 131.9, 129.3, 125.7, 124.4, 122.4, 120.1, 119.8, 119.30, 119.28, 117.2, 111.1, 110.9, 109.3, 57.4, 47.9, 32.1, 29.7, 29.6 (2C), 29.5 (2C), 27.0, 22.9, 14.3; MS [APCI (+)]  $m/z$  (%) 536 ( $^{81}\text{Br}$ ,  $\text{M}^+$ , 100), 534 ( $^{79}\text{Br}$ ,  $\text{M}^+$ , 98); HRMS [EI (+)] calcd for  $\text{C}_{30}\text{H}_{32}\text{BrNO}_3$  533.1566, found 533.1558.

**5.53b**:  $R_f$  = 0.75 (70:30 petroleum ether:EtOAc); mp 154–155 °C; IR  $\nu$  3060 (w), 2920 (m), 2851 (m), 1649 (s), 1625 (s), 1599 (s), 1592 (s), 1601 (w), 1461 (s), 1419 (s), 1358 (m), 1330 (m), 1275 (s), 1169 (s), 1128 (m), 1063 (m), 974 (m), 822 (s), 784 (s), 737 (s) ( $\text{cm}^{-1}$ );  $^1\text{H}$  NMR (500 MHz),  $\delta$  8.81 (s, 1H), 8.52 (d,  $J$  = 2.9 Hz, 1H), 8.16 (d,  $J$  = 7.4 Hz, 1H), 7.80 (dd,  $J$  = 8.8, 2.2 Hz, 1H), 7.53 (t,  $J$  = 7.7 Hz, 1H), 7.49 (d,  $J$  = 8.9 Hz, 1H), 7.43 (d,  $J$  = 8.2 Hz, 1H), 7.31 (t,  $J$  = 7.3 Hz, 1H), 4.58 (t,  $J$  = 8.0 Hz, 2H), 4.12 (s, 3H), 1.94–1.88 (m, 2H), 1.47–1.41 (m, 2H), 1.37–1.33 (m, 2H), 1.28–1.24 (m, 10H), 0.87 (t,  $J$  = 7.0 Hz, 3H);  $^{13}\text{C}$  NMR (125 MHz)  $\delta$  176.3, 154.9, 148.1, 142.6, 137.3, 137.1, 132.6,

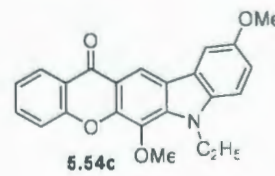
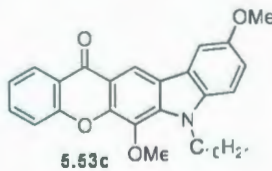
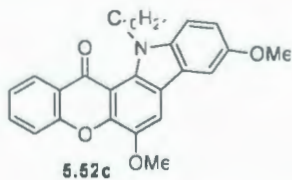
129.6, 127.2, 123.4, 123.1, 122.8, 121.1, 120.8, 119.9, 116.9, 115.7, 114.0, 109.4, 62.8, 45.3, 32.1, 30.2, 29.8 (2C), 29.6, 29.5, 27.3, 22.9, 14.3; MS [APCI (+)]  $m/z$  (%) 536 ( $^{81}\text{Br}$ ,  $\text{M}^+$ , 99), 534 ( $^{79}\text{Br}$ ,  $\text{M}^+$ , 100); HRMS [EI (+)] calcd for  $\text{C}_{30}\text{H}_{32}\text{BrNO}_3$  533.1566, found 533.1559.

**5.54b:**  $R_f$  = 0.55 (70:30 petroleum ether:EtOAc); mp 249–250 °C; IR  $\nu$  2942 (w), 2843 (w), 1650 (s), 1626 (s), 1597 (s), 1592 (s), 1502 (m), 1461 (s), 1451 (s), 1416 (s), 1329 (m), 1277 (s), 1261 (s), 1194 (m), 1166 (m), 1060 (m), 975 (m), 810 (s), 730 (s) ( $\text{cm}^{-1}$ );  $^1\text{H}$  NMR (500 MHz),  $\delta$  8.82 (s, 1H), 8.53 (d,  $J$  = 2.2 Hz, 1H), 8.16 (d,  $J$  = 8.1 Hz, 1H), 7.81 (dd,  $J$  = 8.9, 2.9 Hz, 1H), 7.54 (t,  $J$  = 7.5 Hz, 1H), 7.50 (d,  $J$  = 8.9 Hz, 1H), 7.44 (d,  $J$  = 8.3 Hz, 1H), 7.33 (t,  $J$  = 7.6 Hz, 1H), 4.69 (q,  $J$  = 7.1 Hz, 2H), 4.24 (s, 3H), 1.52 (t,  $J$  = 7.3 Hz, 3H);  $^{13}\text{C}$  NMR (125 MHz)  $\delta$  176.3, 154.9, 148.2, 142.3, 137.3, 136.9, 132.6, 129.6, 127.3, 123.5, 123.2, 122.9, 121.2, 120.9, 120.0, 116.9, 115.8, 114.1, 109.2, 62.8, 40.0, 15.1; MS [APCI (+)]  $m/z$  (%) 424 ( $^{81}\text{Br}$ ,  $\text{M}^+$ , 98), 422 ( $^{79}\text{Br}$ ,  $\text{M}^+$ , 100); HRMS [EI (+)] calcd for  $\text{C}_{22}\text{H}_{16}\text{BrNO}_3$  421.0314, found 421.0312.

**1'-Decyl-5'-methoxy-1'H-indole[2',3'-a]-4-methoxy-9H-xanthene-9-one (5.52c)**

**1'-Decyl-5'-methoxy-1'H-indole[3',2'-b]-4-methoxy-9H-xanthene-9-one (5.53c)**

**1'-Ethyl-5'-methoxy-1'H-indole[3',2'-b]-4-methoxy-9H-xanthene-9-one (5.54c)**



A mixture of xanthone **5.31c** (121.3 mg, 321  $\mu\text{mol}$ ), triethyl phosphite (4 mL) and dichloromethane (1 mL) was microwave irradiated for 60 min and worked up according



to the general procedure. The crude Cadogan products (121.1 mg, 351  $\mu\text{mol}$ ), potassium hydroxide (78.6 mg, 1.40 mmol), and decyl bromide (1.0 mL) in dioxane was heated at 100 °C overnight and worked up according to the general procedure. Column chromatography (80:20 petroleum ether:EtOAc) of the crude product yielded **5.52c** (82.3 mg, 48%), **5.53c** (24.8 mg, 15%) and **5.54c** (16.2 mg, 12%) as yellow solids.

**5.52c**:  $R_f$  = 0.62 (80:20 petroleum ether:EtOAc); mp 108–109 °C; IR  $\nu$  3045 (w), 2948 (m), 2919 (m), 2849 (m), 1659 (s), 1630 (m), 1605 (m), 1588 (m), 1566 (m), 1484 (s), 1465 (s), 1438 (m), 1335 (s), 1310 (m), 1265 (s), 1205 (s), 1162 (s), 1065 (s), 1039 (s), 967 (m), 819 (m), 755 (s) ( $\text{cm}^{-1}$ );  $^1\text{H}$  NMR (500 MHz),  $\delta$  8.37 (dd,  $J$  = 7.6, 1.6 Hz, 1H), 7.93 (s, 1H), 7.75–7.72 (m, 1H), 7.65 (d,  $J$  = 8.3 Hz, 1H), 7.49 (d,  $J$  = 2.3 Hz, 1H), 7.47 (d,  $J$  = 9.7 Hz, 1H), 7.41 (t,  $J$  = 7.6 Hz, 1H), 7.12 (dd,  $J$  = 8.6, 2.3 Hz, 1H), 4.93 (t,  $J$  = 7.7 Hz, 2H), 4.16 (s, 3H), 3.96 (s, 3H), 1.65–1.59 (m, 2H), 1.25–1.12 (m, 14H), 0.85 (t,  $J$  = 7.5 Hz, 3H);  $^{13}\text{C}$  NMR (125 MHz)  $\delta$  177.0, 155.0, 144.5, 147.9, 142.3, 137.9, 134.2, 132.6, 126.8, 124.1, 123.4, 123.2, 118.9, 117.8, 115.0, 112.1, 111.3, 109.2, 101.7, 57.6, 56.3, 47.9, 32.1, 29.7 (2C), 29.5 (2C), 29.4, 27.0, 22.9, 14.3; MS [APCI (+)]  $m/z$  (%) 486 ( $\text{M}^+$ , 100); HRMS [EI (+)] calcd for  $\text{C}_{31}\text{H}_{35}\text{NO}_4$  485.2566, found 485.2561.

**5.53c**:  $R_f$  = 0.70 (80:20 petroleum ether:EtOAc); mp 82–83 °C; IR  $\nu$  3049 (w), 2923 (s), 2853 (s), 1651 (m), 1629 (m), 1599 (s), 1479 (s), 1461 (s), 1412 (s), 1313 (s), 1253 (s), 1212 (s), 1157 (s), 1138 (s), 1071 (s), 1035 (s), 882 (s), 790 (s), 756 (s) ( $\text{cm}^{-1}$ );  $^1\text{H}$  NMR (500 MHz),  $\delta$  8.80 (s, 1H), 8.42 (dd,  $J$  = 7.9, 1.5 Hz, 1H), 7.77–7.72 (m, 1H), 7.67 (d,  $J$  = 2.4 Hz, 1H), 7.60 (d,  $J$  = 8.2 Hz, 1H), 7.40 (t,  $J$  = 7.2 Hz, 1H), 7.32 (d,  $J$  = 8.8 Hz, 1H), 7.14 (dd,  $J$  = 8.8, 2.5 Hz, 1H), 4.55 (t,  $J$  = 7.7 Hz, 2H), 4.22 (s, 3H), 3.95 (s, 3H), 1.92–

1.86 (m, 2H), 1.46–1.38 (m, 2H), 1.34–1.24 (m, 12H), 0.87 (t,  $J = 6.9$  Hz, 3H);  $^{13}\text{C}$  NMR (125 MHz)  $\delta$  177.6, 156.2, 154.9, 148.2, 137.4, 137.3, 134.5, 132.5, 127.1, 124.0, 123.8, 122.7, 121.5, 118.0, 116.1, 115.8, 114.0, 110.1, 103.8, 62.7, 56.3, 45.4, 32.1, 30.2, 29.9, 29.8, 29.6, 29.5, 27.3, 22.9, 14.3; MS [APCI (+)]  $m/z$  (%) 486 ( $\text{M}^+$ , 100); HRMS [EI (+)] calcd for  $\text{C}_{31}\text{H}_{35}\text{NO}_4$  485.2566, found 485.2572.

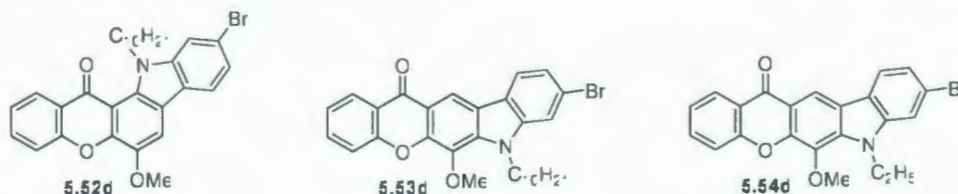
**5.54c:**  $R_f = 0.54$  (80:20 petroleum ether:EtOAc); mp 179–180 °C; IR  $\nu$  2994 (w), 2939 (w), 2829 (w), 1649 (s), 1633 (s), 1607 (s), 1591 (s), 1504 (m), 1482 (s), 1463 (s), 1411 (s), 1317 (s), 1257 (s), 1217 (s), 1185 (s), 1152 (s), 1064 (s), 1032 (s), 1010 (s), 973 (m), 846 (m), 837 (m), 788 (m), 751 (s) ( $\text{cm}^{-1}$ );  $^1\text{H}$  NMR (500 MHz),  $\delta$  8.78 (s, 1H), 8.41 (d,  $J = 8.3$  Hz, 1H), 7.74–7.72 (m, 1H), 7.66 (d,  $J = 2.7$  Hz, 1H), 7.59 (d,  $J = 8.7$  Hz, 1H), 7.39 (t,  $J = 7.8$  Hz, 1H), 7.32 (d,  $J = 8.7$  Hz, 1H), 7.14 (dd,  $J = 8.6, 1.9$  Hz, 1H), 4.65 (q,  $J = 7.1$  Hz, 2H), 4.23 (s, 3H), 3.95 (s, 3H), 1.49 (t,  $J = 7.1$  Hz, 3H);  $^{13}\text{C}$  NMR (125 MHz)  $\delta$  177.5, 156.2, 154.8, 148.1, 137.0, 136.9, 134.4, 132.4, 127.0, 124.1, 123.8, 122.7, 121.5, 117.9, 116.0, 115.8, 114.0, 109.8, 103.9, 62.7, 56.3, 40.0, 15.2; MS [APCI (+)]  $m/z$  (%) 374 ( $\text{M}^+$ , 100); HRMS [EI (+)] calcd for  $\text{C}_{23}\text{H}_{19}\text{NO}_4$  373.1314, found 373.1310.



**1'-Decyl-6'-bromo-1'*H*-indole[2',3'-*a*]-4-methoxy-9*H*-xanthene-9-one (5.52d)**

**1'-Decyl-6'-bromo-1'*H*-indole[3',2'-*b*]-4-methoxy-9*H*-xanthene-9-one (5.53d)**

**1'-Ethyl-6'-bromo-1'*H*-indole[3',2'-*b*]-4-methoxy-9*H*-xanthene-9-one (5.54d)**



A mixture of xanthone **5.31d** (205.6 mg, 482  $\mu\text{mol}$ ), triethyl phosphite (4 mL) and dichloromethane (1 mL) was microwave irradiated for 60 min and worked up according to the general procedure. The crude Cadogan product (106.1 mg, 269  $\mu\text{mol}$ ), potassium hydroxide (56.1 mg, 1.00 mmol), and decyl bromide (1.0 mL) in dioxane was heated at 100 °C overnight and worked up according to the general procedure. Column chromatography (70:30 petroleum ether:EtOAc) of the crude product yielded **5.52d** (75.1 mg, 52%), **5.53d** (6.3 mg, 4%) and **5.54d** (5.5 mg, 5%) as yellow solids.

**5.52d:**  $R_f$  = 0.60 (70:30 petroleum ether:EtOAc); mp 126–127 °C; IR  $\nu$  3029 (w), 2948 (m), 2920 (m), 2848 (m), 1662 (s), 1612 (s), 1586 (s), 1564 (m), 1488 (s), 1467 (s), 1433 (m), 1427 (s), 1367 (s), 1328 (s), 1305 (s), 1279 (s), 1207 (s), 1150 (m), 1131 (m), 1056 (s), 1013 (m), 956 (s), 899 (s), 873 (s), 755 (s) ( $\text{cm}^{-1}$ );  $^1\text{H}$  NMR (500 MHz),  $\delta$  8.36 (dd,  $J$  = 8.4, 1.5 Hz, 1H), 7.90 (s, 1H), 7.87 (d,  $J$  = 8.1 Hz, 1H), 7.76–7.73 (m, 1H), 7.71 (d,  $J$  = 1.2 Hz, 1H), 7.65 (d,  $J$  = 8.0 Hz, 1H), 7.43 (t,  $J$  = 7.6 Hz, 1H), 7.38 (dd,  $J$  = 8.3, 1.5 Hz, 1H), 4.90 (t,  $J$  = 7.6 Hz, 2H), 4.14 (s, 3H), 1.67–1.61 (m, 2H), 1.25–1.14 (m, 14H), 0.85 (t,  $J$  = 7.5 Hz, 3H);  $^{13}\text{C}$  NMR (125 MHz)  $\delta$  177.0, 154.9, 148.0, 143.5, 143.1, 134.4, 132.1, 126.8, 124.3, 123.2, 123.1, 121.9, 120.4, 119.2, 118.5, 117.9, 114.2, 111.5, 108.5,

57.4, 48.0, 32.1, 29.7 (2C), 29.5, 29.4, 29.38, 26.9, 22.9, 14.3; MS [APCI (+)]  $m/z$  (%) 536 ( $^{81}\text{Br}$ ,  $\text{M}^+$ , 100), 534 ( $^{79}\text{Br}$ ,  $\text{M}^+$ , 97); HRMS [EI (+)] calcd for  $\text{C}_{30}\text{H}_{32}\text{BrNO}_3$  533.1566, found 533.1559.

**5.53d:**  $R_f$  = 0.72 (70:30 petroleum ether:EtOAc); mp 139–141 °C; IR  $\nu$  2936 (m), 2921 (s), 2850 (s), 1650 (s), 1627 (s), 1611 (m), 1592 (s), 1502 (m), 1464 (s), 1434 (s), 1413 (s), 1349 (s), 1312 (s), 1279 (s), 1229 (m), 1171 (m), 1147 (m), 1107 (s), 1091 (s), 965 (m), 864 (m), 797 (s), 754 (s) ( $\text{cm}^{-1}$ );  $^1\text{H}$  NMR (500 MHz),  $\delta$  8.80 (s, 1H), 8.41 (dd,  $J$  = 8.4, 1.6 Hz, 1H), 8.00 (d,  $J$  = 8.2 Hz, 1H), 7.77–7.73 (m, 1H), 7.60 (d,  $J$  = 8.4 Hz, 1H), 7.56 (s, 1H), 7.43–7.40 (m, 2H), 4.53 (t,  $J$  = 7.9 Hz, 2H), 4.24 (s, 3H), 1.93–1.87 (m, 2H), 1.47–1.41 (m, 2H), 1.38–1.25 (m, 12H), 0.87 (t,  $J$  = 6.1 Hz, 3H);  $^{13}\text{C}$  NMR (125 MHz)  $\delta$  177.5, 156.1, 148.5, 143.5, 137.0, 134.7, 132.8, 127.1, 124.0, 123.8, 122.5, 122.2, 122.1, 121.5, 120.8, 118.0, 116.7, 114.0, 112.5, 62.8, 45.5, 32.1, 30.1, 29.9, 29.8, 29.6, 29.5, 27.3, 22.9, 14.3; MS [APCI (+)]  $m/z$  (%) 536 ( $^{81}\text{Br}$ ,  $\text{M}^+$ , 100), 534 ( $^{79}\text{Br}$ ,  $\text{M}^+$ , 93); HRMS [EI (+)] calcd for  $\text{C}_{30}\text{H}_{32}\text{BrNO}_3$  533.1566, found 533.1557.

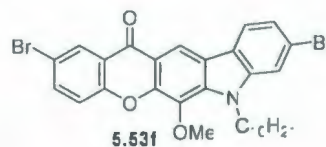
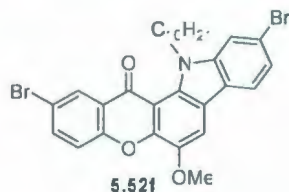
**5.54d:**  $R_f$  = 0.58 (70:30 petroleum ether:EtOAc); mp 255–256 °C; IR  $\nu$  3064 (w), 3010 (w), 2954 (w), 2843 (w), 1649 (s), 1625 (s), 1591 (s), 1502 (m), 1463 (s), 1432 (s), 1412 (s), 1349 (s), 1320 (s), 1280 (s), 1230 (s), 1198 (s), 1172 (s), 1106 (s), 1054 (s), 1004 (s), 966 (s), 905 (s), 861 (s), 840 (s), 798 (s), 783 (s), 749 (s) ( $\text{cm}^{-1}$ );  $^1\text{H}$  NMR (500 MHz),  $\delta$  8.77 (s, 1H), 8.40 (dd,  $J$  = 8.3, 1.7 Hz, 1H), 8.00 (d,  $J$  = 8.2 Hz, 1H), 7.76–7.73 (m, 1H), 7.59 (d,  $J$  = 8.4 Hz, 1H), 7.56 (s, 1H), 7.42–7.39 (m, 2H), 4.63 (q,  $J$  = 7.2 Hz, 2H), 4.25 (s, 3H), 1.51 (t,  $J$  = 7.5 Hz, 3H);  $^{13}\text{C}$  NMR (125 MHz)  $\delta$  177.4, 156.1, 148.5, 143.1, 136.7, 134.6, 132.8, 127.1, 124.0, 123.8, 122.6, 122.2, 122.1, 121.5, 120.8, 118.0, 116.7,

114.0, 112.3, 62.8, 40.2, 15.1; MS [APCI (+)]  $m/z$  (%) 424 ( $^{81}\text{Br}$ ,  $\text{M}^+$ , 100), 422 ( $^{79}\text{Br}$ ,  $\text{M}^+$ , 93); HRMS [EI (+)] calcd for  $\text{C}_{22}\text{H}_{16}\text{BrNO}_3$  421.0314, found 421.0318.

**1'-Decyl-6'-bromo-1'*H*-indole[2',3'-*a*]-7-bromo-4-methoxy-9*H*-xanthene-9-one**  
(**5.52f**);

**1'-Decyl-6'-bromo-1'*H*-indole[3',2'-*b*]-7-bromo-4-methoxy-9*H*-xanthene-9-one**  
(**5.53f**);

and an unidentified product **5.72**



A mixture of xanthone **5.31f** (153.6 mg, 304  $\mu\text{mol}$ ), triethyl phosphite (4 mL) and dichloromethane (1 mL) was microwave irradiated for 40 min and worked up according to the general procedure. The crude Cadogan product (118.2 mg, 250  $\mu\text{mol}$ ), potassium hydroxide (56.3 mg, 1.00 mmol), and decyl bromide (1.0 mL) in dioxane was heated at 100  $^{\circ}\text{C}$  overnight and worked up according to the general procedure. Column chromatography (80:20 petroleum ether:EtOAc) of the crude product yielded **5.52f** (98.4 mg, 64%), **5.53f** (13.3 mg, 9%) and a unidentified product **5.72**<sup>31</sup> (1.6 mg, 1%) as yellow solids.

**5.52f**:  $R_f$  = 0.62 (80:20 petroleum ether:EtOAc); mp 176–177  $^{\circ}\text{C}$ ; IR  $\nu$  3072 (w), 2954 (m), 2922 (s), 2852 (s), 1652 (s), 1623 (m), 1606 (m), 1582 (m), 1564 (m), 1484 (s), 1466 (s), 1439 (s), 1364 (s), 1304 (s), 1256 (s), 1218 (s), 1207 (s), 1171 (s), 1126 (m), 1095 (s), 1057 (s), 962 (s), 905 (s), 877 (s), 811 (s), 795 (s), 721 (s) ( $\text{cm}^{-1}$ );  $^1\text{H}$  NMR (500 MHz),  $\delta$



8.45 (d,  $J = 2.7$  Hz, 1H), 7.86 (s, 1H), 7.84 (d,  $J = 8.1$  Hz, 1H), 7.79 (dd,  $J = 8.9, 2.4$  Hz, 1H), 7.69 (d,  $J = 1.0$  Hz, 1H), 7.51 (d,  $J = 9.4$  Hz, 1H), 7.36 (dd,  $J = 8.3, 1.4$  Hz, 1H), 4.84 (t,  $J = 7.6$  Hz, 2H), 4.12 (s, 3H), 1.68–1.62 (m, 2H), 1.27–1.17 (m, 14H), 0.86 (t,  $J = 7.5$  Hz, 3H);  $^{13}\text{C}$  NMR (125 MHz)  $\delta$  175.6, 153.6, 147.7, 143.5, 143.0, 137.2, 132.0, 129.3, 124.3, 123.3, 121.7, 120.4, 119.8, 119.4, 118.8, 117.4, 114.2, 111.1, 108.8, 57.3, 48.1, 32.1, 29.7 (2C), 29.54, 29.49, 29.45, 26.9, 22.9, 14.3; MS [APCI (+)]  $m/z$  (%) 616 ( $^{81}\text{Br}_2$ ,  $\text{M}^+$ , 57), 614 ( $^{81}\text{Br}^{79}\text{Br}$ ,  $\text{M}^+$ , 100), 612 ( $^{79}\text{Br}_2$ ,  $\text{M}^+$ , 57); HRMS [EI (+)] calcd for  $\text{C}_{30}\text{H}_{31}\text{Br}_2\text{NO}_3$  611.0671, found 611.0673.

**5.53f:**  $R_f = 0.71$  (80:20 petroleum ether:EtOAc); mp 193–194 °C; IR  $\nu$  3074 (w), 2932 (s), 2921 (s), 2851 (s), 1651 (s), 1626 (s), 1592 (s), 1500 (m), 1466 (s), 1434 (s), 1411 (s), 1350 (m), 1315 (m), 1289 (s), 1271 (s), 1126 (s), 1092 (s), 972 (s), 821 (m), 797 (s), 782 (s), 707 (s) ( $\text{cm}^{-1}$ );  $^1\text{H}$  NMR (500 MHz),  $\delta$  8.74 (s, 1H), 8.49 (d,  $J = 2.0$  Hz, 1H), 7.97 (d,  $J = 8.2$  Hz, 1H), 7.80 (dd,  $J = 8.9, 1.9$  Hz, 1H), 7.54 (d,  $J = 2.0$  Hz, 1H), 7.48 (d,  $J = 8.8$  Hz, 1H), 7.41 (dd,  $J = 8.2, 1.6$  Hz, 1H), 4.52 (t,  $J = 8.0$  Hz, 2H), 4.22 (s, 3H), 1.91–1.86 (m, 2H), 1.45–1.41 (m, 2H), 1.39–1.34 (m, 2H), 1.32–1.26 (m, 10H), 0.87 (t,  $J = 6.9$  Hz, 3H);  $^{13}\text{C}$  NMR (125 MHz)  $\delta$  176.1, 154.8, 148.3, 143.4, 137.4, 137.1, 132.8, 129.6, 123.9, 122.7, 122.33, 122.30, 122.1, 121.0, 120.0, 117.0, 116.2, 114.0, 112.6, 62.8, 45.5, 32.1, 30.1, 29.8 (2C), 29.6, 29.5, 27.3, 22.9, 14.3; MS [APCI (+)]  $m/z$  (%) 616 ( $^{81}\text{Br}_2$ ,  $\text{M}^+$ , 52), 614 ( $^{81}\text{Br}^{79}\text{Br}$ ,  $\text{M}^+$ , 100), 612 ( $^{79}\text{Br}_2$ ,  $\text{M}^+$ , 51); HRMS [EI (+)] calcd for  $\text{C}_{30}\text{H}_{31}\text{Br}_2\text{NO}_3$  611.0671, found 611.0668.

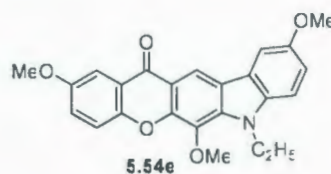
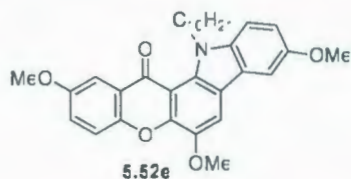
**5.72:**  $R_f = 0.50$  (80:20 petroleum ether:EtOAc); mp > 300 °C; IR  $\nu$  2954 (s), 2923 (s), 2853 (s), 1649 (s), 1628 (s), 1593 (s), 1564 (s), 1498 (s), 1460 (s), 1431 (s), 1347 (s),



1255 (s), 1181 (s), 1126 (s), 1115 (s), 1016 (s), 974 (s), 849 (m), 807 (s), 780 (m), 730 (m) ( $\text{cm}^{-1}$ );  $^1\text{H}$  NMR (500 MHz),  $\delta$  8.55 (d,  $J = 2.5$  Hz, 1H), 8.42 (d,  $J = 8.3$  Hz, 1H), 7.84 (dd,  $J = 8.8, 2.5$  Hz, 1H), 7.70 (s, 1H), 7.69 (d,  $J = 1.4$  Hz, 1H), 7.61 (d,  $J = 8.8$  Hz, 1H), 7.52 (dd,  $J = 8.4, 1.6$  Hz, 1H), 4.73 (q,  $J = 7.1$  Hz, 2H), 4.13 (s, 3H), 1.49 (t,  $J = 7.2$  Hz, 3H);  $^{13}\text{C}$  NMR (insufficient sample for measurement); MS [APCI (+)]  $m/z$  (%) 504 ( $^{81}\text{Br}$ ,  $\text{M}^+$ , 47), 502 ( $^{81}\text{Br}$  and  $^{79}\text{Br}$ ,  $\text{M}^+$ , 100), 500 ( $^{79}\text{Br}$ ,  $\text{M}^+$ , 56); HRMS [EI (+)] calcd for  $\text{C}_{22}\text{H}_{15}\text{Br}_2\text{NO}_3$  498.9419, found 498.9429.

**1'-Decyl-6'-methoxy-1'*H*-indole[2',3'-*a*]-4,7-dimethoxy-9*H*-xanthene-9-one (5.52e)**

**1'-Ethyl-6'-methoxy-1'*H*-indole[2',3'-*b*]-4,7-dimethoxy-9*H*-xanthene-9-one (5.54e)**



A mixture of xanthone **5.31e** (140.5 mg, 345  $\mu\text{mol}$ ), triethyl phosphite (4 mL) and dichloromethane (1 mL) was microwave irradiated for 60 min and worked up according to the general procedure. The crude Cadogan product (131.2 mg, 350  $\mu\text{mol}$ ), potassium hydroxide (79.3 mg, 1.41 mmol), and decyl bromide (1.0 mL) in dioxane was heated at 100  $^{\circ}\text{C}$  overnight and worked up according to the general procedure. Column chromatography (80:20 petroleum ether:EtOAc) of the crude product yielded **5.52e** (115.5 mg, 64%) and **5.54e** (21.8 mg, 15%) as yellow solids.

**5.52e**:  $R_f = 0.55$  (80:20 petroleum ether:EtOAc); mp 142–143  $^{\circ}\text{C}$ ; IR  $\nu$  3004 (w), 2922 (m), 2852 (m), 1651 (s), 1617 (s), 1566 (m), 1484 (s), 1439 (s), 1375 (m), 1334 (s), 1309 (s), 1262 (s), 1220 (s), 1199 (s), 1161 (s), 1064 (s), 1036 (s), 991 (m), 920 (m), 843 (m),

814 (s), 774 (m), 760 (s) ( $\text{cm}^{-1}$ );  $^1\text{H}$  NMR (500 MHz),  $\delta$  7.92 (s, 1H), 7.75 (d,  $J = 3.0$  Hz, 1H), 7.60 (d,  $J = 9.5$  Hz, 1H), 7.49 (d,  $J = 2.1$  Hz, 1H), 7.48 (d,  $J = 7.4$  Hz, 1H), 7.34 (dd,  $J = 9.0, 3.2$  Hz, 1H), 7.12 (dd,  $J = 9.5, 2.6$  Hz, 1H), 4.95 (t,  $J = 7.8$  Hz, 2H), 4.15 (s, 3H), 3.97 (s, 3H), 3.96 (s, 3H), 1.65–1.56 (m, 2H), 1.25–1.12 (m, 14H), 0.84 (t,  $J = 7.5$  Hz, 3H);  $^{13}\text{C}$  NMR (125 MHz)  $\delta$  176.7, 156.4, 154.5, 149.8, 148.0, 142.4, 137.9, 132.6, 124.3, 123.5, 119.3, 118.6, 114.9, 112.1, 110.9, 108.8, 106.1, 101.7, 57.5, 56.3, 56.2, 47.9, 32.1, 29.7 (2C), 29.5 (2C), 29.4, 27.0, 22.8, 14.3 (one signal fewer than expected); MS [APCI (+)]  $m/z$  (%) 516 ( $\text{M}^+$ , 100); HRMS [EI (+)] calcd for  $\text{C}_{32}\text{H}_{37}\text{NO}_5$  515.2672, found 515.2668.

**5.54e:**  $R_f = 0.45$  (80:20 petroleum ether:EtOAc); mp 202–204 °C; IR  $\nu$  2998 (w), 2970 (w), 2941 (w), 2835 (w), 1650 (m), 1606 (s), 1590 (s), 1479 (s), 1459 (s), 1437 (s), 1409 (s), 1366 (m), 1334 (m), 1306 (s), 1285 (s), 1274 (s), 1261 (s), 1247 (s), 1212 (s), 1194 (s), 1145 (s), 1081 (s), 1063 (s), 1032 (s), 948 (m), 862 (m), 824 (s), 782 (s), 765 (m) ( $\text{cm}^{-1}$ );  $^1\text{H}$  NMR (500 MHz),  $\delta$  8.78 (s, 1H), 7.78 (d,  $J = 2.6$  Hz, 1H), 7.67 (d,  $J = 2.4$  Hz, 1H), 7.53 (d,  $J = 9.2$  Hz, 1H), 7.34–7.31 (m, 2H), 7.14 (dd,  $J = 8.5, 2.8$  Hz, 1H), 4.64 (q,  $J = 7.1$  Hz, 2H), 4.22 (s, 3H), 3.95 (s, 6H), 1.84 (t,  $J = 7.2$  Hz, 3H);  $^{13}\text{C}$  NMR (125 MHz)  $\delta$  177.5, 156.0, 154.8, 151.0, 148.2, 137.0, 136.9, 132.3, 124.4, 124.1, 122.7, 121.6, 119.3, 116.0, 115.4, 113.9, 109.8, 106.4, 103.9, 62.6, 56.3, 51.0, 39.9, 15.1; MS [APCI (+)]  $m/z$  (%) 404 ( $\text{M}^+$ , 100); HRMS [EI (+)] calcd for  $\text{C}_{24}\text{H}_{21}\text{NO}_5$  403.1420, found 403.1418.

**General method for Suzuki couplings***a) Coupling with phenylboronic acid 5.66a (compounds 5.67a–c):*

A suspension of aryl bromide (1.0 equiv.), phenylboronic acid (2.0 equiv. for each bromo group), potassium carbonate (10 equiv. for each bromo group) in toluene-ethanol (1.5:1, 2.5 mL) was degassed (N<sub>2</sub>) three times via a “freeze-pump-thaw” cycle. Tetrakis(triphenylphosphine)palladium(0) (5 mol% for each bromo group) was quickly added and the reaction mixture was degassed three times again via a “freeze-pump-thaw” cycle. The resulting yellow reaction mixture was then heated at 80 °C for 2 h.

*b) Coupling with 2-thienylboronic acid 5.66b (compounds 5.68a–c):*

A suspension of aryl bromide (1.0 equiv.), 2-thienylboronic acid (2.0 equiv. for each bromo group), potassium carbonate (5 equiv. or 10 equiv. for each bromo group) in appropriate solvents was degassed three times via a “freeze-pump-thaw” cycle. Tetrakis(triphenylphosphine)palladium(0) (10 mol% or 15 mol% for each bromo group) was quickly added and the reaction mixture was degassed three times again via a “freeze-pump-thaw” cycle. The resulting yellow reaction mixture was then heated at 100 °C for indicated time.

*c) Coupling with 1-pyrenylboronic acid 5.66b (compounds 5.69a–c):*

A suspension of aryl bromide (1.0 equiv.), 1-pyrenylboronic acid (2.0 equiv. for each bromo group), potassium carbonate (10 equiv. for each bromo group) in dioxane-water (2:1, 3 mL) was degassed three times via a “freeze-pump-thaw” cycle. Tetrakis(triphenylphosphine)palladium(0) (10 mol% for each bromo group) was quickly added and the reaction mixture was degassed three times again via a “freeze-pump-thaw”

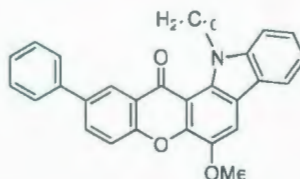


cycle. The yellow resulting reaction mixture was then heated at 100 °C for the indicated time.

*Work up procedure for Suzuki coupling:*

The reaction mixture was cooled to room temperature and water (15 mL) and CH<sub>2</sub>Cl<sub>2</sub> (15 mL) were added. The organic layer was separated and the aqueous layer was extracted with CH<sub>2</sub>Cl<sub>2</sub> (3 x 15 mL). The combined organic layers were washed with water (20 mL), washed with brine (20 mL) and dried over MgSO<sub>4</sub>. The solvent was removed under reduced pressure and the residue was purified by column chromatography to yield desired products as yellow solids.

**1'-Decyl-1'H-indole[2',3'-a]-4-methoxy-7-phenyl-9H-xanthene-9-one (5.67a)**

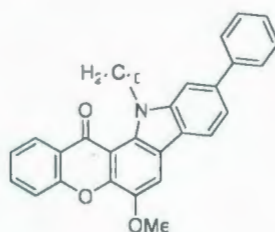


A mixture of bromo compound **5.52b** (26.5 mg, 49.0 μmol), phenylboronic acid **5.66a** (11.9 mg, 98.0 μmol), potassium carbonate (67.7 mg, 490 μmol), and tetrakis(triphenylphosphine)palladium(0) (2.8 mg, 2.5 μmol) in toluene-ethanol was heated and worked up according to the general procedure. Column chromatography (CH<sub>2</sub>Cl<sub>2</sub>) of the crude product yielded **5.67a** (26.0 mg, 100%) as a yellow solid: *R<sub>f</sub>* = 0.66 (CH<sub>2</sub>Cl<sub>2</sub>); mp 133–134 °C; IR ν 3060 (w), 3033 (w), 2950 (w), 2922 (w), 2850 (w), 1657 (s), 1611 (m), 1592 (w), 1566 (m), 1511 (m), 1492 (m), 1471 (s), 1455 (s), 1434 (s), 1323 (s), 1295 (m), 1273 (s), 1260 (s), 1220 (s), 1194 (s), 1067 (s), 1017 (s), 960 (s), 903 (s), 821 (s), 756 (s), 738 (s), 688 (s) (cm<sup>-1</sup>); <sup>1</sup>H NMR (500 MHz) δ 8.59 (d, *J* = 2.9 Hz, 1H),



8.05 (d,  $J = 7.8$  Hz, 1H), 7.99–7.97 (m, 2H), 7.74–7.71 (m, 3H), 7.58 (d,  $J = 8.1$  Hz, 1H), 7.50–7.47 (m, 3H), 7.39 (t,  $J = 7.7$  Hz, 1H), 7.30–7.25 (m, 1H), 4.98 (t,  $J = 7.7$  Hz, 2H), 4.15 (s, 3H), 1.70–1.64 (m, 2H), 1.13–1.25 (m, 14H), 0.82 (t,  $J = 7.3$  Hz, 3H);  $^{13}\text{C}$  NMR (125 MHz)  $\delta$  177.1, 154.4, 147.8, 142.8, 142.6, 139.9, 137.3, 133.1, 132.1, 129.2, 127.8, 127.4, 125.6, 124.7, 123.2, 122.0, 120.0, 119.2, 119.1, 118.4, 111.3, 111.2, 109.1, 57.5, 47.8, 32.0, 29.7, 29.5, 29.4, 27.0, 22.8, 14.3; MS [APCI (+)]  $m/z$  (%) 532 ( $\text{M}^+$ , 100); HRMS [EI (+)] calcd for  $\text{C}_{36}\text{H}_{37}\text{NO}_3$  531.2773, found 531.2775.

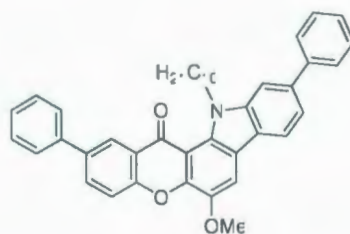
**1'-Decyl-6'-phenyl-1'-H-indole[2',3'-a]-4-methoxy-9H-xanthene-9-one (5.68a)**



A mixture of bromo compound **5.52d** (50.9 mg, 95.0  $\mu\text{mol}$ ), phenylboronic acid **5.56a** (23.2 mg, 190  $\mu\text{mol}$ ), potassium carbonate (131.3 mg, 950  $\mu\text{mol}$ ), and tetrakis(triphenylphosphine)palladium(0) (5.5 mg, 4.8  $\mu\text{mol}$ ) in toluene-ethanol was heated and worked up according to the general procedure. Column chromatography ( $\text{CH}_2\text{Cl}_2$ ) of the crude product yielded **5.68a** (47.0 mg, 93%) as a yellow solid:  $R_f = 0.63$  ( $\text{CH}_2\text{Cl}_2$ ); mp 133–134  $^\circ\text{C}$ ; IR  $\nu$  3000 (w), 2959 (w), 2918 (m), 2849 (m), 1663 (s), 1613 (m), 1589 (s), 1559 (s), 1484 (s), 1465 (s), 1427 (s), 1366 (s), 1329 (s), 1272 (s), 1234 (s), 1220 (s), 1170 (s), 1066 (m), 955 (s), 856 (s), 807 (s), 766 (s), 751 (s), 705 (m) ( $\text{cm}^{-1}$ );  $^1\text{H}$  NMR (500 MHz)  $\delta$  8.36 (dd,  $J = 7.5, 1.6$  Hz, 1H), 8.05 (d,  $J = 8.0$  Hz, 1H), 7.95 (s, 1H), 7.74–7.71 (m, 4H), 7.64 (d,  $J = 7.9$  Hz, 1H), 7.48–7.52 (m, 3H), 7.37–7.42 (m, 2H), 5.01

(t,  $J = 7.5$  Hz, 2H), 4.14 (s, 3H), 1.66–1.72 (m, 2H), 1.14–1.25 (m, 14H), 0.84 (t,  $J = 7.0$  Hz, 3H);  $^{13}\text{C}$  NMR (125 MHz)  $\delta$  177.0, 154.9, 147.8, 143.3, 142.7, 142.4, 139.0, 134.2, 132.6, 129.0, 127.8, 127.3, 126.8, 124.1, 123.2, 122.3, 119.8, 119.5, 118.9, 117.8, 111.4, 109.7, 109.0, 57.4, 47.8, 32.1, 29.7, 29.5, 27.0, 22.9, 14.3; MS [APCI (+)]  $m/z$  (%) 532 ( $\text{M}^+$ , 100); HRMS [EI (+)] calcd for  $\text{C}_{36}\text{H}_{37}\text{NO}_3$  531.2773, found 531.2766.

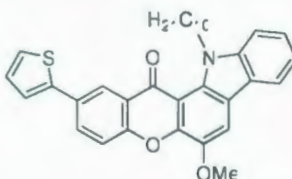
**1'-Decyl-6'-phenyl-1'*H*-indole[2',3'-*a*]-4-methoxy-7-phenyl-9*H*-xanthene-9-one  
(5.69a)**



A mixture of dibromo compound **5.52f** (25.3 mg, 41.2  $\mu\text{mol}$ ), phenylboronic acid **5.66a** (20.0 mg, 164  $\mu\text{mol}$ ), potassium carbonate (113 mg, 818  $\mu\text{mol}$ ), and tetrakis(triphenylphosphine)palladium(0) (4.71 mg, 4.08  $\mu\text{mol}$ ) in toluene-ethanol was heated and worked up according to the general procedure. Column chromatography ( $\text{CH}_2\text{Cl}_2$ ) of the crude product yielded **5.69a** (21.5 mg, 86%) as a yellow solid:  $R_f = 0.66$  ( $\text{CH}_2\text{Cl}_2$ ); mp 145–146  $^\circ\text{C}$ ; IR  $\nu$  3039 (w), 3011 (w), 2951 (w), 2917 (m), 2850 (m), 1661 (s), 1614 (m), 1559 (s), 1509 (m), 1480 (s), 1471 (s), 1435 (s), 1359 (s), 1318 (s), 1258 (s), 1219 (s), 1192 (s), 1068 (m), 1014 (w), 960 (m), 855 (m), 807 (m), 767 (s), 756 (s), 695 (s)  $\text{cm}^{-1}$ ;  $^1\text{H}$  NMR (500 MHz)  $\delta$  8.60 (d,  $J = 2.0$  Hz, 1H), 8.08 (d,  $J = 7.5$  Hz, 1H), 8.00–7.97 (m, 2H), 7.76–7.72 (m, 6H), 7.54–7.48 (m, 5H), 7.41–7.37 (m, 2H), 5.04 (t,  $J = 7.8$  Hz, 2H), 4.17 (s, 3H), 1.73–1.67 (m, 2H), 1.25–1.13 (m, 14H), 0.81 (t,  $J = 7.1$  Hz,

3H);  $^{13}\text{C}$  NMR (125 MHz)  $\delta$  177.0, 154.4, 147.8, 143.4, 142.8, 142.4, 139.8, 139.1, 137.3, 133.1, 132.6, 129.1, 129.0, 127.9, 127.4, 127.3, 124.7, 123.2, 122.3, 119.9, 119.5, 119.0, 118.4, 111.4, 109.7, 109.0, 57.5, 47.8, 32.0, 29.7, 29.48, 29.46, 27.0, 22.8, 14.3; MS [APCI (+)]  $m/z$  (%) 608 ( $\text{M}^+$ , 100); HRMS [EI (+)] calcd for  $\text{C}_{42}\text{H}_{41}\text{NO}_3$  607.3086, found 607.3081.

**1'-Decyl-1'-H-indole[2',3'-a]-4-methoxy-7-(2-thiethyl)-9H-xanthene-9-one (5.67b)**

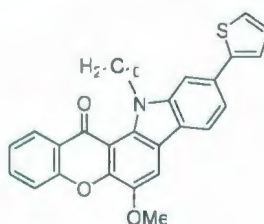


A mixture of bromo compound **5.52b** (20.6 mg, 38.5  $\mu\text{mol}$ ), 2-thienylboronic acid **5.66b** (9.72 mg, 76.0  $\mu\text{mol}$ ), potassium carbonate (26.2 mg, 190  $\mu\text{mol}$ ), and tetrakis(triphenylphosphine)palladium(0) (4.43 mg, 3.83  $\mu\text{mol}$ ) in DMF (3 mL) was heated at 100  $^{\circ}\text{C}$  for 24 h and worked up according to the general procedure. Column chromatography (60:40  $\text{CH}_2\text{Cl}_2$ :petroleum ether) of the crude product yielded **5.67b** (14.5 mg, 71%, 26% recovery of SM or 95% borsm) as a yellow solid:  $R_f$  = 0.41 (60:40  $\text{CH}_2\text{Cl}_2$ :petroleum ether); mp 138–140  $^{\circ}\text{C}$ ; IR  $\nu$  2956 (s), 2917 (s), 2850 (s), 1658 (s), 1611 (m), 1564 (m), 1534 (m), 1492 (s), 1467 (s), 1439 (s), 1322 (s), 1273 (s), 1205 (s), 1178 (s), 1129 (s), 1067 (s), 998 (m), 948 (s), 899 (s), 851 (s), 808 (s), 791 (s), 739 (s), 737 (s), 685 (s) ( $\text{cm}^{-1}$ );  $^1\text{H}$  NMR (500 MHz)  $\delta$  8.58 (d,  $J$  = 1.4 Hz, 1H), 8.06 (d,  $J$  = 7.9 Hz, 1H), 8.00–7.97 (m, 2H), 7.68 (d,  $J$  = 9.0 Hz, 1H), 7.60 (d,  $J$  = 8.0 Hz, 1H), 7.51–7.48 (m, 1H), 7.46–7.45 (m, 1H), 7.34 (dd,  $J$  = 5.1, 1.6 Hz, 1H), 7.30 (t,  $J$  = 7.3 Hz, 1H), 7.14–7.13 (m, 1H), 4.99 (t,  $J$  = 7.5 Hz, 2H), 4.17 (s, 3H), 1.70–1.64 (m, 2H), 1.26–1.14 (m,



14H), 0.83 (t,  $J = 7.5$  Hz, 3H);  $^{13}\text{C}$  NMR (125 MHz)  $\delta$  176.8, 154.2, 147.7, 143.2, 142.9, 142.6, 132.1, 132.0, 130.1, 128.4, 125.62, 125.57, 124.0, 123.32, 123.26, 123.0, 120.1, 119.3, 119.25, 118.5, 111.3, 111.2, 109.2, 57.5, 47.8, 32.1, 29.9, 29.7, 29.48, 29.45, 27.0, 22.9, 14.3; MS [APCI (+)]  $m/z$  (%) 538 ( $\text{M}^+$ , 100); HRMS [EI (+)] calcd for  $\text{C}_{34}\text{H}_{35}\text{NO}_3\text{S}$  537.2338, found 537.2333.

**1'-Decyl-6'-(2-thienyl)-1'H-indole[2',3'-a]-4-methoxy-9H-xanthene-9-one (5.68b)**

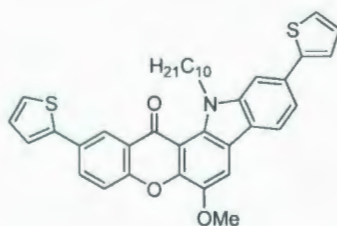


A mixture of bromo compound **5.52d** (20.6 mg, 38.5  $\mu\text{mol}$ ), 2-thienylboronic acid **5.66b** (9.72 mg, 76.0  $\mu\text{mol}$ ), potassium carbonate (52.4 mg, 379  $\mu\text{mol}$ ), and tetrakis(triphenylphosphine)palladium(0) (6.62 mg, 5.73  $\mu\text{mol}$ ) in dioxane-water (2:1 mL) were heated at 100  $^{\circ}\text{C}$  for 2 h and worked up according to the general procedure (extraction with EtOAc instead of  $\text{CH}_2\text{Cl}_2$ ). Column chromatography (80:20  $\text{CH}_2\text{Cl}_2$ :petroleum ether) of the crude product yielded **5.68b** (14.5 mg, 71%) as a yellow solid:  $R_f = 0.53$  (80:20  $\text{CH}_2\text{Cl}_2$ : petroleum ether); mp 144–146  $^{\circ}\text{C}$ ; IR  $\nu$  3069 (w), 2954 (m), 2921 (s), 2851 (s), 1663 (s), 1612 (s), 1587 (s), 1562 (s), 1495 (s), 1464 (s), 1371 (s), 1330 (s), 1272 (s), 1210 (s), 1146 (m), 1065 (m), 952 (s), 900 (m), 849 (m), 801 (s), 757 (s), 719 (s), 683 (s) ( $\text{cm}^{-1}$ );  $^1\text{H}$  NMR (500 MHz)  $\delta$  8.38 (dd,  $J = 7.5, 1.7$  Hz, 1H), 8.03 (d,  $J = 7.9$  Hz, 1H), 7.96 (s, 1H), 7.79 (s, 1H), 7.77–7.73 (m, 1H), 7.66 (d,  $J = 8.6$  Hz, 1H), 7.57 (dd,  $J = 8.3, 0.9$  Hz, 1H), 7.44–7.42 (m, 2H), 7.32 (d,  $J = 4.3$  Hz, 1H), 7.14 (dd,  $J =$



5.2, 3.8 Hz, 1H), 5.00 (t,  $J = 7.2$  Hz, 2H), 4.17 (s, 3H), 1.70–1.67 (m, 2H), 1.24–1.15 (m, 14H), 0.84 (t,  $J = 7.5$  Hz, 3H);  $^{13}\text{C}$  NMR (125 MHz)  $\delta$  177.1, 155.0, 147.9, 145.8, 143.2, 142.9, 134.3, 132.7, 132.1, 128.3, 126.8, 124.8, 124.2, 123.3, 123.2, 122.5, 119.6, 118.9, 118.88, 117.8, 111.4, 108.9, 108.4, 57.5, 47.8, 32.1, 29.9, 29.7, 29.5, 29.44, 29.42, 27.0, 22.9, 14.3; MS [APCI (+)]  $m/z$  (%) 538 ( $\text{M}^+$ , 100); HRMS [EI (+)] calcd for  $\text{C}_{34}\text{H}_{35}\text{NO}_3\text{S}$  537.2338, found 537.2333.

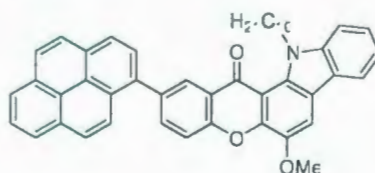
**1'-Decyl-6'-(2-thienyl)-1'H-indole[2',3'-a]-4-methoxy-7-(2-thienyl)-9H-xanthene-9-one (5.69b)**



A mixture of dibromo compound **5.52f** (10.5 mg, 17.1  $\mu\text{mol}$ ), 2-thienylboronic acid **5.66b** (9.2 mg, 71.9  $\mu\text{mol}$ ), potassium carbonate (25.0 mg, 181  $\mu\text{mol}$ ), and tetrakis(triphenylphosphine)palladium (6.31 mg, 5.46  $\mu\text{mol}$ ) in DMF (4 mL) was heated at 120  $^{\circ}\text{C}$  for 26 h and worked up according to the general procedure. Column chromatography (60:40  $\text{CH}_2\text{Cl}_2$ :petroleum ether) of the crude product yielded **5.69b** (8.41 mg, 80%) as a yellow solid:  $R_f = 0.46$  (60:40  $\text{CH}_2\text{Cl}_2$ : petroleum ether); mp 198–200  $^{\circ}\text{C}$ ; IR  $\nu$  2954 (m), 2921 (s), 2852 (s), 1661 (s), 1609 (s), 1563 (s), 1533 (m), 1491 (s), 1485 (s), 1368 (s), 1301 (s), 1275 (s), 1207 (s), 1164 (s), 1065 (m), 1026 (m), 949 (s), 900 (s), 850 (m), 810 (s), 797 (s), 682 (s) ( $\text{cm}^{-1}$ );  $^1\text{H}$  NMR (500 MHz)  $\delta$  8.58 (d,  $J = 2.3$  Hz, 1H), 8.03 (d,  $J = 8.0$  Hz, 1H), 7.99 (dd,  $J = 8.4, 2.0$  Hz, 1H), 7.97 (s, 1H), 7.80 (s, 1H), 7.68

(d,  $J = 8.5$  Hz, 1H), 7.57 (dd,  $J = 8.3, 1.3$  Hz, 1H), 7.46–7.44 (m, 2H), 7.35–7.32 (m, 2H), 7.15–7.13 (m, 2H), 5.02 (t,  $J = 7.3$  Hz, 2H), 4.18 (s, 3H), 1.73–1.67 (m, 2H), 1.23–1.14 (m, 14H), 0.82 (t,  $J = 7.3$  Hz, 3H);  $^{13}\text{C}$  NMR (125 MHz)  $\delta$  176.8, 154.2, 147.8, 145.8, 143.3, 143.1, 142.9, 132.7, 132.1, 132.07, 130.9, 128.5, 128.3, 125.6, 124.9, 124.0, 123.33, 123.29, 123.25, 122.5, 119.7, 119.1, 119.0, 118.6, 111.3, 108.9, 108.5, 57.5, 47.8, 32.2, 32.1, 29.9, 29.7, 29.48, 29.46, 29.42, 27.0, 22.8, 14.3; MS [APCI (+)]  $m/z$  (%) 620 ( $\text{M}^+$ , 100); HRMS [EI (+)] calcd for  $\text{C}_{38}\text{H}_{37}\text{NO}_3\text{S}_2$  619.2215, found 619.2208.

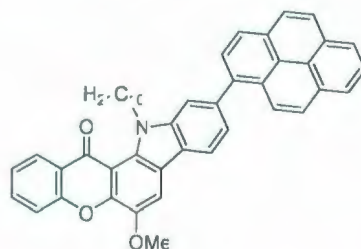
**1'-Decyl-1'H-indole[2',3'-a]-4-methoxy-7-(1-pyrenyl)-9H-xanthene-9-one (5.67c)**



A mixture of bromo compound **5.52b** (10.7 mg, 20.0  $\mu\text{mol}$ ), 1-pyrenylboronic acid **5.66c** (9.8 mg, 39.8  $\mu\text{mol}$ ), potassium carbonate (27.6 mg, 200  $\mu\text{mol}$ ), and tetrakis(triphenylphosphine)palladium (2.3 mg, 1.99  $\mu\text{mol}$ ) in dioxane-water (2:1 mL) were heated and worked up according to the general procedure. Column chromatography (60:40  $\text{CH}_2\text{Cl}_2$ :petroleum ether) of the crude product yielded **5.67c** (13.1 mg, 100%) as a yellow solid:  $R_f = 0.33$  (60:40  $\text{CH}_2\text{Cl}_2$ :petroleum ether); mp 205–207  $^\circ\text{C}$ ; IR  $\nu$  3034 (w), 2952 (s), 2921 (s), 2850 (s), 1650 (s), 1609 (s), 1588 (m), 1565 (s), 1512 (w), 1471 (s), 1468 (s), 1441 (s), 1378 (m), 1322 (s), 1267 (s), 1188 (s), 1128 (m), 1092 (s), 1064 (s), 1020 (s), 973 (s), 960 (s), 862 (s), 820 (s), 794 (s), 758 (s), 729 (s), 682 (m) ( $\text{cm}^{-1}$ );  $^1\text{H}$  NMR (500 MHz)  $\delta$  8.65 (d,  $J = 2.1$ , 1H), 8.26 (d,  $J = 7.8$  Hz, 1H), 8.23–8.17 (m, 3H), 8.12 (s, 2H), 8.10–8.00 (m, 6H), 7.85 (d,  $J = 8.5$ , 1H), 7.59 (d,  $J = 8.2$ , 1H), 7.49 (t,  $J =$

7.3, 1H), 7.31 (t,  $J = 7.4$ , 1H), 4.97 (t,  $J = 7.4$  Hz, 2H), 4.20 (s, 3H), 1.75–1.67 (m, 2H), 1.27–1.08 (m, 14H), 0.76 (t,  $J = 7.1$  Hz, 3H);  $^{13}\text{C}$  NMR (125 MHz)  $\delta$  177.1, 154.4, 147.9, 142.8, 142.7, 137.4, 136.7, 136.3, 132.2, 131.7, 131.2, 131.1, 128.8, 128.2, 128.1, 128.09, 127.9, 127.6, 126.3, 125.6, 125.5, 125.24, 125.22, 125.1, 125.03, 125.0, 123.2, 123.0, 120.1, 119.8, 119.2, 117.9, 111.5, 111.2, 109.3, 57.6, 47.9, 32.0, 29.9, 29.7, 29.6, 29.5, 29.4, 27.0, 22.8, 14.3; MS [APCI (+)]  $m/z$  (%) 656 ( $\text{M}^+$ , 100); HRMS [EI (+)] calcd for  $\text{C}_{46}\text{H}_{41}\text{NO}_3$  655.3086, found 655.3087.

**1'-Decyl-6'-(1-pyrenyl)-1'*H*-indole[2',3'-*a*]-4-methoxy-9*H*-xanthene-9-one (5.68c)**

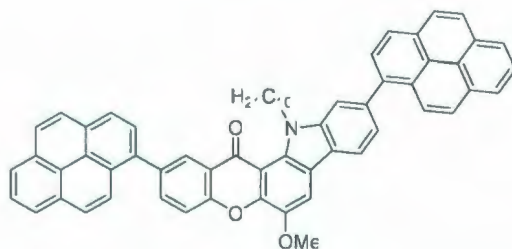


A mixture of bromo compound **5.52d** (10.8 mg, 20.2  $\mu\text{mol}$ ), 1-pyrenylboronic acid **5.66c** (10.0 mg, 40.6  $\mu\text{mol}$ ), potassium carbonate (28.2 mg, 204  $\mu\text{mol}$ ), and tetrakis(triphenylphosphine)palladium(0) (2.41 mg, 2.09  $\mu\text{mol}$ ) in dioxane-water (2:1 mL) were heated and worked up according to the general procedure. Column chromatography (60:40  $\text{CH}_2\text{Cl}_2$ :petroleum ether) of the crude product yielded **5.68c** (12.2 mg, 93%) as a yellow solid:  $R_f = 0.20$  (60:40  $\text{CH}_2\text{Cl}_2$ :petroleum ether); mp 166–167  $^\circ\text{C}$ ; IR  $\nu$  3036 (w), 2921 (s), 2851 (m), 1661 (s), 1613 (m), 1587 (m), 1562 (s), 1491 (m), 1466 (s), 1442 (s), 1427 (s), 1372 (s), 1331 (s), 1273 (s), 1236 (s), 1204 (s), 1187 (m), 1063 (s), 955 (s), 839 (s), 754 (s), 719 (s), 680 (s) ( $\text{cm}^{-1}$ );  $^1\text{H}$  NMR (500 MHz)  $\delta$  8.39 (d,  $J = 7.8$ , 1H), 8.28 (t,  $J = 9.3$  Hz, 2H), 8.21 (dd,  $J = 7.6$ , 2.0 Hz, 2H), 8.17 (d,  $J = 7.5$  Hz,



1H), 8.15–8.09 (m, 3H), 8.05–7.99 (m, 3H), 7.83 (s, 1H), 7.78–7.72 (m, 1H), 7.68 (d,  $J = 8.4$ , 1H), 7.57 (d,  $J = 7.9$ , 1H), 7.43 (t,  $J = 7.4$ , 1H), 5.02 (t,  $J = 7.4$  Hz, 2H), 4.20 (s, 3H), 1.78–1.68 (m, 2H), 1.25–1.10 (m, 14H), 0.80 (t,  $J = 7.1$  Hz, 3H);  $^{13}\text{C}$  NMR (125 MHz)  $\delta$  177.1, 155.0, 147.9, 143.0, 142.9, 138.8, 138.7, 134.3, 132.6, 131.8, 131.3, 130.8, 129.0, 128.2, 127.70, 127.69, 127.6, 126.8, 126.3, 125.8, 125.3, 125.28, 125.2, 125.0, 124.8, 124.2, 123.2, 123.1, 122.2, 119.1, 119.0, 117.9, 113.3, 111.5, 109.1, 57.6, 47.9, 32.0, 29.9, 29.70, 29.67, 29.6, 29.5, 27.0, 22.8, 14.3; MS [APCI (+)]  $m/z$  (%) 656 ( $\text{M}^+$ , 100); HRMS [EI (+)] calcd for  $\text{C}_{46}\text{H}_{41}\text{NO}_3$  655.3086, found 655.3085.

**1'-Decyl-6'-(1-pyrenyl)-1'*H*-indole[2',3'-*a*]-4-methoxy-7-(1-pyrenyl)-9*H*-xanthene-9-one (5.69c)**



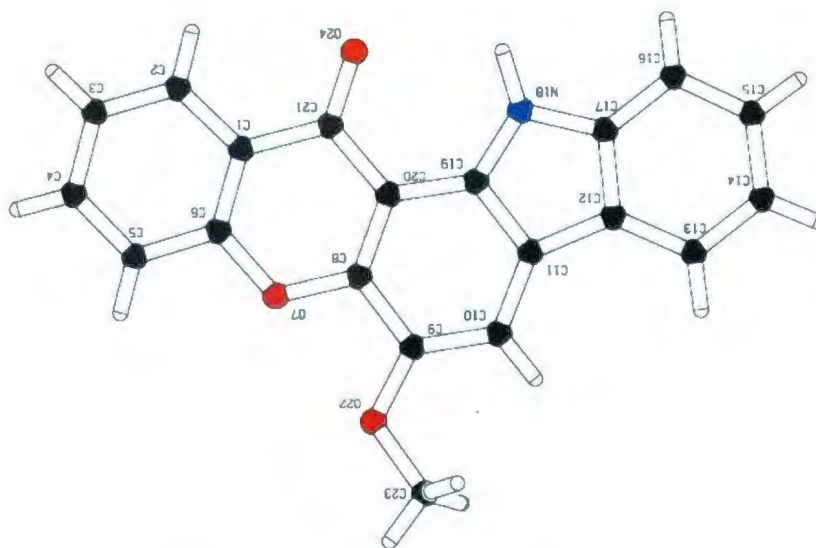
A mixture of dibromo compound **5.52f** (11.3 mg, 18.4  $\mu\text{mol}$ ), 1-pyrenylboronic acid **5.66c** (17.7 mg, 71.9  $\mu\text{mol}$ ), potassium carbonate (49.7 mg, 360  $\mu\text{mol}$ ), and tetrakis(triphenylphosphine)palladium(0) (4.20 mg, 3.63  $\mu\text{mol}$ ) in dioxane-water (2:1 mL) were heated at 100  $^{\circ}\text{C}$  and worked up according to the general procedure. Column chromatography (60:40  $\text{CH}_2\text{Cl}_2$ :petroleum ether) of the crude product yielded **5.69c** (14.1 mg, 92%) as a yellow solid:  $R_f = 0.34$  (60:40  $\text{CH}_2\text{Cl}_2$ :petroleum ether); mp 235–237  $^{\circ}\text{C}$ ; IR  $\nu$  3040 (w), 2947 (w), 2920 (w), 2845 (w), 1643 (s), 1606 (s), 1565 (s), 1483 (s), 1471 (s), 1441 (s), 1370 (s), 1307 (s), 1274 (s), 1255 (s), 1195 (s), 1062 (m), 976 (m), 843 (s),



834 (s), 722 (s), 680 (s) ( $\text{cm}^{-1}$ );  $^1\text{H}$  NMR (500 MHz)  $\delta$  8.67 (d,  $J = 2.1$  Hz, 1H), 8.32–8.01 (m, 21 H), 7.90 (d,  $J = 8.6$  Hz, 1H), 7.84 (s, 1H), 7.61 (dd,  $J = 7.9, 0.9$  Hz, 1H), 5.03 (t,  $J = 7.4$  Hz, 2H), 4.27 (s, 3H), 1.81–1.73 (m, 2H), 1.22–1.01 (m, 14H), 0.71 (t,  $J = 7.1$  Hz, 3H);  $^{13}\text{C}$  NMR (150 MHz,  $\{^1\text{H}\}$  CPMAS (cross-polarization under magic angle spinning), using 100 kHz of  $^1\text{H}$  decoupling and 62.5 kHz for the Hartmann-Hahn matching condition. The spectrum was collected at room temperature (298 K) with a spinning rate  $\nu = 20$  kHz and 10240 scans)  $\delta$  172.4, 148.8, 142.3, 137.7, 133.9, 132.0, 129.2, 123.7, 120.4, 118.3, 113.9, 110.2, 105.8, 54.9, 47.4, 28.5, 25.1, 17.9 (44 signals fewer than expected); MS [APCI (+)]  $m/z$  (%) 856 ( $\text{M}^+$ , 100); HRMS [EI (+)] calcd for  $\text{C}_{62}\text{H}_{49}\text{NO}_3$  855.3712, found 855.3709.

### 5.5.2 Crystallographic Data for Compounds 5.39-5.42.

X-ray crystallographic analysis for compounds **5.39**, **5.40**, **5.41**, and **5.42** were performed by Dr. Dieter Schollmeyer, University of Mainz, Germany. The text and data given below were taken from the reports provided by Dr. Schollmeyer.

**1'*H*- Indole[2',3'-1,2]-4-methoxy-9*H*--9-one (5.39)**Crystal data for JM55F2 (J. Moritz AK Witulski)

formula	$\text{C}_{20}\text{H}_{13}\text{N}_2\text{O}_3$		
molecular weight	$315.3 \text{ g mol}^{-1}$		
absorption	$\mu = 0.82 \text{ mm}^{-1}$		
crystal size	$0.03 \times 0.03 \times 0.8 \text{ mm}^3$ yellow green needle		
space group	$\text{C } 2/c$ (monoclinic)		
lattice parameters	$a = 25.261(3) \text{ \AA}$		
(calculate from 25	$b = 4.8097(4) \text{ \AA}$	$\beta = 97.00(2)^\circ$	
reflections with	$c = 23.376(3) \text{ \AA}$		
$10^\circ < \Theta < 30^\circ$ )	$V = 2819.0(6) \text{ \AA}^3$	$Z = 8$	$F(000) = 1312$
temperature	$-80^\circ\text{C}$		
density	$d_{\text{xray}} = 1.486 \text{ g cm}^{-3}$		

	<u>data collection</u>
diffractometer	Turbo CAD4
radiation	Cu-K $\alpha$ graphite monochromator
scan type	$\omega/2\Theta$
scan – width	$1.1 + 0.16 * \tau \alpha \nu(\Theta)^\circ$
scan range	$2^\circ \leq \Theta < 70^\circ$
	$0 \leq h \leq 30 \quad 0 \leq k \leq 5 \quad -28 \leq l \leq 28$
number of reflections:	
measured	3085
unique	2667 ( $R_\sigma = 0.2059$ )
observed	1300 ( $ F /\sigma(F) > 4.0$ )

daten correction, structure solution and refinement

corrections	Lorentz and polarisation correction.
Structure solution	Program: SIR-97 (Direct methods)
refinement	Program: SHELXL-97 (full matrix). 218 refined parameters, weighting scheme: $w = 1/[\sigma^2(F_o^2) + (0.2 * P)^2]$ with $(\text{Max}(F_o^2, 0) + 2 * F_o^2)/3$ . H-atoms at calculated positions and refined with isotropic displacement parameters, non H- atoms refined anisotropically.
R-values	$wR2 = 0.3788$ ( $R1 = 0.1236$ for observed reflections, 0.2190 for all reflections)
goodness of fit	$S = 1.131$
maximum deviation of parameters	0.001 * e.s.d
maximum peak height in diff. Fourier synthesis	0.82, -0.78 eÅ $^{-3}$

*Table of bond lengths*

Entry	Atom1	Atom2	Length Å
1	C1	C2	1.4064
2	C1	C6	1.3676
3	C1	C21	1.4653
4	C2	H2	0.9300
5	C2	C3	1.3743
6	C3	H3	0.9300
7	C3	C4	1.3676
8	C4	H4	0.9300
9	C4	C5	1.3903
10	C5	H5	0.9300
11	C5	C6	1.3979
12	C6	O7	1.3799
13	O7	C8	1.3666
14	C8	C9	1.4212
15	C8	C20	1.3837
16	C9	C10	1.3978
17	C9	O22	1.3459
18	C10	H10	0.9300
19	C10	C11	1.3951
20	C11	C12	1.4392
21	C11	C19	1.4274
22	C12	C13	1.4082
23	C12	C17	1.4034
24	C13	H13	0.9300
25	C13	C14	1.3844
26	C14	H14	0.9300
27	C14	C15	1.3822
28	C15	H15	0.9300
29	C15	C16	1.3919
30	C16	H16	0.9300
31	C16	C17	1.3857
32	C17	N18	1.3864
33	N18	H18	1.0363
34	N18	C19	1.3498
35	C19	C20	1.4144
36	C20	C21	1.4532
37	C21	O24	1.2393
38	O22	C23	1.4407
39	C23	H23A	0.9600
40	C23	H23B	0.9600
41	C23	H23C	0.9600



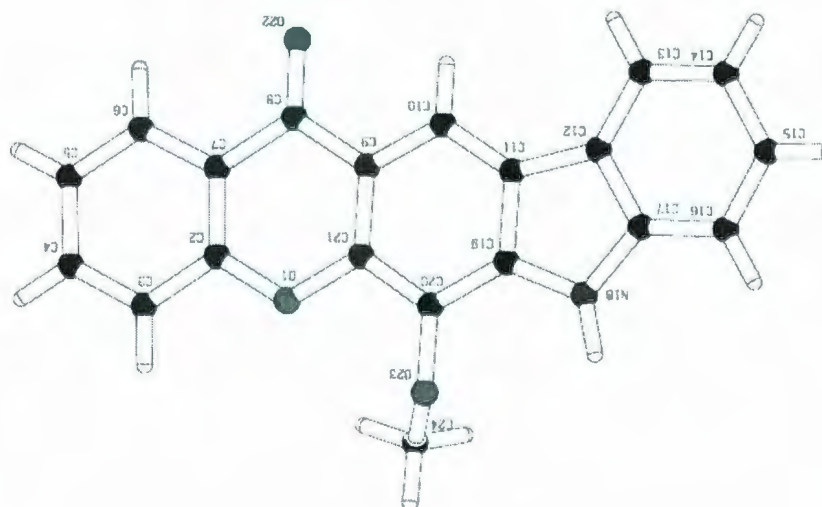
*Table of torsion angles*

Entry	Atom1	Atom2	Atom3	Atom4	Torsion angle (°)
1	C6	C1	C2	H2	-179.87
2	C6	C1	C2	C3	0.13
3	C21	C1	C2	H2	0.76
4	C21	C1	C2	C3	-179.24
5	C2	C1	C6	C5	0.52
6	C2	C1	C6	O7	-177.79
7	C21	C1	C6	C5	179.9
8	C21	C1	C6	O7	1.58
9	C2	C1	C21	C20	178.44
10	C2	C1	C21	O24	-0.97
11	C6	C1	C21	C20	-0.91
12	C6	C1	C21	O24	179.67
13	C1	C2	C3	H3	178.71
14	C1	C2	C3	C4	-1.29
15	H2	C2	C3	H3	-1.29
16	H2	C2	C3	C4	178.71
17	C2	C3	C4	H4	-178.17
18	C2	C3	C4	C5	1.83
19	H3	C3	C4	H4	1.83
20	H3	C3	C4	C5	-178.17
21	C3	C4	C5	H5	178.84
22	C3	C4	C5	C6	-1.16
23	H4	C4	C5	H5	-1.16
24	H4	C4	C5	C6	178.84
25	C4	C5	C6	C1	-0.02
26	C4	C5	C6	O7	178.43
27	H5	C5	C6	C1	179.98
28	H5	C5	C6	O7	-1.57
29	C1	C6	O7	C8	-1.48
30	C5	C6	O7	C8	-179.91
31	C6	O7	C8	C9	179.6
32	C6	O7	C8	C20	0.74
33	O7	C8	C9	C10	179.43
34	O7	C8	C9	O22	-0.62
35	C20	C8	C9	C10	-1.71
36	C20	C8	C9	O22	178.23
37	O7	C8	C20	C19	178.82
38	O7	C8	C20	C21	-0.16
39	C9	C8	C20	C19	0.07
40	C9	C8	C20	C21	-178.92

41	C8	C9	C10	H10	-177.87
42	C8	C9	C10	C11	2.13
43	O22	C9	C10	H10	2.19
44	O22	C9	C10	C11	-177.81
45	C8	C9	O22	C23	-166.77
46	C10	C9	O22	C23	13.17
47	C9	C10	C11	C12	179.3
48	C9	C10	C11	C19	-0.98
49	H10	C10	C11	C12	-0.7
50	H10	C10	C11	C19	179.02
51	C10	C11	C12	C13	-2.76
52	C10	C11	C12	C17	-178.67
53	C19	C11	C12	C13	177.49
54	C19	C11	C12	C17	1.58
55	C10	C11	C19	N18	179.31
56	C10	C11	C19	C20	-0.69
57	C12	C11	C19	N18	-0.9
58	C12	C11	C19	C20	179.1
59	C11	C12	C13	H13	1.19
60	C11	C12	C13	C14	-178.81
61	C17	C12	C13	H13	176.71
62	C17	C12	C13	C14	-3.29
63	C11	C12	C17	C16	-179.29
64	C11	C12	C17	N18	-1.72
65	C13	C12	C17	C16	4.11
66	C13	C12	C17	N18	-178.31
67	C12	C13	C14	H14	-179.05
68	C12	C13	C14	C15	0.95
69	H13	C13	C14	H14	0.95
70	H13	C13	C14	C15	-179.05
71	C13	C14	C15	H15	-179.21
72	C13	C14	C15	C16	0.79
73	H14	C14	C15	H15	0.79
74	H14	C14	C15	C16	-179.21
75	C14	C15	C16	H16	179.89
76	C14	C15	C16	C17	-0.11
77	H15	C15	C16	H16	-0.11
78	H15	C15	C16	C17	179.89
79	C15	C16	C17	C12	-2.36
80	C15	C16	C17	N18	-179.41
81	H16	C16	C17	C12	177.64
82	H16	C16	C17	N18	0.59
83	C12	C17	N18	H18	164.79

84	C12	C17	N18	C19	1.18
85	C16	C17	N18	H18	-17.83
86	C16	C17	N18	C19	178.55
87	C17	N18	C19	C11	-0.14
88	C17	N18	C19	C20	179.86
89	H18	N18	C19	C11	-161.47
90	H18	N18	C19	C20	18.54
91	C11	C19	C20	C8	1.13
92	C11	C19	C20	C21	-179.9
93	N18	C19	C20	C8	-178.88
94	N18	C19	C20	C21	0.09
95	C8	C20	C21	C1	0.23
96	C8	C20	C21	O24	179.65
97	C19	C20	C21	C1	-178.72
98	C19	C20	C21	O24	0.7
99	C9	O22	C23	H23A	-70.32
100	C9	O22	C23	H23B	169.68
101	C9	O22	C23	H23C	49.68

**1'*H*- Indole[3',2'-2,3]-4-methoxy-9*H*--9-one (5.40)**



Crystal data for JM077F3 (J. Moritz AK Witulski)

formula





molecular weight	315.3 gmol <sup>-1</sup>
absorption	$\mu = 0.80 \text{ mm}^{-1}$
crystal size	0.1 x 0.1 x 0.5 mm <sup>3</sup> colourless needle
space group	P 2 <sub>1</sub> /c (monoclinic)
lattice parameters	a = 4.684(3) Å
(calculate from 25	b = 20.106(8) Å $\beta = 90.30(7)^\circ$
reflections with	c = 15.321(8) Å
45° < $\Theta$ < 54°)	V = 1443(1) Å <sup>3</sup> Z = 4      F(000) = 656
temperature	-80 °C
density	d <sub>xray</sub> = 1.452 gcm <sup>-3</sup>

data collection

diffractometer	Turbo CAD4
radiation	Cu-K $\alpha$ graphite monochromator
scan type	$\omega/2\Theta$
scan – width	0.9 + 0.15* $\tau\alpha\nu(\Theta)^\circ$
scan range	2° ≤ $\Theta$ < 70°
	-5 ≤ h ≤ 0    0 ≤ k ≤ 24    -18 ≤ l ≤ 18
number of reflections:	
measured	3188
unique	2736 ( $R_\sigma = 0.0686$ )
observed	2061 ( $ F /\sigma(F) > 4.0$ )

data correction, structure solution and refinement

corrections	Lorentz and polarisation correction.
Structure solution	Program: SIR-97 (Direct methods)
refinement	Program: SHELXL-97 (full matrix). 218 refined parameters, weighting scheme:



$$w=1/[\sigma^2(F_o^2) + (0.0652*P)^2+0.35*P]$$

with  $(\text{Max}(F_o^2, 0)+2*F_o^2)/3$ . H-atoms at calculated positions and refined with isotropic displacement parameters, non H- atoms refined anisotropically.

R-values

$wR2 = 0.1298$  ( $R1=0.0464$  for observed reflections, 0.0671 for all reflections)

goodness of fit

$S = 1.039$

maximum deviation

of parameters

0.001 \* e.s.d

maximum peak height in

diff. Fourier synthesis

0.21, -0.32  $e\text{\AA}^{-3}$

*Table of bond lengths*

Entry	Atom1	Atom2	Length (Å)
1	O1	C2	1.3683
2	O1	C21	1.3741
3	C2	C3	1.3916
4	C2	C7	1.3910
5	C3	H3	0.9500
6	C3	C4	1.3772
7	C4	H4	0.9500
8	C4	C5	1.3955
9	C5	H5	0.9500
10	C5	C6	1.3728
11	C6	H6	0.9500
12	C6	C7	1.4089
13	C7	C8	1.4606
14	C8	C9	1.459
15	C8	O22	1.2300
16	C9	C10	1.3961
17	C9	C21	1.4084
18	C10	H10	0.9500
19	C10	C11	1.3744
20	C11	C12	1.4457
21	C11	C19	1.4246
22	C12	C13	1.3939
23	C12	C17	1.4010

24	C13	H13	0.9500
25	C13	C14	1.3868
26	C14	H14	0.9500
27	C14	C15	1.3936
28	C15	H15	0.9500
29	C15	C16	1.3831
30	C16	H16	0.9500
31	C16	C17	1.3974
32	C17	N18	1.3894
33	N18	H18	0.9676
34	N18	C19	1.3725
35	C19	C20	1.3904
36	C20	C21	1.3969
37	C20	O23	1.3758
38	O23	C24	1.435
39	C24	H24A	0.9800
40	C24	H24B	0.9800
41	C24	H24C	0.9800

*Table of torsion angles*

Entry	Atom1	Atom2	Atom3	Atom4	Torsion angles (°)
1	C21	O1	C2	C3	179.83
2	C21	O1	C2	C7	-0.43
3	C2	O1	C21	C9	1.79
4	C2	O1	C21	C20	-178.39
5	O1	C2	C3	H3	0.45
6	O1	C2	C3	C4	-179.55
7	C7	C2	C3	H3	-179.29
8	C7	C2	C3	C4	0.71
9	O1	C2	C7	C6	-179.67
10	O1	C2	C7	C8	0.2
11	C3	C2	C7	C6	0.05
12	C3	C2	C7	C8	179.92
13	C2	C3	C4	H4	179.21
14	C2	C3	C4	C5	-0.79
15	H3	C3	C4	H4	-0.79
16	H3	C3	C4	C5	179.21
17	C3	C4	C5	H5	-179.9
18	C3	C4	C5	C6	0.1
19	H4	C4	C5	H5	0.1
20	H4	C4	C5	C6	-179.9
21	C4	C5	C6	H6	-179.31

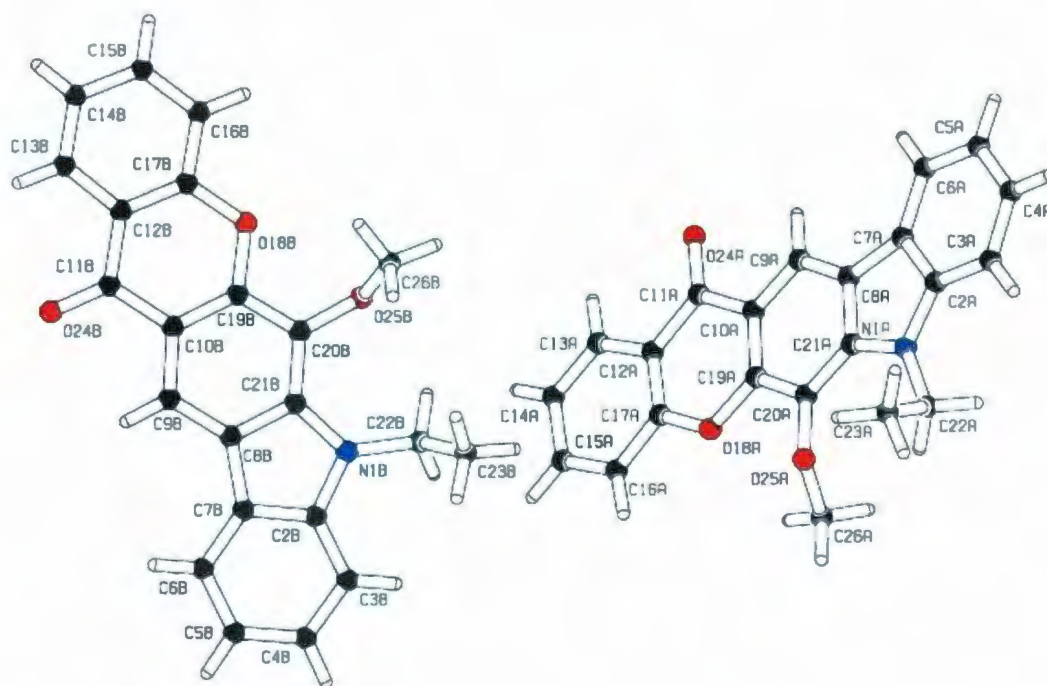
22	C4	C5	C6	C7	0.69
23	H5	C5	C6	H6	0.69
24	H5	C5	C6	C7	-179.31
25	C5	C6	C7	C2	-0.75
26	C5	C6	C7	C8	179.38
27	H6	C6	C7	C2	179.24
28	H6	C6	C7	C8	-0.62
29	C2	C7	C8	C9	-1.19
30	C2	C7	C8	O22	179
31	C6	C7	C8	C9	178.67
32	C6	C7	C8	O22	-1.13
33	C7	C8	C9	C10	-177.34
34	C7	C8	C9	C21	2.46
35	O22	C8	C9	C10	2.46
36	O22	C8	C9	C21	-177.73
37	C8	C9	C10	H10	2.21
38	C8	C9	C10	C11	-177.79
39	C21	C9	C10	H10	-177.6
40	C21	C9	C10	C11	2.4
41	C8	C9	C21	O1	-2.87
42	C8	C9	C21	C20	177.32
43	C10	C9	C21	O1	176.94
44	C10	C9	C21	C20	-2.88
45	C9	C10	C11	C12	179.38
46	C9	C10	C11	C19	0.86
47	H10	C10	C11	C12	-0.62
48	H10	C10	C11	C19	-179.14
49	C10	C11	C12	C13	3.61
50	C10	C11	C12	C17	-177.53
51	C19	C11	C12	C13	-177.73
52	C19	C11	C12	C17	1.13
53	C10	C11	C19	N18	177.61
54	C10	C11	C19	C20	-3.91
55	C12	C11	C19	N18	-1.29
56	C12	C11	C19	C20	177.2
57	C11	C12	C13	H13	-1.08
58	C11	C12	C13	C14	178.92
59	C17	C12	C13	H13	-179.82
60	C17	C12	C13	C14	0.18
61	C11	C12	C17	C16	-179.7
62	C11	C12	C17	N18	-0.58
63	C13	C12	C17	C16	-0.66
64	C13	C12	C17	N18	178.47



65	C12	C13	C14	H14	-179.7
66	C12	C13	C14	C15	0.3
67	H13	C13	C14	H14	0.3
68	H13	C13	C14	C15	-179.7
69	C13	C14	C15	H15	179.66
70	C13	C14	C15	C16	-0.34
71	H14	C14	C15	H15	-0.34
72	H14	C14	C15	C16	179.66
73	C14	C15	C16	H16	179.88
74	C14	C15	C16	C17	-0.12
75	H15	C15	C16	H16	-0.12
76	H15	C15	C16	C17	179.88
77	C15	C16	C17	C12	0.62
78	C15	C16	C17	N18	-178.32
79	H16	C16	C17	C12	-179.38
80	H16	C16	C17	N18	1.68
81	C12	C17	N18	H18	-173.19
82	C12	C17	N18	C19	-0.22
83	C16	C17	N18	H18	5.85
84	C16	C17	N18	C19	178.82
85	C17	N18	C19	C11	0.96
86	C17	N18	C19	C20	-177.38
87	H18	N18	C19	C11	174.06
88	H18	N18	C19	C20	-4.28
89	C11	C19	C20	C21	3.41
90	C11	C19	C20	O23	-172.7
91	N18	C19	C20	C21	-178.43
92	N18	C19	C20	O23	5.45
93	C19	C20	C21	O1	-179.87
94	C19	C20	C21	C9	-0.04
95	O23	C20	C21	O1	-3.87
96	O23	C20	C21	C9	175.95
97	C19	C20	O23	C24	-114.49
98	C21	C20	O23	C24	69.64
99	C20	O23	C24	H24A	-58.91
100	C20	O23	C24	H24B	-178.91
101	C20	O23	C24	H24C	61.09



**1'-N-Ethyl-indole[3',2'-2,3]-4-methoxy-9H--9-one (5.41)**



Crystal data for JM55 (J. Moritz AK Witulski)

formula	$C_{22}H_{17}N_2O_3$		
molecular weight	343.37 $\text{g mol}^{-1}$		
absorption	$\mu = 0.09 \text{ mm}^{-1}$		
crystal size	0.04 x 0.04 x 0.45 $\text{mm}^3$ yellow green plate		
space group	P -1 (triklin)		
lattice parameters	$a = 8.1957(6) \text{ \AA}$	$\alpha = 93.201(6)^\circ$	
(calculate from	$b = 10.0386(8) \text{ \AA}$	$\beta = 89.990(6)^\circ$	
530 reflections with	$c = 20.494(2) \text{ \AA}$	$\gamma = 100.870(6)^\circ$	
$2.3^\circ < \Theta < 17.8^\circ$ )	$V = 1653.2(3) \text{ \AA}^3$	$Z = 4$	$F(000) = 720$
temperature	$-80^\circ\text{C}$		
density	$d_{\text{xray}} = 1.38 \text{ g cm}^{-3}$		

	<u>data collection</u>
diffractometer	SMART CCD
radiation	Mo-K $\alpha$ graphite monochromator
scan type	$\omega, \varphi$ -scans
scan – width	0.5°
scan range	$2^\circ \leq \Theta < 28.15^\circ$ $-10 \leq h \leq 10 \quad -13 \leq k \leq 13 \quad -26 \leq l \leq 24$
number of reflections:	
measured	15999
unique	7940 ( $R_\sigma = 0.1873$ )
observed	1749 ( $ F /\sigma(F) > 4.0$ )

daten correction, structure solution and refinement

corrections	Lorentz and polarisation correction.
Structure solution	Program: SIR-97 (Direct methods)
refinement	Program: SHELXL-97 (full matrix). 472 refined parameters, weighting scheme: $w = 1/[\sigma^2(F_o^2) + (0.071 * P)^2]$ with $(\text{Max}(F_o^2, 0) + 2 * F_o^2)/3$ . H-atoms at calculated positions and refined with isotropic displacement parameters, non H- atoms refined anisotropically.
R-values	$wR2 = 0.1961$ ( $R1 = 0.0518$ for observed reflections, 0.2814 for all reflections)
goodness of fit	$S = 0.602$
maximum deviation of parameters	0.001 * e.s.d
maximum peak height in diff. Fourier synthesis	0.22, -0.25 eÅ <sup>-3</sup>

*Table of bond lengths*

Entry	Atom1	Atom2	Length (Å)
1	N1A	C2A	1.3945
2	N1A	C21A	1.3920
3	N1A	C22A	1.4562
4	C2A	C3A	1.4006
5	C2A	C7A	1.3907
6	C3A	H3A	0.9500
7	C3A	C4A	1.3866
8	C4A	H4A	0.9500
9	C4A	C5A	1.3864
10	C5A	H5A	0.9500
11	C5A	C6A	1.3815
12	C6A	H6A	0.9500
13	C6A	C7A	1.4077
14	C7A	C8A	1.4498
15	C8A	C9A	1.3806
16	C8A	C21A	1.4156
17	C9A	H9A	0.9500
18	C9A	C10A	1.3923
19	C10A	C11A	1.4763
20	C10A	C19A	1.4095
21	C11A	C12A	1.4619
22	C11A	O24A	1.2449
23	C12A	C13A	1.4052
24	C12A	C17A	1.3816
25	C13A	H13A	0.9500
26	C13A	C14A	1.3773
27	C14A	H14A	0.9500
28	C14A	C15A	1.4002
29	C15A	H15A	0.9500
30	C15A	C16A	1.3901
31	C16A	H16A	0.9500
32	C16A	C17A	1.3924
33	C17A	O18A	1.3763
34	O18A	C19A	1.3814
35	C19A	C20A	1.3919
36	C20A	C21A	1.3882
37	C20A	O25A	1.3919
38	C22A	H22A	0.9900
39	C22A	H22B	0.9900
40	C22A	C23A	1.5220
41	C23A	H23A	0.9800



42	C23A	H23B	0.9800
43	C23A	H23C	0.9800
44	O25A	C26A	1.4605
45	C26A	H26A	0.9800
46	C26A	H26B	0.9800
47	C26A	H26C	0.9800
48	N1B	C2B	1.3988
49	N1B	C21B	1.3806
50	N1B	C22B	1.4637
51	C2B	C3B	1.3947
52	C2B	C7B	1.4070
53	C3B	H3B	0.9500
54	C3B	C4B	1.3792
55	C4B	H4B	0.9500
56	C4B	C5B	1.3909
57	C5B	H5B	0.9500
58	C5B	C6B	1.3930
59	C6B	H6B	0.9500
60	C6B	C7B	1.3860
61	C7B	C8B	1.4553
62	C8B	C9B	1.4004
63	C8B	C21B	1.4006
64	C9B	H9B	0.9500
65	C9B	C10B	1.4028
66	C10B	C11B	1.4645
67	C10B	C19B	1.3953
68	C11B	C12B	1.4635
69	C11B	O24B	1.2390
70	C12B	C13B	1.4138
71	C12B	C17B	1.3758
72	C13B	H13B	0.9500
73	C13B	C14B	1.3737
74	C14B	H14B	0.9500
75	C14B	C15B	1.3820
76	C15B	H15B	0.9500
77	C15B	C16B	1.3896
78	C16B	H16B	0.9500
79	C16B	C17B	1.3993
80	C17B	O18B	1.3870
81	O18B	C19B	1.3849
82	C19B	C20B	1.4059
83	C20B	C21B	1.4011
84	C20B	O25B	1.3857



85	C22B	H22C	0.9900
86	C22B	H22D	0.9900
87	C22B	C23B	1.5218
88	C23B	H23D	0.9800
89	C23B	H23E	0.9800
90	C23B	H23F	0.9800
91	O25B	C26B	1.4445
92	C26B	H26D	0.9800
93	C26B	H26E	0.9800
94	C26B	H26F	0.9800

*Table of torsion angles*

Entry	Atom1	Atom2	Atom3	Atom4	Torsion angles (°)
1	C21A	N1A	C2A	C3A	179.03
2	C21A	N1A	C2A	C7A	-0.7
3	C22A	N1A	C2A	C3A	0.86
4	C22A	N1A	C2A	C7A	-178.88
5	C2A	N1A	C21A	C8A	1.22
6	C2A	N1A	C21A	C20A	-178.55
7	C22A	N1A	C21A	C8A	179.32
8	C22A	N1A	C21A	C20A	-0.45
9	C2A	N1A	C22A	H22A	-30.66
10	C2A	N1A	C22A	H22B	-148.05
11	C2A	N1A	C22A	C23A	90.65
12	C21A	N1A	C22A	H22A	151.54
13	C21A	N1A	C22A	H22B	34.15
14	C21A	N1A	C22A	C23A	-87.16
15	N1A	C2A	C3A	H3A	0.23
16	N1A	C2A	C3A	C4A	-179.77
17	C7A	C2A	C3A	H3A	179.94
18	C7A	C2A	C3A	C4A	-0.06
19	N1A	C2A	C7A	C6A	179.98
20	N1A	C2A	C7A	C8A	-0.08
21	C3A	C2A	C7A	C6A	0.22
22	C3A	C2A	C7A	C8A	-179.83
23	C2A	C3A	C4A	H4A	179.91
24	C2A	C3A	C4A	C5A	-0.09
25	H3A	C3A	C4A	H4A	-0.09
26	H3A	C3A	C4A	C5A	179.91
27	C3A	C4A	C5A	H5A	-179.93
28	C3A	C4A	C5A	C6A	0.07
29	H4A	C4A	C5A	H5A	0.07
30	H4A	C4A	C5A	C6A	-179.93

31	C4A	C5A	C6A	H6A	-179.91
32	C4A	C5A	C6A	C7A	0.1
33	H5A	C5A	C6A	H6A	0.09
34	H5A	C5A	C6A	C7A	-179.91
35	C5A	C6A	C7A	C2A	-0.24
36	C5A	C6A	C7A	C8A	179.83
37	H6A	C6A	C7A	C2A	179.76
38	H6A	C6A	C7A	C8A	-0.17
39	C2A	C7A	C8A	C9A	178.8
40	C2A	C7A	C8A	C21A	0.8
41	C6A	C7A	C8A	C9A	-1.27
42	C6A	C7A	C8A	C21A	-179.26
43	C7A	C8A	C9A	H9A	1.11
44	C7A	C8A	C9A	C10A	-178.89
45	C21A	C8A	C9A	H9A	178.87
46	C21A	C8A	C9A	C10A	-1.13
47	C7A	C8A	C21A	N1A	-1.25
48	C7A	C8A	C21A	C20A	178.55
49	C9A	C8A	C21A	N1A	-179.55
50	C9A	C8A	C21A	C20A	0.25
51	C8A	C9A	C10A	C11A	178.15
52	C8A	C9A	C10A	C19A	2.68
53	H9A	C9A	C10A	C11A	-1.85
54	H9A	C9A	C10A	C19A	-177.32
55	C9A	C10A	C11A	C12A	-178.03
56	C9A	C10A	C11A	O24A	4.47
57	C19A	C10A	C11A	C12A	-2.53
58	C19A	C10A	C11A	O24A	179.97
59	C9A	C10A	C19A	O18A	177.13
60	C9A	C10A	C19A	C20A	-3.47
61	C11A	C10A	C19A	O18A	1.59
62	C11A	C10A	C19A	C20A	-179.01
63	C10A	C11A	C12A	C13A	-179.61
64	C10A	C11A	C12A	C17A	1.95
65	O24A	C11A	C12A	C13A	-2.13
66	O24A	C11A	C12A	C17A	179.43
67	C11A	C12A	C13A	H13A	2.36
68	C11A	C12A	C13A	C14A	-177.64
69	C17A	C12A	C13A	H13A	-179.16
70	C17A	C12A	C13A	C14A	0.84
71	C11A	C12A	C17A	C16A	179.22
72	C11A	C12A	C17A	O18A	-0.34
73	C13A	C12A	C17A	C16A	0.74



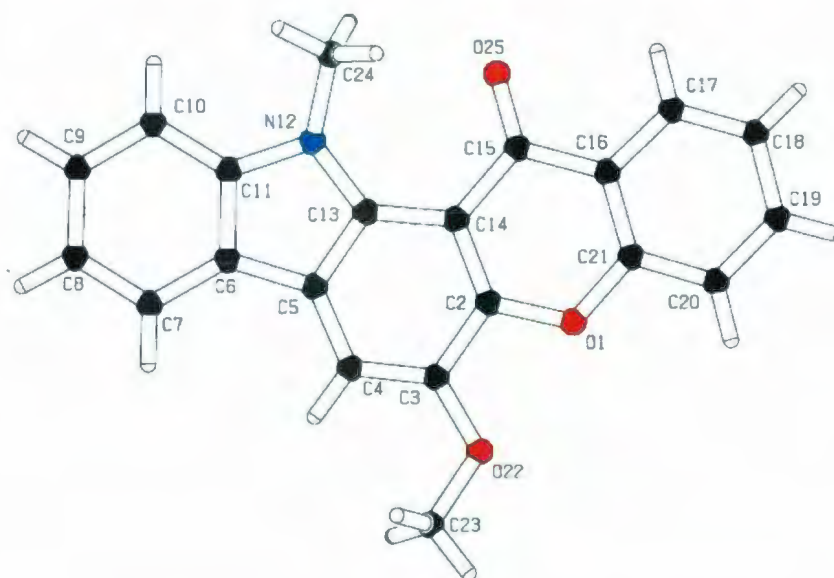
74	C13A	C12A	C17A	O18A	-178.82
75	C12A	C13A	C14A	H14A	178.4
76	C12A	C13A	C14A	C15A	-1.6
77	H13A	C13A	C14A	H14A	-1.6
78	H13A	C13A	C14A	C15A	178.4
79	C13A	C14A	C15A	H15A	-179.2
80	C13A	C14A	C15A	C16A	0.8
81	H14A	C14A	C15A	H15A	0.8
82	H14A	C14A	C15A	C16A	-179.2
83	C14A	C15A	C16A	H16A	-179.28
84	C14A	C15A	C16A	C17A	0.72
85	H15A	C15A	C16A	H16A	0.72
86	H15A	C15A	C16A	C17A	-179.28
87	C15A	C16A	C17A	C12A	-1.51
88	C15A	C16A	C17A	O18A	178.08
89	H16A	C16A	C17A	C12A	178.49
90	H16A	C16A	C17A	O18A	-1.92
91	C12A	C17A	O18A	C19A	-0.78
92	C16A	C17A	O18A	C19A	179.64
93	C17A	O18A	C19A	C10A	0.11
94	C17A	O18A	C19A	C20A	-179.32
95	C10A	C19A	C20A	C21A	2.52
96	C10A	C19A	C20A	O25A	174.89
97	O18A	C19A	C20A	C21A	-178.05
98	O18A	C19A	C20A	O25A	-5.67
99	C19A	C20A	C21A	N1A	178.84
100	C19A	C20A	C21A	C8A	-0.91
101	O25A	C20A	C21A	N1A	6.6
102	O25A	C20A	C21A	C8A	-173.15
103	C19A	C20A	O25A	C26A	71.61
104	C21A	C20A	O25A	C26A	-116.38
105	N1A	C22A	C23A	H23A	179.97
106	N1A	C22A	C23A	H23B	59.97
107	N1A	C22A	C23A	H23C	-60.03
108	H22A	C22A	C23A	H23A	-58.72
109	H22A	C22A	C23A	H23B	-178.72
110	H22A	C22A	C23A	H23C	61.28
111	H22B	C22A	C23A	H23A	58.67
112	H22B	C22A	C23A	H23B	-61.34
113	H22B	C22A	C23A	H23C	178.66
114	C20A	O25A	C26A	H26A	-62.88
115	C20A	O25A	C26A	H26B	177.12
116	C20A	O25A	C26A	H26C	57.12

117	C21B	N1B	C2B	C3B	178.73
118	C21B	N1B	C2B	C7B	0.79
119	C22B	N1B	C2B	C3B	4.73
120	C22B	N1B	C2B	C7B	-173.21
121	C2B	N1B	C21B	C8B	-1.05
122	C2B	N1B	C21B	C20B	-179.76
123	C22B	N1B	C21B	C8B	172.38
124	C22B	N1B	C21B	C20B	-6.33
125	C2B	N1B	C22B	H22C	156.34
126	C2B	N1B	C22B	H22D	38.7
127	C2B	N1B	C22B	C23B	-82.48
128	C21B	N1B	C22B	H22C	-16.21
129	C21B	N1B	C22B	H22D	-133.86
130	C21B	N1B	C22B	C23B	104.97
131	N1B	C2B	C3B	H3B	1.5
132	N1B	C2B	C3B	C4B	-178.5
133	C7B	C2B	C3B	H3B	179.23
134	C7B	C2B	C3B	C4B	-0.77
135	N1B	C2B	C7B	C6B	178.71
136	N1B	C2B	C7B	C8B	-0.23
137	C3B	C2B	C7B	C6B	0.62
138	C3B	C2B	C7B	C8B	-178.31
139	C2B	C3B	C4B	H4B	-179.37
140	C2B	C3B	C4B	C5B	0.63
141	H3B	C3B	C4B	H4B	0.63
142	H3B	C3B	C4B	C5B	-179.37
143	C3B	C4B	C5B	H5B	179.66
144	C3B	C4B	C5B	C6B	-0.34
145	H4B	C4B	C5B	H5B	-0.34
146	H4B	C4B	C5B	C6B	179.66
147	C4B	C5B	C6B	H6B	-179.83
148	C4B	C5B	C6B	C7B	0.17
149	H5B	C5B	C6B	H6B	0.17
150	H5B	C5B	C6B	C7B	-179.83
151	C5B	C6B	C7B	C2B	-0.31
152	C5B	C6B	C7B	C8B	178.23
153	H6B	C6B	C7B	C2B	179.69
154	H6B	C6B	C7B	C8B	-1.77
155	C2B	C7B	C8B	C9B	178.08
156	C2B	C7B	C8B	C21B	-0.41
157	C6B	C7B	C8B	C9B	-0.6
158	C6B	C7B	C8B	C21B	-179.09
159	C7B	C8B	C9B	H9B	1.15



160	C7B	C8B	C9B	C10B	-178.85
161	C21B	C8B	C9B	H9B	179.46
162	C21B	C8B	C9B	C10B	-0.54
163	C7B	C8B	C21B	N1B	0.91
164	C7B	C8B	C21B	C20B	179.75
165	C9B	C8B	C21B	N1B	-177.77
166	C9B	C8B	C21B	C20B	1.07
167	C8B	C9B	C10B	C11B	176.77
168	C8B	C9B	C10B	C19B	-0.19
169	H9B	C9B	C10B	C11B	-3.23
170	H9B	C9B	C10B	C19B	179.81
171	C9B	C10B	C11B	C12B	176.97
172	C9B	C10B	C11B	O24B	-4.38
173	C19B	C10B	C11B	C12B	-6.09
174	C19B	C10B	C11B	O24B	172.55
175	C9B	C10B	C19B	O18B	179.89
176	C9B	C10B	C19B	C20B	0.42
177	C11B	C10B	C19B	O18B	2.92
178	C11B	C10B	C19B	C20B	-176.55
179	C10B	C11B	C12B	C13B	-175.41
180	C10B	C11B	C12B	C17B	4.78
181	O24B	C11B	C12B	C13B	5.96
182	O24B	C11B	C12B	C17B	-173.85
183	C11B	C12B	C13B	H13B	1.26
184	C11B	C12B	C13B	C14B	-178.74
185	C17B	C12B	C13B	H13B	-178.92
186	C17B	C12B	C13B	C14B	1.08
187	C11B	C12B	C17B	C16B	176.39
188	C11B	C12B	C17B	O18B	-0.08
189	C13B	C12B	C17B	C16B	-3.43
190	C13B	C12B	C17B	O18B	-179.9
191	C12B	C13B	C14B	H14B	-179.51
192	C12B	C13B	C14B	C15B	0.49
193	H13B	C13B	C14B	H14B	0.49
194	H13B	C13B	C14B	C15B	-179.51
195	C13B	C14B	C15B	H15B	-179.8
196	C13B	C14B	C15B	C16B	0.2
197	H14B	C14B	C15B	H15B	0.2
198	H14B	C14B	C15B	C16B	-179.8
199	C14B	C15B	C16B	H16B	177.61
200	C14B	C15B	C16B	C17B	-2.39
201	H15B	C15B	C16B	H16B	-2.39
202	H15B	C15B	C16B	C17B	177.61

203	C15B	C16B	C17B	C12B	4.06
204	C15B	C16B	C17B	O18B	-179.2
205	H16B	C16B	C17B	C12B	-175.94
206	H16B	C16B	C17B	O18B	0.8
207	C12B	C17B	O18B	C19B	-3.48
208	C16B	C17B	O18B	C19B	179.81
209	C17B	O18B	C19B	C10B	2.02
210	C17B	O18B	C19B	C20B	-178.47
211	C10B	C19B	C20B	C21B	0.09
212	C10B	C19B	C20B	O25B	174.44
213	O18B	C19B	C20B	C21B	-179.43
214	O18B	C19B	C20B	O25B	-5.08
215	C19B	C20B	C21B	N1B	177.76
216	C19B	C20B	C21B	C8B	-0.82
217	O25B	C20B	C21B	N1B	3.47
218	O25B	C20B	C21B	C8B	-175.11
219	C19B	C20B	O25B	C26B	74.86
220	C21B	C20B	O25B	C26B	-111.05
221	N1B	C22B	C23B	H23D	-64.81
222	N1B	C22B	C23B	H23E	175.19
223	N1B	C22B	C23B	H23F	55.19
224	H22C	C22B	C23B	H23D	56.37
225	H22C	C22B	C23B	H23E	-63.63
226	H22C	C22B	C23B	H23F	176.37
227	H22D	C22B	C23B	H23D	174.02
228	H22D	C22B	C23B	H23E	54.02
229	H22D	C22B	C23B	H23F	-65.98
230	C20B	O25B	C26B	H26D	-66.64
231	C20B	O25B	C26B	H26E	173.36
232	C20B	O25B	C26B	H26F	53.36

**1'-Methyl-1'H-indole[2',3'-a]-4-methoxy-9H-xanthene-9-one (5.42)**Crystal data for Dat031 (Anh-Thu Dang AK Witulski)

formula	$C_{21}H_{15}NO_3$		
molecular weight	$329.3 \text{ g mol}^{-1}$		
absorption	$\mu = 0.79 \text{ mm}^{-1}$		
crystal size	$0.1 \times 0.1 \times 0.4 \text{ mm}^3$ light yellow needle		
space group	$P 2_1/c$ (monoclinic)		
lattice parameters	$a = 15.125(1) \text{ \AA}$		
(calculate from	$b = 4.886(4) \text{ \AA}$	$\beta = 91.258(7)^\circ$	
reflections with 25	$c = 20.397(1) \text{ \AA}$		
$25^\circ < \Theta < 43^\circ$ )	$V = 1507.8(2) \text{ \AA}^3$	$Z = 4$	$F(000) = 688$
temperature	$-80^\circ\text{C}$		
density	$d_{\text{xray}} = 1.451 \text{ g cm}^{-3}$		



	<u>data collection</u>
diffractometer	Turbo CAD4
radiation	Cu-K $\alpha$ graphite monochromator
scan type	$\omega/2\Theta$
scan – width	$0.9 + 0.14 \cdot \tau \alpha \nu(\Theta)^\circ$
scan range	$2^\circ \leq \Theta < 70^\circ$
	$-18 \leq h \leq 0 \quad -5 \leq k \leq 0 \quad -23 \leq l \leq 23$
number of reflections:	
measured	3324
unique	2842 ( $R_\sigma = 0.0583$ )
observed	1979 ( $ F /\sigma(F) > 4.0$ )

daten correction, structure solution and refinement

corrections	Lorentz and polarisation correction.
Structure solution	Program: SIR-97 (Direct methods)
refinement	Program: SHELXL-97 (full matrix). 228 refined parameters, weighting scheme: $w = 1/[\sigma^2(F_o^2) + (0.0992 \cdot P)^2 + 0.14 \cdot P]$ with $(\text{Max}(F_o^2, 0) + 2 \cdot F_o^2)/3$ . H-atoms at calculated positions and refined with isotropic displacement parameters, non H- atoms refined anisotropically.
R-values	$wR2 = 0.1725$ ( $R1 = 0.0556$ for observed reflections, 0.0865 for all reflections)
goodness of fit	$S = 1.023$
maximum deviation of parameters	0.001 * e.s.d
maximum peak height in diff. Fourier synthesis	0.30, -0.31 eÅ <sup>-3</sup>



*Table of bond length*

Entry	Atom1	Atom2	Length (Å)
1	O1	C2	1.3686
2	O1	C21	1.3687
3	C2	C3	1.4217
4	C2	C14	1.4026
5	C3	C4	1.3633
6	C3	O22	1.3624
7	C4	H4	0.9500
8	C4	C5	1.3951
9	C5	C6	1.4358
10	C5	C13	1.4144
11	C6	C7	1.4016
12	C6	C11	1.4013
13	C7	H7	0.9500
14	C7	C8	1.3750
15	C8	H8	0.9500
16	C8	C9	1.3937
17	C9	H9	0.9500
18	C9	C10	1.3767
19	C10	H10	0.9500
20	C10	C11	1.3948
21	C11	N12	1.3871
22	N12	C13	1.3867
23	N12	C24	1.4586
24	C13	C14	1.4263
25	C14	C15	1.4796
26	C15	C16	1.4687
27	C15	O25	1.2180
28	C16	C17	1.4080
29	C16	C21	1.3754
30	C17	H17	0.9500
31	C17	C18	1.3691
32	C18	H18	0.9500
33	C18	C19	1.3884
34	C19	H19	0.9500
35	C19	C20	1.3778
36	C20	H20	0.9500
37	C20	C21	1.3922
38	O22	C23	1.4190
39	C23	H23A	0.9800
40	C23	H23B	0.9800
41	C23	H23C	0.9800
42	C24	H24A	0.9800
43	C24	H24B	0.9800
44	C24	H24C	0.9800

*Table of torsion angles*

Entry	Atom1	Atom2	Atom3	Atom4	Torsion angles (°)
1	C21	O1	C2	C3	-179.54
2	C21	O1	C2	C14	0.94
3	C2	O1	C21	C16	-2.04
4	C2	O1	C21	C20	178.7
5	O1	C2	C3	C4	-178.23
6	O1	C2	C3	O22	1.19
7	C14	C2	C3	C4	1.29
8	C14	C2	C3	O22	-179.29
9	O1	C2	C14	C13	-179.22
10	O1	C2	C14	C15	3.71
11	C3	C2	C14	C13	1.32
12	C3	C2	C14	C15	-175.75
13	C2	C3	C4	H4	178.5
14	C2	C3	C4	C5	-1.5
15	O22	C3	C4	H4	-0.84
16	O22	C3	C4	C5	179.16
17	C2	C3	O22	C23	167.25
18	C4	C3	O22	C23	-13.38
19	C3	C4	C5	C6	-179.01
20	C3	C4	C5	C13	-0.92
21	H4	C4	C5	C6	0.99
22	H4	C4	C5	C13	179.08
23	C4	C5	C6	C7	0.21
24	C4	C5	C6	C11	178.26
25	C13	C5	C6	C7	-178.1
26	C13	C5	C6	C11	-0.05
27	C4	C5	C13	N12	-178
28	C4	C5	C13	C14	3.61
29	C6	C5	C13	N12	0.49
30	C6	C5	C13	C14	-177.9
31	C5	C6	C7	H7	-0.82
32	C5	C6	C7	C8	179.18
33	C11	C6	C7	H7	-178.66
34	C11	C6	C7	C8	1.34
35	C5	C6	C11	C10	179.45
36	C5	C6	C11	N12	-0.42
37	C7	C6	C11	C10	-2.19
38	C7	C6	C11	N12	177.95
39	C6	C7	C8	H8	-179.65
40	C6	C7	C8	C9	0.35

41	H7	C7	C8	H8	0.35
42	H7	C7	C8	C9	-179.65
43	C7	C8	C9	H9	178.72
44	C7	C8	C9	C10	-1.28
45	H8	C8	C9	H9	-1.28
46	H8	C8	C9	C10	178.72
47	C8	C9	C10	H10	-179.55
48	C8	C9	C10	C11	0.45
49	H9	C9	C10	H10	0.45
50	H9	C9	C10	C11	-179.55
51	C9	C10	C11	C6	1.26
52	C9	C10	C11	N12	-178.9
53	H10	C10	C11	C6	-178.74
54	H10	C10	C11	N12	1.1
55	C6	C11	N12	C13	0.73
56	C6	C11	N12	C24	-164.64
57	C10	C11	N12	C13	-179.12
58	C10	C11	N12	C24	15.51
59	C11	N12	C13	C5	-0.75
60	C11	N12	C13	C14	177.37
61	C24	N12	C13	C5	162.7
62	C24	N12	C13	C14	-19.19
63	C11	N12	C24	H24A	-108.06
64	C11	N12	C24	H24B	131.94
65	C11	N12	C24	H24C	11.94
66	C13	N12	C24	H24A	90.09
67	C13	N12	C24	H24B	-29.91
68	C13	N12	C24	H24C	-149.91
69	C5	C13	C14	C2	-3.66
70	C5	C13	C14	C15	173.14
71	N12	C13	C14	C2	178.41
72	N12	C13	C14	C15	-4.8
73	C2	C14	C15	C16	-6.88
74	C2	C14	C15	O25	171.03
75	C13	C14	C15	C16	176.37
76	C13	C14	C15	O25	-5.72
77	C14	C15	C16	C17	-176.12
78	C14	C15	C16	C21	6.09
79	O25	C15	C16	C17	5.91
80	O25	C15	C16	C21	-171.88
81	C15	C16	C17	H17	2.29
82	C15	C16	C17	C18	-177.71
83	C21	C16	C17	H17	-179.85



84	C21	C16	C17	C18	0.15
85	C15	C16	C21	O1	-1.7
86	C15	C16	C21	C20	177.51
87	C17	C16	C21	O1	-179.56
88	C17	C16	C21	C20	-0.35
89	C16	C17	C18	H18	-179.6
90	C16	C17	C18	C19	0.4
91	H17	C17	C18	H18	0.4
92	H17	C17	C18	C19	-179.6
93	C17	C18	C19	H19	179.23
94	C17	C18	C19	C20	-0.77
95	H18	C18	C19	H19	-0.77
96	H18	C18	C19	C20	179.23
97	C18	C19	C20	H20	-179.43
98	C18	C19	C20	C21	0.57
99	H19	C19	C20	H20	0.57
100	H19	C19	C20	C21	-179.43
101	C19	C20	C21	O1	179.25
102	C19	C20	C21	C16	-0.01
103	H20	C20	C21	O1	-0.75
104	H20	C20	C21	C16	179.99
105	C3	O22	C23	H23A	-50.83
106	C3	O22	C23	H23B	-170.83
107	C3	O22	C23	H23C	69.17

### 5.5.3 UV and Fluorescence Experiments

Methods are identical to those described in Chapter 2, page 105–106. Most of the experiments were carried out at Memorial University, unless otherwise indicated in a footnote. Solutions of all xanthenes-carbazole systems in  $\text{CHCl}_3$  were prepared with concentration around  $2\text{--}4 \times 10^{-5}$  M.



*Table of UV data of dienes and xanthones.*

	Compounds	$\lambda_{\max}$ ( $\epsilon$ )
<b>Dienes</b>	<b>5.37</b>	277 (33170), 310 (22571)
	<b>5.32a</b>	283 (27418), 341 (16087)
	<b>5.32b</b>	264 (38019), 351 (4639)
	<b>5.32c</b>	284 (25596), 309 (23813)
	<b>5.32d</b>	279 (30811), 314 (26203)
	<b>5.32e</b>	293 (34250), 334 (22930)
	<b>5.32f</b>	283 (27261), 316 (21838)
<b>Xanthones</b>	<b>5.38</b>	266 (69335), 355 (10573)
	<b>5.31a</b>	273 (66216), 381 (9956)
	<b>5.31b</b>	271 (60172), 362 (7452)
	<b>5.31c</b>	266 (52336), 352 (10116)
	<b>5.31d</b>	268 (57867), 355 (10008)
	<b>5.31e</b>	274 (126367), 368 (21324)
	<b>5.31f</b>	271 (59740), 362 (8600)

*Table of UV data of xanthone-carbazoles.*

	Compounds	$\lambda_{\max}$ ( $\epsilon$ )
<b>Non-substituted xanthone-carbazoles</b>	<b>5.39</b>	252 (55711), 287 (40739), 304 (36734), 412 (12354)
	<b>5.40</b>	251 (29144), 287 (21071), 304 (19007), 412 (6366)
	<b>5.42</b>	252 (41536), 287 (30888), 308 (31430), 412 (10140)
	<b>5.43</b>	253 (60115), 300 (44814), 312 (73464), 365 (15336)
	<b>5.44</b>	254 (45492), 287 (33135), 308 (33756), 412 (11143)
	<b>5.41</b>	253 (60332), 309 (46675), 313 (77773), 366 (15818)
	<b>5.45</b>	254 (45126), 287 (30256), 309 (34366), 412 (9727)
	<b>5.46</b>	254 (181903), 302 (140927), 313 (244105), 366 (47180)
<b>Substituted xanthone-carbazoles</b>	<b>5.52a</b>	243 (60563), 300 (65432), 343 (15209), 418 (16434)
	<b>5.52b</b>	241 (57585), 295 (52433), 333 (17497), 421 (13292)
	<b>5.52c</b>	243 (86106), 290 (47821), 315 (66464), 421 (17979)
	<b>5.52d</b>	260 (57491), 292 (28286), 313 (46112), 409 (12640)
	<b>5.52f</b>	254 (60491), 301 (51020), 316 (52797), 418 (13537)
	<b>5.53b</b>	257 (88019), 316 (112479), 370 (25955)
	<b>5.53c</b>	257 (100880), 324 (91533), 366 (10638)
	<b>5.53d</b>	256 (53147), 304 (45614), 315 (78534), 366 (14043)
	<b>5.53e</b>	244 (51016), 303 (48829), 421 (11761)
	<b>5.53f</b>	259 (191407), 318 (295490), 369 (55025)

*Table of UV data of xanthone-carbazoles.*

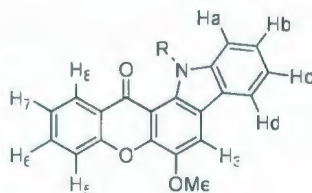
Compounds	$\lambda_{\max}$ (nm)
<b>5.67a</b>	255 (49185), 301 (52524), 419 (11373)
<b>5.68a</b>	266 (51210), 297 (27932), 321 (47997), 416 (13221)
<b>5.69a</b>	258 (61839), 315 (52776), 421 (14160)
<b>5.67b</b>	313 (50579), 421 (10843)
<b>5.68b</b>	216 (34531), 333 (37259), 419 (10930)
<b>5.69b</b>	265 (36903), 333 (45531), 427 (12915)
<b>5.67c</b>	269 (48165), 281 (53709), 308 (37797), 348 (47928), 420 (12269)
<b>5.68c</b>	245 (93669), 280 (57852), 315 (37386), 347 (52548), 412 (15445)
<b>5.69c</b>	244 (362948), 270 (198968), 280 (230819), 348 (238373), 420 (48408)

#### 5.5.4 Cyclic Voltammetry Experiments

CV measurements were performed on a BASi Epsilon-EC Bioanalytical systems in a solution of  $\text{Bu}_4\text{NBF}_4$  (0.1 M), the supporting electrolyte, dissolved in  $\text{CH}_2\text{Cl}_2:\text{CH}_3\text{CN}$  (4:1, v/v) at scan rate  $500 \text{ V}\cdot\text{s}^{-1}$  at room temperature. The solution in the three-electrode cell was purged with  $\text{N}_2$  before each experiment and a blanket of  $\text{N}_2$  was used during the experiment. A Pt wire was used as the counter electrode, glassy carbon as the working electrode, and Ag / AgCl as the reference. HOMO energies were estimated by the empirical equation  $\text{HOMO} = -(4.4 + E_{\text{ox}}^{\text{onset}}) \text{ eV}$ .<sup>46</sup>

### 5.5.5 Aggregation Studies on Compound 5.45

Compound **5.54** (60.9 mg) was dissolved in  $\text{CDCl}_3$  (1.0 mL) in a 1 mL volumetric flask. This solution was then diluted into the indicated concentrations. The H-shifts (ppm) were obtained from  $^1\text{H}$  NMR spectra of each solution.



**5.45**  $\text{R} = \text{C}_6\text{H}_{13}$

Chemical Formula  $\text{C}_{26}\text{H}_{28}\text{NO}_2$   
Exact Mass 427.2147

Entry	Mol / L	H8	Hd	H3	H6	H5	Ha	Hb	H7	Hc	OMe
1	$14.2 \times 10^{-2}$	8.360	8.019	7.943	7.711	7.629	7.564	7.465	7.395	7.266	4.123
2	$7.1 \times 10^{-2}$	8.371	8.040	7.973	7.729	7.649	7.579	7.479	7.411	7.283	4.145
3	$3.55 \times 10^{-2}$	8.376	8.051	7.988	7.739	7.658	7.585	7.486	7.418	7.291	4.155
4	$14.2 \times 10^{-3}$	8.379	8.058	7.996	7.743	7.664	7.590	7.489	7.423	7.296	4.162
5	$7.1 \times 10^{-3}$	8.379	8.059	7.999	7.745	7.665	7.590	7.489	7.424	7.296	4.163

$\Delta\delta$	2-1	0.011	0.021	0.030	0.018	0.020	0.015	0.014	0.016	0.017	0.022
	3-2	0.005	0.011	0.015	0.010	0.009	0.006	0.007	0.007	0.008	0.010
	4-3	0.003	0.007	0.008	0.004	0.006	0.005	0.003	0.005	0.005	0.007
	5-4	0.000	0.001	0.003	0.002	0.001	0.000	0.000	0.001	0.000	0.001
	5-1	0.019	0.040	0.056	0.034	0.036	0.026	0.024	0.029	0.030	0.040



## 5.6 References and Notes

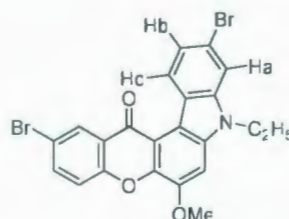
- 
- [1] (a) Kamel, M.; Allam, M. A.; El-Alfi, I. *Egypt. J. Chem.* **1973**, *16*, 91–100.  
 (b) Ahluwalia, V. K.; Mallika, N.; Kumari, S.; Singh, R. P. *Indian J. Chem. Sec. B* **1989**, *28B*, 1021–1025.
- [2] (a) Sun, L.; Liebeskind, L. S. *J. Am. Chem. Soc.* **1996**, *118*, 12473–12474.  
 (b) Vandana, T.; Prasad, K. J. R. *Indian J. Chem. Sec. B* **2005**, *44B*, 815–818.
- [3] (a) Liebermann, H.; Lewin, G.; Gruhn, A.; Gottesmann, E.; Lissner, D.; Schonda, K. *Justus Liebigs Ann. Chem.* **1934**, *513*, 156–179. (b) Singh, T.; Bedi, S. N. *Jour. Indian Chem. Soc.* **1957**, *34*, 321–323. (c) Sharghi, H.; Tamaddon, F.; Eshghi, H. *Iran. J. Chem. & Chem. Eng.* **2000**, *19*, 32–36. (d) Colquhoun, H. M.; Lewis, D. F.; Williams, D. J. *Org. Lett.* **2001**, *3*, 2337–2340.
- [4] (a) Kamel, M.; Allam, M. A.; Issa, R. M.; El-Alfi, E. *Egypt. J. Chem.* **1973**, *16*, 185–195. (b) Abd El-Halim, F. M.; Issa, R. M.; Harfoush, A. A.; Ghoneim, M. M. *Egypt. J. Chem.* **1976**, *17*, 711–715.
- [5] (a) Rohlad, W.; Wuest, H.; Sasse, H. J. (Badische Anilin- & Soda-Fabrik A.-G.), **1963**, GB920851. (b) Bohler, H.; Kehrner, F. (Sandoz Ltd.), **1965**, CH386029. (c) Wakimoto, T. (Pioneer Electronic Corp., Japan), *Jpn. Kokai Tokkyo Koho* **1999**, JP11054279.
- [6] Anthony, J. E. *Chem. Rev.* **2006**, *106*, 5028–5048.
- [7] (a) Wu, Y.; Li, Y.; Gardner, S.; Ong, B. *J. Am. Chem. Soc.* **2005**, *127*, 614–618. (b) Boudreault, P.-L. T.; Wakim, S.; Blouin, N.; Simard, M.; Tessier, C.; Ye, T.; Leclerc, M. *J. Am. Chem. Soc.* **2007**, *127*, 9125–9136.

- 
- [8] Kawaguchi, K.; Nakano, K.; Nozaki, K. *Org. Lett.* **2008**, *10*, 1199–1202.
- [9] Gao, P.; Feng, X.; Yang, X.; Enkelmann, V.; Baumgarten, M.; Müllen, K. *J. Org. Chem.* **2008**, *73*, 9207–9213.
- [10] Adhikari, R. M.; Mondal, R.; Shah, B. K.; Neckers, D. C. *J. Org. Chem.* **2007**, *72*, 4727–4732.
- [11] Shao, H.; Chen, X.; Wang, Z.; Lu, P. *Journal of Luminescence* **2007**, *127*, 349–354.
- [12] Palayangoda, S. S.; Cai, X.; Adhikari, R. M.; Neckers, D. C. *Org. Lett.* **2008**, *10*, 281–284.
- [13] (a) Yu, H.; Zain, S. M.; Eigenbrot, I. V.; Phillips, D. *Chem. Phys. Lett.* **1993**, *202*, 141–147. (b) Howell, R.; Taylor, A. G.; Phillips, D. *Chem. Phys. Lett.* **1992**, *188*, 119–125.
- [14] Zelinsky, N. D.; Titz, I.; Gaverdowskaja, M. *Ber.*, **1926**, *59*, 2590–2593.
- [15] Grotta, H. M. *U. S. Patent* **1960**, *2*, 921, 942.
- [16] Grotta, H. M.; Riggle, C. J.; Bearse, A. E. *J. Org. Chem.* **1961**, *26*, 1509–1511.
- [17] Cadogan, J. I. G.; Cameron-Wood, M.; Mackie, R. K.; Searle, R. J. G. *J. Chem. Soc.* **1965**, 4831–4837.
- [18] (a) Freeman, A. W.; Urvoy, M.; Criswell, M. E. *J. Org. Chem.* **2005**, *70*, 5014–5019. (b) Tsunashima, Y.; Kuroki, M. *J. Heterocycl. Chem.* **1981**, *18*, 315–318. (c) Pukas, I.; Fields, E. K. *J. Org. Chem.* **1968**, *33*, 4237–4242.
- [19] (a) Bouchard, J.; Wakim, S.; Leclerc, M. *J. Org. Chem.* **2004**, *69*, 5705–5711. (b) Blouin, N.; Michaud, A.; Wakim, S.; Boudreault, P. L. T.; Leclerc, M.; Vercelli, B.; Zecchin, S.; Zotti, G. *Macromol. Chem. Phys.* **2006**, *207*, 166–174.

- 
- [20] A review: Knölker, H.-J. *Synlett* **1992**, 371–387.
- [21] Knölker, H.-J.; Bauermeister, M. *J. Chem. Soc. Commun.* **1990**, 664–665.
- [22] Wakim, S.; Bouchard, J.; Blouin, N.; Michaud, A.; Leclerc, M. *Org. Lett.* **2004**, 6, 3413–3416.
- [23] Kuwahara, A.; Nakano, K.; Nozaki, K. *J. Org. Chem.* **2005**, 70, 413–419.
- [24] Department of Chemistry, Johannes Gutenberg University of Mainz, Germany.
- [25] Witulski, B.; Wrobel, N. *manuscript in preparation*.
- [26] (a) Lin, N.-H.; Xia, P.; Kovar, P.; Park, C.; Chen, Z.; Zhang, H.; Rosenberg, S. H.; Sham, H. L. *Bioorganic & Medicinal Chemistry Letters* **2006**, 16, 421–426. (b) Stoll, A.; Troxler, F.; Peyer, J.; Hofmann, A. *Helv. Chim. Acta.* **1955**, 38, 1452–1472. (c) King, L. T.; Parke, D. V.; Williams, R. T. *Biochem. J.* **1966**, 98, 266–277.
- [27] Cadogan reaction of **5.38** and characterization of products **5.39–5.41** were processed in Prof. Witulski's laboratory by Joerg Moritz, an undergraduate student in his group, as a collaborative work.
- [28] The crystals were grown by Joerg Moritz and the X-ray analyses were done by Dr. Dieter Schollmeyer, Mainz University, Germany.
- [29] Kürti, L.; Czakó, B. *Strategic Applications of Named Reactions in Organic Synthesis*, Elsevier Academic Press, USA, **2005**, pp. 468.
- [30] Cadogan reactions of xanthenes **5.31a–f** were processed in Prof. Witulski's laboratory by Dr. Carole Witulski-Alayrac, as a collaborative work.
- [31] There was one unidentified product (1%) was isolated in the Cadogan / *N*-alkylation reactions of xanthone **5.31f**. Although both MS and HRMS spectra showed the



exact molecular mass of the byproduct *N*-ethylated one (see the experimental section, page 322), the  $^1\text{H}$  NMR does not indicate either **5.53f** or **5.54f**. A possible structure, which have very downfield Hc, maybe suggested as below:



- [32] Bunyan, P. J.; Cadogan, J. I. G. *J. Chem. Soc.* **1963**, 42–49.
- [33] In fact, only the angular isomers **5.52b**, **5.52d**, and **5.52f**, the major products, were obtained in sufficient amounts for the coupling reactions.
- [34] (a) Igawa, S; Okada, S; Takiguchi, T; Kamatani, J. (Canon Kabushiki Kaisha, Japan), *U.S. Pat. Appl. Publ.* **2008**, US 2008131731. (b) Tao, S.; Zhou, Y.; Lee, C. S.; Lee, S.-T.; Huang, D.; Zhang, X. *J. Phys. Chem. C* **2008**, *112*, 14603–14606.
- [35] Badone, D.; Baroni, M.; Cardamone, R.; Ielmini, A.; Guzzi, U. *J. Org. Chem.* **1997**, *62*, 7170–7173.
- [36] The procedure was modified from: (a) Tao, B.; Boykin, D. W. *J. Org. Chem.* **2004**, *69*, 4330–4335. (b) Zhu, R.; Qu, F.; Quéléver, G.; Peng, L. *Tetrahedron Lett.* **2007**, *48*, 2389–2393.
- [37] Xiao, K.; Liu, Y.; Qi, T.; Zhang, W.; Wang, F.; Gao, J.; Qiu, W.; Ma, Y.; Cui, G.; Chen, S.; Zhan, X.; Yu, G.; Qin, J.; Hu, W.; Zhu, D. *J. Am. Chem. Soc.* **2005**, *127*, 13281–13286.

- [38] (a) Boudreault, P. T.; Wakim, S.; Blouin, N.; Simard, M.; Tessier, C.; Tao, Y.; Leclerc, M. *J. Am. Chem. Soc.*, **2007**, *129*, 9125–9136. (b) Horowitz, G. *J. Matter. Chem.* **1999**, *9*, 2021–2026.
- [39] Turro, N. J. *Modern Molecular Photochemistry*, University Science Books, **1991**, California, US, pp.136–137.
- [40] Stokes shifts are given by  $E_{\text{abs}} - E_{\text{em}} = 2\lambda_t$ , where  $\lambda_t$  is the total reorganization energy, which is a linear combination of the vibrational ( $\lambda_{\text{vib}}$ ) and solvent reorganization ( $\lambda_o$ ) energies, respectively.
- [41] See the relevant explanation in Chapter 2, page 72.
- [42] Xiao, K.; Liu, Y.; Qi, T.; Zhang, W.; Wang, F.; Gao, J.; Qiu, W.; Ma, Y.; Cui, G.; Chen, S.; Zhan, X.; Yu, G.; Qin, J.; Hu, W.; Zhu, D. *J. Am. Chem. Soc.* **2005**, *127*, 13281–13286.
- [43] These experiments were done using instruments at Mainz University, Germany.
- [44] Cyclic voltammetry experiments of **5.42** and **5.43** were proceeded by Guang Chen in Department of Chemistry, Memorial University. His helpful is highly appreciated.
- [45] The ideal reversible redox process has well defined characteristics:

- (1) The voltage separation between the current peaks is

$$|E_{\text{pc}} - E_{\text{pa}}| = \frac{59 \text{ mV}}{n}, \text{ n is electron process.}$$

- (2) The ratio of the peak currents is equal to one

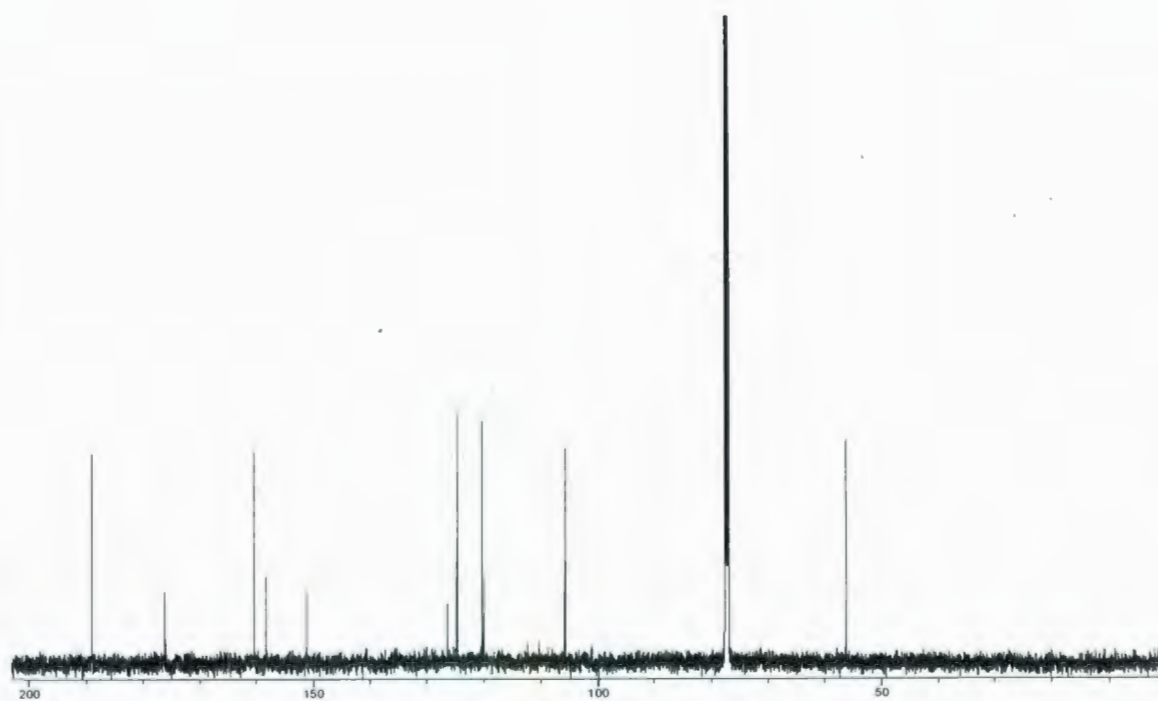
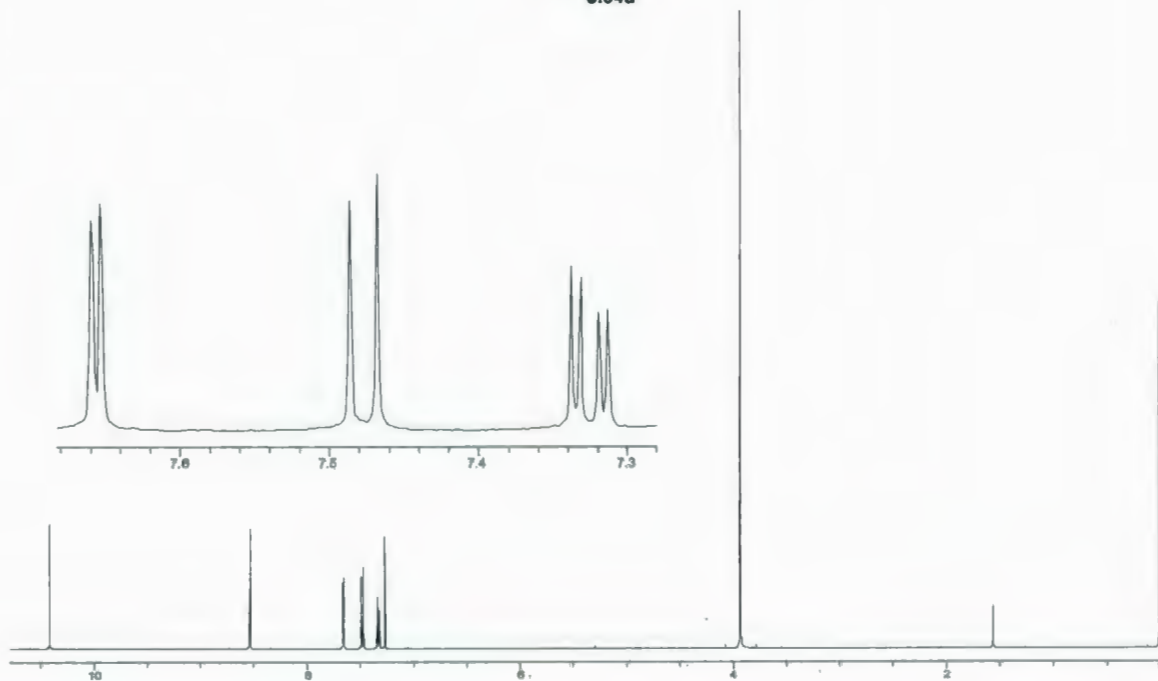
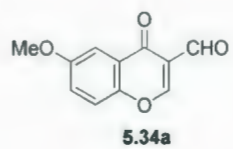
$$\frac{i_{\text{pa}}}{i_{\text{pc}}} = 1$$

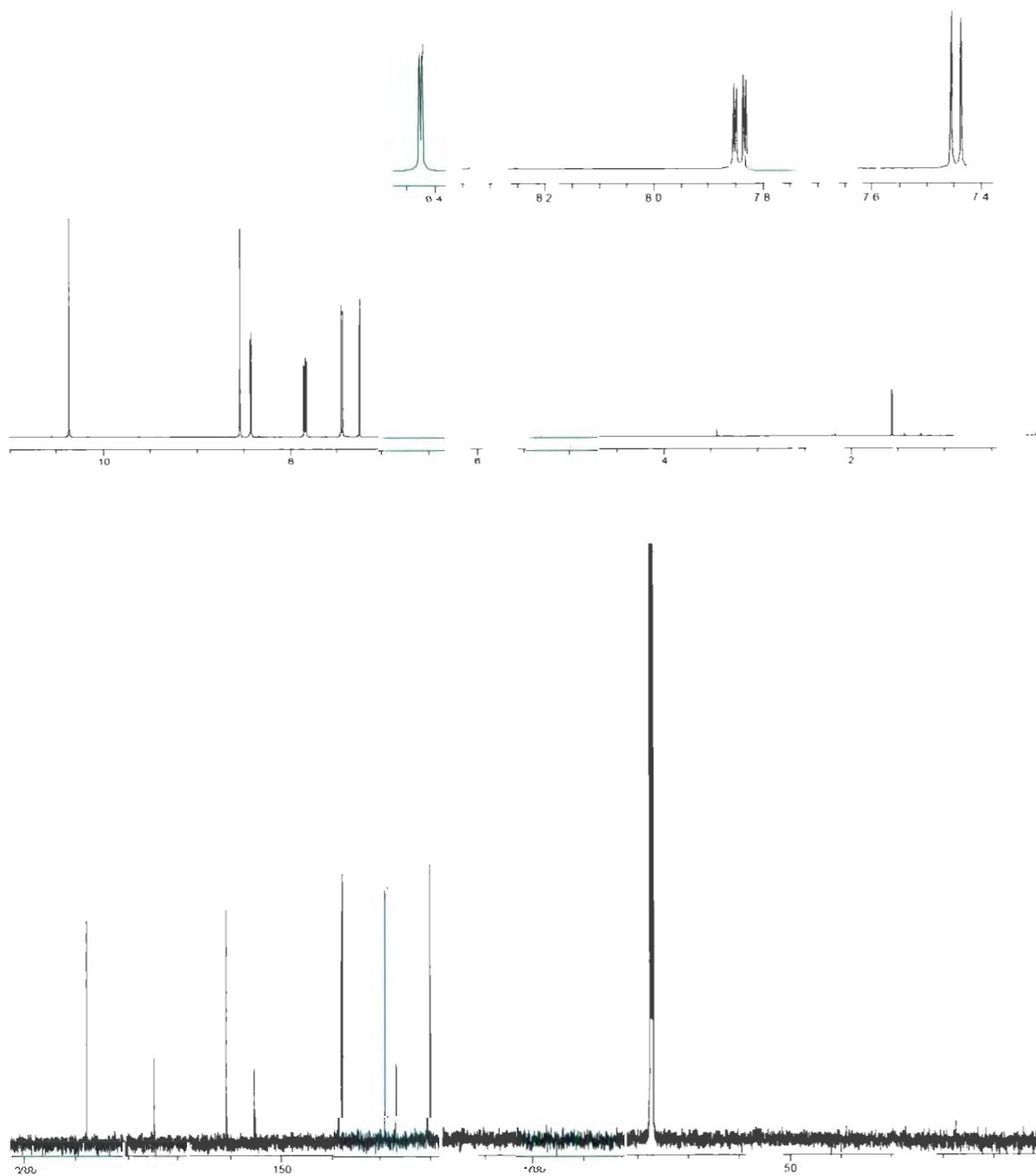
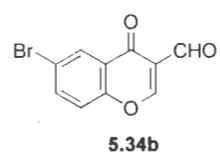
- 
- See: Nicholson, R. S.; Shain, I. *Anal. Chem.* **1964**, *36*, 706–723.
- [46] Gao, P.; Beckmann, D.; Tsao, H. N.; Feng, X.; Enkelmann, V.; Pisula, W.; Müllen, K. *Chem. Commun.* **2008**, 1548–1550.
- [47] Meng, H.; Bendikov, M.; Mitchell, G.; Helgeson, R.; Wudl, F.; Bao, Z.; Siegrist, T.; Kloc, C.; Chen, C. H. *Adv. Mater.* **2003**, *15*, 1090–1093.
- [48] Boudreault, P.-L. T.; Wakim, S.; Blouin, N.; Simard, M.; Tessier, C.; Ye, T.; Leclerc, M. *J. Am. Chem. Soc.* **2007**, *127*, 9125–9136.
- [49] SPARTAN '08 software from Wavefunction, Inc. Irvine, CA, USA.
- [50] For all known compounds, a literature citation is given after the compound name. In all cases, the obtained spectroscopic data were consistent with published data.
- [51] Patonay, T.; Kiss-Szikszai, A.; Silva, V. M. L.; Silva, A. M. S.; Pinto, D. C. G. A.; Cavaleiro, J. A. S.; Jekó, J. *Eur. J. Org. Chem.* **2008**, 1937–1946.
- [52] Araya-Maturana, R.; Heredia-Moya, J.; Pessoa-Mahana, H.; Weiss-López, B.; *Synth. Commun.* **2003**, *33*, 3225–3231.
- [53] <http://www.sigmaaldrich.com/canada-english.html>
- [54] Cravotto, G.; Giovenzana, G. B.; Pilati, T.; Sisti, M.; Palmisano, G. *J. Org. Chem.* **2001**, *66*, 8447–8453.
- [55] Silva, V. L. M., Silva, A. M. S., Pinto, D. C. G. A., Cavaleiro, J. A. S., Patonay, T. *Synlett* **2004**, *15*, 2717–2720.
- [56] The experimental procedure and spectroscopic data of compounds **5.39**, **5.40**, and **5.41** were supplied by Joerg Moritz, Mainz University, Germany.



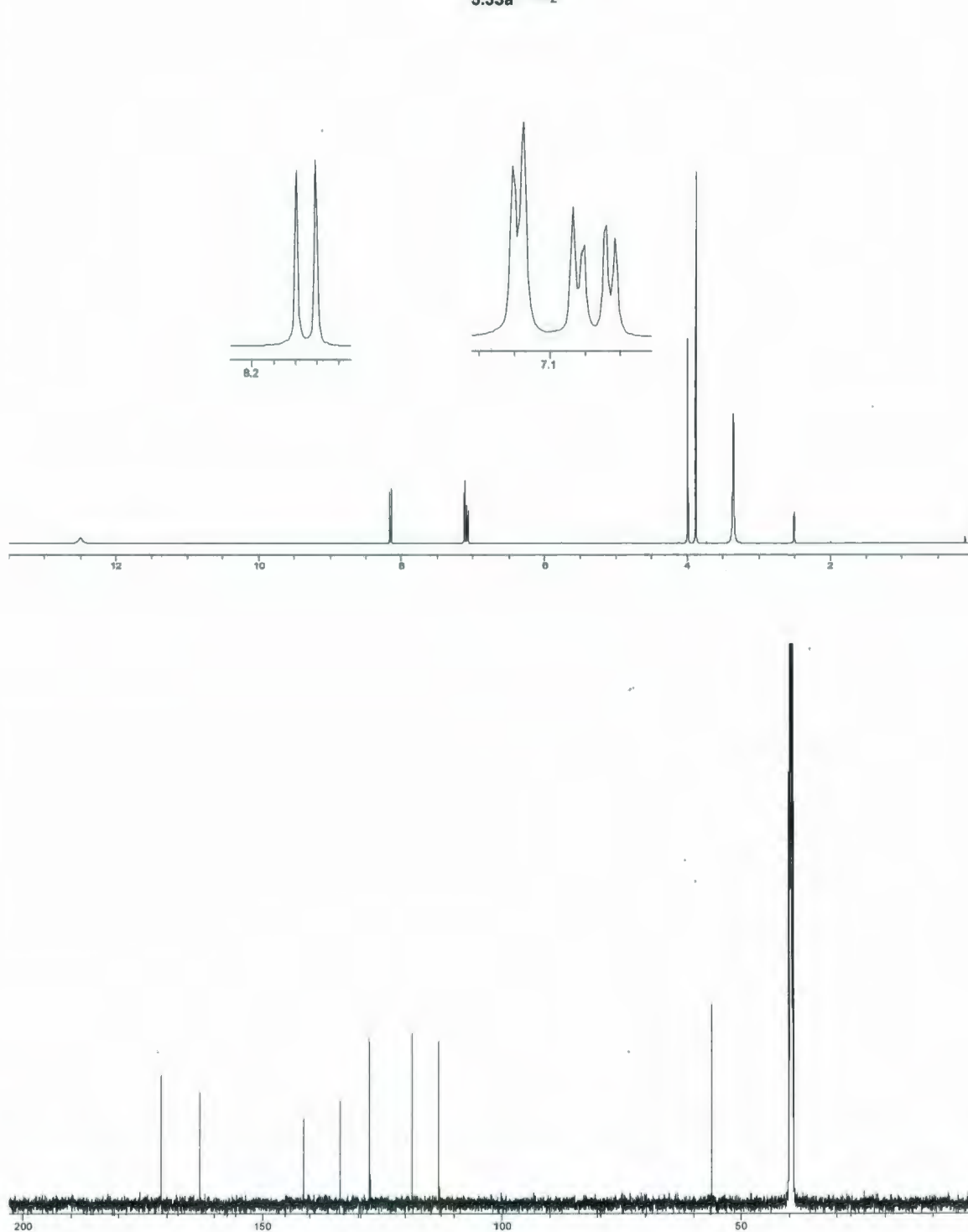
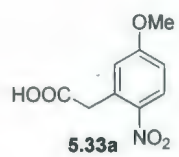
## Appendix

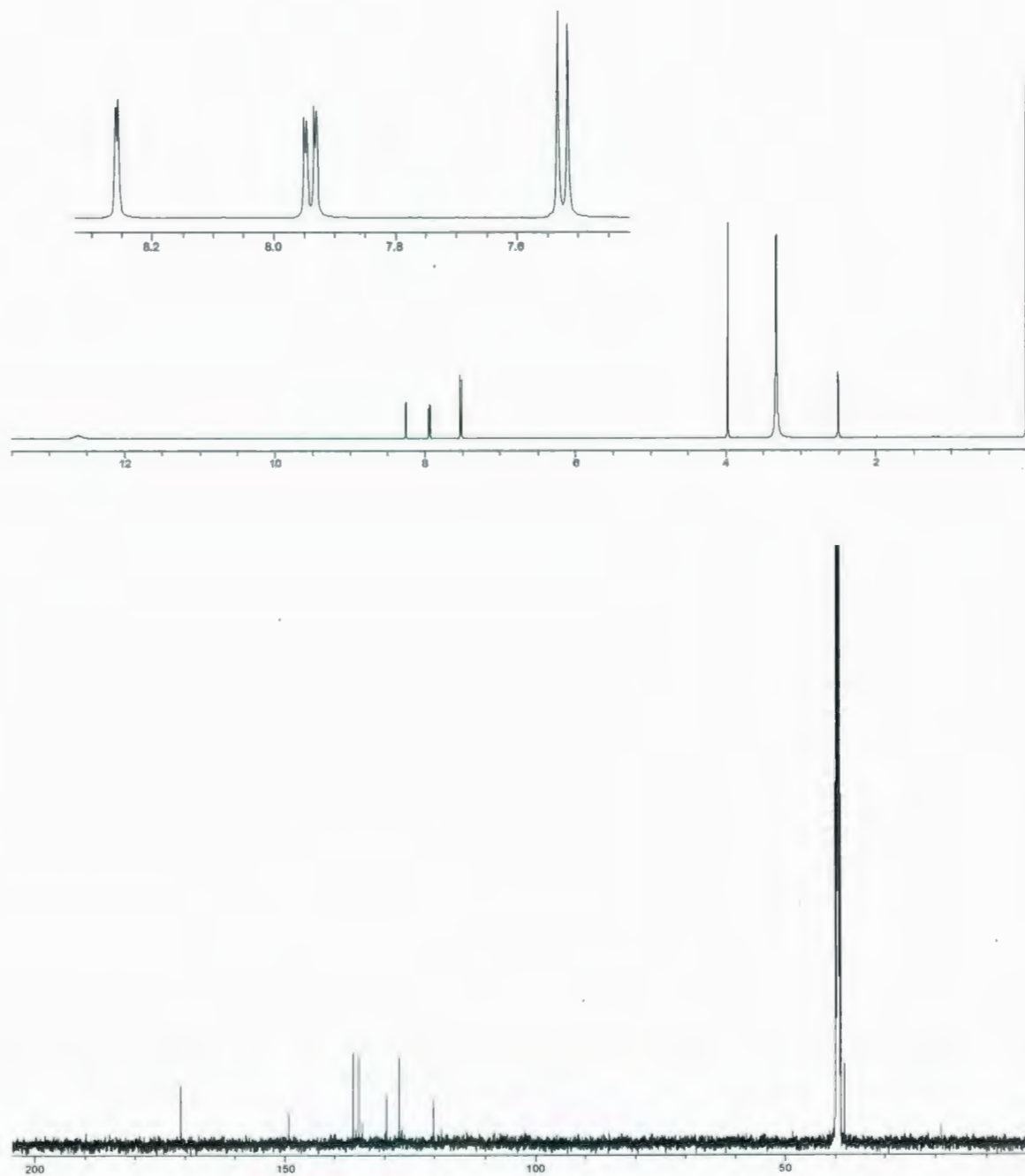
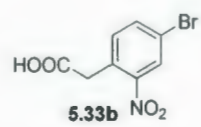
Selected NMR spectra for synthesized compounds

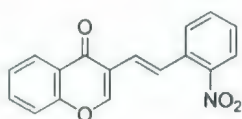




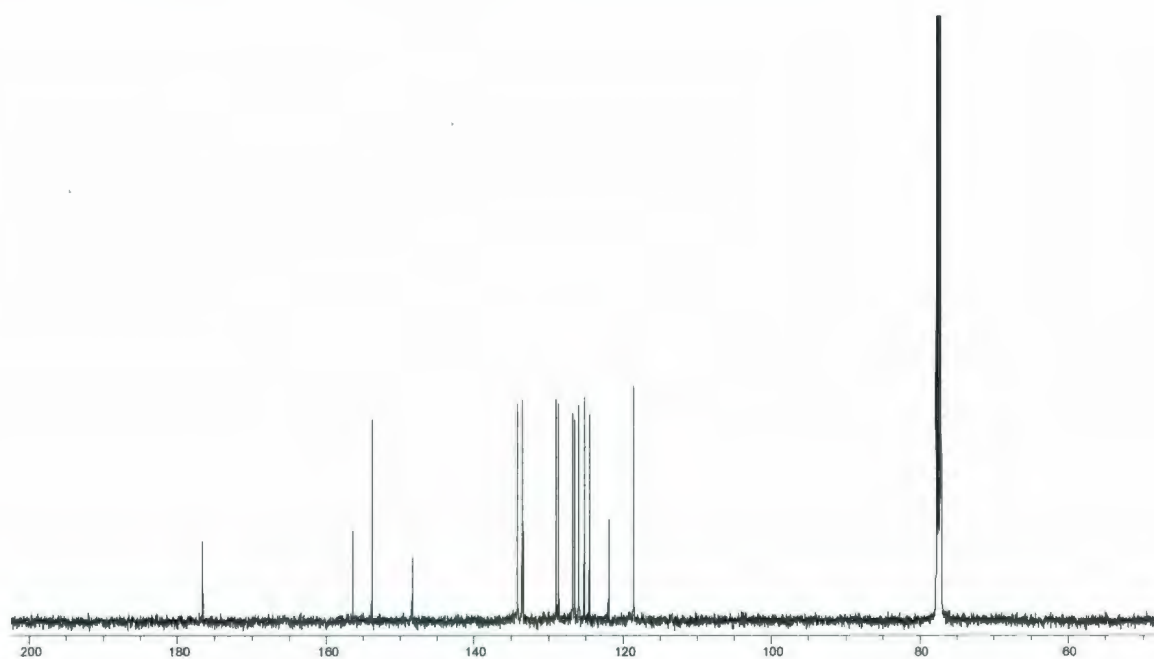
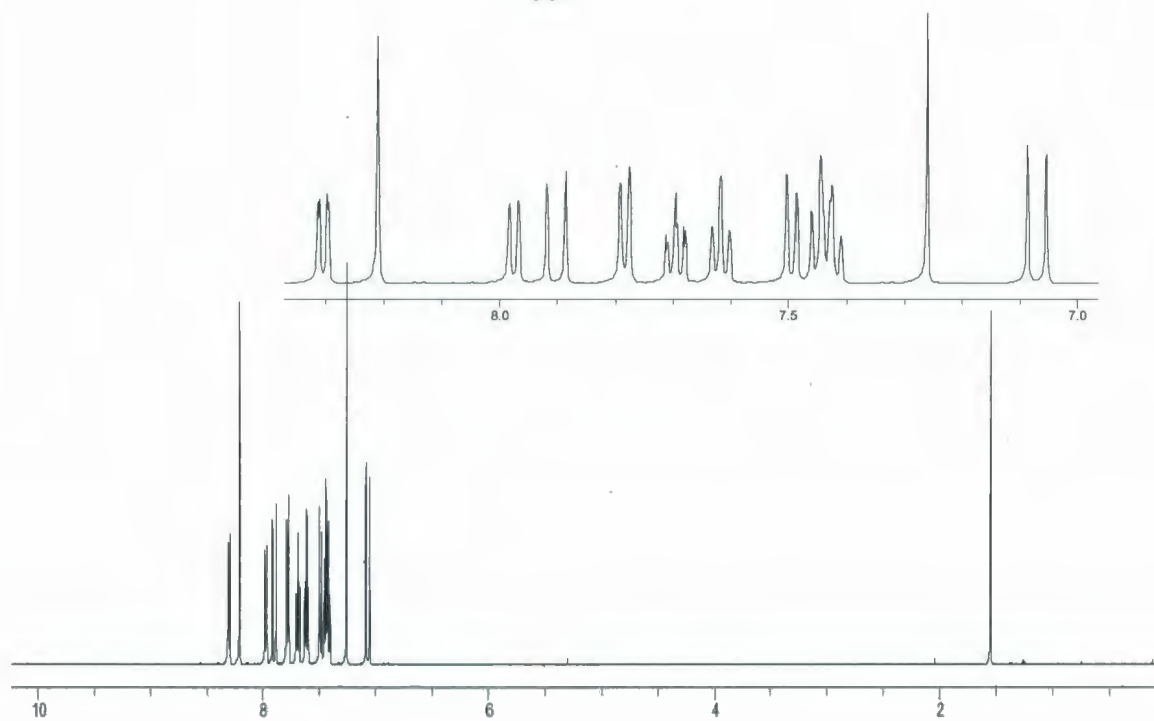


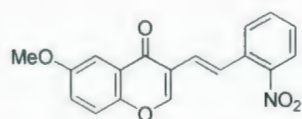




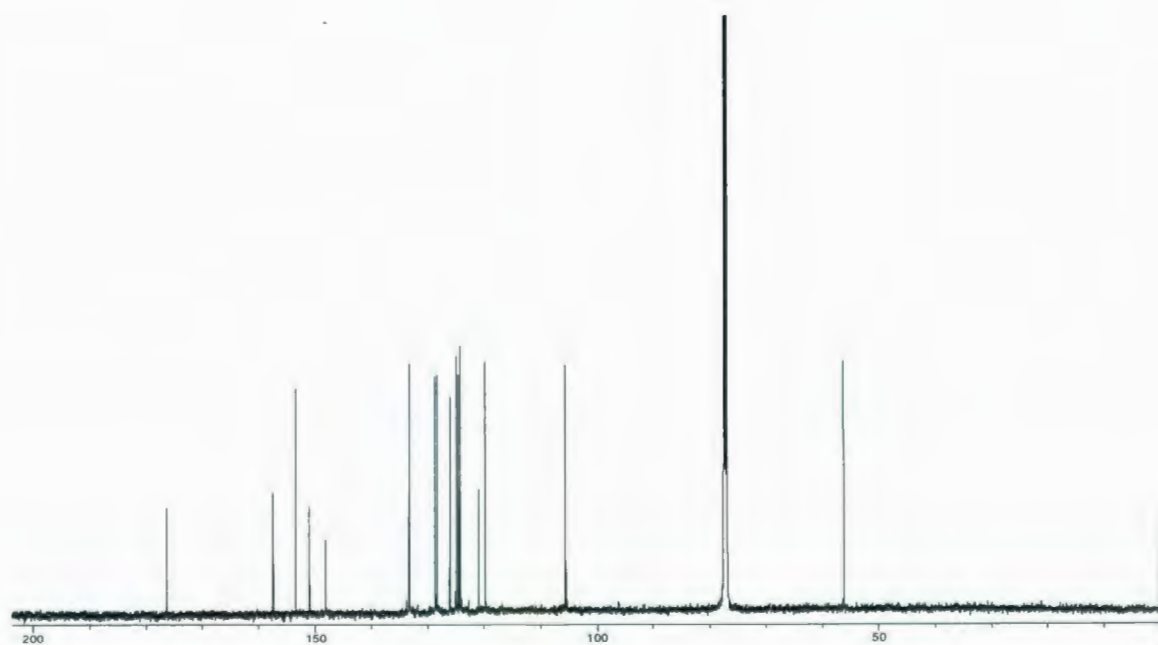
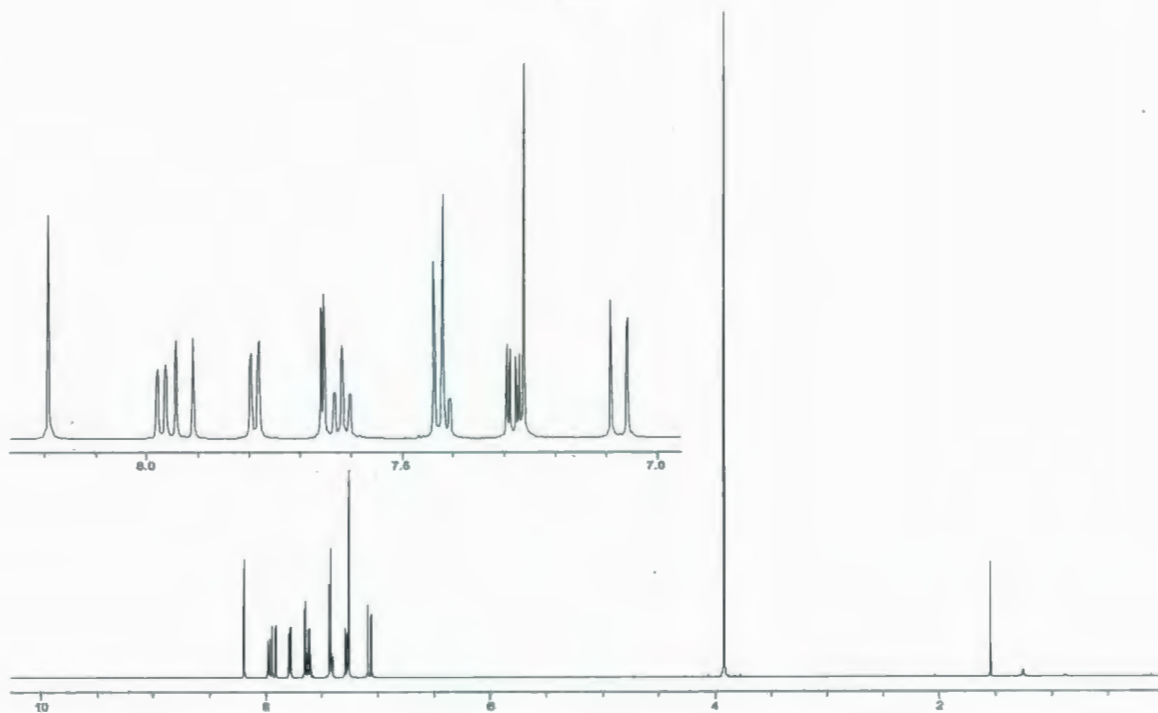


5.37

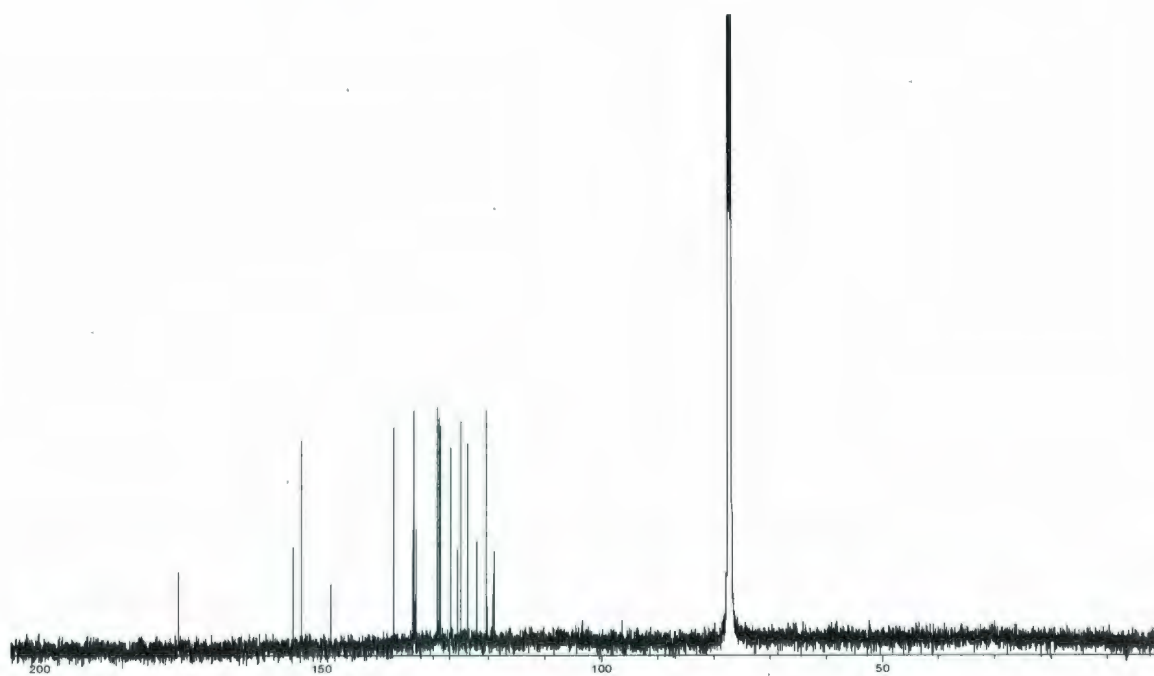
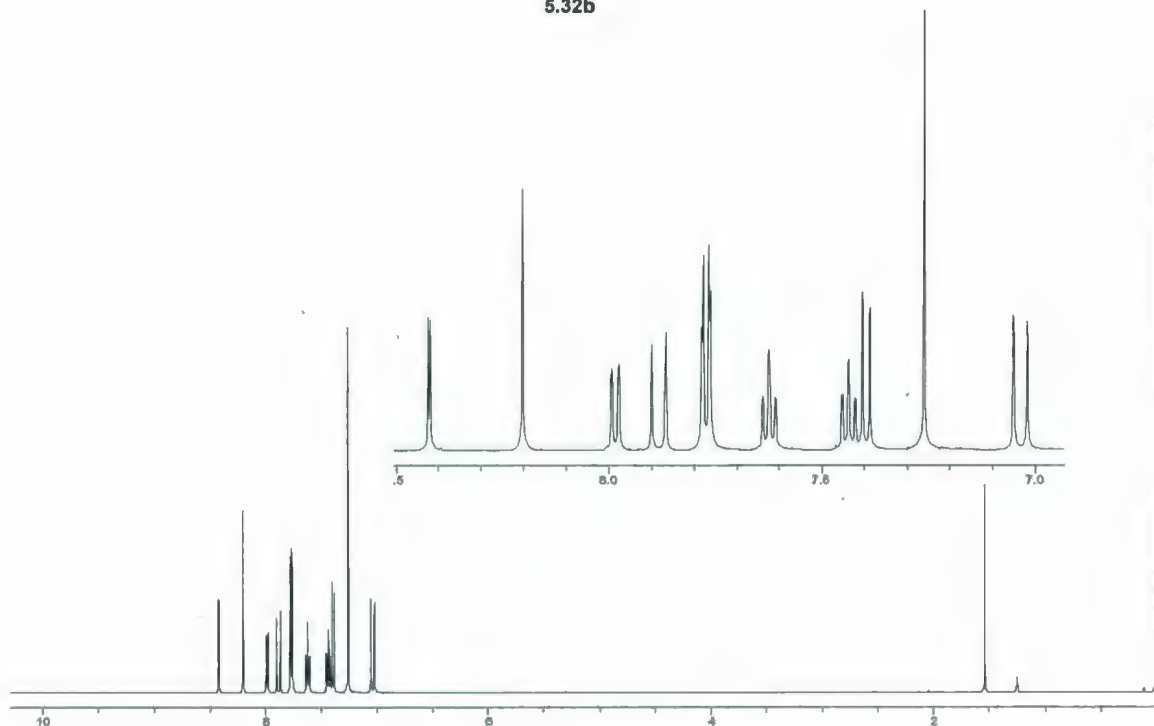
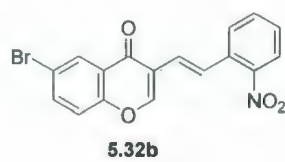


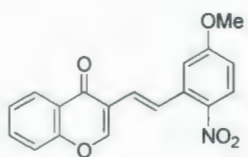


5.32a

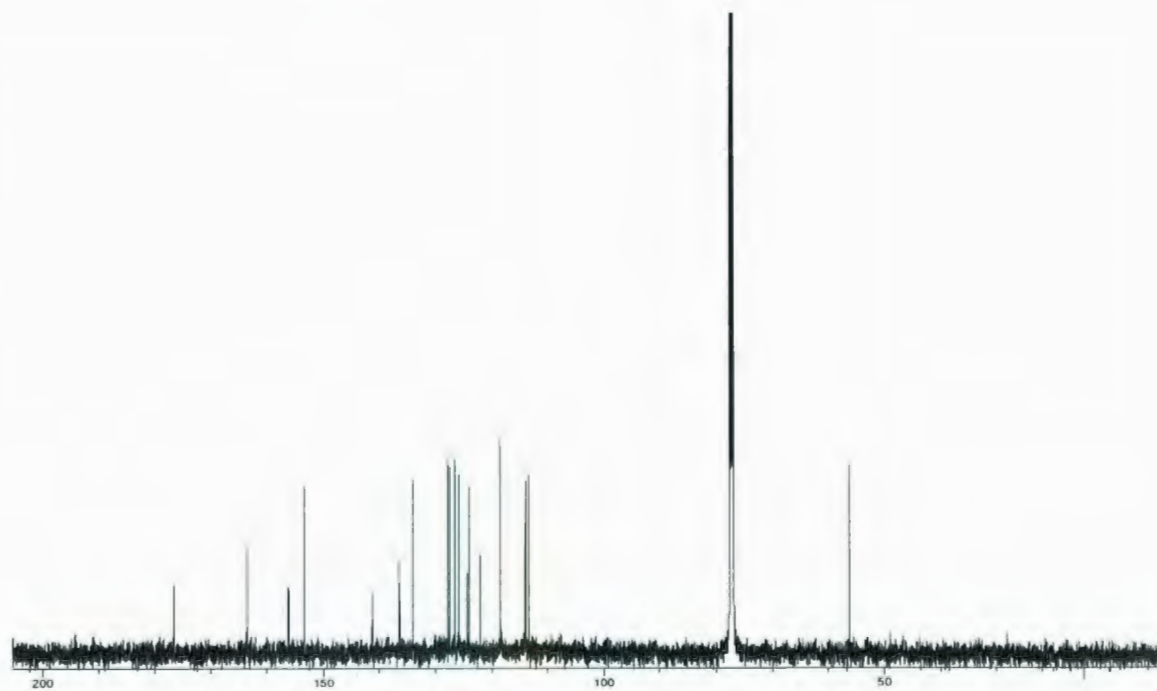
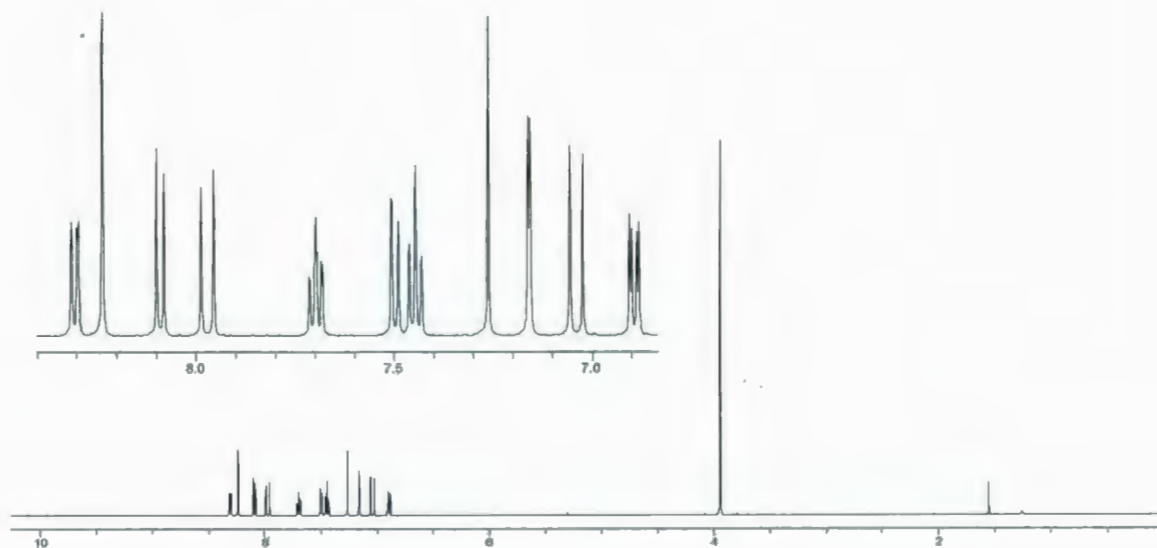


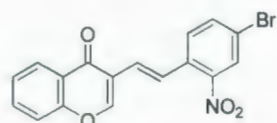




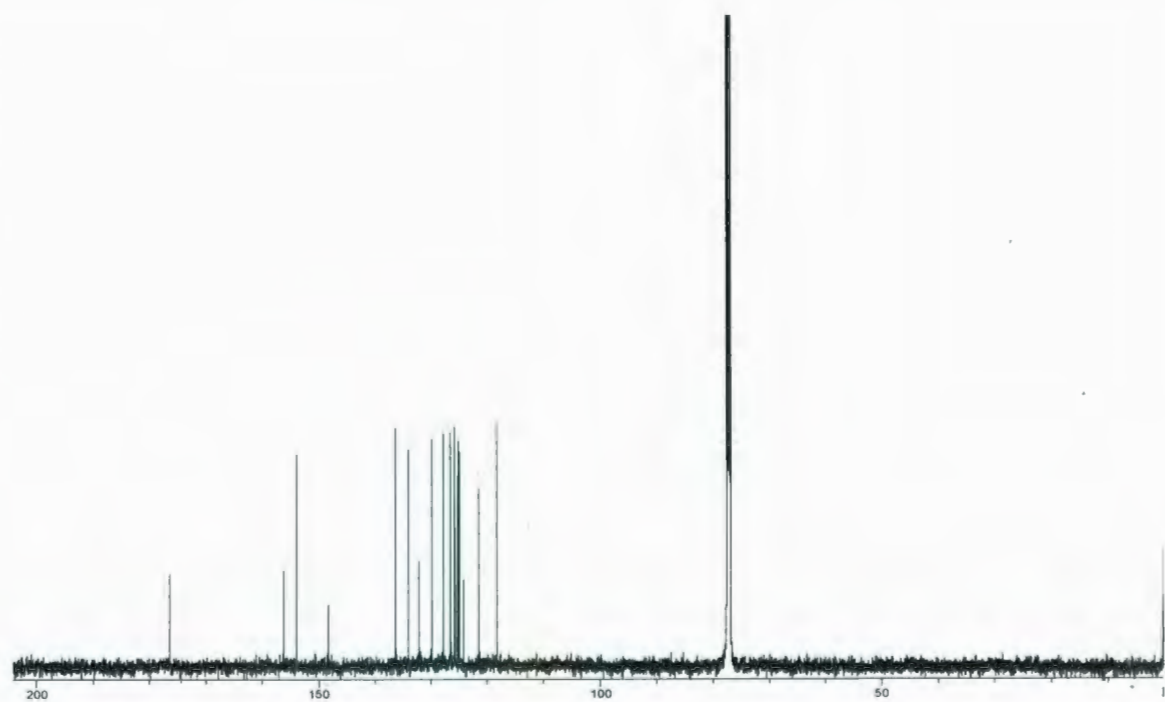
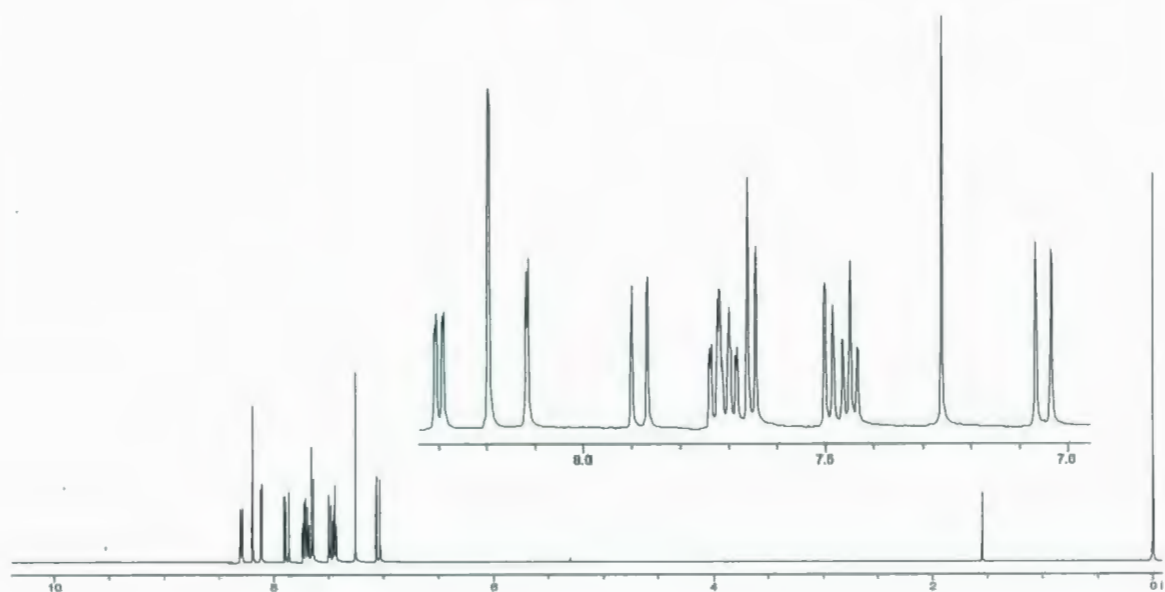


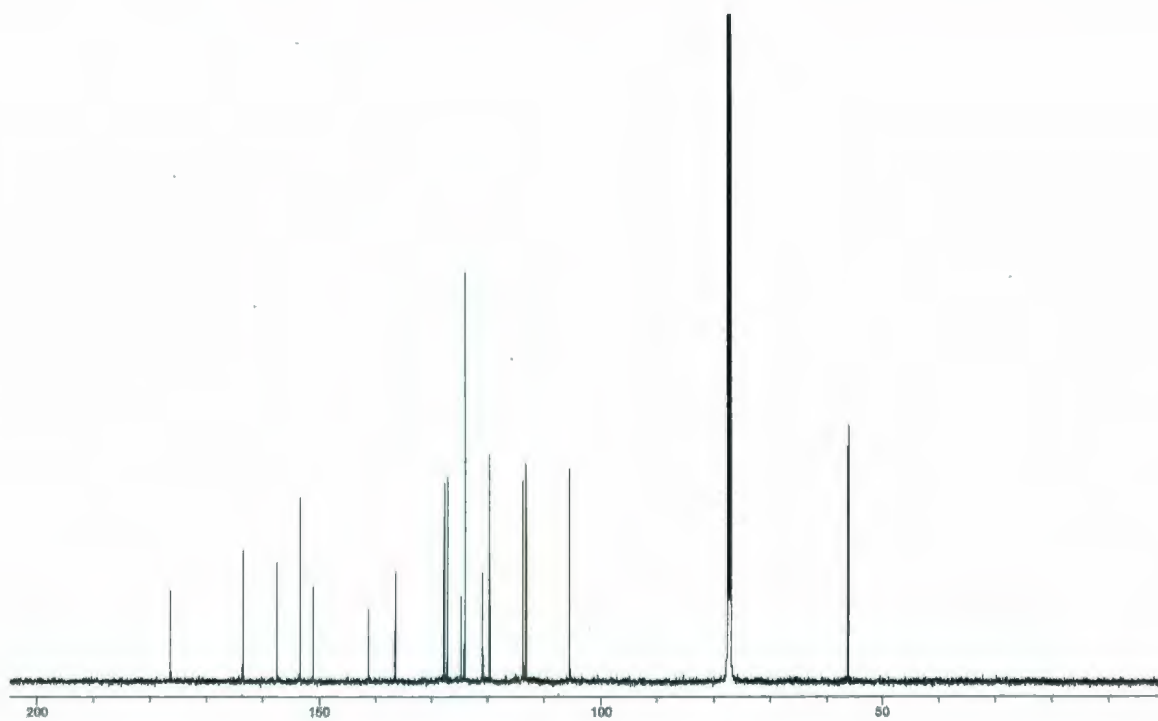
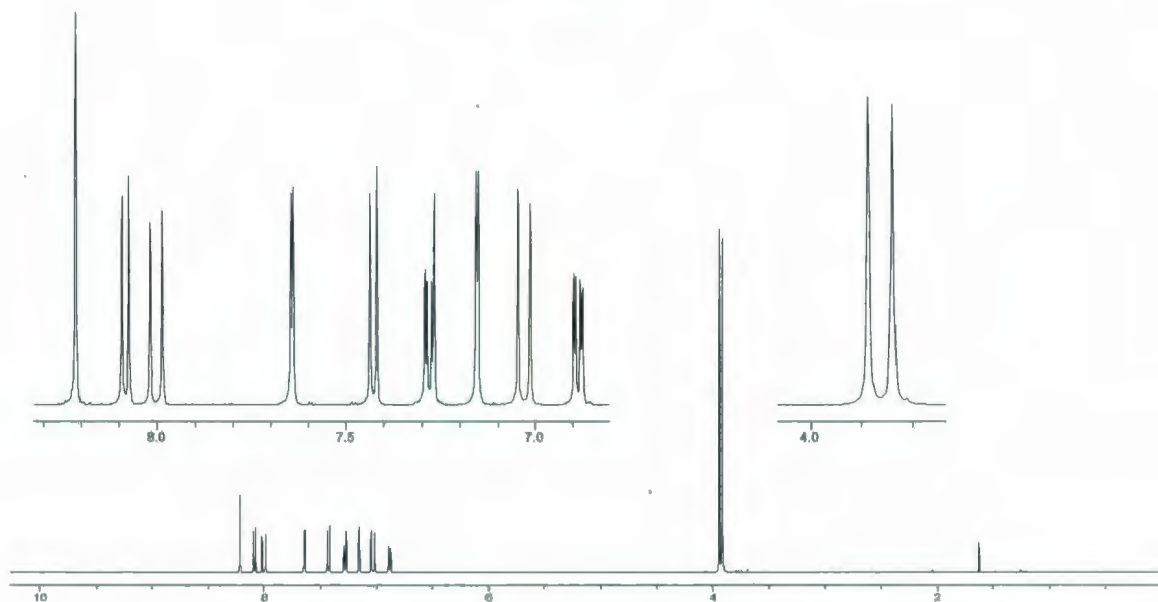
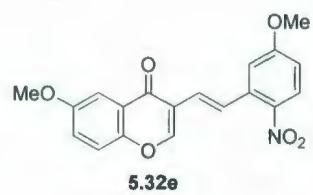
5.32c



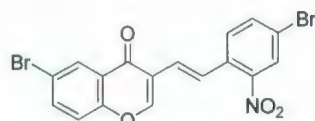


5.32d

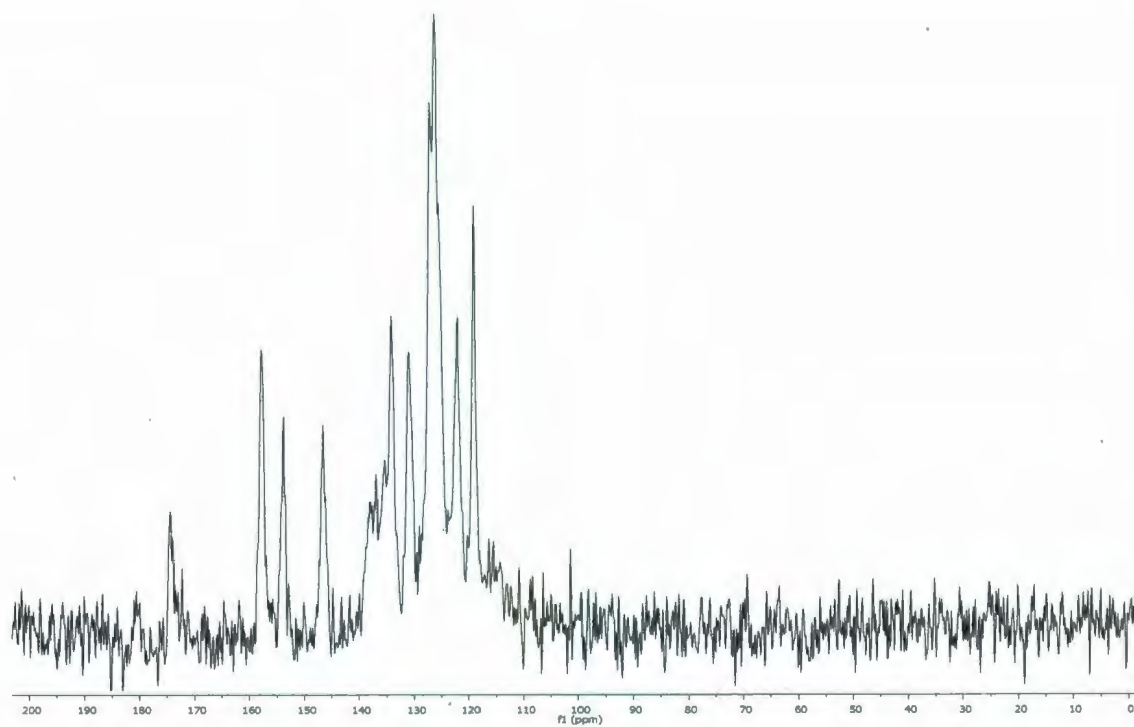
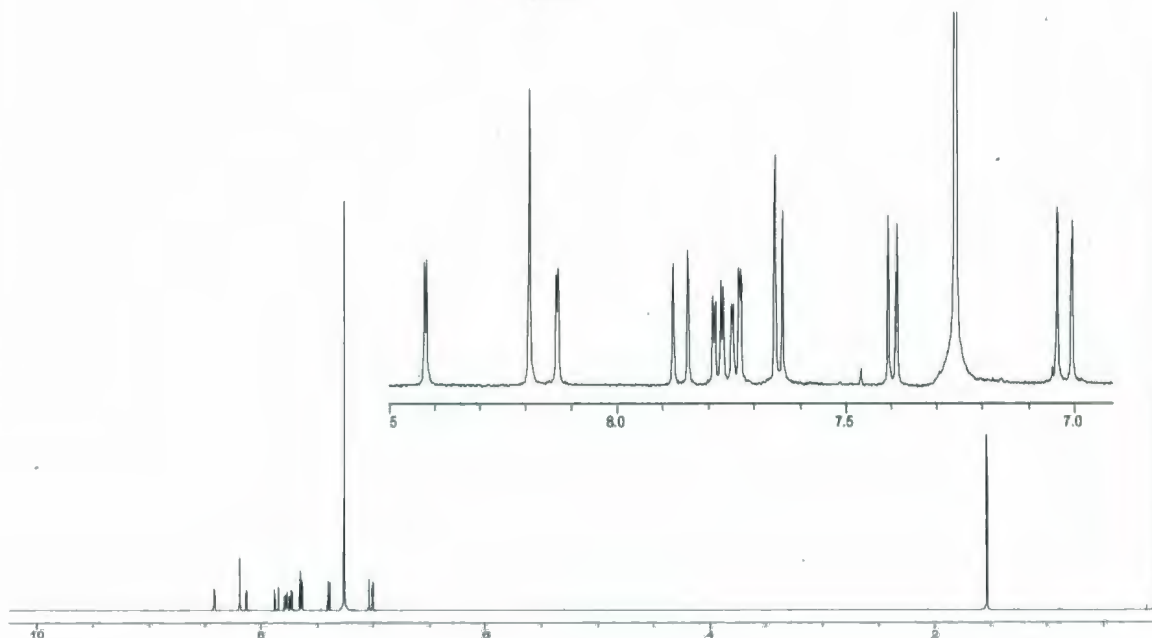


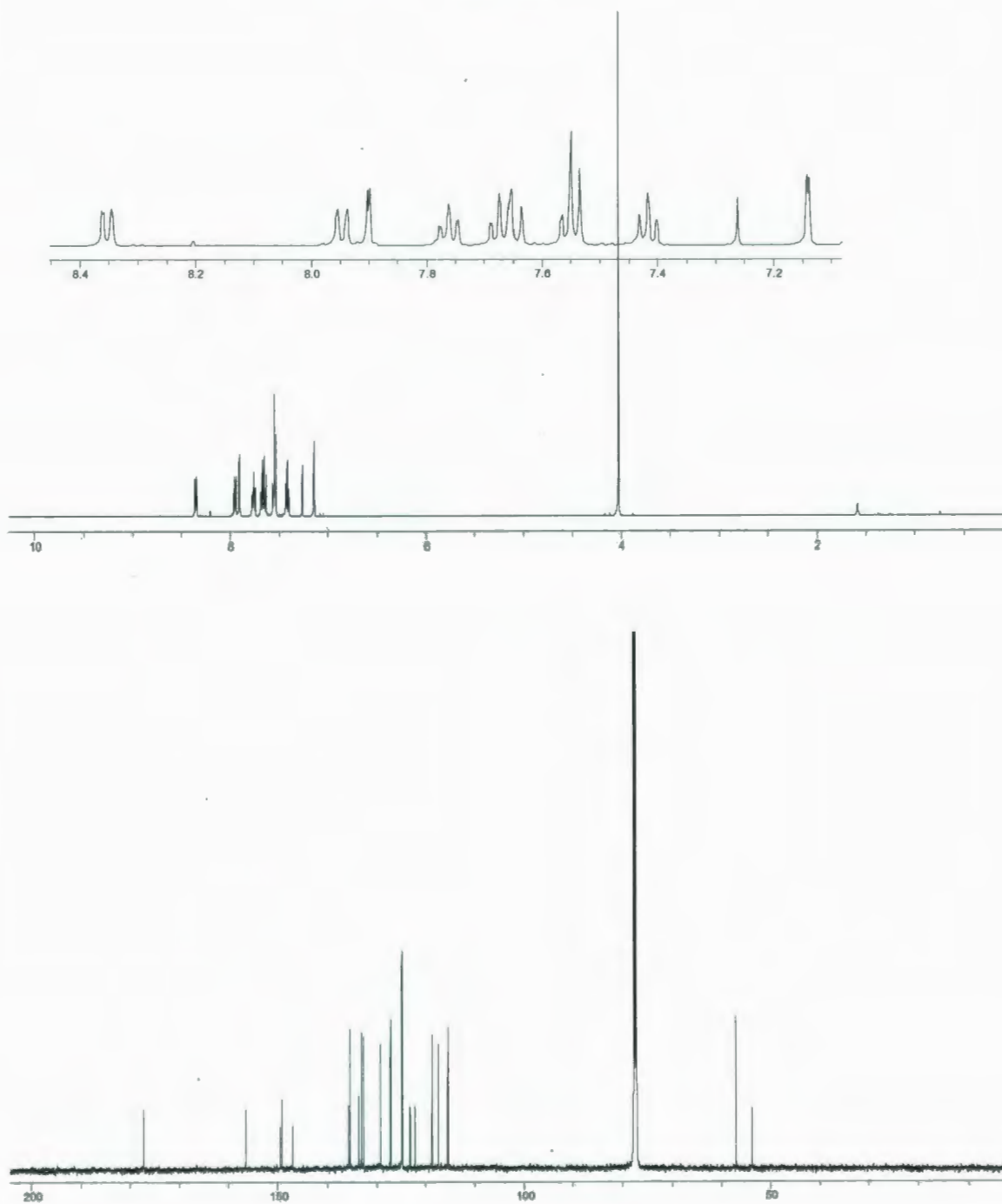
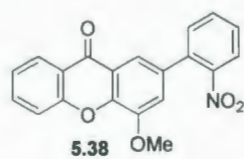


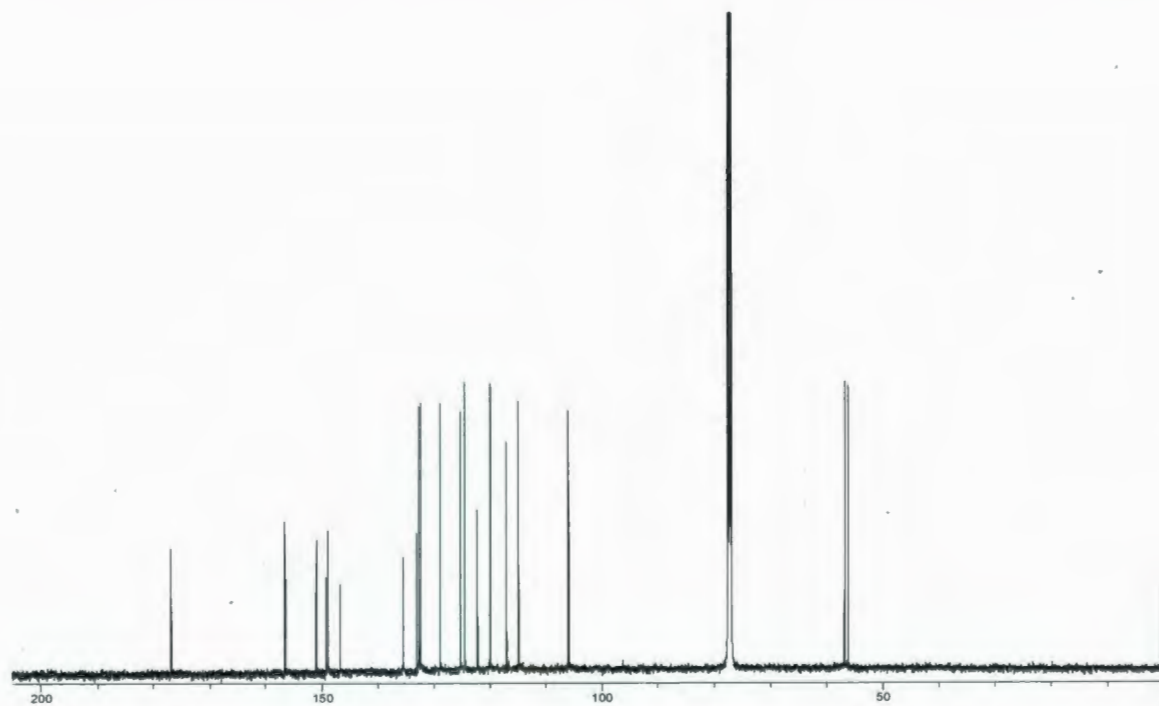
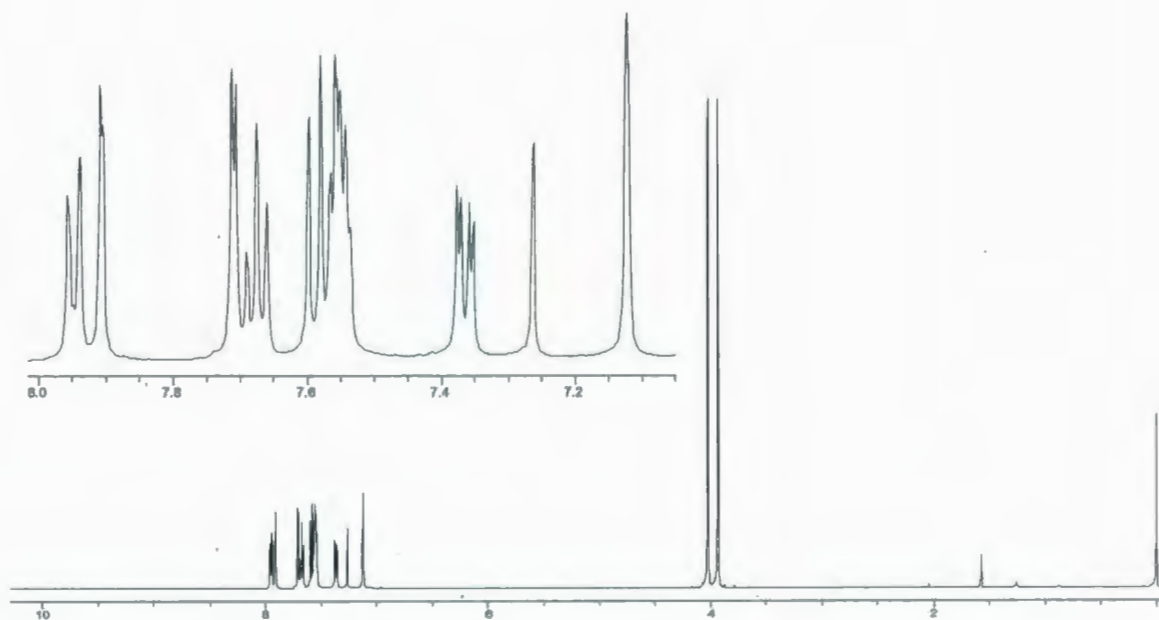
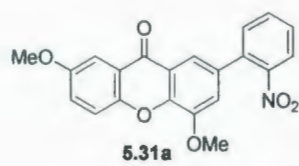


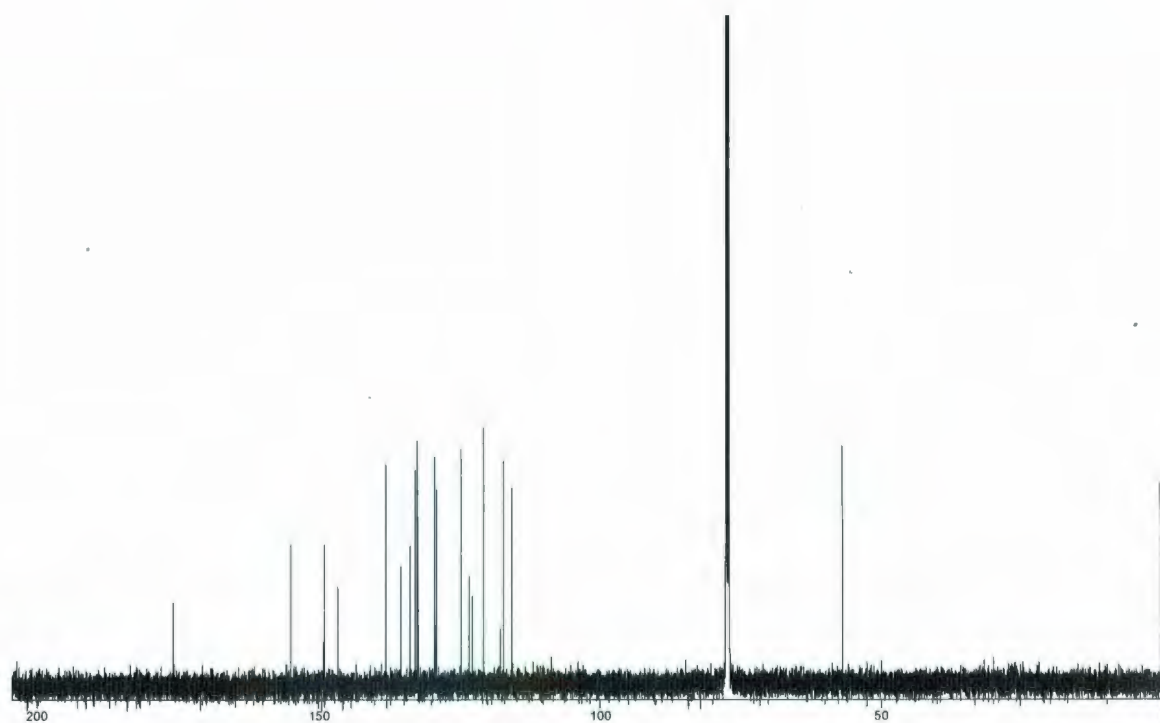
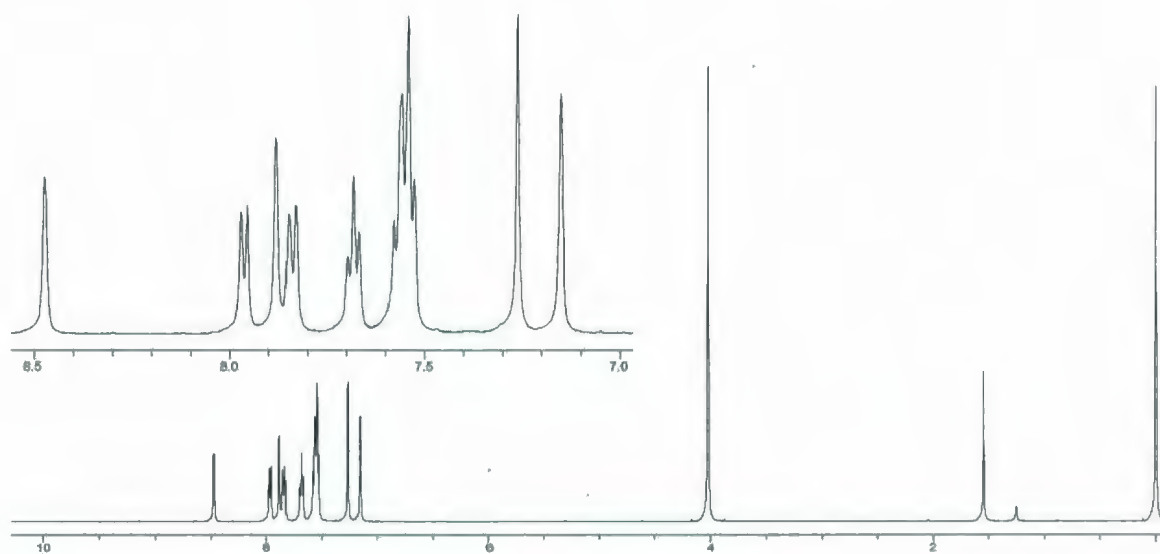
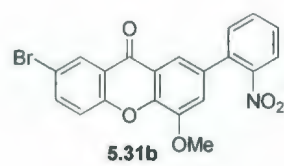


5.32f

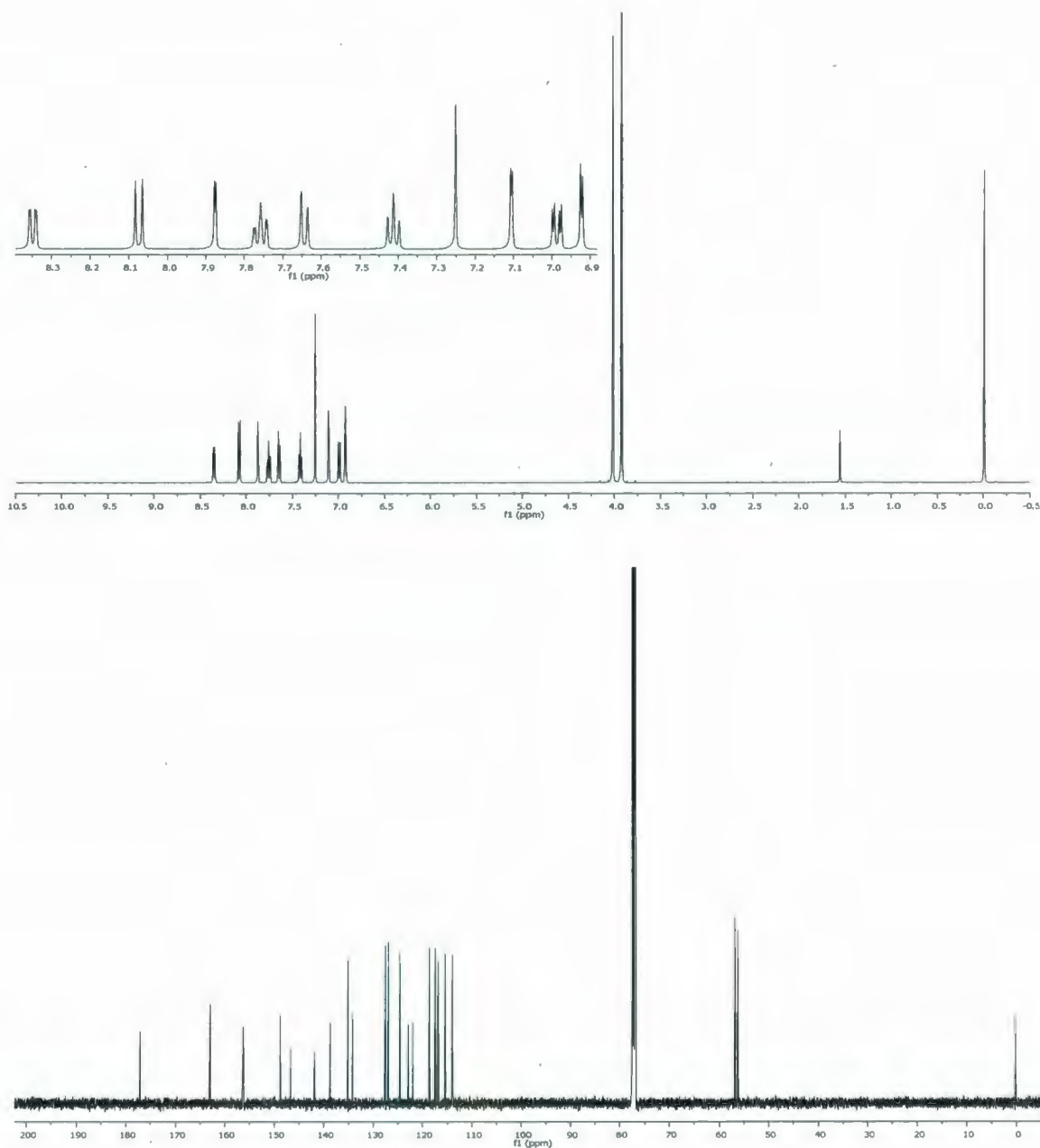
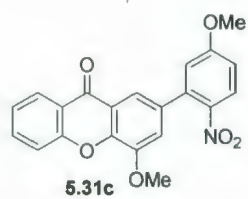


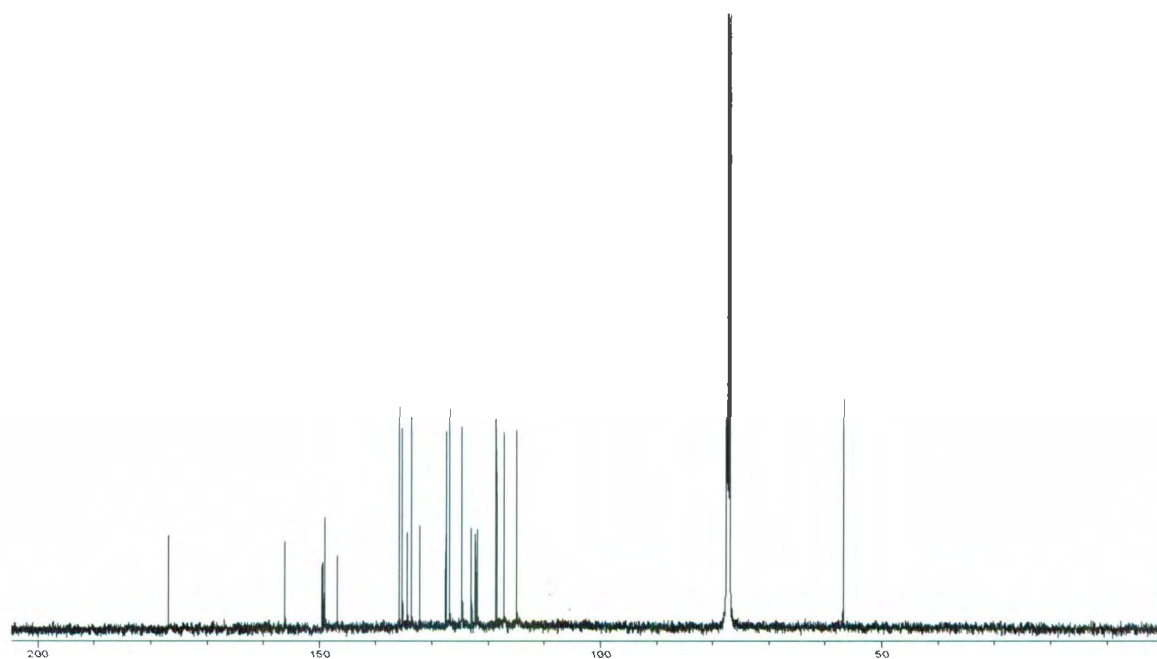
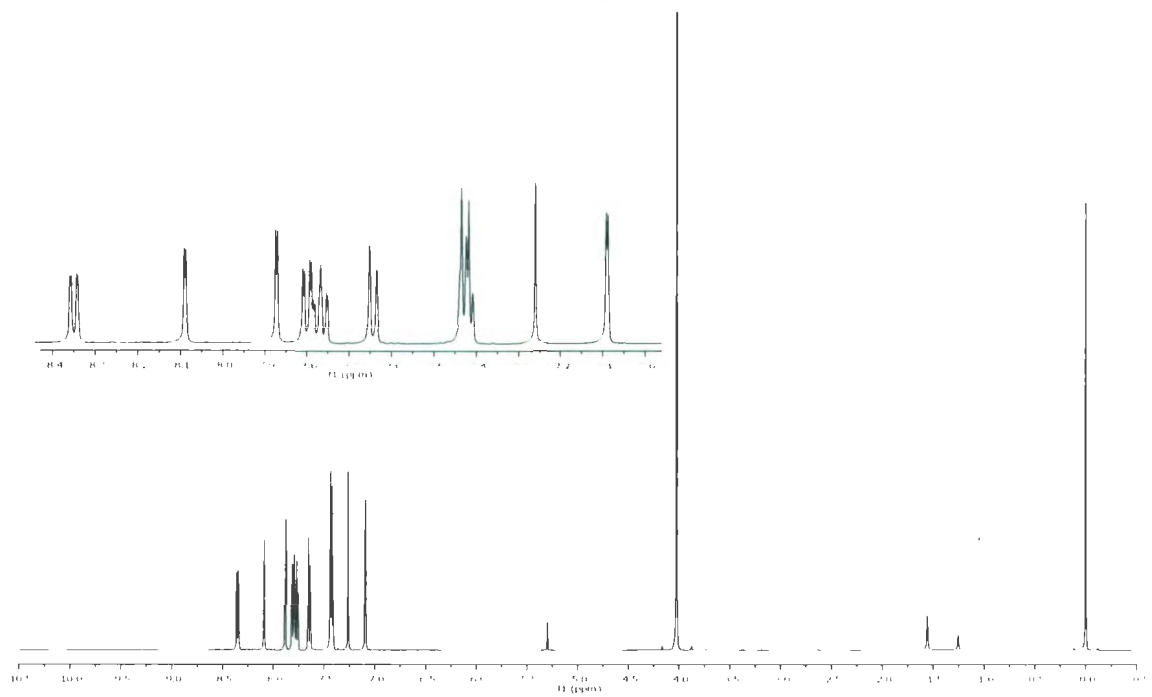
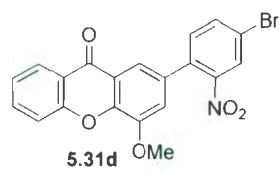


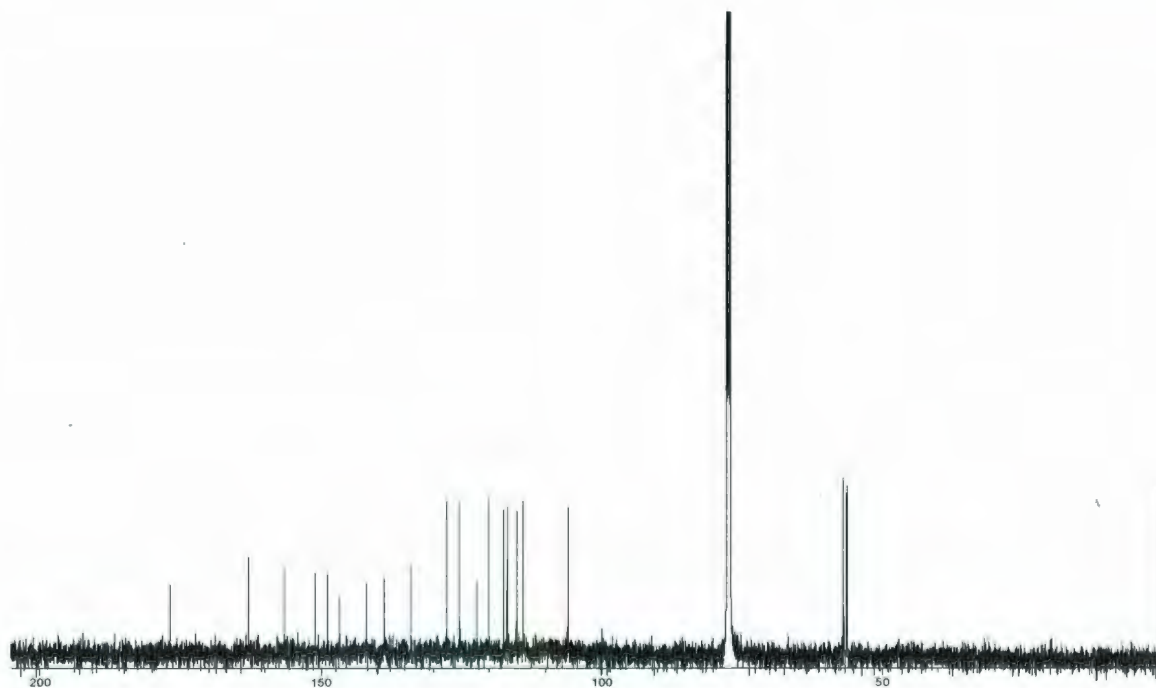
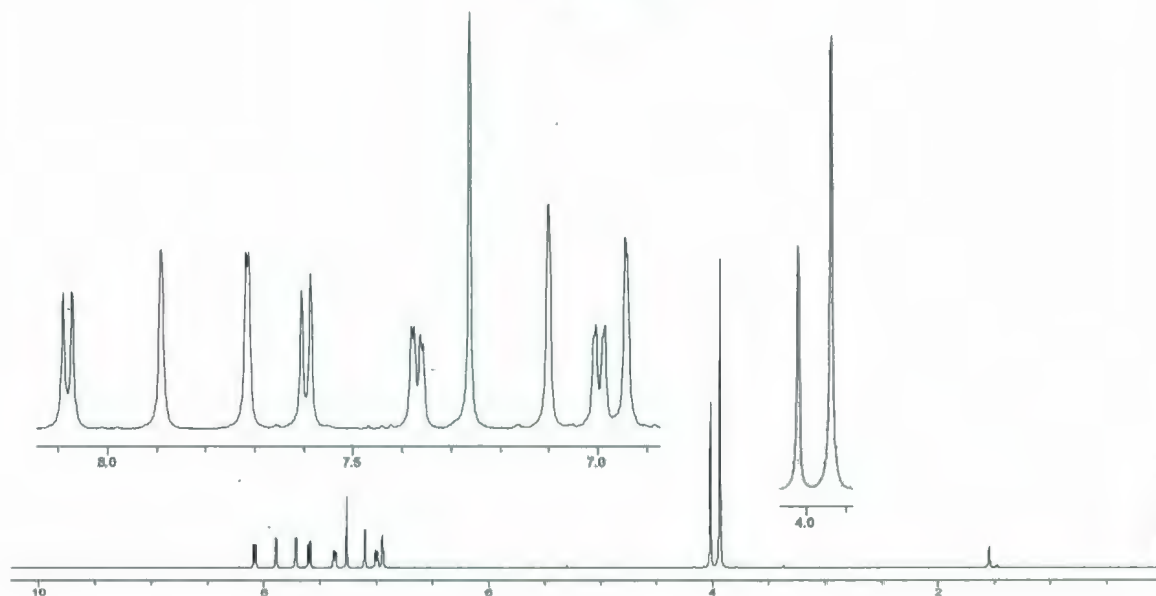
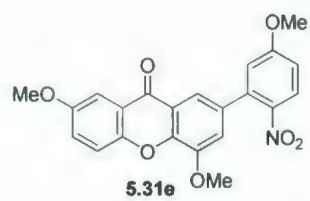


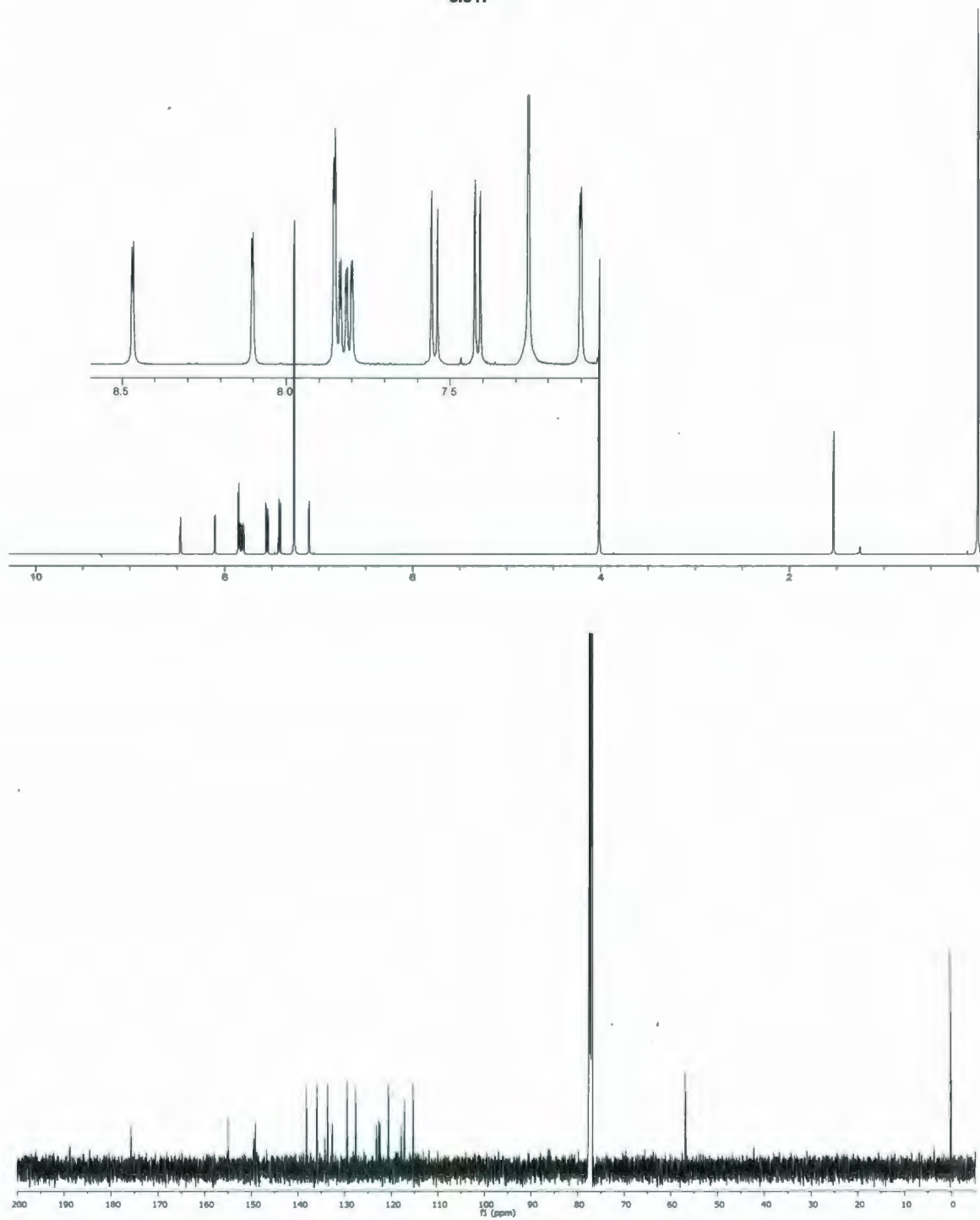
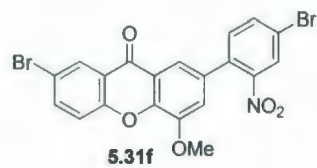




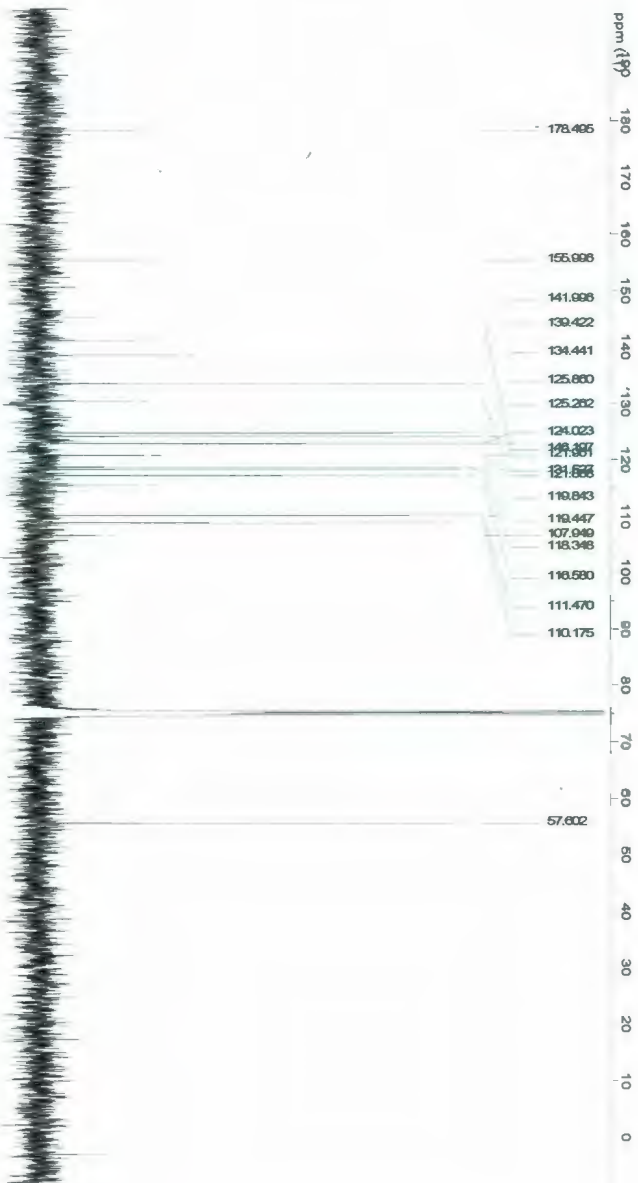
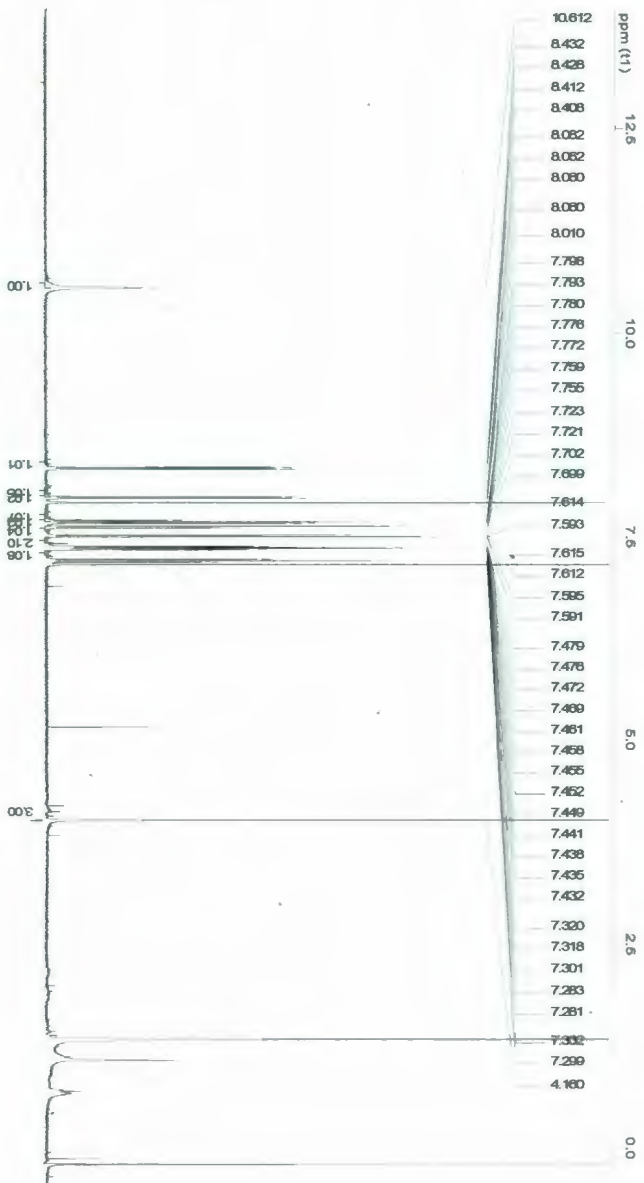
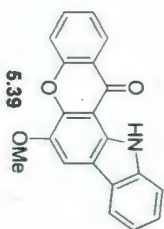


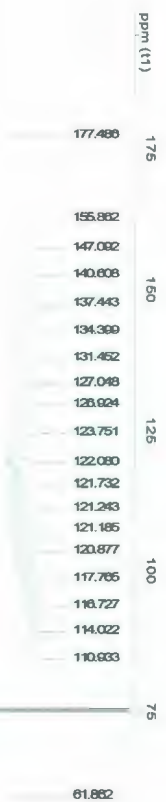
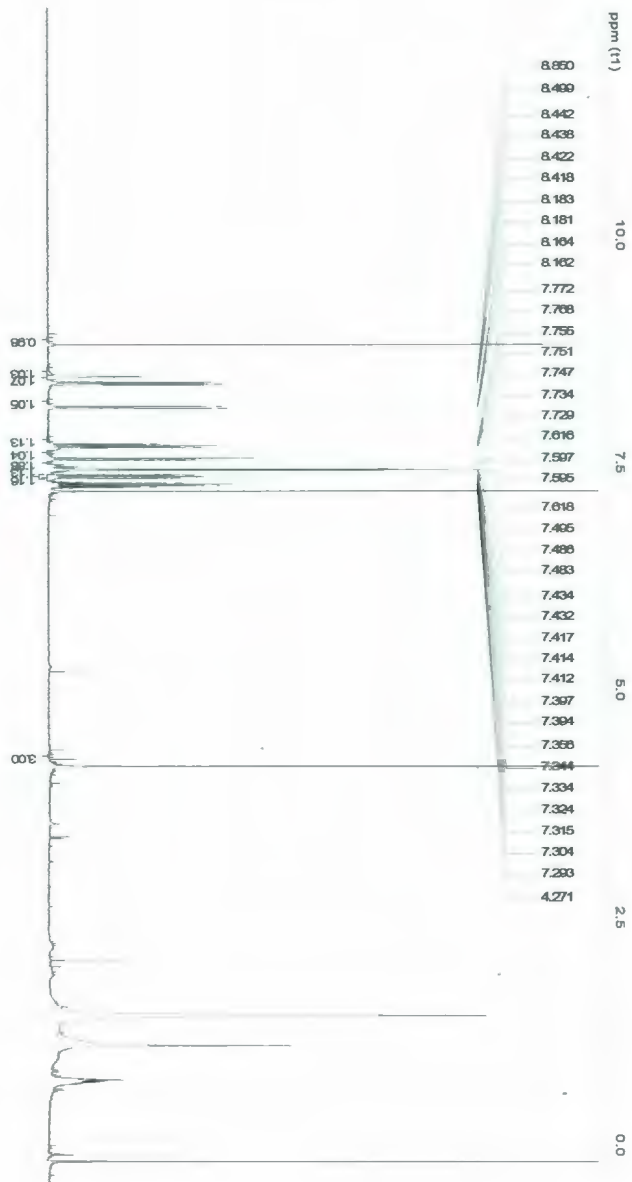
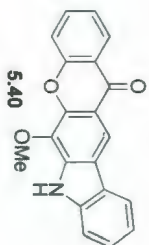


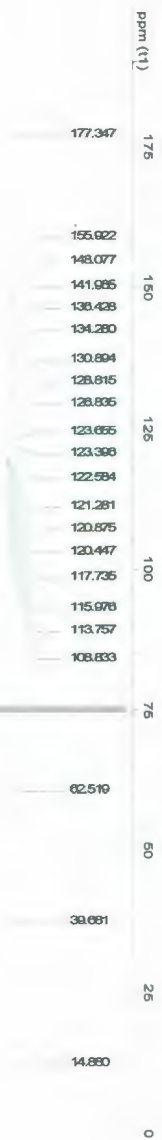
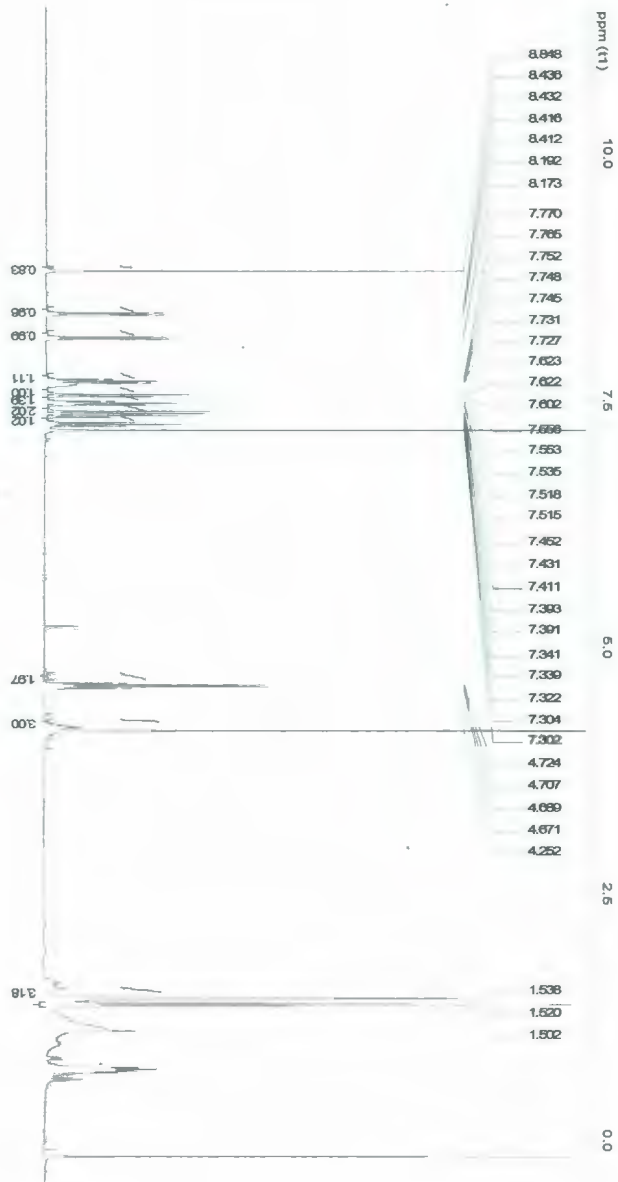
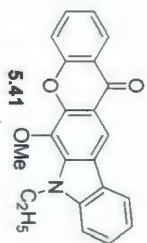


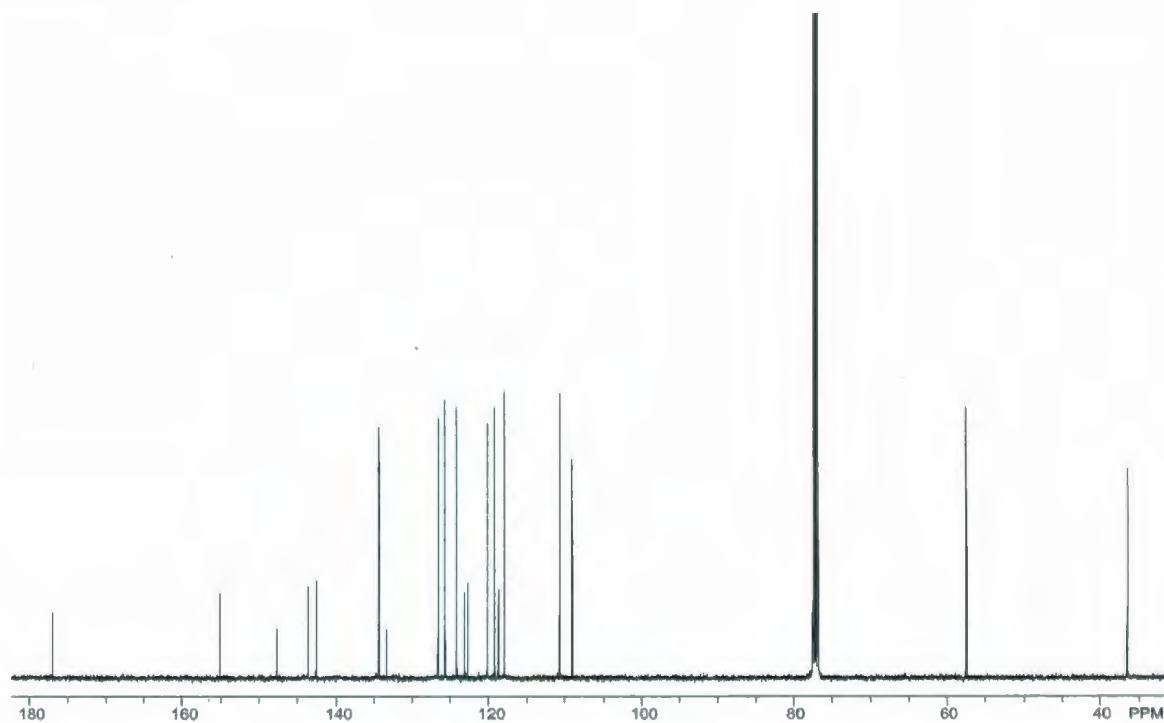
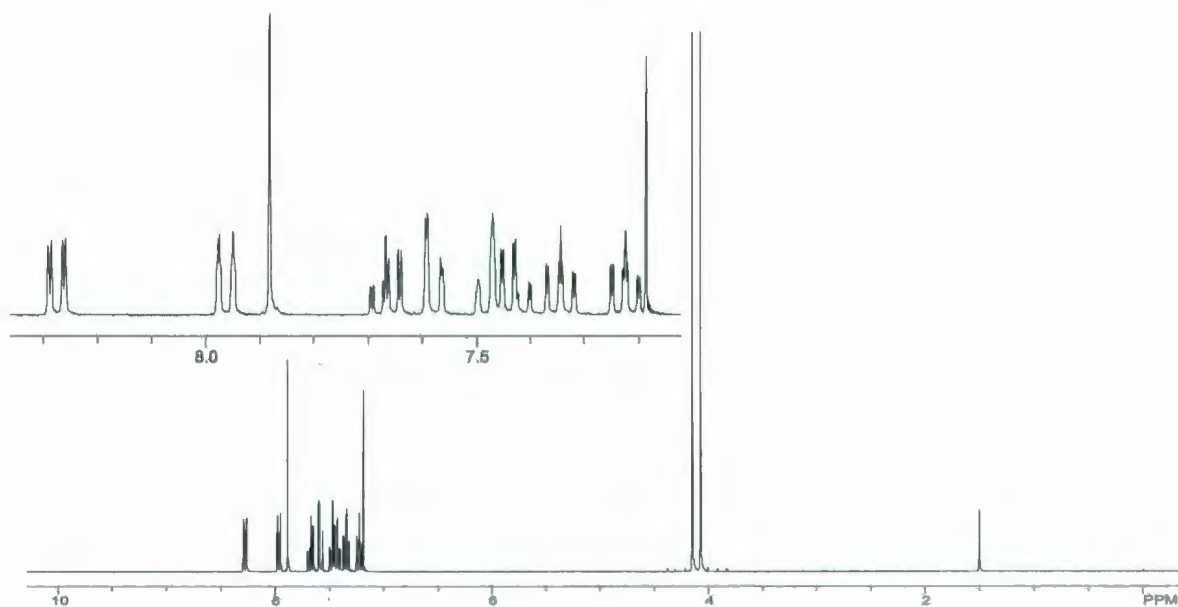
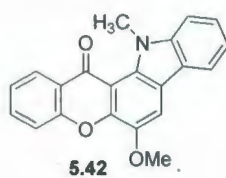




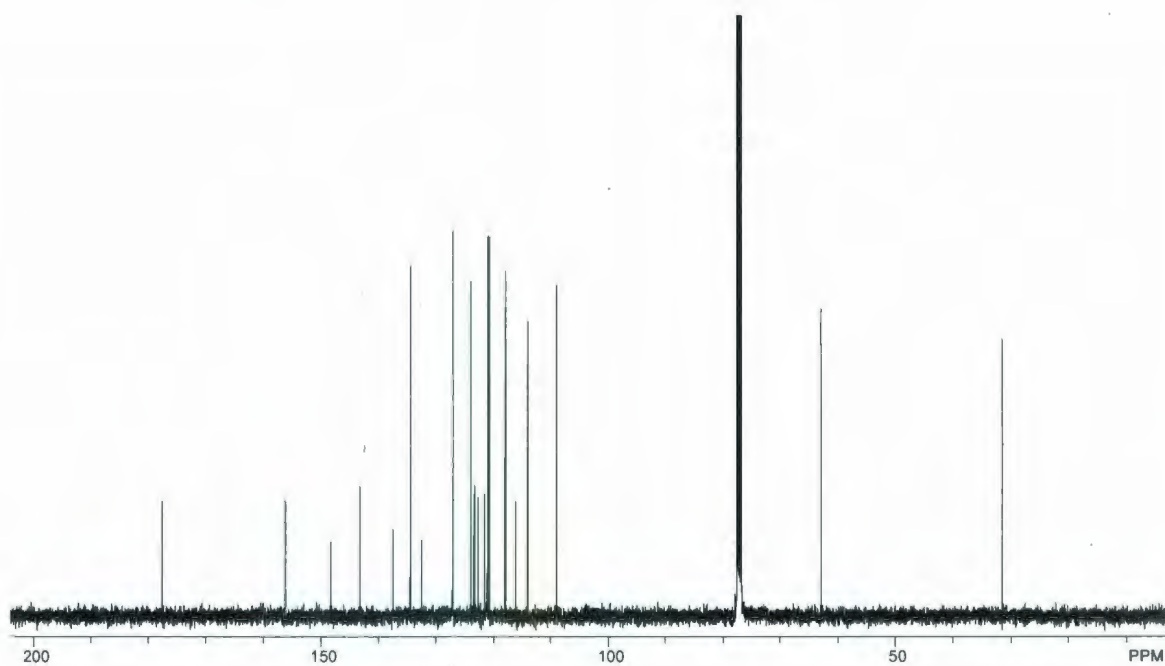
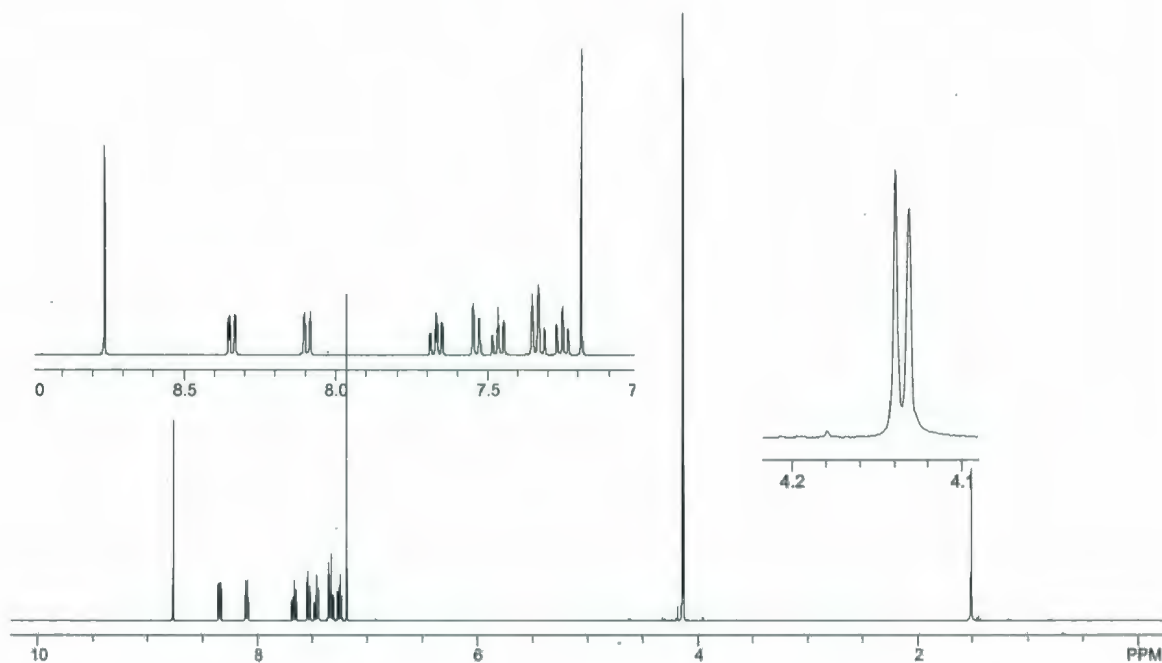
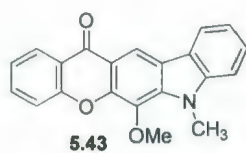


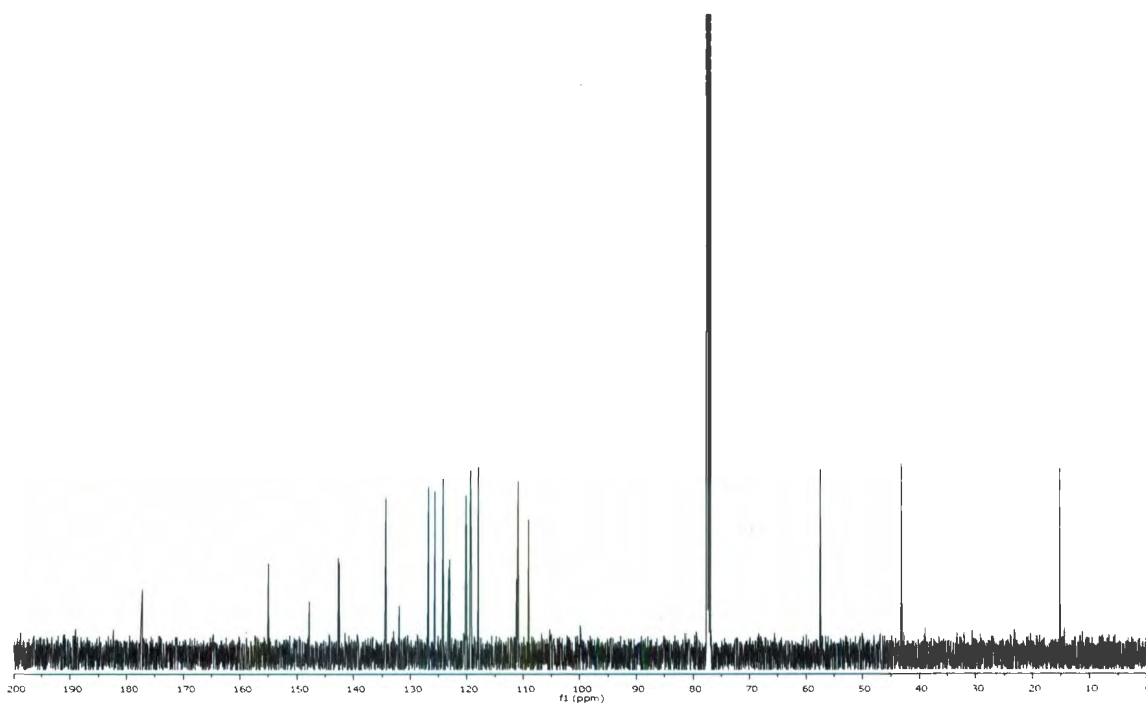
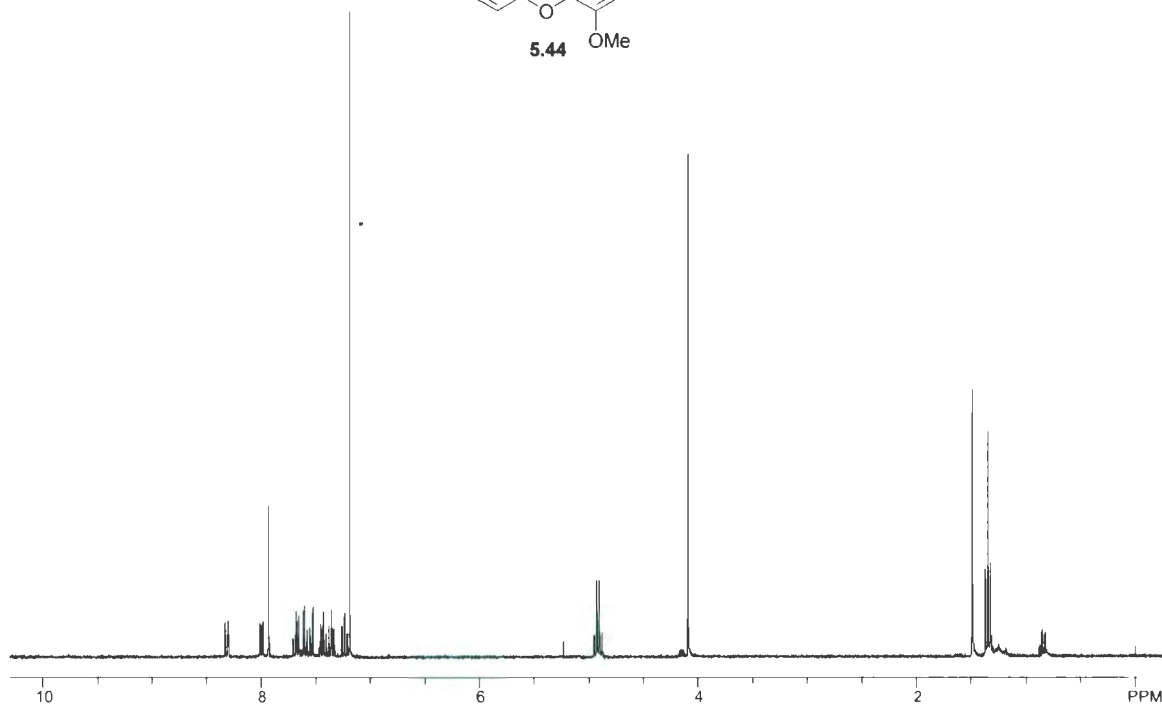
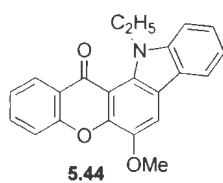


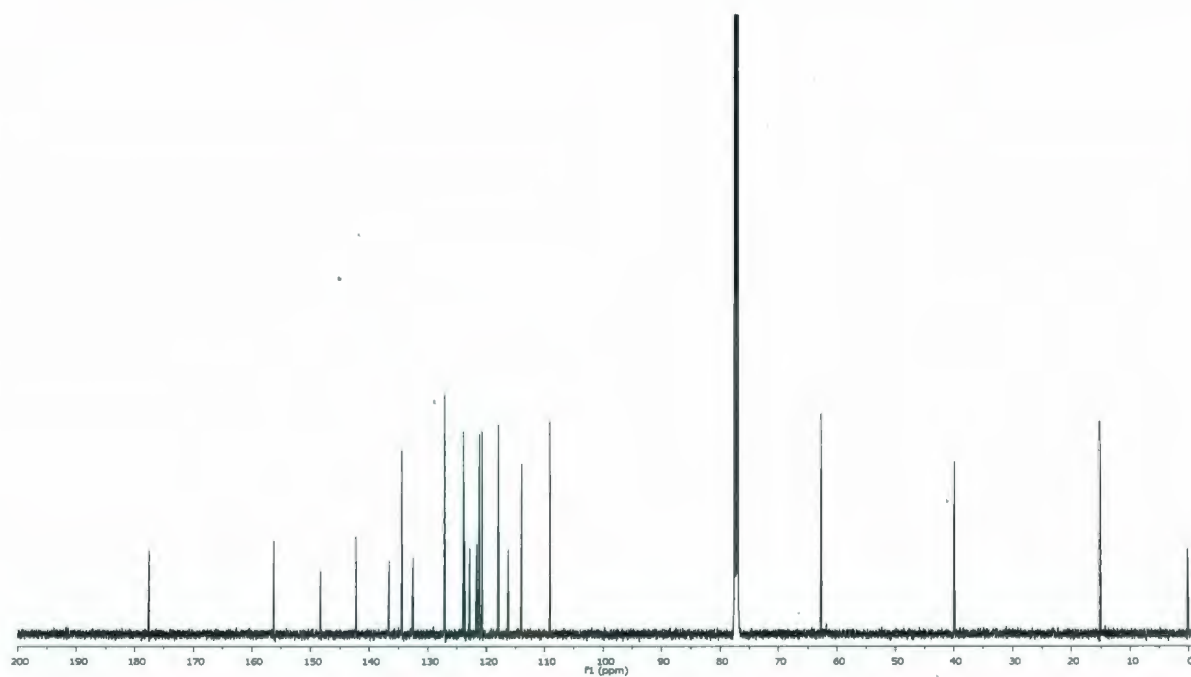
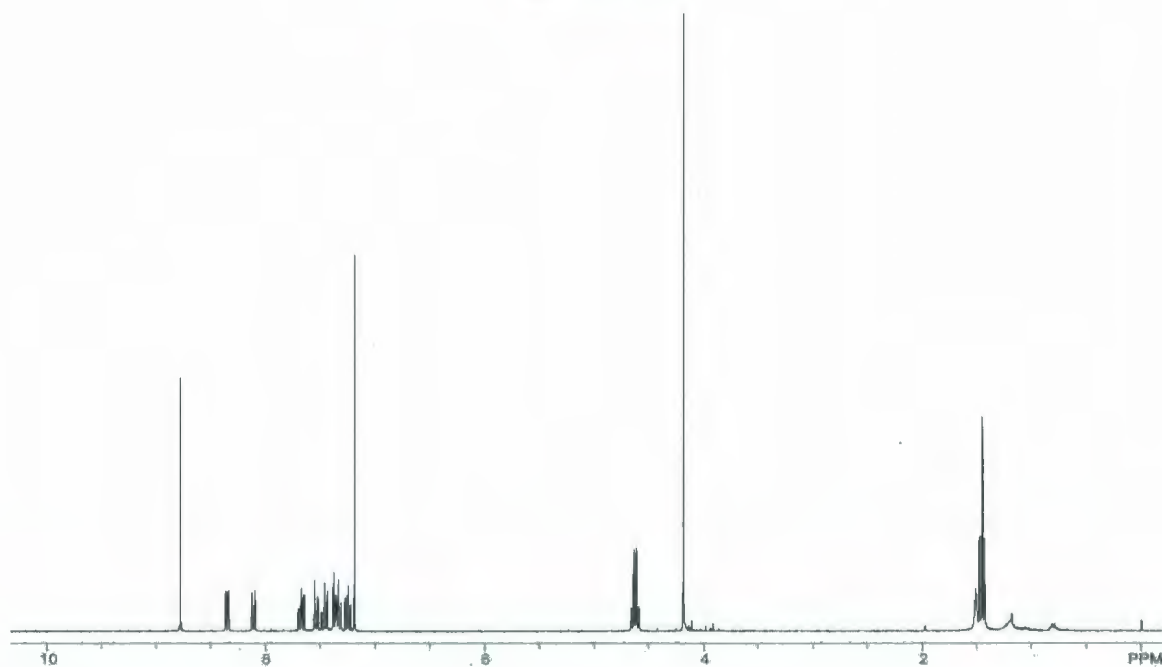
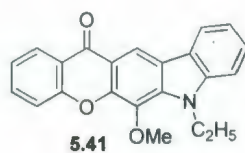


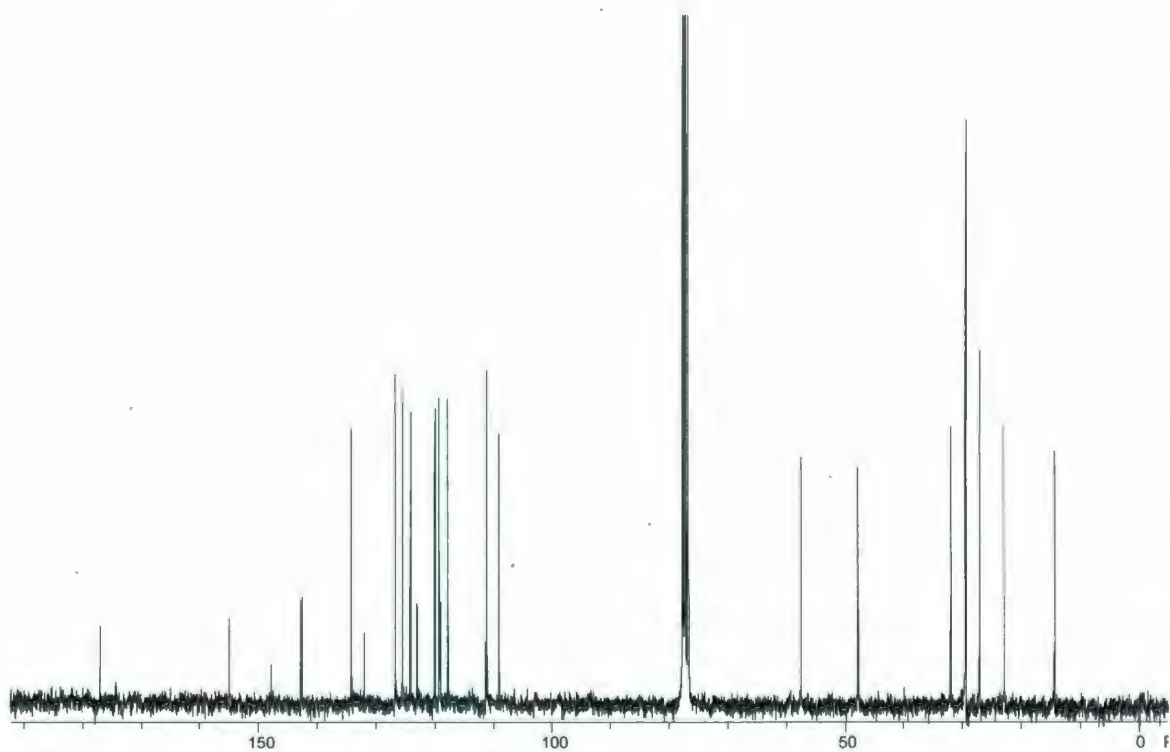
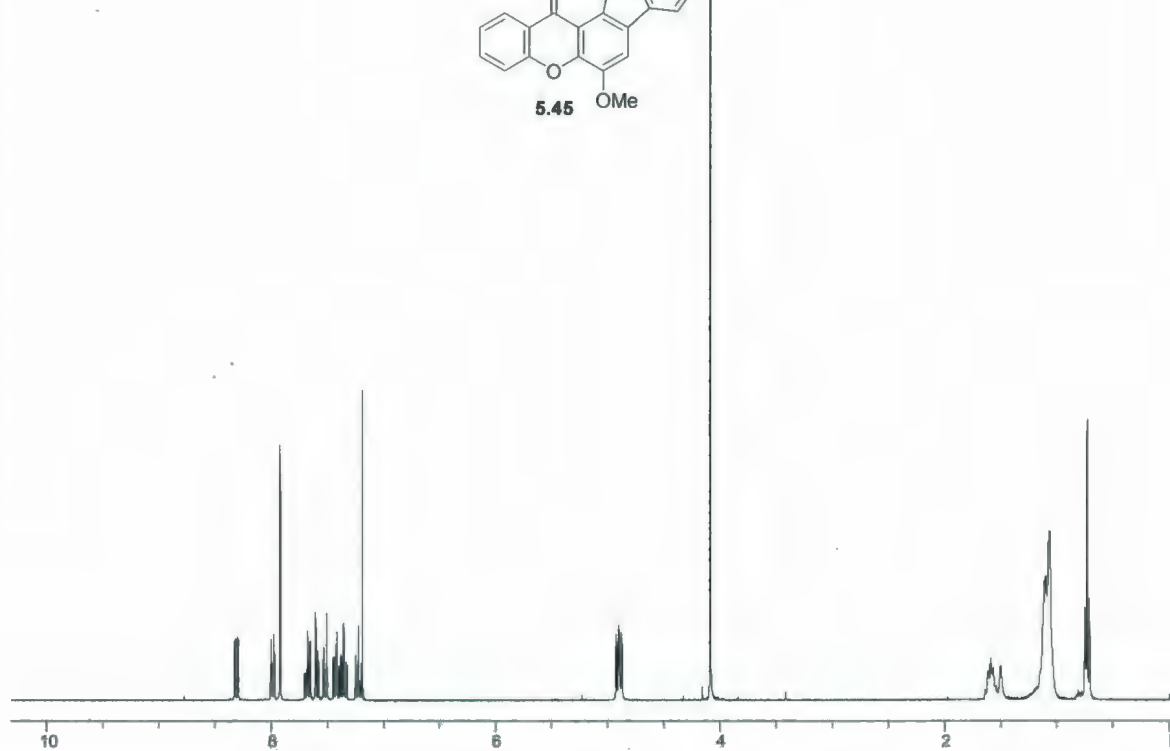
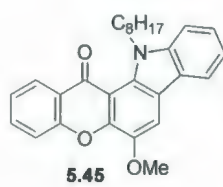




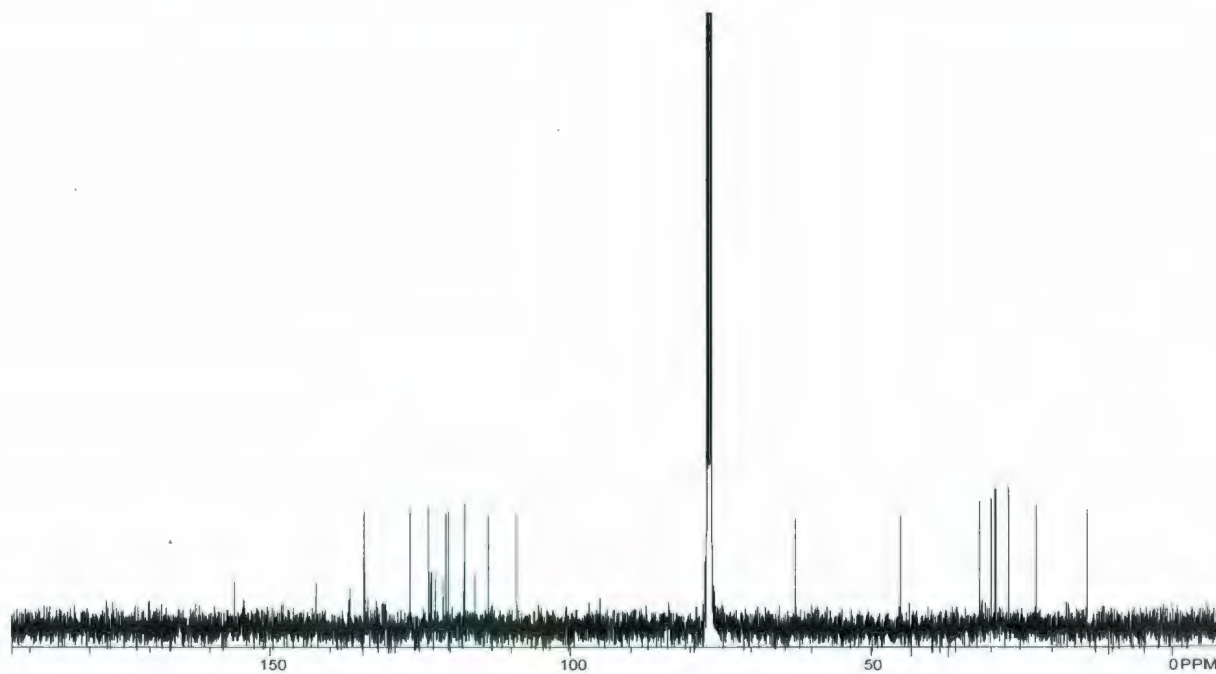
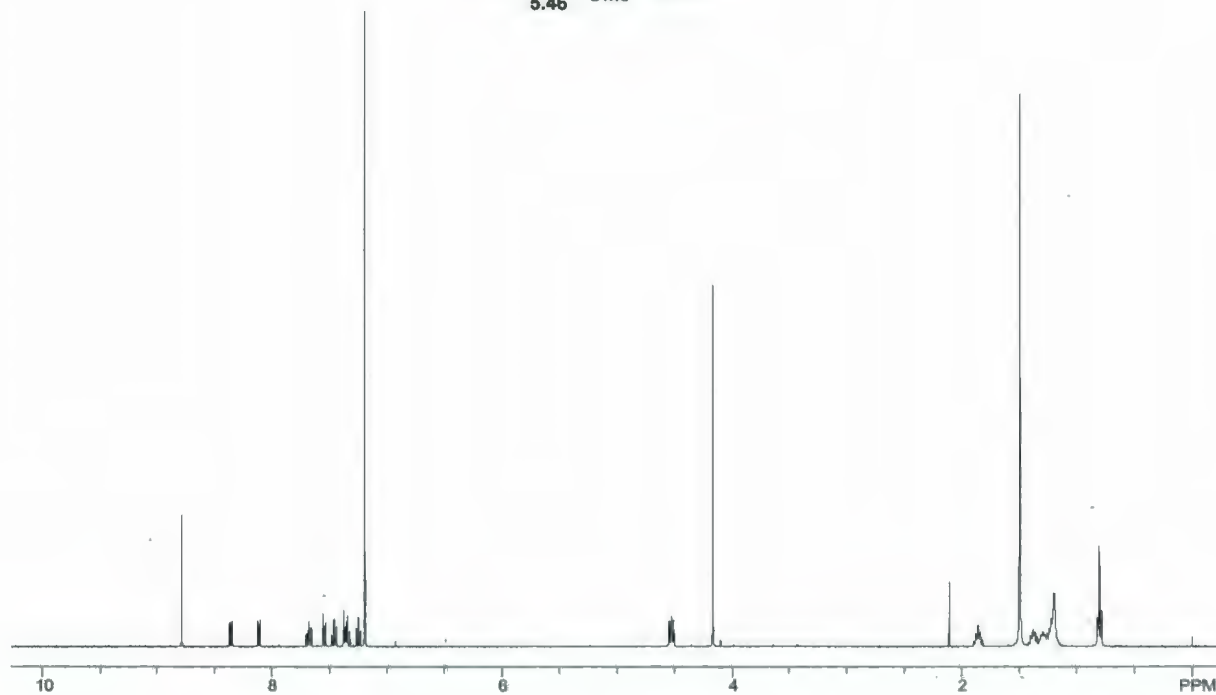
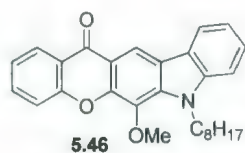


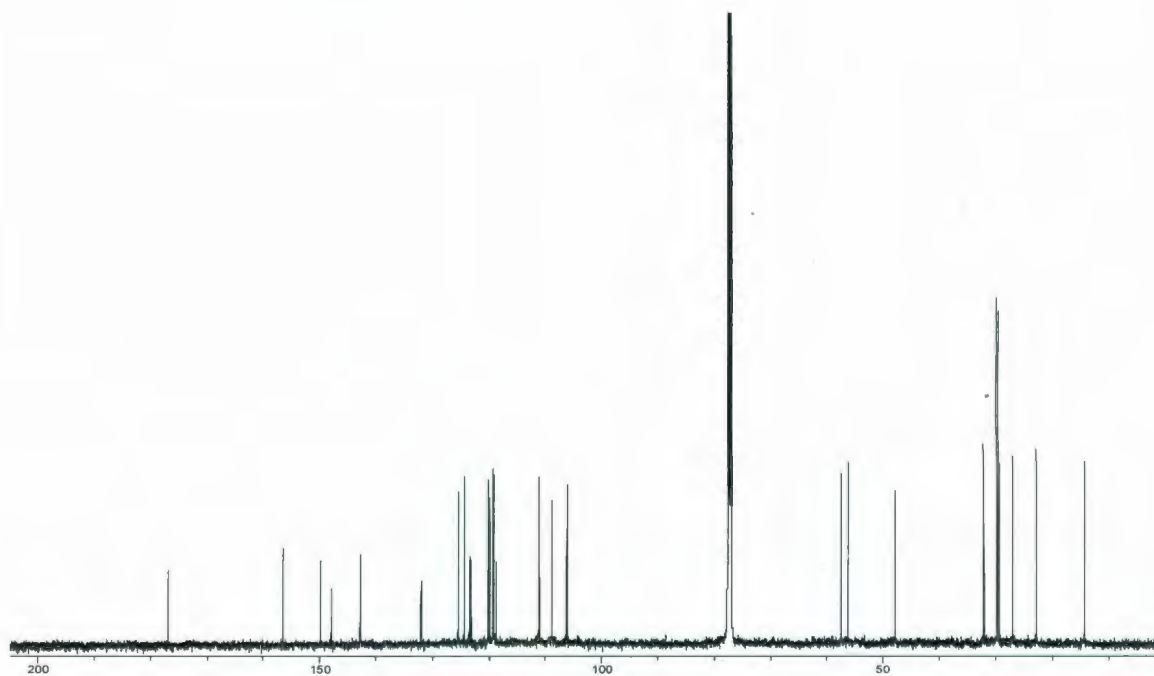
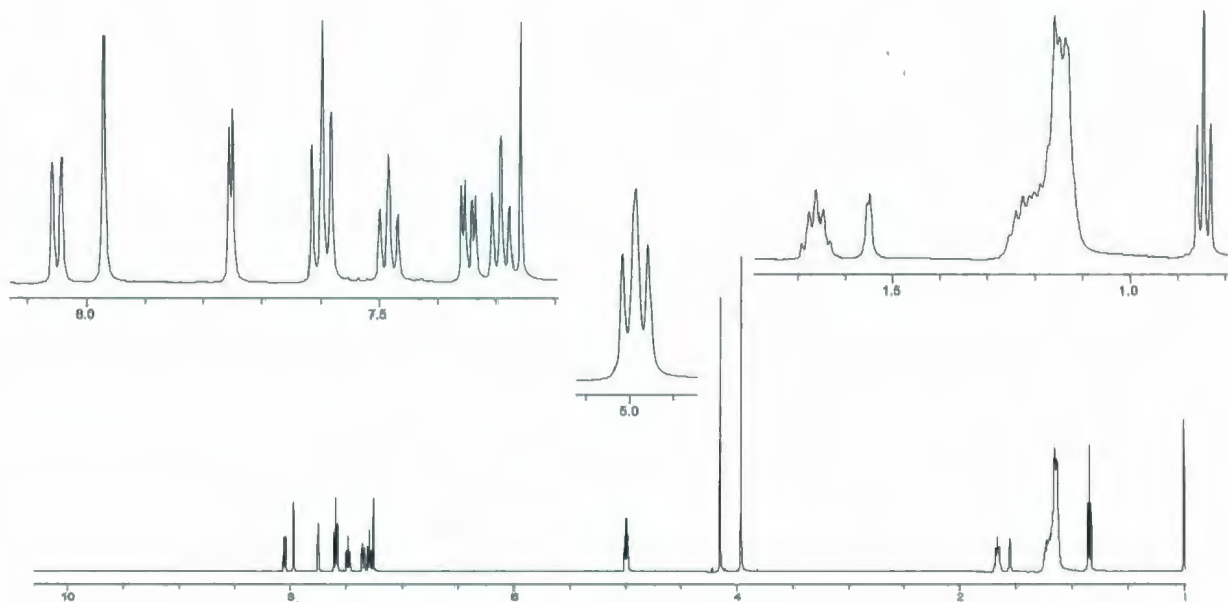
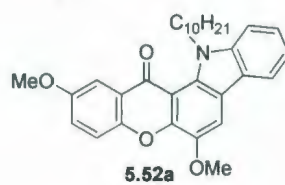


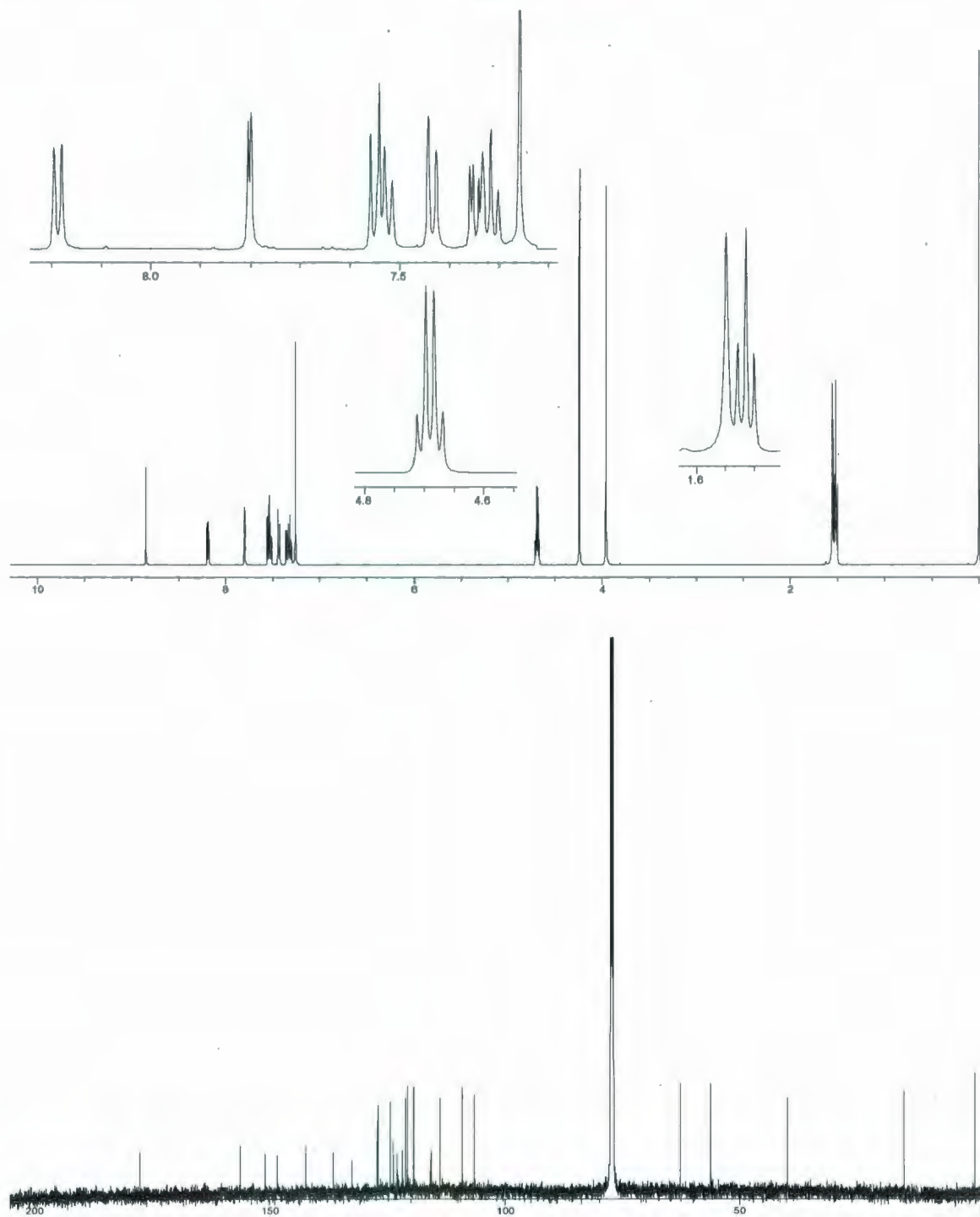
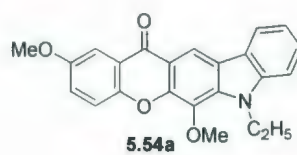


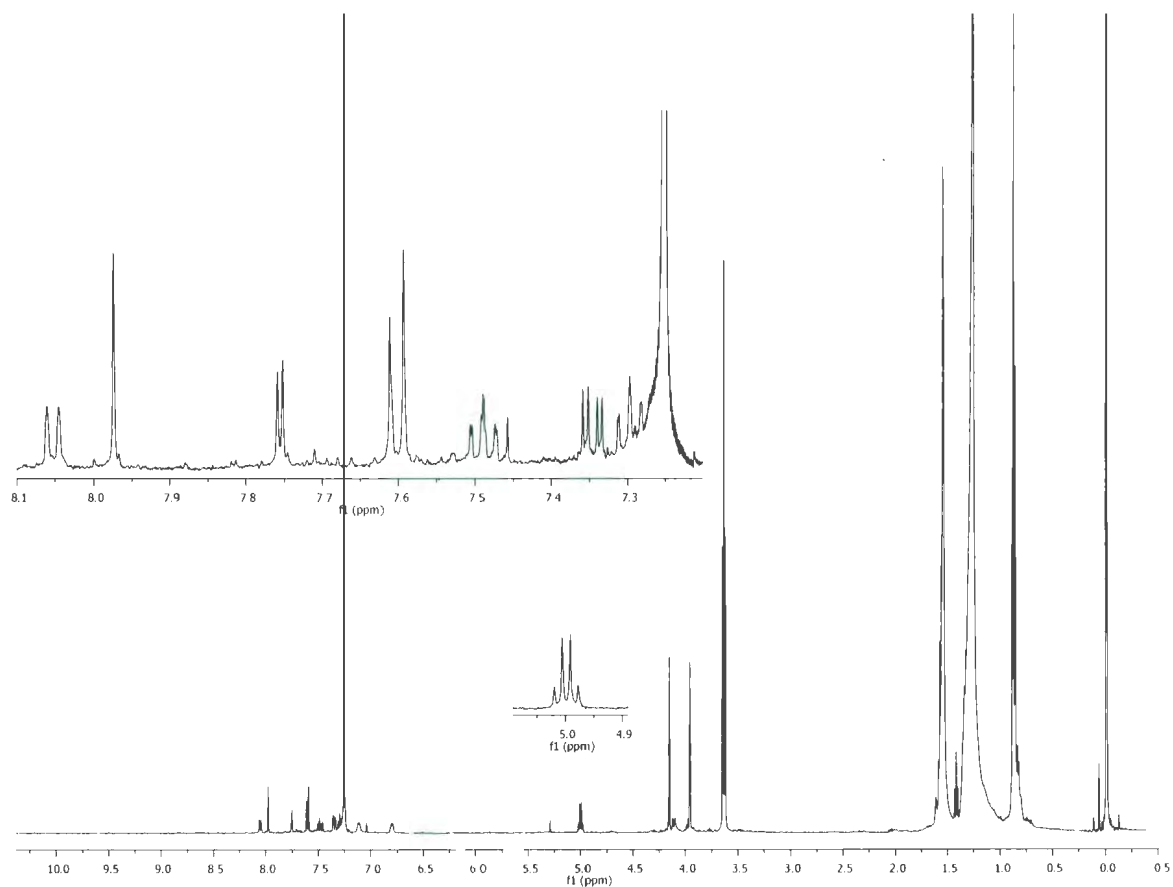
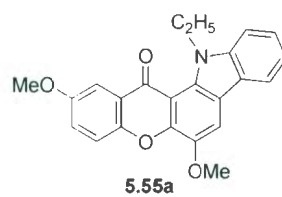




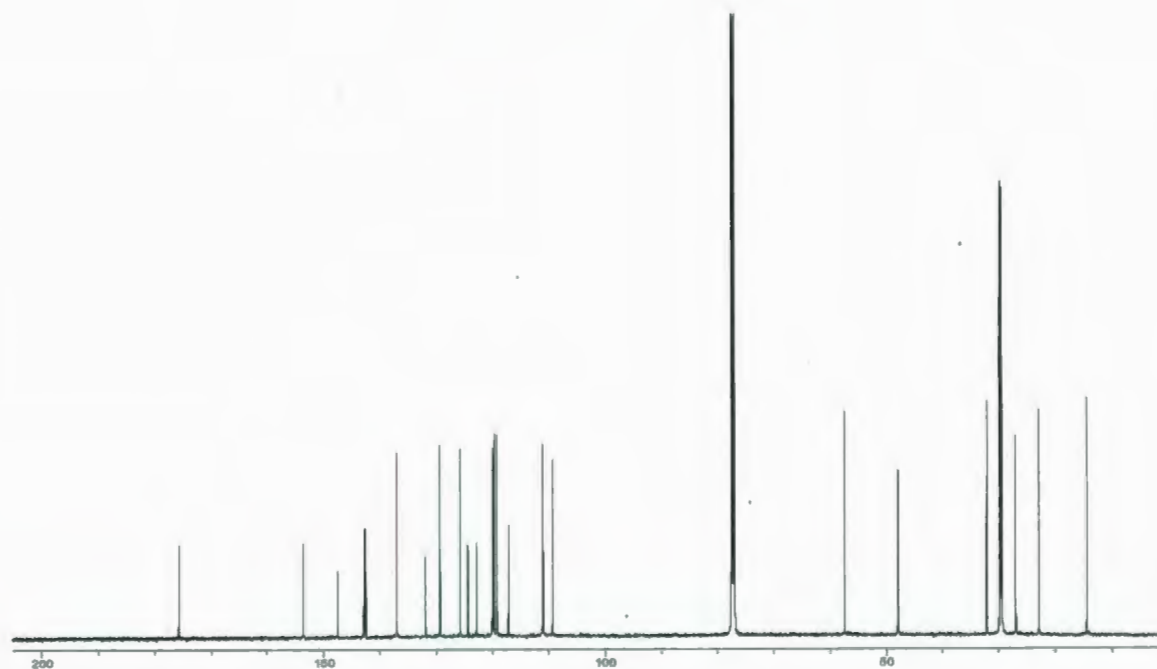
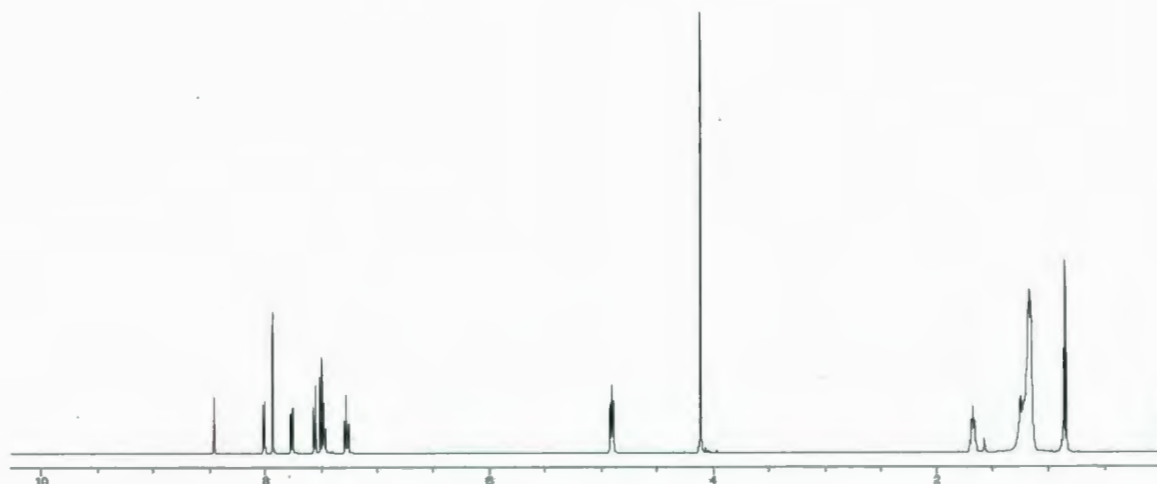
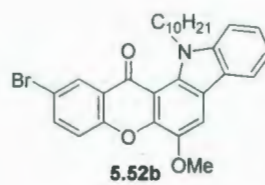


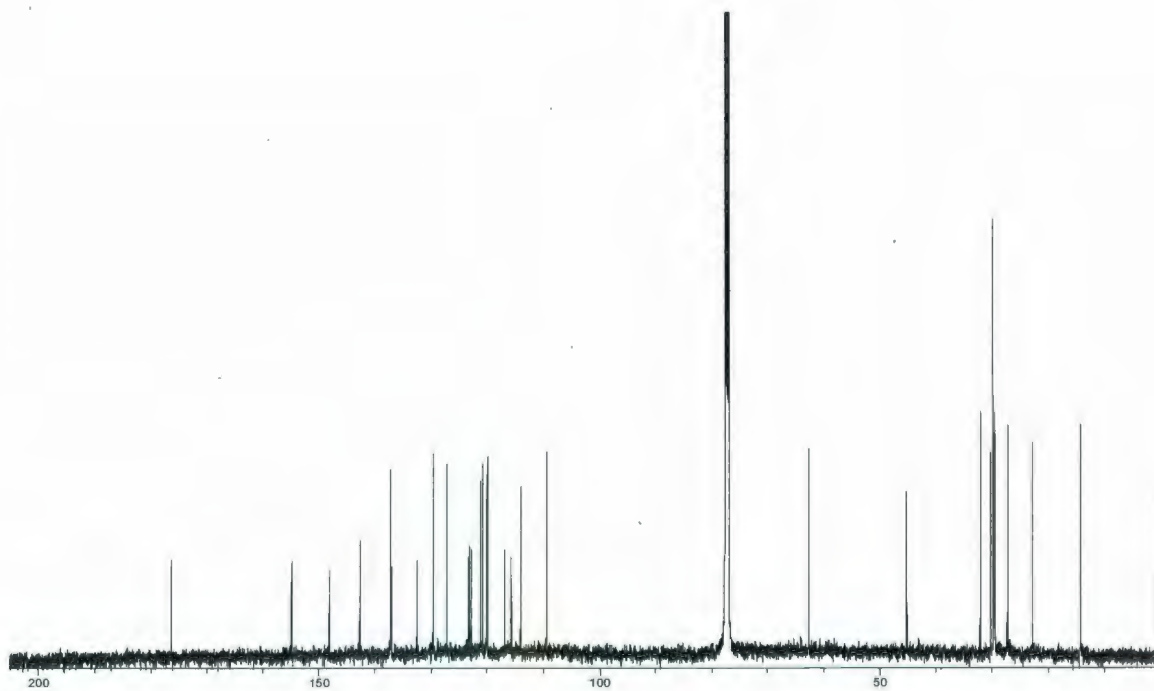
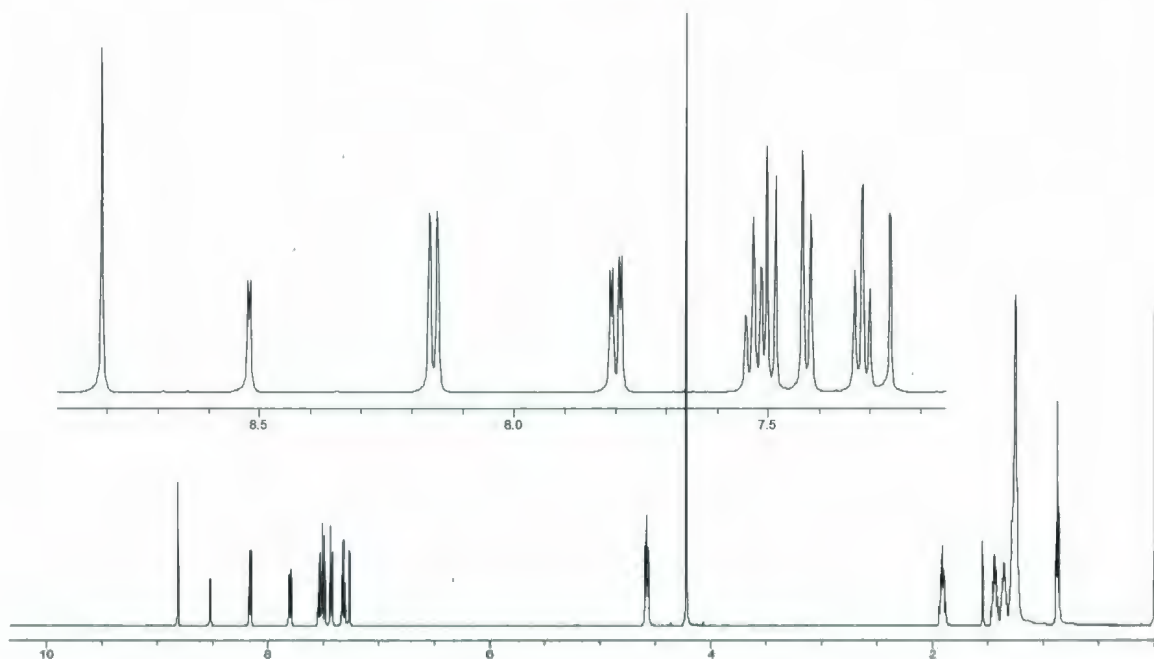
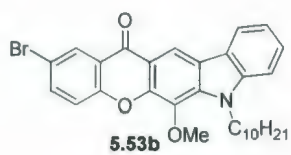


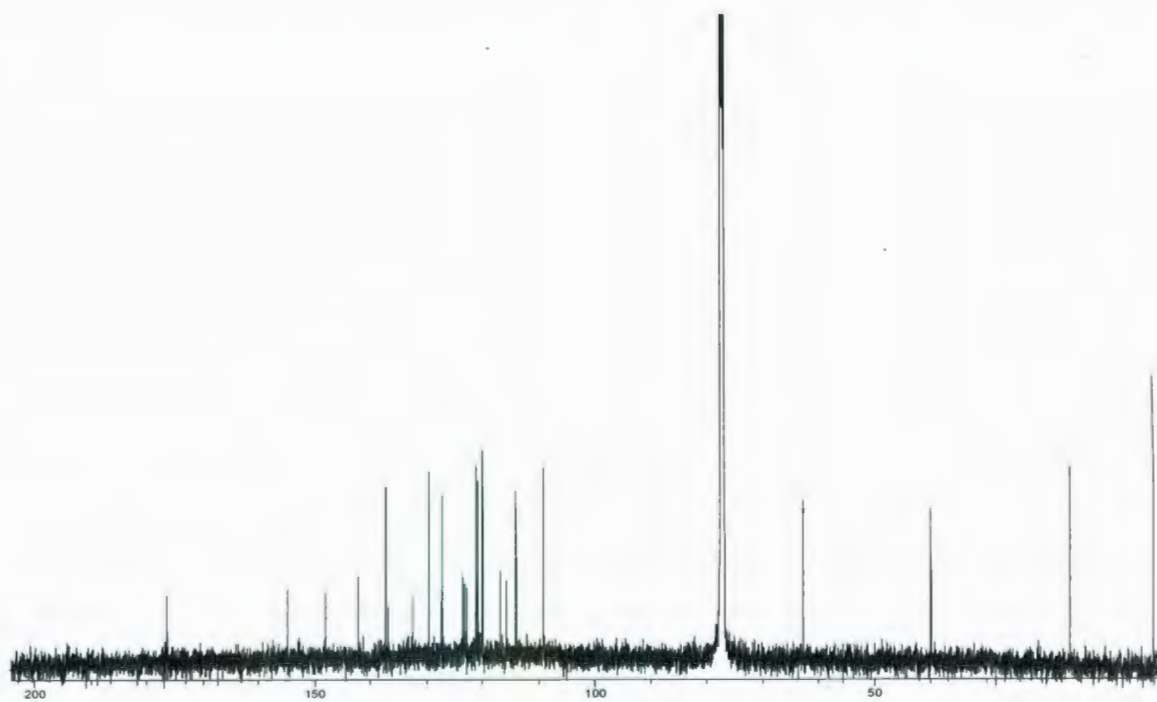
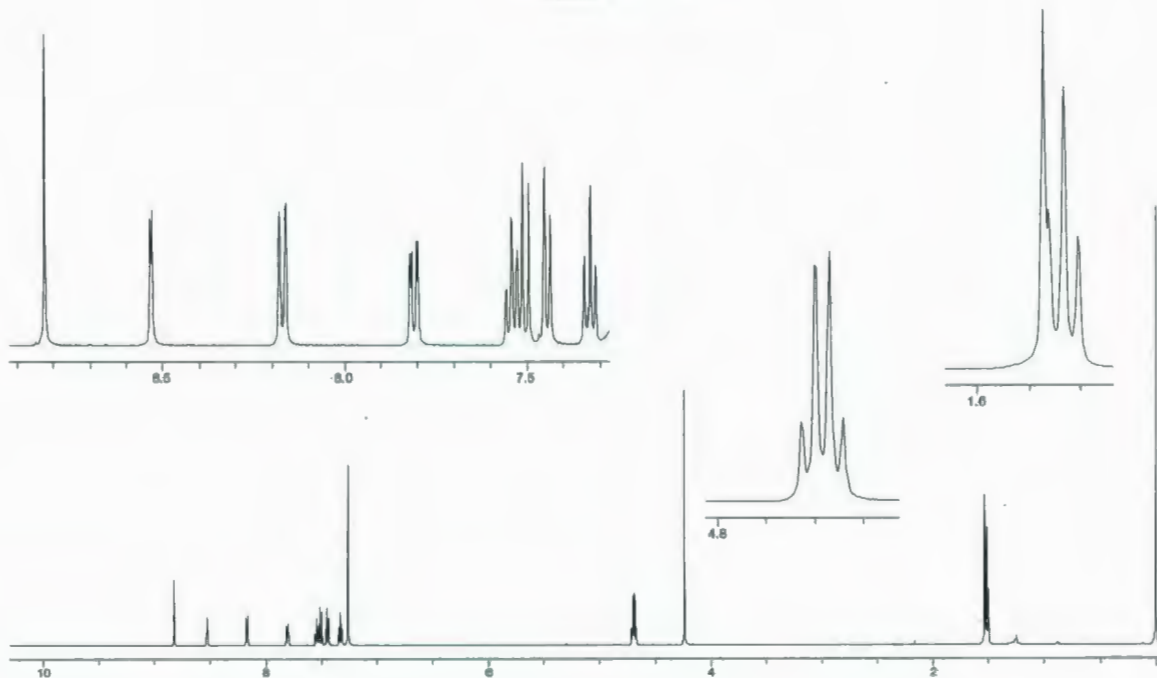
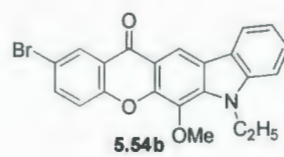


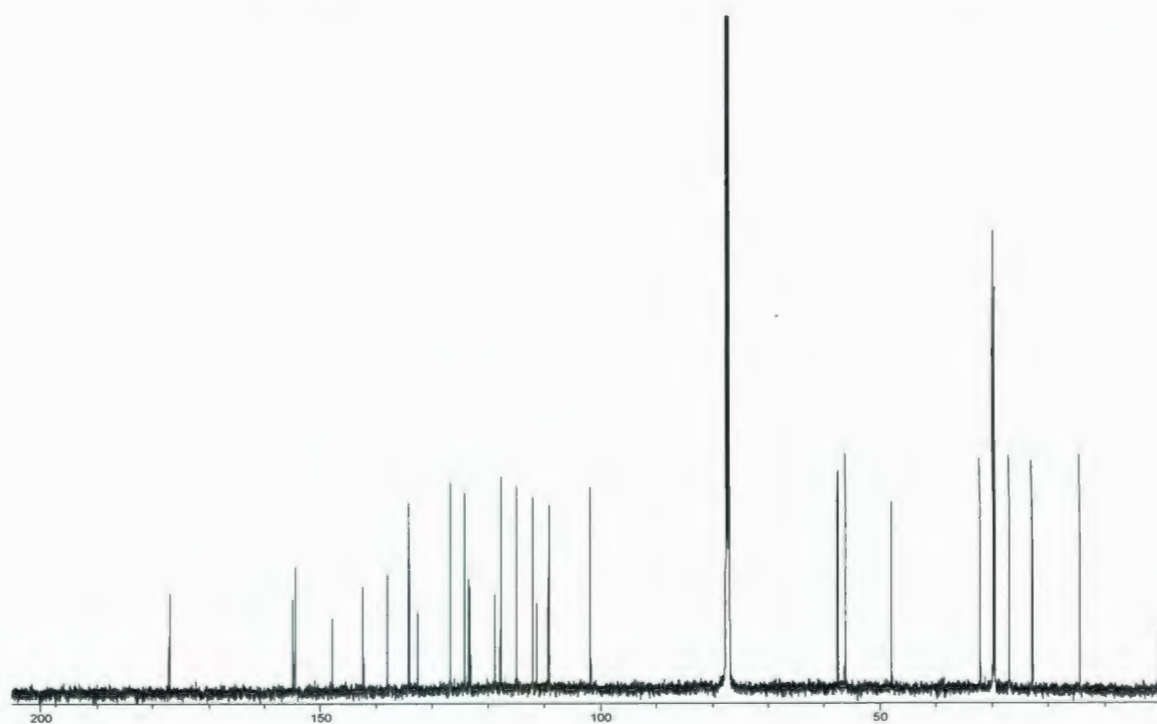
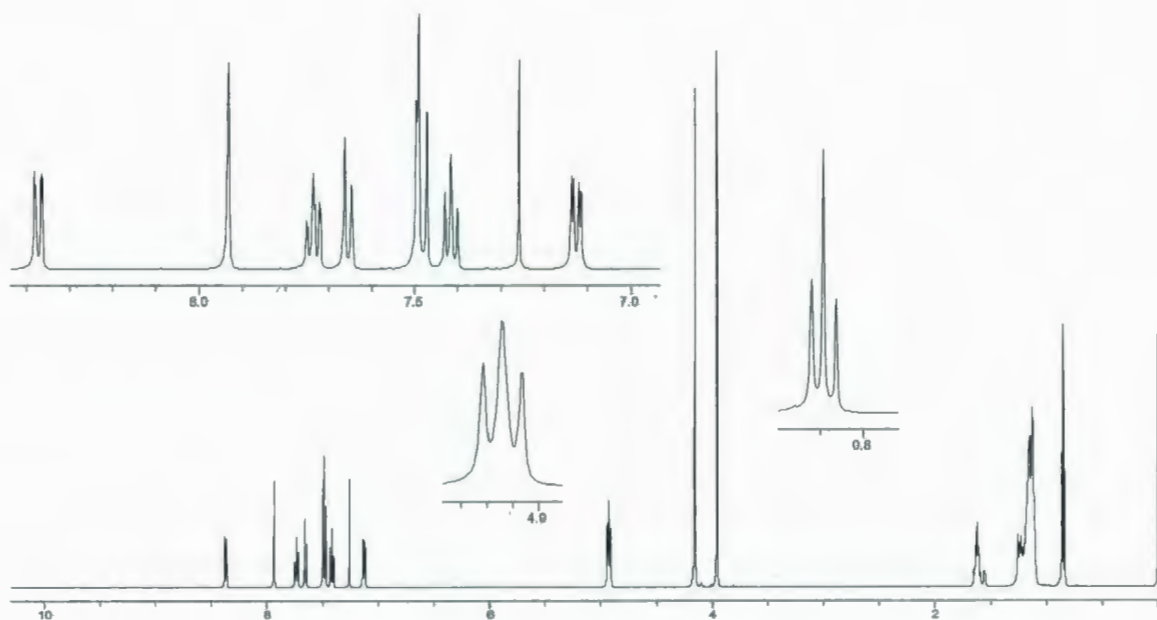
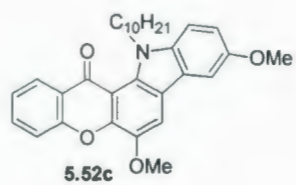




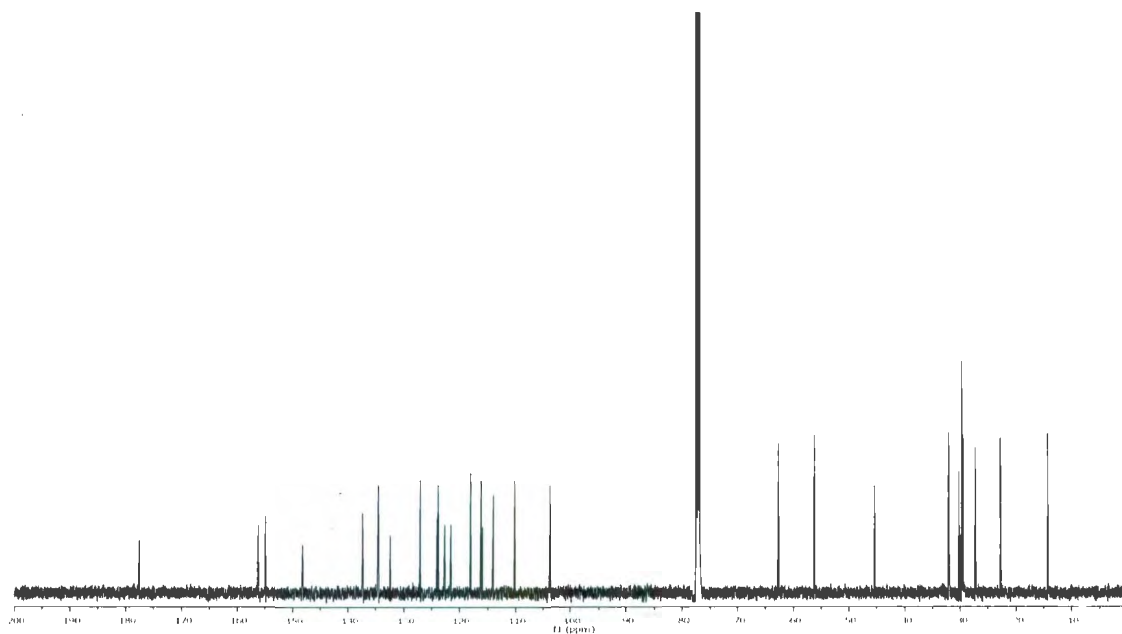
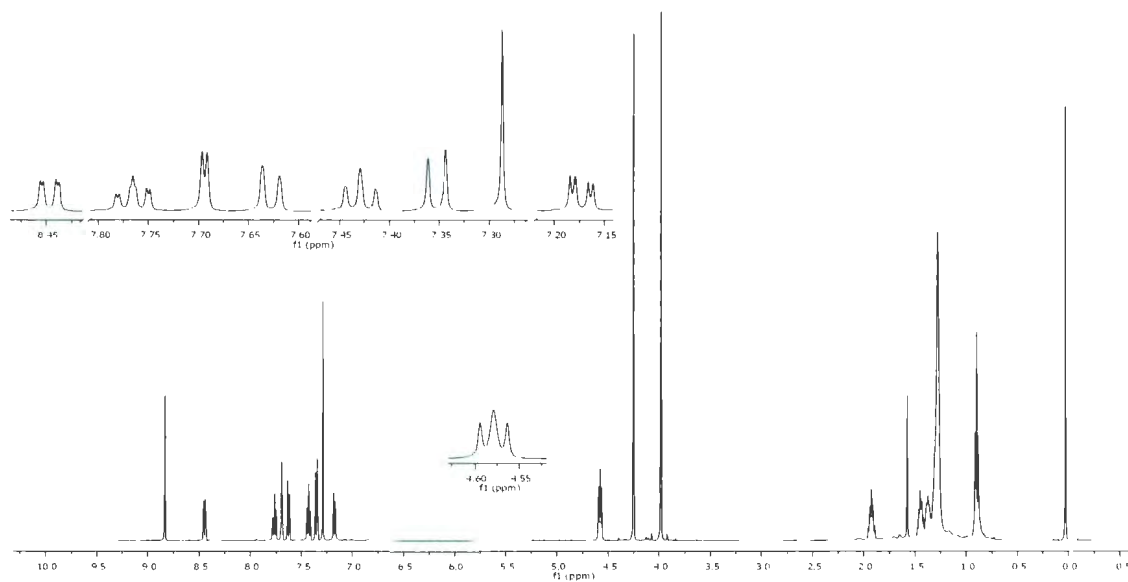
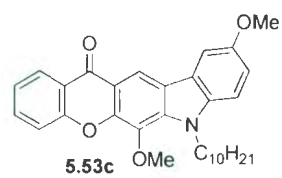


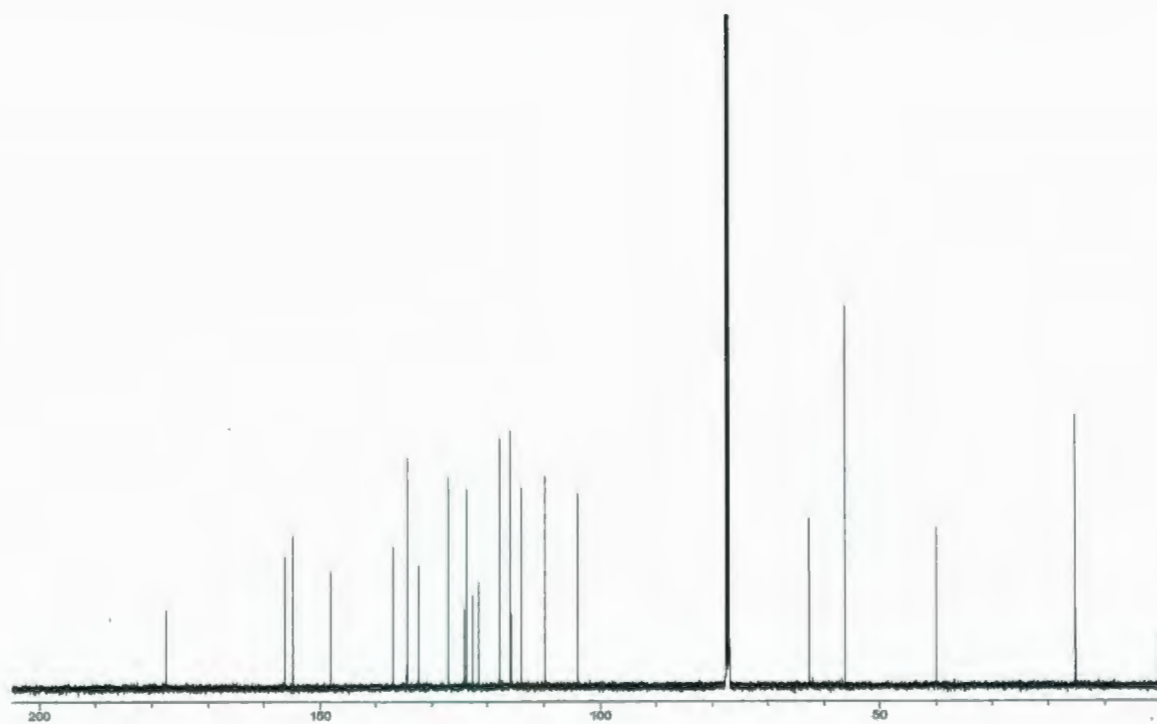
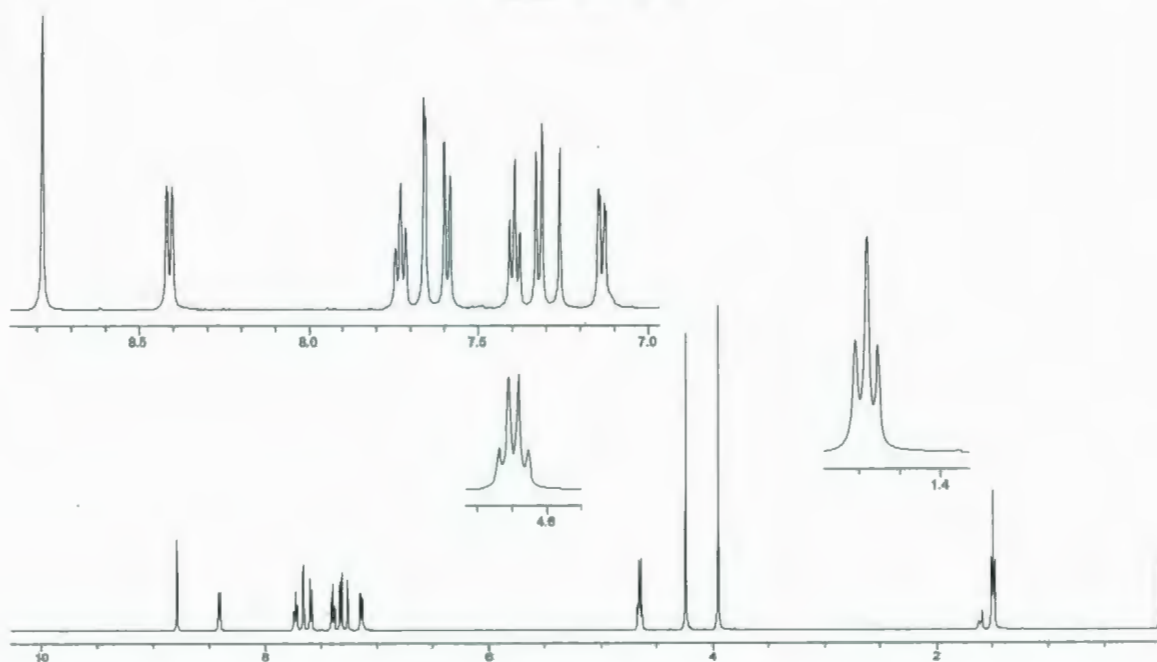
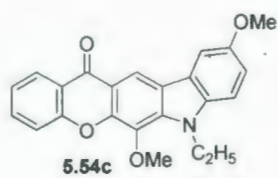


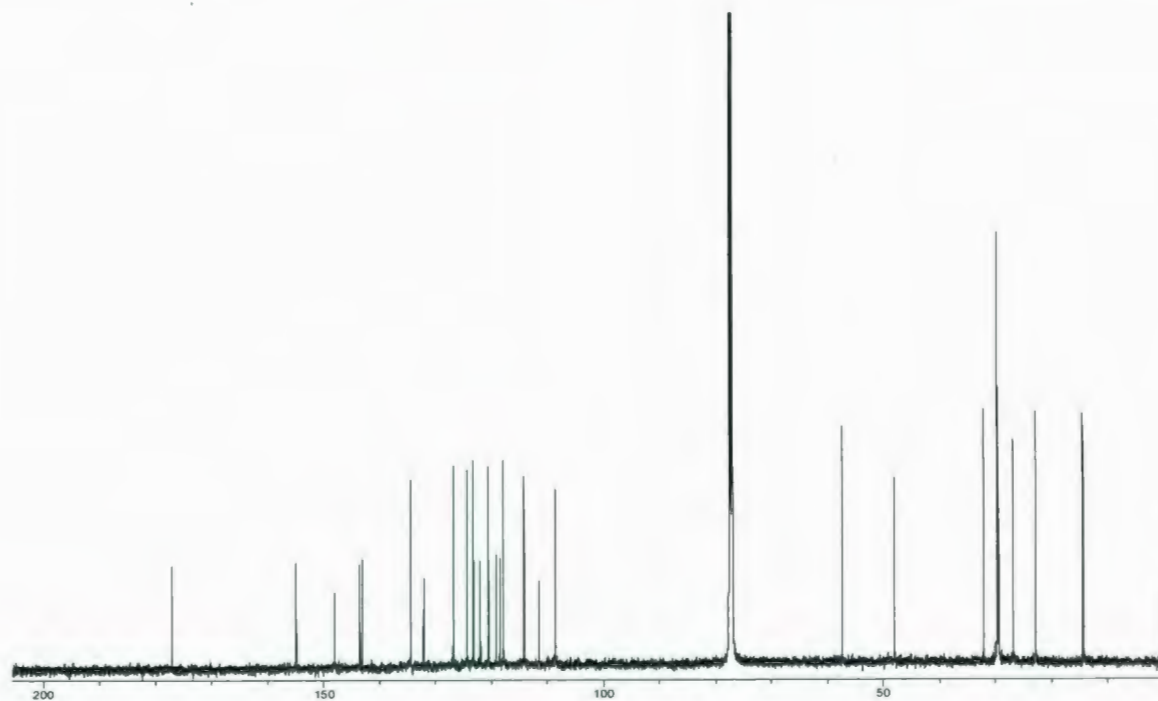
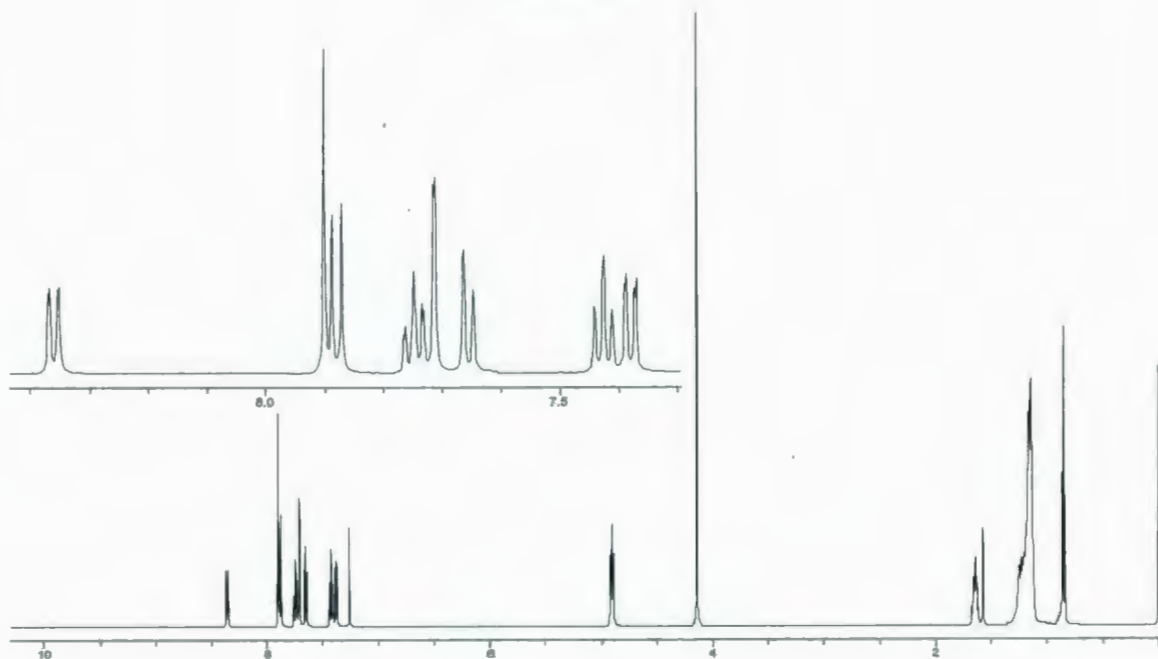
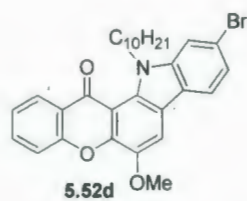


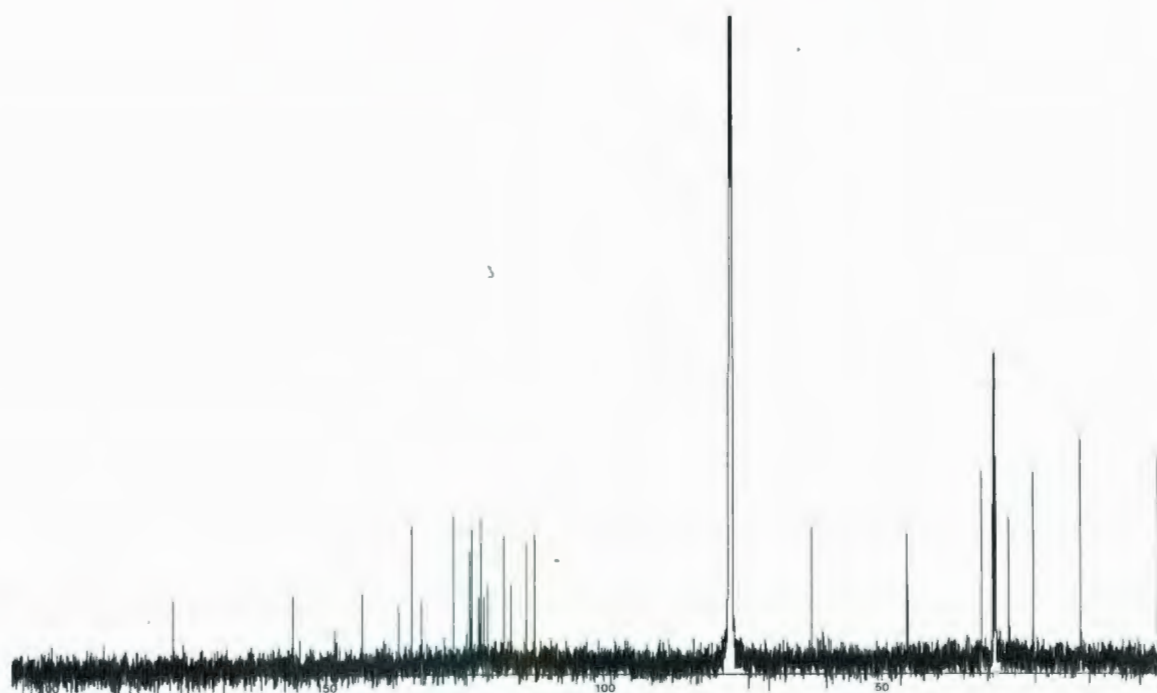
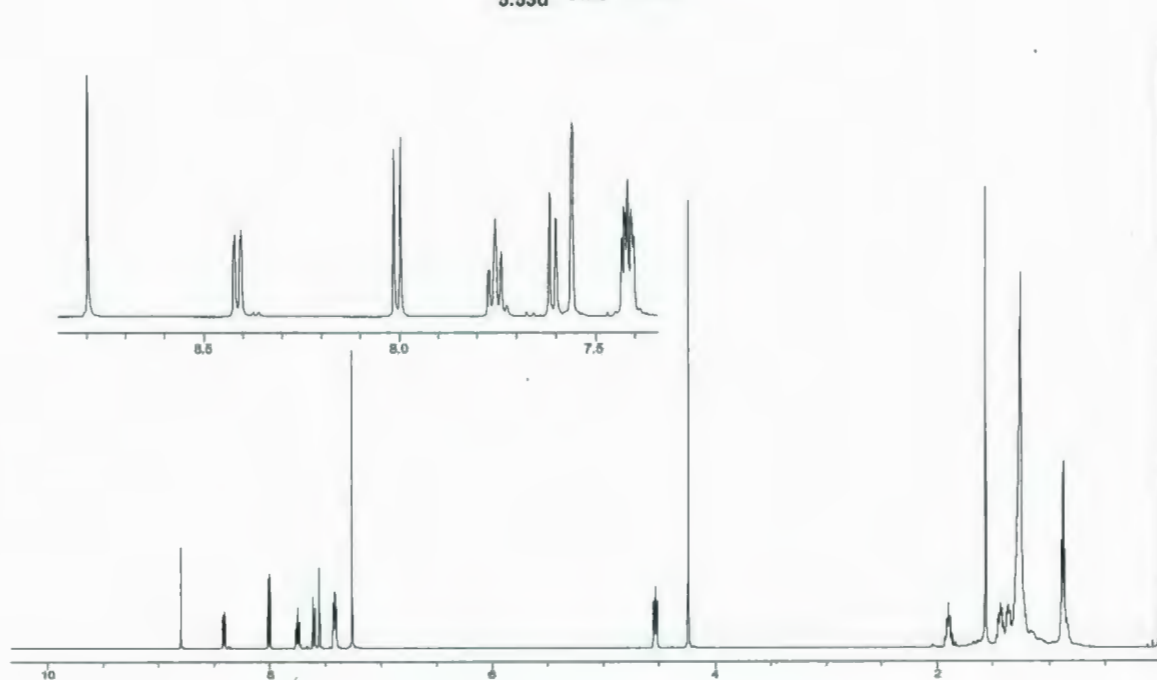
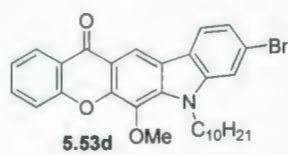




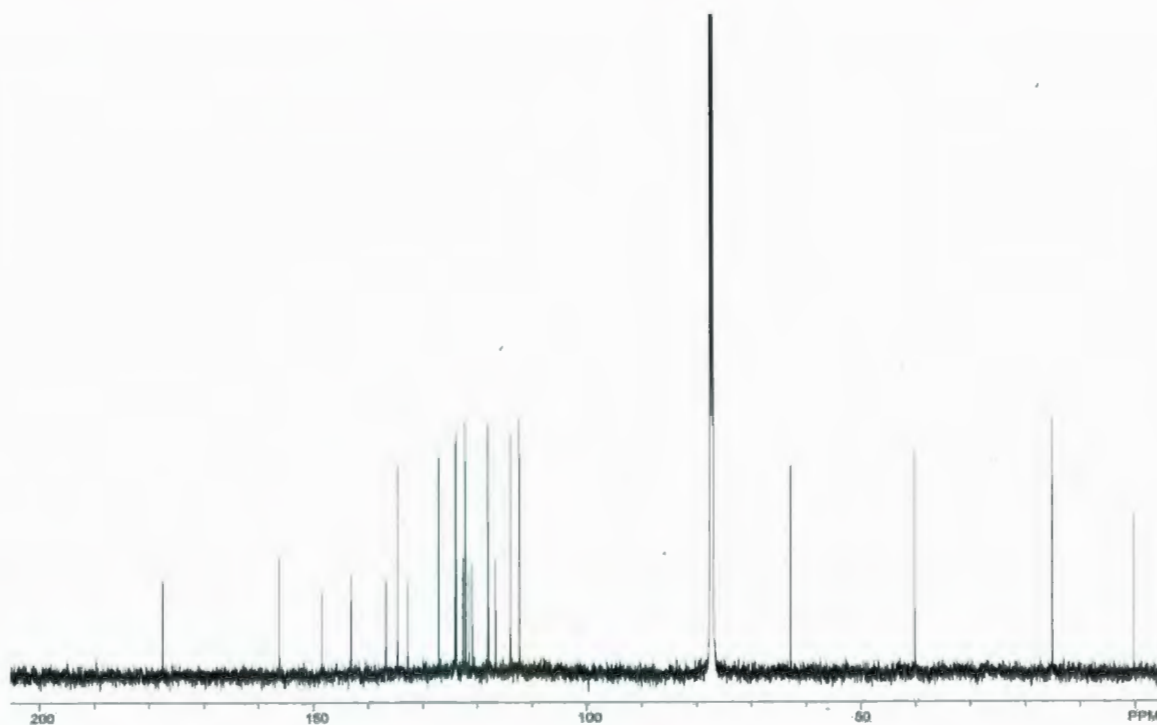
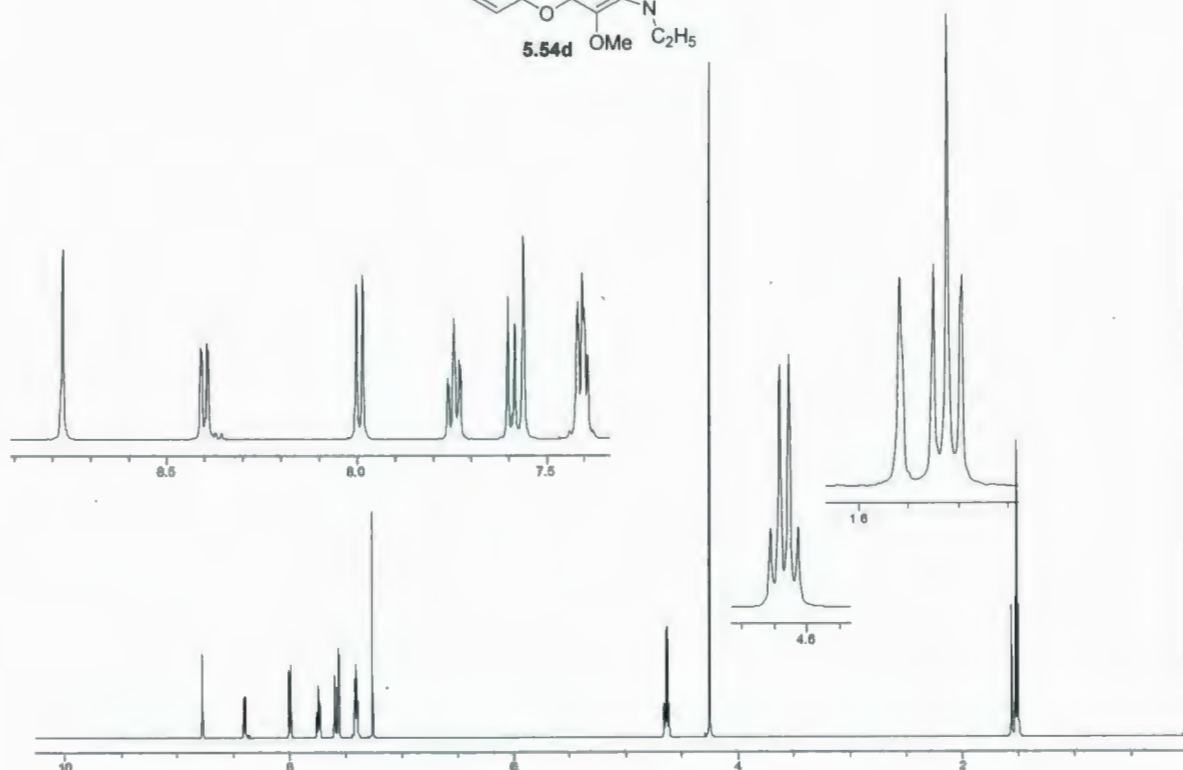
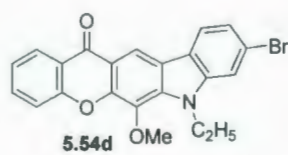


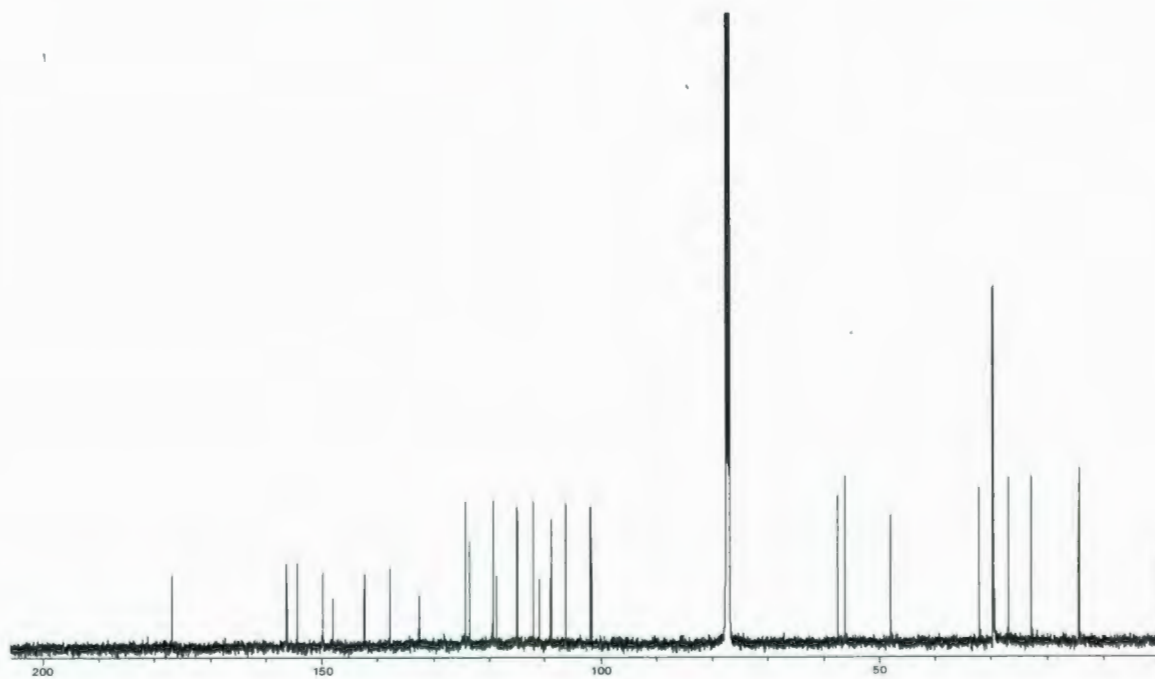
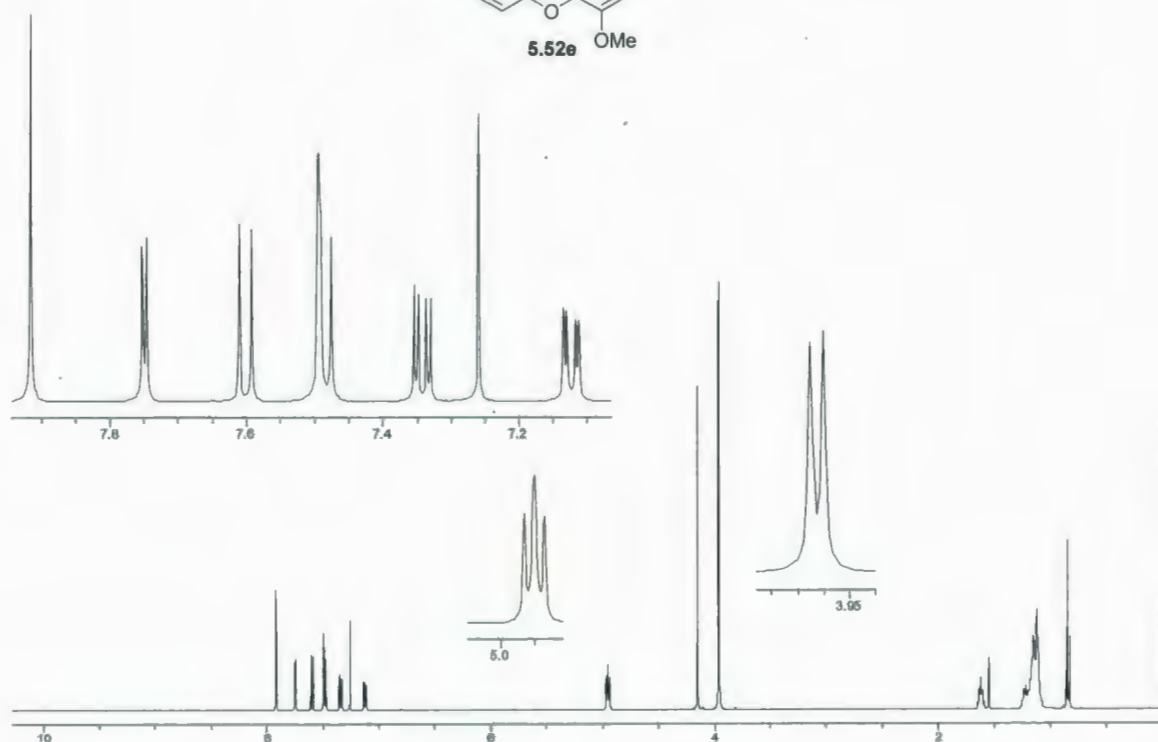
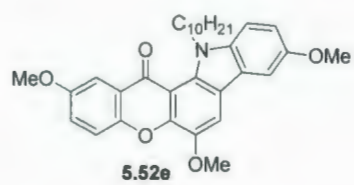


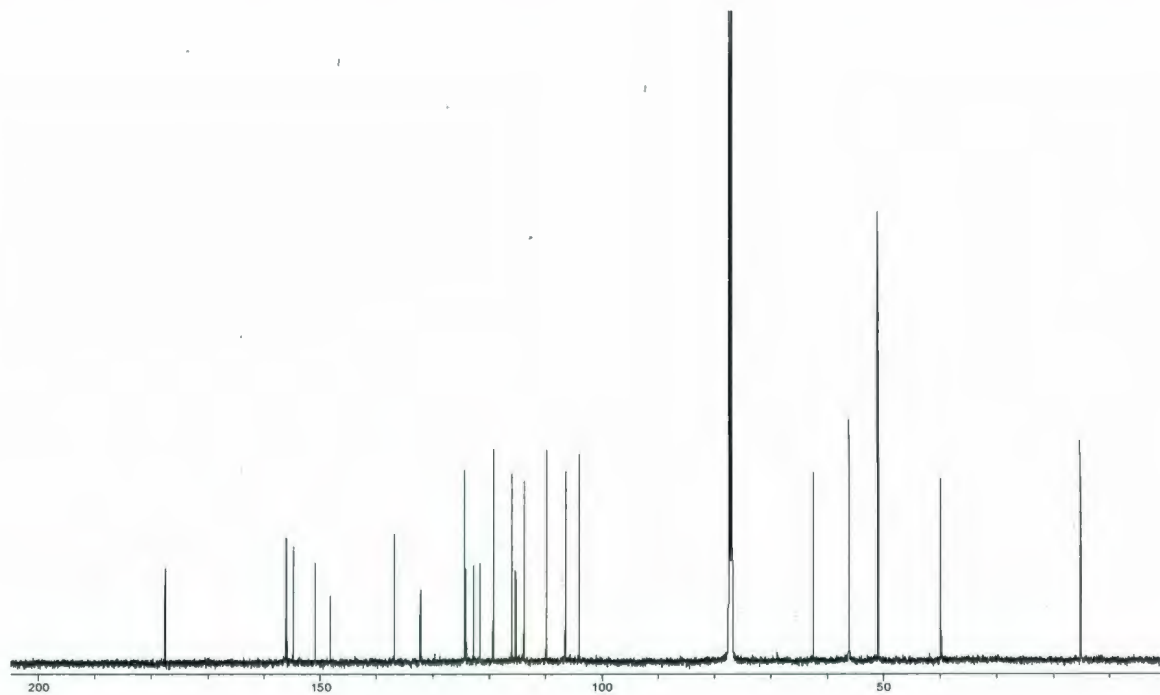
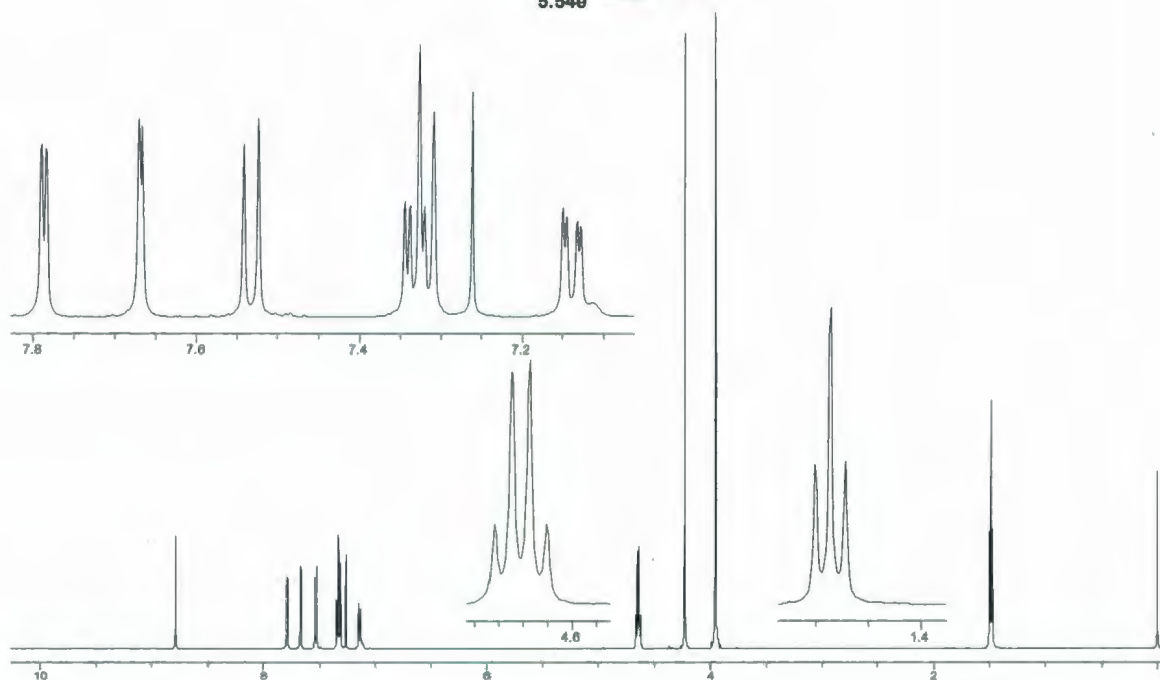
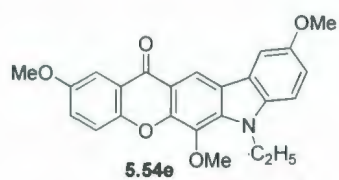


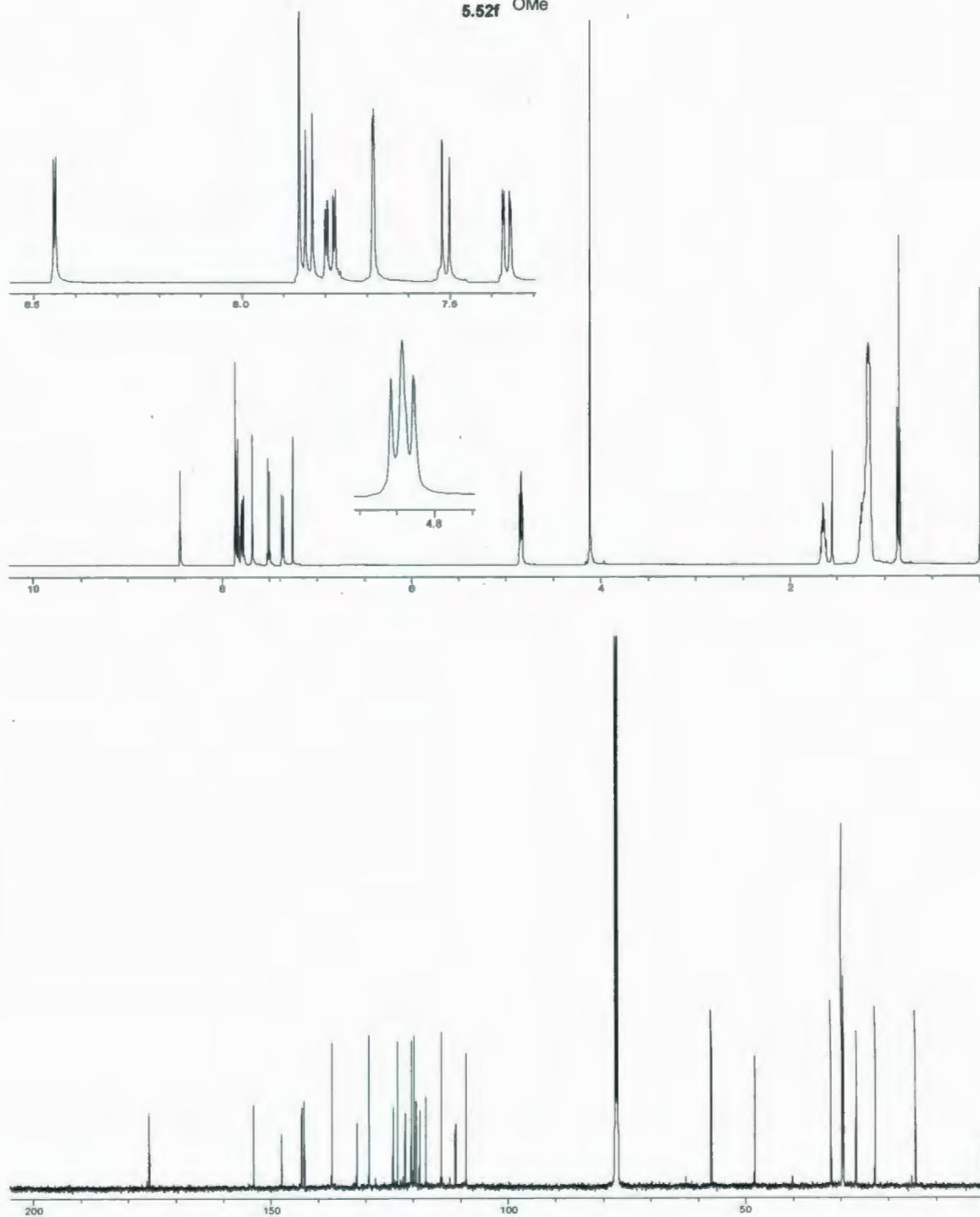
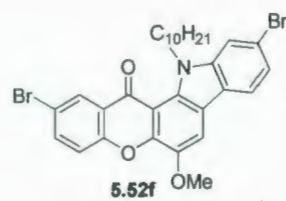




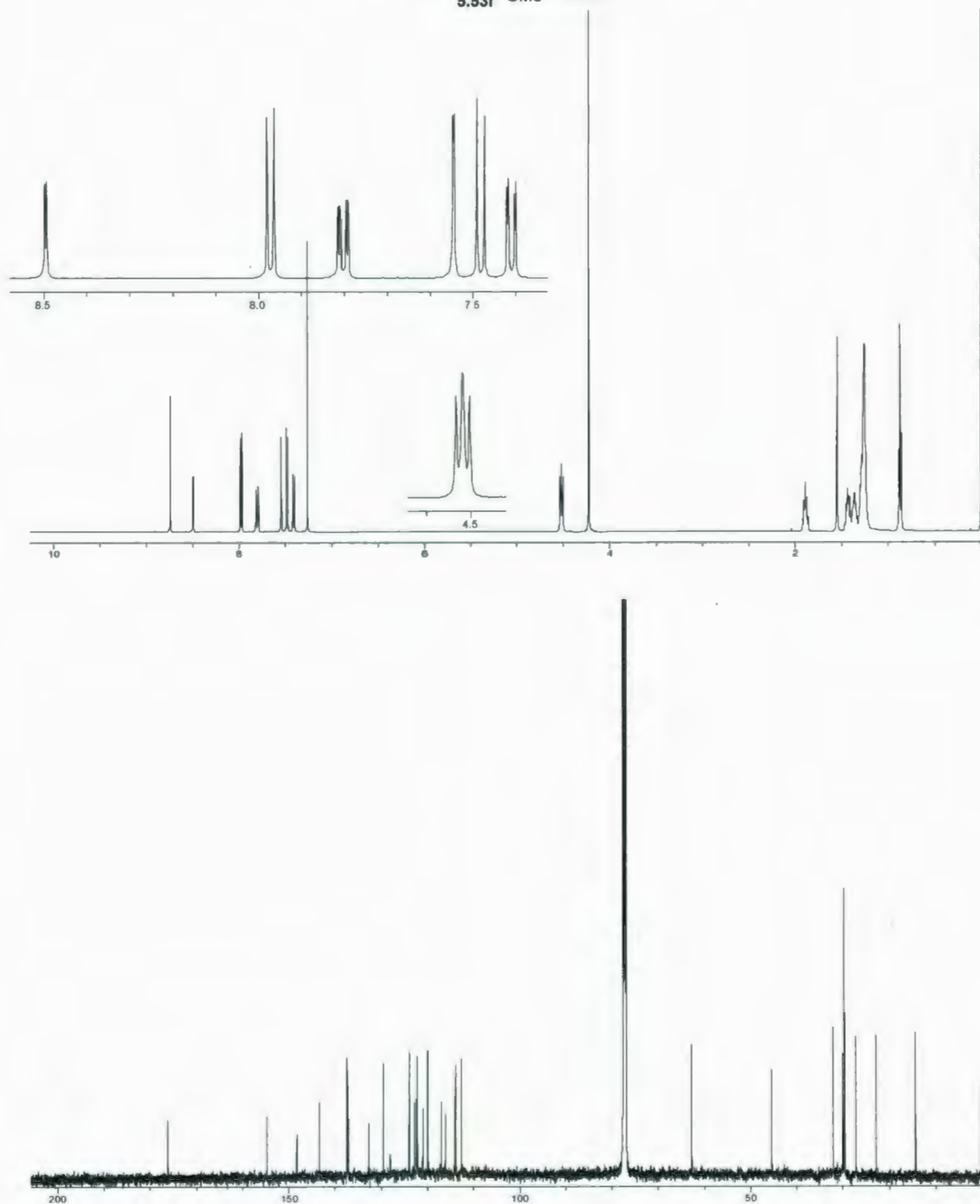
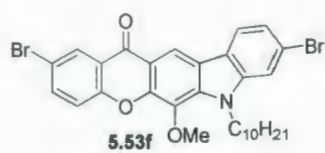


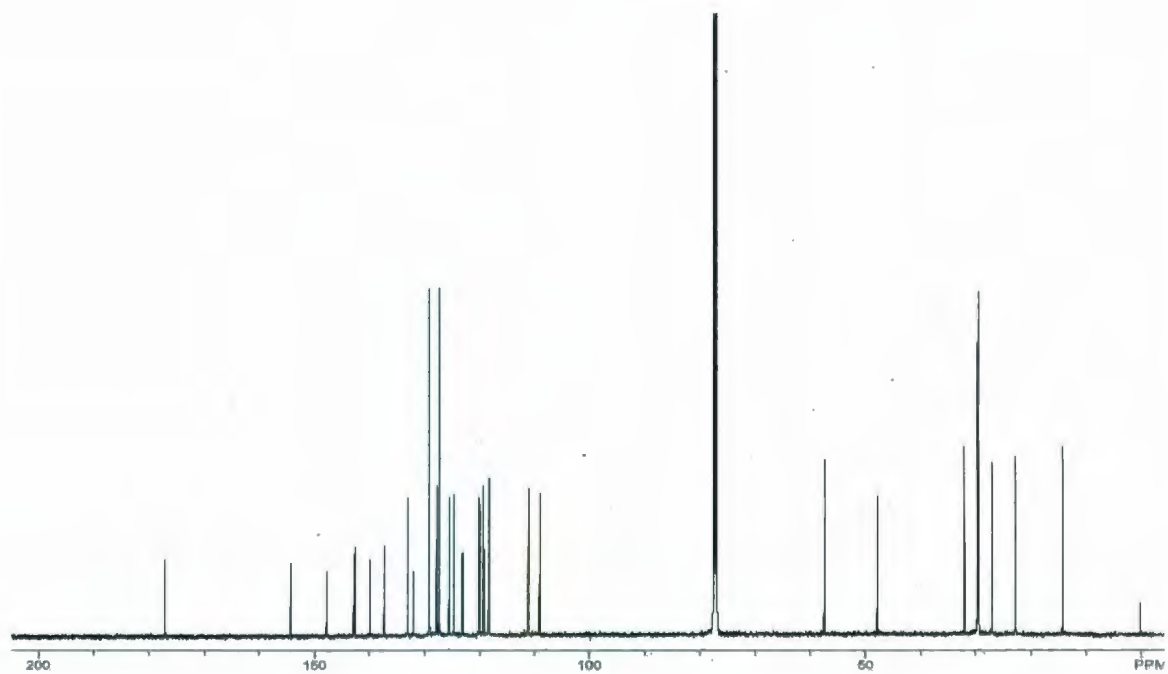
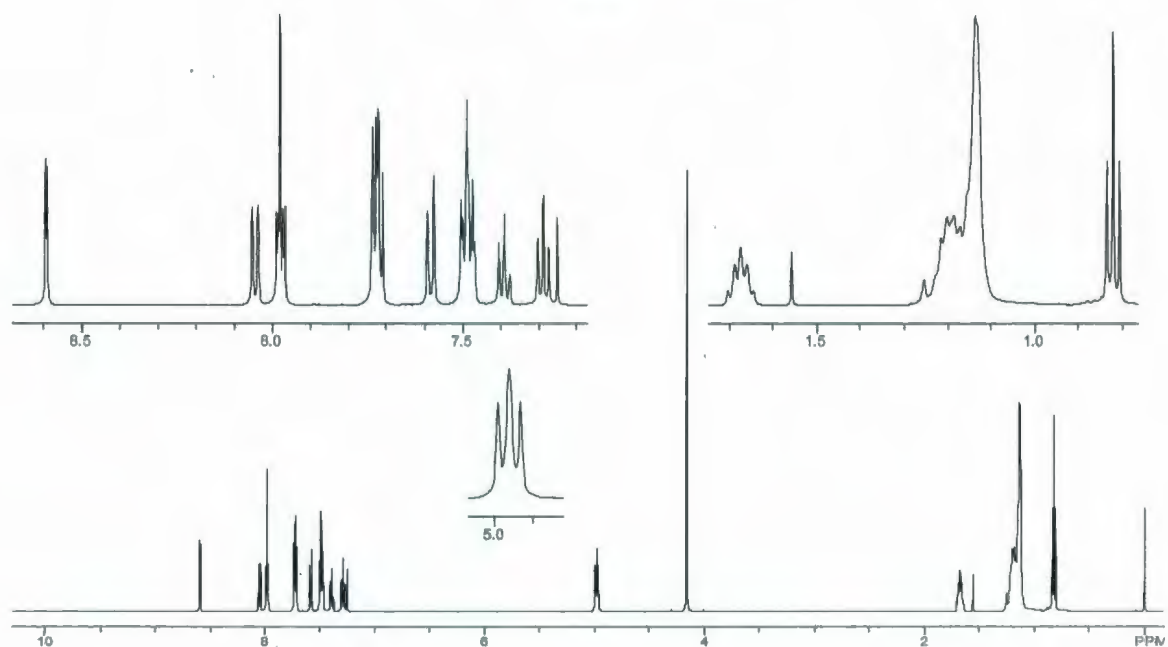
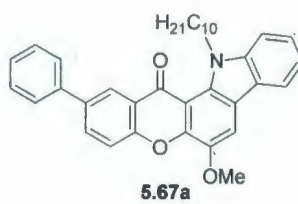


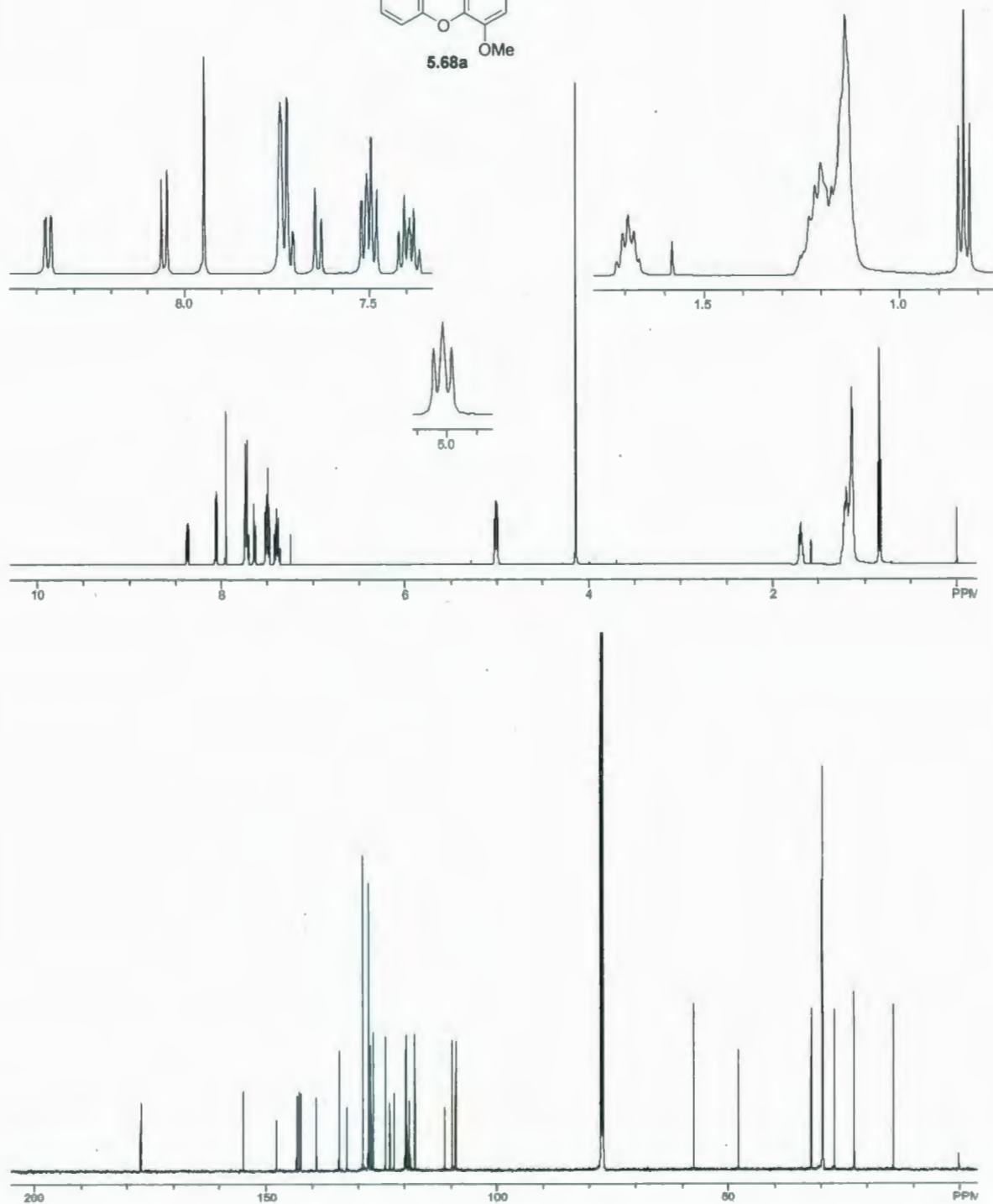
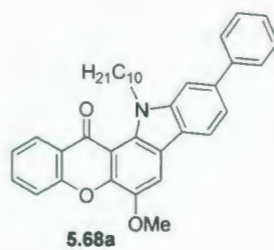


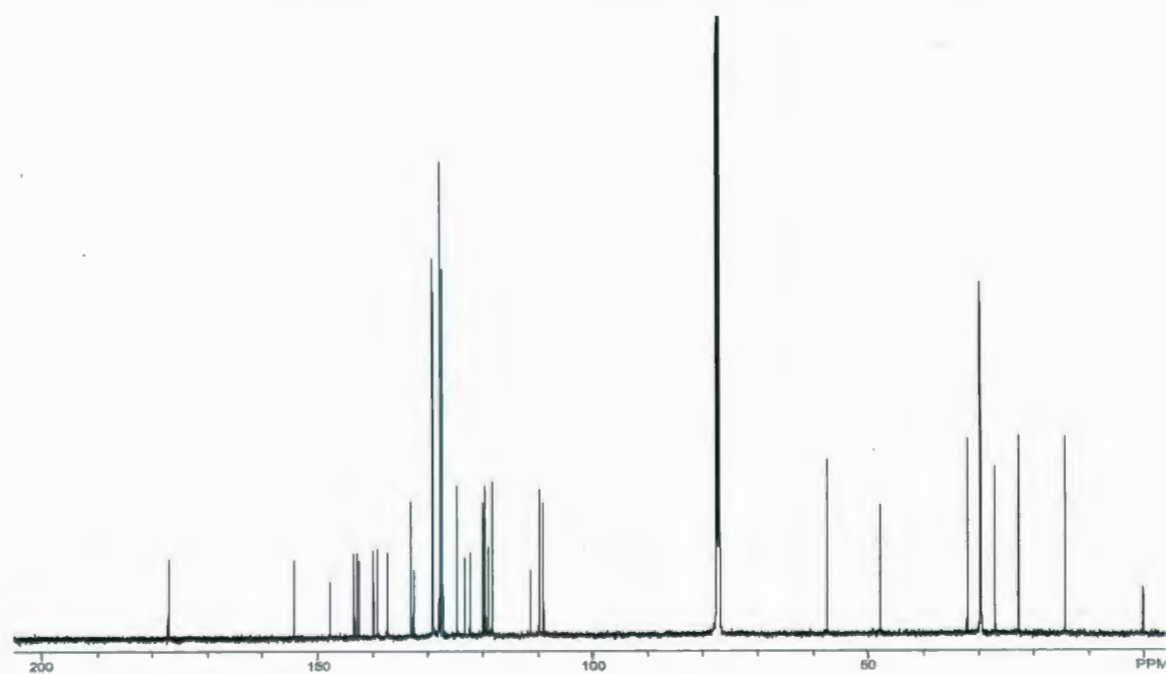
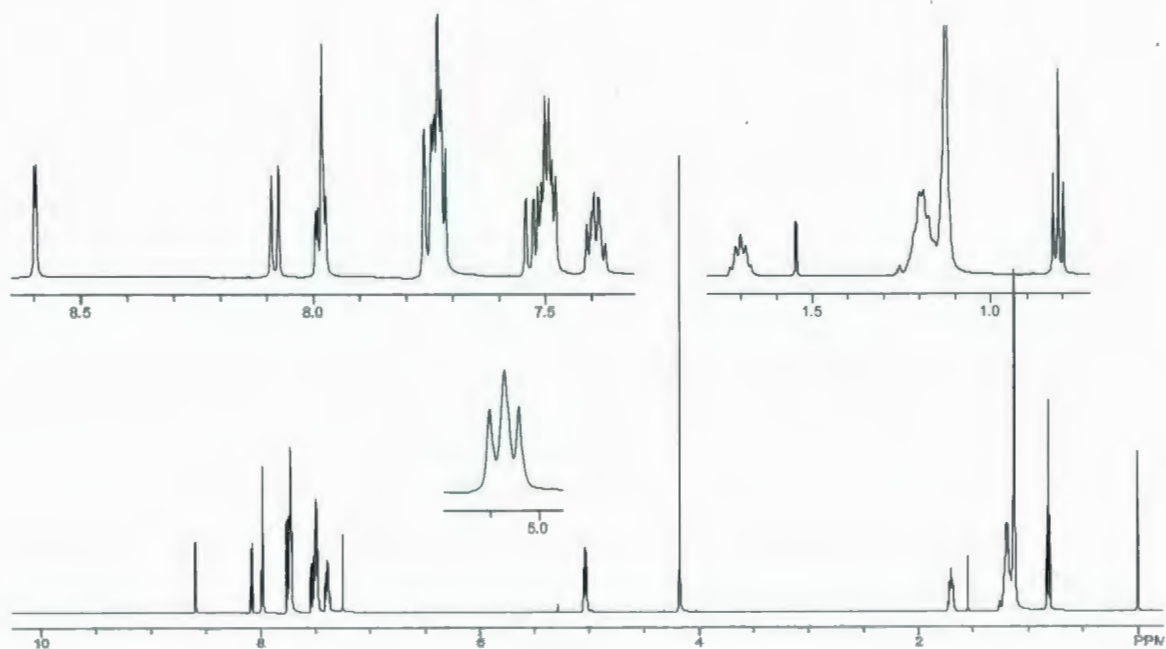
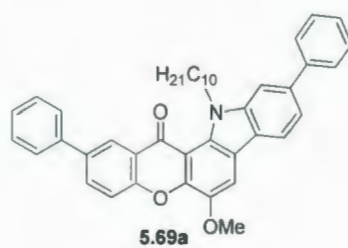




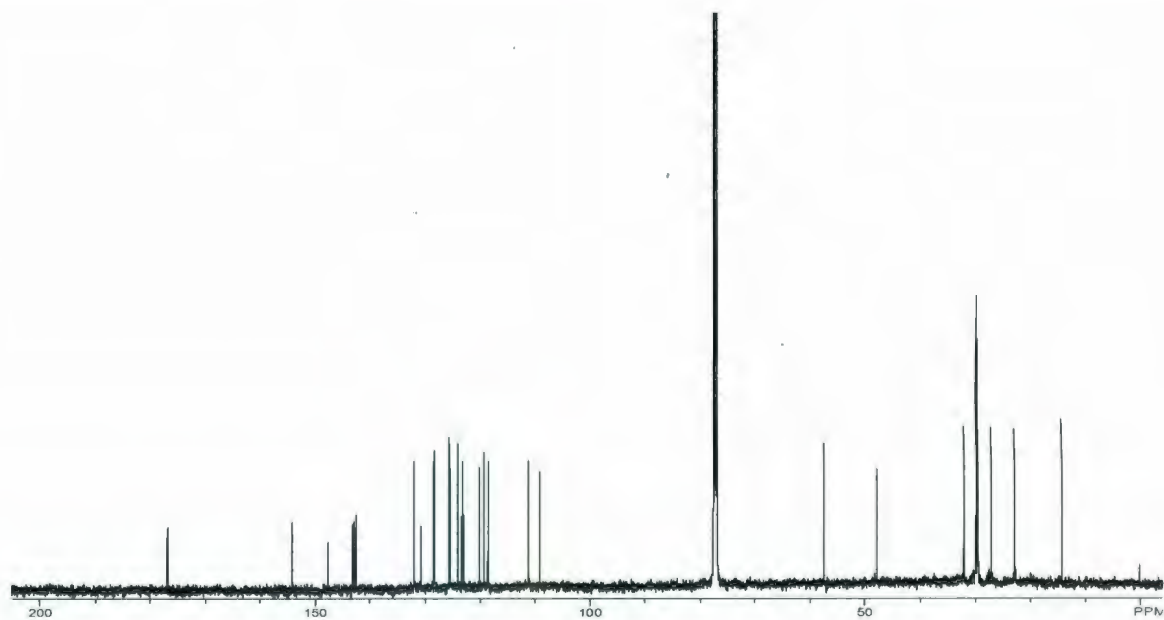
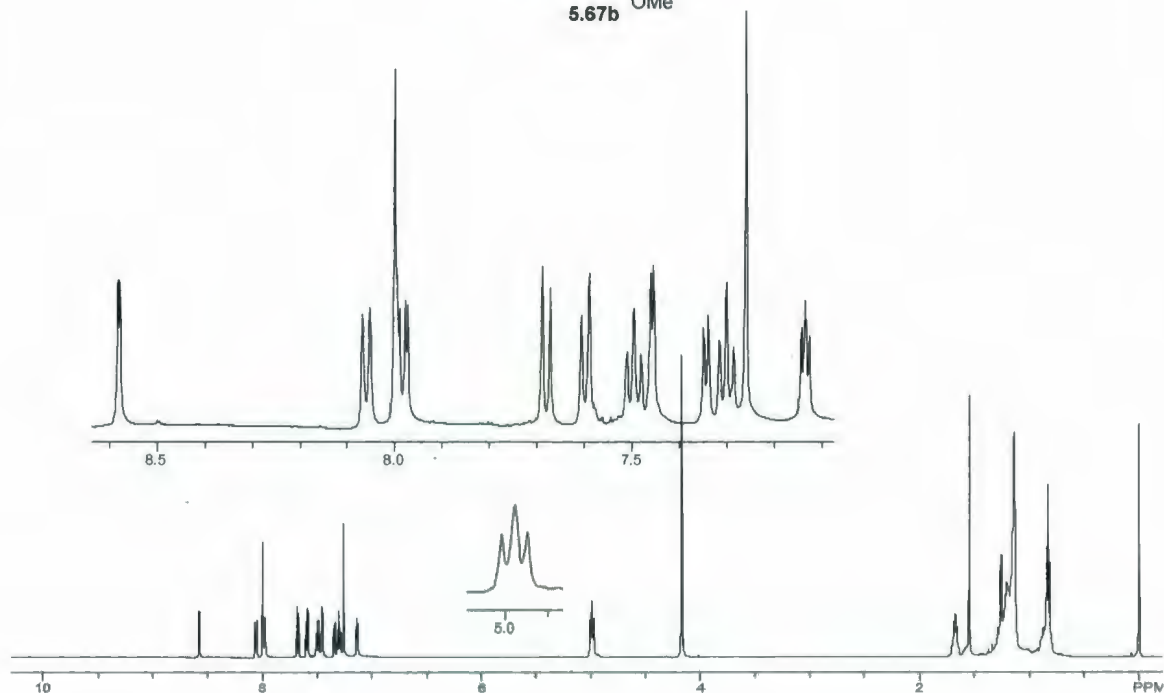
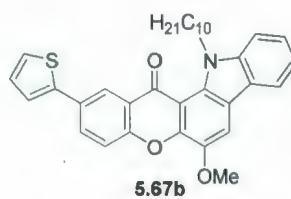


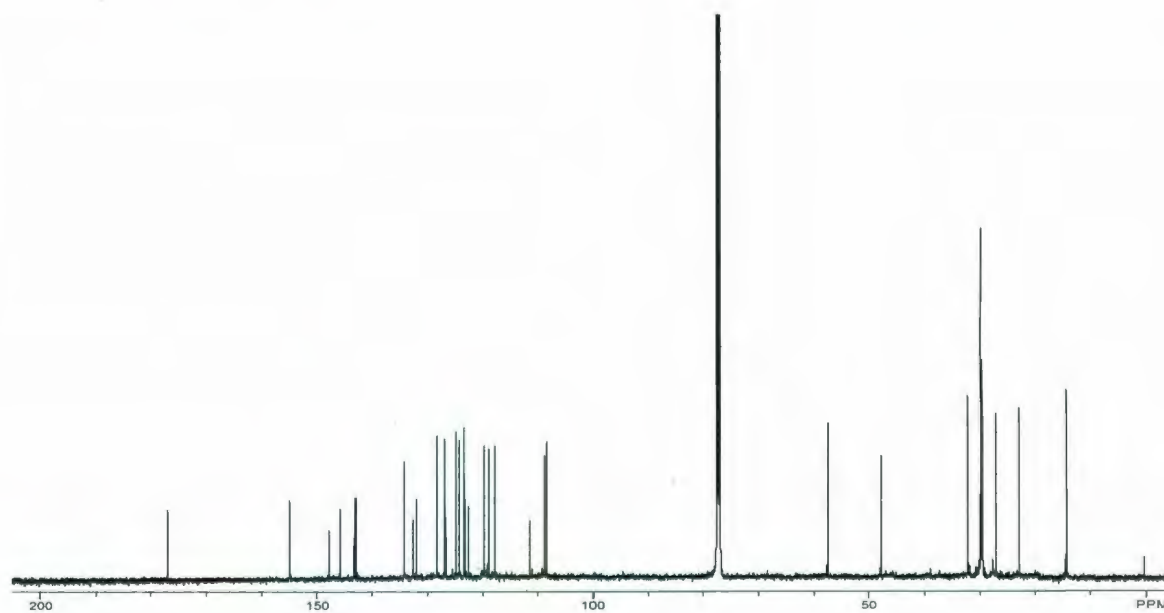
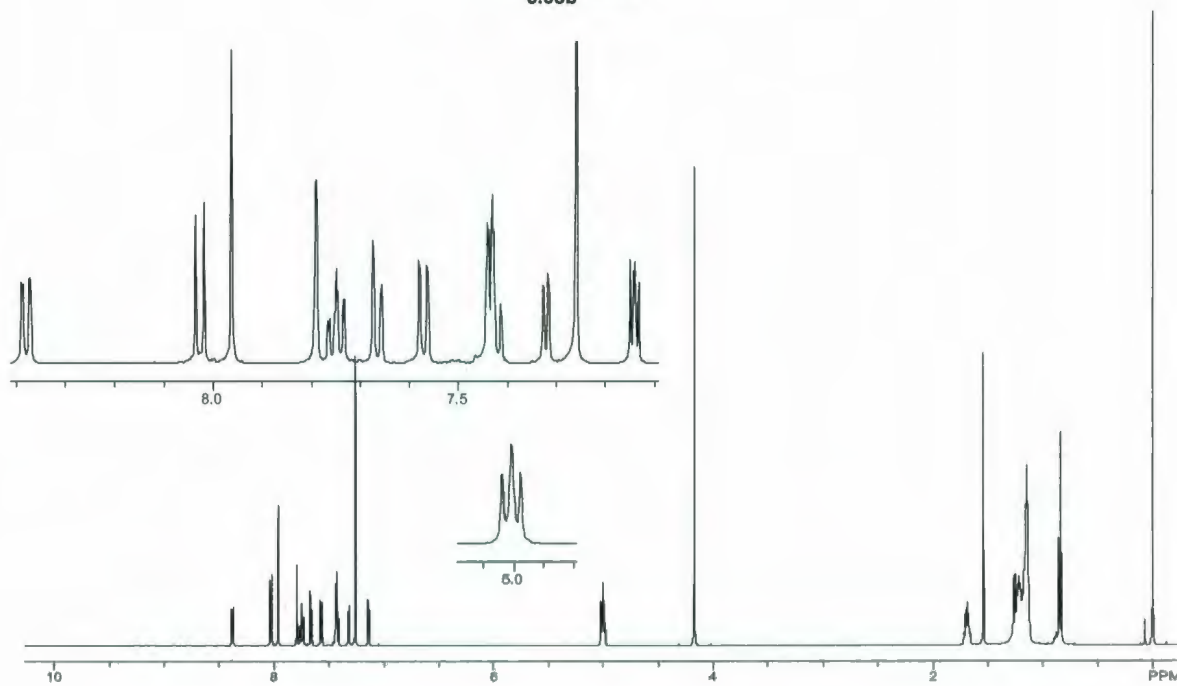
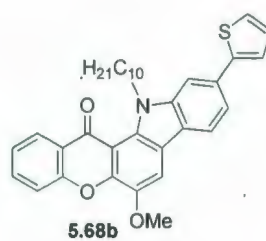


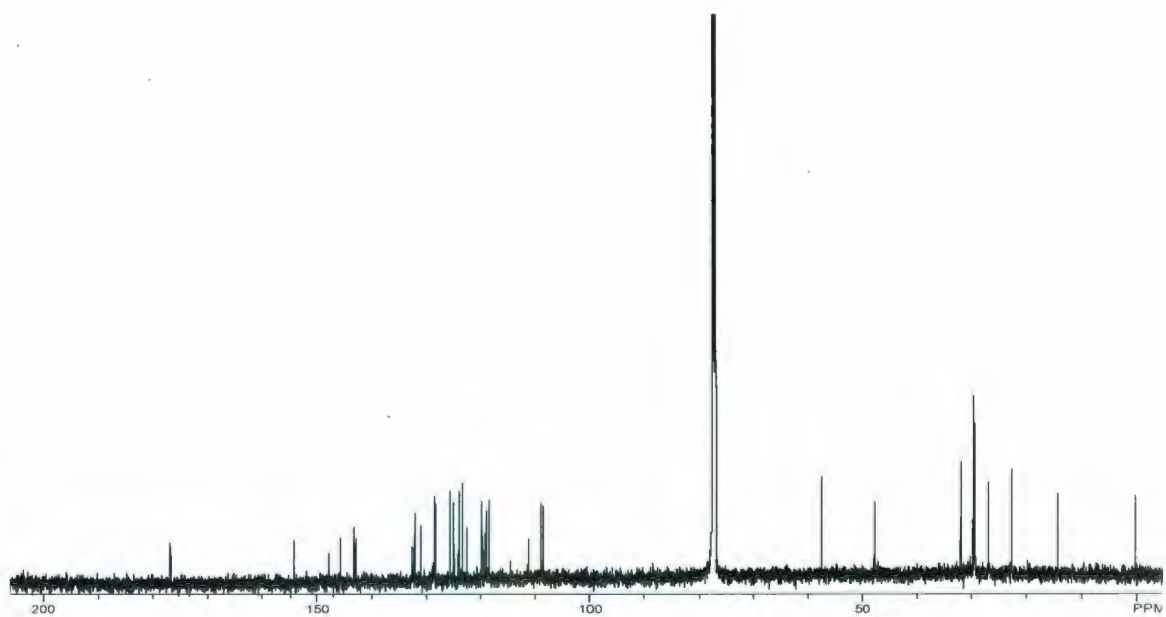
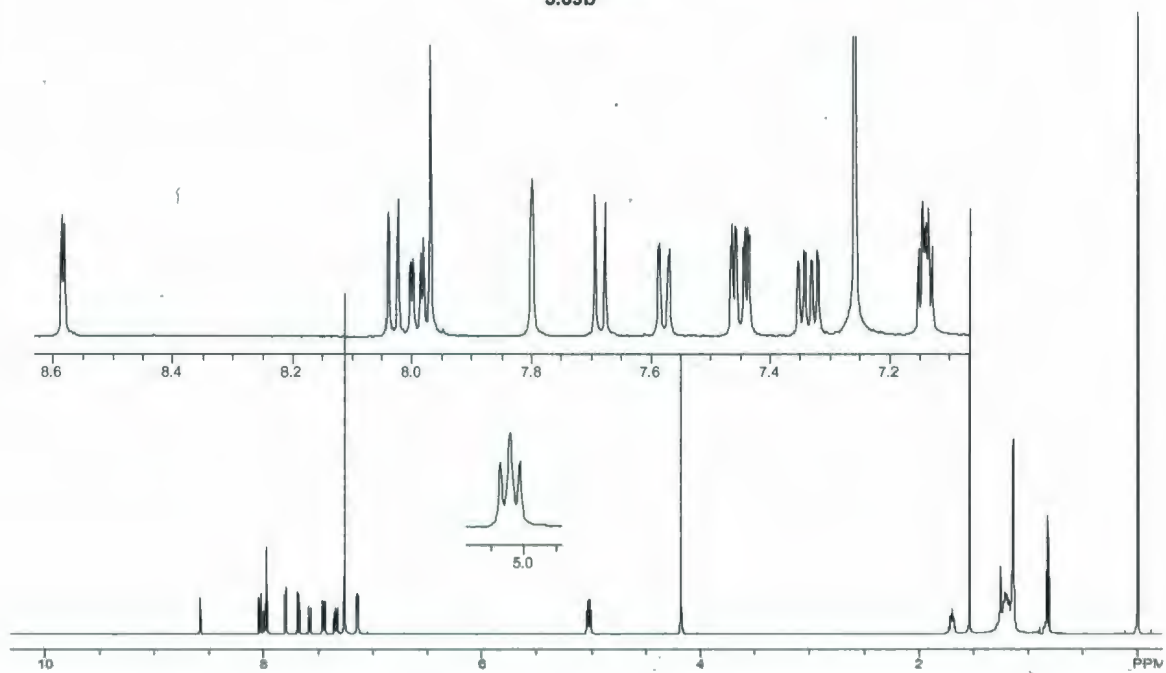
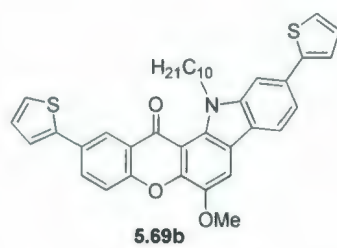


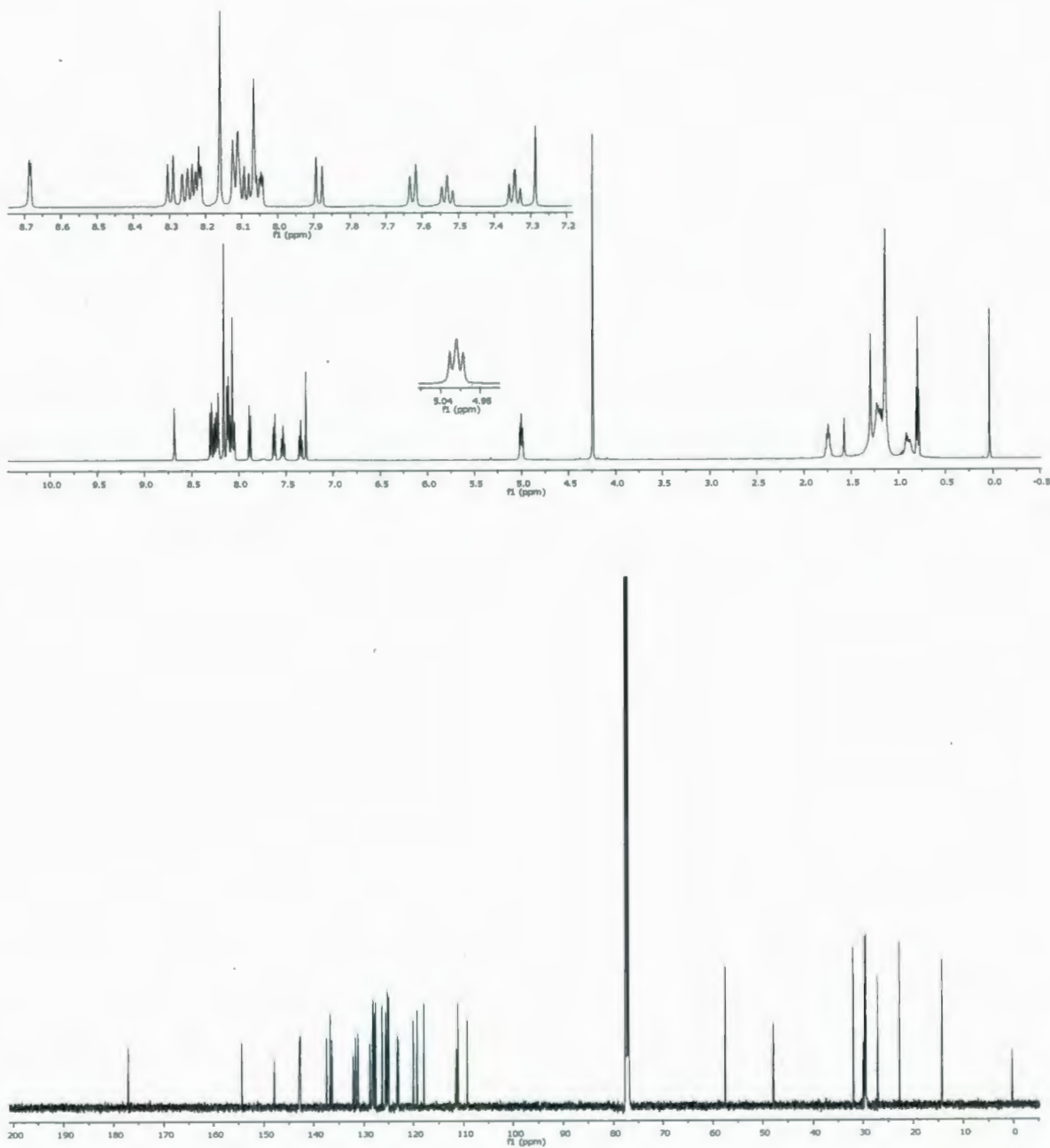
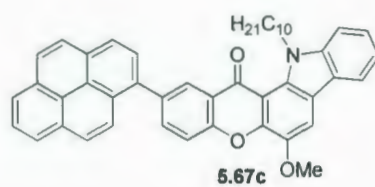




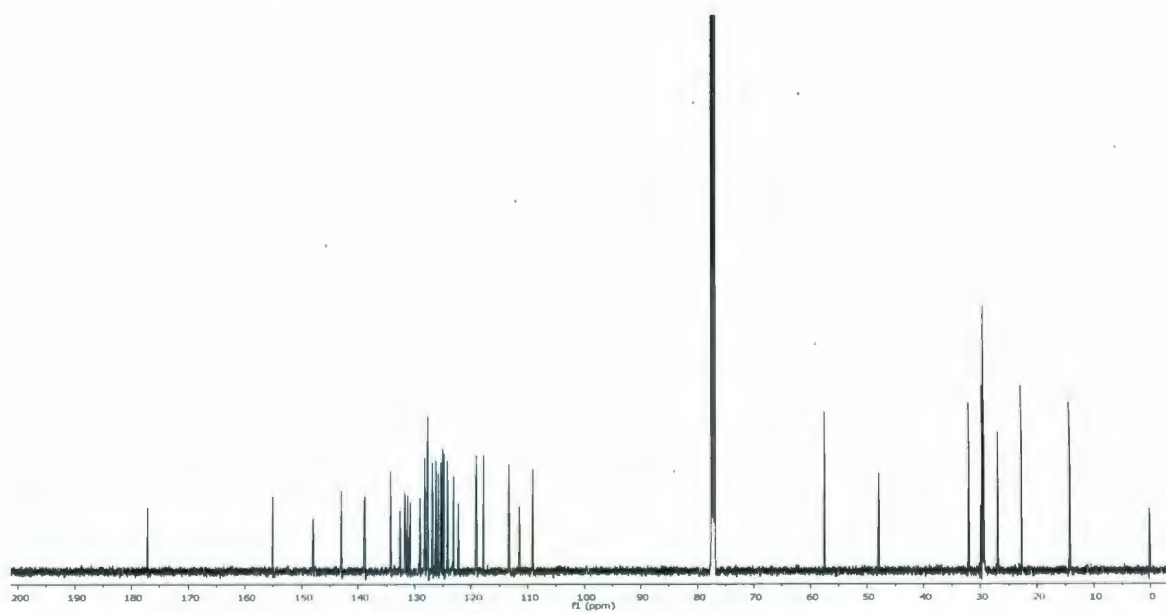
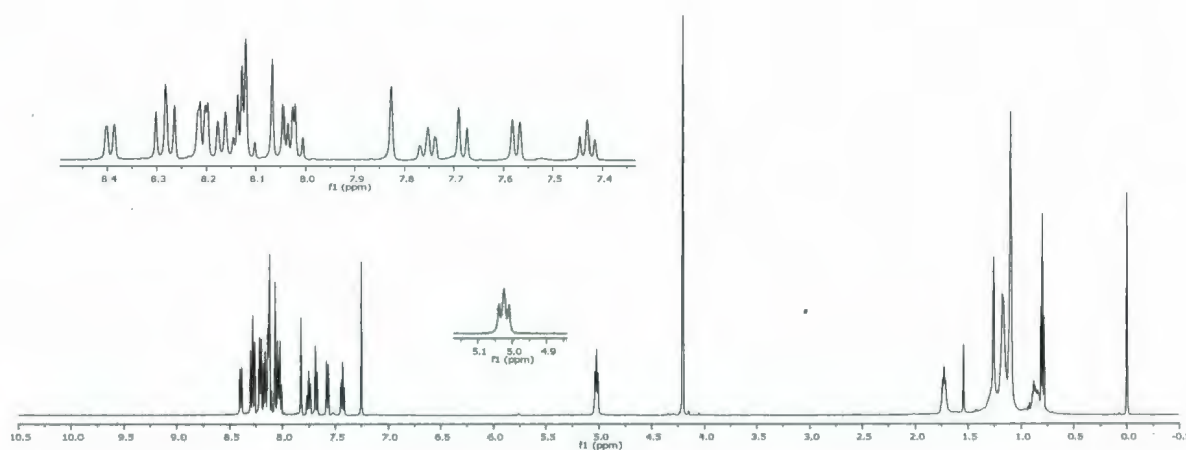
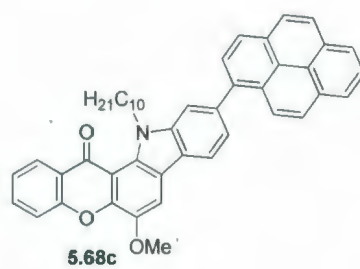


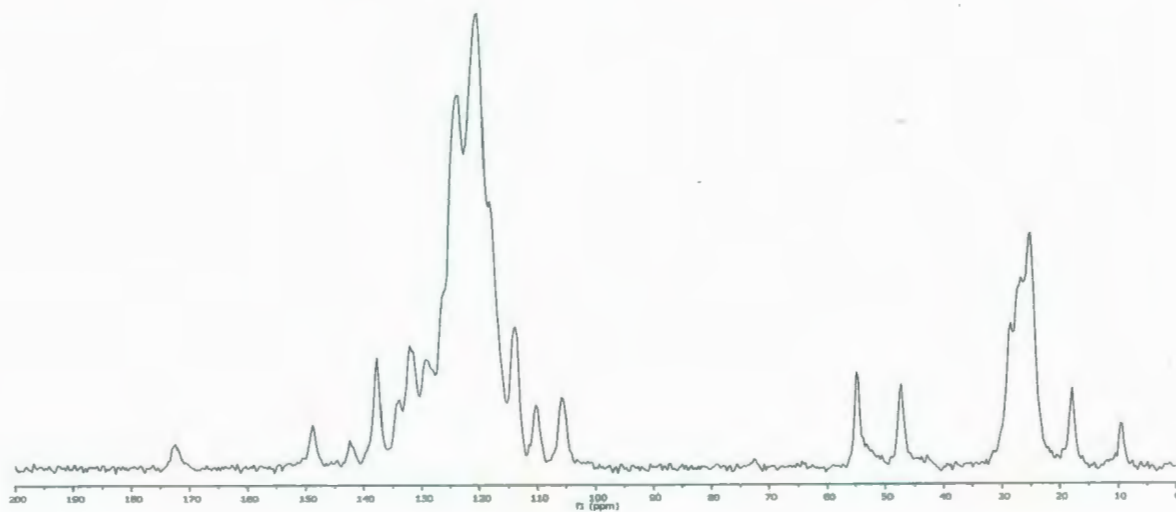
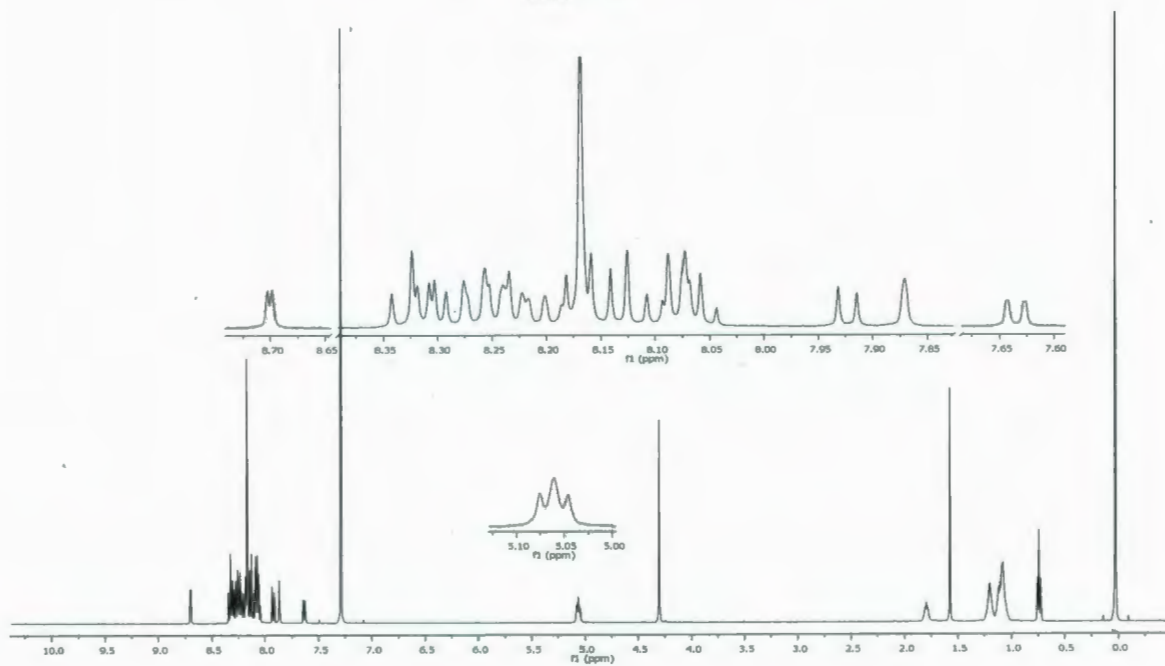
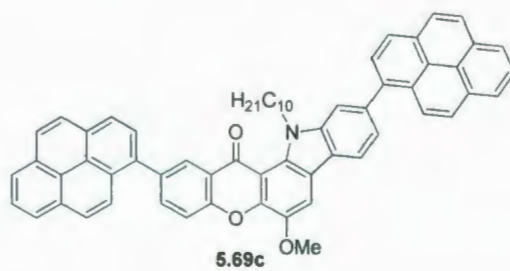












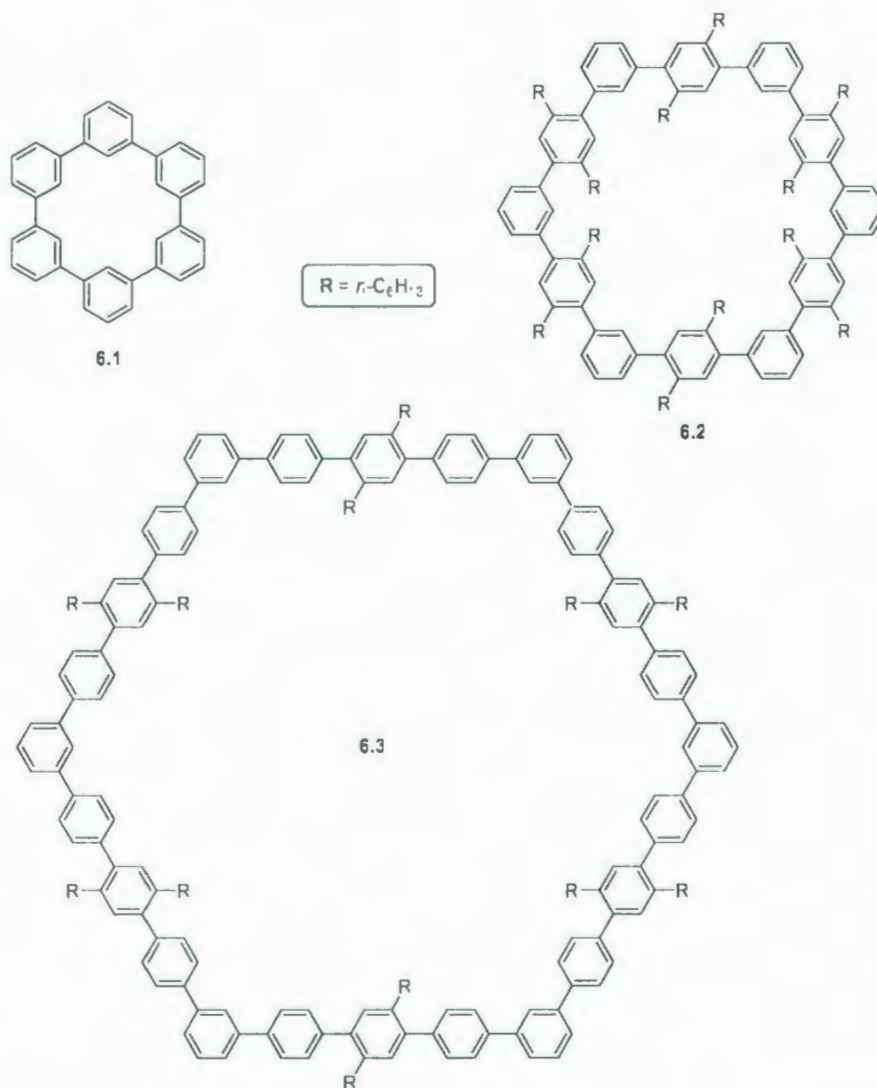
## Chapter 6

### Attempted Synthesis of Cyclic Oligophenylenes

#### Using IEDDA Chemistry

##### 6.1 Introduction

Oligoarylenes are a class of compounds composed entirely of aromatic units connected by single bonds. Most of the work in this area has employed benzene as the aromatic unit and the numerous one-dimensional (linear), two-dimensional (cyclic) and three-dimensional (dendritic) structures that have been synthesized are referred to as oligophenylenes. Cyclic oligophenylenes such as **6.1–6.3** (Figure 6.1)<sup>1</sup> are hexagonal macrocyclic compounds, which consist of phenylene units connected together via *meta*-linkages at their corners and *para*-linkages along their sides.



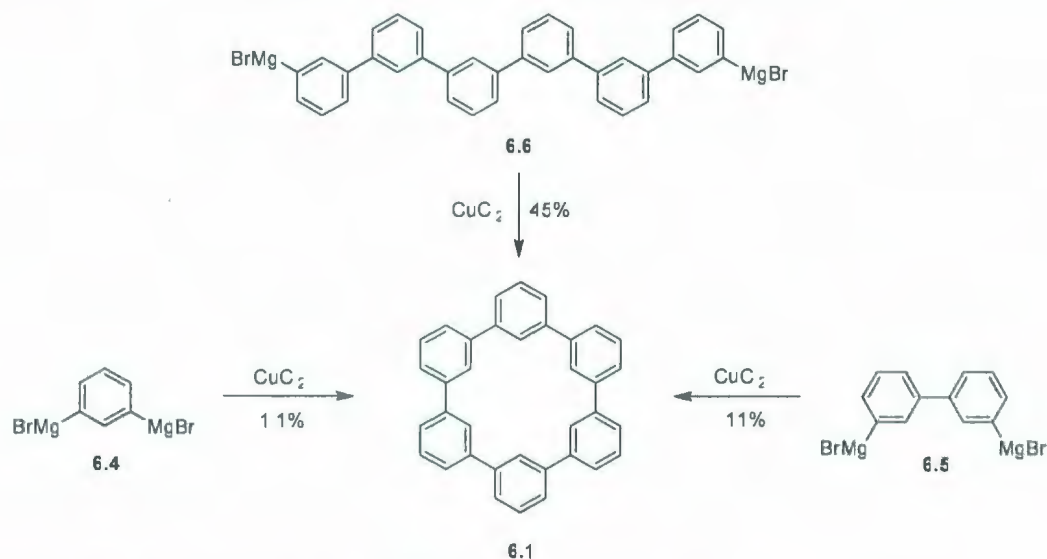
**Figure 6.1** Examples of hexagonal cyclic oligophenylenes **6.1–6.3**.

Although cyclic oligophenylenes were already of interest in the earliest stages of macrocyclic chemistry, only a few of them have been reported. For example, cyclic hexa-*m*-phenylene **6.1**, the first cyclic oligophenylene, was synthesized in 1967 by Staab and Binning.<sup>2</sup> The synthetic strategy relied upon the use of oxidative Grignard-coupling reactions. The desired product **6.1** was obtained in 1.1%, 11% and 45% yields, respectively, from different substrates **6.4–6.6** (Scheme 6.1). The cyclization yields



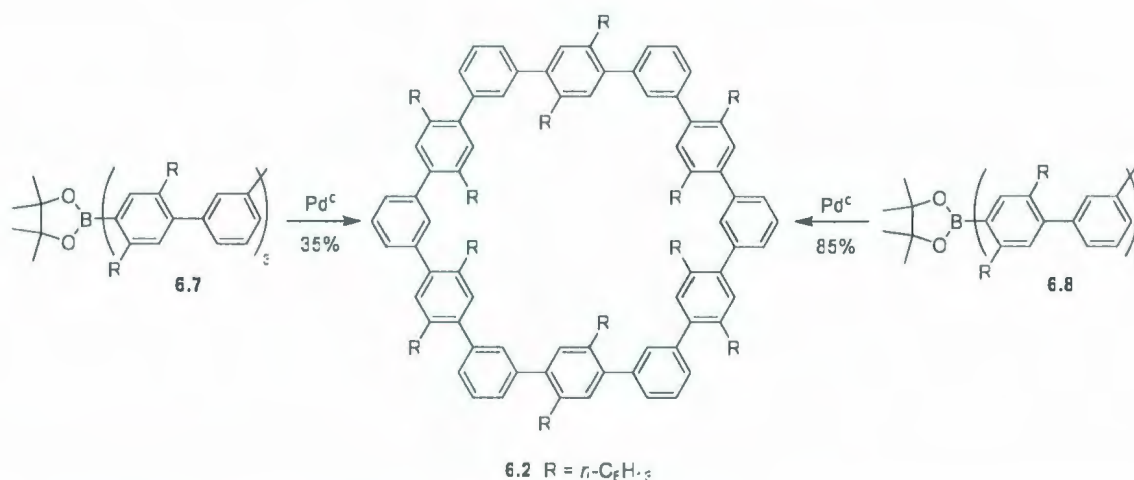
increased along with the number of *m*-phenylene units in the Grignard precursors, *i.e.*

6.4–6.6.



**Scheme 6.1** Staab and Binning's synthesis of cyclic hexaphenylene **6.1**.

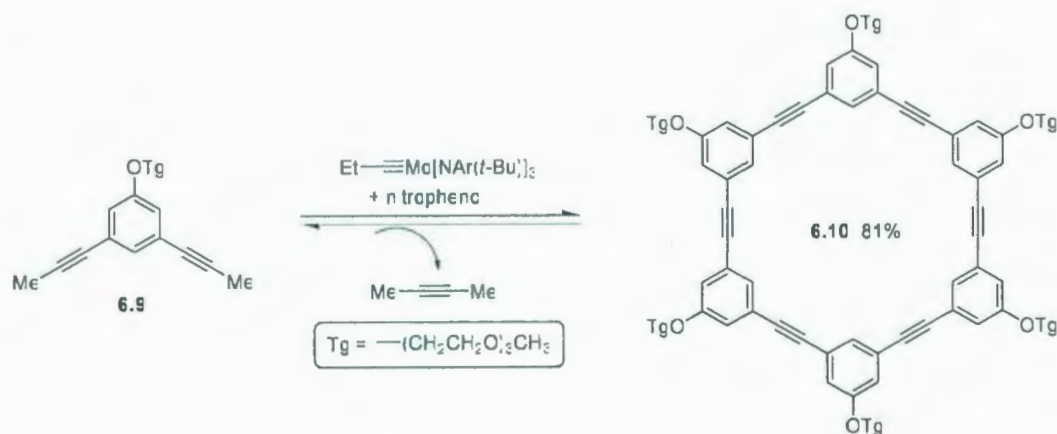
Not until three decades later, Schülter *et al.* reported a convergent synthesis of the cyclic dodecaphenylene **6.2** using Suzuki coupling methodology to form the biaryl bonds (Scheme 6.2).<sup>3</sup> Not surprisingly, a high yield (85%) was achieved in the cyclization of the precursor **6.8**, whereas the cyclodimerization of **6.7** gave the same product, *i.e.* **6.2**, only in 35% yield. A larger macrocycle, cyclic tetraeicosaphenylene **6.3** (Figure 6.1) was also prepared using the same approach, but the yield for the macrocyclization was not reported.



**Scheme 6.2** Schülter's synthesis of cyclic dodecaphenylene **6.2**.

There are two distinct types of synthetic approaches to macrocycles: kinetic and thermodynamic. In the kinetic approach, the building blocks of the macrocycle are connected into a linear oligomer that subsequently undergoes an intramolecular bond formation to produce the cyclic compound. The oligomer can be formed independently and then cyclized in a separate reaction. The advantage of this way is the efficient cyclization to form the desired cyclic compound, normally in high yield. However, multi-step synthesis is required for the preparation of the oligomer, *e.g.* oligomers **6.6**–**6.8** in the syntheses of cyclophenylenes **6.1** and **6.2**. On the other hand, a one-pot reaction can be performed for both oligomer formation and cyclization starting from a small building block. Although this is a short approach, the rings can be formed in different sizes (unless it is a templated reaction) and the cyclization usually competes with oligomerization. All of these features of a one-pot reaction normally lead to low yield of the desired cyclic compound(s). In the kinetic approach, bond-forming reactions are irreversible, which means that the system is unable to “correct” undesired bond

formations. However, the kinetic approach is the most commonly-used approach and has been used for the synthesis of numerous shape-persistent macrocycles,<sup>4</sup> including cyclic oligophenylenes **6.1**–**6.3**. The thermodynamic approach, which was developed recently, involves reversible bond formation. This being the case, the system can undergo a self-healing process. As a result, if the desired structure is the most stable under the given conditions, it might be obtained as a single macrocyclic product in high yield, although the reaction starts with small building blocks. The synthesis of hexameric phenylacetylene macrocycle **6.10** via alkyne metathesis is a good example (Scheme 6.3).<sup>5</sup> However, no cyclic oligophenylenes have been synthesized using the thermodynamic approach.



**Scheme 6.3** Synthesis of macrocycle **6.10** using the thermodynamic approach.

The aim of this research was to synthesize cyclic oligophenylene **1.233** (Figure 6.2), which has the same backbone as **6.2**, using IEDDA-based methodology. If the synthesis is successful, this cyclic compound could conceivably be converted into the hexaacid **6.11**, which has the potential to be a valuable supramolecular building block.

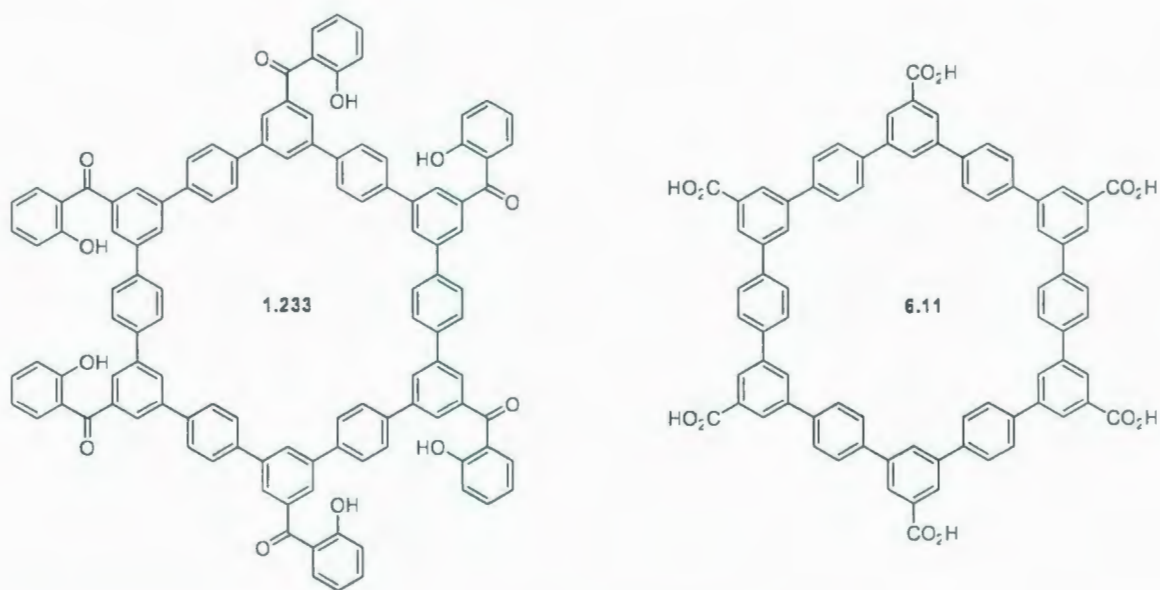
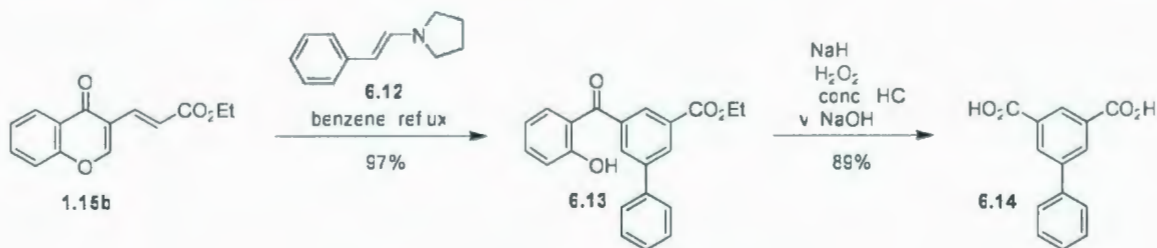


Figure 6.2 Target structures.

## 6.2 Retrosynthetic Analysis of Cyclic Oligophenylenes

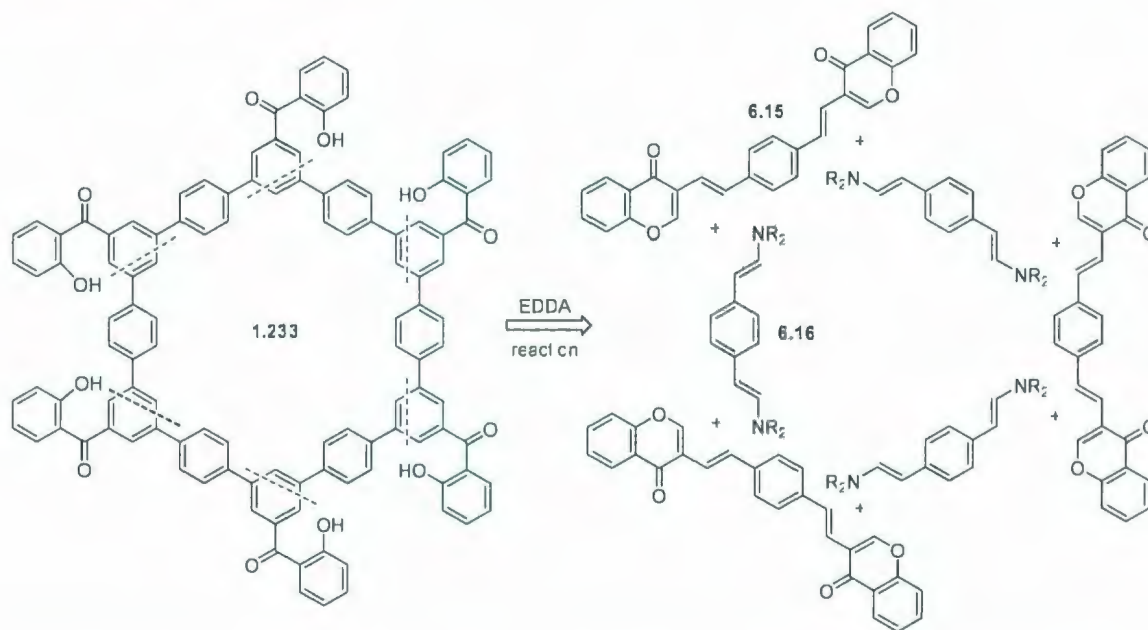
Recently, Bodwell *et al.* reported that 2-hydroxyacetophenone **6.13** was obtained in high yield from the IEDDA-driven domino reaction between chromone diene **1.15b** and enamine **6.12** (Scheme 6.4). The 2-hydroxyacetophenone product **6.13** was then converted into its corresponding diacid **6.14**<sup>6</sup> via a Dakin reaction,<sup>7</sup> followed by a hydrolysis. These transformations formed the basis for the planned synthesis of the target cyclic oligophenylenes **1.233** and **6.11**.



Scheme 6.4 Synthesis of 2-hydroxyacetophenone **6.13** and diacid **6.14**.



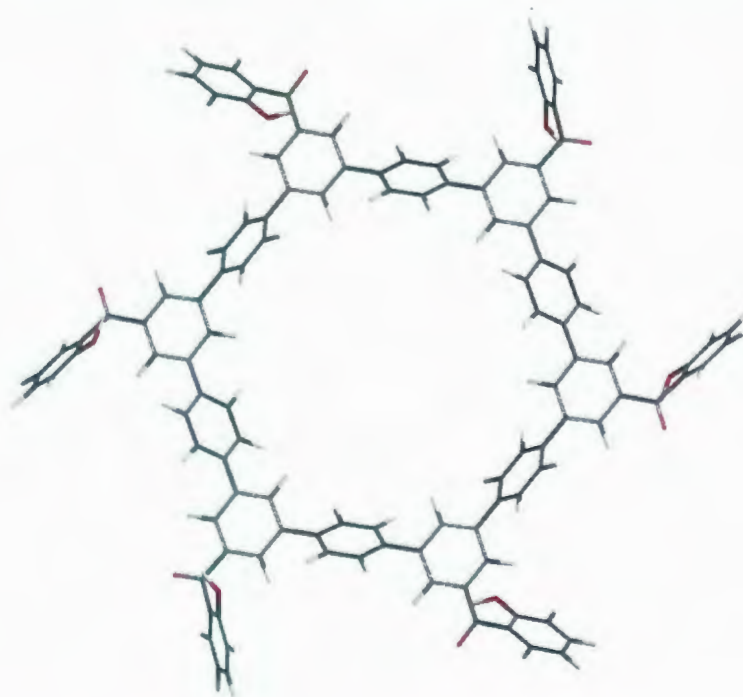
Retrosynthetic analysis of the symmetrical cyclic oligophenylene **1.233** at the indicated bonds revealed bis(diene) **6.15** and bis(enamine) **6.16** as potential precursors for a six-fold IEDDA-driven domino reaction (Scheme 6.5). This is a novel approach to a cyclic oligophenylene because none of the biaryl bonds in the target are formed during the synthesis: they are all present in the starting materials. Instead, the approach being followed here involves the construction of all six of the corner benzene rings via IEDDA-driven domino reactions in the same pot. Furthermore, the final benzene-ring-formation is also the macrocyclization.



**Scheme 6.5** Retrosynthetic analysis of cyclic oligophenylene **1.233** via a six-fold IEDDA-driven domino reaction.

Although the proposed chemistry clearly belongs to a kinetic approach, the six-fold-symmetric macrocycle **1.233** (from 3 units of diene and 3 units of dienophile) was expected to be favoured because it should be essentially free of strain. Indeed, the

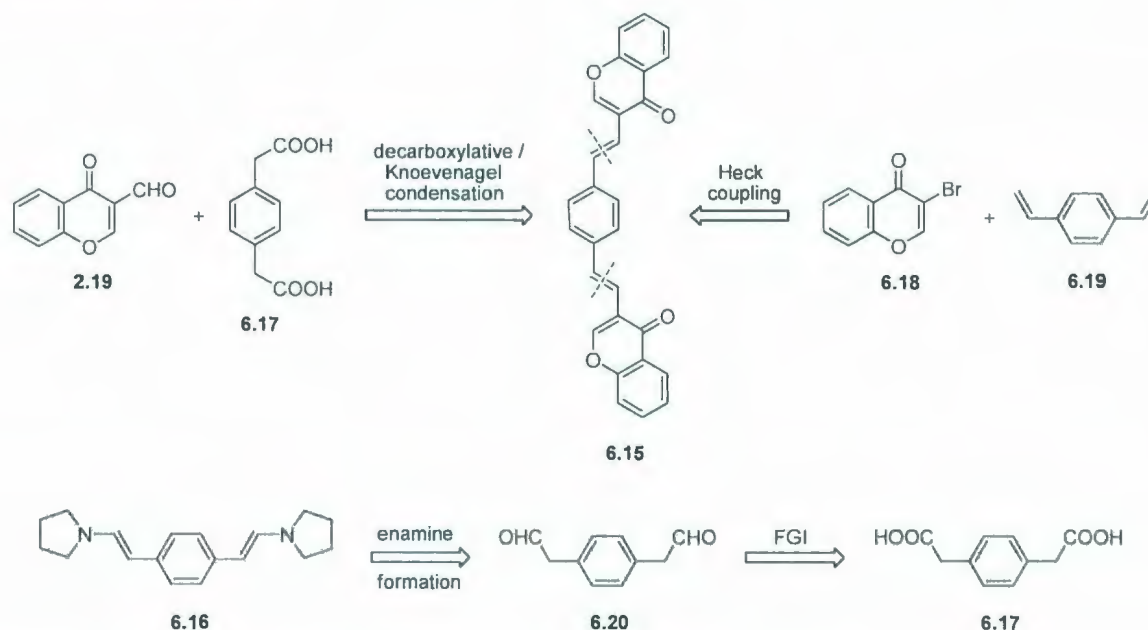
computed structure (MMFF)<sup>8</sup> of **1.233** (Figure 6.3) shows a “happy” molecule without any deformation. The next lower cyclic homolog (a four-fold symmetric cyclic oligoarylene derived from two bis(diene) units and two bis(dienophile) units) and the next higher cyclic homolog (an eight-fold symmetric cyclic oligoarylene derived from four bis(diene) units and four bis(dienophile) units) are quite different from **1.233**, both in size and geometry. Upon simple inspection of models, they both appear to have some strain. As such, the disadvantages in the kinetic approach, *i.e.* the competition from oligomer formation and the formation of other ring sizes, may be minimized.



**Figure 6.3** Computed structure (MMFF) of cyclic oligophenylene **1.233**.

Bis(diene) **6.15**, in turn, could be synthesized via either a decarboxylative / Knoevenagel condensation of 3-formylchromone (**2.19**) and *p*-phenylenediacetic acid (**6.17**) or a Heck coupling of 3-bromo-4*H*-1-benzopyrane-4-one (**6.18**) and 1,4-

divinylbenzene **6.19** (Scheme 6.6). The straightforward synthesis of bis(enamine) **6.16** would start from *p*-phenylenediacetic acid (**6.17**) via the key intermediate 1,4-benzene diacetaldehyde (**6.20**).



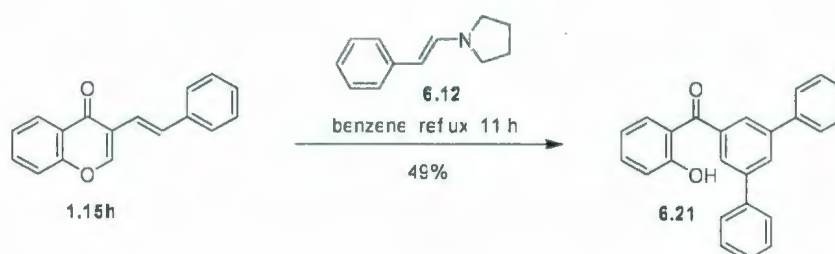
**Scheme 6.6** Retrosynthetic analysis of bis(diene) **6.15** and bis(enamine) **6.16**.

## 6.3 Results and Discussions

### 6.2.1 Synthesis of 2-Hydroxybenzophenone **6.21** as a Model Study

Before embarking on the synthesis of the bis(diene) **6.15** and bis(enamine) **6.16** precursors for the desired target **1.233**, a single IEDDA reaction was tested with diene **1.15h** and enamine **6.12**. The reaction occurred smoothly to give the desired product **6.21** in 49% yield upon heating in benzene for 11 h (Scheme 6.7). In fact, this appears to be a novel approach to the synthesis of *m*-terphenyls.





**Scheme 6.7** IEDDA reaction between diene **1.15h** and enamine **6.12**.

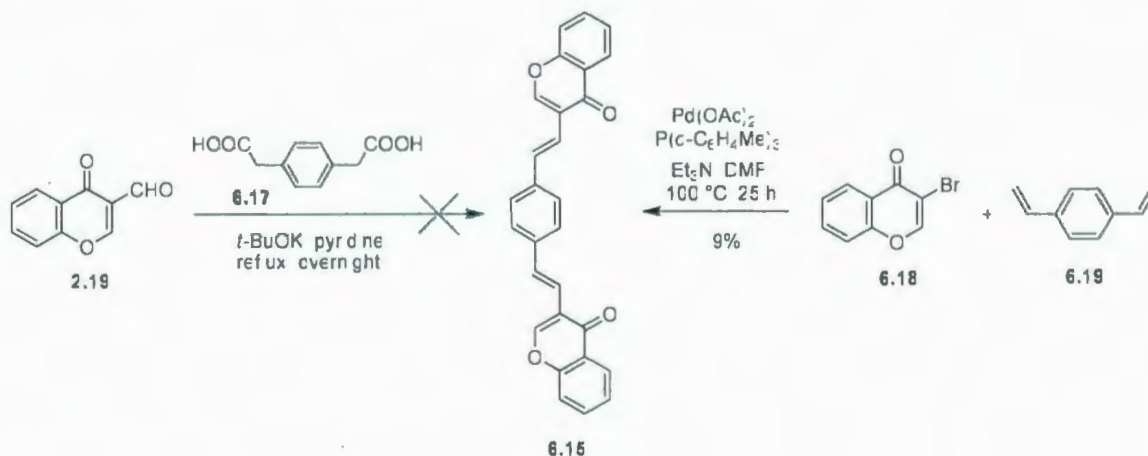
This result is similar to the yield of 4-methoxyxanthone **1.228h** (51%) from the IEDDA reaction between the same diene, *i.e.* **1.15h**, with enamine **1.225** (Chapter 2, page 65). The moderate yield for the IEDDA-driven domino reaction between **6.12** and diene **1.15h**, which bears an electron-neutral phenyl group, did not bode well for the six-fold IEDDA reaction between bis(diene) **6.15** and bis(enamine) **6.16**. Moreover, MO calculations (RHF/3-21G(d)//AM1)<sup>8</sup> of bis(diene) **6.15** ( $E_{\text{LUMO}} = 1.58$  eV) and bis(enamine) **6.16** ( $E_{\text{LUMO}} = -6.25$  eV) gave a similar HOMO-LUMO energy gap (4.67 eV) to that (4.87 eV) of diene **1.15h** and enamine **6.12**. At 50% yield per IEDDA reaction, the overall yield could not exceed 1.6% and would likely be lower due to competition from linear oligomer formation and the formation of other ring sizes. Nevertheless, the planned synthetic route was short enough for the key reaction to be attempted. It was borne in mind that, if the reaction did not occur or occurred in very low yield, electron withdrawing groups could be introduced to bis(diene) **6.15** and electron-donating groups could be introduced to bis(enamine) **6.12** to enhance their reactivity.

### 6.2.2 Synthesis of Bis(diene) **6.15**

Recalling that diene **1.15h** was synthesized in high yield (82%) via a decarboxylative Knoevenagel condensation between 3-formylchromone (**2.19**) and

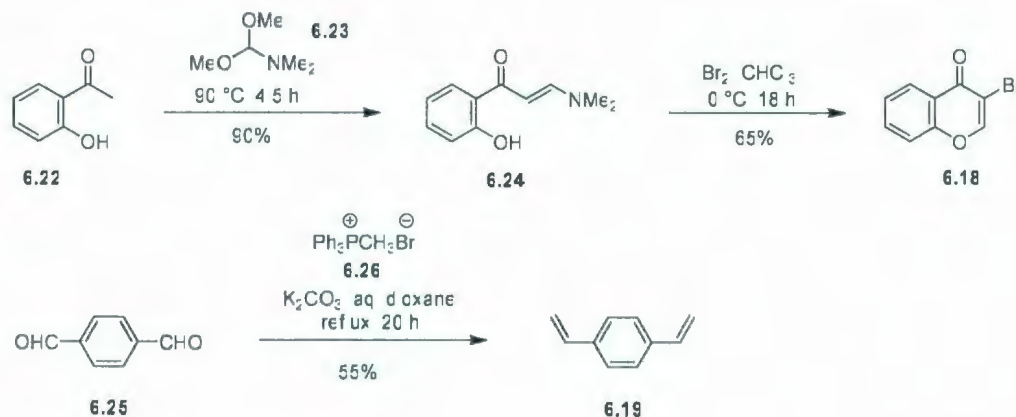


phenylacetic acid (**2.37**) (Chapter 2, page 62), the double condensation between **2.19** and *p*-phenylenediacetic acid (**6.17**) was expected to form bis(diene) **6.15** (Scheme 6.8). The reaction was performed under the same conditions (*t*-BuOK, pyridine, reflux) used for diene **1.15h**, but no trace of the desired product was detected by mass spectrometric analysis, even though the starting materials were completely consumed. Alternatively, Heck coupling between 3-bromo-4*H*-1-benzopyrane-4-one (**6.18**) and 1,4-divinylbenzene **6.19** gave bis(diene) **6.15**, but in just 9% yield. The *trans* geometry of double bonds in newly synthesized bis(diene) **6.15** was confirmed by <sup>1</sup>H NMR analysis (*J* = 16.3 Hz). Unlike the other type of bis(diene) such as **4.26b–c**, which presumably polymerized in the solid state (Chapter 4, pages 191 and 193), bis(diene) **6.15** could be isolated, but not easily purified by column chromatography. The optimization of the Heck coupling conditions was not carried out due to time constraints. However, it is likely that a higher yield of bis(diene) **6.15** could be obtained under the appropriate conditions.



Scheme 6.8 Synthesis of bis(diene) **6.15**.

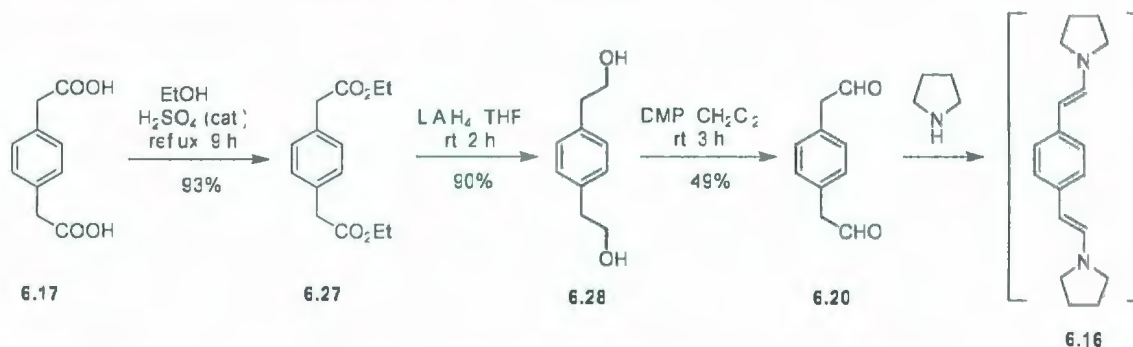
Intermediates **6.18**<sup>9</sup> and **6.19**<sup>10</sup> were prepared according to literature procedures (Scheme 6.9).



**Scheme 6.9** Synthesis of intermediates **6.18** and **6.19**.

### 6.2.3 Synthesis of Bis(enamine) **6.16**

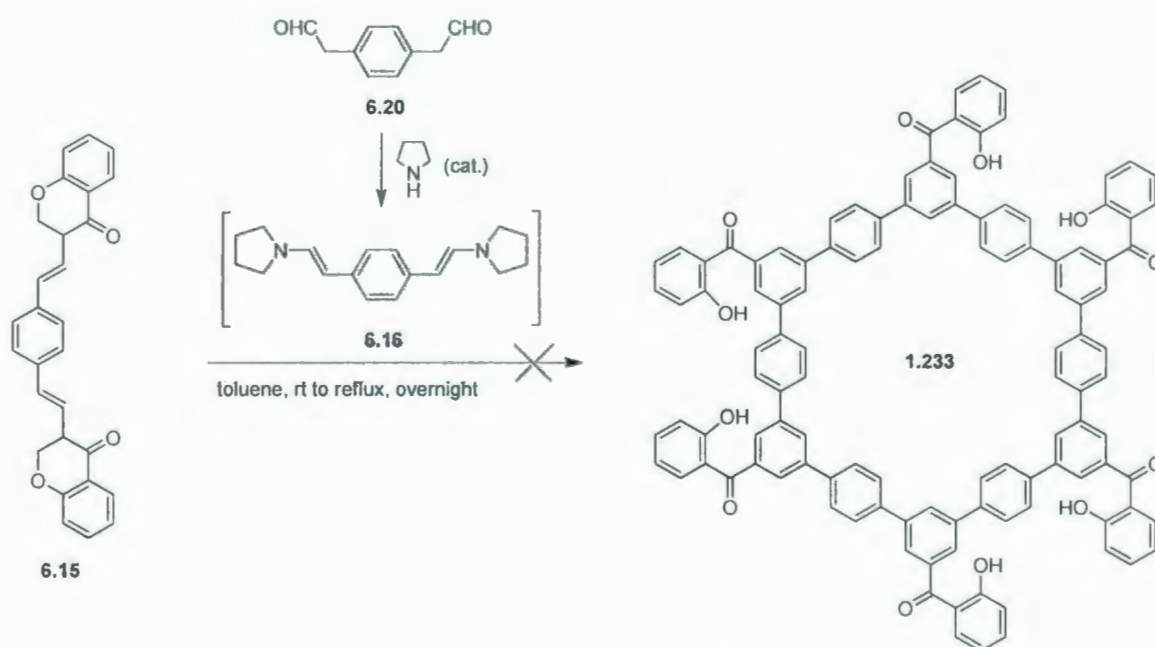
The plan for the macrocyclization reaction was to form bis(enamine) **6.16** from the dialdehyde **6.20** with few drops of pyrrolidine in the presence of bis(diene) **6.15**. Therefore, synthetic work was focused on the synthesis of dialdehyde **6.20**. Commercially available diacid **6.17** was subjected to a series of functional group interconversions, *i.e.* esterification (93%), reduction (90%), and oxidation (49%) to afford the desired dialdehyde **6.20**.<sup>11</sup>



**Scheme 6.10** Synthesis of bis(aldehyde) **6.20** as a prospective precursor to bis(enamine) **6.16**.

#### 6.2.4 Attempted Synthesis of Cyclic Oligophenylene 1.233

The stage was set for the challenging six-fold IEDDA reaction between bis(diene) **6.15** and bis(enamine) **6.16** to construct the target cyclic oligophenylene **1.233** (Scheme 6.11). A mixture of bis(diene) **6.15**, dialdehyde **6.20** and a catalytic amount of pyrrolidine was stirred at room temperature for 2 h, but bis(diene) **6.15** appeared not be consumed (tlc analysis). Upon heating the reaction mixture in toluene at reflux overnight, an insoluble product and small amount of unconsumed bis(diene) **6.15** were obtained. Unfortunately, no evidence for the presence of **1.233** in the insoluble product could be obtained, even using the MALDI-TOF technique for mass spectroscopic analysis. In the hope that the desired product was indeed present, but not detected, the insoluble product was subjected to conditions ( $K_2CO_3$ , 1-bromodecane, DMF, reflux, overnight) that would bring about *O*-alkylation of the hydroxyl groups thereby increasing the solubility. However, this reaction did not show any promise (tlc analysis). With absolutely no evidence to support the formation of cyclic oligophenylene **1.233** or the corresponding hexa-*O*-alkylated analog, work on this project was terminated. Future work will have to involve modified versions of the bis(diene) **6.15** that bear electron-withdrawing groups and modified versions of the dialdehyde **6.20** that bear electron-donating groups. These modifications should not only enhance the reactivity of diene / dienophile pair, but also improve the solubility of the cyclic product.

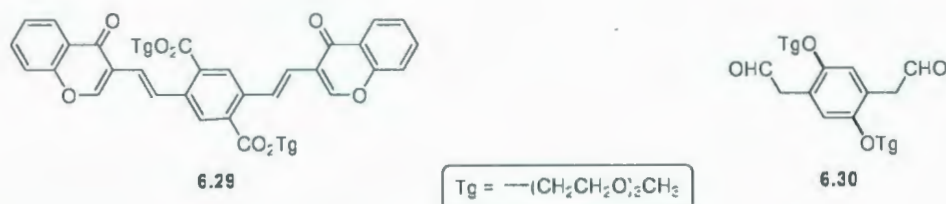


**Scheme 6.11** An attempted six-fold IEDDA reaction between bis(diene) **6.15** and bis(enamine) **6.16**.

### 6.3 Conclusions

A concise six-fold IEDDA strategy was investigated for the synthesis of cyclic oligophenylene **1.233** from two simple building blocks, bis(diene) **6.15** and bis(enamine) **6.16**. Although no evidence for the formation of desired macrocyclic product **1.233** was obtained, this synthetic route still has the potential to open up a new approach to cyclic oligophenylenes such as **1.233**. Optimization of the Heck coupling conditions for bis(diene) formation and the design of new bis(diene)s such as **6.29** and new dialdehydes such as **6.30** (Figure 6.4) should form the basis of the future work.



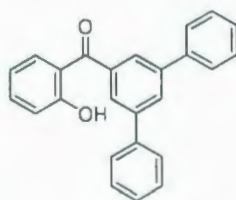


**Figure 6.4** Suggested bis(diene) **6.29** and bis(dienophile) **6.30**.

## 6.4 Experimental Section<sup>12</sup>

General methods and instrumentation used are identical to those described in Chapter 2 (pages 76–77).

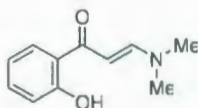
### 3',5'-Diphenyl-2-hydroxybenzophenone (**6.21**)



Enamine **6.12** (20.1 mmol), which was prepared from phenylacetaldehyde (2.41 g, 20.1 mmol) and pyrrolidine (1.43 g, 20.1 mmol), and diene **1.15h** (500 mg, 2.01 mmol) were heated in benzene at reflux for 11 h and worked up according to the general procedure for the xanthone synthesis in Chapter 2. Column chromatography (50:50  $\text{CH}_2\text{Cl}_2$ :hexanes) of the crude product yielded **6.21** (361 mg, 49%) as a yellow solid:  $R_f = 0.71$  ( $\text{CH}_2\text{Cl}_2$ ); mp 158–159 °C; IR  $\nu$  3052 (w), 1622 (m), 1587 (m), 1479 (m), 1450 (m), 1425 (m), 1349 (m), 1287 (m), 1243 (m), 1209 (m), 1193 (m), 1156 (m), 1026 (m), 963 (m), 760 (s), 712 (s), 700 (s), 671 (s) ( $\text{cm}^{-1}$ );  $^1\text{H}$  NMR (500 MHz)  $\delta$  12.03 (s, 1H), 8.02 (d,  $J = 1.4$  Hz, 1H), 7.85 (d,  $J = 1.4$  Hz, 2H), 7.70 (dd,  $J = 8.1, 1.3$  Hz, 1H), 7.68–7.66 (m, 4H), 7.55–7.51 (m, 1H), 7.49 (t,  $J = 7.6$  Hz, 4H), 7.41 (t,  $J = 7.8$  Hz, 2H), 7.10 (d,  $J = 8.0$

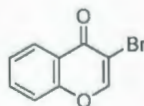
Hz, 1H), 6.90 (t,  $J = 7.6$  Hz, 1H);  $^{13}\text{C}$  NMR (125 MHz)  $\delta$  201.8, 163.6, 142.3, 140.2, 139.3, 136.8, 133.8, 129.6, 129.2, 128.3, 127.5, 126.8, 119.4, 119.1, 118.7; MS [APCI (+)]  $m/z$  (%) 351 ( $\text{M}^+$ , 100); HRMS [EI (+)] calcd for  $\text{C}_{25}\text{H}_{18}\text{O}_2$  350.1307, found 350.1305.

### 2-Hydroxy-*N,N*-dimethylvinylamide (6.24)<sup>9</sup>



A mixture of 2-hydroxyacetophenone (6.22) (20.4 g, 150 mmol) and dimethylformamide dimethyl acetal (6.23) (22.4 g, 188 mmol) was stirred at 90 °C for 4.5 h. The reaction mixture was then cooled to room temperature. The solid, brown crude product was washed with cold methanol (3 x 50 mL) to yield **6.24** (25.8 g, 90%) as bright yellow crystals:  $R_f = 0.45$  (50:50 EtOAc-hexanes); mp 136–138 °C (lit. mp<sup>9</sup> 132–134 °C);  $^1\text{H}$  NMR (500 MHz)  $\delta$  13.96 (s, 1H), 7.86 (d,  $J = 11.7$  Hz, 1H), 7.69 (dd,  $J = 8.3, 1.4$  Hz, 1H), 7.36–7.32 (m, 1H), 6.92 (dd,  $J = 8.2, 1.3$  Hz, 1H), 6.82–6.79 (m, 1H), 5.76 (d,  $J = 12.2$  Hz), 3.16 (s, 3H), 2.94 (s, 3H);  $^{13}\text{C}$  NMR (125 MHz)  $\delta$  191.7, 163.2, 154.9, 134.1, 128.4, 120.5, 118.4, 118.2, 90.3, 45.6, 37.6; MS [APCI (+)]  $m/z$  (%) 192 ( $\text{M}^+$ , 100).

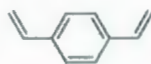
### 3-Bromo-4*H*-1-benzopyran-4-one (6.18)<sup>9</sup>



To a solution of vinylogous amide **6.24** (4.61 g, 24.1 mmol) in  $\text{CHCl}_3$  (40 mL) was added dropwise a solution of bromine (3.82 g, 23.9 mmol) in  $\text{CHCl}_3$  (40 mL) at 0 °C within 40 min. The resulting yellow solution was stirred at 0 °C for 20 min then at room

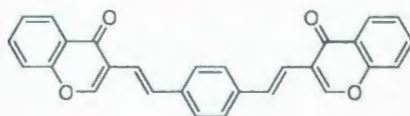
temperature for further 16 h. The solvent was removed under reduced pressure. Column chromatography ( $\text{CHCl}_3$ ) of the crude product yielded **6.18** (3.50 g, 65%) as yellow crystals:  $R_f = 0.75$  (50:50 EtOAc-hexanes); mp 93–94 °C (lit. mp<sup>9</sup> 93–93 °C);  $^1\text{H}$  NMR (500 MHz)  $\delta$  8.27 (dd,  $J = 8.2, 1.8$  Hz, 1H), 8.24 (s, 1H), 7.73–7.70 (m, 1H), 7.50–7.45 (m, 2H);  $^{13}\text{C}$  NMR (125 MHz)  $\delta$  172.5, 156.3, 154.0, 134.3, 126.7, 126.1, 123.4, 118.3, 110.9; MS [APCI (+)]  $m/z$  (%) 225 ( $^{79}\text{Br}, \text{M}^+$ , 100), 227 ( $^{81}\text{Br}, \text{M}^+$ , 98).

### 1,4-Divinylbenzene (**6.19**)<sup>10</sup>



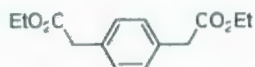
A mixture of terephthalaldehyde (**6.25**) (2.68 g, 20.0 mmol), phosphonium salt **6.26** (14.3 g, 40.0 mmol), and  $\text{K}_2\text{CO}_3$  (7.01 g, 60.0 mmol) in 1,4-dioxane (40 mL) containing  $\text{H}_2\text{O}$  (0.6 mL) was heated at reflux for 20 h. The precipitate was removed by suction filtration and the solvent was removed from the filtrate by vacuum distillation at room temperature. Column chromatography (hexanes) of the crude product yielded **6.19** (1.43 g, 55%) as a colorless liquid:  $R_f = 0.50$  (hexanes);  $^1\text{H}$  NMR (500 MHz)  $\delta$  7.37 (s, 4H), 6.70 (dd,  $J = 17.7, 10.6$  Hz, 2H), 5.74 (d,  $J = 17.7$  Hz, 2H), 5.23 (d,  $J = 11.1$  Hz, 2H);  $^{13}\text{C}$  NMR (125 MHz)  $\delta$  137.4, 136.7, 126.6, 114.0; MS [APCI (+)]  $m/z$  (%) 131 ( $\text{M}^+$ , 100).



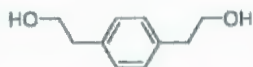
**3,3'-[(1*E*,1'*E*)-2,2'-(1,4-Phenylene)bis(ethenyl)]bis(4*H*-chromen-4-one) (6.15)**


A mixture of 3-bromochromone (**6.18**) (1.02 g, 4.53 mmol), Pd(OAc)<sub>2</sub> (20.2 mg, 90.0 μmol), tri-*o*-tolylphosphine (164 mg, 540 μmol) and triethylamine (800 μL, 5.85 mmol) in DMF (5 mL) was stirred at room temperature and deoxygenated by passing a stream of N<sub>2</sub> through the solution. 1,4-Divinylbenzene (**6.19**) (400 mg, 3.08 mmol) was added and the reaction mixture was heated at 100 °C for 27 h. The solvent was removed under high vacuum. Column chromatography (10:90 EtOAc:hexanes) of the crude product yielded **6.15** (85.2 mg, 9%) as a yellow solid: *R*<sub>f</sub> = 0.24 (35:65 EtOAc:hexanes); mp 283–284 °C; IR ν 3085 (w), 3073 (w), 1642 (s), 1611 (s), 1562 (s), 1509 (w), 1466 (s), 1410 (m), 1356 (s), 1313 (s), 1218 (m), 1184 (m), 1160 (m), 975 (s), 864 (w), 815 (w), 758 (s), 751 (s), 698 (s) (cm<sup>-1</sup>); <sup>1</sup>H NMR (500 MHz) δ 8.32 (dd, *J* = 8.0, 1.3 Hz, 2H), 8.13 (s, 2H), 7.67–7.47 (m, 2H), 7.65 (d, *J* = 16.3 Hz, 2H), 7.53 (s, 4H), 7.48 (d, *J* = 8.4 Hz, 2H), 7.44 (t, *J* = 7.6 Hz, 2H), 7.00 (d, *J* = 16.3 Hz, 2H); <sup>13</sup>C NMR (125 MHz) δ 176.8, 156.1, 153.3, 137.2, 133.7, 131.5, 127.2, 126.5, 125.5, 124.4, 122.1, 119.3, 118.3; MS [APCI (+)] *m/z* (%) 419 (M<sup>+</sup>, 100); HRMS [EI (+)] calcd for C<sub>28</sub>H<sub>18</sub>O<sub>4</sub> 418.1205, found 418.1194.



**1,4-Phenylenediacetic acid diethyl ester (6.27)<sup>11</sup>**

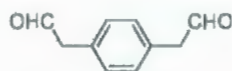
To a solution of *p*-phenylenediacetic acid (**6.17**) (3.12 g, 16.1 mmol) in ethanol (30 mL) was added 2 drops of concentrated sulfuric acid. The reaction mixture was heated at reflux for 9 h. The reaction mixture was cooled to room temperature and poured into ice cold water (150 mL). The white precipitate was collected by suction filtration and dried in air to yield **6.27** (3.71 g, 93%) as a colorless solid:  $R_f$  = 0.54 (35:65 EtOAc:Hexanes); mp 55–56 °C;  $^1\text{H}$  NMR (500 MHz)  $\delta$  7.24 (s, 4H), 4.14 (q,  $J$  = 7.1 Hz, 4H), 3.59 (s, 4H), 1.25 (t,  $J$  = 7.1 Hz, 6H);  $^{13}\text{C}$  NMR (125 MHz)  $\delta$  171.7, 133.1, 129.7, 61.1, 41.3, 14.4; MS [APCI (+)]  $m/z$  (%) 251 ( $\text{M}^+$ , 100).

**1,4-Phenylenediethanol (6.28)<sup>11</sup>**

To a slurry of  $\text{LiAlH}_4$  (1.68 g, 44.4 mmol) in THF (40 mL) was added dropwise a solution of 1,4-phenylenediacetic acid diethyl ester (**6.27**) (3.71 g, 14.8 mmol) in THF (20 mL) at 0 °C. The reaction mixture was stirred at room temperature for 2 h. The reaction mixture was cooled to 0 °C and acidified with cold aqueous 20% HCl and extracted with ether. The organic layer was washed with brine, dried over  $\text{MgSO}_4$  and filtered. The solvent was removed under reduced pressure. Flash column chromatography (EtOAc) of the crude product yielded **6.28** (2.21 g, 90%) as a colorless solid:  $R_f$  = 0.41 (EtOAc); mp 83–84 °C;  $^1\text{H}$  NMR (500 MHz)  $\delta$  7.17 (s, 4H), 3.83 (t,  $J$  = 6.5 Hz, 4H), 2.83 (t,  $J$  = 6.6 Hz, 4H) (OH proton was not observed);  $^{13}\text{C}$  NMR (125

MHz)  $\delta$  136.8, 129.5, 63.8, 39.0; MS [APCI (+)]  $m/z$  (%) 149 ( $M^+$  - OH, 100); 131 ( $M^+$  - 2OH, 80).

### 1,4-Phenylenediactaldehyde (**6.20**)<sup>11</sup>



To a solution of 1,4-benzenediethanol (**6.28**) (659 mg, 3.96 mmol) in  $\text{CH}_2\text{Cl}_2$  (30 mL) was added Dess-Martin periodinane (5.67 g, 13.4 mmol) in one portion. The reaction mixture was stirred at room temperature for 3 h. The solvent was removed under reduced pressure. Column chromatography (95:5  $\text{CH}_2\text{Cl}_2$ :EtOAc) of the crude product yielded **6.20** (314 mg, 49%) as a colorless solid:  $R_f$  = 0.85 (10:90 EtOAc: $\text{CH}_2\text{Cl}_2$ ); mp 48–50 °C;  $^1\text{H}$  NMR (500 MHz)  $\delta$  9.76 (t,  $J$  = 2.2 Hz, 2H), 7.23 (s, 4H), 3.71 (d,  $J$  = 2.2 Hz, 4H);  $^{13}\text{C}$  NMR (125 MHz)  $\delta$  199.4, 131.3, 130.4, 50.3.

## 6.5 References and Notes

- 
- [1] Müller, T. J.J.; Bunz, U. H. F., Eds. *Functional Organic Materials: Syntheses, Strategies and Applications*, Wiley-VCH Verlag GmbH & Co. KGaA, Weinheim, **2007**, pp 230–234.
- [2] Staab, H.; Binning, F. *Chem. Ber.* **1967**, *100*, 293–305.
- [3] Hensel, V.; Lützow, K.; Jakob, J.; Gessler, K.; Saenger, W.; Schlüter, A. D. *Angew. Chem., Int. Ed. Engl.* **1997**, *36*, 2654–2656.
- [4] The term “shape-persistent” in this context means that the average diameter of the compound is equal to the contour length of the molecular backbone divided by  $\pi$ . A

---

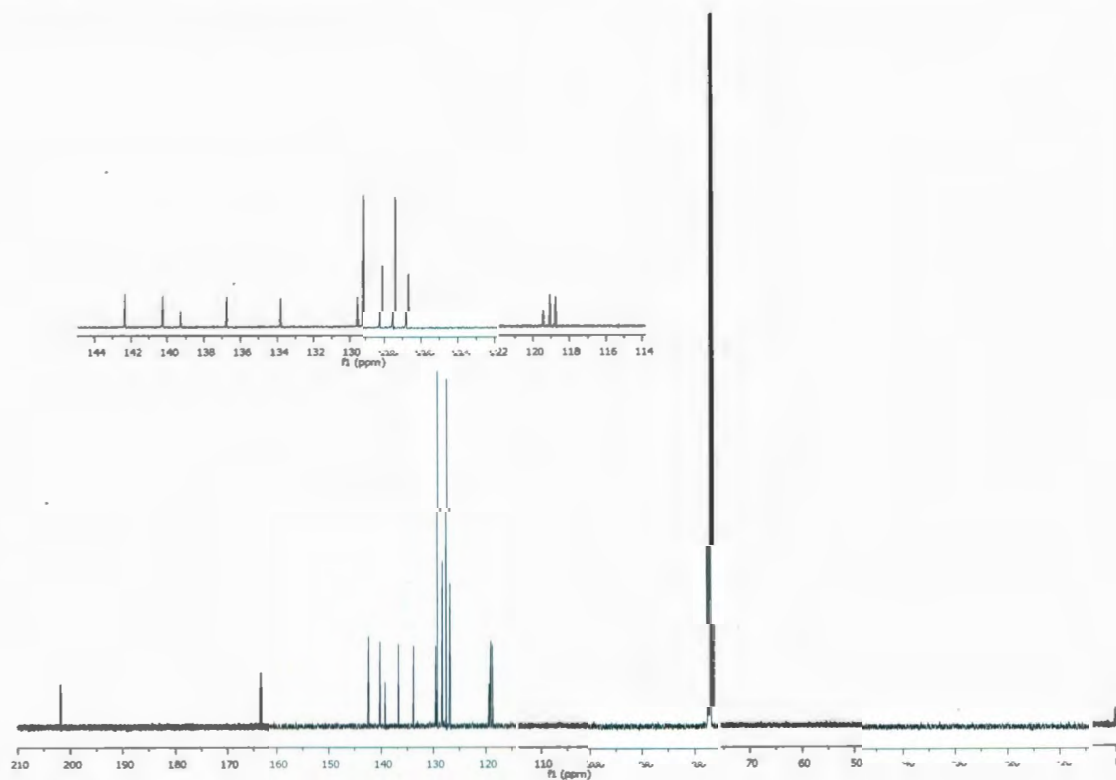
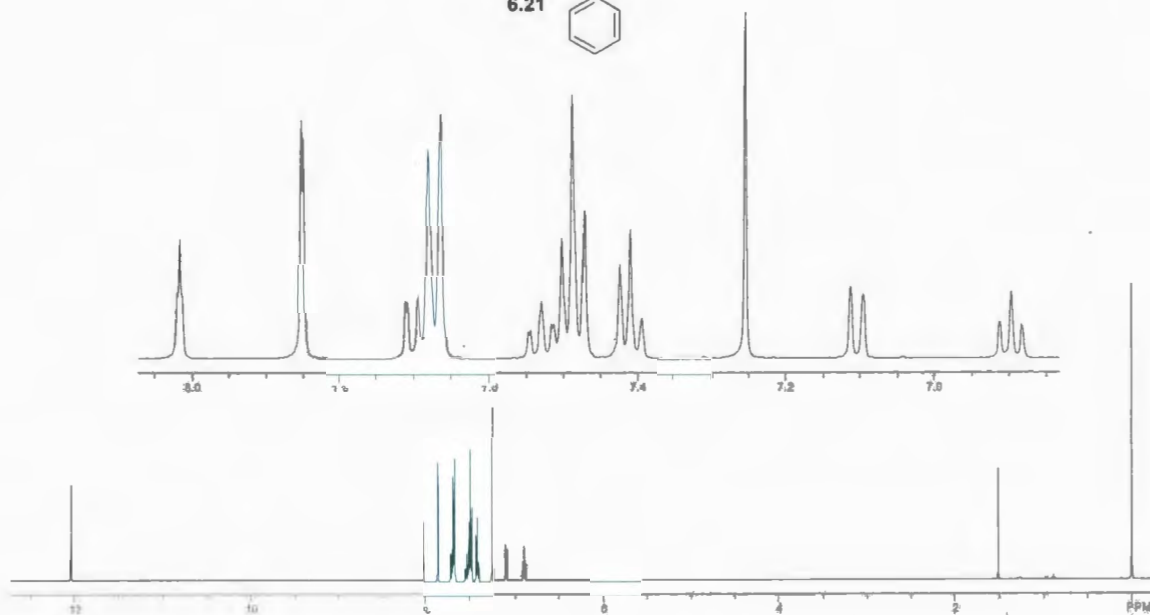
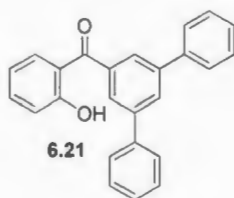
shape-persistent macrocycle's backbone is made of rigid components with a high persistent length. See reference 1, page 225.

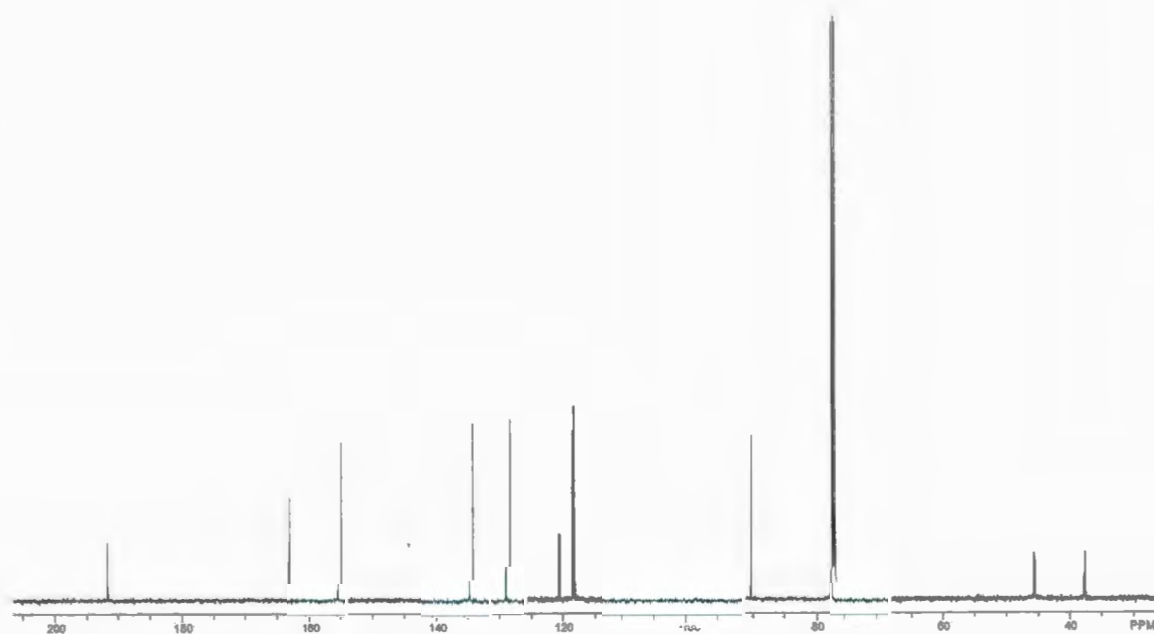
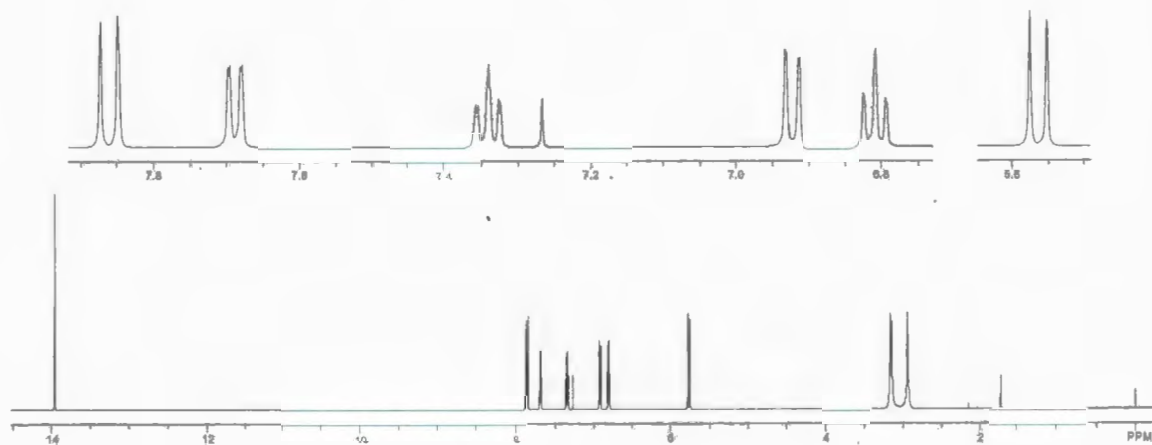
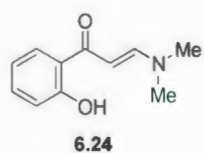
- [5] Zhang, W.; Moore, S. *J. Am. Chem. Soc.* **2004**, *126*, 12796 (1 page).
- [6] Bodwell, G. J.; Hawco, K. M.; Satou, T. *Synlett* **2003**, 879–881.
- [7] For examples of the Dakin reaction, see: Varma, R. S.; Naicker, K. P. *Org. Lett.* **1999**, *1*, 189–191. Lee, J. B.; Uff, B. C. *Quart. Rev.* **1967**, *21*, 429–457. Baker, W.; Bondy, H. F.; Gumb, J.; Miles, D. *J. Chem. Soc.* **1953**, 1615–1619. Dakin, H. D. *Org. Synth., Coll. Vol. 1*; Wiley: New York, **1941**, pp 149.
- [8] SPARTAN '08 software from Wavefunction, Inc. Irvine, CA, USA.
- [9] Gammill, R. B. *Synthesis* **1979**, *11*, 901–903.
- [10] Delmas, M.; Gaset, A. *Synth. Commun.* **1983**, *13*, 177–182.
- [11] Zhang, X.; Sarkar, S.; Larock, R. C. *J. Org. Chem.* **2006**, *71*, 236–243. Melting points of **6.28**, **6.29**, **6.20** were not reported in the literatures.
- [12] For all known compounds, a literature citation is given after the compound name. In all cases, the spectroscopic data is consistent with published data.

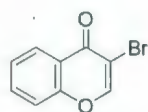
## Appendix

Selected NMR spectra for synthesized compounds

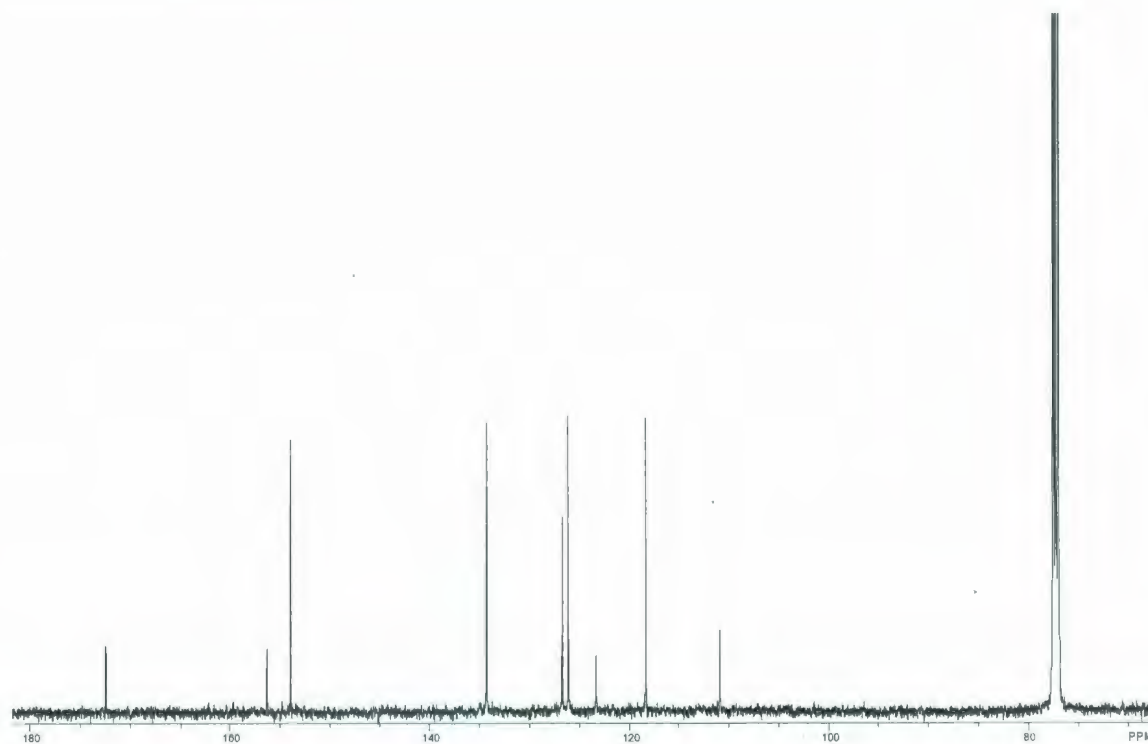
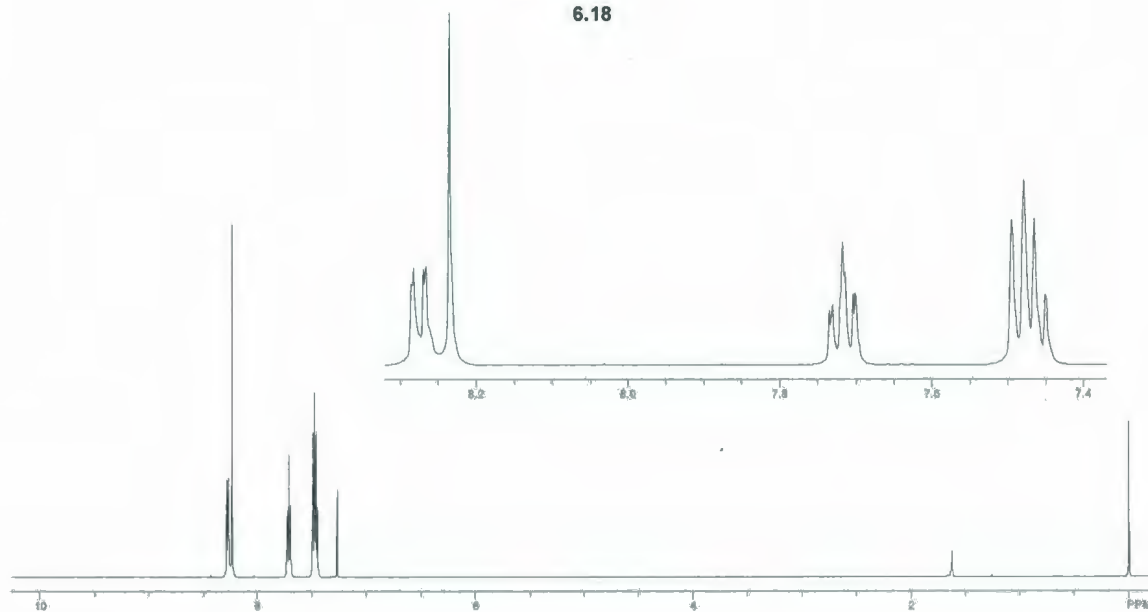


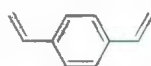




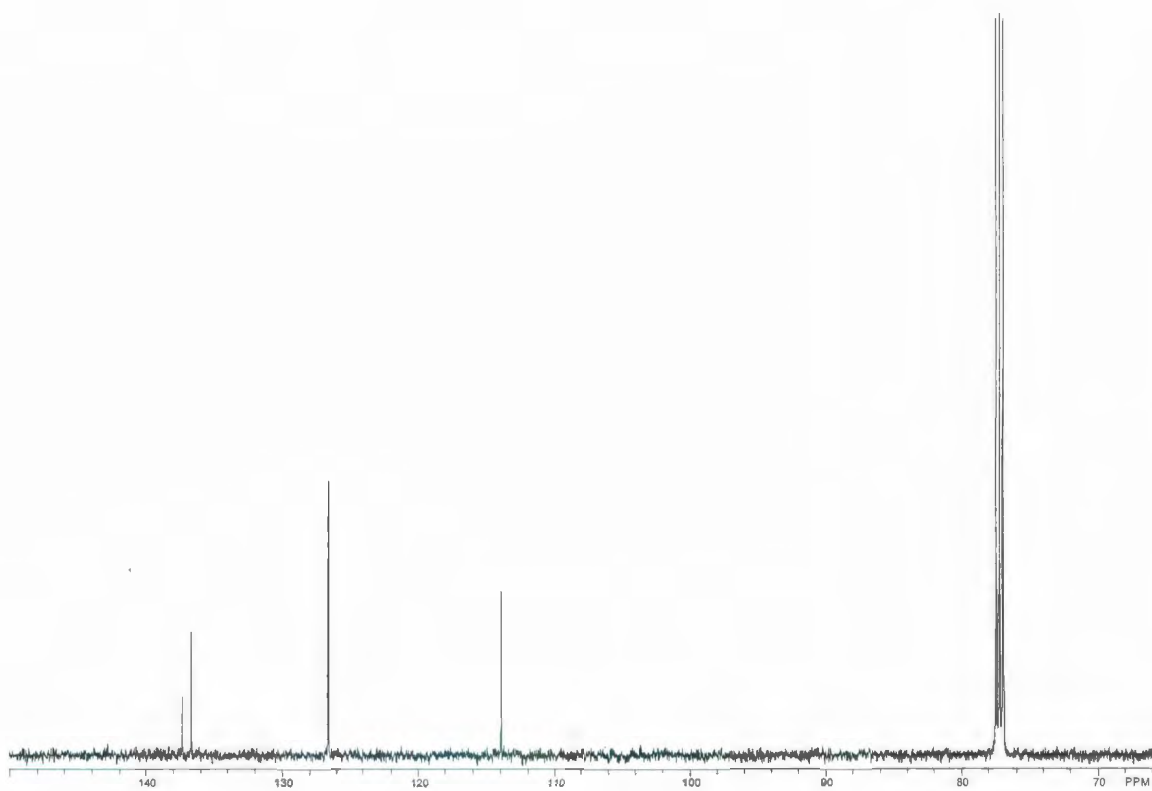
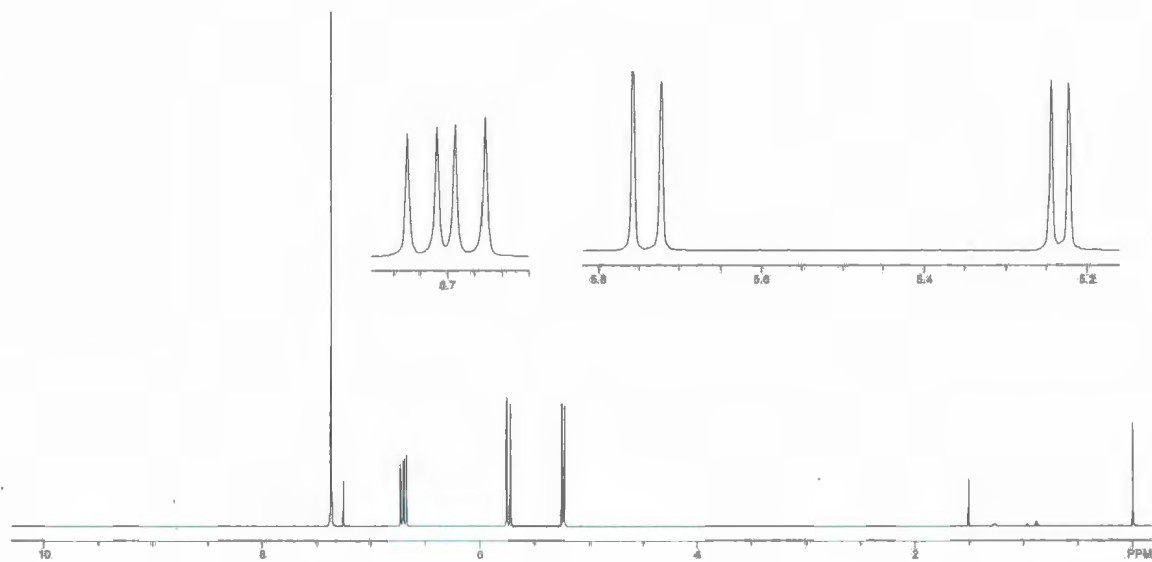


6.18

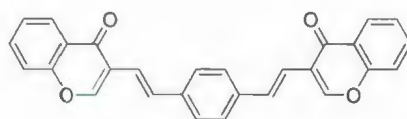




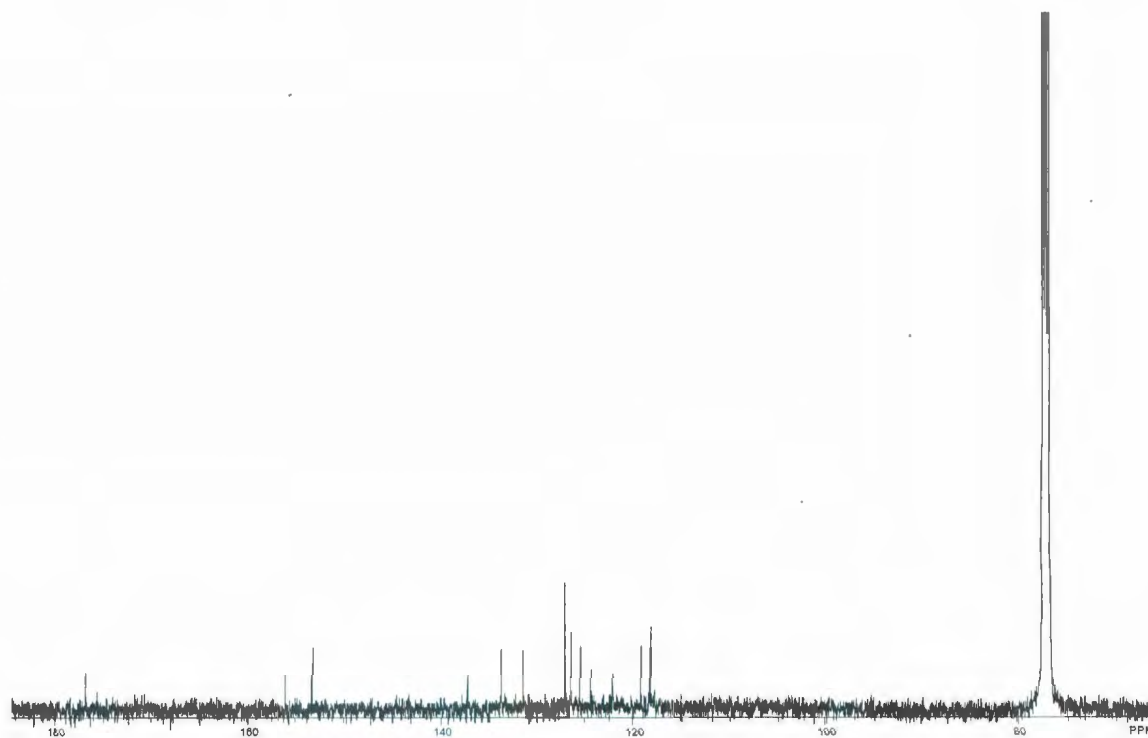
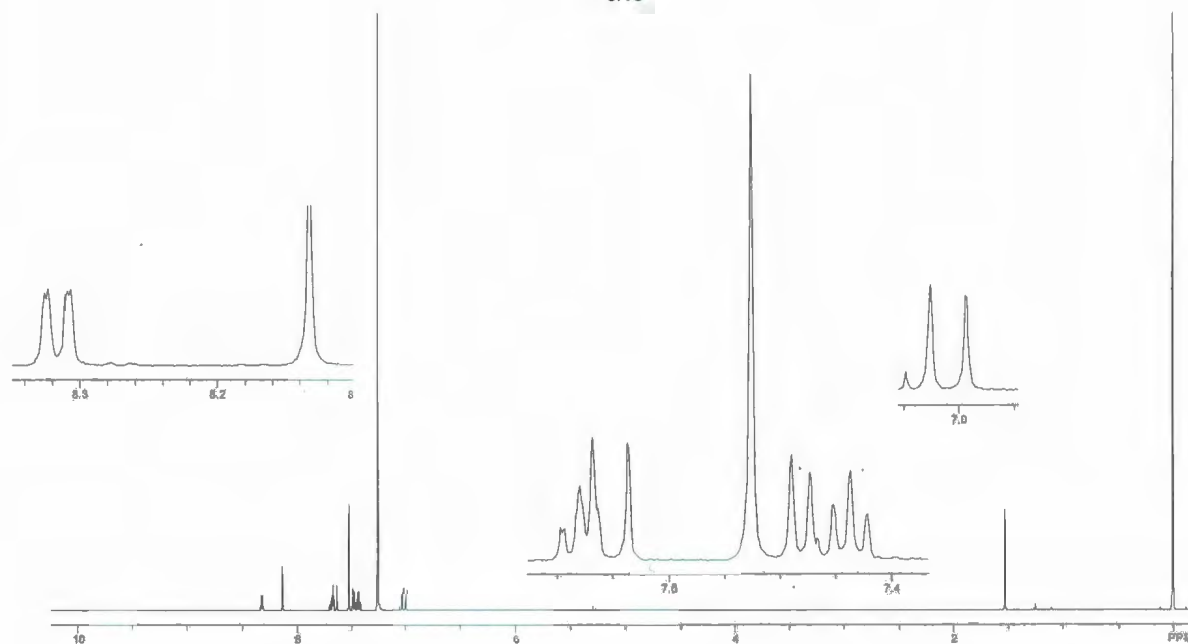
6.19

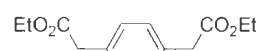




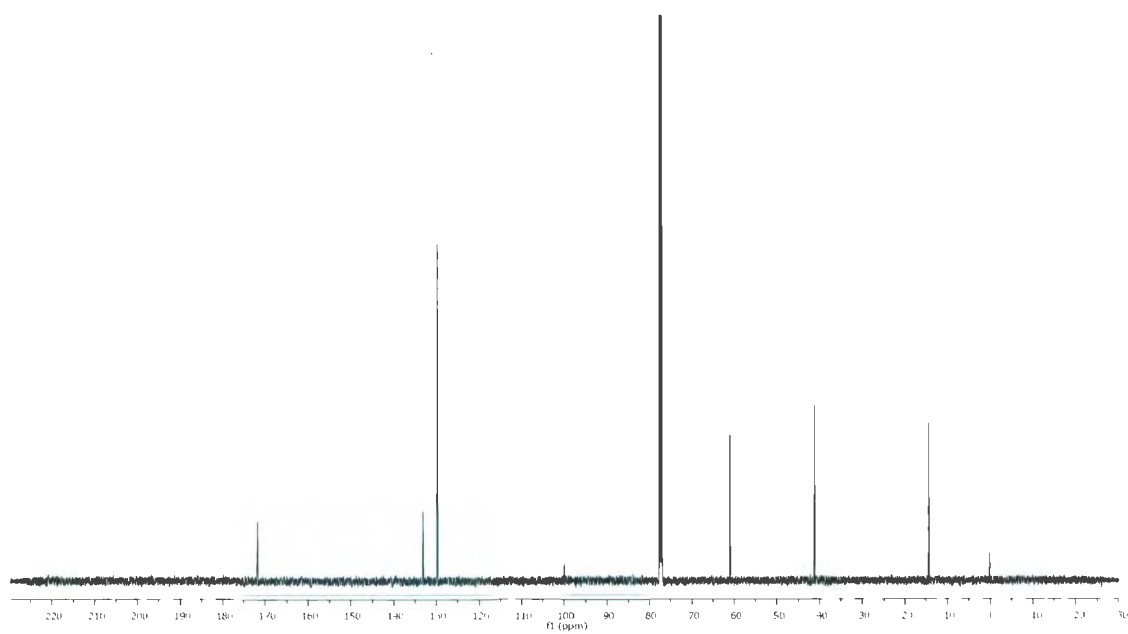
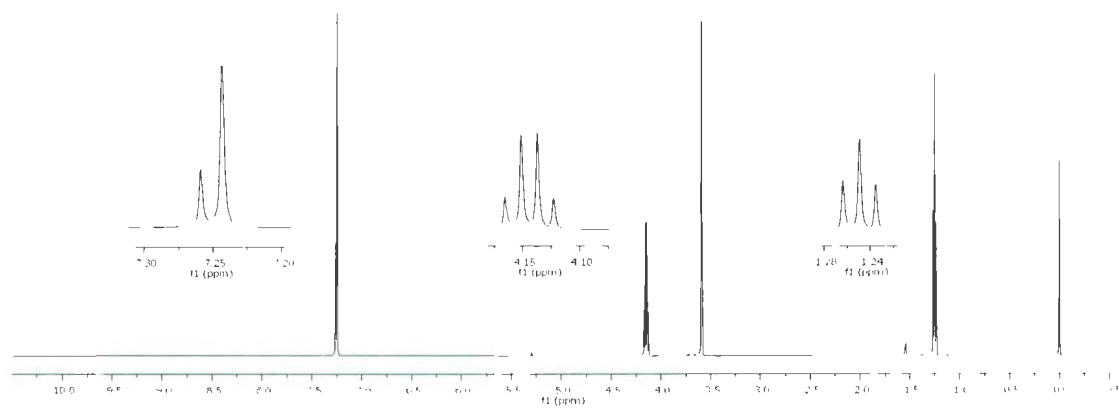


6.15



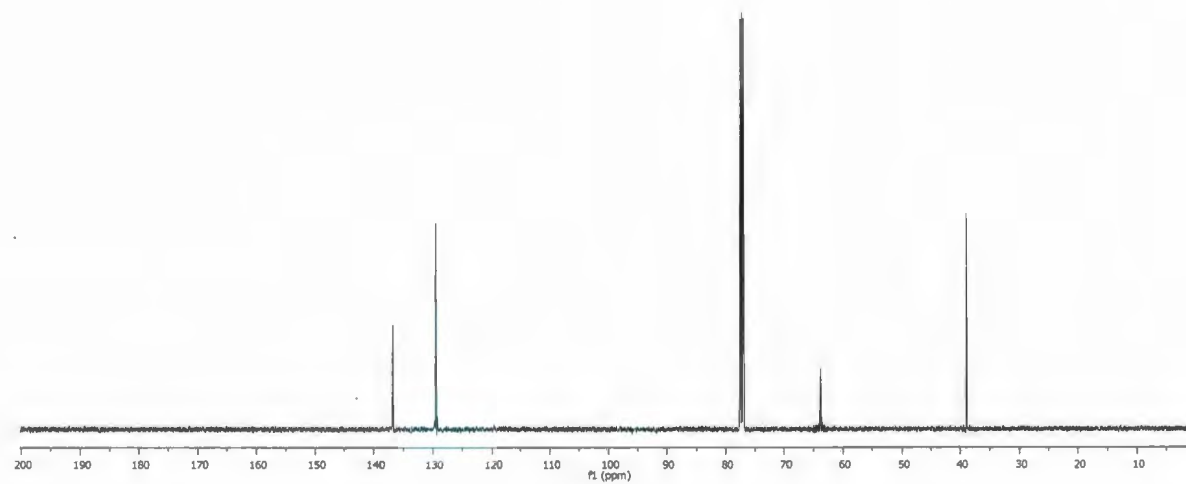
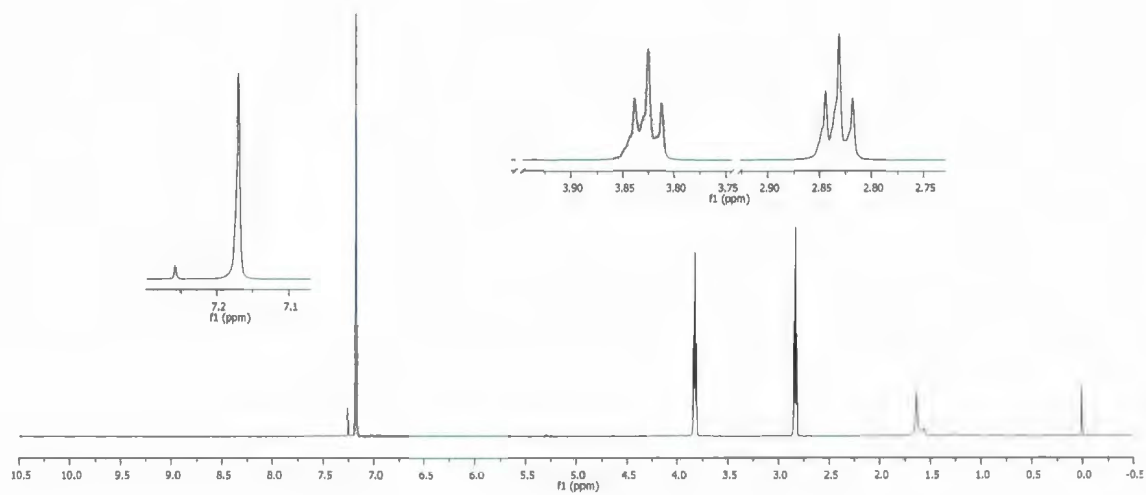


6.27





6.28





6.20

